WILEY-VCH

Edited by Mohammad A. Jafar Mazumder,
Mumtaz A. Quraishi, and Amir Al-Ahmed

# Polymeric Corrosion Inhibitors for Greening the Chemical and Petrochemical Industry

# Polymeric Corrosion Inhibitors for Greening the Chemical and Petrochemical Industry

# Polymeric Corrosion Inhibitors for Greening the Chemical and Petrochemical Industry

*Edited by*

*Mohammad A. Jafar Mazumder*
*Mumtaz A. Quraishi*
*Amir Al-Ahmed*

WILEY-VCH

**The Editors**

***Dr. Mohammad A. Jafar Mazumder***
King Fahd University of Petroleum & Minerals
Chemistry Department
31261 Dhahran
Saudi Arabia

***Dr. Mumtaz A. Quraishi***
King Fahd University of Petroleum
& Minerals
Interdisciplinary Research Center for Advanced Materials
31261 Dhahran
Saudi Arabia

***Dr. Amir Al-Ahmed***
King Fahd University of Petroleum
& Minerals
Interdisciplinary Research Center for Renewable Energy and Power Systems
31261 Dhahran
Saudi Arabia

**Cover Image:** © CHUNYIP WONG/
Getty Images

**Library of Congress Card No.:** applied for

**British Library Cataloguing-in-Publication Data**
A catalogue record for this book is available from the British Library.

**Bibliographic information published by the Deutsche Nationalbibliothek**
The Deutsche Nationalbibliothek lists this publication in the Deutsche Nationalbibliografie; detailed bibliographic data are available on the Internet at <http://dnb.d-nb.de>.

**Print ISBN:** 978-3-527-34992-0
**ePDF ISBN:** 978-3-527-83560-7
**ePub ISBN:** 978-3-527-83561-4
**oBook ISBN:** 978-3-527-83562-1

**Typesetting** Straive, Chennai, India

# Contents

## 10 Green Polymeric Inhibitors for Corrosion of Metals in Alkaline Media *221*

*Refat M. Hassan (El-Moushy)*

# Preface

Corrosion is a destructive phenomenon that causes the degradation of metals and alloys. It potentially affects industrial equipment and reduces the shelf life of the infrastructure assets and the quality of the environment. Corrosion is one of the significant problems for most industrialized countries, particularly considering the economic growth and infrastructure development, which can eventually pose a severe threat to human life and indirectly shade our everyday lives. In the twenty-first century, the primary challenge is to minimize/prevent pipes and other plant systems' failures by adequately dealing with corrosion. Using corrosion inhibitors, particularly polymeric corrosion inhibitors, is a cost-effective, safe, and easy-to-employ approach, among other prevailing corrosion tackling methods.

Corrosion inhibitors in the petrochemical industries are an excellent resource for international experts actively involved in research and development in the fields of material science, chemistry and electrochemistry, and chemical/mechanical/metallurgical engineering to counter the economic and environmental consequences of corrosion. Considering the vast importance of polymeric corrosion inhibitors for greening the chemical and petrochemical industry, this reference book systematically presents the fundamentals, up-to-date development, and industrial applications of polymeric corrosion inhibitors. It covers a comprehensive overview of polymeric corrosion inhibitors' synthesis, properties, process, and applications as innovative sustainable materials for the chemical and petrochemical industry. The primary focus of this book is to provide an overview of the most recent advancement and showcase experimental results based on their applications, which will open new windows for researchers to use polymers as corrosion inhibitors for greening the chemical and petrochemical industry.

Overall, this book will be helpful for senior researchers in industry and academia working in corrosion protection and assist the graduate and senior undergraduate students as a reference book.

King Fahd University
of Petroleum & Minerals
Dhahran 31261
Saudi Arabia
August 2022

*Mohammad A. Jafar Mazumder,*
*PhD, CChem., FRSC*
*Mumtaz A. Quraishi, PhD, DSc, FRSC*
*Amir Al-Ahmed, PhD*

# Acknowledgments

We are thankful to all contributing authors and coauthors for their valued contribution to this book. The project would never have been possible without their sincere support and contributions. We would also like to express our gratitude to the publisher, authors, and others for granting us copyright permission to use their illustrations. Although sincere efforts were made to obtain the copyright permissions from the respective owners to include the citation with the reproduced materials, we would like to apologize to any copyright holder if, unknowingly, their right is being infringed. Among the editors, Dr. Mohammad A. Jafar Mazumder would like to take this opportunity to express his sincere thanks to Drs. Abdulaziz A. Al-Saadi (Dean, College of Chemicals and Materials, KFUPM) and Khalid R. Alhooshani (Chairman, Chemistry Department, KFUPM) and also to his colleagues at the King Fahd University of Petroleum & Minerals (KFUPM), Saudi Arabia. Dr. Mumtaz A. Quraishi would like to take this opportunity to express his sincere thanks to Dr. Ahmad A. Sorour (Director IRC-AM, KFUPM) and also to his colleagues at the King Fahd University of Petroleum & Minerals, Saudi Arabia. Dr. Amir Al-Ahmed expresses his sincere thanks to Dr. Fahad Al-Suliman (Director IRC-HES, KFUPM) and his colleagues at the King Fahd University of Petroleum & Minerals, Saudi Arabia. This book would not have been brought into its final form without their continuous encouragement. We would also like to acknowledge the sincere efforts of the Wiley team, especially Dipl.-Ing. Felix Bloeck and Mrs. Lesley Fenske and others, who were always so helpful and provided us their assistance in evolving this book into its final shape. We are most grateful to all of them.

# About the Editors

## Dr. Mohammad A. Jafar Mazumder

Dr. Mohammad A. Jafar Mazumder has been working as a Professor of Chemistry at KFUPM, Saudi Arabia. His current research interest includes the design, synthesis, and characterization of various organic compounds and polymers for potential use in the inhibition of mild steel corrosion in oil and gas industries and polyelectrolyte-coated membranes/resin for the removal of heavy metals and organic contaminants from aqueous water samples. Dr. Jafar Mazumder secured 7 US patents, published more than 85 articles in peer-reviewed journals, 37 conference abstracts/proceedings, 9 book chapters, and co-edited 4 books with Springer Nature and Trans Tech publications. He has been awarded as a Fellow of the Royal Society of Chemistry, UK, and Chartered Chemist, Association of Chemical Profession of Ontario, Canada. He is currently serving as an Editorial Board member of five international journals. He was awarded numerous national and international scholarships and awards in his academic career, including the prestigious Indian Council for Cultural Relations (ICCR) Scholarship, Govt. of India, for undergraduate studies, and MITACS postdoctoral fellowship (Canada) for pursuing postdoctoral research in chemical and biomedical engineering.

## Dr. Mumtaz A. Quraishi

Dr. Mumtaz A. Quraishi is a Chair Professor at the Interdisciplinary Research Center for Advanced Materials at King Fahd University of Petroleum and Minerals, Saudi Arabia. Before joining KFUPM, he was a Full Professor in Chemistry at the Indian Institute of Technology BHU Varanasi. Dr. Quraishi also served as Head of the Chemistry IIT BHU Varanasi. He obtained a PhD in Chemistry in 1986 at Kurukshetra University and DSc in corrosion inhibition in 2004 from Aligarh Muslim University. He has published more than 300 papers (H index 93, Citations 27416) in reputed journals. Prof. Quraishi is a fellow of the Royal Society of Chemistry, UK. He has received several prestigious awards, including Life Time Achievement Awards (International Science Congress Association, ISCA), and National Corrosion Council of India, Electrochemical Society Bangalore, Meritorious and Excellence awards (NACE India), MASCOT award (Electrochemical Society Bangalore, India), Vigyan Ratna Award (Council of Science and Technology, India). He is a member of Editorial Board of >12 international journals and Associate Editor of current *Material Science Bentham Science*. His current research area is the synthesis and applications of green corrosion inhibitors.

**Dr. Amir Al-Ahmed**

Dr. Amir Al-Ahmed is working as a Research Scientist-II (Associate Professor) in the Interdisciplinary Research Center for Renewable Energy and Power Systems at King Fahd University of Petroleum & Minerals (KFUPM), Saudi Arabia. He graduated in chemistry from the Department of Chemistry, Aligarh Muslim University (AMU), India. Then he completed his MPhil (2001) and PhD (2004) degrees in Applied Chemistry from the Department of Applied Chemistry, AMU, India, followed by three consecutive postdoctoral fellowships in South Africa and Saudi Arabia. He has been working on various multidisciplinary projects, particularly electrochemical sensors, nanomaterials, proton-exchange membranes, electrocatalysis, and solar cells. At present, his research activity is fundamentally focused on third-generation solar cell devices, such as low bandgap semiconductor quantum dot structures, perovskite cells, and tandem cells. At the same time, he also has projects on heat storage, evaluation of electricity storage devices, and dust-repellent coating for PV. He has worked on different KACST, NSTIP, and Saudi Aramco-funded projects in the capacity of co-investigator and principal investigator. Dr. Amir has 8 US patents, over 60 journal articles, invited book chapters, and conference publications. He has edited nine books with Springer, Trans Tech Publication, and Elsevier, and several other books are in progress. He is also the Editor-in-Chief of an international journal, *Nano Hybrids and Composites*, along with Professor Y. H. Kim.

# 1

# Green Polymeric Corrosion Inhibitors: Design, Synthesis, and Characterization

*Dheeraj S. Chauhan*[1,2], *Mumtaz A. Quraishi*[3], *Hussein Al-Qahtani*[1], *and Mohammad A. Jafar Mazumder*[3,4]

[1] *Modern National Chemicals, Second Industrial City, Dammam 31421, Saudi Arabia*
[2] *King Fahd University of Petroleum & Minerals, Center of Research Excellence in Corrosion, Dhahran 31261, Saudi Arabia*
[3] *King Fahd University of Petroleum & Minerals, Interdisciplinary Research Center for Advanced Materials, Dhahran 31261, Saudi Arabia*
[4] *King Fahd University of Petroleum & Minerals, Chemistry Department, Dhahran 31261, Saudi Arabia*

## 1.1 Introduction

Different industrial practices require the use of metals and metal-based structures [1, 2]. In these environments, the metals can directly contact the aggressive acidic, alkaline, saline, etc. media [3]. This can cause considerable damage to the underlying metallic surface that causes significant economic losses and is a potential hazard to the environment. The application of organic molecules as corrosion inhibitors is one of the most effective means to counter corrosion issues. Most effective corrosion inhibitors are based on inorganic and organic molecules, which are toxic and pose serious environmental concerns. Due to strict environmental regulations, there is growing research attention in the area of environment-friendly alternatives as corrosion inhibitors. This includes the categories of naturally occurring plant extracts, drugs, biopolymers, amino acids, proteins, and ionic liquids (ILs) [4–7].

This chapter presents a brief overview of corrosion, impact, and its background, emphasizing green corrosion inhibitors. The significance of biopolymers as corrosion inhibitors is described, and a comprehensive review of literature is presented on the application of biological polymeric corrosion inhibitors derived from polysaccharides and proteins. The importance of the chemical functionalization of corrosion inhibitor molecules and the application of chemically modified biopolymers as corrosion inhibitors are also outlined. This review article is expected to benefit the scientists and researchers working in this area and would act as a reference tool for the chemists/biochemists working in this field.

*Polymeric Corrosion Inhibitors for Greening the Chemical and Petrochemical Industry*, First Edition.
Edited by Mohammad A. Jafar Mazumder, Mumtaz A. Quraishi, and Amir Al-Ahmed.

## 1.2 Corrosion and Its Economic Significance

Corrosion is a major industrial nuisance, and its control is a considerably challenging issue in different industrial applications. The corrosion damage incurred upon the metals and alloys in the presence of aqueous corrosive environments is considered a major concern in several industries. The metals are generally purified from their respective ore forms by applying a considerable amount of energy. Therefore, these metallic surfaces have a significant tendency to revert to their original ore forms when exposed to the environment. This process of natural degradation and deterioration of the metals and alloys to their original forms is referred to as corrosion, which poses enormous economic losses and can even lead to potential structural failure and even loss of human life. According to a study by the National Association of Corrosion Engineers (NACE), the number of developed and developing nations estimated that the global annual loss is due to corrosion amounts to around US$3.4 trillion [8]. A number of different methods are in practice to control and mitigate corrosion. This includes anticorrosion coatings, corrosion inhibitors, corrosion-resistant alloys, and cathodic protection. The use of corrosion inhibitors becomes a preferred choice to counter the aqueous corrosion of metals and alloys in various media. For this reason, many researchers working in chemical engineering, mechanical engineering, materials science, computational studies, and organic chemistry are devoted to developing efficient corrosion inhibitors.

## 1.3 Corrosion Inhibitors

The corrosion inhibitors can be described as chemical additives, when introduced to a corrosive environment, and can minimize corrosion losses [3]. Conventionally, the inorganic chemical compounds from the classes of chromates, nitrites, nitrates, and phosphonates are the preferred choice as corrosion inhibitors [9]. In addition, the organic molecules from the categories of azoles, pyridines, and pyrimidines are also a preferred choice. This is due to the presence of an abundance of heteroatoms (N, S, O, etc.) on the inhibitor backbone and the existence of phenyl rings, $\pi$-bonds, etc. that can aid in the adsorption of the inhibitor molecules on the metallic surface. However, the use of conventional inorganic/organic corrosion inhibitors has caused severe environmental concerns forcing scientists and researchers worldwide to focus on using greener alternatives as corrosion inhibitors.

### 1.3.1 Green Corrosion Inhibitors

Several organic corrosion inhibitors come into the category of environmentally benign molecules. This includes synthetic heterocyclic molecules, amino acids, natural extracts, biological polymers, and ILs. The criteria of greenness include: (i) Toxicity in terms of $EC_{50}$ and $LC_{50}$ values $> 10\ \mathrm{mg\,l^{-1}}$ to North Sea species (algae, fish, crustacean, and seabed worms); (ii) Biodegradability: >60% in 28 days; (iii) Bioaccumulation: $\log(P_{\mathrm{o/w}}) < 3$ or Mol. Wt. $> 600\ \mathrm{g\,mol^{-1}}$. Literature shows the number of natural extracts derived from different plant parts, such as leaves, stems, fruits, flowers, peel, and pulp [7], has been explored as corrosion inhibitors for various media. The presence of different phytochemical constituents in these extracts is responsible for the adsorption and corrosion inhibition behavior.

Another example is the pharmaceutical products that contain a number of heterocycles, heteroatoms, and phenyl rings and can undergo adsorption on the metal surface [10, 11]. The ILs that are the room-temperature liquid molecules containing organic cations and ions are another category of green inhibitors. Their appreciable solubility in the corrosive media has led to the application of several ILs in corrosion inhibition [12]. Some of the examples of IL-based corrosion inhibitors are given in Scheme 1.1. Imidazolium and pyridinium-based ILs were studied for mild steel in 1 M $H_2SO_4$ [13]. High inhibition performance of 82–88% at 100 mg $l^{-1}$ was noticed with chemical adsorption supported from the surface analytical measurements. A pyridazinium-based IL was prepared by El-Hajjaji et al. and evaluated for mild steel in 1 M HCl medium. High inhibition performance at high temperatures was observed [4]. The same group studied two pyridazinium-based ILs 1-decylpyridazin-1-ium iodide (DPI) and 1-tetradecylpyridazin-1-ium iodide (TPI) for mild steel in 1 M HCl using electrochemical and surface analysis [14]. Density functional theory (DFT)–based computational investigation of the inhibitors was in good agreement with the experimental results. Two pyridinium ILs were studied on mild steel in 1 M HCl by electrochemical methods. [15]. Tafel evaluation revealed anodic type of corrosion inhibitors. The experimental studies supported by the computational methods of analysis indicated that the inhibitor having longer alkyl chain length provided better performance. Other examples of green inhibitors are

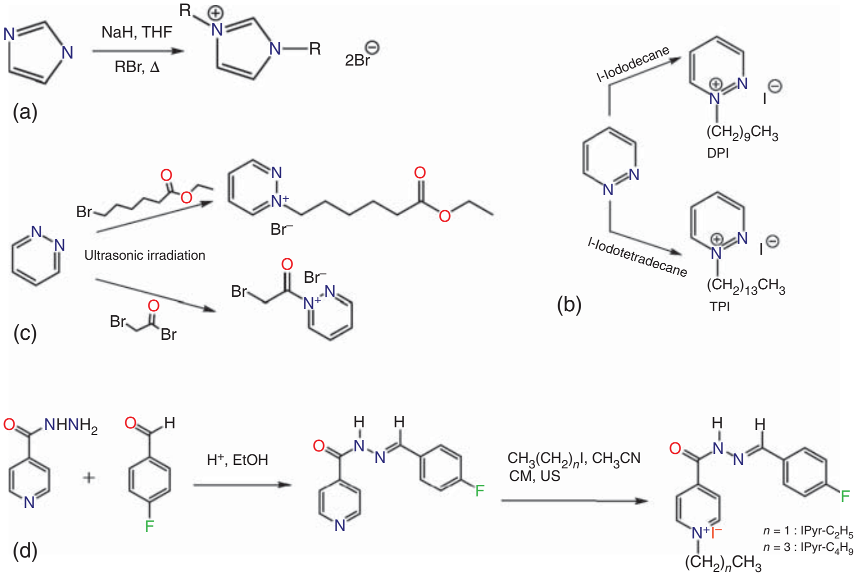

**Scheme 1.1** Synthesis of different ionic liquid-based corrosion inhibitors. Source: (a) Likhanova et al. [13]/Elsevier, (b–d) El-Hajjaji et al. [4, 14, 15]/Elsevier.

bio-derived polymers [16] and amino acids [17] that undergo effective adsorption on the metallic substrates.

### 1.3.2 Importance of Biopolymers as Corrosion Inhibitors

Polymeric corrosion inhibitors find significance due to the high surface coverage and the availability of plenty of adsorption sites to interact with the metallic surface. The biopolymers refer to the polymeric corrosion inhibitors derived from the classes of polysaccharides and proteins. Biopolymers gain their market share by their intrinsic biodegradable nature in combination with the exciting properties that have been applied for specific applications. The biopolymers can be extracted from natural resources, biosynthesized by living organisms, or chemically produced from biological materials [18]. Being of natural origin, biopolymers present a significant advantage over plastic-based materials. Additional advantages include biocompatibility, renewal origin, biocompatibility, barrier action against moisture/gases, low toxicity, and cost-effectiveness. A primary benefit associated with these molecules is the greenness and the environmentally benign nature. Several research articles are focused on the development of corrosion inhibitors based on biopolymers. To further improve the solubility and the corrosion inhibition performance, researchers have also investigated the chemical functionalization of these corrosion inhibitors. The global biopolymers market can be expected to attain around US$10 billion by 2021, at a growth rate of approximately 17% [19]. A detailed account of the corrosion inhibitors developed from polysaccharides, proteins, and chemically modified biopolymers is given in the following sections.

## 1.4 Polysaccharides as Corrosion Inhibitors

Carbohydrates are naturally abundant and are green in nature. Naturally occurring carbohydrate polymers have emerged as a potential class of corrosion inhibitors due to their appreciable biodegradability, biocompatibility, and solubility in aqueous media [16]. Some of these are given in Figure 1.1. A beneficial aspect of using these polymers as corrosion inhibitors is their natural origin, due to which they do not pose any environmental concerns. In addition, being of a polymeric nature, these molecules contain a number of heteroatoms, functional groups, and a large molecular weight that can afford a considerable coverage of the metallic surface. In the below section, a literature review on the application of some of the corrosion inhibitors developed from carbohydrate polymers is discussed. The biopolymer-based corrosion inhibitors are designed using DFT-based computational studies. From these studies, the computational parameters of frontier molecular orbital energies ($E_{\mathrm{HOMO}}$, $E_{\mathrm{LUMO}}$), molecular orbital energy gap ($\Delta E$), electronegativity ($\chi$), hardness ($\eta$), softness ($\sigma$), etc. are evaluated. On that basis, the reactivity and tendency to adsorb on a given metallic substrate can be determined [20]. The synthesis/chemical functionalization of the biopolymers can be accomplished using simple single-step chemical methods. The biopolymers are

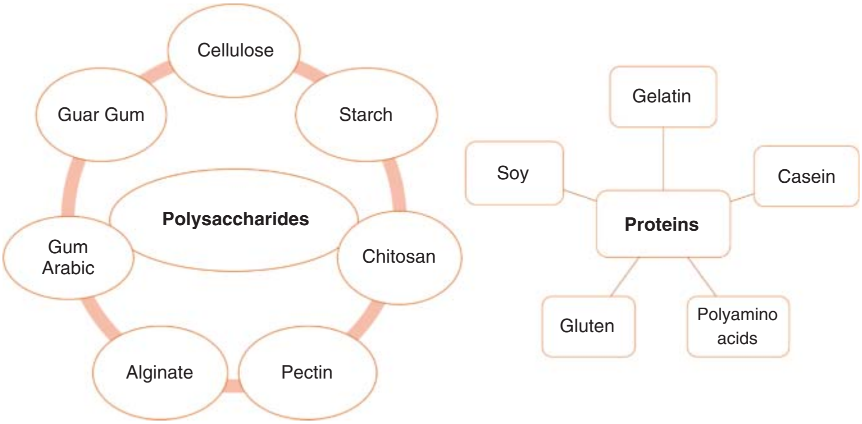

**Figure 1.1** Different types of polysaccharides and proteins-based biopolymers reported as corrosion inhibitors.

characterized using spectral analysis methods, including Fourier-transform infrared spectroscopy (FTIR), nuclear magnetic resonance (NMR) ($^1$H NMR, $^{13}$C NMR), molecular weight analysis, and thermal stability using thermogravimetric analysis (TGA).

Chitosan is a polysaccharide extracted from chitin, which constitutes the exoskeleton of insects, molluscs, shrimps, etc. It was studied on copper corrosion for 0.5 M HCl [21]. Scanning electron microscopy (SEM) and FTIR analyses supported the inhibitor adsorption on the metallic surface. For mild steel substrate, chitosan was studied in 0.1 M HCl, wherein the inhibition efficiency (IE) increases with increasing the inhibitor concentration, and maximum efficiency of 68% was achieved [22]. Chitosan and carboxymethylcellulose were studied for API 5L X60 steel surface in the sweet environment via electrochemical impedance spectroscopy (EIS), potentiodynamic polarization (PDP), and surface analysis [23]. The inhibitor performance was also compared with a commercial inhibitor formulation, and encouraging results were noted. Hydroxyethylcellulose was investigated for zinc surface in ammonium chloride [24]. Electrochemical and surface analysis evidenced the inhibitor adsorption on the metallic surface. The high inhibition efficiency was noticed with the thermodynamic parameters indicating the physical mode of adsorption. Sodium alginate is a polysaccharide carbohydrate extracted from seaweed (such as *sargassum*). It is biodegradable and nontoxic, has good biocompatibility, can reduce blood glucose and lipid levels, clean the intestinal tract, eliminate heavy metals, and have other functions beneficial to health. Sodium alginate is an unbranched binary copolymer of (1–4)-linked β-ᴅ-mannuronic acid (M) and α-l-guluronic acid (G) residues as monomers, constituting of M, G, and MG sequential block structures [25]. Sodium alginate as a corrosion inhibitor was evaluated for Mg alloy AZ31 in NaCl environment [26]. Surface analysis by SEM and FTIR supported the adsorption of sodium alginate on the metal surface. It was also studied for X60 carbon steel in the saline environment using weight loss and electrochemical measurements [27]. The inhibitor adsorption on the metal surface took place by the carboxylate oxygen groups and exhibited a physical mode of adsorption. Ultraviolet (UV)–vis and FTIR verified the adsorption of the corrosion inhibitor on the metallic substrate. Chitosan and carboxymethylcellulose were studied for API 5L X60 steel surface in sweet environment via EIS, PDP, and surface analysis [23]. The inhibitor performance was also compared with a commercial inhibitor formulation, and encouraging results were noted. Hydroxyethylcellulose was investigated for zinc surface in ammonium chloride [24]. Electrochemical and surface analysis evidenced the adsorption of hydroxyethylcellulose on the metallic surface. The high inhibition efficiency was noticed with the thermodynamic parameters indicating the physical adsorption.

Guar gum is a polysaccharide consisting of a straight chain of D-mannopyranose units joined by β-(1 → 4) linkage with a side-branching unit of a single D-galactopyranose unit joined to every other mannose unit by α-(1 → 6) linkages. It was analyzed for carbon steel corrosion in 1 M $H_2SO_4$ by applying weight loss and PDP tests [28]. Guar gum was also studied for pure aluminum in 1 M HCl, and 84.19% protection efficiency was noted at a dose of $0.4\,g\,l^{-1}$ [29]. Gum acacia (GA) is a complex arabinogalactan, which contains a small proportion of proteinaceous materials and has been classified as arabinogalactan–protein complex. Gum acacia was analyzed for steel in 1 M HCl, resulting in 95% inhibition at $1\,g\,l^{-1}$ [30]. Atomic force microscopy (AFM) and X-ray photoelectron spectroscopy (XPS) evidenced the inhibitor adsorption, and the formation of a protective film on the metal surface further supported using the DFT-based computational studies. Gum arabic provided 83.5% inhibition efficiency at $5\,g\,l^{-1}$ when evaluated for carbon steel 1018 [31].

Pectin is a structural heteropolysaccharide contained in the primary cell walls of terrestrial plants. It is produced commercially as a white to light brown powder, mainly extracted from citrus fruits. Electrochemical tests studied pectin as a corrosion inhibitor for X60 steel substrate in a 0.5 M HCl environment [32]. EIS revealed a charge-transfer control of the inhibition performance that was further supported with contact angle measurements, which exhibited an increment in the hydrophobicity with the inhibitor-adsorbed film providing evidence for the formation of inhibitor film on the steel surface. On the aluminum surface, pectin provided 92.1% protection at a dose of $2\,g\,l^{-1}$ [33]. The $\Delta G^0{}_{ads}$ values indicated spontaneous inhibitor adsorption with a primarily mixed type of inhibition. Starch is a natural polymer, available in abundance at low cost, renewable, and biodegradable. Chemically, it is a polysaccharide carbohydrate consisting of a large number of glucose units joined together by glycosidic bonds. All green plants produce starch as an energy store. It contains two structurally different components: amylose (15–20%) and amylopectin (80–85%). The amylose is composed of a large linear chain of a (1–4) linked α-D-glucopyranosyl residue, whereas amylopectin is a branching form of α-glycogen linked by a (1–6) linkage. Amylose was evaluated on mild steel in 0.1 M $H_2SO_{4,}$ and 64.78% protection was achieved at 500 $mg\,l^{-1}$ [34]. The addition of cetyltrimethylammonium bromide (CTAB) surfactant produced a synergistic improvement in the corrosion inhibition performance. Tapioca starch was evaluated for AA6061 alloy in seawater medium using weight loss and electroanalytical measurements [35]. The inhibition efficiency was achieved at 96% at 1000 $\mathrm{mg\,l^{-1}}$, and the adsorption of inhibitor was in agreement with Langmuir isotherm. SEM and energy-dispersive X-ray (EDX) analyses supported the inhibitor film formation on the metallic substrate that supported the surface protection.

Hydroxyethylcellulose (HEC) and sodium alginate (ALG)–based corrosion inhibitor formulations were used as inhibitors for Mg alloy AZ31 in NaCl environment [36]. HEC and ALG formulations provided effective performance with 80.56% and 77.43% efficiencies. Surface examinations using scanning electrochemical microscopy (SECM), AFM, SEM, and EDX revealed that the coexistence of $Mg(OH)_2$ and adsorbed inhibitor complexes protected the alloy surface. Dextran was used to inhibit corrosion of 6061 Al alloy in a 1 M HCl medium [37]. The inhibitor showed a mixed type of performance with physical adsorption and obeyed Langmuir adsorption isotherm. At a dose of $0.4\,\mathrm{g\,l^{-1}}$, an inhibition efficiency of 74.6% was obtained. Some of the different polysaccharides that have been used as corrosion inhibitors for metals and alloys are listed in Table 1.1.

## 1.5 Proteins and Polyamino Acids as Corrosion Inhibitors

Mostly the animal and vegetable wastes are responsible for the protein sources. For example, slaughterhouse wastes can provide a reputable resource for the proteins of animal origin, such as gelatin. These wastes constitute the inedible tissues/parts of the animals that have been slaughtered for meat production [38]. Several reports are available in the literature on the application of protein-based biopolymers as corrosion inhibitors. Figure 1.1 lists the different proteins that have been used as corrosion inhibitors for metals and alloys [39]. Casein was studied as a corrosion inhibitor for mild steel in 0.1 M HCl solution in the range of 50–400 $\mathrm{mg\,l^{-1}}$ concentrations [40]. The corrosion rate decreased from 98.4 to 3.9 mpy in the presence of an inhibitor. EIS studies revealed a charge-transfer control of the electrochemical process, whereas the PDP measurements indicated a mixed mode of inhibition. Casein was also studied as an inhibitor for reinforcing steel 0.1 $\mathrm{mol\,l^{-1}}$ NaOH solution in the presence of varying concentrations of $Cl^-$ ions with 82% inhibition efficiency [41]. Using weight loss and electrochemical measurements, gelatin was explored for X60 steel in a 15% HCl environment wherein the inhibition efficiency increased with increasing the inhibitor concentration [42]. Adding potassium iodide (KI) to gelatin as a synergistic component increased the inhibition efficiency from 70.42% to 84.51%. Gelatin was also evaluated for aluminum and aluminum–silicon alloys in 0.1 M NaOH solution using electrochemical measurements [43]. The inhibitor adsorption was in accordance with the Flory–Huggins isotherm. Gluten hydrolysate was analyzed on mild steel in 1 M HCl solution using weight loss and electrochemical measurements [44]. The inhibitor showed a mixed mode of inhibition performance by forming an inhibitive film on the metallic substrate. It also performed as a mixed mode of physical and chemical adsorption. A high inhibition efficiency of 93% was obtained even at an elevated temperature

**Table 1.1** Performance of different polysaccharides as corrosion inhibitors.

| Name | Metal surface/medium | Inhibition efficiency/ concentration | Adsorption isotherm/type | Reference |
|---|---|---|---|---|
| Chitosan | Cu/0.5 M HCl | 93%/8 μM | Langmuir isotherm/mixed type | [21] |
| Chitosan | Mild steel/0.1 M HCl | 68%/4 μM | Langmuir isotherm/mixed type | [22] |
| Carboxymethylcellulose | API 5L X60 pipeline steel/$CO_2$ saturated 3.5% NaCl | 39%/100 mg $l^{-1}$ | Langmuir isotherm/mixed type | [23] |
| Hydroxyethylcellulose | Zn/26% $NH_4Cl$ | 92.07%/300 mg $l^{-1}$ | Langmuir isotherm/mixed type | [24] |
| Sodium alginate | Mg alloy AZ31/3.5% NaCl | 86.62%/500 mg $l^{-1}$ | Mixed type | [26] |
| Sodium alginate | API X60 steel/3.5% NaCl | 87.23%/1000 mg $l^{-1}$ | — | [27] |
| Guar gum | Carbon steel/1 M $H_2SO_4$ | 93.2%/1000 mg $l^{-1}$ | Langmuir isotherm/mixed type | [28] |
| Guar gum | Aluminum/1 M HCl | 83.19%/400 mg $l^{-1}$ | Temkin isotherm/cathodic type | [29] |
| Gum acacia | Mild steel/1 M HCl | 95%/1000 mg $l^{-1}$ | Langmuir isotherm/mixed type | [30] |
| Gum arabic | Carbon steel 1018/oil-field water | 94.2%/5000 mg $l^{-1}$ | Langmuir isotherm/mixed type | [31] |
| Pectin | X60 steel/0.5 M HCl | 78.7%/1000 mg $l^{-1}$ | Langmuir isotherm/mixed type | [32] |
| Pectin | Aluminum/2 M HCl | 92.1%/2000 mg $l^{-1}$ | Langmuir isotherm | [33] |
| Starch | Mild steel/0.1 M $H_2SO_4$ | 66.21%/300 mg $l^{-1}$ | Langmuir isotherm/mixed type | [34] |
| Tapioca starch | AA6061 alloy/seawater | 91.41%/1000 mg $l^{-1}$ | Langmuir isotherm/mixed type | [35] |

**Table 1.2** Performance of different protein-based biopolymers as corrosion inhibitors.

| Name | Metal surface/ medium | Inhibition efficiency/ concentration | Adsorption isotherm/type | Reference |
|---|---|---|---|---|
| Casein | Mild steel/0.1 M HCl | 96.41%/400 mg $l^{-1}$ | Langmuir isotherm/ mixed type | [40] |
| Casein | Reinforcing steel/ synthetic concrete pore solution | 82%/$9.7 \times 10^{-4}$ M | — | [41] |
| Gelatin | X60 steel/15% HCl | 70.42%/2.5% w/v | Mixed type | [42] |
| Gelatin | Al alloy/0.1M NaOH | 65.71%/2000 mg $l^{-1}$ | Flory–Huggins isotherm/ Mixed type | [43] |
| Gluten hydrolysate | Mild steel/1 M HCl | 92.8%/1000 mg $l^{-1}$ | Langmuir isotherm/ mixed type | [44] |
| Maize-gluten meal extract | Steel/Simulated concrete pore solution in 3% NaCl | 88%/2000 mg $l^{-1}$ | Langmuir isotherm/ mixed type | [45] |
| Soy | Carbon steel/1 M $H_2SO_4$ | 89.51%/5000 mg $l^{-1}$ | Langmuir isotherm/ mixed type | [46] |

of 323 K. Maize-gluten meal extracts were analyzed for steel in simulated concrete pore solutions with 3% NaCl [45]. The inhibition efficiency rose from 69.12% to 88.10% in the concentration range of 0.25–2 g $l^{-1}$. The Langmuir isotherm provided the most appropriate fit of the data and the surface analysis via SEM and AFM studies. Soy polymer and polyvinyl pyrrolidinone were evaluated for carbon steel in a 1 M $H_2SO_4$ environment in the temperature range of 30–60 °C with high efficiency of 89.5% [46]. The inhibitor adsorption on the metal surface obeyed the Langmuir isotherm and the PDP studies revealed a mixed mode of inhibitor action. Table 1.2 lists some of the different protein-based biopolymers that have been used as corrosion inhibitors for metals and alloys.

Among polyamino acids, most of the available literature reports the application of polyaspartic acid as corrosion inhibitors. Polyaspartic acid (PAsp) was reported as a corrosion inhibitor in different molecular weights. Besides, a combination of polyaspartic acid and various amino acids, namely, tyrosine, histidine, phenylalanine, and leucine, resulted in detergent formulations without/with phosphate/silicate have also been reported as corrosion inhibitors [47]. The effect of pH, temperature, and rotation conditions was studied for PAsp as corrosion inhibitors by Silverman et al. [48]. PAsp accelerated the corrosion at pH values lower than neutral pH. In contrast, at the higher pH values, it facilitated corrosion inhibition at a concentration of 1–10% for iron and steel surfaces. In an amino sulfonic acid medium, PAsp was also reported as a corrosion inhibitor for copper surface wherein it provided a high efficiency of 89.8% at 1 g $l^{-1}$ [49]. An amount of 0.5 g $l^{-1}$ PAsp in a synergistic combination with the same imidazole concentration provided an inhibition efficiency of 95.7%. Synergistic corrosion inhibition was also introduced with iodide ions for mild steel in 0.5 M $H_2SO_4$, resulting in a rise in the inhibition efficiency from 87.9% to 96.3% [50]. At a pH value lower than an isoelectric point, the amino acid can get protonated in the corrosive solution, resulting in $PAspH^+$ species in the medium, which would directly adsorb on the metallic surface to provide protection from corrosion. In the presence of KI, $I^-$ ions would first undergo adsorption on the metallic surface and would promote the electrostatic interaction with the protonated form of the polymer. In another study, a combination of polyaspartic acid with $Zn^{2+}$ ions ($0.01\,g\,l^{-1}$) produced the corrosion inhibition of 61% at $2\,g\,l^{-1}$ for mild steel in 3.5% NaCl medium [51]. It was proposed that the amide groups and the carboxylate species of the PAsp played a key role in the interaction of the PAsp with the metallic substrate. This was further evidenced by the DFT-based quantum chemical calculations and Monte Carlo simulations.

## 1.6 Chemically Modified Biopolymers as Corrosion Inhibitors

One of the issues associated with the naturally occurring carbohydrate-based polymers as corrosion inhibitors is their limited solubility in the corrosive solution. The high-molecular weights of these polymers that afford the appreciable surface coverage also render these molecules with limited solubility in the aqueous corrosive medium. A convenient strategy, in this case, is the chemical functionalization of the polymeric backbone using a suitable agent to improve the solubility and the inhibition performance. Herein we have discussed the corrosion inhibition behavior of several organic corrosion inhibitors based on chemically modified biopolymers in the aqueous corrosive media. The synthesis of some chemically modified chitosan-based inhibitors is shown in Scheme 1.2.

A most commonly adopted strategy for chemical modification of chitosan is the Schiff base formation. The pyranose ring present in the chitosan contains attached $-NH_2$ functional groups. These amine groups can be reacted with organic compounds containing free –CHO groups in a single-step reaction to introduce the imine (–HC=N–) linkage in the chitosan polymer. The imine (–HC=N–) linkage present in the Schiff base shows the ability to undergo adsorption on the metal surfaces. The choice of Schiff bases stems from the fact that they are nontoxic and can be synthesized easily, and the introduction of the imine linkage is expected to improve the film-forming capability and anticorrosion behavior [5, 55–58]. A significant advantage of using the chitosan Schiff bases is that the Schiff base preparation is a simple procedure requiring single-step reactions, and the azomethine (–CH=N) linkage is known to show strong adsorption over the metallic surface. Three Schiff bases of chitosan produced via microwave irradiation method using benzaldehyde (CSB-1), vanillin (CSB-2), and *N*,*N*-dimethylaminobenzaldehyde (CSB-3) were utilized as inhibitors against the corrosion of mild steel in 1 M HCl [5]. At a low dose of $50\ mg\,l^{-1}$, all the inhibitors showed high inhibition efficiencies among which, CSB-3 performed the best. The structural aspects in terms of $-N(CH_3)_2$

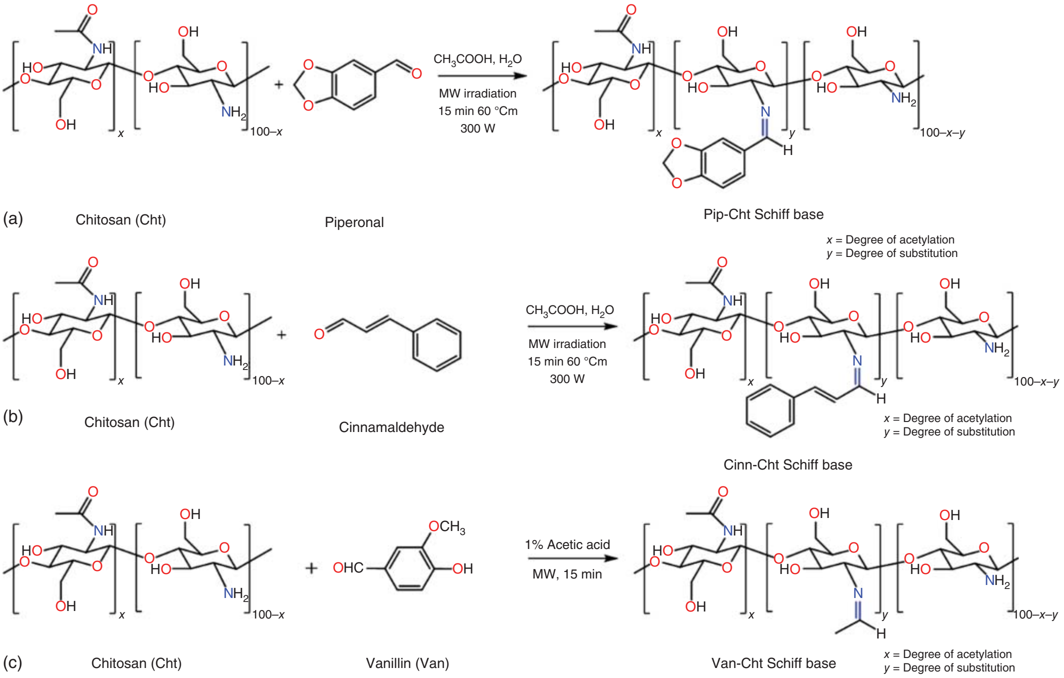

**Scheme 1.2** Synthesis of chemically modified chitosans. Source: (a) Chauhan et al. [52]/Elsevier, (b) Chauhan et al. [53]/Elsevier, (c) Quraishi et al. [54]/Elsevier.

group afforded a planar orientation on the metallic substrate that allowed a better coverage and a superior corrosion inhibition. Two more Schiff bases of chitosan with Piperonal (Pip-Cht) [52] and cinnamaldehyde (Cinn-Cht) [53] were prepared using a single-step microwave synthesis method. They were utilized as corrosion inhibitors for carbon steel in 15% HCl solution. The thermal stability studies indicated both the inhibitors were stable up to 200 °C and revealed high efficiencies at low doses of 500 and 400 mg $l^{-1}$, respectively. In a subsequent study by the same group, vanillin–chitosan (Van–Cht) Schiff base was used as a corrosion inhibitor for carbon steel in 15% HCl solution [54]. Electrochemical studies and computation analyses revealed strong inhibitor adsorption over the metallic substrate. Another

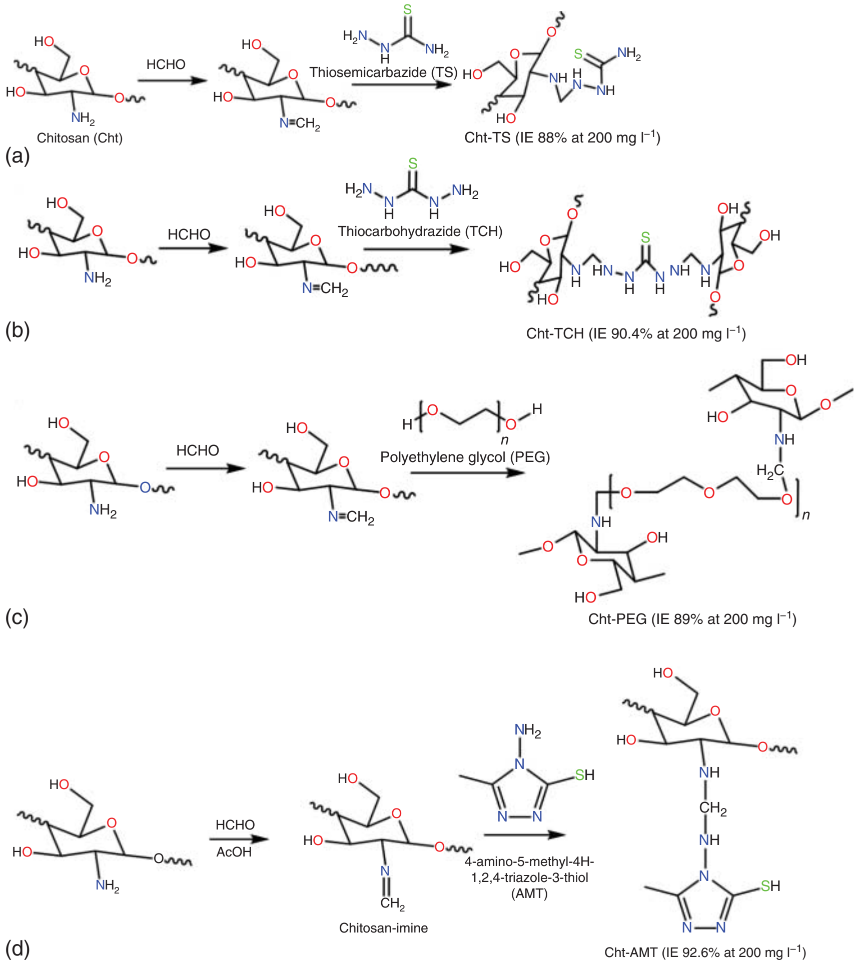

**Scheme 1.3** Structures and inhibition performance of different chemically modified chitosan-based inhibitors on mild steel in 1M HCl. Source: (a) Chauhan et al. [60]/Elsevier, (b) Chauhan et al. [60]/Elsevier, (c) Srivastava et al. [61]/Elsevier, (d) Chauhan et al. [62]/Elsevier.

Schiff base of chitosan was prepared using salicylaldehyde and studied for sweet corrosion of J55 steel [59]. At an elevated temperature of 65 °C, high inhibition efficiency of 95% was obtained at a concentration of 150 $\text{mg}\,\text{l}^{-1}$. The structures and corrosion inhibition performance of different chemically modified chitosan derivatives are shown in Scheme 1.3.

Heterocyclic molecules are generally understood as effective corrosion inhibitors. Several heterocyclic corrosion inhibitors, e.g. azoles, pyridines, and pyrimidines, have been reported for different corrosive media [3]. In a study, chitosan was chemically functionalized using amino-mercapto triazole and utilized as corrosion inhibitor for 1 M HCl on carbon steel environment and in 3.5% NaCl on stainless steel [62, 63]. In both cases, high inhibition performances were obtained. Thiosemicarbazide (CS-TS) and thiocarbohydrazide (CS-TCH) were used to chemically functionalize the chitosan and used as mild steel inhibitors in 1 M HCl medium using gravimetric, electrochemical, and computational studies. The CS-TCH provided a more significant corrosion inhibition with preferential adsorption of the protonated form of the corrosion inhibitor [60]. Using EIS and PDP measurements, the same polymer was further investigated for stainless steel 3.5% NaCl [64]. Chitosan was also modified using polyethylene glycol and was evaluated as an inhibitor for steel surface in 1 M HCl and 1 M sulfamic acid solutions [61, 65]. High efficiencies were obtained at around 200 $\text{mg}\,\text{l}^{-1}$ in both media. Two amino-acid-modified derivatives of dextran (LDT and S-LDT) were studied as inhibitors for corrosion of carbon steel in $CO_2$-saturated oilfield produce water [66].

## 1.7 Biopolymer Nanoparticles as Corrosion Inhibitors

Nanoparticles of chitosan were utilized for corrosion inhibition of mild steel substrate in 3.5% NaCl solution. A 90% protection was achieved with the inhibitor adsorption on the steel surface, obeying the Langmuir isotherm [67]. Nonionic amphiphilic chitosan nanoparticles were synthesized in aqueous medium employing surfactant-free protocol and used for steel surface protection in 1 M HCl. At 250 $\text{mg}\,\text{l}^{-1}$, an inhibition efficiency of 93.5% was afforded [68]. Chitosan nanoparticles were also studied as inhibitors for A6063 alloy corrosion in 3.65% NaCl medium [69]. An inhibition performance of >70% was observed. Glycogen nanoparticles were synthesized via microwave irradiation and studied as corrosion inhibitors for zinc in sulfamic acid medium [70]. At a concentration of 0.20 $\text{mg}\,\text{l}^{-1}$, an inhibition efficiency of 92% was obtained. Maltodextrin nanoparticles were evaluated as inhibitors against acid corrosion of zinc and at high efficiency of 93% was obtained at 50 $\text{mg}\,\text{l}^{-1}$ of concentration [71].

## 1.8 Biopolymer Composites as Corrosion Inhibitors

Nanocomposites of chitosan were prepared with cobalt ($\text{IE} > 95\%$) and $SnS_2$ ($\text{IE} > 80\%$) and investigated for mild steel in 1 M HCl medium [72]. Chitosan composites were also prepared with silver nanoparticles using the simple reduction of silver by honey and were studied for ST37 steel in 15% HCl [73]. A mixed mode of physical and chemical adsorption was obtained at low temperatures, wherein chemical adsorption was observed at higher temperatures. A cathodic type of corrosion inhibition performance was observed at higher temperatures. The chitosan–AgNp composites when evaluated in 15% $H_2SO_4$ provided a 94% inhibition performance [74]. Chitosan (Ch) grafted with poly(ethylene glycol) (Ch-g-mPEG) was assembled over silver nanoparticles and evaluated for carbon steel in 1 M HCl using electrochemical and surface analytical measurements [75]. Starch–silver nanoparticle composites were studied as inhibitors for mild steel in 0.5 M HCl, and 82.806% efficiency was obtained at 70 °C [76]. At 30 °C, a high efficiency of 93.168% was observed. Dextran and its silver nanoparticle composites were utilized as corrosion inhibitors for ST37-2 steel surface in 15% $H_2SO_4$ using weight loss and electrochemical studies [77]. Synergistic effect of KI was also investigated at 25 °C (IE 94.21%) and 60 °C (IE 99.4%). A mixed type of inhibition behavior with predominance of the cathodic control of the reaction was observed.

## 1.9 Adsorption and Protection Mechanism of Biopolymers on the Metal Surface

A general mechanism of the adsorption of the biopolymer-based corrosion inhibitors on the surface of metals and the protection performance can be explained as follows. The gravimetric method of inhibitor analysis reveals the effect of the variation in the inhibitor concentration on the corrosion rate and the inhibition efficiency. The increase in the inhibition efficiency and a corresponding lowering in the corrosion rate with an increase in the inhibitor concentration suggests adsorption of the corrosion inhibitor on the metal surface. The inhibitor molecules adsorb on the metal surface and cover the corrosion active sites, thereby decreasing corrosion. The EIS studies show an increase in the resistance against the charge transfer with the increase in the inhibitor concentration [14]. The PDP method shows a lowering in the corrosion current densities with an increase in the inhibitor concentration. Thus, the EIS and PDP methods also support the inhibitor adsorption and corrosion inhibition. The shift in the corrosion potential can indicate the anodic, cathodic, or mixed type of inhibition behavior [14]. In a corrosive solution, a corrosion inhibitor can exist in the protonated form as shown below:

$$\mathrm{Cinn} - \mathrm{Cht}_{\mathrm{neutral}} \rightleftharpoons \mathrm{Cinn} - \mathrm{Cht}_{\mathrm{protonated}} \tag{1.1}$$

The inhibitor can adsorb on the metallic surface via displacement of the pre-adsorbed water molecules as follows:

$$\mathrm{M}_{\mathrm{H_2O}} + \mathrm{Cinn} - \mathrm{Cht} \rightleftharpoons \mathrm{M}_{\mathrm{Cinn-Cht}} + \mathrm{H_2O} \tag{1.2}$$

The protonated form of corrosion inhibitor can adsorb on the metallic substrate and cover the cathodic sites, protecting them from corrosion. The neutral form

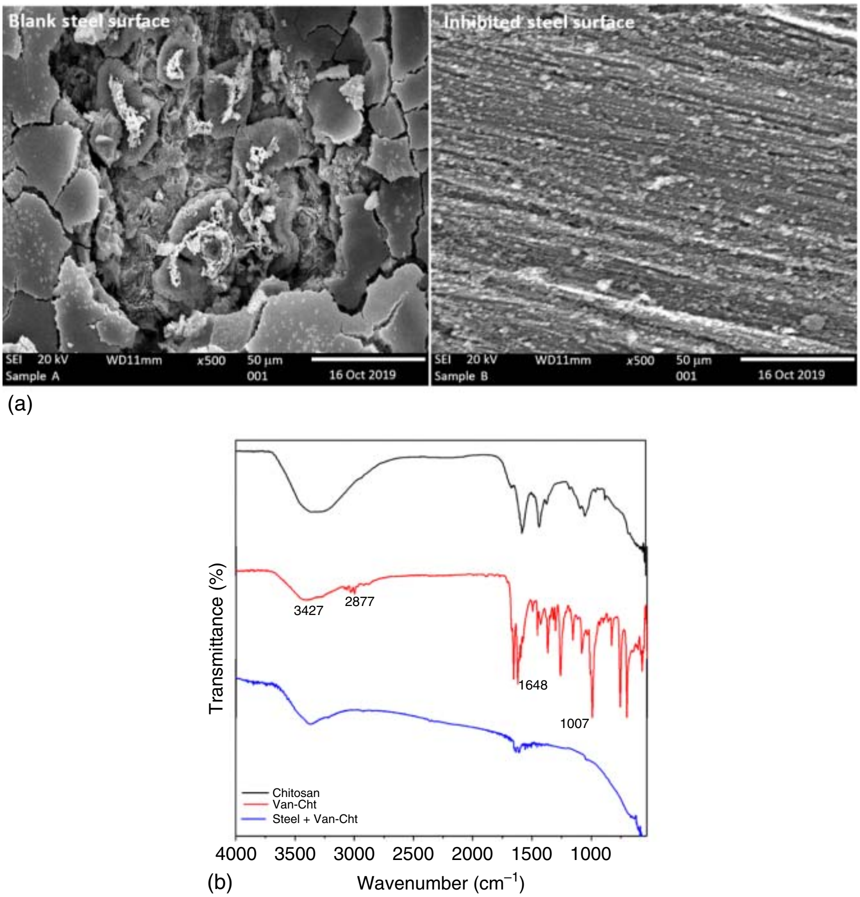

**Figure 1.2** (a) Surface morphology (SEM) of carbon steel samples after immersion in 15% HCl in the absence (A) and the presence of (B) optimum concentration of Van–Cht for 6 h at 25 °C. (b) FTIR spectra of pure chitosan, Van–Cht, and film of Van–Cht adsorbed steel surface after immersion in 15% HCl for 6 h at 25 °C. Source: Quraishi et al. [54]/Springer Nature.

of the inhibitor can adsorb directly at the metal surface by the sharing of the π electrons or the lone pair of electrons. The filled d-orbitals of the metal surface can also back-donate the electrons to the inhibitor molecules. The surface analysis of the metal surface via electron microscopy and spectroscopic analysis can provide further support for inhibitor adsorption (Figure 1.2). The surface morphology of carbon steel substrate after immersion in 15% HCl in the absence and the presence of inhibitor Van–Cht is given in Figure 1.2a. The blank steel surface shows considerable damage, whereas the inhibited surface shows a smooth morphology indicating the adsorption and protection performance of inhibitor. The FTIR spectra of pure chitosan, Van–Cht, and Van–Cht inhibitor after adsorption on carbon steel surface following immersion in 15% HCl are given in Figure 1.2b. The characteristic absorbance maxima of Van–Cht can be seen in the range of 3300–3400 cm$^{-1}$,

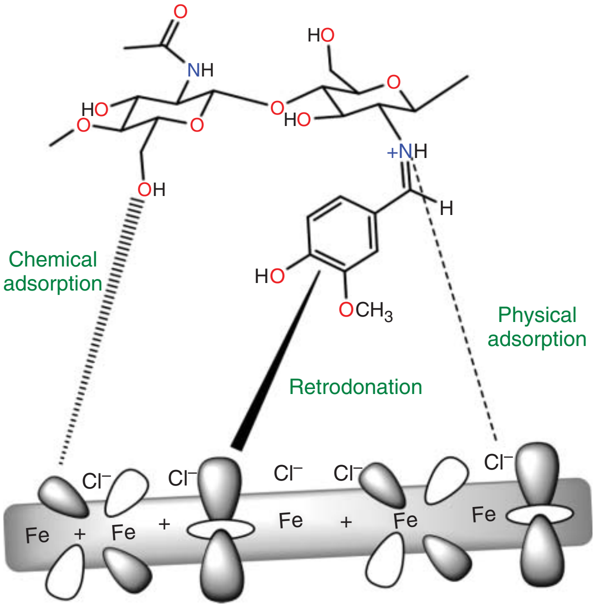

**Figure 1.3** Mechanism of adsorption and inhibition behavior of vanillin-modified chitosan (Van–Cht) on carbon steel surface. Source: Quraishi et al. [54]/Springer Nature.

corresponding to N–H stretch. Small peaks of –HC=N– stretching in the region of 1598–1575 $cm^{-1}$ can be observed in the adsorbed sample. Slight shift in the above band in the adsorbed sample compared to the pure Van–Cht with a lowering in the intensity indicates the involvement of this group in the adsorption of the inhibitor on the steel surface.

Further information can be obtained via computation analysis. The $pK_a$ analysis can indicate the existence of the inhibitor in the protonated form [66]. This observation is supported by the DFT calculations and the molecular simulations, both of which can reveal the active sites present on the inhibitor molecule amenable to undergo adsorption and the inhibitor's preferred alignment on the metal surface [23]. Figure 1.3 shows a tentative mechanism of the adsorption and inhibition behavior of the corrosion inhibitor.

## 1.10 Conclusions and Prospects

Corrosion of metallic structures is a major issue causing significant economic concerns. Most of the available corrosion inhibitors belong to the class of nitrogen-based heterocyclic compounds. However, the use of these inhibitors leads to severe issues related to toxicity and environmental pollution. Therefore, there is a growing interest in the area of corrosion inhibitors based on environmentally benign molecules, such as natural extracts, drugs, and ILs. One of the primary categories is the polymeric corrosion inhibitors derived from carbohydrates and proteins.

The polymer-based corrosion inhibitors find application due to their large molecular size that can afford the considerable coverage of the metallic substrate on the target metal surface. The major categories are chitosan and the exudate gums, among the carbohydrate-based corrosion inhibitors. On the other hand, polyamino acids have found the major application as corrosion inhibitors among the protein-based corrosion inhibitors.

Furthermore, in recent years, to improve the adsorption and the inhibition effect of the polymeric corrosion inhibitors on the metallic surface, the chemical modification of the inhibitor backbone has been applied as a strategy. Namely, the single-step chemical modifications, nanocomposite formations, and copolymer formation are some of the methods commonly adopted to develop the modified polymeric materials with superior corrosion inhibition behavior. The comprehensive experimental studies have been well supported using appropriate computational modeling analysis of the corrosion inhibitors. In recent years, researchers have also targeted industry-relevant research areas, such as sweet corrosion and the oil-well acidizing environments using polymeric corrosion inhibitors. However, the collected literature also shows some knowledge gaps specifically in the realms of the influence of different functional groups, more detailed synergism studies, the effect of temperature, etc. Furthermore, another aspect is the development of inhibitor formulations using the desired surfactant, oil, synergistic agent, etc. as an additive along with the active corrosion inhibitors. Also, detailed comparisons of the newly developed corrosion inhibitors with the literature reported corrosion inhibitors must be carried out before they can be considered for the potential applications in industry.

## Acknowledgment

MAQ wishes to thank the Deanship of Scientific Research (DSR), KFUPM, Saudi Arabia, for the financial assistance received under the project DF191051.

## References

1 Sastri, V.S. (1998). *Corrosion Inhibitors: Principles and Applications*. Wiley.

2 Ansari, K.R., Chauhan, D.S., Singh, A. et al. (2020). Corrosion inhibitors for acidizing process in oil and gas sectors. In: *Corrosion Inhibitors in the Oil and Gas Industry* (ed. V.S. Saji and S.A. Umoren), 153–176. Wiley-VCH Verlag GmbH & Co. KGaA, ISBN 978-3-527-34618-9.

3 Quraishi, M.A., Chauhan, D.S., and Saji, V.S. (2020). *Heterocyclic Organic Corrosion Inhibitors: Principles and Applications*. Amsterdam: Elsevier Inc.

4 El-Hajjaji, F., Messali, M., Aljuhani, A. et al. (2018). Pyridazinium-based ionic liquids as novel and green corrosion inhibitors of carbon steel in acid medium: electrochemical and molecular dynamics simulation studies. *Journal of Molecular Liquids* 249: 997–1008.

**5** Haque, J., Srivastava, V., Chauhan, D.S. et al. (2018). Microwave-induced synthesis of chitosan Schiff bases and their application as novel and green corrosion inhibitors: experimental and theoretical approach. *ACS Omega* 3: 5654–5668.

**6** Singh, A., Ahamad, I., and Quraishi, M.A. (2016). Piper longum extract as green corrosion inhibitor for aluminium in NaOH solution. *Arabian Journal of Chemistry* 9: S1584–S1589.

**7** Verma, C., Ebenso, E.E., Bahadur, I., and Quraishi, M.A. (2018). An overview on plant extracts as environmental sustainable and green corrosion inhibitors for metals and alloys in aggressive corrosive media. *Journal of Molecular Liquids* 266: 577–590.

**8** Verma, C., Olasunkanmi, L., Ebenso, E.E., and Quraishi, M.A. (2018). Substituents effect on corrosion inhibition performance of organic compounds in aggressive ionic solutions: a review. *Journal of Molecular Liquids* 251: 100–118.

**9** Verma, C., Ebenso, E.E., and Quraishi, M.A. (2017). Corrosion inhibitors for ferrous and non-ferrous metals and alloys in ionic sodium chloride solutions: a review. *Journal of Molecular Liquids* 248: 927–942.

**10** Gece, G. (2011). Drugs: a review of promising novel corrosion inhibitors. *Corrosion Science* 53: 3873–3898.

**11** Xhanari, K., Finšgar, M., Hrnčič, M.K. et al. (2017). Green corrosion inhibitors for aluminium and its alloys: a review. *RSC Advances* 7: 27299–27330.

**12** Verma, C., Ebenso, E.E., and Quraishi, M.A. (2017). Ionic liquids as green and sustainable corrosion inhibitors for metals and alloys: an overview. *Journal of Molecular Liquids* 233: 403–414.

**13** Likhanova, N.V., Domínguez-Aguilar, M.A., Olivares-Xometl, O. et al. (2010). The effect of ionic liquids with imidazolium and pyridinium cations on the corrosion inhibition of mild steel in acidic environment. *Corrosion Science* 52: 2088–2097.

**14** El-Hajjaji, F., Salim, R., Messali, M. et al. (2019). Electrochemical studies on new pyridazinium derivatives as corrosion inhibitors of carbon steel in acidic medium. *Journal of Bio-and Tribo-Corrosion* 5: 4.

**15** El-Hajjaji, F., Ech-chihbi, E., Rezki, N. et al. (2020). Electrochemical and theoretical insights on the adsorption and corrosion inhibition of novel pyridinium-derived ionic liquids for mild steel in 1 M HCl. *Journal of Molecular Liquids* 314: 113737.

**16** Umoren, S.A. and Eduok, U.M. (2016). Application of carbohydrate polymers as corrosion inhibitors for metal substrates in different media: a review. *Carbohydrate polymers* 140: 314–341.

**17** El Ibrahimi, B., Jmiai, A., Bazzi, L., and El Issami, S. (2020). Amino acids and their derivatives as corrosion inhibitors for metals and alloys. *Arabian Journal of Chemistry* 13: 740–771.

**18** Jha, A. and Kumar, A. (2019). Biobased technologies for the efficient extraction of biopolymers from waste biomass. *Bioprocess and Biosystems Engineering* 42: 1893–1901.

**19** Martău, G.A., Mihai, M., and Vodnar, D.C. (2019). The use of chitosan, alginate, and pectin in the biomedical and food sector—biocompatibility, bioadhesiveness, and biodegradability. *Polymers* 11: 1837.

**20** Obot, I., Macdonald, D., and Gasem, Z. (2015). Density functional theory (DFT) as a powerful tool for designing new organic corrosion inhibitors. Part 1: an overview. *Corrosion Science* 99: 1–30.

**21** El-Haddad, M.N. (2013). Chitosan as a green inhibitor for copper corrosion in acidic medium. *International journal of Biological Macromolecules* 55: 142–149.

**22** Umoren, S.A., Banera, M.J., Alonso-Garcia, T. et al. (2013). Inhibition of mild steel corrosion in HCl solution using chitosan. *Cellulose* 20: 2529–2545.

**23** Umoren, S.A., AlAhmary, A.A., Gasem, Z.M., and Solomon, M.M. (2018). Evaluation of chitosan and carboxymethyl cellulose as ecofriendly corrosion inhibitors for steel. *International Journal of Biological Macromolecules* 117: 1017–1028.

**24** Deyab, M. (2015). Hydroxyethyl cellulose as efficient organic inhibitor of zinc–carbon battery corrosion in ammonium chloride solution: electrochemical and surface morphology studies. *Journal of Power Sources* 280: 190–194.

**25** Gombotz, W.R. and Wee, S. (1998). Protein release from alginate matrices. *Advanced Drug Delivery Reviews* 31: 267–285.

**26** Dang, N., Wei, Y., Hou, L. et al. (2015). Investigation of the inhibition effect of the environmentally friendly inhibitor sodium alginate on magnesium alloy in sodium chloride solution. *Materials and Corrosion* 66: 1354–1362.

**27** Obot, I., Onyeachu, I.B., and Kumar, A.M. (2017). Sodium alginate: a promising biopolymer for corrosion protection of API X60 high strength carbon steel in saline medium. *Carbohydrate Polymers* 178: 200–208.

**28** Abdallah, M. (2004). Guar gum as corrosion inhibitor for carbon steel in sulfuric acid solutions, Portugaliae. *Electrochimica Acta* 22: 161–175.

**29** Palumbo, G., Berent, K., Proniewicz, E., and Banaś, J. (2019). Guar gum as an eco-friendly corrosion inhibitor for pure aluminium in 1-M HCl solution. *Materials* 12: 2620.

**30** Azzaoui, K., Mejdoubi, E., Jodeh, S. et al. (2017). Eco friendly green inhibitor Gum Arabic (GA) for the corrosion control of mild steel in hydrochloric acid medium. *Corrosion Science* 129: 70–81.

**31** Shen, C., Alvarez, V., Koenig, J.D., and Luo, J.-L. (2019). Gum Arabic as corrosion inhibitor in the oil industry: experimental and theoretical studies. *Corrosion Engineering, Science and Technology* 54: 444–454.

**32** Umoren, S.A., Obot, I.B., Madhankumar, A., and Gasem, Z.M. (2015). Performance evaluation of pectin as ecofriendly corrosion inhibitor for X60 pipeline steel in acid medium: experimental and theoretical approaches. *Carbohydrate Polymers* 124: 280–291.

**33** Fares, M.M., Maayta, A., and Al-Qudah, M.M. (2012). Pectin as promising green corrosion inhibitor of aluminum in hydrochloric acid solution. *Corrosion Science* 60: 112–117.

**34** Mobin, M., Khan, M., and Parveen, M. (2011). Inhibition of mild steel corrosion in acidic medium using starch and surfactants additives. *Journal of Applied Polymer Science* 121: 1558–1565.

**35** Rosliza, R. and Nik, W.W. (2010). Improvement of corrosion resistance of AA6061 alloy by tapioca starch in seawater. *Current Applied Physics* 10: 221–229.

**36** Umoren, S.A., Solomon, M.M., Madhankumar, A., and Obot, I.B. (2020). Exploration of natural polymers for use as green corrosion inhibitors for AZ31 magnesium alloy in saline environment. *Carbohydr Polym* 230: 115466.

**37** Charitha, B., Rao, P.J.S.E., and Electrochemistry, A. (2017). Electrochemical and adsorption studies for the corrosion control of 6061 Al alloy using eco-friendly inhibitor. *Surface Engineering and Applied Electrochemistry* 53: 551–559.

**38** Adhikari, B.B., Chae, M., and Bressler, D.C. (2018). Utilization of slaughterhouse waste in value-added applications: recent advances in the development of wood adhesives. *Polymers* 10: 176.

**39** Nishinari, K., Fang, Y., Guo, S., and Phillips, G. (2014). Soy proteins: a review on composition, aggregation and emulsification. *Food Hydrocolloids* 39: 301–318.

**40** Rabizadeh, T. and Asl, S.K. (2019). Casein as a natural protein to inhibit the corrosion of mild steel in HCl solution. *Journal of Molecular Liquids* 276: 694–704.

**41** Zomorodian, A., Bagonyi, R., and Al-Tabbaa, A. (2021). The efficiency of eco-friendly corrosion inhibitors in protecting steel reinforcement. *Journal of Building Engineering* 38: 102171.

**42** Haruna, K., Obot, I., Ankah, N. et al. (2018). Gelatin: a green corrosion inhibitor for carbon steel in oil well acidizing environment. *Journal of Molecular Liquids* 264: 515–525.

**43** Abdallah, M., Kamar, E., El-Etre, A., and Eid, S. (2016). Gelatin as corrosion inhibitor for aluminum and aluminum silicon alloys in sodium hydroxide solutions. *Protection of Metals and Physical Chemistry of Surfaces* 52: 140–148.

**44** Roy, P., Maji, T., Dey, S., and Sukul, D. (2015). Adsorption behaviour of gluten hydrolysate on mild steel in 1 M HCl and its role as a green corrosion inhibitor. *RSC Advances* 5: 61170–61178.

**45** Zhang, Z., Ba, H., and Wu, Z. (2019). Sustainable corrosion inhibitor for steel in simulated concrete pore solution by maize gluten meal extract: electrochemical and adsorption behavior studies. *Construction and Building Materials* 227: 117080.

**46** Nwanonenyi, S., Obasi, H., Chukwujike, I. et al. (2019). Inhibition of carbon steel corrosion in 1 M $H_2SO_4$ using soy polymer and polyvinylpyrrolidone. *Chemistry Africa* 2: 277–289.

**47** Freeman, M.B., Hann, W.M., Paik, Y.H., and Swift, G. (1996). Method of inhibiting corrosion in aqueous systems using poly (amino acids), in, United States Patent, United States.

**48** Silverman, D., Kalota, D., and Stover, F. (1995). Effect of pH on corrosion inhibition of steel by polyaspartic acid. *Corrosion* 51: 818–825.

**49** Wang, H., Wu, Q., Li, C., and Gu, N. (2013). Copper corrosion inhibition by polyaspartic acid and imidazole. *Materials and Corrosion* 64: 347–352.

**50** Qian, B., Wang, J., Zheng, M., and Hou, B. (2013). Synergistic effect of polyaspartic acid and iodide ion on corrosion inhibition of mild steel in $H_2SO_4$. *Corrosion Science* 75: 184–192.

**51** Zeino, A., Abdulazeez, I., Khaled, M. et al. (2018). Mechanistic study of polyaspartic acid (PASP) as eco-friendly corrosion inhibitor on mild steel in 3% NaCl aerated solution. *Journal of Molecular Liquids* 250: 50–62.

**52** Chauhan, D.S., Mazumder, M.J., Quraishi, M.A. et al. (2020). Microwave-assisted synthesis of a new Piperonal-Chitosan Schiff base as a bio-inspired corrosion inhibitor for oil-well acidizing. *International Journal of Biological Macromolecules* 158: 231–243.

**53** Chauhan, D.S., Mazumder, M.J., Quraishi, M.A., and Ansari, K. (2020). Chitosan-cinnamaldehyde Schiff base: a bioinspired macromolecule as corrosion inhibitor for oil and gas industry. *International Journal of Biological Macromolecules* 158: 127–138.

**54** Quraishi, M.A., Ansari, K.R., Chauhan, D.S. et al. (2020). Vanillin modified chitosan as a new bio-inspired corrosion inhibitor for carbon steel in oil-well acidizing relevant to petroleum industry. *Cellulose* 27: 6425–6443.

**55** Ansari, K.R. and Quraishi, M.A. (2014). Bis-Schiff bases of isatin as new and environmentally benign corrosion inhibitor for mild steel. *Journal of Industrial and Engineering Chemistry* 20: 2819–2829.

**56** Ansari, K.R., Quraishi, M.A., and Singh, A. (2014). Schiff's base of pyridyl substituted triazoles as new and effective corrosion inhibitors for mild steel in hydrochloric acid solution. *Corrosion Science* 79: 5–15.

**57** Gupta, N.K., Verma, C., Quraishi, M.A., and Mukherjee, A.K. (2016). Schiff's bases derived from L-lysine and aromatic aldehydes as green corrosion inhibitors for mild steel: experimental and theoretical studies. *Journal of Molecular Liquids* 215: 47–57.

**58** Singh, P. and Quraishi, M.A. (2016). Corrosion inhibition of mild steel using Novel Bis Schiff's Bases as corrosion inhibitors: electrochemical and surface measurement. *Measurement* 86: 114–124.

**59** Ansari, K.R., Chauhan, D.S., Quraishi, M.A. et al. (2020). Chitosan Schiff base: an environmentally benign biological macromolecule as a new corrosion inhibitor for oil & gas industries. *International Journal of Biological Macromolecules* 144: 305–315.

**60** Chauhan, D.S., Ansari, K.R., Sorour, A.A. et al. (2018). Thiosemicarbazide and thiocarbohydrazide functionalized chitosan as ecofriendly corrosion inhibitors for carbon steel in hydrochloric acid solution. *International Journal of Biological Macromolecules* 107: 1747–1757.

**61** Srivastava, V., Chauhan, D.S., Joshi, P.G. et al. (2018). PEG-functionalized chitosan: a biological macromolecule as a novel corrosion inhibitor. *ChemistrySelect* 3: 1990–1998.

**62** Chauhan, D.S., Quraishi, M.A., Sorour, A.A. et al. (2019). Triazole-modified chitosan: a biomacromolecule as a new environmentally benign corrosion inhibitor for carbon steel in a hydrochloric acid solution. *RSC Advances* 9: 14990–15003.

**63** Chauhan, D.S., Mouaden, K.E., Quraishi, M.A., and Bazzi, L. (2020). Aminotriazolethiol-functionalized chitosan as a macromolecule-based bioinspired corrosion inhibitor for surface protection of stainless steel in 3.5% NaCl. *International Journal of Biological Macromolecules* 152: 234–241.

**64** Mouaden, K.E.L., Chauhan, D.S., Quraishi, M.A., and Bazzi, L. (2020). Thiocarbohydrazide-crosslinked chitosan as a bioinspired corrosion inhibitor for protection of stainless steel in 3.5% NaCl. *Sustainable Chemistry and Pharmacy* 15: 100213.

**65** Chauhan, D.S., Srivastava, V., Joshi, P.G., and Quraishi, M.A. (2018). PEG cross-linked Chitosan: a biomacromolecule as corrosion inhibitor for sugar industry. *International Journal of Industrial Chemistry* 9: 363–377.

**66** Zhang, Q., Hou, B., Li, Y. et al. (2021). Dextran derivatives as highly efficient green corrosion inhibitors for carbon steel in $CO_2$-saturated oilfield produced water: experimental and theoretical approaches. *Chemical Engineering Journal* 130519: 130519.

**67** Fayomi, O., Akande, I., Oluwole, O., and Daramola, D. (2018). Effect of water-soluble chitosan on the electrochemical corrosion behaviour of mild steel. *Chemical Data Collections* 17: 321–326.

**68** Atta, A.M., El-Mahdy, G.A., Al-Lohedan, H.A., and Ezzat, A.-R.O. (2015). Synthesis of nonionic amphiphilic chitosan nanoparticles for active corrosion protection of steel. *Journal of Molecular Liquids* 211: 315–323.

**69** Fayomi, O., Akande, I., and Popoola, A. (2018). Corrosion protection effect of chitosan on the performance characteristics of A6063 alloy. *Journal of Bio-and Tribo-Corrosion* 4: 1–6.

**70** Pais, M., George, S.D., and Rao, P. (2021). Glycogen nanoparticles as a potential corrosion inhibitor. *International Journal of Biological Macromolecules* 182: 2117–2129.

**71** Pais, M., George, S.D., and Rao, P. (2021). Interfacial adsorption of nanoparticles of maltodextrin for enhanced protection of metal surface. *Surfaces and Interfaces* 26: 101418.

**72** Srivastava, M., Srivastava, S.K., Nikhil, G., and Ji, R.P. (2019). Chitosan based new nanocomposites for corrosion protection of mild steel in aggressive chloride media. *International Journal of Biological Macromolecules* 140: 177–187.

**73** Solomon, M.M., Gerengi, H., Kaya, T., and Umoren, S.A. (2016). Performance evaluation of a chitosan/silver nanoparticles composite on St37 steel corrosion in a 15% HCl solution. *ACS Sustainable Chemistry & Engineering* 5: 809–820.

**74** Solomon, M.M., Gerengi, H., Kaya, T., and Umoren, S.A. (2017). Enhanced corrosion inhibition effect of chitosan for St37 in 15% $H_2SO_4$ environment by silver nanoparticles. *International Journal of Biological Macromolecules* 104: 638–649.

**75** Hefni, H.H., Azzam, E.M., Badr, E.A. et al. (2016). Synthesis, characterization and anticorrosion potentials of chitosan-g-PEG assembled on silver nanoparticles. *International Journal of Biological Macromolecules* 83: 297–305.

**76** Paul, E., Egbuniwe, A., and Ekwumemgbor, P. (2018). The use of starch silver nanoparticles for the inhibition of mild steel corrosion using weight loss technique. *ATBU Journal of Science, Technology and Education* 6: 176–182.

**77** Solomon, M.M., Umoren, S.A., Obot, I.B. et al. (2018). Exploration of dextran for application as corrosion inhibitor for steel in strong acid environment: effect of molecular weight, modification, and temperature on efficiency. *ACS Applied Materials & Interfaces* 10: 28112–28129.

# 2

# Natural Polymers and Their Derivatives as Corrosion Inhibitors for the Oil and Gas Industry

*Ali F.S.A. Rahiman*[1], *Menaka Ramanathan*[2], *and Sethumanickam Subhashini*[1]

[1] *Avinashilingam Institute for Home Science and Higher Education for Women, Department of Chemistry, Bharathi Park Road Tatabad, Forest College Campus, Saibaba Colony, Coimbatore, Tamil Nadu, 641043, India*
[2] *Dr. N.G.P Arts and Science College, Department of Chemistry, Kalapatti Road, Coimbatore, Tamil Nadu 641048, India*

## 2.1 Introduction

Oil and gas are extremely momentous not just to an individual and their business, but also to the country's global standing. The economic growth of a nation is closely related to its energy demand; therefore, its prices hold captive a direct impact on the overall health of the economy. Oil and natural gas power the globe, as they together produce more than half of the world's energy, and without them, many countries would not be able to carry on with their everyday activities. The need for oil and gas is projected to grow more, thereby making the sector quite inevitable for investments and research. The exploration and development of new oil fields to satisfy the growing demands of energy are found to be too difficult, costly, or politically unstable to justify operations. On the back of the continuous growing demand for energy and robust economic growth of each nation, it is extremely prime to maintain the existing oil fields under operable conditions.

In recent years, offshore operators have constructed offshore facilities, including offshore platforms, pipelines, ships, and undersea storage, and shore facilities to support their exploration and drilling activities. The oil and gas industries starting from drilling activities and pipeline transportation to storage tanks and their distribution are confronted with corrosion challenges in every inevitable aspect. The general corrosion issues of the offshore structures include the crevice corrosion of drill pipe joints, localized corrosion of drilling equipment and well casing, uniform deterioration of transmission pipelines, and storage tanks in hostile environments. Hydraulic fracturing, often known as fracking, is the technique of pumping water, sand, and/or chemical additives, such as alkali metal chlorides, borates, and cross-linking agents, into a well to fracture subterranean bedrock and release oil or gas deposits. To stimulate the production of oil and gases in new and aging wells and also to remove scales, acidic solutions were employed in practice during the operational procedures where the metallic structures are exposed to a

*Polymeric Corrosion Inhibitors for Greening the Chemical and Petrochemical Industry*, First Edition.
Edited by Mohammad A. Jafar Mazumder, Mumtaz A. Quraishi, and Amir Al-Ahmed.

serious corrosive attack by fracturing liquids and acids. Corrosion is exacerbated by the drilling process's high temperatures, pressures, and strains, which will aggravate all the possible ways of corrosion.

Corrosion may cause life-menacing deterioration to metal and alloy structures, resulting in financial penalties, including product losses, replacement, restructuring, safety, and environmental contamination. Metal deterioration can cause malfunctioning of corroded instruments and contamination of major industrial products (e.g. chemical compounds) by aqueous corrosion products, which would result in increased productivity loss. Recently, offshore facility operators have focused on cost savings through the implementation of technologies and solutions to extend the life of existing assets and infrastructures. This can be well achieved by minimizing the risk of general and localized corrosion by material selection, cathodic protection, coatings, and use of various corrosion inhibitors to the solution during fracturing [1], oil-well acidizing [2], and acid descaling [3]. It is also suitable for specialized applications, such as interior corrosion control, where the use of conventional methods may be impractical. In the oil and gas industries, corrosion inhibitors are generally used of inorganic nature (borates, chromates, phosphates, etc.) [4] with high toxicity and environmental incompatibility or of organic nature (amines, amides, imidazoles, etc.) [5, 6], which are expensive due to the tangle in their preparation methods.

The use of polymeric compounds as corrosion inhibitors in the oil and gas industries [7, 8] are reported by various authors as they possess multifunctionality and better film-forming capabilities, which could significantly improve protective barrier properties, but their use is restricted due to its nonbiodegradable nature. These inevitable drawbacks can be overcome by the use of natural polymers, which are biodegradable and eco-friendly. The presence of polar functional groups (e.g. –OH, –COOH, $-(C{=}O)\ NH_2$) in the polymer plays an important role and provides strong interaction with the surface of the metal with which it comes in contact. Thus, several natural polymers, such as cellulose and cellulose derivatives, gelatine, alginate, pectin, lignin, chitin, and chitosan (CS), have proved their corrosion inhibition for sour and sweet corrosions in acidic and brine solutions. This chapter focuses on their specific application of natural polymeric materials and their derivatives as corrosion inhibitors in acidic and brine solutions media, which are of high importance in the oil and gas production sectors. This chapter also includes the various practices for the provision of the most rampant and avant-garde polymeric inhibitors with tunned corrosion mitigation efficiency, which can be extended to its applications as corrosion inhibitors in the oil and gas sectors.

## 2.2 Reliable Methods for the Study of Polymeric Corrosion Inhibitors

The gravimetric or weight-loss method, electrochemical techniques, gasometric or hydrogen-evolution method, and different surface techniques were used to examine the corrosion mitigation capability of the majority of the natural polymeric materials, as mentioned in this chapter. The commonly used techniques and the required conditions for the methods are described below.

### 2.2.1 Gravimetric Method

In the gravimetric method, the metal specimens of a particular dimension were weighed and exposed to the corrosive medium with and without natural polymeric inhibitors. After exposure for a specified time period, the specimens were cleaned, dried, and weighed to find the weight loss. Using the observed weight-loss corrosion rate and inhibitor efficiencies were calculated for different systems studied.

### 2.2.2 Electrochemical Methods

The electrochemical measurements were carried out using the metal specimens as a working electrode. The working electrode was immersed along with reference and standard electrodes and the responsive current was measured for the specified potentials ranging from its negative value to the positive potential. Anodic and cathodic Tafel segments were extrapolated to obtain corrosion potential and corrosion current density, which, in turn, were used to calculate the inhibition efficiency (IE) of the polymer under study. In impedance spectroscopy techniques, small amplitude of alternating current (AC) signals was swept through specified frequency region. The observed plots were fitted to various circuit models based on their nature to find the charge-transfer resistance and double-layer capacitance.

### 2.2.3 Gasometric Method

The hydrogen evolution method was also employed for the study; the metal specimens were dropped in the acid with and without inhibitors and the hydrogen ($H_2$) gas evolved due to the corrosion of the metal were collected. The reduced volume of $H_2$ gas evolved in presence of inhibitor was used to calculate the IE.

### 2.2.4 Surface Morphological Studies

Surface morphological studies were also employed as a tool for the study of corrosion inhibition performance of the polymers. The polymers being a large molecule with more functional groups, which provide multicentric adsorption leading to the formation of film over the surface of the metals under study. Thus, the formed polymeric film protects against the attack of the corrosive medium on the metal surface thereby inhibiting the corrosion process. The formed film showed a large difference in the surface morphology of the exposed metal. The surface morphologies were studied by scanning electron microscopy (SEM), laser profilometry, atomic force microscopy (AFM), transition electron microscopy (TEM), and X-ray photoelectron spectroscopy (XPS). The surface hydrophobicity was measured by contact angle measurements. SEM proved the formation of polymeric films over the metal surfaces and the energy-dispersive X-ray analysis (EDX) further evidencing the existence of the film by providing the elemental composition of C, H, and other heteroatoms along with the metal under consideration. Any other common methods employed for the corrosion studies and the inhibitor adsorbed surface characterization are discussed in brief in the following sessions.

## 2.3 Natural Polymeric Corrosion Inhibitors

The various natural polymeric materials are grouped based on their structures and the works reported for their corrosion inhibition process are discussed in the following sections (Figure 2.1).

### 2.3.1 Chitosan and its Derivatives

Chitin is a natural polysaccharide found particularly in the shells of crustaceans, such as crab and shrimp, the cuticles of insects, and the cell walls of fungi. Chitosan is the N-deacetylated product of chitin and it is a polysaccharide bearing-(1–4)-linked *N*-acetyl-D-glucosamine units as its monomeric moiety. Chitosan is an attractive material for many applications because of its immunological activity, wound healing, biocompatibility, low toxicity, and biodegradability. Chitosan is also employed in the textile, paper, and food industries for various applications. Chitosan's anticorrosive ability could be drawn from its molecular structure; it bears electron-rich hydroxyl and amino groups capable of bonding with the metal surface and subsequent corrosion inhibition via coordinating its lone pair electrons to the empty or partially occupied metal orbitals. The chitosan contains the special groups amidogen and hydroxyl, and both groups contain active hydrogen atoms and lone pairs that pay the way for structural modifications to generate different derivatives with the required properties. Chitosan derivatives are easily synthesized since their amine-bound glucosamine molecular units allow for the introduction of reactive chemical groups within their polymer chains. Moreover, due to the unique physiological activity, degradability, and adsorbability, chitosan and its derivatives have better corrosion inhibition performance. Among the natural

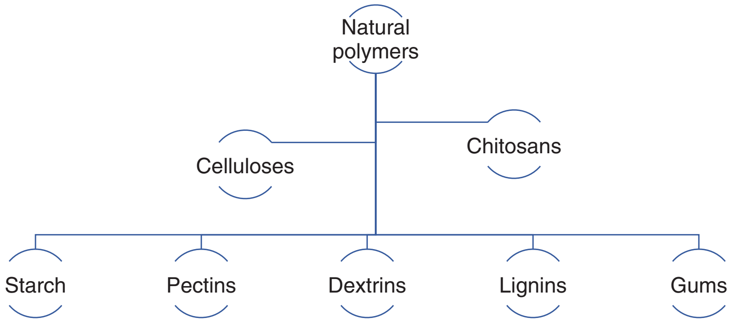

**Figure 2.1** Broad class of natural polymeric corrosion inhibitors.

polymeric anticorrosive materials, chitosan derivatives are the one variety, which was widely studied for their application in the oil-well acidizing process.

Umoren et al. have investigated Chitosan for mild steel (MS) corrosion inhibition in 0.1 M HCl using gravimetric, potentiodynamic polarization, electrochemical impedance spectroscopy (EIS) measurements, SEM, and ultraviolet (UV)–visible analysis [9]. The IE increased with temperature to 96% at 60 °C and then dropped to 93% at 70 °C. Chemical adsorption was proposed as the mechanism for corrosion inhibition as there was an increase in the trend of protection efficiency with temperature. The inhibition performance of water-soluble chitin (WSC) and its synergistic inhibition with potassium iodide (KI) in 1 M HCl was studied using gravimetric and electrochemical measurements [10]. Results revealed the improvised inhibition on the addition of KI due to the observed synergism between the WSC and KI. Chitin from crab shells was deacetylated to obtain water-soluble chitosan and deployed for their corrosion inhibition toward carbon steel in 1 M HCl. The results revealed that WSC optimum efficiency of about 98.94% with 500 ppm concentrated at 303 K. The calculated thermodynamic factors suggested endothermic spontaneous physisorption [11].

Carboxymethyl chitosan, the derivative of chitosan, was used to synthesize chitosan-modified Schiff bases with citral (CHC) and others with cinnamaldehyde (CAHC) [12]. This modification enhances the solubility of chitosan, thereby enhancing its inhibition performance. CHC and CAHC were tested for their anticorrosion efficiency on P110 steel in 3.5% NaCl medium with a carbon dioxide environment. Various test methods revealed around 82–87% IE for CHC and 90–94% for CAHC. AFM, SEM analysis evidenced the adsorbed chitosan derivative layer on the surface of the metal. Quantum mechanical and simulation methods were used to predict the ranking of the studied inhibitors [12]. Four chitosan Schiff base derivatives were synthesized using cinnamyl aldehyde, vanillic aldehyde, CHC, and anisaldehyde to yield chitosan cinnamyl aldehyde Schiff base (CTBR), chitosan vanillic aldehyde Schiff base (CTBS), chitosan citral Schiff base (CTBN), and chitosan anisaldehyde Schiff base (CTBH) [13]. The corrosion inhibition performance of these chitosan derivatives was evaluated for P110 steel in 15% HCl. The interaction mechanism between the inhibitor molecule and steel surface was investigated by the theoretical calculation method of molecular dynamics simulation. FLUENT software was used to simulate the erosion of liquid on the tube wall corrosion inhibitor film under different flow rates during acidizing at different pipeline positions in oil and gas wells using the transient simulation with the VOF model. The simulation results show that the adsorption energies of four inhibitors on the Fe (110) surface are CTBR ($-1109.64\ \text{kJ mol}^{-1}$), CTBS ($-1259.86\ \text{kJ mol}^{-1}$), CTBN ($-1285.66\ \text{kJ mol}^{-1}$), and CTBH ($-1175.36\ \text{kJ mol}^{-1}$). The results showed that these chitosan-modified base molecules have an excellent adsorption capacity [13].

Chitosan oligosaccharide derivatives, such as benzaldehyde-modified chitosan oligosaccharide quaternary ammonium salt (BHC) and propionaldehyde-modified chitosan oligosaccharide quaternary ammonium salt (PHC), were synthesized and tested for their inhibition performance on P110 steel corrosion in 3.5% NaCl medium saturated with $CO_2$ environment [14]. SEM, AFM, and contact angle measurements evidenced its inhibition performance of BHC and PHC. Usual corrosion monitoring methods reported 91.5% IE for PHC and 93.3% for BHC inhibitor molecules. Quantum mechanical calculations showed that $\Delta E_{\mathrm{PHC}}$ is greater than $\Delta E_{\mathrm{BHC}}$, indicating that the adsorption of BHC on the surface of P110 steel is greater than that of PHC [14]. Salicylaldeyde-chitosan Schiff base (SCSB) was synthesized by the reaction of chitosan and salicylaldehyde [15] and their corrosion inhibition performance was tested in 3.5% NaCl saturated with $CO_2$ on P110 steel. A maximum of 95.2% IE was reported for SCSB. The surface analysis was carried out using SEM, AFM, scanning Kelvin probe (SKP), and XPS to corroborate the formation of inhibitor film on the metal surface. Computational studies showed the effective adsorption of the protonated form of the inhibitor [15].

Carboxymethyl chitosan-grafted poly(2-methyl-1-vinylimidazole) (polyCMCh-graft-polyMVI) copolymer was synthesized from carboxymethyl chitosan backbone. *N*-(3-aminopropyl)imidazole (APM) was synthesized from imidazole via hydrogenation using Raney nickel catalyst [16]. Eduok et al., in the study, evaluated the corrosion inhibition of the polyCMCh-graft-polyMVI; APM and APM/graft copolymer conjugate against pipeline steel corrosion has been investigated in $CO_2$-saturated acidic oilfield formation water. APM showed about 70% inhibition; copolymer showed 88% inhibition, whereas APM/graft copolymer conjugate was found to possess higher efficiency of 93.5%. Synergism was observed and a greater total inhibition effect was attained compared to one of the inhibitors investigated independently. The observed superior protective performance could be attributed to the formation of more stable organic–inorganic APM/polyCMCh-graft-polyMVI hybrid film clusters on the metal surface, which was confirmed by morphological studies, such as SEM, AFM, XPS, and contact angle measurements [16]. Carboxymethyl chitosan was grafted with water-soluble poly(*N*-vinyl imidazole) – (CMCh-g-PVI) using the procedure reported by Sabaa et al. [17] and was deployed as a corrosion inhibitor for API X70 corrosion in 1 M HCl [18]. CMCh-g-PVI processes good solubility upon constant stirring, which increases its inhibitive effect to 93% on electrochemical measurements. SEM, AFM, and XPS studies confirmed the film-forming ability of chitosan derivatives through the adsorption phenomenon. The authors suggested a mechanism for adsorption involving physisorption, chemisorption, and retrodonation process [18].

Eduok et al. synthesized glucosyloxyethyl acrylate graft chitosan (GA-CHS) polymer and studied their anticorrosive nature on API5L X70 pipeline steel in chloride enriched 1 M HCl medium [19]. On exposure to corrosive electrolytes, the steel coupons are corroded due to unrestricted chloride-induced attacks, leading to severe surface pits. The enhanced corrosion inhibition and the greater edge over unmodified chitosan could have been due to the linear GA-CHS polysaccharide moiety and its hydroxyl/amino chemical groups in combination with its acrylate functionality [19].

Allyl sulfonate graft chitosan (CH(S)) was synthesized by a reaction involving CH and allyl sulfonate, catalyzed homogeneously by acetic acid in alkaline pH using sodium persulfate initiator. CH(S) was subsequently grafted onto graphene oxide (GO) nanosheets and utilized as a corrosion inhibitor for X70, the extensively used steel in the various oilfield in a $CO_2$-saturated NaCl electrolyte at 60 °C. This nanocomposite significantly inhibited corrosion, and this was attributed to the molecular adsorption and formation of protective polymeric chitosan–GO hybrid nanocomposite films on the metallic surface. The (CH(S)–GO) polymer nanocomposite ensured a more compact coverage on steel surfaces, hence was an effective corrosion inhibitor [20].

Chitosan is inactive at the interfaces, while carboxymethyl chitosan was found to have a little surface activity. Carboxymethyl chitosan was further modified by introducing a hydrophobic moiety to become surface-active polymers. The resulting amphiphilic polymer further decreases the surface tension. Seven different hydrophobic substitutions were used to modify chitosan and carboxymethyl chitosan. As the length of the hydrophobic portion increases, the surface activity increases. The modified polymers are carboxymethyl chitosan–benzaldehyde (cmch–benz); carboxymethyl chitosan–chlorobenzaldehyde (cmch–chloro); carboxymethyl chitosan–anisaldehyde (cmch–aniz); carboxymethyl chitosan–butyraldehyde (cmch–but); and carboxymethyl chitosan–octanaldehyde (cmch–oct). The thio-derivative of carboxymethyl chitosan (thio-cmch) was also prepared and used as carbon steel corrosion inhibitor for oil-field applications in 1 M HCl [21]. The inhibition efficiencies of the studied chitosan derivatives are depicted in Figure 2.2.

The IE of all the prepared polymers was in the following order: ch < cmch < cmch–chloro < cmch–benz < cmch–aniz < cmch–but < cmch–oct < thio-cmch while that

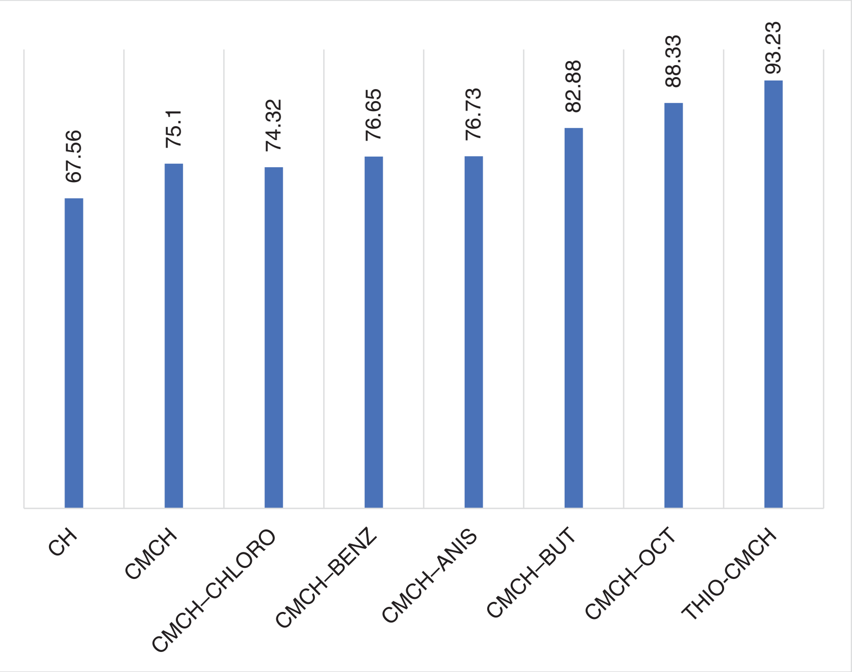

**Figure 2.2** Inhibition efficiencies of hydrophobically modified chitosan surfactants.

of surface activity was: cmch < cmch–chloro < cmch–benz < cmch–Aniz < cmch–but < thio-cmch < cmch–oct. Quantum chemical calculations of the selected inhibitors support the observed inhibition efficiencies trends of the polymers.

Chitosan derivative, piperonal-chitosan Schiff base (Pip-Cht), was synthesized via a microwave-based method and was tested for its application as a novel environmentally benign corrosion inhibitor in oil-well acidizing for carbon steel in 15% HCl and found to show 83% IE, which was further enhanced by the addition of KI to 91% [22]. Chitosan was modified with cinnamaldehyde (Cinn-Cht) and deployed as a corrosion inhibitor for carbon steel in 15% HCl. The studies showed that Cinn-Cht provided IE of about 85%, which was enhanced to 92.45% with addition of KI. The computational studies carried out via density functional theory (DFT) revealed that mainly the protonated form of inhibitor adsorbs on the metal surface. Monte Carlo simulation studies also showed that the protonated form of the inhibitor molecule exhibited higher adsorption energy than the neutral inhibitor [23]. Environmentally benign vanillin-modified chitosan (Van-Cht) was synthesized using a microwave-induced green synthetic protocol and has been evaluated as a corrosion inhibitor for carbon steel in 15% HCl. Van-Cht acted by adsorption on the surface of carbon steel with about 93% efficiency to inhibit corrosion and exhibited a mixed-type behavior with cathodic predominance [24]. Chauhan et al. synthesized triazole-modified chitosan, chitosan-4-amino-5-methyl-1,2,4-triazole-3-thiol (CS–AMT), and was evaluated as an inhibitor against corrosion of carbon steel in 1 M hydrochloric acid. Results showed IE of about 95%, which was supported by DFT calculations, Fukui indices analysis, and molecular dynamics simulations [25].

Chitosan ionic liquid polymers are attractive materials to apply as green corrosion inhibitors. Chitosan-*p*-toluene sulfonate salt (CSPTA) was prepared by refluxing PTA with CS polymeric ionic liquids (PIL) were prepared by amidation of CSPTA with fatty acids, such as stearic (C18), palmitic (C16), myristic (C14), and lauric (C12) acids. Fatty acid-modified chitosans were tested for their control of hydrogen evolution. The results revealed that the volume of hydrogen gas evolved was reduced with the rise in the prepared PILs concentrations. The order of effectiveness of the inhibitors was CSPTA-lauric > CSPTA-myristic > CSPTA-palmitic > CSPTA-stearic. This indicates that CSPTA-lauric is the most efficient inhibitor, which has the shortest chain among the prepared PILs. The difference between the inhibitors' efficiency may be attributable to the spacer length. Due to the long distance between the two head hydrophobic groups in the structure decreases the charge density of the head groups and lowers the adsorption of the inhibitor [26].

β-Cyclodextrin-modified natural chitosan was synthesized and investigated for its corrosion-mitigating property on carbon steel in 0.5 M HCl. The results declared a higher IE of about 96% due to both physisorption and chemisorption [27]. Polyaspartic acid [28]/chitosan complex (PASP/CS) was synthesized by the reaction of PASP, chitosan, and glutaraldehyde. PASP/CS is an anodic corrosion inhibitor in sodium chloride solution with 83.5% IE. The hydrophobic groups in the complexes can interact with the hydrophilic polar groups so that the PASP/CS composite forms a compact protective film on the metal surface. The PASP/CS inhibits the diffusion of water and dissolved oxygen to the metal surface by steric hindrance, thereby inhibiting corrosion [28].

Chitosan biguanidine hydrochloride (CBG-HCl) was prepared by Elhebshia et al. and explored for its corrosion inhibition performance on low-carbon steel in 0.5 M $H_2SO_4$. CBG-HCl was found to protect the metal with 66% efficiency which upon addition of 0.1 M NaCl enhanced its efficiency to about 93% due to the synergism exists between CBG-HCl and NaCl [29]. Methyl acrylate graft chitosan copolymer (CS-MAA) was prepared by the reaction of chitosan (CS) and methyl acrylate (MAA) via the Michael addition reaction followed by the action of ethylenediamine (EN) and triethylenetetramine (TN), respectively, with CS-MMA to synthesize ethylenediamine-grafted chitosan copolymer (CS-MAA-EN) and triethylenetetramine-grafted chitosan copolymer (CS-MAA-TN). The compounds CS-MAA-EN and CS-MAA-TN showed an appreciable corrosion inhibition property against corrosion of Q235 carbon steel in 5% HCl providing nearly 85% protection [30].

Water-soluble chitosan derivatives 2-*N,N*-diethyl benzene ammonium chloride *N*-oxoethyl chitosan, and 12-ammonium chloride *N*-oxododecan chitosan were tested for the corrosion inhibition of carbon steel by Hussein et al. The IE 2-*N,N*-diethyl benzene ammonium derivative in 1 M HCl at varying temperatures was higher than for chitosan and 12-ammonium chloride *N*-oxododecan chitosan [31]. Li et al. synthesized two new CS derivatives modified with thiosemicarbazide (TSFCS) and thiocarbohydrazide (TCFCS) by a simple method using formaldehyde as linkage. The results showed that the compound TCFCS acted as a mixed-type metal anticorrosion inhibitor by providing an IE of 92% with $60\,\mathrm{mg\,l^{-1}}$ concentration [32]. Migahed et al. synthesized a new chitosan-based ionic liquid and investigated for corrosion of X-65 steel in 1 M HCl using electrochemical techniques. Results of electrochemical measurements revealed the reduction of metal dissolution in presence of chitosan-based ionic liquid. Quantum calculation was also carried out to support the adsorption of inhibitors on the metal surface [33]. Chitosan (Ch)-grafted poly(ethylene glycol) (Ch-g-mPEG) and its respective silver nanoparticles were synthesized and examined as corrosion inhibitors for carbon steel in 1 M HCl solution using potentiodynamic polarization and electrochemical methods. The results revealed that the IE obtained by Ch-g-mPEG self-assembled on silver nanoparticles was higher than that of Ch-g-mPEG [34].

A large number of chitosan derivatives were synthesized by structure modification techniques and were used as an MS corrosion inhibitor. The inhibitor systems of chitosan includes water-soluble chitosan [35, 36], chitosan with KI [37, 38], chito-oligosaccharide [39], thiourea-chitosan [40], acetyl thiourea chitosan [41], *O*-fumaryl-chitosan [42], anionic chitosan surfactant [43], chitosan salicylaldehyde Schiff base [44, 45], polyethylene glycol (PEG)-functionalized chitosan [46], disodium ethylene diamine tetraacetic acid (EDTA) functionalized chitosan [47], hydroxyquinoline derivative of chitosan [48], stearic acid-grafted chitosan [49], (2-pyridyl)-acetyl chitosan [50], chitosan thiophene carboxaldehyde [51], polyaniline/chitosan [52], carboxymethyl hydroxypropyl chitosan [53],

**Table 2.1** Chitosan derivatives for mild steel corrosion inhibition.

| Inhibitor system | Corrosive medium | Inhibition efficiency (%) | Reference |
|---|---|---|---|
| Water-soluble chitosan | 3.65% NaCl | 90 | [35] |
| Water-soluble chitosan | 1 M HCl | 74.6 | [36] |
| Chitosan + potassium iodide | $H_2SO_4$ | >90 | [37] |
| Chitosan + iodide ion | 15% $H_2SO_4$ | 97.68 | [38] |
| Chito-oligosaccharide | 3.5% NaCl | 89 | [39] |
| Thiourea-chitosan | 1 M HCl | >90 | [40] |
| Acetyl thiourea chitosan | $H_2SO_4$ | 94 | [41] |
| *O*-fumaryl-chitosan | 1 M HCl | 93.2 | [42] |
| Anionic chitosan surfactant | 1.0 M HCl | >90 | [43] |
| Chitosan salicylaldehyde Schiff base | 1 M HCl | 76 and 90 | [44, 45] |
| PEG-functionalized chitosan | 1 M HCl | 93.9 | [46] |
| Disodium EDTA-functionalized chitosan | 1 M HCl | 96.63 | [47] |
| Chitosan ferulic acid amide | 1 M HCl | 95.96 | [48] |
| Stearic acid- grafted chitosan | 1 N HCl | 83 | [49] |
| (2-Pyridyl)-acetyl chitosan | 1 M HCl | 85 | [50] |
| Chitosan thiophene carboxaldehyde | 1 M HCl | >80 | [51] |
| Polyaniline/chitosan | 0.5 M HCl | >85 | [52] |
| Carboxymethyl hydroxypropyl chitosan | 1 M HCl | 95 | [53] |
| Polyaniline/salicylaldehyde chitosan | 1 M HCl | 76 | [54] |
| *N*-(2-hydroxy-3-trimethyl ammonium) propyl chitosan chloride | 1 M HCl | 98.9 | [55] |
| Amylose-acetate-blended carboxymethyl chitosan | 0.25 M $H_2SO_4$ | 89 | [56] |

polyaniline/salicylaldehyde chitosan [54], *N*-(2-hydroxy-3-trimethyl ammonium) propyl chitosan chloride [55], and amylose-acetate-blended carboxymethyl chitosan [56]. The polymeric inhibitor systems and the resulted inhibition efficiencies in the specified corrosive media are tabulated in Table 2.1.

Three chitosan Schiff bases, such as chitosan benzaldehyde (CSB-1), 4-(dimethylamino) benzaldehyde (CSB-2), and 4-hydroxy-3-methoxy benzaldehyde (CSB-3), were synthesized by microwave irradiation by Haque et al. [57]. The IE of the inhibitors followed the order CSB-1 < CSB-2 < CSB-3 in gravimetric and electrochemical studies. Theoretical studies and molecular dynamics simulation studies supported the order of IE. The formation of the inhibitor film was corroborated by Fourier-transform infrared spectroscopy (FTIR)–attenuated total reflectance (ATR) and SEM/EDX [57]. Cross-linked poly(*N*-alkyl-4-vinyl pyridinium) iodides, namely, as P4-VPMI, P4-VPOI, and P4-VPDI, were synthesized from quaternization of poly(4-vinyl pyridine) cross-linked with 2% divinyl benzene (DVB), by three alkyl iodides (methyl iodide [MI], octan iodide [OI], and decan iodide [DI]) in acetonitrile at room temperature and were deployed for their corrosion protection of ST37 steel in 1 M $H_2SO_4$. The results showed that IE was decreased by increasing the length of carbon chain of the alkyl group. Thus, among the three inhibitors, P4VPMI showed the best inhibition effect on the corrosion of St-37 [58].

Cobalt and tin sulfide nanoparticles are used to synthesize chitosan-cobalt sulfide and chitosan-$SnS_2$ nanocomposites and are used for corrosion protection of MS in 1 M HCl at room temperature. Chitosan provided only 77% inhibition to MS, while the efficiency increases for chitosan cobalt composites (95%) and chitosan-$SnS_2$ composites (80%) [59]. Amphiphilic chitosan (CS) nanogels were synthesized in water using the surfactant-free method by Atta et al. First amidation of CS with unsaturated fatty acids, such as oleic and linolenic acids, were done to prepare hydrophobic CS. These CS fatty amides were grafted with polyoxyethylene aldehyde monomethyl ether to prepare CSLA-MPEG and CSOA-MPEG amphiphilic CS surfactants. These produced surfactants were converted to nanoparticles by emulsification followed by cross-linking and were tested for their corrosion inhibition performance for steel in the acid medium [60].

*N*-vanillyl-*O*-2′-hydroxypropyl trimethyl ammonium chloride chitosan (VHTC) was synthesized and evaluated for corrosion inhibition performance on Q235 steel in 1 M HCl solution. Weight-loss, polarization, EIS, and stereomicroscope analysis were used to evaluate the inhibition performance. The results showed VHTC as a better inhibitor than chitosan with 90% IE [61]. Ionic liquid of chitosan was synthesized by the amidation of chitosan *p*-toluene sulfonate salt with oleic acid. The corrosion inhibitive effect of the prepared PIL on steel corrosion in acid chloride solution was studied using different electrochemical techniques. Potentiodynamic polarization data revealed that the prepared ionic liquid reduced both dissolution and hydrogen-evolution corrosion reactions [62].

### 2.3.2 Cellulose and its Derivatives

Cellulose is the major component in lignocellulosic biomass and is the most abundant natural renewable polymer on earth [63]. The chemical structure of cellulose is composed of D-glucopyranosyl units linked through β-1,4-glycosidic bonds. Cellulose is a natural polymer that has prominent physiochemical characteristics, such as high chemical resistance, thermal stability, durability, biocompatibility, and biodegradability [64]. Because of the strong intramolecular or intermolecular hydrogen bonding, virgin cellulose is insoluble in water, and less soluble in organic solvents, which limits its processing for their applications [65]. The cellulose chains were modified structurally and the prepared derivatives could achieve the desired solubility which increased its potential usage in the oil and gas industries as corrosion inhibitors. The most common derivatives of cellulose include carboxymethyl cellulose (CMC), hydroxyethyl cellulose (HEC), aminated hydroxyethyl cellulose (AHEC), hydroxypropyl cellulose (HPC), and hydroxypropyl methylcellulose (HPMC), their structures are depicted in Figure 2.3.

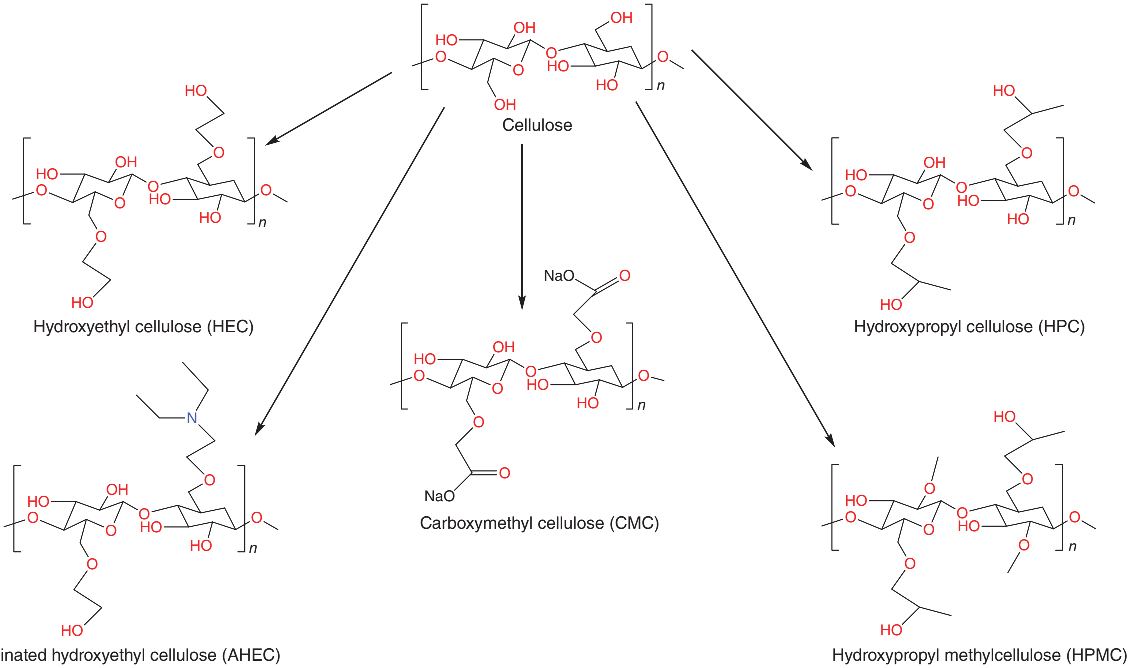

**Figure 2.3** Structure of cellulose and its derivatives.

Cellulose and lignin extracted from pistachio nut were tested for their MS corrosion inhibition in hydrochloric acid medium, with a marked inhibition of about 92.7%. Cellulose and lignin present in the extract together act synergistically providing higher inhibition performance for the extract [66]. CMC [67] and its sodium salt (Na-CMC) [68] were reported for their corrosion-mitigating effect on metal structures. The improvised corrosion protective efficiency for CMC was achieved due to the synergistic effect with iodide ions [69] and $Zn^{2+}$ ions [70]. The CMC along with 1-hydroxyethane-1,1-diphosphonicacid-$Zn^{2+}$ binary system [71] were reported for their effective corrosion inhibition performance of about 97% for Fe-alloys. CMC was incorporated with $Fe_3O_4$, CuO, and NiO nanoparticles via in situ deposition. The incorporation of these nanoparticles enhanced the corrosion inhibition performance of CMC from 76% to more than 94% with a maximum of 98% with NiO nanoparticles [72]. CMC/silver nanoparticles composite was explored as a benign corrosion inhibitor for ST37 steel corrosion in 15% sulfuric acid medium with a maximum of 96.4% efficiency [73].

HEC was reported for their corrosion inhibition of MS [74–77], 1018 C-steel [78]. The corrosion inhibition performance of CMC was improved on synergism with surfactant additives, such as triton X100, cetyl pyridinium chloride, and sodium dodecyl sulfate, and found to increase the IE attributed to the resultant interaction between the HEC and surfactant molecules [79]. Ethyl hydroxyethyl cellulose (EHEC) [80] and AHEC [81] are found to provide more than 80% IE. HPC [82] and hydroxypropyl methylcellulose [83] showed higher inhibition efficiencies of about 90%. Recently, chemically modified hydroxyethyl cellulose (CHEC) has been prepared from polyurethane prepolymer with cellulose and its corrosion inhibition of MS in 15% HCl was reported to be about 90–93% even under higher temperatures. The inhibition performance of CHEC was high when compared with the other carbohydrate polymers [84]. Cellulose tetrazole was tested as a carbon steel corrosion inhibitor in the hydrochloric acid medium, which showed a maximum of 94% inhibition [85]. The reported corrosion inhibitive performances of the reported cellulose derivatives for various metals are tabulated in Table 2.2. The higher inhibition efficiencies were reported for the cellulose derivatives at higher temperatures in acid medium, which promises its applications in acid-well acidizing and descaling process in oil-well industries.

### 2.3.3 Starch and Its Derivatives

Starch is a natural and biodegradable polymer available in abundance at a low cost. It is a polysaccharide consisting of a large number of glucose units linked by glycosidic bonds. Normally, starch consists of two components, namely, amylase (linear and helical) and amylopectin (branched), and the composition of the components will vary with the sources from which the polymer is derived. The unique molecular structure, with several hydroxyl groups, presents in the starch suggested that the compound can be used in corrosion inhibition applications.

Cassava starch graft copolymer with acrylamide was prepared and tested for their anticorrosive nature on cold-rolled steel in sulfuric acid medium with more than

**Table 2.2** Cellulose derivatives as corrosion inhibitors for metal structures.

| Inhibitor system | Type of metal | Corrosive medium | Inhibition efficiency (%) | Reference |
|---|---|---|---|---|
| CMC | Mild steel | 0.5 M $H_2SO_4$ | <70 | [67] |
| Na-CMC | Mild steel | 1 M HCl | 80.00 | [68] |
| CMC + $I^-$ | Mild steel | 0.5 M $H_2SO_4$ | 89 | [69] |
| CMC + $Zn^{2+}$ | Carbon steel | Neutral chloride | 97 | [70] |
| CMC + HEDP+$Zn^{2+}$ | Mild steel | Neutral aqueous | 80 | [71] |
| CMC + $Fe_2O_3$a) | Carbon steel | 1 M HCl | 94.9 | [72] |
| CMC + CuOa) | | | 96.2 | |
| CMC + NiOa) | | | 98.4 | |
| CMC + Aga) | ST37 steel | 15% $H_2SO_4$ | 96.4 | [73] |
| HEC | Mild steel | 1 M HCl | 68; 69 | [74, 75] |
| | Mild steel | 0.5 M $H_2SO_4$ | 93.99 | [76, 77] |
| | 1018C-steel | Neutral chloride | 96.7 | [78] |
| HEC + surfactant | A1020C-steel | 1 M HCl | 91.62 | [79] |
| EHEC; EHEC + $I^-$ | Mild steel | 1 M HCl | 72; 91 | [80] |
| AHEC | Mild steel | 1 M HCl | 91.8 | [81] |
| HPC | Cast iron | 1 M HCl | 89.6 | [82] |
| HPMC | Mild steel | 0.5 M $H_2SO_4$ | 71, 91 | [83] |
| HPMC + $I^-$ | | 1 M HCl | 64, 69 | |

a) Nanoparticles.

90% efficiency was reported even at a higher temperature, 50 °C [86]. Cassava starch ternary graft copolymer of cassava starch-sodium allyl sulfonate-acryl amide graft copolymer was synthesized and its inhibition performance on cold-rolled steel in hydrochloric acid was reported by Li et al. [87]. Glycerin-grafted starch was studied as a corrosion inhibitor of C—Mn steel in 1 M HCl solution with enhanced inhibition performance of about 94% [88]. Cassava starch was modified as activated starch and carboxymethylated starch was tested for their corrosion inhibition of XC 35 carbon steel in NaCl medium. Activated starch was found to be a better inhibitor than the carboxymethylated starch and the reason for better inhibition was attributed to the interaction of the active groups present in the molecule [89]. Carboxymethylated cassava starch and activated starch were prepared from native cassava starch and explored for their corrosion inhibition performance for carbon steel in HCl medium and were found to possess inhibition above 85% [90].

The synergistic effect of various compounds was studied on the corrosion inhibition performance of starch molecules. Surfactants, such as sodium dodecyl sulfate and cetyl trimethyl ammonium bromide, were used to enhance the corrosion-mitigating power of starch [91] in an acid medium for MS. The effect of synergism was more pronounced at low concentrations of the starch. The synergistic effect between starch and 2,6-diphenyl-3-methylpiperidin-4-one was investigated for the MS corrosion in the acid medium [92]. Corrosion protection of natural sweet potato starch, alkaline-modified starch, and the synergistic study of the starch with KI were rumored for MS corrosion in acidic media. Natural starch showed inhibition of about 30% and its alkaline modification enhances its efficiency to about 60%, whereas its synergistic effect showed a good enhancement in the inhibition behavior of the starch to about 84% [93]. The work on the action of millet starch extracted from the millet grains was reported for MS corrosion inhibition in sulfuric acid medium. The maximum IE of 87.14% was obtained for $1.4\,\mathrm{g\,l^{-1}}$ millet starch and the IE was increased to 94.03% with the addition of $0.4\,\mathrm{g\,l^{-1}}$ of KI [94]. As expected from the structure of starch due to the presence of more hydroxyl groups, the experimental observation proved its high inhibition performance greater than 80%, which promises its applications in the simulated conditions in the oil fields.

### 2.3.4 Pectin and Its Derivatives

Pectin is a structural heteropolysaccharide present in the primary cell walls of terrestrial plants and contains a large amount of poly(D-galacturonic acid) bonded via α-1,4-glycosidic linkage. Pectin possesses carboxylic (–COOH) and carboxymethyl ($-COOCH_3$) functional groups on its carbohydrate backbone, making it a possible candidate for corrosion inhibition processes. It is mainly extracted from citrus fruits and other fruits, including apples and berries. It is used in the food industry as a gelling agent, particularly in jams and jellies. Pectin was reported as an inhibitor for X60 pipeline steel corrosion in an acidic environment and IE increased with increasing pectin concentration and solution temperature with a maximum of 85% IE [95]. Pectin was extracted from lemon peel and was used for the MS corrosion inhibition and the performance of the inhibitor showed an efficiency of 90% [96]. Pectin-g-polyacrylamide (Pec-g-PAAm) and pectin-g-polyacrylic acid (Pec-g-PAA) were synthesized and their corrosion behavior was electrochemically evaluated to about 94%for MS in 3.5% NaCl [97]. A synergistic mixture of pectin along with propyl phosphonic acid (PPA) and $Zn^{2+}$ was studied for carbon steel corrosion and reported to provide 90% efficiency [98]. Pectin extracted from *Opuntia cladodes* was used as a corrosion inhibitor for MS corrosion in 1 M HCl showing 96% IE [99]. Poloxamers and pectins were explored for carbon steel corrosion inhibition of more than 80% in hydrochloric acid solution [100]. Three sunflower head pectins with different molecular weights (Mw = 4.50, 97.23, and 254.64 kDa) were obtained by enzyme-assisted extraction and they were examined for carbon steel corrosion inhibition providing more than 90% efficiency [101].

Pectin and ceria were tested for their X60 steel corrosion inhibition in hydrochloric acid and were found to be a maximum of 52%, whereas their synergistic effect enhanced their performance by about 60% even with a low concentration of pectin [102]. Pectin extracted from sugar beet pulp using enzymatic or acid hydrolysis was evaluated as corrosion inhibitor for MS under acidic conditions and were examined for their higher temperature corrosion inhibition performance, the results showed more than 90% efficiency [103]. Corrosion inhibition of pectin on AISI1040 dual-phase steel was studied in 0.5 M sulfuric acid solution, which was reported to possess more than 83% efficiency [104].

### 2.3.5 Dextrin and Its Derivatives

Dextrin, low-molecular-weight carbohydrate polymers formed from D-glucose units linked by α-(1 → 4) or α-(1 → 6) glycosidic linkages. Various forms of dextrin exist in nature ranging from maltodextrin, amylodextrin, α/β-dextrin, cyclic, and highly branched cyclic dextrin compounds [105]. As the dextrin molecules have hetero atoms in their polymeric structure, they are forming a film on the surface of the metal, thereby inhibiting the corrosion process. A favorable synergistic effect of floxacins along with dextrin was reported for the MS corrosion inhibition in the sulfuric acid medium [106]. Ciprofloxacin, levofloxacin, and norfloxacin were monitored for their synergism with dextrin. Among the studied floxacins, ciprofloxacin was found to possess higher efficiency followed by levofloxacin and norfloxacin [106]. Dextrin and caprolactam-grafted dextrin were studied as corrosion inhibitors for J55 Steel in acid solution with a notable enhancement of inhibition performance from 67% (dextrin) to 83% (caprolactam-g-dextrin) [107]. Dextrin was grafted by polyvinyl acetate and their corrosion reticence was explored for MS corrosion in HCl medium. On grafting polyvinyl acetate to dextrin, its inhibition efficiency was reported to show enhanced inhibition from 43 to 64% at lower concentrations and 84 to 98% at higher concentrations [108].

Cyclodextrin is a cyclic oligosaccharide consisting of glucose units linked by α-1,4-glycosidic bonds. The most abundant cyclodextrins are α-, β-, and γ-cyclodextrin, which are comprised of six, seven, and eight glucose units, respectively. The inhibition behavior of the divinyl sulfone cross-linked β-cyclodextrin polymer (bCDS-P) in [poly(AA–AM–AMPS—MAH–β-CD)] prepared from acrylic acid, acrylamide, polyacrylamide, and β-cyclodextrin and was found to achieve good P110 carbon steel corrosion inhibition [109].

### 2.3.6 Natural Gums and Their Derivatives

Gums are naturally occurring polysaccharides obtained from the plant's source in solid form. These naturally occurring polymers are either water-soluble or absorb water and swell up to form a gel-like texture in the water. Naturally occurring gums can be either ionic [110] or neutral uncharged [111] in nature. It is capable of increasing the viscosity of the solutions even in presence of low concentrations. Many researchers have reported the natural gums as effective corrosion inhibitors for different metallic surfaces in corrosive media.

The inhibition effect of gum arabic (GA) on the corrosion of API 5L X42 pipeline steel in 1 M HCl solution was investigated using EIS and potentiodynamic polarization curves. The maximum IE obtained was 92% at $2\,\mathrm{g\,l^{-1}}$. The adsorption of GA on pipeline API 5L X42 steel surface obeyed Langmuir adsorption isotherm and involved physical adsorption [112]. The influence of temperature (25–65 °C) on the adsorption and the IE of GA for the corrosion of API 5L X42 pipeline steel in 1 M HCl was potentiodynamic polarization curves and EIS. GA was a good inhibitor for API 5L X42 pipeline steel, and its IE was significantly stable, with a maximum IE of 93% [113]. Arabic gum (ArG) was extracted and evaluated for its anticorrosive performance of MS and aluminum, which showed around 80% inhibition for MS [114]. GA and synthetic PEG were tested for their MS corrosion inhibition in sulfuric acid medium. The synergistic inhibitor efficiency was also tested with halide ions, which resulted because of the growing surface coverage caused by the collaborations between the pair of ions [115].

Guar gum was tested as a corrosion inhibitor for carbon steel in sulfuric acid [116]. Guar-gum-grafted polyacrylamide was evaluated for their corrosion mitigation effect on MS corrosion in HCl, which showed more than 90% efficiency [117]. Guar-gum-grafted 2-acrylamido-2-methylpropanesulfonic acid (GG-AMPS) were tested to mitigate the corrosion of carbon steel in ASTM standard D1141-98(2013) artificial seawater and the studies revealed 95% mitigation performance [118]. Guar gum-methylmethacrylate (GG-MMA) composite was synthesized and used as an eco-friendly corrosion inhibitor for P110 steel in 3.5% NaCl solution saturated with carbon dioxide. The corrosion inhibition performance of GG-MMA alone is 90% at 400 mg $l^{-1}$, and that of formulation with KI (5 mM) thorn GG-MMA (300 mg $l^{-1}$) is 96.8%. The adsorption of GG-MMA over P110 steel is a spontaneous and mixed-type process [119].

The MS corrosion inhibition using gum acacia in different strengths (0.5, 1, 2 M) of HCl and $H_2SO_4$ was investigated by Abu-Dalo et al. using weight-loss and hydrogen-evolution techniques to evaluate the IE. The effect of the magnetic field on both techniques was also studied. The weight-loss and hydrogen-evolution measurements for ArG showed the same trend in the presence and absence of an externally applied magnetic field, with a remarkable reduction in the weight-loss in presence of the magnetic field. The corrosion rate decreased considerably due to the adsorption of GA on the metal surface, which provides 63% IE in 2 M HCl [120]. The inhibiting effect of gum acacia grafted with polyacrylamide was investigated on MS corrosion in 15% HCl using gravimetric and electrochemical measurements. Among different grafted copolymers, gum acacia and acrylamide resulted in maximum corrosion IE of 94% at 0.3 g $l^{-1}$ [121].

Natural polymer xanthan gum (XG) was investigated as an eco-friendly corrosion inhibitor for MS in 1 M HCl, resulted in adsorption of XG onto the metal surface. The addition of surfactant (sodium dodecyl sulfate, cetyl pyridinium chloride, and Triton X-100) synergistically improved the efficiency of XG to about 84% [122]. Xanthan exudate gum and its graft polyacrylamide copolymer were tested on MS corrosion in a very high concentration of acid (15% HCl) using chemical, electrochemical, and surface analytical techniques. The IE was increased with inhibitor concentration and exhibited maximum of 92% IE, which was remarkably higher for the corrodent concentration (15% HCl). Theoretical evaluation of associated monomeric units using DFT to correlate inhibitor molecular structure with corrosion inhibition was done [123]. Phosphorylated xanthan gum (PXG) has been synthesized by the simple addition of phosphate groups on the XG backbone. The ability of PXG in combating MS corrosion in a 200 ppm NaCl corrosive environment was examined and showed its inhibition to a maximum of 92.5% [124].

Umoren et al. extracted exudates gum from *Raphia hookeri* (RH) and deployed it for the corrosion inhibition of MS in $H_2SO_4$ at 30–60 °C. Results from weight-loss and thermometric techniques showed that the performance of RH improved with concentration and upon addition of the halide ions due to synergistic effect [125]. *Anogessus leocarpus* gum (AL gum) was reported to be a good adsorption inhibitor for the corrosion of MS in HCl solution. FTIR studies confirmed the formation of Fe–AL gum complex on the MS surface, which provides around 76% IE [126]. Ameh et al. studied the inhibitive effect of *Ficus glumosa* (FG) gum for MS corrosion in $H_2SO_4$ medium using weight-loss, gasometric, and thermometric techniques. The results obtained revealed that the gum was a potential adsorption inhibitor with 76% IE [127]. *Ficus platyphylla* gum was investigated by Eddy et al. for its MS corrosion in HCl solution using gravimetric and gasometric methods. The inhibitor worked moderately in this medium, which offered the maximum efficiency of 78% for the concentration of $0.5\,\mathrm{g\,l^{-1}}$ [128]. They also studied *Daniella oliverri* (DO) gum exudate and explored its corrosion IE toward MS corrosion in an acid medium. The better IE shown by the gum was due to the presence of aromatic, suitable functional groups, and heteroatoms in its chemical constituents that facilitated its adsorption [129].

MS corrosion inhibition by *Anacardium occidentale* gum (cashew gum) was reported by Arthur et al. The evaluation of the inhibitor was carried out using weight-loss methods. The corrosion rate of the MS decreased with the increase in the concentration of cashew gum and reached a maximum IE of 89% at the concentration of $1.0\,\mathrm{g\,l^{-1}}$ [130]. Cashew tree gum (CTG), poly(acrylamide) (PAM), and cashew-tree-gum-grafted poly(acrylamide) (CTG-g-PAM) copolymer were tested for their corrosion mitigation effect on MS in hydrochloric acid. PAM was found to have higher IE than CTG and upon grafting; the CTG-g-PAM copolymer showed better inhibition than the individual polymers [131]. The synergistic study of *Acacia Senegal* (ArG) and *A. occidentale* (cashew gum) combination in corrosion inhibition of MS was carried out to determine the IE of their combination, their results showed 83% protection efficiency [132].

*Azadirachta indica* gum exudates were deployed as corrosion inhibitors for MS in 1 M HCl, which provided maximum of 92% protection [133]. *A. indica* was also tested against carbon steel corrosion by Malarvizhi and Mallika showed 83% protection [134]. A binary inhibitor system of *A. indica* gum and four different substituted piperidin-4-one derivatives was reported for the corrosion protection of MS in HCl medium. The results revealed that the protection level of *A. indica* gum depended on the conformation of piperidin-4-one derivatives [135]. They also reported the inhibition performance of gum exudate of *Araucaria columnaris* (AC) for MS corrosion in 1 M $H_2SO_4$ and also studied the synergistic effect with halides and metal cations. The maximum IE of the gum was 400 ppm and inhibition was attributed to the adsorption at the electrode/solution interface. The addition of halides and metal cations enhanced the IE and was endorsed to the complex formation between the gum and the metal [136].

Ameh carried out a comparative study of the exudate gums of *Albizia ferruginea* (AF) and *Khaya senegalensis* (KS) for the corrosion inhibition of MS. Weight-loss and gasometric methods were used to evaluate the effect of inhibition and the results proved them to be better inhibitors. In comparison, maximum IE was found in KS with 82.56% IE at 0.5% $\mathrm{g\,l^{-1}}$ concentration of the gum. The better performance was attributed to the fact that more compounds with heteroatoms were identified in the gas chromatography–mass spectroscopy (GCMS) spectrum of KS gum compared to the AF gum [137]. *Iraqi apricot tree* GA was reported as a corrosion inhibitor for MS substrate in 1 M HCl and the results revealed [138].

Other miscellaneous gum exudates include *Pachylobus edulis* for MS [139], locust bean gum for carbon steel [140], and steel-Q235 [141], *Albizia zygia* for MS [142], *Tragacanth* gum for MS [143], *Boswellia serrata* gum for MS [144], and carbon steel [145] were tested for their corrosion inhibition of the metal surfaces in acid media.

## 2.4 Mechanism for Natural Polymeric Corrosion Inhibition

The corrosion inhibition mechanism of natural polymers and their derivates were discussed based on the adsorption process in the reviewed works of literature. All the discussed natural polymeric inhibitors contain a large number of heteroatoms, especially N and O. Upon addition of these inhibitors to the fracturing liquids or oil-well-acidizing fluids, these inhibitors get protonated and exist in their protonated forms in solutions. The protonated inhibitors replace the already adsorbed water molecules from the surface and get adsorbed ensuing in physisorption. Each polymeric molecule has nonprotonated OH/NH, which is involved in the donation of their lone pair electrons to metal atoms, thereby resulting in chemisorption. Meanwhile, the protonated OH/NH groups are involved in physical adsorption through the electrostatic interaction of protonated polymeric centers with already adsorbed anions of the medium. The adsorption of anions on the MS surface creates an excess negative charge on the surface, thus leading to adsorption of cations (protonated inhibitors). The protonated inhibitor molecules are, thus, adsorbed via anions acting as an interconnecting bridge between positively charged MS surface and protonated inhibitors [146]. The schematic representation for the proposed mechanism for natural polymers is depicted in Figure 2.4. The surface morphology studies, such as SEM–EDX, AFM, XRD, and XPS, in the discussed research works provide evidence for the adsorption of the polymeric inhibitors, which form a film on the metal surface, thereby protecting the metallic structure from the corrosive attack of the fluids.

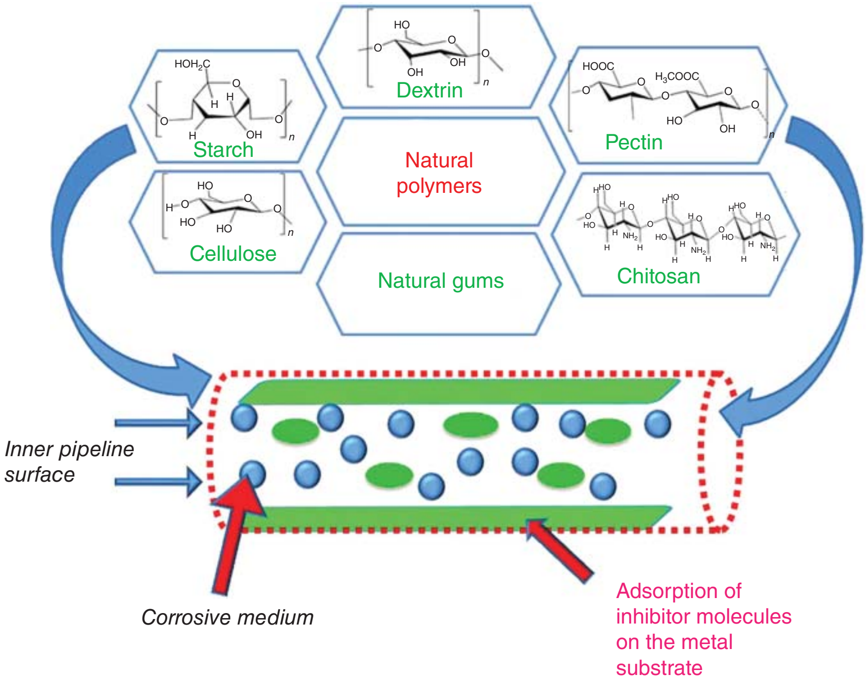

**Figure 2.4** Schematic representation for the mechanism of corrosion inhibition.

## 2.5 Conclusion and Outtake for Future Work

This chapter discussed the various natural occurring polymers and their derivatives for corrosion inhibition of metals, such as steel, MS, carbon steel, and other various alloys of steel, used in the oil-well acidizing and gas pipelines of the industries. Polymers being macromolecules with a large number of functional groups give rise to a way for multicentric adsorption of the polymers on the metal surfaces. Natural polymeric materials being biodegradable and biocompatible with the environment provide their eco-friendly and green-centric approach in the field of oil and gas industries corrosion inhibitors. Chitosan is the most studied natural polymeric material for its better exploration in tunning its corrosion IE by adopting various methods for the preparation of modified chitosan with enhanced corrosion inhibition performance. Grafting, compositing copolymerizing, and activation through functionalization were adopted for the natural polymers, such as chitosan, starch, cellulose, dextrin, and others, to overcome the drawbacks of insolubility. For most of the polymers, the above-mentioned studies were employed for the exploration of the corrosion inhibition effect. For a few discussed natural polymers, some special methods were employed for the better exploration of their corrosion inhibition performances under the stimulated corrosive environments. The good corrosion IE of these natural polymeric materials at elevated temperatures suggests their applications for the oil-well-acidizing process.

## References

1. Barati, R. and Liang, J.T. (2014). A review of fracturing fluid systems used for hydraulic fracturing of oil and gas wells. *Journal of Applied Polymer Science* 131: 40735.
2. Haruna, K., Obot, I., Ankah, N. et al. (2018). Gelatin: a green corrosion inhibitor for carbon steel in oil well acidizing environment. *Journal of Molecular Liquids* 264: 515–525.
3. Deyab, M. (2020). Understanding the anti-corrosion mechanism and performance of ionic liquids in desalination, petroleum, pickling, de-scaling, and acid cleaning applications. *Journal of Molecular Liquids* 309: 113107.
4. Costello, M.T. (2017). *Corrosion Inhibitors and Rust Preventatives, Lubricant Additives*, 393–408. CRC Press.
5. Olajire, A.A. (2017). Corrosion inhibition of offshore oil and gas production facilities using organic compound inhibitors - a review. *Journal of Molecular Liquids* 248: 775–808.
6. Goyal, M., Kumar, S., Bahadur, I. et al. (2018). Organic corrosion inhibitors for industrial cleaning of ferrous and non-ferrous metals in acidic solutions: a review. *Journal of Molecular Liquids* 256: 565–573.
7. Umoren, S.A. and Solomon, M.M. (2020). Polymeric corrosion inhibitors for oil and gas industry. In: *Corrosion Inhibitors in the Oil and Gas Industry* (ed. V.S. Saji and S.A. Umoren), 303–320. Wiley.
8. Tiu, B.D.B. and Advincula, R.C. (2015). Polymeric corrosion inhibitors for the oil and gas industry: design principles and mechanism. *Reactive and Functional Polymers* 95: 25–45.
9. Umoren, S.A., Banera, M.J., Alonso-Garcia, T. et al. (2013). Inhibition of mild steel corrosion in HCl solution using chitosan. *Cellulose* 20: 2529–2545.
10. Sangeetha, Y., Meenakshi, S., and Sundaram, C. (2016). Synergistic effect of water soluble chitin and iodide ion on the corrosion inhibition of mild steel in acid medium. *Advanced Materials Letters* 7: 164–176.
11. Awaliah, T., Asnawati, D., and Hamdiani, S. (2020). Effectivity of water-soluble chitosan from rajungan shell waste as corrosion inhibitor on iron in 1 M HCl. *Journal of Physics: Conference Series* 1594: 012004.
12. Zhao, Q., Guo, J.X., Cui, G.D. et al. (2020). Chitosan derivatives as green corrosion inhibitors for P110 steel in a carbon dioxide environment. *Colloids and Surfaces B-Biointerfaces* 194: 111150.
13. Wang, D.L., Li, Y.M., Chang, T., and Luo, A. (2021). Experimental and theoretical studies of chitosan derivatives as green corrosion inhibitor for oil and gas well acid acidizing. *Colloids and Surfaces A-Physicochemical and Engineering Aspects* 628: 127308.
14. Cui, G.D., Guo, J.X., Zhang, Y. et al. (2019). Chitosan oligosaccharide derivatives as green corrosion inhibitors for P110 steel in a carbon-dioxide-saturated chloride solution. *Carbohydrate Polymers* 203: 386–395.
15. Ansari, K., Chauhan, D.S., Quraishi, M. et al. (2020). Chitosan Schiff base: an environmentally benign biological macromolecule as a new corrosion inhibitor

for oil & gas industries. *International Journal of Biological Macromolecules* 144: 305–315.

**16** Eduok, U., Ohaeri, E., and Szpunar, J. (2019). Conversion of imidazole to *N*-(3-aminopropyl)imidazole toward enhanced corrosion protection of steel in combination with carboxymethyl chitosan grafted poly(2-methyl-1-vinylimidazole). *Industrial & Engineering Chemistry Research* 58: 7179–7192.

**17** Sabaa, M.W., Mohamed, N.A., Mohamed, R.R. et al. (2010). Synthesis, characterization and antimicrobial activity of poly (*N*-vinyl imidazole) grafted carboxymethyl chitosan. *Carbohydrate Polymers* 79: 998–1005.

**18** Eduok, U., Ohaeri, E., and Szpunar, J. (2018). Electrochemical and surface analyses of X70 steel corrosion in simulated acid pickling medium: effect of poly (*N*-vinyl imidazole) grafted carboxymethyl chitosan additive. *Electrochimica Acta* 278: 302–312.

**19** Eduok, U., Ohaeri, E., Szpunar, J., and Akpan, I. (2020). Synthesis, characterization and application of glucosyloxyethyl acrylate graft chitosan against pipeline steel corrosion. *Journal of Molecular Liquids* 315: 113772.

**20** Eduok, U., Ohaeri, E., and Szpunar, J. (2021). Anticorrosion allyl sulfonate graft chitosan/graphene oxide nanocomposite material. *Materials Advances* 2: 1621–1634.

**21** Alsabagh, A.M., Elsabee, M.Z., Moustafa, Y.M. et al. (2014). Corrosion inhibition efficiency of some hydrophobically modified chitosan surfactants in relation to their surface active properties. *Egyptian Journal of Petroleum* 23: 349–359.

**22** Chauhan, D.S., Mazumder, M.A.J., Quraishi, M.A. et al. (2020). Microwave-assisted synthesis of a new piperonal-chitosan Schiff base as a bio-inspired corrosion inhibitor for oil-well acidizing. *International Journal of Biological Macromolecules* 158: 231–243.

**23** Chauhan, D.S., Mazumder, M.A.J., Quraishi, M.A., and Ansari, K.R. (2020). Chitosan-cinnamaldehyde Schiff base: a bioinspired macromolecule as corrosion inhibitor for oil and gas industry. *International Journal of Biological Macromolecules* 158: 127–138.

**24** Quraishi, M.A., Ansari, K.R., Chauhan, D.S. et al. (2020). Vanillin modified chitosan as a new bio-inspired corrosion inhibitor for carbon steel in oil-well acidizing relevant to petroleum industry. *Cellulose* 27: 6425–6443.

**25** Chauhan, D.S., Quraishi, M.A., Sorour, A.A. et al. (2019). Triazole-modified chitosan: a biomacromolecule as a new environmentally benign corrosion inhibitor for carbon steel in a hydrochloric acid solution. *RSC Advances* 9: 14990–15003.

**26** Elsaeed, S.M., El Tamany, E.H., Ashour, H. et al. (2018). Corrosion and hydrogen evolution rate control for X-65 carbon steel based on chitosan polymeric ionic liquids: experimental and quantum chemical studies. *RSC Advances* 8: 37891–37904.

**27** Liu, Y., Zou, C.J., Yan, X.L. et al. (2015). Beta-cyclodextrin modified natural chitosan as a green inhibitor for carbon steel in acid solutions. *Industrial & Engineering Chemistry Research* 54: 5664–5672.

**28** Chen, T.S., Zeng, D.F., and Zhou, S.J. (2018). Study of polyaspartic acid and chitosan complex corrosion inhibition and mechanisms. *Polish Journal of Environmental Studies* 27: 1441–1448.

**29** Elhebshia, A., El Nemrb, A., El-Deabc, M.S., and Ashoura, I. (2019). CBG-HCl as a green corrosion inhibitor for low carbon steel in 0.5 MH. *Desalination and Water Treatment* 164: 240–248.

**30** Li, H., Li, H., Liu, Y., and Huang, X. (2015). Synthesis of polyamine grafted chitosan copolymer and evaluation of its corrosion inhibition performance. *Journal of the Korean Chemical Society* 59: 142–147.

**31** Hussein, M.H.M., El-Hady, M.F., Shehata, H.A.H. et al. (2013). Preparation of some eco-friendly corrosion inhibitors having antibacterial activity from sea food waste. *Journal of Surfactants and Detergents* 16: 233–242.

**32** Li, M.L., Xu, J., Li, R.H. et al. (2014). Simple preparation of aminothiourea-modified chitosan as corrosion inhibitor and heavy metal ion adsorbent. *Journal of Colloid and Interface Science* 417: 131–136.

**33** Migahed, M., Al-Sabagh, A., Khamis, E., and Zaki, E. (2015). Quantum chemical calculations, synthesis and corrosion inhibition efficiency of ethoxylated-[2-(2-{2-[2-(2-benzenesulfonylamino-ethylamino)-ethylamino]-ethylamino}-ethylamino)-ethyl]-4-alkyl-benzenesulfonamide on API X65 steel surface under $H_2S$ environment. *Journal of Molecular Liquids* 212: 360–371.

**34** Hefni, H.H.H., Azzam, E.M., Badr, E.A. et al. (2016). Synthesis, characterization and anticorrosion potentials of chitosan-g-PEG assembled on silver nanoparticles. *International Journal of Biological Macromolecules* 83: 297–305.

**35** Fayomi, O., Akande, I., Oluwole, O., and Daramola, D. (2018). Effect of water-soluble chitosan on the electrochemical corrosion behaviour of mild steel. *Chemical Data Collections* 17: 321–326.

**36** Amanah, N.L., Widharyanti, I.D., and Nugroho, A. (2021). Synthesis of water soluble chitosan inhibitor from shrimp shells and its corrosion rate on mild steel in acidic solution. *Journal of Physics: Theories and Applications* 5: 9–17.

**37** Yavari, Z., Nematiyan, S., Saraveni, H., and Noroozifar, M. (2020). A simple strategy to increase inhibitory activity of chitosan towards iron corrosion in acidic media. *Indian Journal of Chemical Technology* 27: 227–234.

**38** Solomon, M.M., Gerengi, H., Kaya, T. et al. (2017). Synergistic inhibition of St37 steel corrosion in 15% $H_2SO_4$ solution by chitosan and iodide ion additives. *Cellulose* 24: 931–950.

**39** Ma, F.B., Li, W.H., Tian, H.W. et al. (2012). Inhibition behavior of chito-oligosaccharide Schiff base derivatives for mild steel in 3.5% NaCl solution. *International Journal of Electrochemical Science* 7: 10909–10922.

**40** Wang, M., Zhang, J., Wang, Q.H., and Dui, M. (2019). Synthesis, characterization and corrosion inhibition performance of the thiourea-chitosan in acidic medium. *International Journal of Electrochemical Science* 14: 8852–8868.

**41** Fekry, A.M. and Mohamed, R.R. (2010). Acetyl thiourea chitosan as an eco-friendly inhibitor for mild steel in sulphuric acid medium. *Electrochimica Acta* 55: 1933–1939.

**42** Sangeetha, Y., Meenakshi, S., and Sundaram, C.S. (2016). Interactions at the mild steel acid solution interface in the presence of *O*-fumaryl-chitosan: electrochemical and surface studies. *Carbohydrate Polymers* 136: 38–45.

**43** Badr, E.A., Hefni, H.H.H., Shafek, S.H., and Shaban, S.M. (2020). Synthesis of anionic chitosan surfactant and application in silver nanoparticles preparation and corrosion inhibition of steel. *International Journal of Biological Macromolecules* 157: 187–201.

**44** Menaka, R. and Subhashini, S. (2016). Chitosan Schiff base as eco-friendly inhibitor for mild steel corrosion in 1 M HCl. *Journal of Adhesion Science and Technology* 30: 1622–1640.

**45** Chen, N., Kong, P., Feng, H. et al. (2019). Corrosion mitigation of chitosan Schiff base for Q235 steel in 1.0 M HCl. *Journal of Bio-and Tribo-Corrosion* 5: 27.

**46** Srivastava, V., Chauhan, D.S., Joshi, P.G. et al. (2018). PEG-functionalized chitosan: a biological macromolecule as a novel corrosion inhibitor. *Chemistryselect* 3: 1990–1998.

**47** Jessima, S., Subhashini, S., Berisha, A. et al. (2021). Corrosion mitigation performance of disodium EDTA functionalized chitosan biomacromolecule - experimental and theoretical approach. *International Journal of Biological Macromolecules* 178: 477–491.

**48** Rbaa, M., Fardioui, M., Verma, C. et al. (2020). 8-Hydroxyquinoline based chitosan derived carbohydrate polymer as biodegradable and sustainable acid corrosion inhibitor for mild steel: Experimental and computational analyses. *International Journal of Biological Macromolecules* 155: 645–655.

**49** Shamsheera, K., Prasad, A.R., Jaseela, P., and Joseph, A. (2020). Development of self-assembled monolayer of stearic acid grafted chitosan on mild steel and inhibition of corrosion in hydrochloric acid. *Chemical Data Collections* 28: 100402.

**50** Sangeetha, Y., Meenakshi, S., and Sundaram, C.S. (2016). Corrosion inhibition of (2-pyridyl)-acetyl chitosan on the acid corrosion of mild steel. *Journal of Chitin and Chitosan Science* 4: 22–27.

**51** Menaka, R. and Subhashini, S. (2017). Chitosan Schiff base as effective corrosion inhibitor for mild steel in acid medium. *Polymer International* 66: 349–358.

**52** Kong, P., Feng, H., Chen, N. et al. (2019). Polyaniline/chitosan as a corrosion inhibitor for mild steel in acidic medium. *RSC Advances* 9: 9211–9217.

**53** Wan, K., Feng, P.P., Hou, B.R., and Li, Y.T. (2016). Enhanced corrosion inhibition properties of carboxymethyl hydroxypropyl chitosan for mild steel in 1.0 M HCl solution. *RSC Advances* 6: 77515–77524.

**54** Kong, P., Chen, N., Lu, Y. et al. (2019). Corrosion by polyaniline/salicylaldehyde modified chitosan in hydrochloric acid solution. *International Journal of Electrochemical Science* 14: 9774–9784.

**55** Sangeetha, Y., Meenakshi, S., and SairamSundaram, C. (2015). Corrosion mitigation of N-(2-hydroxy-3-trimethyl ammonium)propyl chitosan chloride as inhibitor on mild steel. *International Journal of Biological Macromolecules* 72: 1244–1249.

**56** Erna, M., Herdini, H., and Futra, D. (2019). Corrosion inhibition mechanism of mild steel by amylose-acetate/carboxymethyl chitosan composites in acidic media. *International Journal of Chemical Engineering* 2019: 8514132.

**57** Haque, J., Srivastava, V., Chauhan, D.S. et al. (2018). Microwave-induced synthesis of chitosan Schiff bases and their application as novel and green corrosion inhibitors: experimental and theoretical approach. *ACS Omega* 3: 5654–5668.

**58** Hamidi, Z., Mosavian, S.Y., Sabbaghi, N. et al. (2020). Cross-linked poly(*N*-alkyl-4-vinylpyridinium) iodides as new eco-friendly inhibitors for corrosion study of St-37 steel in 1 M $H_2SO_4$. *Iranian Polymer Journal* 29: 225–239.

**59** Srivastava, M., Srivastava, S.K., Nikhil et al. (2019). Chitosan based new nanocomposites for corrosion protection of mild steel in aggressive chloride media. *International Journal of Biological Macromolecules* 140: 177–187.

**60** Atta, A.M., El-Mahdy, G.A., Al-Lohedan, H.A., and Ezzat, A.R.O. (2015). Synthesis of nonionic amphiphilic chitosan nanoparticles for active corrosion protection of steel. *Journal of Molecular Liquids* 211: 315–323.

**61** Wang, Q.H., Zhang, J., Shi, D.L., and Du, M. (2015). Synthesis, characterization and inhibition performance of vanillin-modified chitosan quaternary ammonium salts for Q235 steel corrosion in HCl solution. *Journal of Surfactants and Detergents* 18: 825–835.

**62** El-Mahdy, G.A., Atta, A.M., Al-Lohedan, H.A., and Ezzat, A.O. (2015). Influence of green corrosion inhibitor based on chitosan ionic liquid on the steel corrodibility in chloride solution. *International Journal of Electrochemical Science* 10: 5812–5826.

**63** Zu, G., Shen, J., Zou, L. et al. (2016). Nanocellulose-derived highly porous carbon aerogels for supercapacitors. *Carbon* 99: 203–211.

**64** Haishun, D., Chao, L., Miaomiao, Z. et al. (2018). Preparation and industrialization status of nanocellulose. *Progress in Chemistry* 30: 448.

**65** Arca, H.C., Mosquera-Giraldo, L.I., Bi, V. et al. (2018). Pharmaceutical applications of cellulose ethers and cellulose ether esters. *Biomacromolecules* 19: 2351–2376.

**66** Shahmoradi, A., Talebibahmanbigloo, N., Javidparvar, A. et al. (2020). Studying the adsorption/inhibition impact of the cellulose and lignin compounds extracted from agricultural waste on the mild steel corrosion in HCl solution. *Journal of Molecular Liquids* 304: 112751.

**67** Solomon, M., Umoren, S., Udosoro, I., and Udoh, A. (2010). Inhibitive and adsorption behaviour of carboxymethyl cellulose on mild steel corrosion in sulphuric acid solution. *Corrosion Science* 52: 1317–1325.

**68** Bayol, E., Gürten, A., Dursun, M., and Kayakirilmaz, K. (2008). Adsorption behavior and inhibition corrosion effect of sodium carboxymethyl cellulose on mild steel in acidic medium. *Acta Physico-Chimica Sinica* 24: 2236–2243.

**69** Umoren, S., Solomon, M., Udosoro, I., and Udoh, A. (2010). Synergistic and antagonistic effects between halide ions and carboxymethyl cellulose for the corrosion inhibition of mild steel in sulphuric acid solution. *Cellulose* 17: 635–648.

**70** Anthony, N., Sherine, H.B., and Rajendran, S. (2010). Investigation of the inhibiting effect of carboxymethyicellulose-$Zn^{2+}$ system on the corrosion of carbon steel in neutral chloride solution. *Arabian Journal for Science and Engineering* 35: 41–53.

**71** Rajendran, S., Joany, R., Apparao, B., and Palaniswamy, N. (2002). Corrosion inhibition by carboxymethyl cellulose-1-hydroxyethane-1, 1-diphosphonic acid-$Zn^{2+}$ system. *Bulletin of Electrochemistry* 18: 25–28.

**72** Abd El-Lateef, H.M., Albokheet, W., and Gouda, M. (2020). Carboxymethyl cellulose/metal (Fe, Cu and Ni) nanocomposites as non-precious inhibitors of C-steel corrosion in HCl solutions: synthesis, characterization, electrochemical and surface morphology studies. *Cellulose* 27: 8039–8057.

**73** Solomon, M.M., Gerengi, H., and Umoren, S.A. (2017). Carboxymethyl cellulose/silver nanoparticles composite: synthesis, characterization and application as a benign corrosion inhibitor for St37 steel in 15% $H_2SO_4$ medium. *ACS Applied Materials & Interfaces* 9: 6376–6389.

**74** Arukalam, I.O., Nleme, I.K., and Anyanwu, A.E. (2011). Comparative inhibitive effect of hydroxyethylcellulose on mild steel and aluminium corrosion in 0.5 M HCl solution. *Academic Research International* 1: 492.

**75** Arukalam, I.O. (2012). The inhibitive effect of hydroxyethylcellulose on mild steel corrosion in hydrochloric acid solution. *Academic Research International* 2: 35–42.

**76** Arukalam, I., Madufor, I., Ogbobe, O., and Oguzie, E. (2014). Experimental and theoretical studies of hydroxyethyl cellulose as inhibitor for acid corrosion inhibition of mild steel and aluminium. *The Open Corrosion Journal* 6: 1–10.

**77** Arukalam, I., Madufor, I., Ogbobe, O., and Oguzie, E. (2015). Inhibition of mild steel corrosion in sulfuric acid medium by hydroxyethyl cellulose. *Chemical Engineering Communications* 202: 112–122.

**78** El-Haddad, M.N. (2014). Hydroxyethylcellulose used as an eco-friendly inhibitor for 1018 C-steel corrosion in 3.5% NaCl solution. *Carbohydrate Polymers* 112: 595–602.

**79** Mobin, M. and Rizvi, M. (2017). Adsorption and corrosion inhibition behavior of hydroxyethyl cellulose and synergistic surfactants additives for carbon steel in 1 M HCl. *Carbohydrate Polymers* 156: 202–214.

**80** Arukalam, I., Madu, I., Ijomah, N. et al. (2014). Acid corrosion inhibition and adsorption behaviour of ethyl hydroxyethyl cellulose on mild steel corrosion. *Journal of Materials* 14: 1–11.

**81** Sangeetha, Y., Meenakshi, S., and Sundaram, C.S. (2016). Corrosion inhibition of aminated hydroxyl ethyl cellulose on mild steel in acidic condition. *Carbohydrate Polymers* 150: 13–20.

**82** Rajeswari, V., Kesavan, D., Gopiraman, M., and Viswanathamurthi, P. (2013). Physicochemical studies of glucose, gellan gum, and hydroxypropyl cellulose—inhibition of cast iron corrosion. *Carbohydrate Polymers* 95: 288–294.

**83** Arukalam, I., Madufo, I., Ogbobe, O., and Oguzie, E. (2014). Adsorption and inhibitive properties of hydroxypropyl methylcellulose on the acid corrosion of mild steel. *International Journal of Applied Science and Engineering Research* 3: 241–256.

**84** Farhadian, A., Kashani, S.A., Rahimi, A. et al. (2021). Modified hydroxyethyl cellulose as a highly efficient eco-friendly inhibitor for suppression of mild steel corrosion in a 15% HCl solution at elevated temperatures. *Journal of Molecular Liquids* 338: 116607.

**85** Al Kiey, S.A., Hasanin, M.S., and Dacrory, S. (2021). Potential anticorrosive performance of green and sustainable inhibitor based on cellulose derivatives for carbon steel. *Journal of Molecular Liquids* 338: 116604.

**86** Li, X. and Deng, S. (2015). Cassava starch graft copolymer as an eco-friendly corrosion inhibitor for steel in $H_2SO_4$ solution. *Korean Journal of Chemical Engineering* 32: 2347–2354.

**87** Li, X., Deng, S., Lin, T. et al. (2020). Cassava starch ternary graft copolymer as a corrosion inhibitor for steel in HCl solution. *Journal of Materials Research and Technology* 9: 2196–2207.

**88** Lahrour, S., Benmoussat, A., Bouras, B. et al. (2019). Glycerin-grafted starch as corrosion inhibitor of C-Mn steel in 1 M HCl solution. *Applied Sciences* 9: 4684.

**89** Bello, M., Ochoa, N., Balsamo, V. et al. (2010). Modified cassava starches as corrosion inhibitors of carbon steel: an electrochemical and morphological approach. *Carbohydrate Polymers* 82: 561–568.

**90** Ochoa, N., Bello, M., Sancristóbal, J. et al. (2013). Modified cassava starches as potential corrosion inhibitors for sustainable development. *Materials Research* 16: 1209–1219.

**91** Mobin, M., Khan, M., and Parveen, M. (2011). Inhibition of mild steel corrosion in acidic medium using starch and surfactants additives. *Journal of Applied Polymer Science* 121: 1558–1565.

**92** Brinda, T., Mallika, J., and Sathyanarayana Moorthy, V. (2015). Synergistic effect between starch and substituted piperidin-4-one on the corrosion inhibition of mild steel in acidic medium. *Journal of Material and Environmental Science* 6: 191–120.

**93** Anyiam, C., Ogbobe, O., Oguzie, E., and Madufor, I. (2020). Synergistic study of modified sweet potato starch and KI for corrosion protection of mild steel in acidic media. *Journal of Bio-and Tribo-Corrosion* 6: 1–10.

**94** Nwanonenyi, S., Madufor, I., Uzoma, P., and Chukwujike, I. (2016). Corrosion inhibition of mild steel in sulphuric acid environment using millet starch and potassium iodide. *International Research Journal of Pure and Applied Chemistry* 12: 1–15.

**95** Umoren, S.A., Obot, I.B., Madhankumar, A., and Gasem, Z.M. (2015). Performance evaluation of pectin as ecofriendly corrosion inhibitor for X60 pipeline steel in acid medium: experimental and theoretical approaches. *Carbohydrate Polymers* 124: 280–291.

**96** Fiori-Bimbi, M.V., Alvarez, P.E., Vaca, H., and Gervasi, C.A. (2015). Corrosion inhibition of mild steel in HCl solution by pectin. *Corrosion Science* 92: 192–199.

**97** Geethanjali, R., Sabirneeza, A., and Subhashini, S. (2014). Water-soluble and biodegradable pectin-grafted polyacrylamide and pectin-grafted polyacrylic acid: electrochemical investigation of corrosion-inhibition behaviour on mild steel in 3.5% NaCl media. *Indian Journal of Materials Science* 2014: 356075.

**98** Prabakaran, M., Ramesh, S., Periasamy, V., and Sreedhar, B. (2015). The corrosion inhibition performance of pectin with propyl phosphonic acid and $Zn^{2+}$ for corrosion control of carbon steel in aqueous solution. *Research on Chemical Intermediates* 41: 4649–4671.

**99** Saidi, N., Elmsellem, H., Ramdani, M. et al. (2015). Using pectin extract as eco-friendly inhibitor for steel corrosion in 1 M HCl media. *Der Pharma Chemica* 7: 87–94.

**100** Abdallah, M., Fawzy, A., Hawsawi, H. et al. (2020). Estimation of water-soluble polymers (poloxamer and pectin) as corrosion inhibitors for carbon steel in acidic medium. *International Journal of Electrochemical Science* 15: 8129–8144.

**101** Ma, X., Wang, J., Xu, J. et al. (2019). Sunflower head pectin with different molecular weights as promising green corrosion inhibitors of carbon steel in hydrochloric acid solution. *ACS Omega* 4: 21148–21160.

**102** Umoren, S.A. and Madhankumar, A. (2016). Effect of addition of $CeO_2$ nanoparticles to pectin as inhibitor of X60 steel corrosion in HCl medium. *Journal of Molecular Liquids* 224: 72–82.

**103** Abou-Elseoud, W.S., Abdel-karim, A.M., Hassan, E.A., and Hassan, M.L. (2021). Enzyme-and acid-extracted sugar beet pectin as green corrosion inhibitors for mild steel in hydrochloric acid solution. *Carbohydrate Polymer Technologies and Applications* 2: 100072.

**104** Prabhu, D., Sharma, S., Prabhu, P. et al. (2021). Analysis of the inhibiting action of pectin on corrosion of AISI1040 dual-phase steel with ferrite–martensite and ferrite–bainite structure: a comparison in 0.5 M sulphuric acid. *Journal of the Iranian Chemical Society* 19: 1–20.

**105** Umoren, S.A. and Eduok, U.M. (2016). Application of carbohydrate polymers as corrosion inhibitors for metal substrates in different media: a review. *Carbohydrate Polymers* 140: 314–341.

**106** Devi, G.N., Unnisa, C.B.N., Roopan, S.M. et al. (2020). Floxacins: as mediators in enhancing the corrosion inhibition efficiency of natural polymer dextrin. *Macromolecular Research* 28: 1–9.

**107** Liu, M., Xia, D., Singh, A., and Lin, Y. (2021). Analysis of the anti-corrosion performance of dextrin and its graft copolymer on J55 steel in acid solution. *Processes* 9: 1642.

**108** Biswas, A., Das, D., Lgaz, H. et al. (2019). Biopolymer dextrin and poly (vinyl acetate) based graft copolymer as an efficient corrosion inhibitor for mild steel in hydrochloric acid: electrochemical, surface morphological and theoretical studies. *Journal of Molecular Liquids* 275: 867–878.

**109** He, Y., Yang, Q., and Xu, Z. (2014). A supramolecular polymer containing β-cyclodextrin as corrosion inhibitor for carbon steel in acidic medium. *Russian Journal of Applied Chemistry* 87: 1936–1942.

**110** Hamer, G.K., Bhattacharjee, S.S., and Yaphe, W. (1977). Analysis of the enzymic hydrolysis products of agarose by13C-NMR spectroscopy. *Carbohydrate Research* 54: C7–C10.

**111** Tripathy, S. and Das, M. (2013). Guar gum: present status and applications. *Journal of Pharmaceutical and Scientific Innovation* 2: 24–28.

**112** Bentrah, H., Rahali, Y., and Chala, A. (2014). Gum Arabic as an eco-friendly inhibitor for API 5L X42 pipeline steel in HCl medium. *Corrosion Science* 82: 426–431.

**113** Bentrah, H., Chala, A., Djellab, M. et al. (2017). The influence of temperature on the corrosion inhibition of API 5L X42 pipeline steel in HCl medium by gum Arabic. *Anti-Corrosion Methods and Materials* 64: 409–417.

**114** Umoren, S.A. (2008). Inhibition of aluminium and mild steel corrosion in acidic medium using gum Arabic. *Cellulose* 15: 751–761.

**115** Umoren, S.A., Ogbobe, O., Igwe, I.O., and Ebenso, E.E. (2008). Inhibition of mild steel corrosion in acidic medium using synthetic and naturally occurring polymers and synergistic halide additives. *Corrosion Science* 50: 1998–2006.

**116** Abdallah, M. (2004). Guar gum as corrosion inhibitor for carbon steel in sulfuric acid solutions. *Portugaliae Electrochimica Acta* 22: 161–175.

**117** Roy, P., Karfa, P., Adhikari, U., and Sukul, D. (2014). Corrosion inhibition of mild steel in acidic medium by polyacrylamide grafted guar gum with various grafting percentage: effect of intramolecular synergism. *Corrosion Science* 88: 246–253.

**118** Singh, A., Mohamed, H.S., Singh, S. et al. (2020). Corrosion inhibition using guar gum grafted 2-acrylamido-2-methylpropanesulfonic acid (GG-AMPS) in tubular steel joints. *Construction and Building Materials* 258: 119728.

**119** Singh, A., Ansari, K.R., and Quraishi, M.A. (2020). Inhibition effect of natural polysaccharide composite on hydrogen evolution and P110 steel corrosion in 3.5 wt% NaCl solution saturated with $CO_2$: combination of experimental and surface analysis. *International Journal of Hydrogen Energy* 45: 25398–25408.

**120** Abu-Dalo, M.A., Othman, A.A., and Al-Rawashdeh, N.A.F. (2012). Exudate gum from acacia trees as green corrosion inhibitor for mild steel in acidic media. *International Journal of Electrochemical Science* 7: 9303–9324.

**121** Biswas, A., Mourya, P., Mondal, D. et al. (2018). Grafting effect of gum acacia on mild steel corrosion in acidic medium: gravimetric and electrochemical study. *Journal of Molecular Liquids* 251: 470–479.

**122** Mobin, M. and Rizvi, M. (2016). Inhibitory effect of xanthan gum and synergistic surfactant additives for mild steel corrosion in 1 M HCl. *Carbohydrate Polymers* 136: 384–393.

**123** Biswas, A., Pal, S., and Udayabhanu, G. (2015). Experimental and theoretical studies of xanthan gum and its graft co-polymer as corrosion inhibitor for mild steel in 15% HCl. *Applied Surface Science* 353: 173–183.

**124** Kumar, K.V. and Rao, B.A. (2019). Phosphorylated xanthan gum, an environment-friendly, efficient inhibitor for mild steel corrosion in aqueous 200 ppm NaCl. *Materials Today: Proceedings* 15: 155–165.

**125** Umoren, S., Obot, I., and Obi-Egbedi, N. (2009). *Raphia hookeri* gum as a potential eco-friendly inhibitor for mild steel in sulfuric acid. *Journal of Materials Science* 44: 274–279.

**126** Eddy, N.O., Ameh, P., Gimba, C.E., and Ebenso, E.E. (2011). GCMS studies on *Anogessus leocarpus* (AL) gum and their corrosion inhibition potential for mild steel in 0.1 M HCl. *International Journal of Electrochemical Science* 6: 5815–5829.

**127** Ameh, P.O., Magaji, L., and Salihu, T. (2012). Corrosion inhibition and adsorption behaviour for mild steel by *Ficus glumosa* gum in $H_2SO_4$ solution. *African Journal of Pure and Applied Chemistry* 6: 100–106.

**128** Eddy, N.O., Ameh, P., Gimba, C.E., and Ebenso, E.E. (2012). Chemical information from GCMS of *Ficus platyphylla* gum and its corrosion inhibition potential for mild steel in 0.1 M HCl. *International Journal of Electrochemical Science* 7: 5677–5691.

**129** Eddy, N.O., Odiongenyi, A.O., Ameh, P.O., and Ebenso, E.E. (2012). Corrosion inhibition potential of *Daniella oliverri* gum exudate for mild steel in acidic medium. *International Journal of Electrochemical Science* 7: 7425–7439.

**130** Arthur, D.E., Adedayo, A., Igelige, G., and Ogwuche, E. (2014). Corrosion inhibition of mild steel in 0.1 M $H_2SO_4$solution by *Anacardium occidentale* gum. *American Chemical Science Journal* 4: 847–854.

**131** Ramesan, M. and Surya, K. (2016). Studies on electrical, thermal and corrosion behaviour of cashew tree gum grafted poly (acrylamide). *Polymers from Renewable Resources* 7: 81–99.

**132** Arthur, D.E. (2020). Computational and experimental study on corrosion inhibition potential of the synergistic 1:1 combination of Arabic and cashew gums on mild steel. *Petroleum Research* 5: 170–180.

**133** Manickam, M., Sivakumar, D., Thirumalairaj, B., and Jaganathan, M. (2016). Corrosion inhibition of mild steel in 1 mol $L^{-1}$ HCl using gum exudates of *Azadirachta indica*. *Advances in Physical Chemistry* 2016: 5987528.

**134** Malarvizhi, M. and Mallika, J. (2018). Efficacy of corrosion inhibitive properties of gum exudates of *Azadirachta indica* on carbon steel in 1N hydrochloric acid. *Oriental Journal of Chemistry* 34: 2487.

**135** Thirumalairaj, B. and Jaganathan, M. (2016). Corrosion protection of mild steel by a new binary inhibitor system in hydrochloric acid solution. *Egyptian Journal of Petroleum* 25: 423–432.

**136** Brindha, T., Revathi, P., and Mallika, J. (2015). Corrosion inhibition of naturally occurring gum exudates of *Araucaria columnaris* on mild steel in 1 M $H_2SO_4$. *International Journal of Environmental Science* 4: 36–43.

**137** Ameh, P.O. (2015). A comparative study of the inhibitory effect of gum exudates from *Khaya senegalensis* and *Albizia ferruginea* on the corrosion of mild steel in hydrochloric acid medium. *International Journal of Metals* 2015: 1–13.

**138** Alwaan, I. and Mahdi, F.K. (2016). Natural polymer of *Iraqi apricot* tree gum as a novel corrosion inhibitor for mild steel in 1 M HCl solution. *International Journal of Chemical Engineering* 2016: 5706432.

**139** Umoren, S.A. and Ekanem, U.F. (2010). Inhibition of mild steel corrosion in $H_2SO_4$ using exudate gum from *Pachylobus edulis* and synergistic potassium halide additives. *Chemical Engineering Communications* 197: 1339–1356.

**140** Jano, A., Lame, A., and Kokalari, E. (2012). Use of extracted green inhibitors as a friendly choice in corrosion protection of low alloy carbon steel. *Kemija u Industriji* 61: 497–503.

**141** Guo, L., Zhang, R., Tan, B. et al. (2020). Locust bean gum as a green and novel corrosion inhibitor for Q235 steel in 0.5 M $H_2SO_4$ medium. *Journal of Molecular Liquids* 310: 113239.

**142** Ameh, P.O. (2014). Inhibitory action of *Albizia zygia* gum on mild steel corrosion in acid medium. *African Journal of Pure and Applied Chemistry* 8: 37–46.

**143** Manickam, M., Jaganathan, M., and Sivakumar, D. (2017). Gum tragacanth powder as a green corrosion inhibitor for mild steel in 1N sulphuric acid solution. *International Journal of Innovative Science and Research Technology* 2: 132–140.

**144** Basik, M., Mobin, M., and Aslam, J. (2017). *Boswellia serrata* gum: an eco-friendly corrosion inhibitor for mild steel in 1 M HCl medium. *NIGIS CORCON*. PP4.

**145** Mobin, M., Basik, M., and Aslam, J. (2018). *Boswellia serrata* gum as highly efficient and sustainable corrosion inhibitor for low carbon steel in 1 M HCl solution: experimental and DFT studies. *Journal of Molecular Liquids* 263: 174–186.

**146** Solmaz, R., Kardas, G., Yazici, B., and Erbil, M. (2008). Adsorption and corrosion inhibitive properties of 2-amino-5-mercapto-1,3,4-thiadiazole on mild steel in hydrochloric acid media. *Colloids and Surfaces A-Physicochemical and Engineering Aspects* 312: 7–17.

# 3

# Current Applications of Carbohydrates as Green Corrosion Inhibitors for the Oil and Gas Industry

*Ruby Aslam*[1], *Mohammad Mobin*[1], *Saman Zehra*[1], *and Jeenat Aslam*[2]

[1] *Aligarh Muslim University, Corrosion Research Laboratory, Department of Applied Chemistry,*
*Faculty of Engineering and Technology, Aligarh, Uttar Pradesh 202002, India*
[2] *Taibah University, Department of Chemistry, College of Science, Yanbu 30799, Al-Madina, Saudi Arabia*

## 3.1 Introduction

### 3.1.1 Corrosion: An Introduction and Associated Social and Economic Issues

The oxidation of metallic materials that leads them to deteriorate has long been defined as corrosion [1]. Because so much of the world's population lives near water and humidity, corrosion of metallic items is an inescapable part of human existence [2, 3]. While iron oxidation (rust) has been the most immediately recognized type of corrosion, it accounts for just a small but significant portion of total material losses. Today, the impact of corrosion on society and the associated degradation of materials are of far-reaching importance owing to the increased complexity and diversity of materials systems, including metallic materials and ceramics, polymers, and composites. Advancing technology and the need for global sustainability bring with new and emerging corrosion issues whose negative impacts must be minimized through appropriate materials selection, mitigation and monitoring, and new materials development [4]. The effect of corrosion is often described in economic terms. Several studies have assessed financial losses, which concluded that premature materials degradation costs industrialized nations approximately [5] 3–5% of their gross domestic product (GDP). In the United States, it is estimated that between US$2 and US$4 trillion are lost due to corrosion. National Association of Corrosion Engineers (NACE) International reported that the cost of corrosion for different countries [6] in which the cost of corrosion for India is estimated to be 4.2% of India's GDP (Figure 3.1). However, the actual costs of corrosion to society are even more pervasive and, in practice, difficult to compile. Corrosion can affect public health, the environment, and global sustainability in ways that cannot be quantified simply in terms of GDP loss.

*Polymeric Corrosion Inhibitors for Greening the Chemical and Petrochemical Industry*, First Edition.
Edited by Mohammad A. Jafar Mazumder, Mumtaz A. Quraishi, and Amir Al-Ahmed.

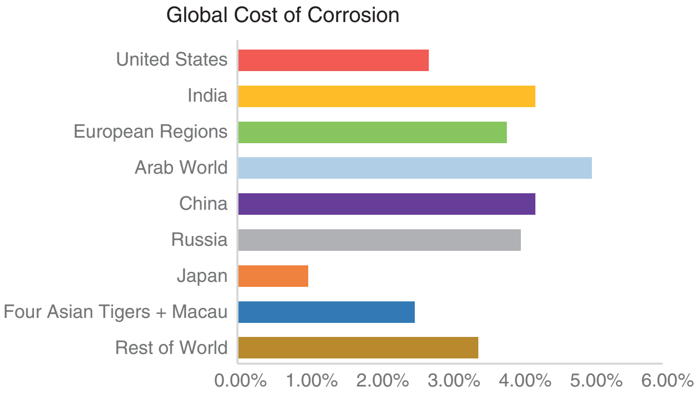

**Figure 3.1** Combined cost of corrosion [6].

### 3.1.2 Strategies to Control Corrosion

Corrosion prevention technologies typically employ one or more of the following methods:

1. Using metals reinforced with elements that provide a corrosion-resistant aspect to the metal surface throughout the corrosion process;
2. Addition of aqueous inhibitors, which adsorb strongly onto the metal surface and prevent the reaction with the corrosion-inducing agent;
3. Deposition of protective coatings on metal substrates.

Choosing the most effective method is not always easy. This choice is partly governed by the ambient environmental conditions and economic considerations. The latter includes the initial cost of application and the replacement of corroded parts and, in some cases, the renewal frequency of the protecting medium. These are frequently determining factors, and the corrosion engineer/scientist will use economic parameters and familiarity with science to determine the ultimate choice. According to a report by Grand View Research, Inc., the global corrosion inhibitors market size was valued at US$7.4 billion in 2019 and is expected to grow at a compound annual growth rate (CAGR) of 3.8% from 2020 to 2027 (https://www.grandviewresearch.com/industry-analysis/corrosion-inhibitors-market). The growth in the market can be attributed to the development of biobased and more eco-friendly corrosion inhibitors. A gradual shift toward the development of environment-friendly corrosion inhibitors may potentially lead the market toward sustainable development and increase the acceptance of corrosion inhibitors among sustainable end users. The product finds widespread application in the industry as its components used in oil and gas exploration are exposed to extreme climatic conditions and require protection against corrosion. The overall corrosion inhibitors market size for oil and gas is forecast to witness more than 5.5% CAGR over the projected timeframe.

There have been plenty of corrosion inhibitors based on organic molecules possessing several types of functional groups and geometrical structures developed and synthesized by various synthetic procedures and used as corrosion inhibitors for decades. As the search for metals corrosion inhibitors that can replace the inorganic and synthetic organic metal corrosion inhibitors found to influence the natural ecosystem or be too expensive continues negatively, the searchlight is beamed on polymers, particularly the natural polymers. Therefore, the current chapter focuses on the anticorrosive applications of carbohydrate polymers for various metals.

## 3.2 Carbohydrate Polymers: A Sustainable Alternatives

The synthetic compounds often employed in daily activities, such as plastics, come to mind when thinking of polymers. You might be amazed to know that nature contains a vast store of sustainable and nontoxic polymers (Figure 3.2). Biopolymers are ample and biodegradable compounds, such as proteins, polysaccharides, and nucleic acids (DNA and RNA) produced by living organisms (e.g. fungi, animals, bacteria, and green plants). Carbohydrate polymers are the most abundant class of natural polymers, which are made of carbon, hydrogen, and oxygen. They are the primary and most essential components of a healthy diet. In biochemistry, the term “carbohydrate” is synonymous with “saccharide.” Based on the number of building units, the saccharides are subcategorized into “mono-,” “di-,” “oligo-,” and “polysaccharides.”

Among these four subcategories of the saccharides, it has been observed that the polysaccharides are most known carbohydrate polymers that have made their mark in various scientific and industrial processes ranging from being vessels for drug

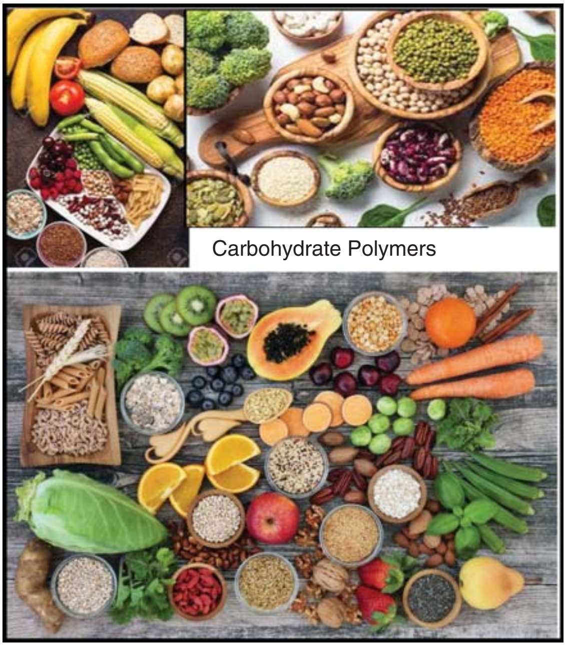

**Figure 3.2** Sources of naturally occurring carbohydrate polymers. Source: Yulia Furman/Adobe Stock; nadianb/Adobe Stock; marilyn barbone/Adobe Stock.

delivery, forming corrosion-resistant films on metals, starting materials for fuel cells, and forming active surfaces for heterogeneous catalysis. Natural polymers have the advantage of being derived from renewable sources as well as being biodegradable. The existence of oxygen and nitrogen atoms in the biopolymers' architecture makes them biodegradable. Some biopolymers applications are used as nanostructures for drug delivery, tissue engineering, nanocontainer, coating, composite, etc. However, a critical purpose of employing biopolymers is to exploit their potential as corrosion inhibitors. Because of heteroatoms exist in the biopolymer's large molecules, they exhibit adsorption capability, which is an essential step in hindering the corrosion by inhibitors [7]. It has been shown that polymers, especially the water-soluble ones, i.e. carboxymethyl cellulose, chitosan, pectin, tannins, starch, Raphia hookeri gum, gum arabic, Gellan gum, hydroxypropyl cellulose, xanthan gum, alginate, and iota-carrageenan, are efficient corrosion inhibitors in different aqueous media. The attractive features of polymers are: (i) availability, (ii) cost-effectiveness, (iii) eco-friendliness, (iv) inherent stability, and (iv) presence of multiple adsorption centers [8]. The mechanism of inhibition depends on the adsorption. It depends on the type of metal, physicochemical properties of the molecule, such as functional groups, steric factors, aromaticity at the donor atom, and the electronic structure of the molecules. In other words, the efficiency of polymers as corrosion inhibitors depends on the characteristics of the environment in which it acts, the nature of the metal surface, and electrochemical potential at the interface. It also depends on the structure of the inhibitor itself, which includes the number of adsorption active centers in the molecule, their charge density, the molecular size, the mode of adsorption, the formation of metallic complexes, and the projected area of the inhibitor on the metallic surface.

### 3.2.1 Limitations of Using Carbohydrate Polymers as Anticorrosive Material

Carbohydrate polymers are less expensive, environmentally benign, and nontoxic. As is well known, most polysaccharides can withstand temperatures of up to 150 °C, and many of them can withstand temperatures of up to 40–50 °C. Because carbohydrate polymers have little mechanical strength, their usage is restricted [9]. Furthermore, botanists warned that if carbohydrate polymers, some directly derived from plants, have been used in abundance as corrosion inhibitors to avoid metal corrosion, the plant kingdom will gradually diminish. Therefore, metals will be safeguarded at the expense of the plant kingdom.

Furthermore, polymer application suffers from low solubility when stored for days, i.e. they may not be viable in highly aggressive testing medium, such as 1 or 2 M mineral acids, after a given duration, which impairs anticorrosion behavior. Furthermore, adding polymers at concentrations ranging from 500 to 1000 ppm frequently may cause the solutions to become turbid or possibly impair equipment performance. As a result, contemporary research has begun to apply modified carbohydrate polymers, which effectively protect the metal surface at low concentrations [10].

### 3.2.2 Emerging Trends in Corrosion Protection Offered by Carbohydrates Polymer

Scientists in corrosion have created several methods for improving the stability and efficacy of polymers as metal corrosion inhibitors. Researchers all over the world advocated compositing and chemical modification to enhance polymer water solubility. The usage of carbohydrate polymer-based compounds as corrosion inhibitors is currently trending toward functionalization. This unique approach intends to improve biocompound solubilization in almost all corrosive conditions and their adsorption and adhesion properties to metallic surfaces. Functionalized carbohydrate polymer-based inhibiting additives can be divided into several categories based on their molecular structures. The class includes carbohydrate polymer Schiff bases, heterocyclic compound-modified carbohydrate polymers, grafted carbohydrate polymer, poly(ethylene glycol) (PEG) cross-linked carbohydrate polymer, carbohydrate polymer surfactants, and carbohydrate–nanoparticle composites. The inhibitory efficacies of several sets of functionalized polymers will be addressed in the following section.

#### 3.2.2.1 Carbohydrate Polymer Schiff Bases

Chitosan Schiff bases derivatives have been synthesized using a condensation process and microwave irradiation. It was discovered that adding a Schiff bases functional group to the chitosan skeleton significantly improves the inhibitory property and polymer film adherence on metal surfaces. In general, the prevention efficiencies reached with those chitosan-based derivatives were greater than 80%, indicating that chitosan Schiff base could be a good choice for use as anticorrosion agents [11].

Recently, salicylaldehyde-functionalized chitosan (Salicylaldehyde-Chitosan Schiff base, SCSB) was reported as an inhibitor for application in 3.5% NaCl saturated with $CO_2$ corrosion at 65 °C [12]. The method of synthesis is presented in Scheme 3.1.

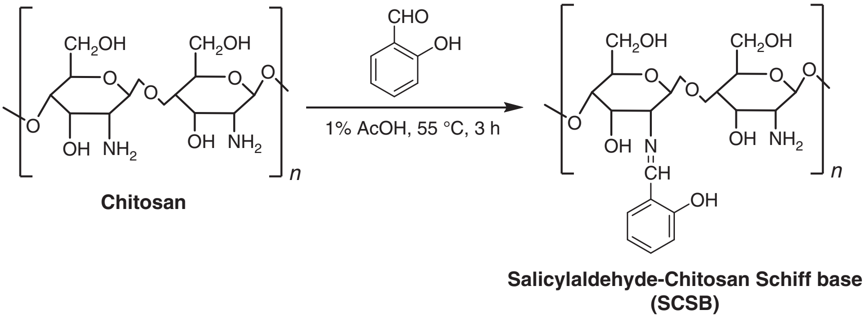

**Scheme 3.1** Synthetic scheme of SCSB [12].

SCSB operated as a mixed type of inhibitor and efficiently decreased the corrosion process at 150 mg $l^{-1}$ concentration, with an inhibition efficiency of 95.2% and a corrosion rate of 0.444 mm $y^{-1}$, according to the potentiodynamic polarization (PDP)

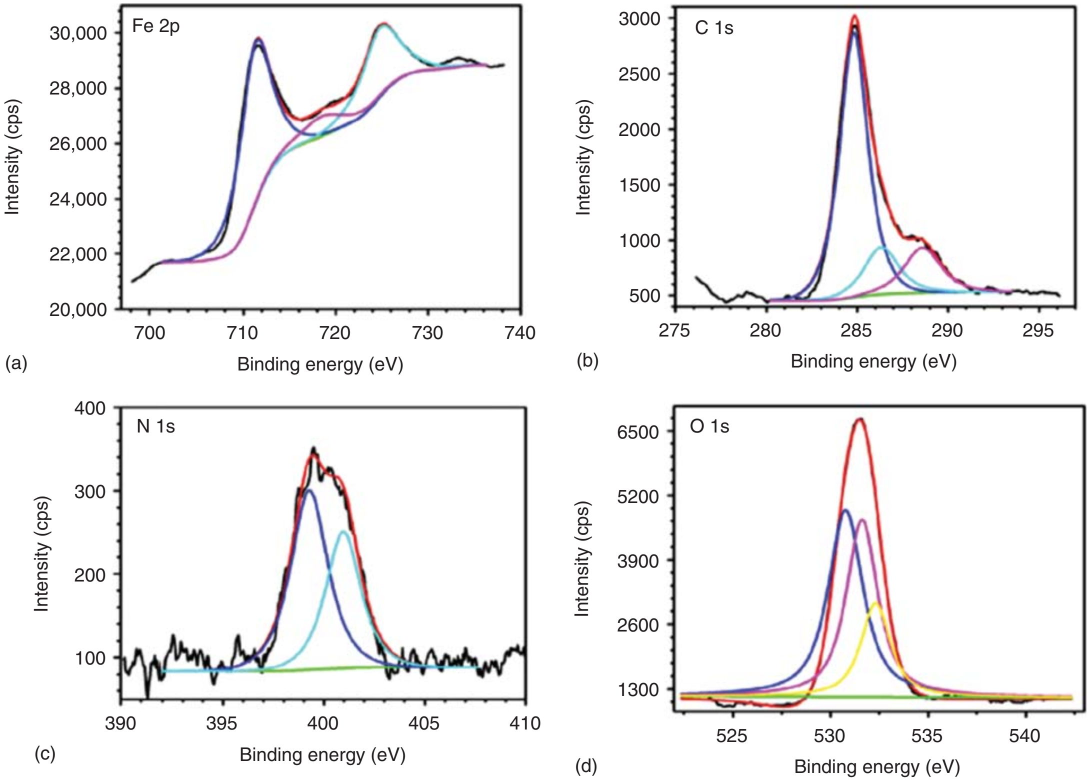

**Figure 3.3** XPS spectra images (a) Fe 2p (b) C 1s (c) N 1s (d) O 1s. Source: Republished from Ansari et al. [12] with permission from Elsevier.

data. X-ray photoelectron spectroscopy (XPS) demonstrated the adsorption of SCSB molecules on the metal surface. The XPS spectra of Fe 2p, O 1s, C 1s, and N 1s of SCSB adsorbed on the J55 steel surface are shown in Figure 3.3.

Chitosan-cinnamaldehyde Schiff base was employed as a corrosion inhibitor for mild steel in 0.5 M $H_2SO_4$ solution [13]. Scheme 3.2 shows the schematic representation of synthesis method.

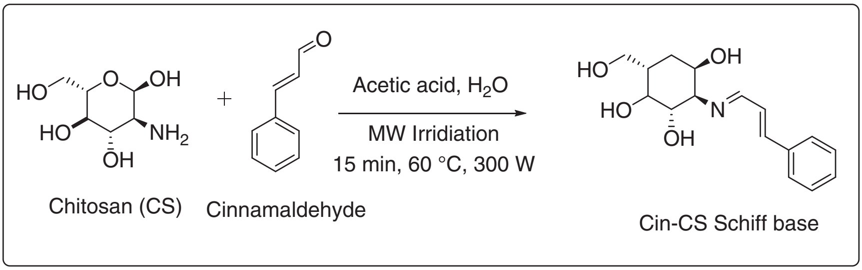

**Scheme 3.2** Schematic representation of the synthesis of Cinn-Cht Schiff base [13].

The authors tested its inhibition performances by varying the concentration of cinnamaldehyde. All the inhibitors acted as mix-type inhibitors, and the XPS study confirmed inhibitor components' adsorption on the metal's surface. Scanning electrochemical microscopy (SECM) results suggested the inductive behavior of mild steel surfaces in the presence of synthesized biopolymers. In another study [14], chitosan-cinnamaldehyde Schiff base was synthesized following microwave irradiation and tested for its corrosion inhibition performance for CS in 15% HCl solution. Schiff base exhibited 85.1% inhibition efficacy at 400 ppm, which further improved (92.4%) on adding potassium iodide (KI). Theoretical methods further supported the inhibition mechanism. Three chitosan Schiff bases, namely, [chitosan benzaldehyde (CSB-1), 4-(dimethylamino)benzaldehyde (CSB-2), and 4-hydroxy-3-methoxy benzaldehyde (CSB-3)] derivatives, have been synthesized under microwave irradiations. The authors further tested them as corrosion inhibitors for mild steel in acidic solutions. According to the obtained experimental data, these modified chitosan compounds were exhibited significant tendencies to reduce metallic corrosion even at a lower concentration, in which the maximum prevention efficiencies of 91%, 87%, and 85% (at 50 ppm) were attained for CSB-3, CSB-2, and CSB-1, respectively [15].

In another study, Piperonal-chitosan as a Schiff base [16] was added to the HCl solution to protect the steel surface. The proposed synthesis method was schematically represented in Scheme 3.3.

The weight loss test showed that the inhibitor suppressed the corrosion, and the inhibition efficiency increased with increasing the inhibitor concentration to 600 mg $l^{-1}$. However, a higher amount of inhibitor exhibited an insignificant alteration in the inhibition efficiency. The corrosion inhibitory impact of Vanillin-modified chitosan on the steel in HCl was tested. The authors obtained the corrosion inhibition efficiency of 98.3% in the presence of an inhibitor based on the weight loss test. Langmuir was calculated to be the best possible adsorption

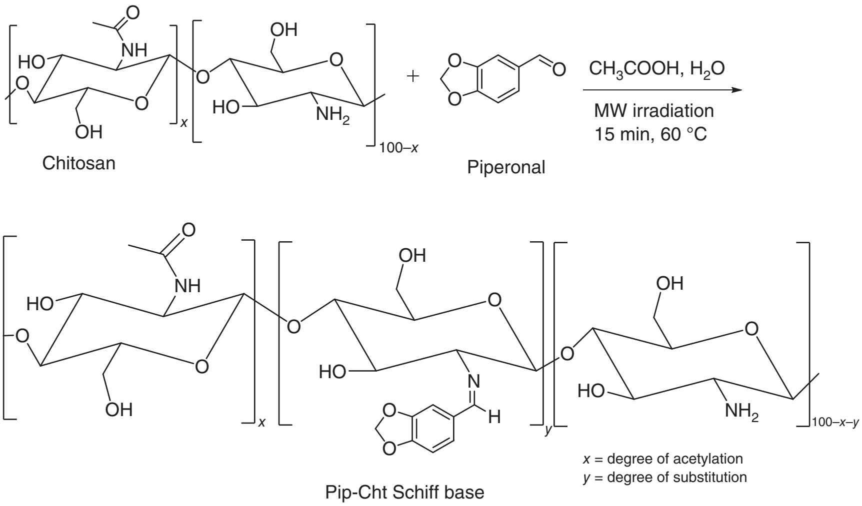

**Scheme 3.3** Schematic representation of the synthesis of Piperonal-chitosan Schiff base [16].

isotherm. Moreover, the capacitive loop was seen in the Nyquist plot for the blank and low-inhibitor concentrations in the electrochemical impedance spectroscopy (EIS) test. In contrast, the capacitive and inductive loop was reported for the high concentrations [17].

#### 3.2.2.2 Heterocyclic Compound-Modified Carbohydrate Polymers

8-hydroxyquinoline-based chitosan is another inhibitor that was reported to increase corrosion inhibition compared with the blank sample for the steel surface. Moreover, compared to the chitosan, the 8-hydroxyquinoline-based chitosan exhibited a higher polarization resistance in the EIS test and lower $i_{\text{corr}}$ in the potentiodynamic polarization test [18].

Cinnamaldehyde-modified chitosan ([Cinn-CS] (Scheme 3.4 exhibits the synthesis route) as a bio-derived corrosion inhibitor for acid pickling of copper in 1 M HCl was reported by Mouaden et al. [19]. The inhibitor Cinn-CS functioned by adsorption on the copper surface and showed an inhibition efficiency of >89% at a dose of 1000 mg $\text{l}^{-1}$. The charge-transfer resistance showed a rise with the increase in inhibitor dosage to the corrosive medium, and the corrosion currents showed a significant decrease with the addition of the inhibitor. The Cinn-CS displayed a mixed type of inhibition performance with cathodic nature.

Two new chitosan (CS) derivatives modified, namely, thiosemicarbazide (TSFCS) and thiocarbohydrazide (TCFCS) were synthesized by the modification of CS using formaldehyde as a coupling link reagent. Scheme 3.5 exhibited the synthesis method. The authors further extended their study on the anticorrosive applications of synthesized compounds for 304 steel in 2% acetic acid [20]. The obtained results exhibited that carbon steel, TSFCS, and TCFCS can be used as inhibitors for 304 steel in acidic medium, TCFCS being more effective. TCFCS acted as a mixed-type metal anticorrosion inhibitor; its inhibition efficiency was 92% at 60 mg $\text{l}^{-1}$.

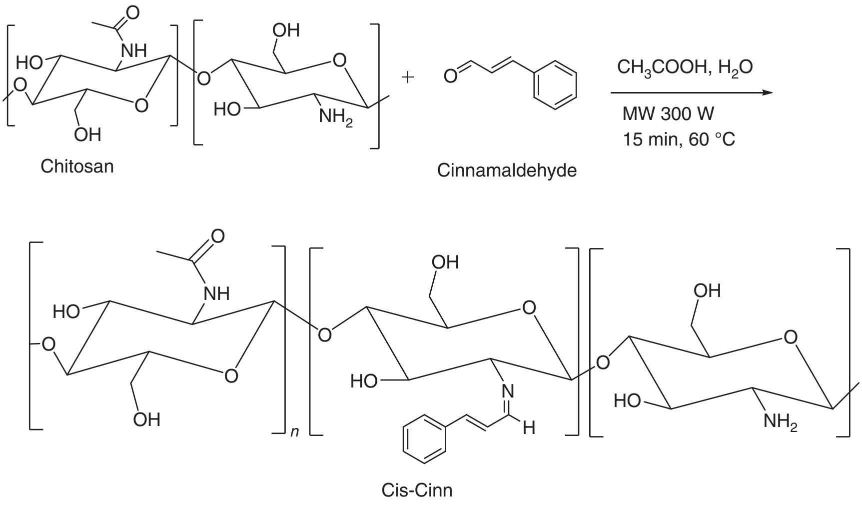

**Scheme 3.4** Schematic representation of the synthesis of Cinn-CS [19].

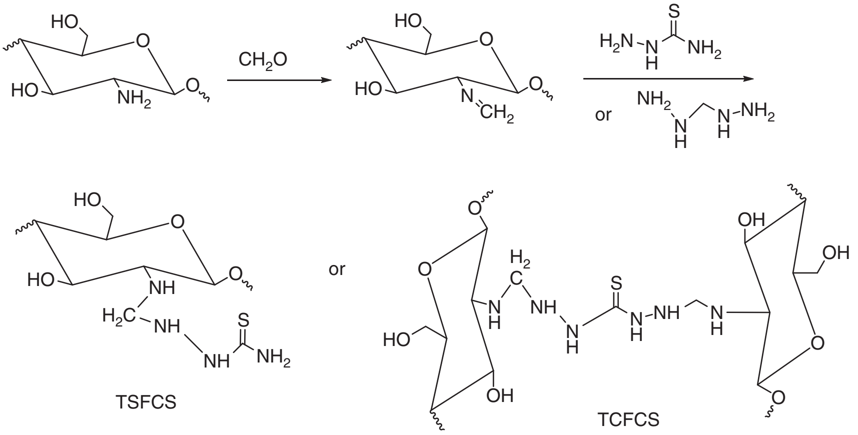

**Scheme 3.5** Synthesis of TSFCS and TCFCS by using formaldehyde as linkages [20].

Acetyl thiourea chitosan (ATUCS) polymer has been synthesized and evaluated as a corrosion inhibitor [21] for mild steel in naturally aerated 0.5 M $H_2SO_4$ media. Inhibition efficiency (IE) of this compound has been found to vary with the concentration of the polymer solution, immersion time, and temperature and reached 94.5% for 0.76 mM concentration.

In another study, different cinnamaldehyde concentrations were used to modify the chitosan as a corrosion inhibitor [13] for the mild steel surface in the $H_2SO_4$ solution. The result was indicative of higher corrosion inhibition efficiency for the chitosan solution with a higher concentration of cinnamaldehyde. Moreover, the addition of inhibitors to the solution reduced the roughness of the surface based on the atomic force microscopy (AFM) study.

Surface protection of American Iron and Steel Institute (AISI) 304 stainless steel in 3.5% NaCl was studied using aminotriazolethiol-functionalized chitosan as a macromolecule-based bioinspired corrosion inhibitor [22]. The aminotriazolethiol-modified chitosan (ATT-Cht) had excellent solubility in water and was an effective inhibitor of stainless steel corrosion in 3.5% NaCl, with a corrosion inhibition efficacy 97.8% at a concentration of $100\,\mathrm{mg\,l^{-1}}$. The authors described the passivation and pitting behavior. According to the results, the pitting potential shows an apparent change from 0.12 to 0.23 V, and an enhancement in the passive region was caused by the addition of different quantities of ATT-Cht inhibitor to the corrosive electrolyte. It is well documented that metals and alloys with higher $E_{\mathrm{pit}}$ values have a broader and more stable passive zone, indicating an improvement in resistance to pit nucleation. In the presence of increasing ATT-Cht dosage to 3.5% NaCl, the pitting currents likewise showed an apparent decrease. This backs up the ATT-Cht molecules' suppression and protection of the stainless steel (SS) surface in 3.5% NaCl. The Langmuir isotherm provided the best fitting of the obtained electrochemical data.

Novel triazole-modified chitosan was synthesized following chemical modification of chitosan using 4-amino-5-methyl-1,2,4-triazole-3-thiol referred to as CS–AMT (Scheme 3.6) and characterized employing Fourier-transform infrared spectroscopy (FTIR) and nuclear magnetic resonance (NMR) spectroscopy. The anticorrosive application was further tested via varying experimental techniques.

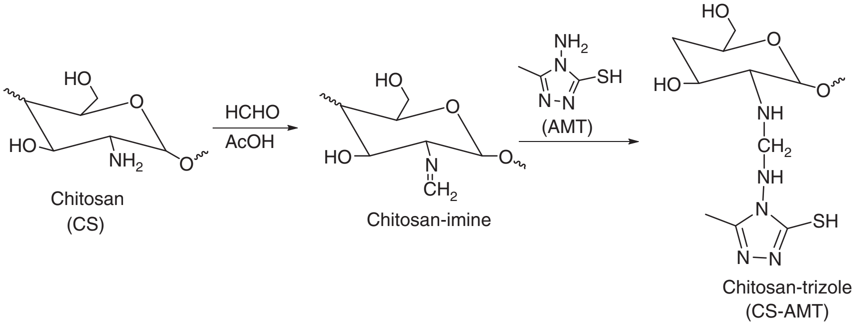

**Scheme 3.6** Synthesis of CS-AMT [23].

The results suggested that CS–AMT acted as an efficient retarder of carbon steel corrosion exhibiting a maximum inhibition efficiency of 97% at 200 ppm of developed chitosan derivative [23]. According to the results of Tafel study, the inhibitor has a mixed type of behavior with cathodic prevalence. The scanning electron microscopy (SEM) confirmed that the presence of CS–AMT improved the surface uniformity of carbon steel. The results of the density functional theory (DFT) analysis corroborated what the experimental approaches had found. The inhibitor adsorbs over the carbon steel surface with heteroatoms, according to Fukui indices. Molecular dynamics simulations revealed that the inhibitor had higher binding energy implying that the inhibitor had an easier way of adsorbing to the metal surface.

Yadav et al., carried out the studies on the preparation of three carbohydrate compounds, namely, 5,6-bis(2-(1*H*-benzo[*d*]imidazol-2-yl)hydrazono)hexane-1,2,3,4-tetraol (BIHT) and 5,6-bis(2-(1-methyl-1*H*-imidazol-2-yl)hydrazono)hexane-1,2,3,4-tetraol (MIHT) and their anticorrosive applications on N80 steel in 15% HCl [24]. The structure was confirmed by 1H-NMR and FTIR spectroscopy. The antimicrobial studies were also assessed. BIHT and MIHT showed 98.3% and 91.5% efficiency, respectively. Various kinetic and thermodynamic parameters were calculated. XPS, DFT, and molecular dynamics (MD) studies were done to explore the inhibition mechanism of the inhibitors.

### 3.2.2.3 Grafted Polymer

Biopolymer dextrin-based graft copolymer (Dxt-g-pVAc) has been synthesized through atom-transfer radical polymerization (ATRP) (Scheme 3.7) and was applied as a corrosion inhibitor for mild steel in 15% HCl medium [26]. The results suggested the mixed type of behavior of inhibitors. The electrochemical measurements have been exploited to compare the anticorrosion properties of dextrin and its copolymer.

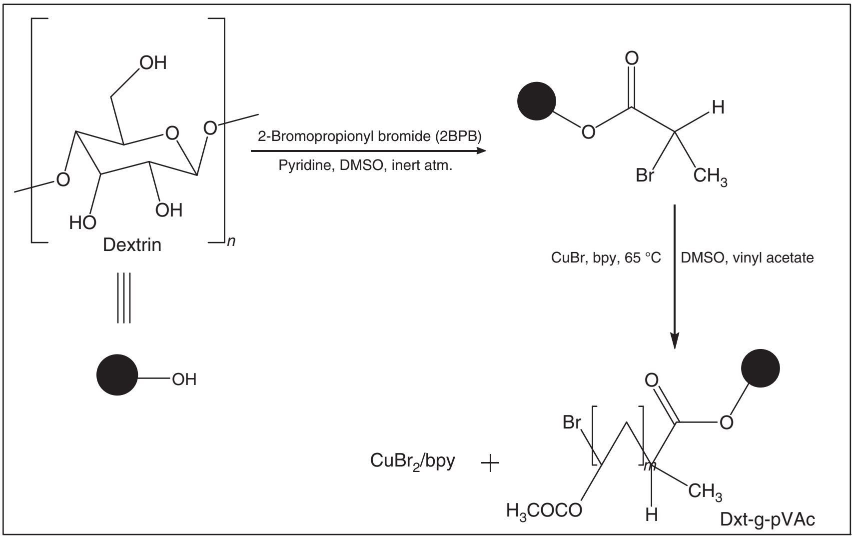

**Scheme 3.7** Synthesis of Dxt-g-pVAc copolymer [25].

Inhibitors formed protective layers on the metal surface through adsorption as per Langmuir model. The metal dissolution and inhibitor adsorption phenomena have been studied through the estimation of thermodynamic parameters. The changes in surface morphology have been followed by field emission scanning electron microscopy (FE-SEM) and AFM analyses. The synthesized graft copolymer showed excellent anticorrosion efficiency (98.39%) compared to native dextrin (84.56%). The results of the MD simulation result suggested that chemical and physical adsorption occurs through heteroatoms and hydroxyl groups. In another publication, chitosan oligosaccharide macromolecule with a glucose moiety (COS-g-Glu) has been synthesized and used as a nontoxic, durable, and biodegradable inhibitor of mild steel corrosion 1.0 M HCl [26]. Electrochemical tests show that the inhibition efficiency increases with the increasing concentration of the inhibitor and reaches an optimum value of 97% at $10^{-3}$ M. The thermodynamic parameters and steel surface characterization methods confirmed the adsorption of COS-g-Glu. The results obtained from the DFT, and MD calculations correlate with the results obtained experimentally. Inductively coupled plasma - optical emission spectrometry (ICP-OES) analysis shows that the amount of dissolved iron in the corrosive solution before the addition of biopolymer (COS-g-Glu) is 259.939 mg $l^{-1}$; after the addition of biopolymer, the amount of dissolved iron is l3.135 mg $l^{-1}$ that clearly showed that the employment of COS-g-Glu decreased the amount of dissolved iron. Furthermore, the scanning electron microscopy (SEM) and energy dispersive X-ray spectroscopy (SEM–EDS) and AFM microscopic results confirmed that a dense and orderly COS-g-Glu barrier could effectively protect steel. The authors further supported the mechanism of inhibition utilizing the DFT and MD simulation methods.

The glucosyloxyethyl acrylate graft chitosan was also researched as an inhibitor for the steel in HCl solution. According to the obtained EIS data, $R_{ct}$ increased, and elements of constant phase (CPE) decreased as the concentration of the inhibitor increased; moreover, because of the corrosion mitigation taking place due to the inhibitor's presence, the roughness of the metal surface decreased in comparison with its absence, according to the AFM study [27].

#### 3.2.2.4 PEG Cross-linked Polymer

PEG cross-linked chitosan was studied as a novel eco-friendly corrosion inhibitor for mild steel in hydrochloric acid solution [28] and sulfamic acid [29]. The maximum corrosion inhibition efficiency of 93.9% was obtained at a concentration of 200 mg $l^{-1}$ in both the acid solution. The inhibitor was found to obey Langmuir adsorption isotherm and exhibited both physical and chemical adsorption. EIS study showed an increase in the polarization resistance, which supported the adsorption and inhibition behavior. Tafel data showed a mixed type of behavior with cathodic predominance.

#### 3.2.2.5 Polymer-Based Surfactant

A sequence of seven-modified chitosan surfactants was produced, and their anti-corrosion property was measured for carbon steel in 1 M HCl. As compared to pure chitosan, good inhibition efficiencies between 93 and 74% at 250 ppm were achieved for those surfactants functionalized chitosan derivatives [30]. It was found that carboxymethyl chitosan thio-derivative provided the highest protection. This finding was related to its high surface activity and the presence of more active adsorption centers within its molecular skeleton.

#### 3.2.2.6 Carbohydrate Polymer–Nanoparticle Composites

Researchers also took advantage of nanotechnology concerning biopolymers as an innovative approach for enhancing the corrosion inhibition of the metals, whether as coating or corrosion inhibitor. The most recent is an inorganic substance in minute size infusion into a polymer matrix [31, 32]. Carbohydrate polymers can be considered a perfect choice for stabilizing corrosion-inhibiting nanoparticles because polymeric compounds showed great effectiveness as low cost and stable corrosion inhibitors for metallic materials. Inorganic nanomaterials can be dispersed in a polymer matrix or chemically bonded to the polymer matrix to form a metal complex [33]. The inhibitive effect of polymers is directly correlated to the structure of polymers that possess different active centers of adsorption, such as cyclic rings and heteroatoms, such as oxygen and nitrogen. Such polymers can form complexes with metal ions. These complexes occupy a large surface area on the metal surface, thereby isolating the surface and protecting the metals from corrosive medium [34, 35].

The section given below will discuss the anticorrosive application of previously studied carbohydrate polymer/nanoparticles formulations.

In the pursuit of enhancing the corrosion-inhibitive characteristic of the carboxymethyl cellulose (CMC), the addition of the silver to the matrix in the form of nanoparticles resulted in the formation of a CMC/Ag nanocomposite [36]. The anticorrosive application of nanocomposite in the 15% $H_2SO_4$ solution for the ST37 steel surface was investigated. At 25 °C, optimum inhibition efficiency of 93.94% was afforded by 1000 ppm CMC/AgNPs. CMC/AgNPs were found to retard both the anodic and cathodic reactions (Figure 3.4) and the adsorption is explained using Langmuir adsorption isotherm.

Nyquist plots revealed the enhancement of semicircle diameters after the introduction of nanocomposite to the solution. Also, phase-angle values in the Bode

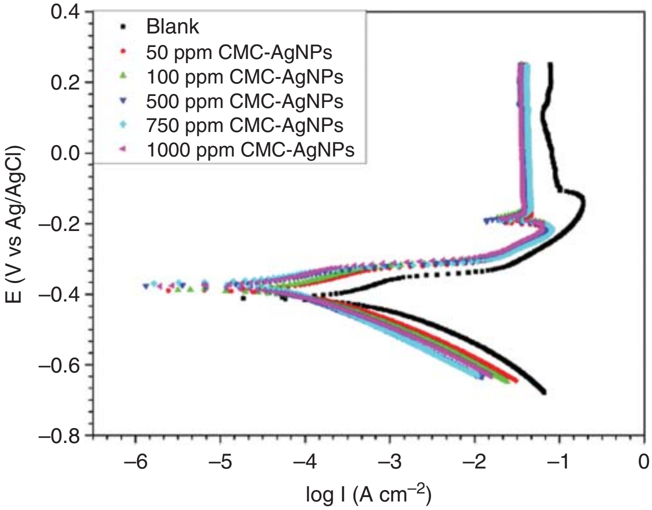

**Figure 3.4** Potentiodynamic polarization curves obtained for ST37 steel in 15% $H_2SO_4$ solution without and with different concentrations of CMC/AgNPs at 25 °C. Source: Republished from Solomon et al. [36] with permission from Elsevier.

plots increased after inhibitor addition. Moreover, potentiodynamic polarization demonstrated that nanocomposite existence diminished cathodic and anodic current densities (Figure 3.4). Finally, in comparison with the blank sample, the surface experienced more smoothness in the presence of nanocomposite.

As an inhibitor, Chitosan–silver nanocomposite was also employed to reduce corrosion damage on ST37 steel surfaces in 15% HCl [37]. The corrosion rate decreased in the presence of nanocomposite and reached the lowest 57.49 mpy at 1000 ppm compared to a blank (391.4 mpy). The inhibition of both anodic and cathodic reactions with predominant prevention of cathodic reactions and inhibition efficiency with nanocomposite concentration was reported. Nyquist plots also indicated an increment in the corrosion inhibition and the rise of inhibitor amount correlated with the higher inhibition efficiency. Solomon et al. [38] prepared the gum Arabic and silver nanoparticle (GA-AgNP) composite and confirmed its preparation using FTIR and EDS spectroscopy in another publication. Further, they tested its corrosion-inhibiting properties for MS in 15%HCl and 15%$H_2SO_4$ media employing various experimental techniques, such as FTIR, ultraviolet (UV)–vis, gravimetric, EIS, electrochemical frequency modulation (EFM), DEIS, and Tafel polarization, SEM, EDAX, AFM, and XPS. Results from Tafel polarization measurement suggested different behavior of GA-AgNPs for MS in 15%HCl (anodic type) and 15%$H_2SO_4$ (cathodic type) media. The authors suggested physisorption of the inhibitor molecules by increasing the temperature. XPS results disclose that the corrosion products in the absence of composite are FeO, $FeCO_3$, $Fe_2O_3$, and $FeSO_4$ ($H_2SO_4$ medium) or $FeCl_3$ (HCl medium). In the adsorbed film of the nanocomposite, gum Arabic was present in both ionic and neutral forms, while AgNPs were present in the form Ag°, $Ag_2O$, and AgO.

Several nanoparticles, such as Cu, Fe, and Ni, were deposited in the matrix of CMC. Then, they were used as inhibitors for the carbon steel in the 2 N HCl solution. The potentiodynamic polarization result demonstrated superior performance in the presence of the inhibitor with or without the nanoparticles compared with the blank sample. Both cathodic and anodic reactions were influenced and the $i_{corr}$ decreased considerably in the presence of inhibitors, and it was more significant for the CMC/Ni nanoparticles. Moreover, increasing the concentration of inhibitors to 400 ppm led to a lower $i_{corr}$. More protective performance of CMC/Ni nanoparticles was also confirmed in the EIS results, and the corrosion mitigation obtained in the presence of inhibitors was in the order of CMC/Ni > CMC/Cu > CMC/Fe > CMC [39].

#### 3.2.2.7 Synergistic Effect of Salts/Surfactants with Carbohydrate Polymer

The synergistic effect is a method through which two materials' modifications combine to produce a more significant result than the mere sum of the impact that each material is capable of alone. The method can be used to enhance the inhibition capability of polymers. This section will discuss the results of previously published research articles on the topic. Chitosan (CS) and the effect of KI on its inhibition performance were tested for corrosion inhibition of mild steel in 1 M sulfamic acid. Chitosan alone exhibited an inhibition efficiency of 73.8%, which was increased synergistically (90.3%) on adding 5 mM KI [40]. The adsorption of CH and CH + KI followed Langmuir adsorption isotherm and acted as a mixed-type inhibitor with cathodic predominance. The SEM and AFM results further confirmed the better adsorption of CH + KI in comparison to CH. Mobin and Alam [41] made an effort to increase the inhibition efficacy of gum acacia (GA) by employing two cationic (cetyltrimethylammonium bromide, CTAB) and anionic (sodium dodecylbenzene sulfonate [SDBS]) surfactants to inhibit MS corrosion in 0.1 M $H_2SO_4$. The experiment was done in the temperature range of 30–60 °C. Inhibiting action of GA was synergistically improved with the addition of a small number of surfactants. Moreover, the adsorption of GA alone and with SDS and CTAB followed the Freundlich adsorption model. Further, Mobin and Rizvi [42] studied the effect of sodium dodecyl sulfate (SDS), cetyl pyridinium chloride (CPC), and Triton X-100 (TX) on the inhibition effect of Xanthan gum (XG) employing various experimental and theoretical techniques. The authors reported that the minimal concentration of surfactants i., 5 ppm increased inhibition performance of XG appreciably and followed the order $\mathrm{XG} \geq \mathrm{XG} + \mathrm{CPC} < \mathrm{XG} + \mathrm{TX} < \mathrm{XG} + \mathrm{SDS}$. The values of synergistic parameters ($S_1$) calculated from the Aramaki equation supported the synergistic inhibition performance. The same authors [43] further tried to enhance the corrosion inhibition properties of hydroxyethyl cellulose (HEC) by using CPC, TX, and SDS for A1020 CS corrosion in 1 M HCl. It is noted that the combination of HEC and surfactants increased the IE more than either HEC or surfactants alone, suggesting a synergistic effect between HEC and surfactants. The effect was attributed to the resultant interaction between the HEC and surfactant molecules that further led to the improved adsorption on the steel surface. The results of PDP measurements suggested that the HEC and HEC + surfactants get adsorbed on the CS surface via mixed-type adsorption (Figure 3.5).

The spectroscopic analysis (UV–vis and FTIR spectroscopy) suggested the formation of a complex between iron and inhibitor molecules and the functional group responsible for the adsorption of inhibitor on CS surface. The authors further supported protective film formation on the metal surface because of inhibitor molecules using SEM and AFM studies. To suggest the adsorption of inhibitor molecules on the metal surface, a theoretical calculation was carried out.

Aslam et al. [44] studied the collective effect of polymer and green cationic Gemini surfactants for the very first time. The effect of cationic di-ester bonded Gemini surfactants, i.e. ethane-1,2-diylbis(*N*,*N*-dimethyl-*N*-alkylammoniumacetoxy) dichloride, referred to as *m*-E2-*m*, where $m = 12, 14, 16$ is the number of carbon atoms in the hydrophobic chain on the inhibition properties of the sodium salt of carboxymethylcellulose was tested for mild steel in 1 M HCl solution. The results suggested that the inhibition effect of NaCMC increased by adding a

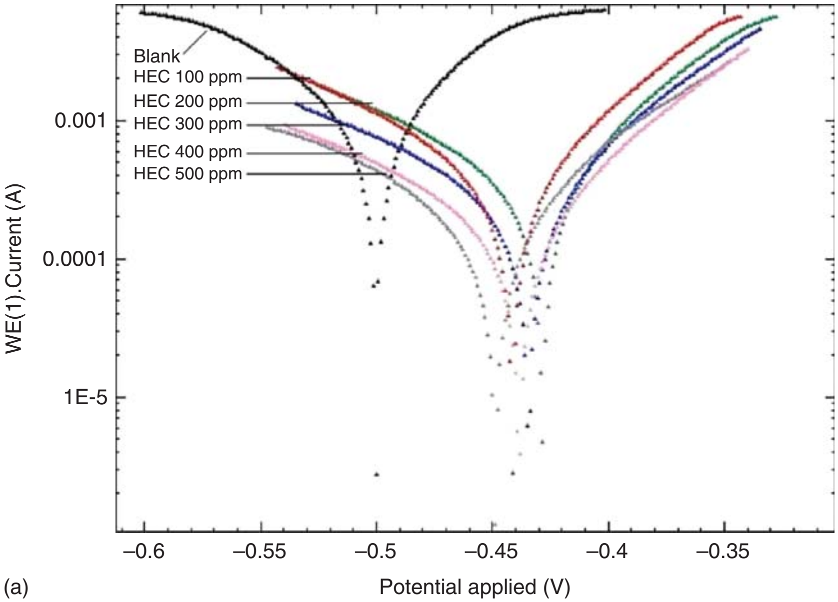

(a)

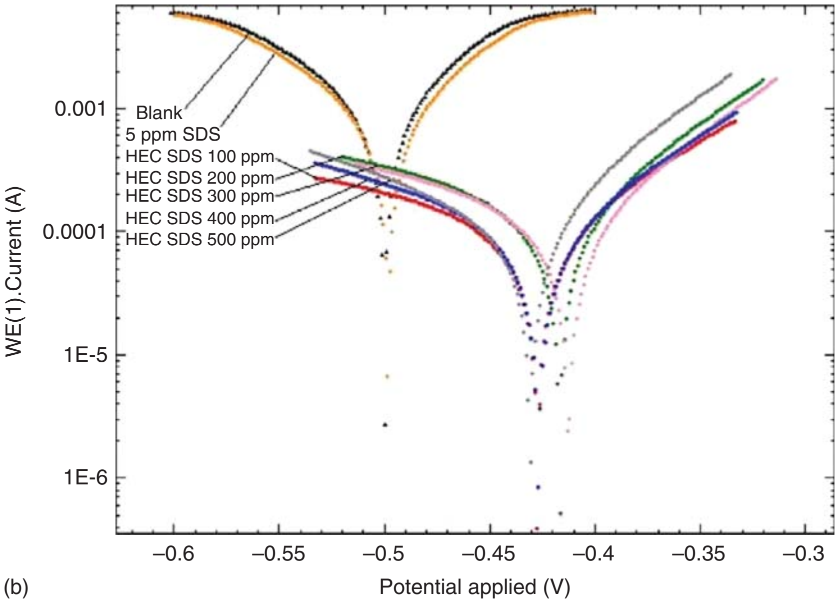

(b)

**Figure 3.5** Potentiodynamic polarization curves for carbon steel in 1 M HCl (a) HEC (b) HEC + CPC (c) HEC + SDS (d) HEC + TX. Source: Republished from Mobin and Rizvi [43] with permission from Elsevier.

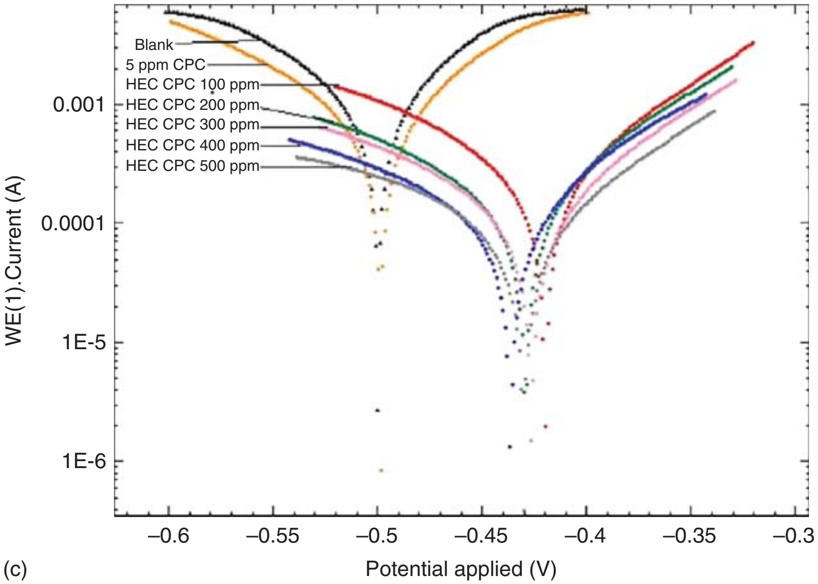

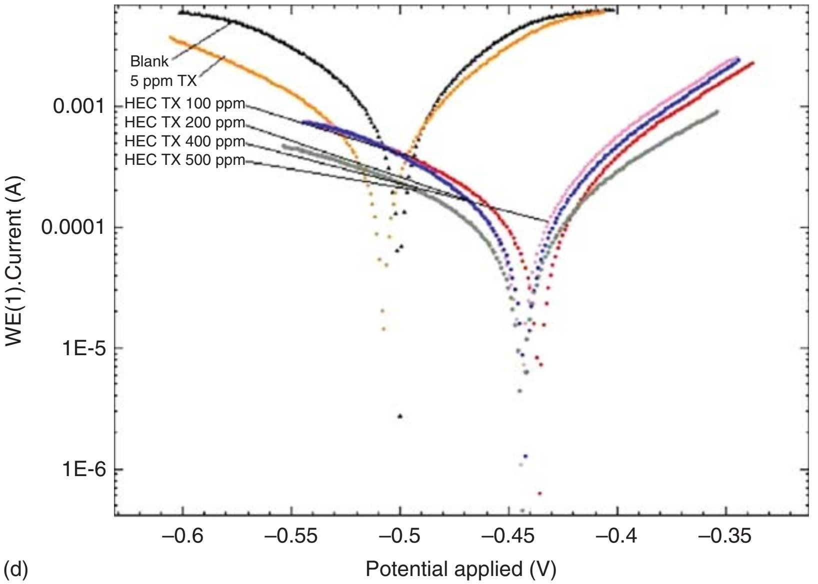

**Figure 3.5** (*Continued*)

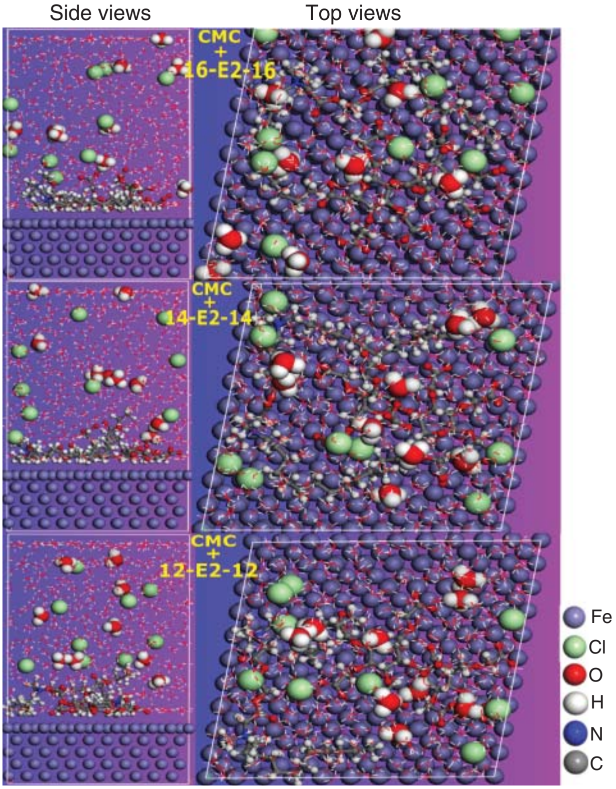

**Figure 3.6** Side and top view of the final adsorption of 12-E2-12, 14-E2-14, and 16-E2-16 in combination with NaCMC on Fe(110) surface in solution. Source: Republished from Aslam et al. [44] with permission from Elsevier.

minimal concentration, i.e. 1 ppm of GS. The NaCMC/16-E2-16 exhibited the maximum inhibition efficiency (90.1%) followed by NaCMC/14-E2-14 (84.8%), NaCMC/12-E2-12 (73.5%), and NaCMC (57.3%). The adsorption occurred following the Langmuir adsorption isotherm. To provide a complete inhibitor function, the authors carried out the MD simulation study. Figure 3.6 shows all molecules that are adsorbed in a roughly parallel manner on the Fe-atoms of the first-layer surface, ensuring strong interactions and, as a result, a substantial inhibitory effect.

Moreover, inhibitor molecules are adsorbed through several adsorption centers, as evidenced by the great magnitude of their binding energies. The distance between oxygen, nitrogen, and carbon in inhibitor molecules and Fe atom was observed by radial distribution function. As exhibited in Figure 3.7, the radial distribution function (RDF) of heteroatoms and carbon atoms exhibited a sharp initial peak suggesting inhibitors' significant affinity for iron atoms. Moreover, the bonding lengths of Fe—C, and Fe—O are all less than 3.5, but Fe—N distances are greater than 3.5. These findings indicate that inhibitor molecules are in close contact with the iron surface.

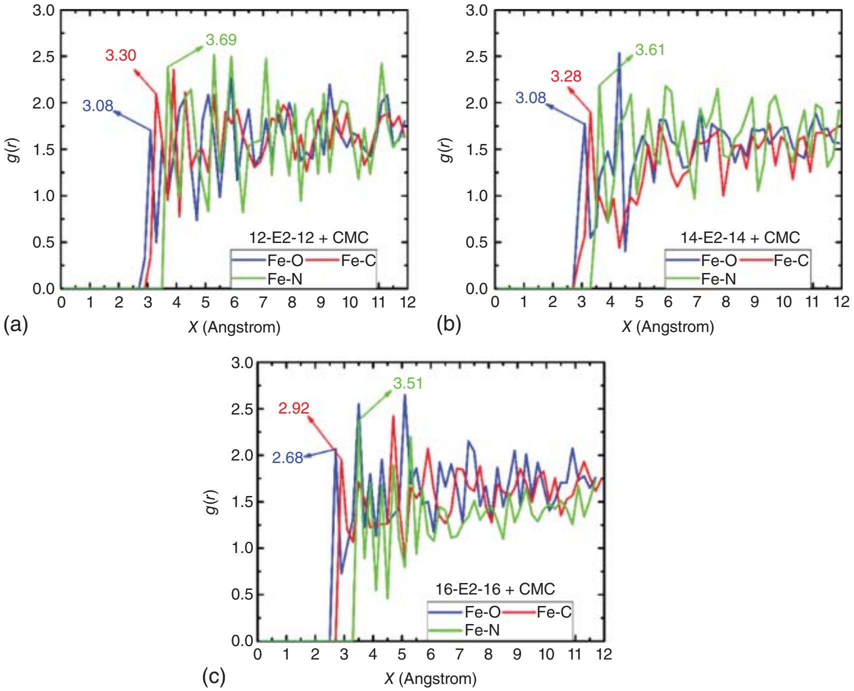

**Figure 3.7** Radial distribution function ($g(r)$) of inhibitor molecules adsorbed on the Fe (110) surface. Source: Republished from Aslam et al. [44] with permission from Elsevier.

## 3.3 Conclusion

For years, extensive research has been conducted with the aim of developing innovative methods to diminish the risk of conventional toxic corrosion inhibitors. Up to now, various substitutes for unsafe inhibitors have been proposed, among them, biopolymers are considered effective, environment-friendly, and available in abundance. This chapter intended to report the recent investigations in this area of research to put the recent progress into a broad perspective as an effort made to promote new ideas to push the boundaries. The various carbohydrate polymer Schiff bases, heterocyclic compound-modified carbohydrate polymer, grafted carbohydrate polymer, PEG cross-linked carbohydrate polymer, carbohydrate polymer surfactants, and carbohydrate–nanoparticle composites were explored. The experimental conditions, such as electrolyte type, temperature, pH, inhibitor concentration, and exposure time in which the biopolymer is playing the role of inhibitor, were emphasized. The media used for biopolymers as corrosion inhibitors in the literature were mainly HCl, NaCl, and seawater; however, their concentrations differed in several papers, which were reported to influence the outcome. Although metals, such as copper and aluminum, were also used as substrates in the existing studies, most of the research was conducted on mild steel. The studies undertaken mainly are weight loss, potentiodynamic polarization, EIS, UV–vis, FTIR SEM, EDS, AFM, and XPS studies. Thermodynamic ($\Delta H$, $\Delta S$, $E_a$) and activation parameters were also calculated in many studies. The proposed mechanisms taking place in the process of inhibitor adsorption were reported. Replacing the water molecules on the surface with inhibitor molecules as an essential step for the adsorption of inhibitors was emphasized in several studies. Despite using theoretical methods widely in many green inhibitors' studies, these are limited to few investigations in the current advancement, and further research should be undertaken using these promising methods.

## Acknowledgments

Ruby Aslam acknowledges the Council of Scientific & Industrial Research, New Delhi, India for providing financial aid under the Research Associate fellowship (09/112(0616)2K19 EMR-I).

## References

1. National Research Council (2009). *Assessment of Corrosion Education*. Washington, DC: The National Academies Press.
2. Abubakirov, R., Yang, M., and Khakzad, N. (2019). A risk-based approach to determination of optimal inspection intervals for buried oil pipelines. *Process Safety and Environmental Protection* 134: 95–107.
3. Dearnaley, G. (1978). Corrosion. *Interdisciplinary Science Reviews* 3: 20–30.
4. Bowman, E., Koch, G., Varney, J. et al. (2016). *International Measures of Prevention, Application, and Economics of Corrosion Technologies Study*, A-19, 201. NACE Int.
5. Koch, G.H., Brongers, M.P.H., Thompson, N.G., Virmani, Y.P., Payer, J.H. (2001). Corrosion cost and preventive strategies in the united state, national technical information service, Report No. FHWA-RD-01-156.
6. White, T. (2019). The cost of corrosion https://www.zerust.com/blog/2019/10/02/the-cost-of-corrosion
7. Solomon, M.M., Umoren, S.A., Israel, A.U., and Ebenso, E.E. (2015). Polypropylene glycol-silver nanoparticle composites: a novel anti-corrosion material for aluminum in acid medium. *Journal of Materials Engineering and Performance* 24: 4206–4218.
8. Umoren, S.A. and Eduok, U.M. (2016). Application of carbohydrate polymers as corrosion inhibitors for metal substrates in different media: a review. *Carbohydrate Polymer* 140: 314–341.
9. Ituen, E., Singh, A., Yuanhua, L., and Akaranta, O. (2021). Biomass-mediated synthesis of silver nanoparticles composite and application as green corrosion inhibitor in oilfield acidic cleaning fluid. *Cleaner Engineering and Technology* 3: 100119.

**10** Banerjee, S., Srivastava, V., and Singh, M.M. (2012). Chemically modified natural polysaccharide as green corrosion inhibitor for mild steel in acidic medium. *Corrosion Science* 59: 35–41.

**11** Chen, N.L., Kong, P.P., Feng, H.X. et al. (2019). Corrosion mitigation of chitosan Schiff base for Q235 steel in 1.0 M HCl. *Journal of Bio- and Tribo-Corrosion* 5: 27.

**12** Ansari, K.R., Chauhan, D.S., Quraishi, M.A. et al. (2020). Chitosan Schiff base: an environmentally benign biological macromolecule as a new corrosion inhibitor for oil & gas industries. *International Journal of Biological Macromolecules* 144: 305–315.

**13** Chugh, B., Singh, A.K., Poddar, D. et al. (2020). Relation of degree of substitution and metal protecting ability of cinnamaldehyde modified chitosan. *Carbohydrate Polymer* 234: 115945.

**14** Chauhan, D.S., Mazumder, M.A.J., Quraishi, M.A., and Ansari, K.R. (2020). Chitosan cinnamaldehyde Schiff base: a bioinspired macromolecule as corrosion inhibitor for oil and gas industry. *International Journal of Biological Macromolecules* 158: 127–138.

**15** Haque, J., Srivastava, V., Chauhan, D.S. et al. (2018). Microwave induced synthesis of chitosan Schiff bases and their application as novel and green corrosion inhibitors: experimental and theoretical approach. *ACS Omega* 5: 5654–5668.

**16** Chauhan, D.S., Mazumder, M.A.J., Quraishi, M.A. et al. (2020). Microwave-assisted synthesis of a new Piperonal-Chitosan Schiff base as a bio-inspired corrosion inhibitor for oil-well acidizing. *International Journal of Biological Macromolecules* 158: 231–243.

**17** Quraishi, M.A., Ansari, K.R., Chauhan, D.S. et al. (2020). Vanillin modified chitosan as a new bio-inspired corrosion inhibitor for carbon steel in oil-well acidizing relevant to petroleum industry. *Cellulose* 27: 6425–6443.

**18** Rbaa, M., Fardioui, M., Verma, C. et al. (2020). 8-Hydroxyquinoline based chitosan derived carbohydrate polymer as biodegradable and sustainable acid corrosion inhibitor for mild steel: experimental and computational analyses. *International Journal of Biological Macromolecules* 155: 645–655.

**19** Mouaden, K.E.L., Chauhan, D.S., Quraishi, M.A. et al. (2020). Cinnamaldehyde-modified chitosan as a bio-derived corrosion inhibitor for acid pickling of copper: microwave synthesis, experimental and computational study. *International Journal of Biological Macromolecules* 164: 3709.

**20** Li, M., Xu, J., Li, R. et al. (2014). Simple preparation of aminothiourea-modified chitosan as corrosion inhibitor and heavy metal ion adsorbent. *Journal of Colloid and Interface Science* 417: 131–136.

**21** Fekry, A.M. and Mohamed, R.R. (2010). Acetyl thiourea chitosan as an eco-friendly inhibitor for mild steel in sulphuric acid medium. *Electrochimica Acta* 55: 1933–1939.

**22** Chauhan, D.S., Mouaden, K.E.L., Quraishi, M.A., and Bazzi, L. (2020). Aminotriazolethiol functionalized chitosan as a macromolecule-based bioinspired corrosion inhibitor for surface protection of stainless steel in 3.5% NaCl. *International Journal of Biological Macromolecules* 152: 234–241.

**23** Chauhan, D.S., Quraishi, M.A., Sorour, A.A. et al. (2019). Triazole-modified chitosan: a biomacromolecule as a new environmentally benign corrosion inhibitor for carbon steel in a hydrochloric acid solution. *RSC Advances* 9: 14990–15003.

**24** Yadav, M., Sarkar, T.K., and Obot, I.B. (2016). Carbohydrate compounds as green corrosion inhibitors: electrochemical, XPS, DFT and molecular dynamics simulation studies. *RSC Advances* 6: 110053–110069.

**25** Biswas, A., Das, D., Lgaz, H. et al. (2019). Biopolymer dextrin and poly (vinyl acetate) based graft copolymer as an efficient corrosion inhibitor for mild steel in hydrochloric acid: electrochemical, surface morphological and theoretical studies. *Journal of Molecular Liquids* 275: 867–878.

**26** Rbaa, M., Benhiba, F., Hssisoua, R. et al. (2021). Green synthesis of novel carbohydrate polymer chitosan oligosaccharide grafted on D-glucose derivative as bio-based corrosion inhibitor. *Journal of Molecular Liquids* 322: 114549.

**27** Eduok, U., Ohaeri, E., Szpunar, J., and Akpan, I. (2020). Synthesis, characterization, and application of glucosyloxyethyl acrylate graft chitosan against pipeline steel corrosion. *Journal of Molecular Liquids* 315: 113772.

**28** Srivastava, V., Chauhan, D.S., Joshi, P.G. et al. (2018). PEG-Functionalized Chitosan: a biological macromolecule as a novel corrosion inhibitor. *Chemistry Select* 3: 1990–1998.

**29** Chauhan, D.S., Srivastava, V., Joshi, P.G., and Quraishi, M.A. (2018). PEG cross-linked chitosan: a biomacromolecule as corrosion inhibitor for sugar industry. *International Journal of Industrial Chemistry* 9: 363–377.

**30** Alsabagh, A.M., Elsabee, M.Z., Moustafa, Y.M. et al. (2014). Corrosion inhibition efficiency of some hydrophobically modified chitosan surfactants in relation to their surface-active properties. *Egyptian Journal of Petroleum* 23: 349–359.

**31** Hefni, H.H.H., Azzam, E.M., Badr, E.A. et al. (2016). Synthesis, characterization and anti-corrosion potentials of chitosan-g-PEG assembled on silver nanoparticles. *International Journal of Biological Macromolecules* 83: 297–305.

**32** Solomon, M.M. and Umoren, S.A. (2016). In-situ preparation, characterization and anti-corrosion property of polypropylene glycol/silver nanoparticles composite for mild steel corrosion in acid solution. *Journal of Colloid and Interface Science* 462: 29–41.

**33** Radheshkumar, C. and Münstedt, H. (2005). Morphology and mechanical properties of antimicrobial polyamide/silver composites. *Materials Letters* 59: 1949–1953.

**34** Espuche, E., David, L., Rochas, C. et al. (2005). In situ generation of nanoparticulate lanthanum(III) oxide-polyimide films: characterization of nanoparticle formation and resulting polymer properties. *Polymer* 46: 6657–6665.

**35** Rajendran, S., Sridevi, S.P., Anthony, N. et al. (2005). Corrosion behaviour of carbon steel in polyvinyl alcohol. *Anti-Corrosion Methods and Materials* 52: 102.

**36** Solomon, M.M., Gerengi, H., and Umoren, S.A. (2017). Carboxymethyl cellulose/silver nanoparticles composite: synthesis, characterization and application as a benign corrosion inhibitor for st37 steel in 15% $H_2SO_4$ medium. *ACS Applied Materials & Interfaces* 9: 6376–6389.

**37** Solomon, M.M., Gerengi, H., Kaya, T., and Umoren, S.A. (2017). Performance evaluation of a chitosan/silver nanoparticles composite on St37 steel corrosion in a 15% HCl solution. *ACS Sustainable Chemistry & Engineering* 5: 809–820.

**38** Solomon, M.M., Gerengi, H., Umoren, S.A. et al. (2018). Gum Arabic-silver nanoparticles composite as a green anti-corrosive formulation for steel corrosion in strong acid media. *Carbohydrate Polymer* 181: 43–55.

**39** El-Lateef, H.M.A., Albokheet, W.A., and Gouda, M. (2020). Carboxymethyl cellulose/metal (Fe, Cu and Ni) nanocomposites as non-precious inhibitors of C-steel corrosion in HCl solutions: synthesis, characterization, electrochemical and surface morphology studies. *Cellulose* 27: 8039–8057.

**40** Gupta, N.K., Joshi, P.G., Srivastava, V., and Quraishi, M.A. (2017). Chitosan: a macromolecule as green corrosion inhibitor for mild steel in sulfamic acid useful for sugar industry. *International Journal of Biological Macromolecules* 106: 704–711.

**41** Mobin, M. and Khan, M.A. (2013). Investigation on the adsorption and corrosion inhibition behavior of gum acacia and synergistic surfactants additives on mild steel in 0.1 M $H_2SO_4$. *Journal of Dispersion Science and Technology* 34: 1496–1506.

**42** Mobin, M. and Rizvi, M. (2016). Inhibitory effect of xanthan gum and synergistic surfactant additives for mild steel corrosion in 1 M HCl. *Carbohydrate Polymer* 136: 384–393.

**43** Mobin, M. and Rizvi, M. (2017). Adsorption and corrosion inhibition behavior of hydroxyethyl cellulose and synergistic surfactants additives for carbon steel in 1 M HCl. *Carbohydrate Polymer* 156: 202–214.

**44** Aslam, R., Mobin, M., Aslam, J. et al. (2019). Inhibitory effect of sodium carboxymethylcellulose and synergistic biodegradable gemini surfactants as effective inhibitors for MS corrosion in 1 M HCl. *Journal of Materials Research and Technology* 8: 4521–4533.

# 4

# Poly(Amino Acid) Corrosion Inhibitors

*Brahim El Ibrahimi*[1,2] *and Nada K. Sebbar*[3,4]

*[1] Ibn Zohr University, Department of Applied Chemistry, Faculty of Applied Sciences, Av. Azrou,*
*Aït Melloul 86153, Morocco*
*[2] Ibn Zohr University, Department of Chemistry, Team of Physical Chemistry and Environment,*
*Faculty of Sciences, Av. Dakhla, Agadir 80000, Morocco*
*[3] Ibn Zohr University, Department of Chemistry, Laboratory of Applied Chemistry and Environment,*
*Applied Bioorganic Chemistry of Team, Faculty of Sciences, Av. Dakhla, Agadir 80000, Morocco*
*[4] Mohammed V University, Department of Chemistry, Drug Science Research Center,*
*Pharmacochemistry Competence Center, Laboratory of Heterocyclic Organic Chemistry, Faculty of Sciences,*
*Av. Ibn Battouta Rabat BP 1014, Morocco*

## 4.1 Introduction

The utilization of corrosion inhibitors is one of the most practical and economic methods to prevent the corrosion of metallic materials. In this regard, several compounds (organic and inorganic substances) have been used as anticorrosion agents for metals and alloys from the corrosion attack. In general, organic-based inhibitors containing heteroatoms, such as oxygen and nitrogen atoms, are widely employed to decline the spontaneous degradation of these materials. The key mechanism by which these compounds reduce the corrosion is based on their interfacial interactions with the surface of the protected metal, resulting in their adsorption at the active sites of corrosion, which enhances the corrosion-resisting property of the metal and retards the corrosion processes [1].

Small-molecule organic inhibitors, such as amino acid, triazole, and imidazole, have attracted extensive attention [2–6]. Nevertheless, in recent years, corrosion inhibitors based on polymer materials have attracted more attention from many researchers [7]. In general, polymers with long-chain molecules exhibit higher inhibition performance than corresponding simple organic compounds. Based on the source, these polymeric compounds can be categorized into natural polymers (e.g. proteins and polysaccharides) and synthetic polymers (e.g. polyethylene, polyurethane, and polysiloxanes). With the growing concern about environmental protection, the use of eco-friendly and nontoxic polymers as anticorrosion agents were gained research interest as the available literature demonstrates. Up to now, many authors reported the successful application of chitosan, alginate, gum Arabic,

*Polymeric Corrosion Inhibitors for Greening the Chemical and Petrochemical Industry*, First Edition.
Edited by Mohammad A. Jafar Mazumder, Mumtaz A. Quraishi, and Amir Al-Ahmed.

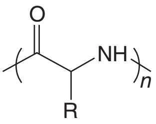

**Figure 4.1** Repeated unit of a simple poly(amino acid) polymer.

and pectin, as well as other ecological polymers, as effective inhibitors for various metals in different corrosive environments [8]. For instance, the corrosion inhibition performance of alginate and chitosan biopolymers on copper in molar HCl solution was investigated and inhibition efficiencies up to 80% were achieved with a concentration of 0.1 ppm at 298 K [9, 10].

Various approaches have been applied to enhance the inhibitive effect of simple amino acids, which are environment-friendly, nontoxic, biodegradable, and relatively cheap biocompounds [11]. Among these, there is the development of their corresponding polymeric forms, called poly(amino acid) polymers (Figure 4.1), which are a novel class of environment-friendly inhibitors against corrosion. Such a demarche leads to amplifying the number of sites of adsorption on the inhibitor molecule, which simplifies and reinforces their adhesion on the surface of corroding metal; and then prevents the attack of corrosive agents contained in the surrounding environment. For instance, while glutamic acid (a simple amino acid) does not show any anticorrosive effect for mild steel alloy in acidic solution, its polymer (poly-$\gamma$-glutamic acid) is found to be a good corrosion inhibitor [12]. Poly(amino acid) polymers exhibit distinct features, such as good biocompatibility and flexible physicochemical modification, as well as biodegradability that was influenced by the hydrophilicity of the amino acids that make up these eco-polymers [13].

The unique characteristics of these poly(amino acid) polymers have motivated scientists to study the usefulness of these polymers for several industrial applications. These amino acid-based polymers are the most frequently utilized polyamides in the formulation of chemotherapeutics to achieve selective delivery for an appropriate duration of time to lessen the drug-related side effects and increase the antitumor efficacy. Poly(amino acid) polymers are able to degrade inside the body resulting in amino acids that are biologically active and are often used as drugs. Furthermore, poly(amino acid) polymers are extensively used in several areas, such as in the cosmetics industry, food industry, construction industry, water treatment, paper processing, and paint additives. Table 4.1 collects the industrial applications of some specific poly(amino acid) polymers.

In the case of some inhibiting systems (i.e. metal, solution, and inhibitor), these eco-friendly polymer inhibitors can show good corrosion inhibition performance only with extremely high concentrations. This results in consuming more material and financial resources. For this purpose and to overcome such a weakness, the application of poly(amino acid) polymers as anticorrosion compounds is extended to the use of their chemical-modified forms or graft copolymerization. This leads to multiplying further the adsorption centers, caused by the incorporated functional groups, within the polymer chains. Besides, their mixture with other compounds of different natures (i.e. composite inhibitors) is also reported to be a helpful strategy to improve their inhibition capacity even at low dosages.

**Table 4.1** The industrial applications of some poly(amino acid) polymers.

| Poly(amino acid) | Applications |
|---|---|
| 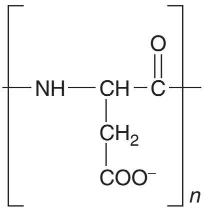 Poly(α-L-aspartic acid) | • Due to its ability to aggregate sand particles, it is applied as a sand-fixing agent or cementing agent<br>• Used as a super-absorbent material, fertilizer, corrosion, and scale inhibitors<br>• Pharmaceutical preparations, such as drug-delivery systems |
| 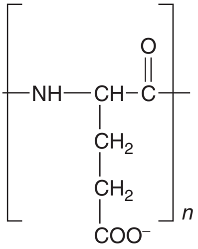 Poly(glutamic acid) | • Applied in skin, body, and hair care products<br>• Food industries, such as food additive<br>• Used as an additive in paints and concrete products<br>• Employed in tablet coating and controlled delivery of drugs as polymer conjugates |
| 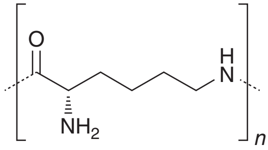 Poly(lysine) | • Used as an antimicrobial agent in pharmaceutical and food industry<br>• Employed in manufacturing of sanitation napkins and diapers<br>• Used as a carrier for cosmetics |

## 4.2 Poly(Amino Acid) Homopolymers as Corrosion Inhibitors

One of the most used poly(amino acid) homopolymers[1] as an anticorrosion agent for metallic materials is polyaspartic acid polymer (PASP, Figure 4.2). This is a kind of environment-friendly polymer that exists naturally in the shell of mollusks and multifunctional polymer material, which characterizes by its excellent biocompatibility, biodegradability, low-toxicity profile, and nonantigenic, as well as it possesses the property of chelation and dispersion [14–16]. PASP can be synthesized by a simple thermal condensation reaction method starting from L-aspartic acid (ASP, Figure 4.2). Currently, tons of PASP can be obtained by chemical synthesis. The application of PASP as an anticorrosive additive has been shown a protective effect

---

[1] The homopolymer’s term refers to a polymer that makes up from the same type of monomer, i.e. an amino acid.

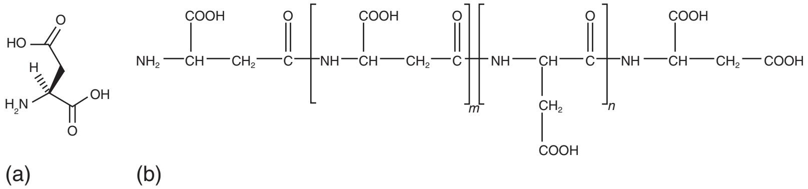

**Figure 4.2** Molecular structure of (a) aspartic acid (ASP) monomer and (b) PASP polymer.

on different metals and alloys (e.g. copper, iron, and magnesium alloys) under the exposition of various corrosive environments (e.g. HCl, $H_2SO_4$, and 3% NaCl solutions) [17, 18]. For example, a higher inhibitor efficiency of 91.5% was reached using PASP at $1\,g\,l^{-1}$ for copper immersed in 3% citric acid solution [19].

To improve the inhibitory effect of poly(amino acid) homopolymers without conducting chemical modifications (i.e. insertion of functional groups) on these polymers and at low concentration, the synergistic effect with other additional compounds, such as halide and metallic ions, is largely adopted. It was reported that the combination of PASP with another environment-friendly compound, namely, sodium tungstate, at a low dosage (total inhibitor concentration of 20 ppm) exhibited an interesting inhibition impact on the corrosion of copper alloys in simulated cooled water solutions. This outlines that there exists a good synergistic effect between components of the inhibition system [20]. Furthermore, the beneficial effect of zinc ion addition into the PASP-based inhibition system was also approved due to a synergistic effect mechanism. In the presence of this ion, the inhibition efficiency of PASP enhances from 61% (at $2\,g\,l^{-1}$ PASP) to 97% (at $0.5\,g\,l^{-1}$ PASP) for mild steel in saline solution [21]. The conjoint addition of tungstate and zinc ions also increased the corrosion inhibition efficiency of PASP from 72.4% to 92.6% for mild steel in seawater [22]. The presence of iodide ion at 1 mM has also contributed to improving the inhibition capacity of PASP for mild steel in acidic solution. As can be seen in Figure 4.3, the diameter of semicircles increases with the addition of PASP polymer, and remarkably in the presence of potassium iodide (KI) compared with the uninhibited solution. This means effective protection of metal using PASP/KI synergistic formulate in such an aggressive medium [23].

Aminosulfonic acid is largely used as an acidic cleaning agent typically for metals and ceramics. The contact of copper, which constitutes one of the major commercial metals, with this acid leads to its spontaneous degradation. To limit that, the addition of PASP into the aggressive acid was demonstrated a beneficial effect, which the inhibition efficiency can reach 89.8% when used along with or up to 95.4% when combined with imidazole compound (a heterocyclic organic compound with two nitrogen atoms) with a total concentration of $1.0\,g\,l^{-1}$. The enhanced anti-corrosion property offered by the coexistence of PASP and imidazole benefits the more stable composite formation on copper surface. Furthermore, it was found that it acts as a mixed-type inhibitor of predominant cathodic effect [24]. Another inhibition formulation, containing PASP and sulfuric acid high cerium, was exhibited a very good prevention effect for copper in citric acid solution, which at a total concentration of $0.1\,g\,l^{-1}$, the inhibition efficiency reached 80.8% [25].

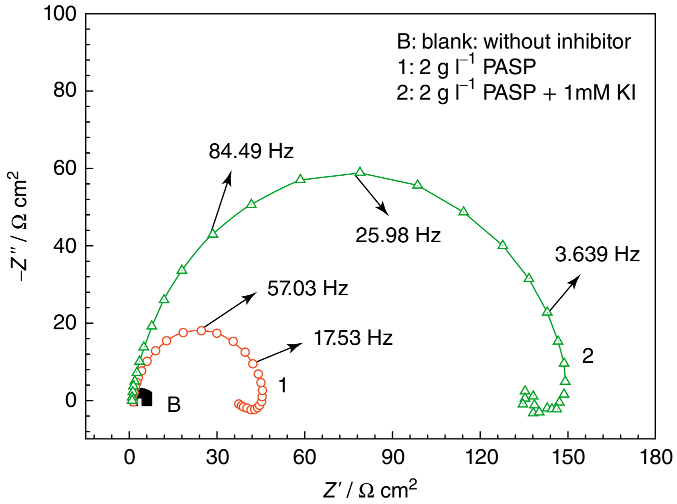

**Figure 4.3** Recorded EIS spectra (Nyquist plots) of mild steel in 0.5 M $H_2SO_4$ in the absence and presence of PASP/KI. Source: Republished from Qian et al. [23] with permission from Elsevier.

Aluminum and its alloys are important metallic materials, which are used in various human activities, such as in construction, transportation, and packing sections, as well as in the refinery equipment in the petroleum industry. Nevertheless, under special environments (e.g. acid or alkali systems in aerated stagnant conditions), these metals undergo disintegration. In this regard, the ability of poly(amino acid) to stop or decline the corrosion of aluminum-based materials has been outlined. Here, we can list the application of polylysine polymer as inhibitor, which is biodegradable, easily available, and shows lesser toxicity. It was found that the presence of this homopolymer at 4 ppm for 10 h (at 303 K) can suppress the almost corrosion (by 92.07%) of aluminum in the industrial acidic pickling environment. Under such conditions, the polylysine blocks the anodic dissolution process of aluminum [26]. On the other hand, a negligible anticorrosion effect is observed for glutamic acid (i.e. monomer) for mild steel in 1 M HCl, whereas its polymeric form (i.e. poly-γ-glutamic acid) was exhibited a remarkable inhibition efficiency of 90%. Such observed result is attributed to an intramolecular synergism within the polymer itself caused by the formed amide linkages. At the electronic scale, this has been explained by the low-energy gap, an increase in dipole moment, and chain length. These molecular features lead to the effective surface coverage of the metallic surface, resulting in its corrosion mitigation [12]. The capability of poly-γ-glutamate *Bacillus* biofilms secreting to decrease the pitting corrosion rate of aluminum 2024 alloy has been outlined [27].

On another side, poly(amino acid) homopolymer can be also used as an additional additive to improve the inhibition efficiency of other inhibitors at lower concentrations. This has been applied in the case of tannic acid, which, its mixture with PASP, shows a better inhibitive effect for mild steel in the cooling systems [28].

## 4.3 Modified Poly(Amino Acid) and Poly(Amino Acid) Copolymers as Corrosion Inhibitors

In many cases, the inhibition efficiency of poly(amino acid) polymers was limited even at higher concentrations. For example, inhibition effectiveness of 80.33% for PASP, which is used as a pickling corrosion inhibitor for carbon steel in $H_2SO_4$ medium, was obtained at an extremely high concentration of $6\,g\,l^{-1}$ (at 283 K) [17]. In this regard, some effective strategies were utilized to enhance the inhibition capacity of those eco-friendly polymers, such as the synergistic effect with other additional compounds as discussed above. Moreover, the inhibitive property of poly(amino acid) polymers can be improved by conducting chemical modification (e.g. introducing a functional group into the polymer chains) or graft copolymerization. In addition, PASP derivatives can exhibit varying physicochemical properties, which are easy to synthesize using simple chemical procedures [29]. In this regard, the corrosion inhibition performance of threonine-modified PASP (Figure 4.4a) for carbon steel in simulated cooling water has been approved. According to the experimental data, it was found that the developed PASP–threonine copolymer act as a mixed-type inhibitor and shows higher prevention capability (i.e. 93.06% at 200 ppm) than unmodified PASP. The formation of a copolymer-based protective film on the metal surface was justified using different surface analysis techniques. Based on computational calculations using density functional theory (DFT) method, the excellent observed performance of PASP–threonine copolymer was attributed to its grafted amino acid and the newly formed amide group [30]. In another recent study, a novel thiol functionalized PASP derivative (cysteamine-modified PASP polymer, Figure 4.4b) has been synthesized via a simple and effective pathway, which is a ring-opening reaction of polysuccinimide with cysteamine. Afterward, it was tested as a green acid pickling inhibitor for mild steel in sulfuric acid medium. The inhibition activity of the modified PASP is greatly improved with high efficiency even with low consumption (93.9% at 100 ppm) at different working temperatures in comparison with unmodified one. The excellent inhibition performance of PASP–cysteamine polymer was related to the presence of pendant functional sulfhydryl group. Such a chemical modification method may also be an effective method to enhance the efficiency of other poly(amino acid) polymer-based inhibitors for acid pickling [31].

Less or more complex molecular fragments were grafted into the main chain of poly(amino acid) polymers to increase their number of active sites of adsorption, which are involved in the improvement of observed prevention effect even at elevated temperatures. In this regard, dopamine-modified PASP (Figure 4.4c) is an excellent corrosion inhibitor for mild steel in 0.5 M $H_2SO_4$ as can be clearly revealed from the obtained scanning electron microscopy (SEM) images of metal surfaces in Figure 4.5a,b. Its inhibition efficiency at 100 ppm is up to 90.9% at 298 K and shows good temperature adaptability in comparison with unmodified PASP. This was explained by the effective adsorption of as-synthesized green macromolecules at the metal/solution interface. Figure 4.5c illustrates a simplified schema of the adsorption behaviors of dopamine-modified PASP on the metal surface [32]. The inclusion

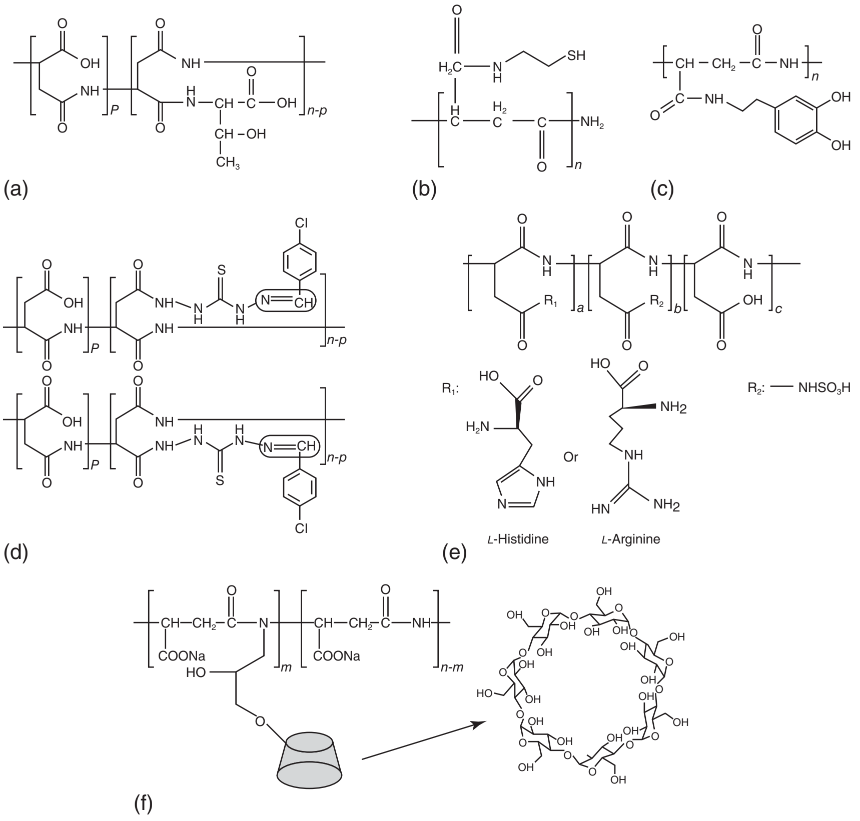

**Figure 4.4** Molecular structure of (a) threonine, (b) cysteamine, (c) dopamine, (d) Schiff base, (e) histidine or arginine/sulfamic acid, and (f) β-cyclodextrin-modified PASP polymers.

of Schiff base with the aromatic ring was also enhanced the corrosion inhibition performance of PASP (Figure 4.4d) to attain 90.39% at low dosage (80 ppm), which is much higher than that of unmodified PASP (i.e. 39.39%), on carbon steel in HCl solution. The temperature and flow of solution were slightly affected the inhibitive performance of Schiff base-modified PASP as compared to PASP. Such findings are attributed to the newly added functional groups on the side chain of modified PASP as demonstrated by using quantum chemical calculations [33]. Another modified PASP polymer by β-cyclodextrin (Figure 4.4f) has approved its acceptability to hinder corrosion (68.4% at 800 ppm) in simulated oilfield water [34].

The introduction of amino acid by itself within the poly(amino acid) polymer chain to improve the corrosion inhibition and to synthesize new eco-friendly inhibitors was also pointed out. For instance, the functionalization through histidine or arginine amino acid with sulfamic acid of PASP (Figure 4.4e) has been demonstrated as an enhancement in its inhibitive effect on carbon steel in industrial circulating cooling water. The chemical modification using arginine has better corrosion inhibition performance (75%) than histidine one (53%) at the same dosage (100 ppm), which points out the key role of grafted functional groups in

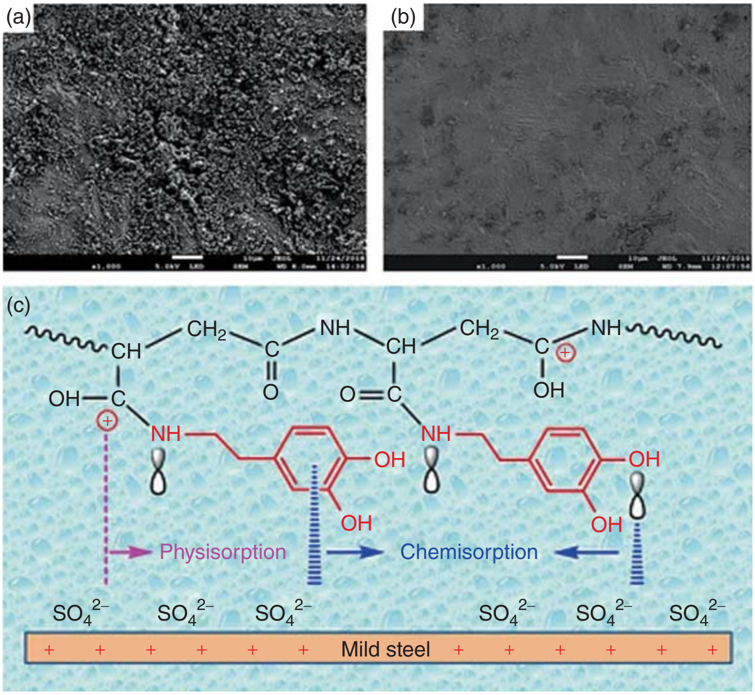

**Figure 4.5** SEM images of mild steel surface after immersion in sulfuric acid solution (a) without and (b) with addition of dopamine-modified PASP. (c) Simplified illustration of the adsorption behavior of modified PASP. Source: Chai et al. [32], Reproduced with permission from Elsevier.

the inhibition process. Furthermore, these modified PASP polymers possess the dual effects of corrosion and scale inhibitions [35]. The application of other amino acid-grafted PASP polymers as corrosion inhibitors at lower concentrations in desalination systems has been reported, they include valine- and leucine-modified PASP macromolecules (Figure 4.6). At 250 ppm, the reached inhibition efficiencies for carbon steel are 86.94% and 88.62% for valine– and leucine–PASP derivatives, respectively [36].

A novel methionine-based zwitterionic cocyclopolymer (Figure 4.6) was found to act as a promising corrosion inhibitor of mild steel in molar hydrochloride acid solution. The attained corrosion inhibition efficiency is 99.5% at $4.50 \times 10^{-4}$ mol $l^{-1}$, which is higher than those of used homo cyclopolymers. The protective behavior of the developed polyzwitterionic cocyclopolymer relates to its adsorption on metal through physisorption and chemisorption processes [37].

The chemical functionalization of PASP by introducing imidazole-based derivatives has also been found to improve effectively its inhibition efficiency and to develop eco-friendly inhibitors. Here, the example of two imidazole derivatives functionalized PASP can be listed; namely, PASP/*N*-(3-aminopropyl)-imidazole (PD-1) and PASP/*N*-(3-aminopropyl)-imidazole-*co*-ndodecylamine (PD-2) (Figure 4.7). It was outlined that the presence of either modified PASP polymers, especially PD-2

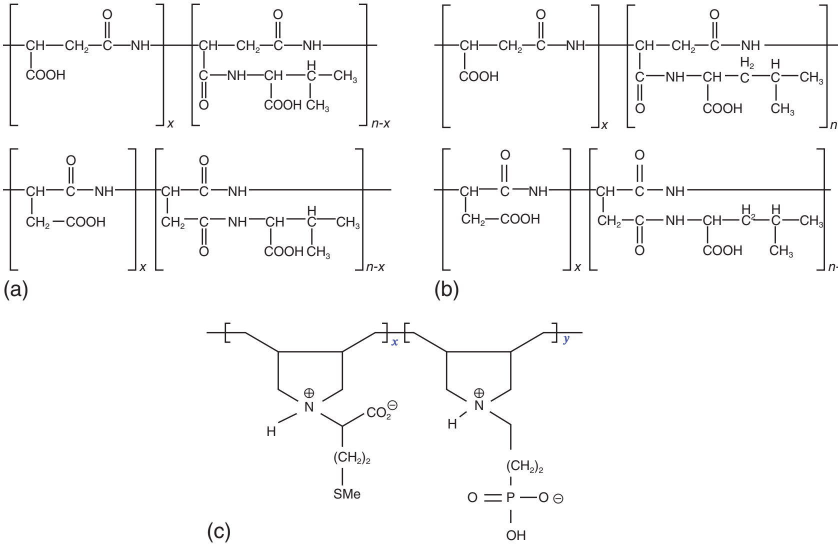

Figure 4.6 Molecular structure of (a) Val-PASP, (b) Leu-PASP, and (c) methionine-based zwitterionic cocyclopolymer.

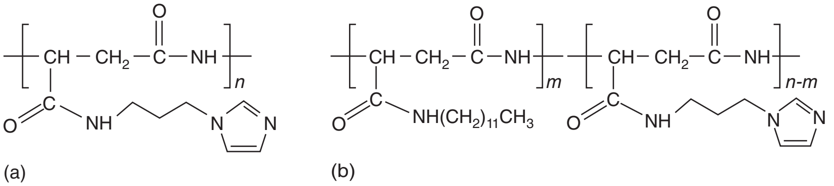

Figure 4.7 Molecular structure of (a) PD-1 and (b) PD-2-modified PASP polymers.

one, exhibit superior inhibition capacity compared to unmodified poly(amino acid) polymer for mild steel in 0.5 M $H_2SO_4$ solution, in which the efficiency is up to 94% at a relatively low dosage (100 ppm) of PD-2 derivative. This was attributed to the presence of additional functional groups in their molecular skeleton. According to the X-ray photoelectron spectroscopy (XPS) analysis, the adsorption of PD-2 macromolecules on the mild steel surface is approved, which effectively inhibits its corrosion. Such results can encourage the application of this novel green PASP–imidazole derivative (i.e. PD-2) during the acid cleaning, de-scaling, and in the pickling industries [38]. Table 4.2 collects other employed decorated poly(amino acid) polymers as corrosion inhibitors for different metal/solution systems and their corresponding inhibition efficiency [39–41].

Sometimes, the conducted chemical modification on poly(amino acid) polymers cannot result in an excellent improvement of the inhibition properties, which can due to the complexity of inhibition process of corrosion and the implication of other factors in this interfacial process (e.g. nature of the corrosive media). This was noted in the case of PASP/furfurylamine graft copolymer (Figure 4.8) for carbon steel in 0.336 g of NaCl, 1.11 g of $CaCl_2$, 0.4815 g of $MgSO_4$, and

**Table 4.2** The corrosion inhibition performance of some modified poly(amino acid) polymers.

| Modified poly(amino acid) polymer | Metal/ solution | Inhibition efficiency |
|---|---|---|
| Polyaspartic acid/4-(2-aminoethyl) morpholine graft copolymer 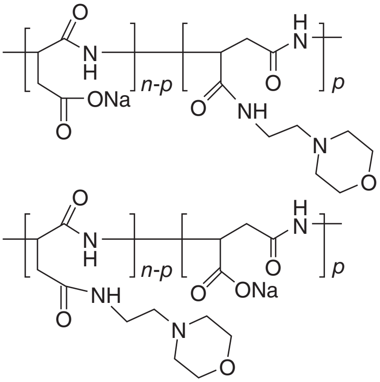 | Carbon steel in 0.5 M $H_2SO_4$ solution | 93.1% at 100 ppm |
| Polyaspartic acid–glycine adduct 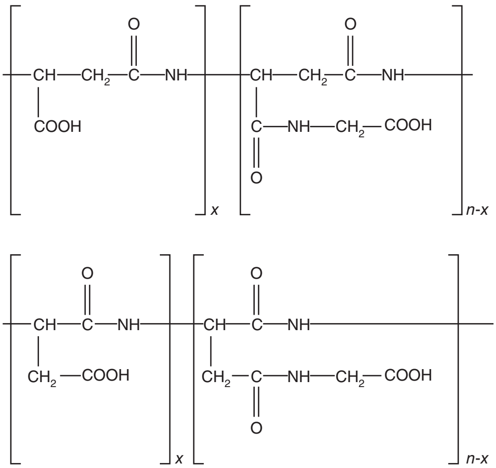 | X-65 carbon steel in seawater | 83.8% at 250 ppm |
| Curcumin–citric acid–aspartic acid/glutamic acid/glycine polymer 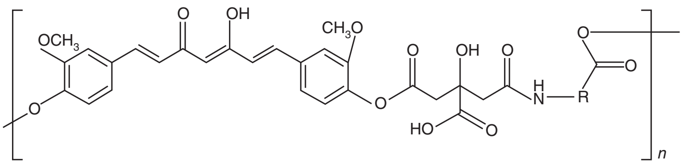 PCCA: R=$CHCH_2COOH$ PCCG: R=$CHCH_2CH_2COOH$ PCCG: R=$CH_2$ | Q235A carbon steel | 84.1% at 50 ppm of PCCA |

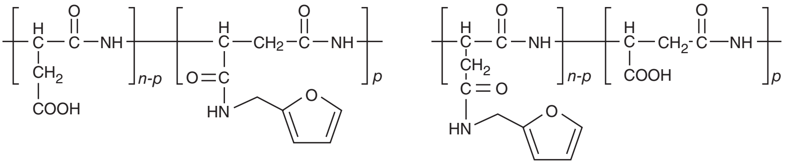

Figure 4.8 Molecular structure of the tested furfurylamine-grafted PASP copolymers.

0.336 g of $NaHCO_3$ solution. The variation of the inhibition effect of PASP and its modified form as a function of additive dosage were shown that the inhibition ability of PASP was slightly enhanced by crafting furfurylamine, as well as the maximum efficiency of 30% reached when the concentration was 16 ppm [42]. PASP/2-amino-2-methyl-1,3-propanediol graft copolymer has also demonstrated lower corrosion inhibition (<20% at 16 ppm) for mild steel in comparison with PASP/furfurylamine derivative in similar solution [43].

## 4.4 Poly(Amino Acid) Composite Polymers as Corrosion Inhibitors

To improve the corrosion inhibition performance of poly(amino acid) polymers, their mixture with other compounds to produce composite materials of different compositions was reported to be a helpful method. This was attributed to an increased number of possible mechanisms working in unison, including retardation of the metal dissolution and formation of protective films and compounds at the anodic/cathodic sites. For instance, a ternary composite of PASP with acrylic acid and acrylicester was demonstrated good corrosion inhibition performance (97.9% at 6 ppm) for A3 carbon steel, which makes it a suitable eco-friendly candidate for high temperature and hardness circulating cooling water system [44]. Furthermore, an environment-friendly corrosion inhibitor based on a PASP-derivative composite has demonstrated the capacity to act as a potent inhibitor for carbon steel in seawater environments, which can be subsequently used in desalination systems. The last one was prepared by mixing the synthesized PASP derivative with zinc sulfate and 2-hydroxyphosphonoacetic acid. The composite showed a considerable corrosion suppression effect than its constituents alone, which reaches 95% at 100 ppm even after a longer exposure time [45]. Another potent used composite is poly(butylene succinate)-L-histidine extended with 1,6-diisocynatohexane polymer. Using this composite, a maximum inhibition efficiency of 78% was obtained at a concentration level of 600 ppm for mild steel in 1 M HCl solution. Such interesting results are related to the existence of multiple C=O and N—H functional groups within the composite, which act as active sites of adsorption [46].

On the other hand, the water-soluble-conducting polymer composites, including poly(amino acid), are also applied to inhibit the metallic dissolution in acidic media. For instance, poly(vinyl alcohol–amino acid) composites of histidine,

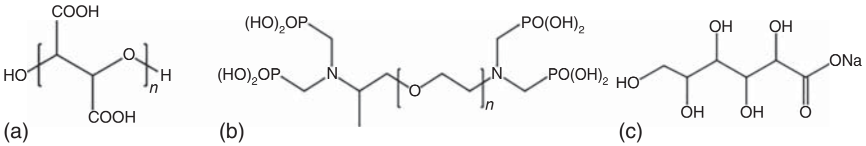

**Figure 4.9** Molecular structure of used compounds to formulate a poly(amino acid)-based composite. (a) Polyepoxysuccinic acid, (b) polyamino polyether methylenephosphonate, and (c) sodium gluconate.

leucine, cysteine, and proline were found to reduce the corrosion of mild steel in molar hydrochloric acid solution to greater extents, in which the inhibition efficiency is around 95% at 0.6 wt% of the inhibitor. The high performance of these composites was attributed to the presence of poly(amino acid) polymers, which act synergistically with the other composite constituents. Furthermore, these poly(amino acid)-based composites act as mixed-type inhibitors and their inhibition ability did not change significantly with a rise in temperature. Besides, the conjoint addition of halide ions with poly(vinyl alcohol–leucine) composite was shown a synergistic effect in retarding the corrosion of mild steel. This is attributed to the pre-adsorption of these ions onto the metal surface that in turn facilitates adsorption of composite via coulombic attraction [47–50].

More complex polymeric composites containing poly(amino acid) polymers without and with additional compounds (e.g. metallic ions) are developed and listed to act as good corrosion inhibitors. An environment-friendly composite of PASP, polyepoxysuccinic acid, polyamino polyether methylenephosphonate, and sodium gluconate (Figure 4.9) is used to retarded the corrosion of carbon steel in the recirculating cooling water, which a remarkable inhibition efficiency of 97.32% at low dosage (30 ppm in a total of composite) was reached. It was found that the composite components demonstrated synergistic effects when blended and a homogeneous protective film containing the composite is formed on the metal surface. The appropriate formulation is determined using an $L_9$ $(3^4)$ orthogonal array settled via the Taguchi method [51]. Moreover, the addition of zinc ions into the above-developed composite helped to suppress almost corrosion [52]. The employed poly(amino acid)-based composites as inhibitors were not limited to the combination with other polymeric materials but also with plant extracts, such as *tobacco* stem extract. The last one was blended with PASP and polyepoxysuccinic acid to construct an effective composite inhibitor to protect A3 carbon steel against corrosion in the recirculating cooling water system. This ternary composite could not only hinder the dissolution of carbon steel but also had an exceptional inhibition effect against the formation of calcium carbonate scales [53].

The employed poly(amino acid)-based composites as corrosion inhibitors are extended to the implementation of their multi-functionalized forms (i.e. of poly(amino acid)) in the complex mixture to achieve excellent results in terms of corrosion inhibition. Here, the example of a derivative of PASP (i.e. PASP–SEA[2]–ASP,

---

[2] SEA = 2-aminoethanesulfonic acid.

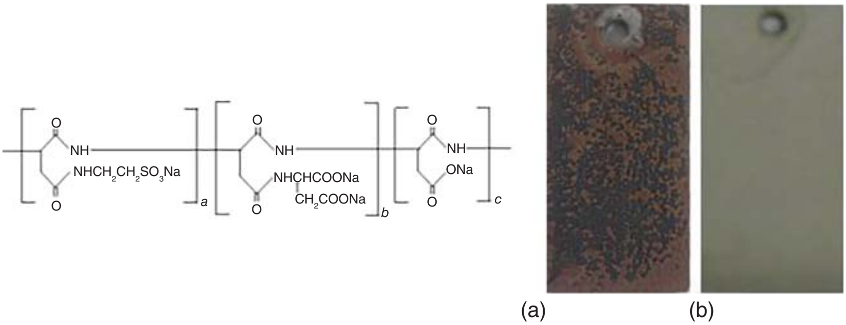

**Figure 4.10** (Left) Molecular structure of PASP–SEA–ASP copolymer. (Right) Images of carbon steel after immersion in seawater (a) without and (b) with PASP–SEA–ASP composite at 100 ppm. Source: Gao et al. [54], Reproduced with permission from Elsevier.

Figure 4.10) can be listed with zinc sulfate, 2-hydroxy phosphonoacetic acid, and hexadecylldimethyl (2-sulfite) ethyl ammonium. The evaluation of this multicomponents composite shows an outstanding inhibitory effect (97% at 100 ppm) for A3 carbon steel in seawater compared with PASP–SEA–ASP (49% at 100 ppm). The retardation effect of the developed composite can be easily revealed from the images of metal surfaces exposed to seawater in its absence and presence. This encourages its utilization in desalination water plants [54]. Table 4.3 collects other employed poly(amino acid) (especially, PASP) composite materials as corrosion inhibitors for different metal/solution systems [55–58].

**Table 4.3** The corrosion inhibition performance of some eco-friendly poly(amino acid) multicomponent materials.

| Poly(amino acid) composite material | Metallic material | Medium | Inhibition efficiency at (total concentration) |
|---|---|---|---|
| PASP + sodium gluconate + zinc sulfate + hydroxyphosphonoacetic acid + benzotriazole | A3 carbon steel and H62 copper | Seawater | 93.3% (carbon steel)<br>93.6% (H62 copper)<br>at 150 ppm |
| PASP + acrylic acid–acrylic ester–itaconic acid tripolymer + 2-phosphonobutane-1,2,4-tricarboxylic acid | Mild steel | 639 ppm $Ca^{2+}$ solution | 96.5% at 40 ppm |
| PASP derivative + itaconic acid homopolymer + polyepoxysuccinic acid + sodium gluconate | Carbon steel | 463 ppm $Ca^{2+}$ + 142 ppm $SO_4^{2-}$ + 154 ppm $Cl^-$ | 97.1% at 150 ppm |
| PASP + polyepoxysuccinic acid + hydrolyzed polymaleic anhydride + benzotriazole | Carbon steel | 62.5 ppm $Ca^{2+}$ + 104.5 ppm $Cl^-$ | 93.0% at 40 ppm |

## 4.5 Conclusion

Poly(amino acid) polymer-based inhibitors have attracted much attention since they are acceptable for the natural ecosystem. The macromolecules of this inhibitor class are equipped with multiple active adsorption centers, which could let them absorb strongly on the metal surface and then form an adherent film, which inhibits the metal corrosion. In some situations, poly(amino acid) polymer can exhibit poor inhibitive effect or a good inhibition performance only with extremely high concentrations. Therefore, chemical modification of poly(amino acid) polymer provides an effective and practical method for preparing high-efficiency inhibitors even at low concentrations. Furthermore, the combination of these polymers with additional organic and/or inorganic compounds to develop composite materials has also been reported to be an effective strategy to improve their inhibition efficiencies. Among the utilized poly(amino acid), PASP is largely employed as a green corrosion inhibitor. Depending on the considered metal/solution system, both chemical-modified or unmodified forms of PASP, as well as its associated composite materials, were demonstrated good abilities to prevent metallic corrosion in different aggressive environments, especially acidic media. Nevertheless, the capacity of other simple poly(amino acid) polymers or their derivatives to act as corrosion inhibitors is still unexplored and needs to be investigated; therefore, more attention should be devoted to this subject.

## References

1. El Mouaden, K., El Ibrahimi, B., Oukhrib, R. et al. (2018). Chitosan polymer as a green corrosion inhibitor for copper in sulfide-containing synthetic seawater. *International Journal of Biological Macromolecules* 119: 1311–1323.
2. El Ibrahimi, B., Soumoue, A., Jmiai, A. et al. (2016). Computational study of some triazole derivatives (un- and protonated forms) and their copper complexes in corrosion inhibition process. *Journal of Molecular Structure* 1125: 93–102.
3. El Ibrahimi, B., Jmiai, A., El Mouaden, K. et al. (2019). Effect of solution's pH and molecular structure of three linear α-amino acids on the corrosion of tin in salt solution: a combined experimental and theoretical approach. *Journal of Molecular Structure* 1196: 105–118.
4. El Ibrahimi, B., El Mouaden, K., Jmiai, A. et al. (2019). Understanding the influence of solution's pH on the corrosion of tin in saline solution containing functional amino acids using electrochemical techniques and molecular modeling. *Surfaces and Interfaces* 17: 100343.
5. El Ibrahimi, B., Bazzi, L., and EL Issam, S. (2020). The role of pH in corrosion inhibition of tin using the proline amino acid: theoretical and experimental investigations. *RSC Advances* 10: 29696.
6. El Ibrahimi, B. and Guo, L. (2020). Azole-based compounds as corrosion inhibitors for metallic materials. In: *Azoles - Synthesis, Properties, Applications and Perspectives* (ed. A. Kuznetsov). London: IntechOpen.

**7** Aljeaban, N.A., Goni, L.K.M.O., Alharbi, B.G. et al. (2020). Polymers decorated with functional motifs for mitigation of steel corrosion: an overview. *International Journal of Polymer Science* 2020: 9512680.

**8** El Ibrahimi, B., Guo, L., Nardeli, J.V., and Oukhrib, R. (2021). The application of chitosan-based compounds against metallic corrosion. In: *Chitin and Chitosan - Physicochemical Properties and Industrial Applications* (ed. M. Berrada). IntechOpen: London.

**9** Jmiai, A., El Ibrahimi, B., Tara, A. et al. (2018). Alginate biopolymer as green corrosion inhibitor for copper in 1 M hydrochloric acid: experimental and theoretical approaches. *Journal of Molecular Structure* 1157: 408–417.

**10** Jmiai, A., El Ibrahimi, B., Tara, A. et al. (2017). Chitosan as an eco-friendly inhibitor for copper corrosion in acidic medium: protocol and characterization. *Cellulose* 24: 3843–3867.

**11** El Ibrahimi, B., Jmiai, A., Bazzi, L., and El Issami, S. (2020). Amino acids and their derivatives as corrosion inhibitors for metals and alloys. *Arabian Journal of Chemistry* 13: 740–771.

**12** Roy, P., Saha, S.K., Banerjee, P. et al. (2017). Experimental and theoretical investigation towards anti-corrosive property of glutamic acid and poly-G-glutamic acid for mild steel in 1 M HCl: intramolecular synergism due to copolymerization. *Research on Chemical Intermediates* 43: 4423–4444.

**13** Boddu, S.H.S., Bhagav, P., Karla, P.K. et al. (2021). Polyamide/poly(amino acid) polymers for drug delivery. *Journal of Functional Biomaterials* 12: 58.

**14** Zheng, Y., Yang, W., Wang, C. et al. (2007). Nanoparticles based on the complex of chitosan and polyaspartic acid sodium salt: preparation, characterization and the use for 5-fluorouracil delivery. *European Journal of Pharmaceutics and Biopharmaceutics* 67: 621–631.

**15** Wheeler, A.P. and Koskan, L.P. (1993). Large scale thermally synthesized polyaspartate as a biodegradable substitute in polymer applications. *Materials Research Society Symposium Proceedings* 292: 277.

**16** Hater, W., Mayer, B., and Schweinsberg, M. (2000). Development of environmentally benign scale inhibitors for industrial applications. *Power Plant Chemistry* 12: 721.

**17** Cui, R., Gu, N., and Li, C. (2011). Polyaspartic acid as a green corrosion inhibitor for carbon steel. *Materials and Corrosion* 62: 362–369.

**18** Yang, L., Li, Y., Qian, B., and Hou, B. (2015). Polyaspartic acid as a corrosion inhibitor for WE43 magnesium alloy. *Journal of Magnesium and Alloys* 3: 47–51.

**19** He, R., Gao, Y., Yan, M. et al. (2020). Electrochemical impedance spectroscopy study of copper corrosion inhibition by PASP in 3% citric acid. *Desalination and Water Treatment* 175: 189–195.

**20** Xu, Q.-J., Zhou, G.-D., Wang, H.-F., and Cai, W.-B. (2006). Electrochemical studies of polyaspartic acid and sodium tungstate as corrosion inhibitors for brass and Cu30Ni alloy in simulated cooled water solutions. *Anti-Corrosion Methods and Materials* 53: 207–211.

**21** Zeino, A., Abdulazeez, I., Khaled, M. et al. (2018). Mechanistic study of polyaspartic acid (PASP) as eco-friendly corrosion inhibitor on mild steel in 3% NaCl aerated solution. *Journal of Molecular Liquids* 250: 50–62.

**22** Ma, X., Qian, B., Zhang, J. et al. (2016). The inhibition effect of polyaspartic acid and its mixed inhibitor on mild steel corrosion in seawater wet/dry cyclic conditions. *International Journal of Electrochemical Science* 11: 3024–3038.

**23** Qian, B., Wang, J., Zheng, M., and Hou, B. (2013). Synergistic effect of polyaspartic acid and iodide ion on corrosion inhibition of mild steel in $H_2SO_4$. *Corrosion Science* 75: 184–192.

**24** Wang, H.P., Wu, Q., Li, C.M., and Gu, N. (2012). Copper corrosion inhibition by polyaspartic acid and imidazole. *Materials and Corrosion* 62: 9999.

**25** He, R., Liu, Z., and Gu, N. (2013). Corrosion inhibition effect of PASP and sulfuric acid high cerium on copper in citric acid. *Advanced Materials Research* 681: 3–6.

**26** Raghavendra, N., Chitnis, S.R., and Sheelimath, D.S. (2021). Anti-corrosion investigation of polylysine (amino acid polymer) as efficacious corrosion inhibitor for Al in industrial acidic pickling environment. *Journal of Bio- and Tribo-Corrosion* 7: 1–17.

**27** Örnek, D., Jayaraman, A., Syrett, B.C. et al. (2002). Pitting corrosion inhibition of aluminum 2024 by *Bacillus* biofilms secreting polyaspartate or G-polyglutamate. *Applied Microbiology and Biotechnology* 58: 651–657.

**28** Sezerand, E. and Öztürk, I. (2019). Mild steel protection with tannic and polyaspartic acid in cooling systems. *Anti-Corrosion Methods and Materials* 66: 583–594.

**29** Wang, Y., Wu, G., Fan, Y., and Ma, J. (2009). pH-responsive self-assembly and conformational transition of partially propyl-esterified poly(α,β-L-aspartic acid) as amphiphilic biodegradable polyanion. *Colloids and Surfaces, B: Biointerfaces* 68: 13–19.

**30** Chen, J., Wang, C., Han, J. et al. (2018). Corrosion inhibition performance of threonine-modified polyaspartic acid for carbon steel in simulated cooling water. *Journal of Applied Polymer Science* 136: 47242.

**31** Chai, C., Xu, Y., Li, D. et al. (2019). Cysteamine modified polyaspartic acid as a new class of green corrosion inhibitor for mild steel in sulfuric acid medium: synthesis, electrochemical, surface study and theoretical calculation. *Progress in Organic Coatings* 129: 159–170.

**32** Chai, C., Xu, Y., Xu, Y. et al. (2020). Dopamine-modified polyaspartic acid as a green corrosion inhibitor for mild steel in acid solution. *European Polymer Journal* 137: 109946.

**33** Wang, C., Chen, J., Han, J. et al. (2019). Enhanced corrosion inhibition performance of novel modified polyaspartic acid on carbon steel in HCl solution. *Journal of Alloys and Compounds* 771: 736–746.

**34** Fu, L., Lv, J., Zhou, L. et al. (2020). Study on corrosion and scale inhibition mechanism of polyaspartic acid grafted *b*-cyclodextrin. *Materials Letters* 264: 127276.

**35** Chen, J., Chen, F., Han, J. et al. (2020). Evaluation of scale and corrosion inhibition of modified polyaspartic acid. *Chemical Engineering and Technology* 43: 1048–1058.

**36** Migahed, M.A., Rashwan, S.M., Kamel, M.M., and Habib, R.E. (2017). Synthesized polyaspartic acid derivatives as corrosion and scale inhibitors in desalination operations. *Cogent Engineering* 4: 1366255.

**37** Mazumder, M.A.J. (2019). New, amino acid based zwitterionic polymers as promising corrosion inhibitors of mild steel in 1 M HCl. *Coatings* 9: 675.

**38** Chai, C., Xu, Y., Shi, S. et al. (2018). Functional polyaspartic acid derivatives as ecofriendly corrosion inhibitors for mild steel in 0.5 M $H_2SO_4$ solution. *RSC Advances* 8: 24970–24981.

**39** Shi, S., Li, D., Chai, C. et al. (2018). Synthesis of a polyaspartic acid/4-(2-aminoethyl) morpholine graft copolymer and evaluation of its scale and corrosion inhibition performance. *Polymers for Advanced Technologies* 29: 2838–2847.

**40** Migahed, M.A., Rashwan, S.M., Kamel, M.M., and Habib, R.E. (2016). Synthesis, characterization of polyaspartic acid-glycine adduct and evaluation of their performance as scale and corrosion inhibitor in desalination water plants. *Journal of Molecular Liquids* 224: 849–858.

**41** Yuan, X., Dong, S., Zheng, Q. et al. (2020). Novel and efficient curcumin based fluorescent polymer for scale and corrosion inhibition. *Chemical Engineering Journal* 389: 124296.

**42** Shi, S., Zhao, X., Wang, Q. et al. (2016). Synthesis and evaluation of polyaspartic acid/furfurylamine graft copolymer as scale and corrosion inhibitor. *RSC Advances* 6: 102406.

**43** Zhang, B., Li, J., Lv, X. et al. (2015). Synthesis of polyaspartic acid/2-amino-2-methyl-1,3-propanediol graft copolymer and evaluation of its scale inhibition and corrosion inhibition performance. *Desalination and Water Treatment* 54: 1998–2004.

**44** Liu, Z.-F., Bai, X., Zhang, L.-H., and Zhang, Y.-L. (2014). Synthesis and properties of environmentally friendly scale and corrosion inhibitor. *Applied Mechanics and Materials* 618: 180–183.

**45** Gao, Y., Ward, L., Fan, L. et al. (2019). A study of the use of polyaspartic acid derivative composite for the corrosion inhibition of carbon steel in a seawater environment. *Journal of Molecular Liquids* 294: 111634.

**46** Tsoeunyane, M.G., Makhatha, M.E., and Arotiba, O.A. (2019). Corrosion inhibition of mild steel by poly(butylene succinate)-L-histidine extended with 1,6-diisocynatohexane polymer composite in 1 M HCl. *International Journal of Corrosion* 2019: 7406409.

**47** Sabirneeza, A.A.F. and Subhashini, S. (2013). A novel water-soluble, conducting polymer composite for mild steel acid corrosion inhibition. *Journal of Applied Polymer Science* 127: 3084–3092.

**48** Sabirneeza, A.A.F., Subhashini, S., and Rajalakshmi, R. (2013). Water soluble conducting polymer composite of polyvinyl alcohol and leucine: an effective acid corrosion inhibitor for mild steel. *Materials and Corrosion* 64: 74–82.

**49** Rahiman, A.F.S.A. and Sethumanickam, S. (2017). Corrosion inhibition, adsorption and thermodynamic properties of poly(vinyl alcoholcysteine) in molar HCl. *Arabian Journal of Chemistry* 10: S3358–S3366.

**50** Sabirneeza, A.A.F. and Subhashini, S. (2014). Poly(vinyl alcohol–proline) as corrosion inhibitor for mild steel in 1M hydrochloric acid. *International Journal of Industrial Chemistry* 5: 111–120.

**51** He, C., Tian, Z., Zhang, B. et al. (2015). Inhibition effect of environment-friendly inhibitors on the corrosion of carbon steel in recirculating cooling water. *Industrial and Engineering Chemistry Research* 54: 1971–1981.

**52** Zhang, B., He, C., Wang, C. et al. (2015). Synergistic corrosion inhibition of environment-friendly inhibitors on the corrosion of carbon steel in soft water. *Corrosion Science* 94: 6–20.

**53** Chen, Y., Xing, W., Wang, L., and Chen, L. (2019). Experimental and electrochemical research of an efficient corrosion and scale inhibitor. *Materials* 12: 1821.

**54** Gao, Y., Fan, L., Ward, L., and Liu, Z. (2015). Synthesis of polyaspartic acid derivative and evaluation of its corrosion and scale inhibition performance in seawater utilization. *Desalination* 365: 220–226.

**55** Wang, X., Liu, Z., Liu, Z. et al. (2013). The preparation and performance of a multifunctional corrosion inhibitor in seawater. *Advanced Materials Research* 773: 704–708.

**56** Liu, Z., Liu, H., Zhang, L., and Yan, M. (2011). Study on performance of scale and corrosion inhibition of polyaspartic acid composite material. *Advanced Materials Research* 233–235: 50–53.

**57** Liu, Z., Wu, Y., Zhang, L. et al. (2013). Research on performance of environmentally friendly multi-component corrosion inhibitor. *Advanced Materials Research* 813: 382–386.

**58** Chen, Y., Sun, C., Xu, H. et al. (2014). Preparation and performance research of the environment-friendly corrosion and scale inhibitor. *Advanced Materials Research* 881–883: 604–609.

# 5

# Water-Soluble Polymeric Corrosion Inhibitors

*Lipiar K.M.O. Goni[1], Mohammad A. Jafar Mazumder[1,2], Shaikh A. Ali[1,2], and Dheeraj S. Chauhan[3,4]*

[1] *King Fahd University of Petroleum & Minerals, Chemistry Department, Dhahran 31261, Saudi Arabia*
[2] *King Fahd University of Petroleum & Minerals, Interdisciplinary Research Center for Advanced Materials, Dhahran 31261, Saudi Arabia*
[3] *Modern National Chemicals, Second Industrial City, Dammam 31421, Saudi Arabia*
[4] *King Fahd University of Petroleum & Minerals, Center of Research Excellence in Corrosion, Dhahran 31261, Saudi Arabia*

## 5.1 Introduction

Corrosion, in general, is referred to as the destruction or loss of metals or metallic structures by their reaction to the environment. In a more technical sense, simultaneous transfer of mass and charge across a metal/solution interface constitutes the phenomenon of corrosion [1]. Chemical species, such as acids (HCl, $H_2SO_4$, and $HNO_3$), bases (NaOH, $NaHCO_3$, and $CaCO_3$), table salts (NaCl), moisture/water ($H_2O$), gases (formaldehyde, ammonia, sulfur-containing gases), and aggressive metal polishes, attack the surface of metals upon coming in contact with them [2]. Every industrialized country has to deal with the menaces of corrosion affecting all aspects of production, processing, and production of many commercial products and equipment. It has been reported that the cost of corrosion for any country is in the range of 1–5% of its GNP [3]. A 2013 study conducted by the National Association of Corrosion Engineers (NACE) showed that the global cost of corrosion was 2.8% of the global GDP of that year [4]. It is also worth mentioning that corrosion-mediated infrastructure collapses claimed many lives in the past.

There are several methods, such as cathodic protection, anodic protection, coating, alloying, proper design and materials selection, and using corrosion inhibitors to counter the menaces of corrosion. However, the use of corrosion inhibitors is a very straightforward, economical, and popular approach to mitigating the negative impacts of corrosion [5]. A corrosion inhibitor is a chemical substance that, when added in small amounts to systems, such as cooling systems, refineries, boilers, chemicals, oil and gas production units, diminishes or prevents and controls the dissolution of metals in corrosive media [6]. Corrosion inhibitors can be ramified into two classes based on their chemical nature – organic and inorganic. Organic corrosion inhibitors are film-forming inhibitors, and some common examples include

*Polymeric Corrosion Inhibitors for Greening the Chemical and Petrochemical Industry*, First Edition.
Edited by Mohammad A. Jafar Mazumder, Mumtaz A. Quraishi, and Amir Al-Ahmed.

fatty amides, pyridines, 1,3-azoles, and imidazolines. On the other hand, inorganic anions, such as molybdate ($MoO_3^-$), chromates ($CrO_4^{2-}$), phosphate ($H_2PO_4^-$), silicates ($SiO_4^{4-}$), and nitrate ($NO_2^-$) are some of the ordinary instances of inorganic inhibitors [7]. However, the challenges of high toxicity and environmental incompatibility associated with inorganic inhibitors and complexity in the synthetic route of organic inhibitors are shifting the focus to a new and exciting class of corrosion inhibitors – polymers.

Polymers are macromolecules made up of long chains of repeating units known as monomers. Polymeric materials possess a diverse range of architectures, such as linear chains, comb-like, branched, hyperbranched, cross-links, rotaxanes, and dendrimeric. Because of an increased number of attachment points repeated along with the chain length, polymers can cover a larger surface area and provide better protection compared to the traditionally used small-molecule corrosion inhibitors [8]. Polymers used for this purpose are of two types – natural and synthetic. Some common examples of natural polymers derived from plant or animal sources include chitosan, Dextran, and carboxymethyl cellulose.

On the contrary, synthetic polymers synthesized in laboratories include polyurethane and polyethylene glycol. Some common examples of widely used polymeric corrosion inhibitors include polyaminoacids, polysaccharides, polyaspartates, polyamine derivatives, polyvinylamide derivatives, polysulfides, polycarboxylates, and conducting polymers. Here this chapter focuses on the discussion of water-soluble polymers, including synthetic and natural polymers as corrosion inhibitors of metals and metal alloys in different corrosive media.

## 5.2 Polymers as Water-Soluble Corrosion Inhibitors

Water-soluble polymers have been defined as "substances that dissolve, disperse, or swell in water and, thus, modify the physical properties of aqueous systems in the form of gelation, thickening, or emulsification/stabilization" [9]. It is worth mentioning that for a polymer to function as a water-soluble corrosion inhibitor, it must contain either a coordination group that is capable of chelating with the metal or has an ionizable group or group with a permanent charge that can allow the polymer to undergo electrostatic interaction with other ionic species in the aqueous corrosive media [10]. Amino acids, amines, amides, alcohols, carboxylic acids, and pyridines are some groups that can impart water solubility to a particular polymer and make it function as a water-soluble corrosion inhibitor (Figure 5.1). Throughout the rest of this section, a diverse range of water-soluble synthetic and natural polymers will be highlighted in terms of their application as corrosion inhibitors of various metals and metal alloys used across many industries.

### 5.2.1 Mild Steel

Mild steel, also known as low carbon steel because of having a low carbon content of 0.05–0.25%, is a prevalent type of steel. Because of its high malleability and

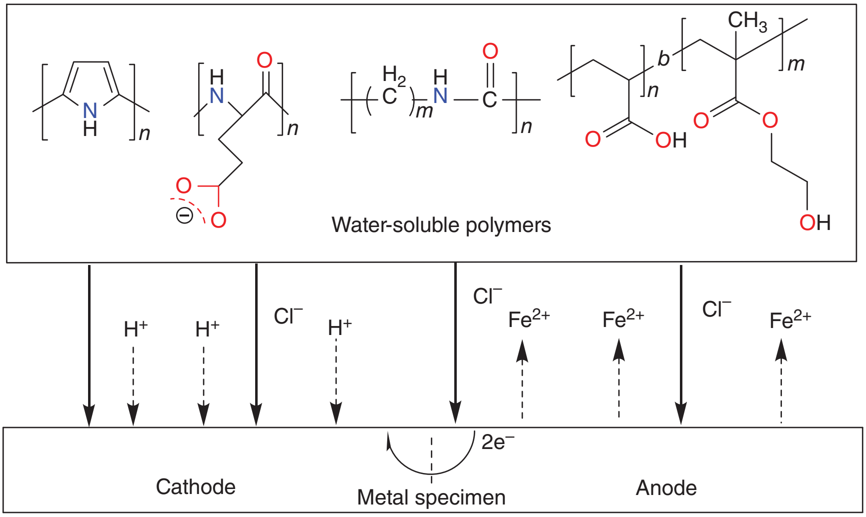

**Figure 5.1** Different water-soluble polymers undergo adsorption onto the metal surface to protect corrosive electrolytes.

ductility, it can be used to create products across a wide range of industries. Therefore, it is an excellent choice of material for steel frame buildings, gates and fencing, machinery parts, pipelines, and structural steel. Industries that carry out oil-well acidizing, acid pickling, acid descaling, and industrial acid cleaning suffer severely from mild steel corrosion, causing material loss and structural damage, leading to enormous economic loss. Acid solutions are commonly used to remove undesirable scale and rust in metalworking and chemical-cleaning scales in metallurgy and the petrochemical industry. However, inhibitors are added to acid solutions to prevent excess acid consumption and unwanted metal dissolution in the pickling process of mild steel. Geethanjali and Subhashini [11] prepared a terpolymer that has a poly(vinyl sulfonate-*co*-*p*-vinyl benzene sulfonate) grafted to polyvinyl alcohol (PVA) backbone. The terpolymer PVA-VSA-PVSB was designed to accommodate heteroatoms, such as S and O, and aromatic rings, which render the terpolymer water-soluble and effective through multiple anchoring points. This idea of polymerizing/blending/compositing originates from the concept of numerous adsorption sites or instilling special functional groups that promote solubility, degradability, and processability. Inhibition efficiencies (IE) from different techniques, such as weight loss (WL), potentiodynamic polarization (PDP), and electrochemical impedance spectroscopy (EIS), were between 80% and 85% when PVA-VSA-PVSB terpolymer was used to protect mild steel in 1 M HCl. The IE increased with an increasing inhibitor concentration, and the polarization study proved that the inhibitor acted as a mixed-type reducing the extent of both anodic and cathodic reactions. The fact that charge-transfer phenomenon-controlled corrosion reactions were validated by EIS spectra exhibiting one capacitive loop, which was strengthened by the finding that the charge-transfer resistance ($R_{ct}$)

and the double-layer capacitance ($C_{\mathrm{dl}}$) increased and decreased, respectively, with increasing inhibitor concentration.

Sabirneeza and Subhashini [12] prepared poly(vinyl alcohol – proline) (PVAP) polymer composite for the protection of mild steel in 1 M HCl for hydrochloric acid is the most commonly used pickling acid in industries. It is well recognized that amino acids are good sources of heteroatoms with excellent IE and nontoxic nature. Therefore, the PVAP composite achieved a maximum IE of 94% at 303 K. Moreover, the IEs from experimental techniques were in good agreement. It was found that the addition of PVAP did not change the values of corrosion potential ($E_{\mathrm{corr}}$) significantly (less than 85 mV), and hence, the composite was regarded as a mixed-type inhibitor. The adsorption of PVAP onto mild steel was found to follow Langmuir adsorption isotherm and the value of free energy of adsorption ($\Delta G^{\circ}_{\mathrm{ads}}$) indicated that the adsorption of the inhibitor was spontaneous. The doping/compositing of PVA with L-cysteine led to the production of water-soluble conducting polymer composite poly(vinyl alcohol – cysteine) [PVAC] that was used for the protection of mild steel in 1 M HCl [13]. A maximum IE of 94% was achieved for an inhibitor concentration as low as 0.6 wt%. PDP study revealed that the inhibitive nature of the polymer composite was of mixed-type. The free energy ($\Delta G_{ads}$), enthalpy ($\Delta H_{ads}$), and entropy of adsorption ($\Delta S_{\mathrm{ads}}$) were found to be $-16.28\ \mathrm{kJ\ mol^{-1}}$, $-1.08\ \mathrm{kJ\ mol^{-1}}$, and $44.68\ \mathrm{kJ\ mol^{-1}}$ at 323 K. The negative value of $\Delta G_{\mathrm{ads}}$, low negative value $\Delta H_{\mathrm{ads}}$, and large positive value of $\Delta S_{\mathrm{ads}}$ proved that the adsorption process was spontaneous. Moreover, the value of $\Delta G_{\mathrm{ads}}$ being less than $-40\ \mathrm{kJ\ mol^{-1}}$ proved that the interaction between the inhibitor and metal surface was electrostatic in nature i.e. physisorption.

Even though poly-methylaniline (PMA) is a good corrosion inhibitor of iron, its instability and insolubility in water make it a somewhat less exploited corrosion inhibitor. Keeping that in mind, Karthikaiselvi and Subhashini [14] prepared a new water-soluble polymer composite poly-(vinylpyrrolidone–methylaniline) (PVPMA), as polyvinyl pyrrolidone (PVP) acted as a steric stabilizer and prevented the dispersion of PMA in solution. The resulting composite showed a maximum IE of 88.8% through the EIS study and appeared mixed-type inhibitive nature. In acidic solutions, PMA usually exists as protonated species. These protonated species get adsorbed on the cathodic sites of mild steel and reduce the evolution of molecular hydrogen. This adsorption phenomenon is often aided by the presence of chloride ions adsorbed onto the positively charged metal surface. The anodic dissolution of the mild steel surface is retarded by the π-electrons of aromatic rings and lone pair of electrons on nitrogen atoms. Two water-soluble acryl terpolymers, polyvinyl alcohol-g-poly(acrylamide-vinyl sulphonate) (PVA-AAm-VSA) and polyvinyl alcohol-g-poly(acrylic acid-vinyl sulphonate) (PVA-AA-VSA), were prepared to study their corrosion inhibitive properties for mild steel in 1 M HCl [15]. Both terpolymers showed IE around 90% through gravimetric technique, and the PDP study confirmed the composites' inhibitive nature to be of mixed-type. Geethanjali et al. [16] synthesized pectin-g-polyacrylamide (Pec-g-PAAm) and pectin-g-polyacrylic acid (Pec-g-PAA) by grafting nontoxic pectin with PAAm and PAA, respectively. The composites were tested for IE of mild steel in neutral 3.5% NaCl. Both the polymers showed IE around 85%, with the graft polymer containing

PAAm showing relatively higher IE, probably due to the presence of nitrogen atoms in the polymer chain. Kumar et al. [17] prepared two polyurethane-based tri-block copolymers, namely, poly(dimethylaminoethylmethacrylate)-*b*-polyurethane-*b*-poly (dimethylaminoethylmethacrylate) (PDMAEMA-PU) and poly(N-vinylpyrrolidone)-*b*-polyurethane-*b*-poly(*N*-vinylpyrrolidone) (PNVP-PU) for their inhibition efficacy test for mild steel in 0.5 M $H_2SO_4$. Both (PDMAEMA-PU) and (PNVP-PU) showed very high IEs of 99.53% and 98.23% at 298 K for a relatively higher concentration of 1600 ppm. Some other polymer composites and their inhibitive action toward mild steel in different corrosive media are given in Table 5.1. Both inhibitors acted as mixed-type and were found to follow Langmuir adsorption isotherm.

Due to highly reactive primary and secondary amine groups, polyethyleneimine (PEI) is an excellent water-soluble polymeric corrosion inhibitor. However, its modest performance of imparting only 81.9% IE to ASTM 420 stainless steel for a high concentration of 1000 ppm in a neutral medium [33] inspired Chen et al. [34] to modify PEI with phosphorous acid to make polyethyleneimine phosphorous acid (PEIPA). PEIPA, owing to its improved adsorption due to the introduction of phosphorous and oxygen atoms, imparted an improved IE of 88.0% to mild steel for a much lower concentration of 200 ppm. The energy difference between the highest occupied molecular orbital (HOMO) and the lowest unoccupied molecular orbital (LUMO), denoted as $\Delta E$, is a good indicator of how good a corrosion inhibitor is in terms of electron donation to the metal surface, with small $\Delta E$ indicating at a better performance of a corrosion inhibitor. $\Delta E$ of PEI and PEIPA was found to be 7.4902 and 6.6668 eV, respectively. The binding energy between PEIPA and mild steel surface, denoted as $E_{\text{binding}}$ for the binding between any inhibitor and metal surface to be protected, was found to be a very high value of 737.46 kJ mol$^{-1}$ through molecular dynamics (MD) study, meaning strong adsorption of PEIPA onto mild steel surface. Polyamide resins, due to the possession of surface-active polar amine and amide groups and hydrophobic fatty acid tail, can act as excellent corrosion inhibitors of mild steel. Those fatty acid tails can prevent the access of water, oxygen, hydrogen sulfide, and other corrosive media from coming into contact with the steel surface. In light of these properties of polyamide resins, two water-soluble, biodegradable, and nontoxic polyamidoaminoepichlorohydrin (PAE) polymeric resins were prepared as corrosion inhibitor of mild steel in 0.5 M $H_2SO_4$ [35]. Both resins imparted IEs of more than 90% and followed Langmuir adsorption isotherm. Dwivedi et al. [36] studied the corrosion inhibition behavior of water-soluble PAA on mild steel in 0.5 M $H_2SO_4$. With increasing concentration, PAA showed increased efficiency, and a maximum IE of 96.8% was achieved for a modest concentration of 100 ppm. PDP study revealed that PAA altered both anodic and cathodic reactions.

Naturally occurring substances, also known as “green corrosion inhibitors,” have received enormous attention over the last few years because they are environmentally benign and relatively cheaper. Additionally, they are renewable sources of materials and readily available [2]. Therefore, biopolymers, a class of polymers that occur naturally, possess the characteristics of environment-friendly and cost-effectivity, and additionally, they are well-known for their exceptional functionality. Anyiam et al. [37] extracted starch from sweet potatoes and investigated the corrosion IE of

**Table 5.1** Corrosion IE of different synthetic polymer composites toward mild steel in various corrosive media.

| Composite | Corrosive medium | Adsorption behavior | $IE_{max}$(%) [concentration] | Reference |
|---|---|---|---|---|
| Polyaniline – poly(acrylic acid) (PANI – PAA) | 0.5 M HCl | Langmuir | 91.68 [200 ppm] | [18] |
| Polypropylene glycol/silver nanoparticles (PPG – AgNPs) | 0.5 M $H_2SO_4$ | Temkin | 94 [1000 ppm] | [19] |
| Polyvinyl alcohol – sulfanilic acid (PVASA) | 1 M HCl | Langmuir | 84 [6000 ppm] | [20] |
| Poly(vinyl alcohol – histidine) | 1 M HCl | Temkin | 95 [0.6 wt.%] | [21] |
| Poly(butylene succinate) – L-Histidine (PBSLH) | 1 M HCl | Langmuir | 78 [600 ppm] | [22] |
| Poly(vinylpyrrolidone)/zinc oxide nanoparticles (ZnO/PVP) | 5% HCl | Langmuir | 90.81 [1000 ppm] | [23] |
| Xanthan gum-graft-poly(acrylamide) (XG-g-PAM) | 15% HCl | Langmuir | 94.79 [0.4 g $l^{-1}$] | [24] |
| Poly(ethylene glycol) – tyrosine (PEGT) | 1 M HCl | Langmuir | 91.33 [600 ppm] | [25] |
| Poly (vinyl alcohol-*o*-methoxy aniline) (PVAMOA) | 1 M HCl | Langmuir | 91.60 [2000 ppm] | [26] |
| Melamine formaldehyde–hybrid graphene oxide (MF–GO) | 3.5 wt.% NaCl | — | 100 [500 ppm] | [27] |
| Urea-formaldehyde–hybrid graphene oxide (UF–GO) | 3.5 wt.% NaCl | — | 100 [500 ppm] | [27] |
| Stearic acid-graft-chitosan/epoxy blend [(SA-g-CS)/epoxy] | 3.5 wt.% NaCl | — | 94.59 [coating] | [28] |
| Polyaniline/CdTe (PANI/CdTe) | 3.5 wt.% NaCl | — | 75 [coating] | [29] |
| Polyaniline/$TiO_2$ nanoparticles/epoxy (PANI/$TiO_2$ NPs/epoxy) | 3.5 wt.% NaCl | — | 98.64 [coating] | [30] |
| Sulfonated polyaniline (SPANI)/epoxy | 3.5 wt.% NaCl | — | 98.26 [coating] | [31] |
| β-Cyclodextrin–octadecylamine (CPD–DA) | Condensate water | Langmuir | 92.87 [150 ppm] | [32] |

native starch (NS) and alkaline-modified starch (AMS) on the mild steel in 0.25 M $H_2SO_4$. Due to the alkaline modification, AMS had active alkoxy functionalities that helped it to impart better IE than NS. However, the maximum IE of 62.8% imparted by AMS (0.5 $g\,l^{-1}$) is not impressive enough in practical applicability. Therefore, the authors exploited the synergistic IE of AMS and iodide ions, as halide ions have been reported to have promoted the IE by forming interconnecting bridges between organic cations and positively charged metal surfaces. Therefore, a combination of 0.5 $g\,l^{-1}$ of AMS and 0.4 $g\,l^{-1}$ of KI showed a superior IE of 84.2%. However, interestingly, the inhibitive behavior of AMS was found to be mixed-type with cathodic predominance, whereas that of AMS + KI was found to be mixed-type with anodic predominance.

Nevertheless, both types of inhibitors demonstrated Langmuir adsorption isotherm. Sodium carboxy methyl cellulose (NaCMC), derived from the partial substitution of 2, 3, and 6 hydroxyl groups of cellulose by hydrophilic carboxymethyl groups, contains —OH and —COOH groups in its chemical structure and can impart impressive IE. However, previous literature [38] has shown that CMC and NaCMC showed only a moderate IE of 64.8% and 78.1% for concentrations of 500 and 400 ppm in 2 M $H_2SO_4$ and 1 M HCl, respectively, at approximately 300 K. Aslam et al. [39] studied the synergistic IE of NaCMC and Gemini surfactants for mild steel corrosion in 1 M HCl. Gemini surfactants are cationic and contain diester functional groups in the spacer part with 12, 14, or 16 carbon atoms in the alkyl tail. A combination of 500 ppm of NaCMC and 1 ppm of Gemini surfactant (16-E2-16, 16 refers to the number of carbon atoms in the alkyl tail and E2 refers to the diester functionality) imparted a superior IE of 91.61%. MD study found out that the $E_{\text{adsorption}}$ to be 507.5 $kJ\,mol^{-1}$, indicating a strong interaction between the inhibitor system and the mild steel surface.

Xanthan gum (XG), a naturally occurring polymer, comprises pentasaccharide repeat units consisting of glucose, mannose, and glucuronic acid in the molar ratio of 2 : 2 : 1. XG is soluble in hot and cold water, stables over a broad pH range, and is completely biodegradable. Mobin and Rizvi [40] studied the synergistic IE of XG and some surfactants, such as sodium dodecyl sulfate (SDS), cetyl pyridinium chloride (CPC), and Triton X-100 (TX) for mild steel corrosion in 1 M HCl. Even though all the surfactants caused the IE of XG to go up, the best IE (90.4%) was achieved for a combination of 1000 ppm of XG and 5 ppm of SDS. The inhibitor systems worked as mixed-type inhibitors and followed Langmuir adsorption isotherm. Pal et al. [41] studied the corrosion inhibition characteristics of gelatin on mild steel 1 M HCl. Gelatin is obtained by the thermal denaturation of collagen from animal skin, bones, and fish scales. It is a heterogeneous mixture of single or multistranded polypeptides and has a nonuniform distribution of at least 18 amino acids. A maximum IE of 96% was achieved for 100 ppm of gelatin at 303 K. Involvement of the polyamide groups of the protein backbone and side-chain amino acids was confirmed by Fourier-transform infrared (FTIR) study. Gelatin was found to be of mixed-type inhibitor and followed Langmuir adsorption isotherm. Pectin, a naturally occurring polysaccharide found in the primary cell walls of higher plants, is another popular biopolymer that has recently been used as a corrosion inhibitor of mild steel in 1 M HCl [42]. A maximum IE of 94.2% was achieved for 2 $g\,l^{-1}$ of pectin at 318 K. Pectin acted as a mixed-type inhibitor and adsorbed onto mild steel through chemisorption. Basik and Mobin [43] exploited chondroitin sulfate (CS), a mucopolysaccharide found both in vertebrates and invertebrates, as a corrosion inhibitor of mild steel in 1 M HCl. The presence of different surface-active moieties, such as —OH, —NH, —C=O, —$OSO_{3,}$ and aromatic rings made CS impart an impressive IE of 95.4% at a concentration of 500 ppm at 333 K. The adsorption of CS was found to follow Langmuir adsorption isotherm. It acted as a mixed-type inhibitor with cathodic predominance. The examples of naturally occurring polymers tested as corrosion inhibitors of mild steel are plenty in literature and very challenging to discuss them all here. However, some additional naturally occurring polymers reported as corrosion inhibitors of mild steel are mentioned in Table 5.2.

### 5.2.2 Carbon Steel

Carbon steel is a type of steel with carbon content from about 0.05%–2.1% by weight. Carbon steel can be classified into four types based on the carbon content: (i) low-carbon steel or mild steel, (ii) medium-carbon steel (~0.3–0.5% carbon content) used for forging, large parts, and automotive components, (iii) high-carbon steel (~0.6–1.0% carbon content), which is very strong and used for high-strength wires, springs, and edged tools, and (iv) ultrahigh-carbon steel (~1.25–2.0% carbon content), which is of extraordinary hardness and used for particular purposes, such as punches, axles, and knives. However, like mild steel, carbon steel can also undergo severe corrosion when exposed to highly acidic or alkaline conditions [58]. Polymers, primarily naturally occurring polymers or nontoxic polymers, are being significantly explored for their application as corrosion inhibitors of carbon steel in different corrosive media.

Ma et al. [59] studied the corrosion behavior of carbon steel in 1 M HCl in the presence of low-ester pectin derived from a sunflower head. Using enzyme-assisted extraction, the authors derived pectin with three different molecular weights ($M_w$ = 4.50, 97.2, and 254.6 kDa). However, the WL study showed that pectins with $M_w$ of 97.2 and 254.6 kDa were less efficient than those with $M_w$ of 4.50 kDa. This has been attributed to the fact that pectins with higher $M_w$ were more entangled in the acidic solution and hence less soluble. On the contrary, pectins with low $M_w$ were less entangled and more uncoiled, leading to increased solubility in the solution. Thus, the pectin with $M_w$ of 4.50 kDa showed an impressive IE of 92.1% for a moderate concentration of 2.0 $g\,l^{-1}$. PDP study showed that the pectin acted as a mixed-type corrosion inhibitor, and the adsorption of pectin was found to follow Langmuir adsorption isotherm. Mobin et al. [60] synthesized a biopolymer called arabinogalactan (AG) from tragacanth gum and studied its IE for carbon steel corrosion in 1 M HCl. AG is a highly branched anionic polysaccharide comprised of L-arabinose, D-galactose, D-xylose, L-rhamnose, D-glucose, L-fucose, and D-galacturonic acid. It is complex, hydrophilic, and heterogeneous. The tragacanth gum-derived AG is water-soluble and creates low-viscosity solutions. Many hydroxyl groups (OH) and heteroatoms (O) are found in the primary constituents of AG. With

**Table 5.2** Some recently reported naturally occurring polymers as corrosion inhibitors of mild steel.

| Naturally occurring polymers | Corrosive medium | Adsorption behavior | $IE_{max}$(%) [concentration] | Reference |
|---|---|---|---|---|
| *Okra* mucilage – graft – PAM (O-g-PAM) | 0.5 M $H_2SO_4$ | Langmuir | 96.6 [100 ppm] | [44] |
| Glucomannan (GL) + Bisquaternary ammonium salt (BQAS) | Simulated seawater | Langmuir | 99.1 [80 ppm] | [45] |
| Chitosan derivative | 1 M HCl | Langmuir | 98.81 [200 ppm] | [46] |
| Dopamine-modified polyaspartic acid (PASP-Dop) | 0.5 M HCl | Langmuir | 90.9 [100 ppm] | [47] |
| 5-Chloromethyl-8-hydroxyquinoline derivative of chitosan (CH-HQ) | 1 M HCl | Langmuir | 93.9 [0.001 ppm] | [48] |
| Aminated hydroxyethyl cellulose (AHEC) | 1 M HCl | Frumkin | 93 [900 ppm] | [49] |
| Amino acid-modified konjac glucomannan (KGMH) | 0.5 M HCl | Langmuir | 92.4 [2000 ppm] | [50] |
| Pig cartilage-derived CS (CS-PC) + sodium alginate (SA) | 1 M HCl | — | 95.18 [400 + 200 ppm] | [51] |
| Polyaspartic acid-glycine adduct (GLY-PASP) | Simulated seawater | — | 83.8 [250 ppm] | [52] |
| Iota-carrageenan (IC) | 0.5 M $H_2SO_4$ | Langmuir | 97.40 [1000 ppm] | [53] |
| Gum acacia-graft-polyacrylamide (GA-g-PAM) | 15% HCl | Langmuir | 94.08 [0.3 $g\,l^{-1}$] | [54] |
| Silver nanoparticles – chitosan nanocomposite (SNPs-CTNC) | Cooling-water system | Langmuir | 80 [100 ppm] | [55] |
| Soluble cyclodextrin polymer (SCDP) + cinnamaldehyde (CA) | 3.5 wt.% NaCl | Langmuir | 92.2 [125 ppm] | [56] |
| Amylose-acetate-blended carboxymethyl chitosan (AA-CMCh) | 0.25 M $H_2SO_4$ | Langmuir | 97.65 [400 ppm] | [57] |

its colossal size, many reactive groups and abundance of unshared lone pairs of electrons from O, the AG macromolecule was projected to get adsorbed over a large area on the carbon steel surface and slow corrosion rates at low concentrations. AG was found to be so effective that it imparted an amazing IE of 96.3% at temperatures as high as 60 °C, confirmed by gravimetric analysis. EIS study showed higher values of $C_{dl}$ and $R_{ct}$ for inhibited solutions with respect to that of blank and indicated the accumulation of AG at the metal/solution interface. PDP study revealed that AG worked mainly as a mixed-type inhibitor with anodic predominance.

Nwanonenyi et al. [58] studied the IE of CMC and additives PVP, PAA, and PVA for corrosion protection of carbon steel in 1 M HCl and 1 M KOH corrosive media. At a concentration of 2.5 g $l^{-1}$, CMC alone showed an IE of 79.7% and 72.5% at 30 and 60 °C, in 1 M HCL, and 71.1% and 62.6% at temperatures of 30 and 60 °C, in 1 M KOH, respectively. However, PVP (0.5 g $l^{-1}$) as additives to CMC (2.5 g $l^{-1}$) improved the IE more than the addition of PAA and PVA. The mixture of CMC and PVP improved the IE in 1 M HCl to 89.6% and 80.4% for temperatures 30 and 60 °C, and the IE in 1 M KOH to 86.2% and 75.1% for temperatures 30 and 60 °C. The presence of multiple adsorption centers present in both CMC and PVP led to increased surface coverage and hence increased IE. A similar type of study [61] where HEC and PAA were mixed in different ratios was also carried out to see the synergistic IE of HEC and PAA for carbon steel in 1 M HCl. The best IE of 92.0% was achieved when HEC and PAA were mixed in a 4 : 1 ratio. This IE was far better than what individual polymers would offer because a mixture of polymers is far better in terms of blanketing the metal surface with respect to individual polymers. MD study also showed that the binding energies for Fe (110) surface and HEC, PAA, and HEC/PAA were −490.79, −162.84, and −660.24 kJ $mol^{-1}$, bolstering the efficacy of polymer composite found through experimental study. Quraishi et al. [62] developed vanillin-modified chitosan (Van-Cht) as a bioinspired corrosion inhibitor of carbon steel for use during the oil-well acidizing that involves approximately 15% HCl. This green corrosion inhibitor contains several —OH and —$OCH_3$ groups that are readily available for adsorption onto carbon steel surfaces via chemisorption facilitated by lone pair of electrons on oxygen atoms. The inhibitor was so effective that it imparted an IE of more than 98% for a concentration of 500 ppm at 25 °C, as confirmed by the WL study. DFT analysis showed that the adsorption of Van-Cht occurs through the protonated form. This means that electrostatic interaction between the protonated form of Van-Cht and chloride ions pre-adsorbed onto the carbon steel surface facilitates the adsorption of Van-Cht. PDP study showed that Van-Cht acts as a mixed-type inhibitor with cathodic predominance. Due to its strong affinity, good solubility, and adsorption capability on metal surfaces, Dextran is found to be a suitable corrosion inhibitor. However, because of numerous strong hydrogen bonds in the dextral molecule, it is highly hydrophilic in nature and suffers a significant decrease in its corrosion IE. One of the ways to get around this problem is to reduce the number of —OH groups in the dextran molecule. Zhang et al. [63] developed two amino acid-modified dextran derivatives (LDT and S-LDT; Scheme 5.1) green inhibitors and used electrochemical testing and surface analysis to investigate their anticorrosion performance for carbon steel in $CO_2$-saturated oilfield produced water. Amino

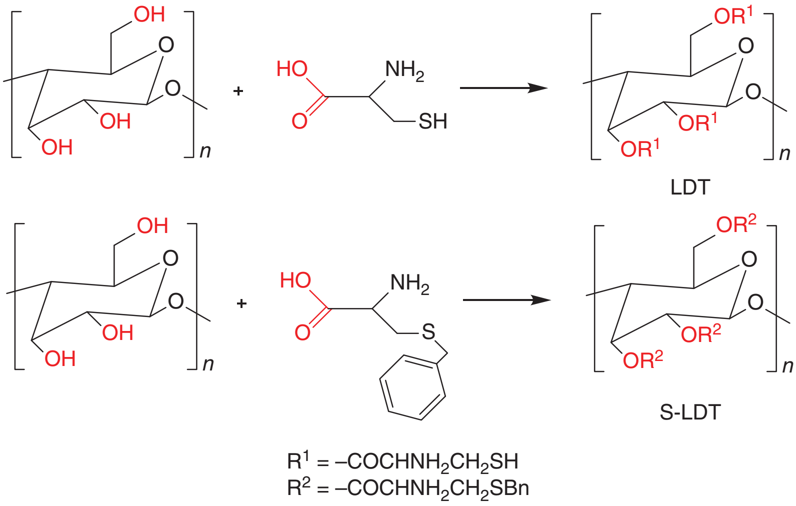

**Scheme 5.1** Synthetic routes of two dextran derivatives (LDT and S-LDT).

acid carboxyl groups can react with hydroxyl groups in the dextran structure, resulting in a green alteration of dextran-based corrosion inhibitors. Based on the foregoing, L-cysteine and S-benzyl-L-cysteine were utilized as esterification reagents to change the dextran molecule and produce two environmentally safe inhibitors (LDT and S-LDT). S-LDT was found to impart an amazing IE of 99.5% for the concentration of 250 mg $l^{-1}$ via electrochemical measurements. Additionally, S-LDT showed an extraordinary corrosion inhibition stability (99.7% after 72 hours of immersion).

### 5.2.3 Iron

Iron is utilized in various industries, including construction, bridges, tunnels, and agricultural equipment. Unfortunately, with the exception of a few metals, such as gold, silver, and platinum, most metallic elements are chemically unstable and react spontaneously with the surrounding environment, resulting in relatively stable corrosion products, such as rusts and scales. Metals naturally tend to oxidize, accounting for their spontaneous corroding tendency. The change in the value of standard Gibb's free energy ($\Delta G^{\circ}$) determines the relative rate of metallic corrosion. In general, a higher corroding tendency is related to a lower ($\Delta G^{\circ}$) value, and *vice versa* [64]. Umoren et al. [65] studied the corrosion behavior of pure iron in 0.5 M $H_2SO_4$ in the presence of PAM. A maximum IE of 76% was achieved in the presence of $1 \times 10^{-6}$ M of PAM. However, upon adding 5.0 mM of KI to the solution, the IE dramatically increased to 97%, attributed to the increased adsorption aided by the presence of iodide ions on the iron surface that helped more PAM adsorbed in turn (cooperative adsorption). The adsorption of PAM onto iron surface followed El-Awady kinetic–thermodynamic adsorption isotherm model via chemisorption mechanism, and the PDP study revealed that PAM acted as a mixed-type inhibitor. Another similar study by Jeyaprabha et al. [66] showed that the IE of PANI at 10 ppm increased to 90% from 53% upon the addition of $0.5 \times 10^{-3}$ M $I^-$ ions. The improved adsorption of polyaniline by the adsorbed halide ions was due to the synergistic effect.

WL, PDP, and EIS techniques were used to investigate the effect of hydroxypropyl cellulose (HPC) on acid (1 M HCl) corrosion of cast iron [67]. The IE was observed to rise as the inhibitor concentration was increased, with a maximum IE of 89.6% reported for 500 ppm of HPC. When potassium iodide was added to the corrosion-inhibition system, it produced antagonistic and synergistic effects in IE. HPC's mixed-type inhibitory nature was discovered through polarization research. In the presence and absence of KI, the adsorption of inhibitors on the cast-iron surface followed the Langmuir adsorption isotherm model. The inhibitor performance of chemically produced water-soluble poly(aminoquinone) (PAQ) on iron corrosion in 0.5 M $H_2SO_4$ was investigated in relation to inhibitor concentration [68]. When the inhibitory performance of PAQ was compared to that of the monomer *o*-phenylenediamine (OPD), the OPD showed an IE of 80% for 1000 ppm while it was 90% for 100 ppm of PAQ. PAQ was found to be a mixed-type inhibitor.

Furthermore, PAQ was able to significantly increase the passivation tendency of iron in 0.5 M $H_2SO_4$. Recently, PEG and PVA have been tested as corrosion inhibitors of iron in 1 M NaCl, with PEG and PVA showing an IE of 93% and 86%, respectively, for the concentration of 500 ppm [69]. Both inhibitors followed Langmuir adsorption isotherm and were adsorbed via mixed-type inhibition. The greater IE of PEG was attributed to its higher molar mass. To prevent the internal corrosion of the piping system, used in the petroleum mining industry for the distribution of crude oil from drilling fields to processing refineries, polyethylene oxide (PEO) was tested as a corrosion inhibitor of iron in 1% NaCl electrolyte [70]. An optimum IE of 80.2% was achieved for a small concentration of 16 ppm at 25 °C. With free adsorption energy of $-21.38$ kJ $mol^{-1}$, PEO showed adsorption qualities that conform with the Langmuir adsorption isotherm.

PANI and metal cations, such as $Zn^{2+}$ and $Mn^{2+}$ ions, have moderately prevented iron corrosion in $H_2SO_4$. Metal cations have been found to interact directly with PANI via protonation of the imine nitrogen atom of PANI's quinoid groups, causing chemical and structural changes in the polymer. Following this, Sathiyanarayanan et al. [71] exploited EIS, linear polarization resistance (LPR), and Tafel polarization methods to investigate the inhibition of iron in 0.5 M $H_2SO_4$ by PANI in the presence of $Zn^{2+}$ and $Mn^{2+}$ ions ($1 \times 10^{-3}$ M). PANI showed 40% IE at 10 ppm and 72% IE at 100 ppm. However, in the presence of metal cations, the IE of PANI increased to 80% for 10 ppm and more than 90% for 100 ppm. The higher IE of PANI in the presence of metal cation was due to higher electron-rich benzenoid groups that absorbed more efficiently on the iron surface, lowering the corrosion rate significantly. When PANI was tested in the absence of any metal cations by Jeyaprabha et al. [72], for the protection of pure iron in 0.5 M $H_2SO_4$ showed a moderate IE of 84% at a concentration of 100 ppm. The shift of the benzenoid–quinonoid ring's distinctive band from 1560–1490 $cm^{-1}$ to 1560–1460 $cm^{-1}$ verified PANI was heavily adsorbed onto the iron surface. In light of the good IE imparted by polymer amines, two water-soluble polymer amines, namely, poly(*p*-phenylenediamine) [73] and poly(*p*-toluidine) [74], were studied as corrosion inhibitors of iron in 1 M HCl.

Poly(*p*-phenylenediamine) imparted a maximum IE of 92.7% at a concentration of 500 ppm, whereas poly(*p*-toluidine) showed a maximum IE of 94.6% at a concentration of 500 ppm. Both inhibitors followed Langmuir adsorption isotherm and showed mixed-type inhibitive behavior.

### 5.2.4 Aluminum

Aluminum and its alloys, because of their unique properties, are widely utilized in various industrial applications, including machine tools and components, reaction vessels, reaction tanks, storage tanks, pipelines, fittings, nuts, bolts, and cooking pots and plates. In the presence of atmospheric air, aluminum is a passive metal; however, severe corrosion occurs on aluminum surfaces in aqueous conditions [75]. Because of the damage caused to the passive layer of aluminum oxide in an alkaline medium, Punitha et al. [76] studied the corrosion behavior of aluminum using PAA as a corrosion inhibitor in a 1 M NaOH solution. PAA, known for its stability, adhesion, and anticorrosion nature, was modified to bear triazole pendant moieties by means of reacting polyacryloyl chloride with 3-amino-1,2,4-triazole-5-thiol. The modified PAA (ACTP) showed the maximum IE of 90.97% at a concentration of 0.05%. The fact that the destruction of the aluminum oxide passive layer is possible in aqueous acidic environments, there are efforts to make inhibitors that are good enough to protect aluminum metal in acidic environments. Nwanonenyi et al. [75] studied the IE of HPC for aluminum in 0.5 M HCl and 2 M $H_2SO_4$. HPC showed the maximum IE of 84.39% and 95.92% in 0.5 M HCl and 2 M $H_2SO_4$, at a concentration of $5\,g\,l^{-1}$, respectively. HPC inhibitor followed Langmuir adsorption isotherm in both acidic solutions and showed mixed-type inhibitive behavior. Some additional aluminum corrosion inhibitors and their structures and IE are reported in Table 5.3.

### 5.2.5 Copper

Due to its strong electrical and thermal conductivities, mechanical workability, and comparatively noble qualities, copper is one of the most essential metallic elements in the industry. Due to their mechanical qualities and thermal conductivity, copper and its alloys are used in home and industrial water utilities, such as condensers, heat exchangers, marine environments, agriculture machinery, and water-treatment technologies. However, despite having a relatively good corrosion-resistant nature, copper can still undergo severe corrosion in acidic, highly alkaline, and saline water conditions. Therefore, there is a good amount of effort to make inhibitors to protect metallic copper in aggressive corrosive conditions [84]. Metallic copper can undergo serious corrosion in the presence of chloride ions in pitting and stress corrosion cracking. Samide et al. studied the coating performance of poly (vinyl butyral-*co*-vinyl alcohol-*co*-vinyl acetate) (PVBA; Figure 5.2) for copper corrosion in 0.9% NaCl solution.

PVBA consists of three distinct structural units: hydrophobic polyvinyl butyral macromolecular chain, hydrophilic polyvinyl alcohol, and polyvinyl acetate. PVBA was chemically coated on the copper surface by dipping the metal sample in a

**Table 5.3** Polymeric corrosion inhibitors of aluminum for different corrosive media.

| Structure and name | Corrosive medium | $IE_{max}$(%) [concentration] | Reference |
|---|---|---|---|
| 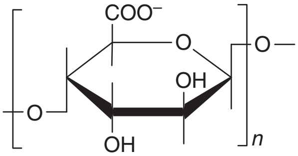<br>Pectate | 1 M NaOH | 88.67 [1.6%] | [77] |
| 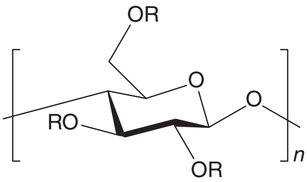<br>R = H or $CH_2CH_2OH$<br>HEC | 0.5 M HCl | 60.8 [$2.5 \times 10^{-3}$ M] | [78] |
| 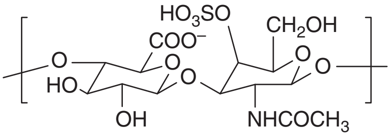<br>CS | 3 M HCl | 64.12 [0.8%] | [79] |
| 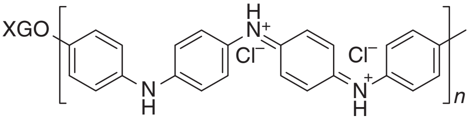<br>XG-g-PANI | 1 M HCl | 95.32 [0.1%] | [80] |
| 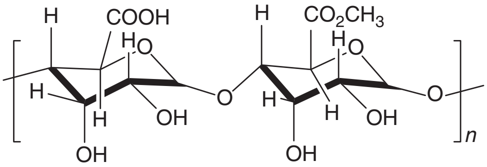 | 2 M HCl | 91 [8 g l$^{-1}$] | [81] |
| 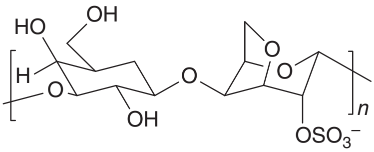<br>i-Carrageenan | 2 M HCl | 66.7 [400 ppm] | [82] |

**Table 5.3** (Continued)

| Structure and name | Corrosive medium | $IE_{max}$(%) [concentration] | Reference |
|---|---|---|---|
| 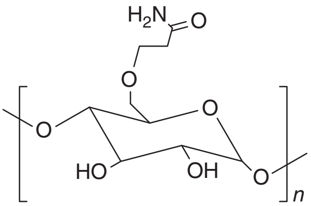<br>Cassava starch – acrylamide graft copolymer (CS-AAGC) | 1 M $H_3PO_4$ | 90.6 [$1\,g\,l^{-1}$] | [83] |

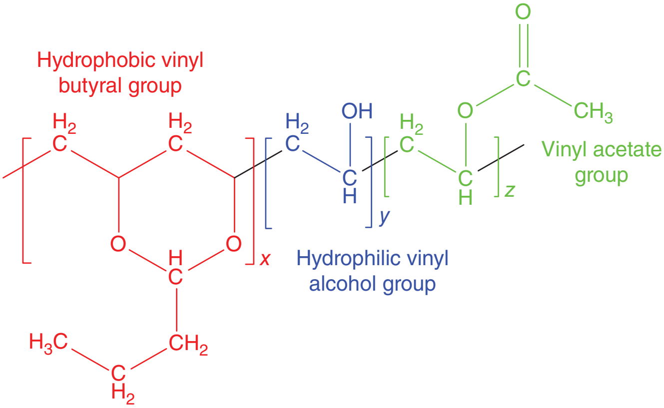

**Figure 5.2** Molecular structure of PVBA.

methanol-containing dissolved polymer at a concentration of 6%. PVBA protection performance was calculated to be around 81% using EIS and PDP. PVBA acted through adsorption on copper surfaces, involving noncovalent interactions between methanol hydroxyl groups and polyvinyl alcohol hydroxyl groups and hydrophobic interactions owing to vinyl butyral groups, with the metallic network acting as a suitable matrix for polymer macromolecules. Ghelichkhah et al. [85] studied polydopamine (PDA)'s coating performance for copper corrosion in 3.5% NaCl solution using PDP and EIS techniques. However, before PDA was coated onto the surface of metallic copper, nontoxic L-cysteine was first coated onto bare copper to improve PDA adhesion. The combined L-cysteine/PDA coating provided a high IE of 97.34%, whereas L-cysteine alone was 77.7%. Aromatic polyamides, also known as aramids, are good corrosion inhibitors due to the presence of π-electron-rich aromatic rings, nonbonding electrons containing oxygen and nitrogen.

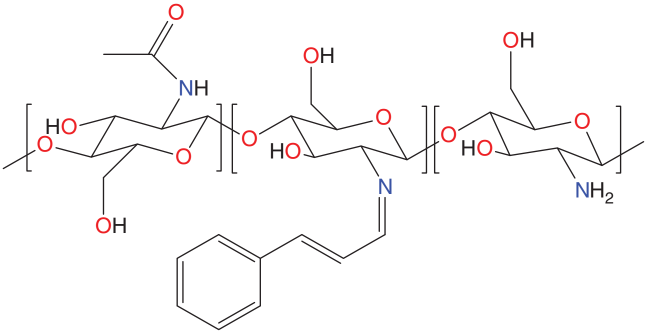

Figure 5.3 Molecular structure of CS-Cinn.

Additionally, they are categorized as high-performance polymers due to high mechanical and chemical resistance, excellent thermal stability, and low flammability. Farahati et al. [86] studied the corrosion of copper using sulfonated aromatic polyamide (SAP) as a corrosion inhibitor in 1 M HCl. SAP showed a good IE of 92% at a reasonable concentration of 500 ppm. SAP followed Langmuir adsorption isotherm and acted as a mixed-type inhibitor with cathodic predominance.

Being famous for its biocompatibility, biodegradability, and low toxicity, CS is an excellent corrosion inhibitor for it possesses amino and hydroxyl groups in the polymer structure. As CS has been reported to have an extraordinary affinity for copper, El Mouaden et al. [87] studied the influence of CS on copper corrosion in sulfide-polluted synthetic seawater (SSW). CS showed an IE of 89% at a concentration of 800 ppm following physical adsorption. El-Haddad [88] also studied the corrosion of copper using CS as a green corrosion inhibitor in 0.5 M HCl. CS was found to provide an IE of 95% for a meager concentration of $8 \times 10^{-6}$ M and acted as a mixed-type corrosion inhibitor. It is noteworthy that CS cannot impart IE to a great extent because of poor solubility in aqueous media and usually needs to be used at a high concentration. However, CS-forming Schiff bases with cinnamaldehyde (CS-Cinn), as reported by El Mouaden et al. [89], can increase its solubility and enable it to impart good IE in a more aggressive corrosive solution. CS-Cinn (Figure 5.3) showed an IE of about 90% at a concentration of $1000\,\mathrm{mg\,l^{-1}}$ in a very aggressive 1 M HCl solution. Sodium alginate, another green carbohydrate biopolymer, has been used by Jmiai et al. [90] as a corrosion inhibitor of copper in 1 M HCl. Different electrochemical measurements showed that the IE increased with increasing concentration, with the maximum IE of 83% being achieved at a concentration of $0.1\,\mathrm{mg\,l^{-1}}$.

### 5.2.6 Brass

Due to their superior electrical and thermal conductivities, good corrosion resistance, and ease of manufacturing, copper-based alloys are among the most important commercial metals. Brass, a $Cu_{30}Zn$ alloy, is suited for pipework, tube plates, water boxes, flanges, and pump casings in circulating systems, such as condensers, heat exchangers, and desalination plants because of its outstanding reliability and low maintenance. It is, nevertheless, sensitive to several types of corrosion, including chloride-induced pitting [91]. Corrosion inhibitors, much like they are used to protect other metals and alloys, are used for the protection of brass in different corrosive media as well. Fouda et al. [92] studied the corrosion behavior of α-brass in 1 M $HNO_3$ and PEG presence using different electrochemical techniques. A maximum IE of 85.2% was achieved for a PEG concentration of 300 ppm using the electrochemical frequency modulation (EFM) test. PEG was found to act as a mixed-type inhibitor and follow Langmuir adsorption isotherm. Atomic force microscopy (AFM) studied revealed the average surface roughness of the polished α-brass before 24 hours after immersion in 1 M $HNO_3$ to be 2.7 and 117.6 nm, and that of α-brass after 24 hours immersion in 1 M $HNO_3$ and 300 ppm to be 3.9 ppm, indicating the surface coverage provided by PEG in drastically corrosive 1 M $HNO_3$. Xu et al. [91] investigated the inhibitory impact of environment-friendly inhibitors PASP and $Na_2WO_4$ as well as the complex of PASP and $Na_2WO_4$ on brass corrosion in simulated cooled water solutions. Whereas 20 ppm of PASP and 20 ppm of $Na_2WO_4$ showed IEs of 50.3% and 61.4% separately, that of 20 ppm of mixed inhibitors (17.14 ppm PASP + 2.86 ppm $Na_2WO_4$) was found to be 93.4%. The inhibitor mix was found to be anodic in nature.

## 5.3 Industrial Applications of Water-Soluble Polymeric Corrosion Inhibitors

Corrosion is responsible for enormous economic and structural losses across many industries, such as pulp and paper, petroleum refining, food processing, oil and gas exploration, production and chemical, and petroleum and pharmaceuticals. However, these losses can be minimized and even stopped by accepting appropriate corrosion control methods. Corrosion inhibitors have tremendous implications in minimizing corrosion rate and saving economy and structures. The highly concentrated acidic solution is used for various industrial purposes. Acid pickling is a widely known acidic process used to remove rust and surface impurities of wires, metal plates, pipelines, and metal equipment in various industries. Different acidic solutions, such as sulfuric acid, nitric acid, hydrochloric acid, phosphoric acid, sulfamic acid, hydrofluoric acid, and citric acid, are used for this purpose. However, these acidic solutions are highly aggressive toward metallic structures and can cause structural failures.

Additionally, the acid treatment procedure can produce molecular hydrogen that can penetrate the metallic structures to cause hydrogen embrittlement. Therefore, corrosion inhibitors are added to the acid solutions to protect the metals. Another process in the petroleum industries known as oil-well acidizing requires the addition of highly concentrated hydrochloric acid (mostly 15–28%) to the well through a metallic pipe to enhance oil flow. This high concentration of hydrochloric acid can cause extensive corrosion of the metallic surface during the acidification

**Table 5.4** Some water-soluble polymers for different industrial applications.

| Structure and name | Corrosive medium | Metal | Applications | Reference |
|---|---|---|---|---|
| 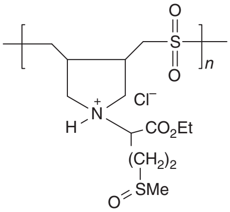 Poly(*N*,*N*-diallylmethionine sulfoxide ethyl ester hydrochloride-alt-sulfur dioxide) | 1 M HCl | Mild steel | Acid cleaning | [94] |
| 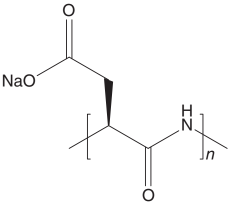 PASP | 3% NaCl aerated solution | Mild steel | Cooling systems | [95] |
| 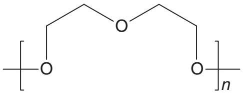 Polyethylene oxide | 1% NaCl | Iron | Pipeline corrosion | [70] |

|  |  |  |  |  |
|---|---|---|---|---|
| 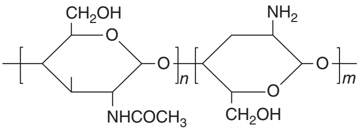<br>Chitosan | Sulfide-containing synthetic seawater | Copper | Marine application | [87] |
| 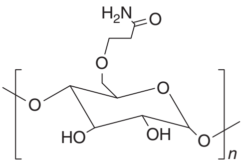<br>Cassava starch-acrylamide graft copolymer (CS-AAGC) | 1 M $H_3PO_4$ | Aluminum | Acid pickling and electro-polishing | [83] |
| 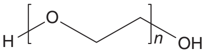<br>PEG | 1 M $HNO_3$ | α-Brass alloy | Acid pickling and cleaning | [92] |

process. Hence, external additives known as corrosion inhibitors are required to be added to the acidizing solution [93]. Corrosion is almost inevitable happen to materials located on or near water bodies and is a big issue in the field of marine engineering. Salt in water and air is corrosive to the exposed metal surfaces and can also contribute to the growth of different corrosive organisms. The instrument, electronic gadgets, wiring, and other equipment become useless if they get exposed to marine corrosion. Polymers containing different metal-binding moieties repeated along with the chain length and extraordinary surface-coverage ability are a significant focus of today's corrosion inhibition research. Some of the water-soluble polymers that have been developed for applications across different industries are tabulated in Table 5.4.

## 5.4 Conclusions

This chapter focused on the application of different categories of water-soluble polymers, both synthetic and natural, as corrosion inhibitors of various metals and alloys, including mild steel, carbon steel, iron, aluminum, copper, and brass. It was realized that polymers should have certain hydrophilic functionalities, such as carboxylic, alcoholic, amine, and ester, that would render them water-soluble. Basically, these same functionalities are also the ones that would help water-soluble polymers to undergo adsorption onto metal surfaces for protection against different corrosive media. Additionally, it is also expected that the polymers would have hydrophobic moiety that can repel water away from the metal surface in a corrosive solution. Since mild steel and carbon steel have widespread applications across many industries, it is natural that water-soluble polymers developed for their protection are present in plenty of literature. However, we believe that researchers should also focus on finding suitable water-soluble polymers for pure metals and other alloys. Polymers' unique advantage of possessing multiple adsorption centers repeated along with the entire chain length helps them to blanket the metal surface better than other small-molecule inhibitors. A significant trend in the corrosion protection research community is finding green corrosion inhibitors to replace the existing toxic ones that pose a threat to human health and the environment. Besides, this chapter also discussed green, naturally occurring water-soluble polymers to a great extent. Even though naturally occurring polymers are not yet on par with the synthetic ones in terms of IE, researchers are continually trying to prepare different modified natural polymers that offer the best of both worlds. With increased industrialization and infrastructure development happening across the globe, corrosion research will inevitably draw more attention. As one of the significant classes of corrosion inhibitors, polymers will also keep drawing attention.

## Acknowledgments

The authors gratefully acknowledge the research facilities provided by King Fahd University of Petroleum & Minerals (KFUPM), Dhahran, Saudi Arabia.

## References

**1** McCafferty, E. (2010). *Introduction to Corrosion Science*. New York: Springer-Verlag.

**2** Aljeaban, N.A., Goni, L.K.M.O., Alharbi, B.G. et al. (2020). Polymers decorated with functional motifs for mitigation of steel corrosion: an overview. *International Journal of Polymer Science* 2020: 1–23.

**3** Javaherdashti, R. (2000). How corrosion affects industry and life. *Anti-Corrosion Methods and Materials* 47 (1): 30–34.

**4** Koch, G., Varney, J., Thompson, N. et al. (2016). *International Measures of Prevention, Application, and Economics of Corrosion Technologies Study*. NACE International.

**5** Umoren, S.A. and Solomon, M.M. (2020). Polymeric corrosion inhibitors for oil and gas industry. In: *Corrosion Inhibitors in the Oil and Gas Industry* (ed. V.S. Saji and S.A. Umoren), 303–320. Weinheim: Wiley-VCH.

**6** Goni, L.K.M.O., Mazumder, M.A.J., Quraishi, M.A., and Rahman, M.M. (2021). Bioinspired heterocyclic compounds as corrosion inhibitors: a comprehensive review. *Chemistry, An Asian Journal* 16: 1324–1364.

**7** Goni, L.K.M.O. and Mazumder, M.A.J. (2019). Green corrosion inhibitors. In: *Corrosion Inhibitors* (ed. A. Singh), 77–94. London: IntechOpen.

**8** Tiu, B.D.B. and Advincula, R.C. (2015). Polymeric corrosion inhibitors for the oil and gas industry: Design principles and mechanism. *Reactive & Functional Polymers* 95: 25–45.

**9** Sudhakar, C.K., Upadhyay, N., Jain, A. et al. (2015). Hydrogels-promising candidates for tissue engineering. In: *Nanotechnology Applications for Tissue Engineering* (ed. S. Thomas, Y. Grohens and N. Ninan), 77–94. Oxford: Elsevier Inc.

**10** Rivas, B.L., Urbano, B.F., and Sánchez, J. (2018). Water-soluble and insoluble polymers, nanoparticles, nanocomposites and hybrids with ability to remove Hazardous inorganic pollutants in water. *Frontiers in Chemistry* 6 (JUL): 1–13.

**11** Geethanjali, R. and Subhashini, S. (2018). Synthesis and kinetics of corrosion inhibition of water-soluble terpolymer of polyvinyl alcohol functionalized with vinyl sulfonate and p-vinyl benzene sulfonate, in molar HCl. *Journal of Bio- and Tribo-Corrosion* 4 (4): 1–13.

**12** Sabirneeza, A.A.F. and Subhashini, S. (2014). Poly(vinyl alcohol–proline) as corrosion inhibitor for mild steel in 1M hydrochloric acid. *International Journal of Industrial Chemistry* 5 (3–4): 111–120.

**13** Abdul Rahiman, A.F.S. and Sethumanickam, S. (2017). Corrosion inhibition, adsorption and thermodynamic properties of poly(vinyl alcohol-cysteine) in molar HCl. *Arabian Journal of Chemistry* 10: S3358–S3366.

**14** Karthikaiselvi, R. and Subhashini, S. (2017). The water-soluble composite poly(vinylpyrrolidone–methylaniline): a new class of corrosion inhibitors of mild steel in hydrochloric acid media. *Arabian Journal of Chemistry* 10: S627–S635.

**15** Geethanjali, R. and Subhashini, S. (2016). Synthesis of water-soluble acryl terpolymers and their anticorrosion properties on mild steel in 1 mol·L-1 HCl. *Chinese Journal of Chemical Engineering* 24 (4): 543–552.

**16** Geethanjali, R., Sabirneeza, A.A.F., and Subhashini, S. (2014). Water-soluble and biodegradable pectin-grafted- polyacrylamide and pectin-grafted polyacrylic acid: electrochemical investigation of corrosion-inhibition behaviour on mild steel in 3.5% NaCl media. *Indian Journal of Materials Science* 2014: 1–9.

**17** Kumar, S., Vashisht, H., Olasunkanmi, L.O. et al. (2016). Experimental and theoretical studies on the inhibition of mild steel corrosion by some synthesized polyurethane tri-block copolymers. *Scientific Reports* 6 (March): 1–18.

**18** Syed, J.A., Tang, S., Lu, H., and Meng, X. (2015). Water-soluble polyaniline-polyacrylic acid composites as efficient corrosion inhibitors for 316ss. *Industrial & Engineering Chemistry Research* 54 (11): 2950–2959.

**19** Solomon, M.M. and Umoren, S.A. (2016). In-situ preparation, characterization and anticorrosion property of polypropylene glycol/silver nanoparticles composite for mild steel corrosion in acid solution. *Journal of Colloid and Interface Science* 462: 29–41.

**20** Srimathi, M., Rajalakshmi, R., and Subhashini, S. (2014). Polyvinyl alcohol-sulphanilic acid water-soluble composite as corrosion inhibitor for mild steel in hydrochloric acid medium. *Arabian Journal of Chemistry* 7 (5): 647–656.

**21** Ali Fathima Sabirneeza, A. and Subhashini, S. (2013). A novel water-soluble, conducting polymer composite for mild steel acid corrosion inhibition. *Journal of Applied Polymer Science* 127 (4): 3084–3092.

**22** Tsoeunyane, M.G., Makhatha, M.E., and Arotiba, O.A. (2019). Corrosion inhibition of mild steel by poly(butylene succinate)-L-histidine extended with 1,6-diisocynatohexane polymer composite in 1 M HCl. *International Journal of Corrosion* 2019: 7406409.

**23** Quadri, T.W., Olasunkanmi, L.O., Fayemi, O.E. et al. (2017). Zinc oxide nanocomposites of selected polymers: synthesis, characterization, and corrosion inhibition studies on mild steel in HCl solution. *ACS Omega* 2 (11): 8421–8437.

**24** Biswas, A., Pal, S., and Udayabhanu, G. (2015). Experimental and theoretical studies of xanthan gum and its graft copolymer as corrosion inhibitor for mild steel in 15% HCl. *Applied Surface Science* 353: 173–183.

**25** Sanumi, O.J., Saliu, O.D., and Makhatha, M.E. (2021). Alternative surface localization studies and electrochemical investigation of tyrosine hybridized poly (ethylene glycol) for corrosion inhibition of mild steel. *Journal of Materials Reserach and Technology* 13: 700–715.

**26** Karthikaiselvi, R. and Subhashini, S. (2014). Study of adsorption properties and inhibition of mild steel corrosion in hydrochloric acid media by water-soluble composite poly (vinyl alcohol-o-methoxy aniline). *Journal of the Association of Arab Universities of Basic and Applied Sciences* 16: 74–82.

**27** Sharifi, Z., Pakshir, M., Amini, A., and Rafiei, R. (2019). Hybrid graphene oxide decoration and water-based polymers for mild steel surface protection in saline environment. *Journal of Industrial and Engineering Chemistry* 74: 41–54.

**28** Shamsheera, K.O., Prasad, A.R., Garvasis, J. et al. (2019). Stearic acid grafted chitosan/epoxy blend surface coating for prolonged protection of mild steel in saline environment. *Journal of Adhesion Science and Technology* 33 (20): 2250–2264.

**29** Mekhiche, L., Maouche, N., Nessark, B. et al. (2021). Composites of polyanine/CdTe for corrosion protection of mild steel XC 70 in a 3.5% NaCl solution. *Journal of Adhesion Science and Technology* 35 (23): 2602–2624.

**30** Rangel-Olivares, F.R., Arce-Estrada, E.M., and Cabrera-Sierra, R. (2021). Synthesis and characterization of polyaniline-based polymer nanocomposites as anti-corrosion coatings. *Coatings* 11 (6): 1–20.

**31** Qiu, S., Chen, C., Zheng, W. et al. (2017). Long-term corrosion protection of mild steel by epoxy coating containing self-doped polyaniline nanofiber. *Synthetic Metals* 229 (May): 39–46.

**32** Ma, Y., Zhou, T., Zhu, W. et al. (2020). Understanding the anticorrosive mechanism of a cross-linked supramolecular polymer for mild steel in the condensate water: comprehensive experimental, molecular docking, and molecular dynamics investigations. *Journal of Molecular Modeling* 26 (4): 81.

**33** Finšgar, M., Fassbender, S., Nicolini, F., and Milošev, I. (2009). Polyethyleneimine as a corrosion inhibitor for ASTM 420 stainless steel in near-neutral saline media. *Corrosion Science* 51 (3): 525–533.

**34** Chen, T., Chen, M., Chen, Z., and Fu, C. (2021). Comprehensive investigation of modified polyethyleneimine as an efficient polymeric corrosion inhibitor in neutral medium: synthesis, experimental and theoretical assessments. *Journal of Molecular Liquids* 339: 116803.

**35** Devi, G.N., Saranya, J., Manjubaashini, N. et al. (2017). Polyamidoamino-epichlorohydrin resin a novel synthetic anti-corrosive water-soluble polymer for mild steel. *Progress in Organic Coatings* 109 (April): 117–125.

**36** Dwivedi, A., Bharti, P.K., and Shukla, S.K. (2018). Interaction of water-soluble polyacrylic acid with mild steel / hydrochloric acid interface. *IOP Conference Series: Materials Science and Engineering* 404 (1): 1–11.

**37** Anyiam, C.K., Ogbobe, O., Oguzie, E.E., and Madufor, I.C. (2020). Synergistic study of modified sweet potato starch and KI for corrosion protection of mild steel in acidic media. *Journal of Bio- and Tribo-Corrosion* 6 (3): 1–10.

**38** Umoren, S.A. and Solomon, M.M. (2015). Effect of halide ions on the corrosion inhibition efficiency of different organic species - a review. *Journal of Industrial and Engineering Chemistry* 21: 81–100.

**39** Aslam, R., Mobin, M., Aslam, J. et al. (2019). Inhibitory effect of sodium carboxymethylcellulose and synergistic biodegradable Gemini surfactants as effective inhibitors for MS corrosion in 1 M HCl. *Journal of Materials Research and Technology* 8 (5): 4521–4533.

**40** Mobin, M. and Rizvi, M. (2016). Inhibitory effect of xanthan gum and synergistic surfactant additives for mild steel corrosion in 1 M HCl. *Carbohydrate Polymers* 136: 384–393.

**41** Pal, A., Dey, S., and Sukul, D. (2016). Effect of temperature on adsorption and corrosion inhibition characteristics of gelatin on mild steel in hydrochloric acid medium. *Research on Chemical Intermediates* 42 (5): 4531–4549.

**42** Fiori-Bimbi, M.V., Alvarez, P.E., Vaca, H., and Gervasi, C.A. (2015). Corrosion inhibition of mild steel in HCL solution by pectin. *Corrosion Science* 92: 192–199.

**43** Basik, M. and Mobin, M. (2020). Chondroitin sulfate as potent green corrosion inhibitor for mild steel in 1 M HCl. *Journal of Molecular Structure* 1214: 128231.

**44** Banerjee, S., Srivastava, V., and Singh, M.M. (2012). Chemically modified natural polysaccharide as green corrosion inhibitor for mild steel in acidic medium. *Corrosion Science* 59: 35–41.

**45** Luo, X., Pan, X., Yuan, S. et al. (2017). Corrosion inhibition of mild steel in simulated seawater solution by a green eco-friendly mixture of glucomannan (GL) and bisquaternary ammonium salt (BQAS). *Corrosion Science* 125 (October 2016): 139–151.

**46** Zhang, Q.H., Hou, B.S., Li, Y.Y. et al. (2020). Two novel chitosan derivatives as high efficient eco-friendly inhibitors for the corrosion of mild steel in acidic solution. *Corrosion Science* 164: 108346.

**47** Chai, C., Xu, Y., Xu, Y. et al. (2020). Dopamine-modified polyaspartic acid as a green corrosion inhibitor for mild steel in acid solution. *European Polymer Journal* 137 (April): 109946.

**48** Rbaa, M., Fardioui, M., Verma, C. et al. (2020). 8-Hydroxyquinoline based chitosan derived carbohydrate polymer as biodegradable and sustainable acid corrosion inhibitor for mild steel: experimental and computational analyses. *International Journal of Biological Macromolecules* 155: 645–655.

**49** Sangeetha, Y., Meenakshi, S., and Sairam Sundaram, C. (2016). Corrosion inhibition of aminated hydroxyl ethyl cellulose on mild steel in acidic condition. *Carbohydrate Polymers* 150: 13–20.

**50** Zhang, K., Yang, W., Yin, X. et al. (2018). Amino acids modified konjac glucomannan as green corrosion inhibitors for mild steel in HCl solution. *Carbohydrate Polymers* 181 (September 2017): 191–199.

**51** Zhang, W., Nie, B., Li, H.J. et al. (2021). Inhibition of mild steel corrosion in 1 M HCl by chondroitin sulfate and its synergistic effect with sodium alginate. *Carbohydrate Polymers* 260 (December 2020): 117842.

**52** Migahed, M.A., Rashwan, S.M., Kamel, M.M., and Habib, R.E. (2016). Synthesis, characterization of polyaspartic acid-glycine adduct and evaluation of their performance as scale and corrosion inhibitor in desalination water plants. *Journal of Molecular Liquids* 224: 849–858.

**53** Gowraraju, N.D., Jagadeesan, S., Ayyasamy, K. et al. (2017). Adsorption characteristics of Iota-carrageenan and Inulin biopolymers as potential corrosion inhibitors at mild steel/sulphuric acid interface. *Journal of Molecular Liquids* 232: 9–19.

**54** Biswas, A., Mourya, P., Mondal, D. et al. (2018). Grafting effect of gum acacia on mild steel corrosion in acidic medium: gravimetric and electrochemical study. *Journal of Molecular Liquids* 251: 470–479.

**55** Fetouh, H.A., Hefnawy, A., Attia, A.M., and Ali, E. (2020). Facile and low-cost green synthesis of eco-friendly chitosan-silver nanocomposite as novel and promising corrosion inhibitor for mild steel in chilled water circuits. *Journal of Molecular Liquids* 319: 114355.

**56** Ma, Y., Fan, B., Zhou, T. et al. (2019). Molecular assembly between weak crosslinking cyclodextrin polymer and Trans-cinnamaldehyde for corrosion inhibition towards mild steel in 3.5% NaCl solution: experimental and theoretical studies. *Polymers (Basel)* 11 (4, 635).

**57** Erna, M., Herdini, H., and Futra, D. (2019). Corrosion inhibition mechanism of mild steel by amylose-acetate/carboxymethyl chitosan composites in acidic media. *International Journal of Chemical Engineering* 2019: 1–12.

**58** Nwanonenyi, S.C., Obasi, H.C., and Chidiebere, A.M. (2018). Inhibitive performance of carboxymethyl cellulose and additives on corrosion of carbon steel in acidic and alkaline environments. *Journal of Bio- and Tribo-Corrosion* 4 (3): 1–12.

**59** Ma, X., Wang, J., Xu, J. et al. (2019). Sunflower head pectin with different molecular weights as promising green corrosion inhibitors of carbon steel in hydrochloric acid solution. *ACS Omega* 4 (25): 21148–21160.

**60** Mobin, M., Rizvi, M., Olasunkanmi, L.O., and Ebenso, E.E. (2017). Biopolymer from Tragacanth gum as a green corrosion inhibitor for carbon steel in 1 M HCl solution. *ACS Omega* 2 (7): 3997–4008.

**61** Nwanonenyi, S.C., Obasi, H.C., Udochukwu, M. et al. (2022). Protection by a polymer composite on carbon steel surface in 1.0 M HCl environment: a combined experimental and theoretical approach. *Brazilian Journal of Chemical Engineering* 39 (1): 159–173.

**62** Quraishi, M.A., Ansari, K.R., Chauhan, D.S. et al. (2020). Vanillin modified chitosan as a new bio-inspired corrosion inhibitor for carbon steel in oil-well acidizing relevant to petroleum industry. *Cellulose* 27 (11): 6425–6443.

**63** Zhang, Q.H., Hou, B.S., Li, Y.Y. et al. (2021). Dextran derivatives as highly efficient green corrosion inhibitors for carbon steel in CO2-saturated oilfield produced water: experimental and theoretical approaches. *Chemical Engineering Journal* 424: 130519.

**64** Verma, C., Ebenso, E.E., and Quraishi, M.A. (2017). Corrosion inhibitors for ferrous and non-ferrous metals and alloys in ionic sodium chloride solutions: a review. *Journal of Molecular Liquids* 248: 927–942.

**65** Umoren, S.A., Li, Y., and Wang, F.H. (2010). Electrochemical study of corrosion inhibition and adsorption behaviour for pure iron by polyacrylamide in H2SO4: synergistic effect of iodide ions. *Corrosion Science* 52 (5): 1777–1786.

**66** Jeyaprabha, C., Sathiyanarayanan, S., and Venkatachari, G. (2005). Co-adsorption effect of polyaniline and halide ions on the corrosion of iron in 0.5 M H2SO4 solutions. *Journal of Electroanalytical Chemistry* 583 (2): 232–240.

**67** Rajeswari, V., Kesavan, D., Gopiraman, M., and Viswanathamurthi, P. (2013). Physicochemical studies of glucose, gellan gum, and hydroxypropyl cellulose - inhibition of cast iron corrosion. *Carbohydrate Polymers* 95 (1): 288–294.

**68** Jeyaprabha, C., Sathiyanarayanan, S., Phani, K.L.N., and Venkatachari, G. (2005). Influence of poly(aminoquinone) on corrosion inhibition of iron in acid media. *Applied Surface Science* 252 (4): 966–975.

**69** Al-Gorair, A.S., Hawsawi, H., Fawzy, A. et al. (2021). Evaluation of the anticorrosion and adsorption properties of polyethylene glycol and polyvinyl alcohol for corrosion of iron in 1.0 M NaCl solution. *International Journal of Electrochemical Science* 16: 1–19.

**70** Sudiarti, T., Silviayanadewi, A.Y., and Supriadin, A. (2019). The effect of concentration and temperature on the activities of polyethylene oxide (PEO) as iron corrosion inhibitor in electrolyte solution of NaCl. *Journal of Physics: Conference Series* 1402 (5): 1–6.

**71** Sathiyanarayanan, S., Jeyaprabha, C., and Venkatachari, G. (2008). Influence of metal cations on the inhibitive effect of polyaniline for iron in 0.5 M $H_2SO_4$. *Materials Chemistry and Physics* 107 (2–3): 350–355.

**72** Jeyaprabha, C., Sathiyanarayanan, S., and Venkatachari, G. (2006). Polyaniline as corrosion inhibitor for iron in acid solutions. *Journal of Applied Polymer Science* 101 (4): 2144–2153.

**73** Manivel, P., Sathiyanarayanan, S., and Venkatachari, G. (2008). Synthesis of poly(p-phenylenediamine) and its corrosion inhibition effect on iron in 1M HCl. *Journal of Applied Polymer Science* 110 (5): 2807–2814.

**74** Manivel, P. and Venk (2007). The inhibitive effect of poly(p-toluidine) on corrosion of iron in 1M HCl solutions. *Journal of Applied Polymer Science* 104 (4): 2595–2601.

**75** Nwanonenyi, S.C., Obasi, H.C., and Eze, I.O. (2019). Hydroxypropyl cellulose as an efficient corrosion inhibitor for aluminium in acidic environments: experimental and theoretical approach. *Chemistry Africa* 2 (3): 471–482.

**76** Punitha, R., Kirupha, S.D., Vivek, S., and Ravikumar, L. (2019). Synthesis and corrosion inhibition studies of modified polyacrylic acid bearing triazole moieties on aluminium in alkaline medium. *Journal of Polymer Reserach* 26 (12): 1–12.

**77** Zaafarany, I. (2012). Corrosion inhibition of aluminum in aqueous alkaline solutions by alginate and pectate water-soluble natural polymer anionic polyelectrolytes. *Portugaliae Electrochimica Acta* 30 (6): 419–426.

**78** Arukalam, I.O., Nleme, I.K., and Anyanwu, A.E. (2011). Comparative inhibitive effect of hydroxyethylcellulose on mild steel and aluminium corrosion in 0.5 M HCl solution. *Academic Research International* 1 (3): 492–498.

**79** Hassan, R.M., Ibrahim, S.M., Takagi, H.D., and Sayed, S.A. (2018). Kinetics of corrosion inhibition of aluminum in acidic media by water-soluble natural polymeric chondroitin-4-sulfate as anionic polyelectrolyte inhibitor. *Carbohydrate Polymers* 192 (March): 356–363.

**80** Babaladimath, G., Vishalakshi, B., and Nandibewoor, S.T. (2018). Electrical conducting Xanthan Gum-graft-polyaniline as corrosion inhibitor for aluminum in hydrochloric acid environment. *Materials Chemistry and Physics* 205: 171–179.

**81** Fares, M.M., Maayta, A.K., and Al-Qudah, M.M. (2012). Pectin as promising green corrosion inhibitor of aluminum in hydrochloric acid solution. *Corrosion Science* 60: 112–117.

**82** Fares, M.M., Maayta, A.K., and Al-Mustafa, J.A. (2012). Corrosion inhibition of iota-carrageenan natural polymer on aluminum in presence of zwitterion mediator in HCl media. *Corrosion Science* 65: 223–230.

**83** Deng, S., Li, X., and Du, G. (2021). An efficient corrosion inhibitor of cassava starch graft copolymer for aluminum in phosphoric acid. *Chinese Journal of Chemical Engineering* 37: 222–231.

**84** Chauhan, D.S., Madhan Kumar, A., and Quraishi, M.A. (2019). Hexamethylenediamine functionalized glucose as a new and environmentally benign corrosion inhibitor for copper. *Chemical Engineering Reserach and Design* 150: 99–115.

**85** Ghelichkhah, Z., Sharifi-Asl, S., Farhadi, K. et al. (2015). L-cysteine/polydopamine nanoparticle-coatings for copper corrosion protection. *Corrosion Science* 91: 129–139.

**86** Farahati, R., Ghaffarinejad, A., Rezania, H.(J.). et al. (2019). Sulfonated aromatic polyamide as water-soluble polymeric corrosion inhibitor of copper in HCl. *Colloids and Surfaces A: Physicochemical and Engineering Aspects* 578: 1–8.

**87** El Mouaden, K., El Ibrahimi, B., Oukhrib, R. et al. (2018). Chitosan polymer as a green corrosion inhibitor for copper in sulfide-containing synthetic seawater. *International Journal of Biological Macromolecules* 119: 1311–1323.

**88** El-Haddad, M.N. (2013). Chitosan as a green inhibitor for copper corrosion in acidic medium. *International Journal of Biological Macromolecules* 55: 142–149.

**89** El Mouaden, K., Chauhan, D.S., Quraishi, M.A. et al. (2020). Cinnamaldehyde-modified chitosan as a bio-derived corrosion inhibitor for acid pickling of copper: microwave synthesis, experimental and computational study. *International Journal of Biological Macromolecules* 164: 3709–3717.

**90** Jmiai, A., El Ibrahimi, B., Tara, A. et al. (2018). Alginate biopolymer as green corrosion inhibitor for copper in 1 M hydrochloric acid: experimental and theoretical approaches. *Journal of Molecular Structure* 1157: 408–417.

**91** Xu, Q.J., Zhou, G.D., Wang, H.F., and Cai, W.-B. (2006). Electrochemical studies of polyaspartic acid and sodium tungstate as corrosion inhibitors for brass and Cu30Ni alloy in simulated cooled water solutions. *Anti-Corrosion Methods and Materials* 53 (4): 207–211.

**92** Fouda, A.S., El-Dossoki, F.I., and Shady, I.A. (2018). Adsorption and corrosion inhibition behavior of polyethylene glycol on α-brass alloy in nitric acid solution. *Green Chemistry Letters and Reviews* 11 (2): 67–77.

**93** Verma, C., Ebenso, E.E., Quraishi, M.A., and Hussain, C.M. (2021). Recent developments in sustainable corrosion inhibitors: design, performance, and industrial-scale applications. *Materials Advances* 2 (12): 3806–3850.

**94** Goni, L.K.M.O., Mazumder, M.A.J., Ali, S.A. et al. (2019). Biogenic amino acid methionine-based corrosion inhibitors of mild steel in acidic media. *International Journal of Minerals, Metallurgy, and Materials* 26 (4): 467–482.

**95** Zeino, A., Abdulazeez, I., Khaled, M. et al. (2018). Mechanistic study of polyaspartic acid (PASP) as eco-friendly corrosion inhibitor on mild steel in 3% NaCl aerated solution. *Journal of Molecular Liquids* 250: 50–62.

# 6

# High-Temperature Polymeric Corrosion Inhibitors

*Jiyaul Haque*[1], *Mumtaz A. Quraishi*[2], *and Wan M.N.B. Wan Nik*[1]

[1] *Universiti Malaysia Terengganu, Faculty of Ocean Engineering Technology and Informatics, Kuala Nerus 21030, Malaysia*
[2] *King Fahd University of Petroleum and Minerals, Interdisciplinary Research Center for Advanced Materials, Dhahran 31261, Saudi Arabia*

## 6.1 Introduction

The oil and gas industries have corrosion issues in every sector, such as production, refinery, transportation, and storage, due to the presence of corrosion-causing agents: acids, brine, $CO_2$, $H_2S$, and naphthenic acid [1]. Although steel is more susceptible to corrosion, commonly used in oil and gas industries. High temperature involves in oil-well acidizing and refinery sections cause serious corrosion on metallic equipment.

Corrosion cannot be completely stopped, it can be minimized using different techniques, such as proper design, material section, cathodic protection, coating, and inhibitor. The use of inhibitors is economical and easy to apply in the oil and gas sector compare to other techniques. Moreover, in internal corrosion, the inhibitor is used as the first line of defense.

In the oil and gas industries, inhibitor formulation for high temperatures is a big challenge, because the rate of corrosion is very high at elevated temperatures [2]. So, few inorganic and organic inhibitors have been developed for high-temperature corrosion. However, these inhibitors have some issues, such as inorganic-based inhibitors: chromate, phosphate, and molybdenum, which are highly toxic, and the organic-based inhibitors: amine, triazole, and imidazolines, which are costly due to tedious synthesis process [3, 4].

Polymer is a macromolecule that is made up of repeating units of atoms and groups (monomers), which link together chemically. The polymer has a great significance to use as a corrosion inhibitor for high-temperature corrosion because of its thermally stability, availability, eco-friendly, cost-effective, and possess multiple adsorption centers [5]. This chapter discusses the application of polymer corrosion

*Polymeric Corrosion Inhibitors for Greening the Chemical and Petrochemical Industry*, First Edition.
Edited by Mohammad A. Jafar Mazumder, Mumtaz A. Quraishi, and Amir Al-Ahmed.

inhibitors in the mitigation of high-temperature corrosion in oil-well acidizing, sweet and sour corrosion, naphthenic acids corrosion, and computational studies of polymer corrosion inhibitors.

## 6.2 Polymer as Corrosion Inhibitor for High-Temperature Oil-Well Acidization

Acidization is a technique, which enhances the oil production from the oil well. It is done by forcing the hot acid solution into the down well. This solution breakdown the rock and open the new oil-flow channels for reaching oil and gas to the well. The acids are used based on the dissolution of formation materials. For carbonate formation, hydrochloric acid (HCl) is used, which reacts with carbonate to form salt, carbon dioxide, and water. The metal chloride salt exhibits good solubility in water. Many other acids, such as sulfate, nitrate, and phosphate, are used, but they show low solubility compare to chloride [6]. Therefore, HCl or combined HCl and hydrofluoric acid (HF) are preferably used to dissolve the rock and other blockages. Generally, the oil-well tubing and casing are made up of low-carbon steel that is very susceptible to corrosion in acid solution. Hence, during acidization, hot acid corrodes very fast the well equipment. The deep well operates at a high temperature of up to 200 °C due to the tiredness of the primary well. This is a very challenging task, sometimes the acidization is failed. Overcoming the severe action of corrosive solution on low-carbon steel, the corrosion inhibitor is added to the acid solution during acidization.

Generally, thermally stable inhibitors are used at high concentrations, when processing temperature is 100 °C or higher. Some of the successful organic inhibitors have been implied at high temperatures, such as acetylenic alcohol [7–9], aromatic alcohol [10, 11], and the condensation product of aldehyde and ketone [12–17]. Most of these inhibitors are toxic in nature and non-eco-friendly. Therefore, researchers focus on developing environmentally benign corrosion inhibitors. Polymer is one of the most effective classes of corrosion inhibitors [18–20]. They contain many functional groups (alcohol, ether, amine, etc.) and a long hydrophobic carbon chain. These functional groups can help the inhibitor molecule to effectively interact with the metal surface and their hydrophobic carbon chain can cover the metallic surface resulted retard the interaction of corrosive ions.

Quaternary polymer is an effective acidizing corrosion inhibitor, which can show the corrosion inhibitor and achieve around 90% inhibition performance. Polyquaternary inhibitors have a cationic group that makes them easily dissolve in an aqueous solution and/or disperse over the metal surface. The quaternary polyamine has hydrophilic cationic sites and a long-corban chain. Hydrophilic cationic sites help polymer inhibitors to strongly adsorb on the metal surface and make the inhibitors thermally stable for longer protection. Annand and Woodson patented [21] for the study of corrosion inhibition of polyquaternary amine polymers, as shown in Figure 6.1. The polymers were prepared by the reaction of different alkyl halides and polyamines. The incorporated polyamines are derived from dipropylene

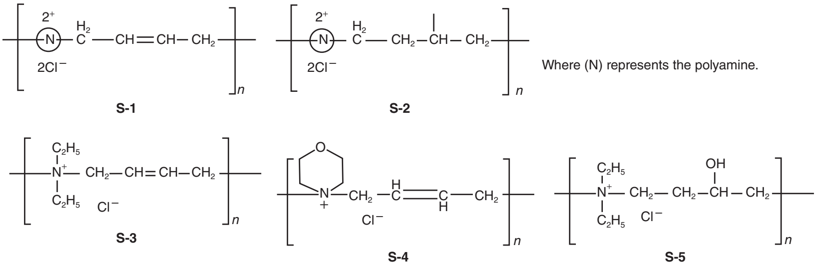

**Figure 6.1** Structure of polyquaternary amine polymers.

triamine, tripropylene tetramine, triethylenetetramine, tetrapropylene pentamine, and tetraethylene pentamine. Polyethyleneimines and polypropyleneimines are used as source of higher molecular weight polyamines. The author found that the partially quaternized amine polymers (S-1 and S-2) are less effective corrosion inhibitors compared to fully quaternized (S-3, S-4, and S-5). There are five inhibitors (S-1, S-2, S-3, S-4, and S-5) molecules that have been studied at 200 °F (Table 6.1).

Quinlan studied the difference between quaternary polymers (Figure 6.2) [22]. It found that the quaternary polyamines (Ex-1 and Ex-3) are more effective corrosion inhibitors and exhibited high inhibition efficiency (>90%) compared to nonquaternary polymers (Py2VP and Py2M5VP), which show an inhibition efficiency of less than 80% (Table 6.1). It has been observed that the quaternary polymer derived from poly(vinylpyridine–methylacrylate), poly(vinylpyridine–acrylic acid), and poly(vinylpiperidine) shows the effective inhibition performance. For example, the inhibition performance of Ex-2 (reaction product of 4-vinylpyridine and ethyl iodide) IE: 78% at inhibitor concentration of 2500 ppm at 200 °C. The polymer derived from the vinylalkylenimines, piperidine, vinylpyridine (having a nitrogen-containing heterocyclic compound), and polymers containing five of these heterocyclic groups of every 20 carbon in carbon chains, exhibit an excellent corrosion inhibitor.

Recently, Odewunmi et al. [23] studied the *N*1,*N*1-diallyl-*N*6,*N*6,*N*6-tripropylhexane-1,6-diaminium chloride (NDTHDC) and its polymer poly(*N*1,*N*1-diallyl-*N*6,*N*6,*N*6-tripropylhexane-1,6-diaminium chloride) (poly-NDTHDC) as corrosion inhibitors for API X60 steel in 15 wt% HCl using weight loss, electrochemical and surface analysis techniques. The structure of inhibitors is represented in Figure 6.3. It was found that the poly-NDTHDC exhibits better inhibition performance compared to NDTHDC. Temperature effect results (Figure 6.4a) show that corrosion rate increases with increasing the temperature and in presence of inhibitors, the corrosion rate decreased significantly at elevated temperature (90 °C). The corresponding inhibition efficiency and corrosion rate were found in presence of NDTHDC and poly-NDTHDC (Figure 6.4b).

Polysaccharides (e.g. chitosan and cellulose) are environmentally benign corrosion inhibition. Although it has several polar adsorption centers, shows low solubility and poor inhibition performance. Researchers have developed some modified forms of polysaccharides to improve their solubility, thermal stability, and

**Table 6.1** High-temperature corrosion inhibitors for oil-well acidization.

| Inhibitors | Metal/medium | Inhibition performance | Reference |
|---|---|---|---|
| Reaction product of polyethylenepolyamines (contain 1°, 2°, 3° amino and heterocyclic amines) and 1,4-dichlorobutene (S-1) | Mild steel in $H_2SO_4$ | Conc.: 0.25%<br>IE: 71.0% at 200 °F | [21] |
| Reaction product of polyethylene polyamines (contain 1°, 2°, 3° amino and heterocyclic amines) and with epichlorohydrin (S-2) | Mild steel in $H_2SO_4$ | Conc.: 0.25%<br>IE: 71.0% at 200 °F | [21] |
| Reaction product of diethylamine and 1,4-dichlorobutene (S-3) | Mild steel in $H_2SO_4$ | Conc.: 0.25%<br>IE: 90.0% at 200 °F | [21] |
| Reaction product of morpholine and 1,4-dichlorobutene (S-4) | Mild steel in $H_2SO_4$ | Concentration: 0.25%<br>IE: 85.0% at 200 °F | [21] |
| Reaction product of diethylamine and epichlorohydrin (S-5) | Mild steel in $H_2SO_4$ | Conc.: 0.25%<br>IE: 90.0% at 200 °F | [21] |
| Poly-2-methyl-5-vinylpyridine (Py2M5VP) | Mild steel in 15% HCl | Conc.: 4000 ppm<br>IE: 78.0% at 200 °F | [22] |
| Poly-2-vinylpyridine (Py2VP) | Mild steel in 15% HCl | Conc.: 4000 ppm<br>IE: 79.5.0% at 200 °F | [22] |
| Reaction product of 4-vinylpyridine and benzyl chloride (Ex-1) | Mild steel in 15% HCl | Conc.: 2000 ppm<br>IE: 93.0% at 200 °F | [22] |
| Reaction product of 4-vinylpyridine and ethyl iodide (Ex-2) | Mild steel in 15% HCl | Conc.: 2500 ppm<br>IE: 99.50% at 200 °F | [22] |
| *N*1,*N*1-Diallyl-*N*6,*N*6,*N*6-tripropylhexane-1,6-diaminium chloride (NDTHDC) | API X60 carbon in 15 wt% HCl | Conc.: 1000 ppm<br>IE: 89.2% at 60 °C,<br>IE: 73.4% at 90 °C | [23] |
| Poly(*N*1,*N*1-diallyl-*N*6,*N*6,*N*6-tripropylhexane-1,6-diaminium chloride) (poly-NDTHDC) | API X60 carbon in 15 wt% HCl | Conc.: 100 ppm<br>IE: 90.2% at 60 °C,<br>IE: 87.5% at 90 °C | [23] |
| Schiff base of chitosan with cinnamaldehyde (Cinn-Cht) | Carbon steel corrosion in 15% HCl | Conc.: 400 mg $l^{-1}$<br>IE: 85.16% at 35 °C | [24] |
| Schiff base of chitosan with cinnamaldehyde (Cinn-Cht) + KI | Carbon steel corrosion in 15% HCl | Conc.: 400 mg $L^{-1}$ + 10 mM KI<br>IE: 92.45% at 35 °C | [24] |
| Chitosan/silver nanoparticles (AgNPs/chitosan) composite | ST37 steel in 15% HCl | Conc.: 1000 ppm<br>IE: 87.88% at 25 °C,<br>IE: 97.09% at 60 °C | [25] |
| Carboxymethyl cellulose/silver nanoparticles composite (CMC/AgNPs) | ST37 steel in 15% $H_2SO_4$ | Conc.: 1000 ppm<br>IE: 93.94% 25 °C,<br>IE = 96.37% at 60 °C | [26] |

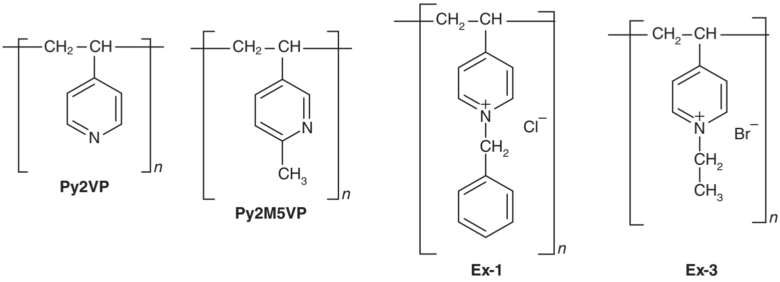

**Figure 6.2** Structure of nonquaternary polymers (Py2VP and Py2M5VP) and quaternary polyamines (Ex-1 and Ex-3).

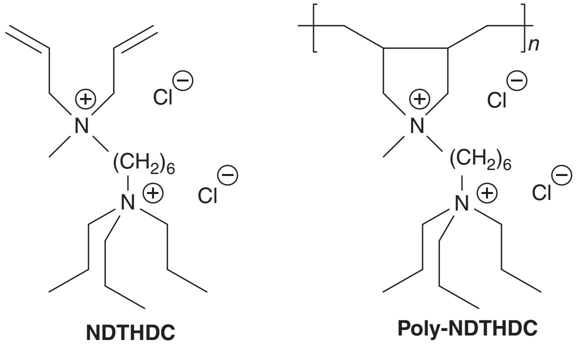

**Figure 6.3** Structure of monomer (NDTHDC) and polymer (poly-NDTHDC) inhibitors.

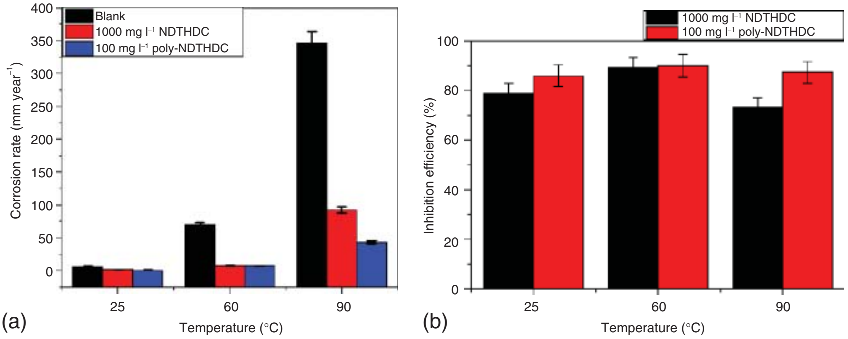

**Figure 6.4** Comparative bar chart showing the effect of temperature on the (a) corrosion rate of API X60 steel and (b) inhibition efficiency of NDTHDC and poly-NDTHDC in 15 wt% HCl solution. Source: Nurudeen et al. [23]/American Chemical Society / Licensed under CC BY 4.0.

inhibition performance. Chauhan et al. [24] evaluated the corrosion inhibition of Schiff base of chitosan with cinnamaldehyde (Cinn-Cht) on carbon steel in 15% HCl. The inhibitor was synthesized by the condensation reaction of chitosan and cinnamaldehyde in the microwave (Figure 6.5). The corrosion inhibition studies were done using weight loss and electrochemical techniques. The maximum inhibition efficiency was reported at 85.16% at 400 $\mathrm{mg\,l^{-1}}$. The inhibition efficiency

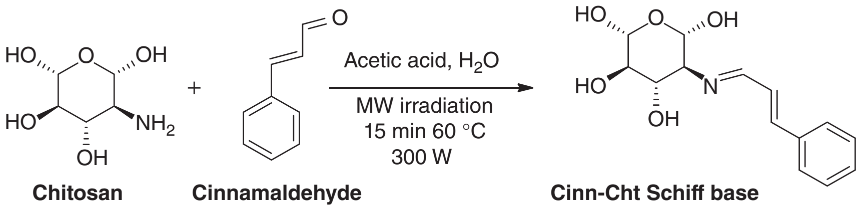

**Figure 6.5** Schematic representation of the synthesis of Cinn-Cht Schiff base. Source: Reproduced with permission from Chauhan et al. [24]. Copyright 2020 Elsevier.

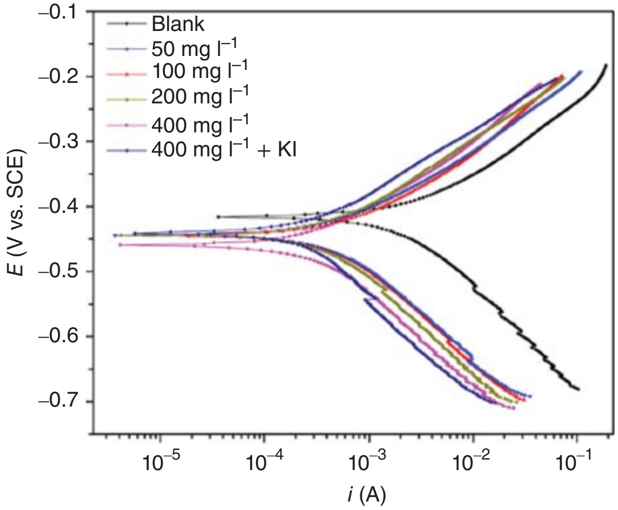

**Figure 6.6** Potentiodynamic polarization curves were recorded for the carbon steel surface on the addition of the different concentrations of Cinn-Cht and with 10 mM KI to the 15% HCl. Source: Reproduced with permission from Chauhan et al. [24]. Copyright 2020 Elsevier.

further increased to 92.45% after the addition of 10 mM of KI. The intensifier KI was applied to both temperatures 308 and 338 K along with inhibitor and it found that the inhibition efficiency increases at both the temperatures. Polarization study was done on different inhibitor concentrations. The result shows that the inhibitor mitigates both the anodic and cathodic corrosion reactions (Figure 6.6).

Solomon et al. [25] evaluated the corrosion inhibition of chitosan/silver nanoparticles (AgNPs/chitosan) composite on ST37 steel in 15% HCl at 25 and 60 °C using weight loss, electrochemical impedance spectroscopy, and potentiodynamic polarization techniques. The structure of carboxymethyl cellulose is shown in Figure 6.7. Researchers found that the studied inhibitor act as a cathodic type inhibitor. The surface studies: AFM, SEM, and EDS results confirm the formation of protective inhibitor film over the metallic surface. The inhibition efficiency increased with temperature from 87.88% (at 25 °C) to 97.09% (at 60 °C) at 1000 ppm. The adsorption of the inhibitor obeys the Temkin adsorption isotherm. Further, Solomon et al. [26] studied the corrosion inhibition effect of carboxymethyl cellulose/silver

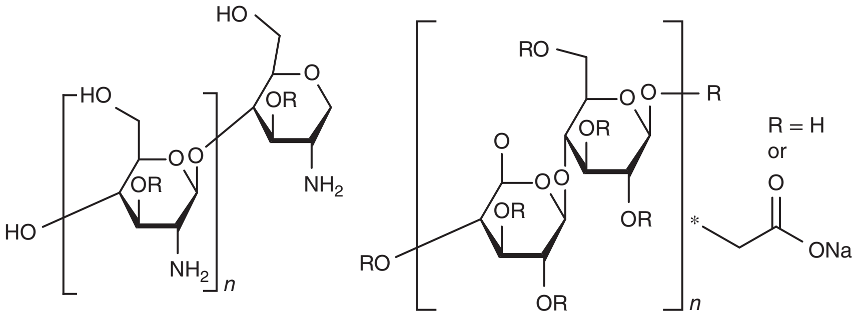

**Chitosan** **CMC**

**Figure 6.7** Structure of chitosan and carboxymethyl cellulose (CMC).

nanoparticles composite (CMC/AgNPs) on ST37 steel in 15% $H_2SO_4$. The structure of carboxymethyl cellulose is shown in Figure 6.7. The weight loss and electrochemical results show that CMC/AgNPs exhibit better corrosion protection compared to CMC. CMC/AgNPs shows 96.37% inhibition efficiency at 60 °C. Potentiodynamic polarization results reveal that CMC/AgNPs inhibit both the anodic and cathodic reactions.

## 6.3 Polymer as Corrosion Inhibitor for High-Temperature Sour and Sweet Environment

Oil and gas production from the deep oil well is corrosive due to the presence of carbon dioxide ($CO_2$) and hydrogen sulfide ($H_2S$) gases, dissolved in water. Depending upon the ratio of partial pressure of these gases, the system can be categorized as sweet, sour, and mixed corrosion. If the ratio of $CO_2/H_2S$ is greater than 500, known as sweet corrosion, while, the ratio of $CO_2/H_2S$ is less than 20, known as sour corrosion [27]. In sour corrosion, the formation of iron sulfide ($F_xS_y$) takes place as a dominant corrosion product. Although the $F_xS_y$ scale is porous, it acts as protecting layer, particularly in absence of chloride salt and oxygen, and at low temperatures. However, the iron sulfide protective layer can be disrupted from the metal surface under certain conditions, such as a high temperature, in presence of chloride, resulted localize corrosion occurs. $H_2S$ gas easily enters the oil-well reservoir from the formation, sulfur-reducing bacteria and water [28]. Moreover, the production of hydrogen gas in sour corrosion causes embrittlement, resulting in stress corrosion cracking is occurred [28].

In sweet corrosion, $CO_2$ dissolves in water and causes corrosion, resulting in the formation of iron carbonate and siderite as the main corrosion product on the metal surface. Like $H_2S$, its corrosion product also acts as a protective layer. However, at high temperatures and highly acidic conditions, the protective layer is swept out, resulting in localized corrosion is occurred. Hence, sweet corrosion can visible in a crevice and pitting corrosion [29].

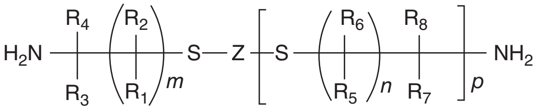

**Figure 6.8** Structure of polyaspartate with thiol and disulfide functionalities. Where $R_1$, $R_2$, $R_3$, $R_4$, $R_5$, $R_6$, $R_7$, and $R_8$ are independent members of the different alkyl groups and the hydrogen atom.

Prevention of sour and sweet corrosion problems requires batch inhibitor or continuous inhibitor injection method. Nitrogen-containing polymer compounds consider an effective class of nontoxic and environmentally benign corrosion inhibitors for iron alloys at high temperatures in sour and sweet environments. Polyaspartate, a biodegradable and nontoxic amino acid polymer, has been investigated as an effective corrosion inhibitor for mild steel in brine solution at 56 °C, studied by Fan et al. [30]. The polyaspartate mixed with amino acids, such as amino thiol and amino disulfide inhibitors, to formulate a more effective corrosion inhibitor compared to polyaspartate. The high degree of effective inhibition performance (>95%) was achieved by using the mixture of sodium polyapartate and amino thiol. The structure of biodegradable low-toxic polyaspartate corrosion inhibitor consists of thiol (Z as a hydrogen bond) and disulfide (Z as a hydrogen bond) functionalities (Figure 6.8).

Aniline, formaldehyde, and piperazine-based polymer (ADPD) have been found effective corrosion inhibitors for N-80 steel in 3.5% NaCl solution containing $CO_2$, studied by Singh et al. [31]. The polymeric ligand (ADPD) has been synthesized by reaction of aniline formaldehyde and piperazine in an alkaline medium (Figure 6.9). The ADPD inhibitor shows 68% inhibition performance at higher temperatures (60 °C).

Imidazoline is low toxicity and exhibits a high degree of corrosion inhibition. Therefore, imidazoline uses intensively as a corrosion inhibitor in continuous and batch treatment for sour and sweet corrosion. Maddox and Schoen [32] have synthesized *N*-imidazolinylpolymeric acid amides by the reaction of polymeric acid and 1-aminoalkyl-2-alkyl-2-imidazoline. The synthesized imidazoline polymer was studied as a continuous treatment corrosion inhibitor for mild steel in a sweet and sour environment. The inhibitor is mixed with other additives to enhance the heat resistance at high temperatures (120 °F for sour and 160 °F for sweet corrosion). Potential corrosion performance was obtained in addition to 1% Brij 35 and 79% light gas oil aromatic solvent. In the general structure of inhibitor, $R$ and $R'$ are hydrocarbon and m is an integer, Figure 6.10.

Overcoming the issues of poor solubility and bioincompatibility of corrosion inhibitors in sweet and sour corrosion, quaternary amine derivatives have been investigated as potential inhibitors. Naraghi and Obeyesekere [33] reported a reaction product of polyepihalohydrin with a tertiary amine is a biodegradable corrosion inhibitor as well as a biocide. The inhibitor implied continuous treatment with effective dosages between 1 to 3000 ppm and batch treatment with effective dosages between 200 to 15 000 ppm. The potential inhibition performance was 89%

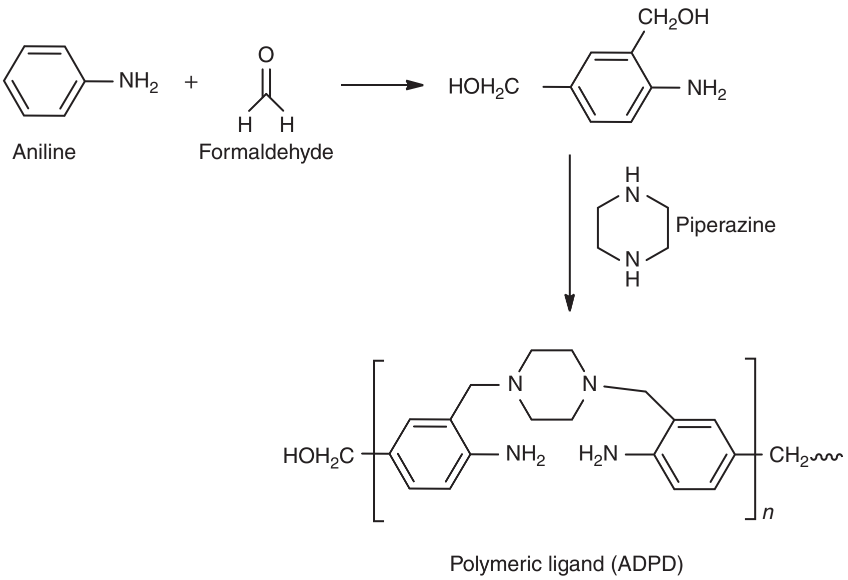

**Figure 6.9** Synthetic scheme of piperazine-based polymer inhibitor.

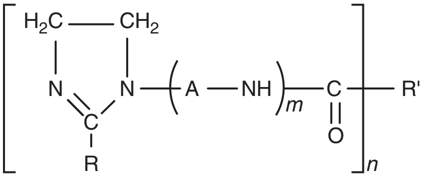

**Figure 6.10** Structure of *N*-imidazolinylpolymeric acid amides.

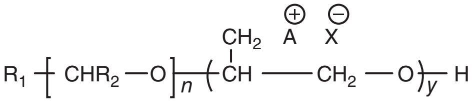

$$R_1 \left[ CHR_2 - O \right]_n \left( \underset{\substack{| \\ CH_2A^{\oplus}X^{\ominus}}}{CH} - CH_2 - O \right)_y - H$$

**Figure 6.11** Structure of polymeric quaternary ammonium salt. Where $R_1$ and $R_2$ are organic moieties or H of the polyalcohol R (CHOH), R, $n = 1$ to 10, $y = 3$ to 150, A is the tertiary amine and X is a halide. Preferably, $n$ may range between about 3 and 10 and $y$ may range between about 6 and 42.

at 15 ppm in wheel test process at 39 °C. Moreover, the invested inhibitor also kills the microorganism to reduce or terminate the microbial-induced corrosion (MIC). Polymeric quaternary ammonium salt represents in Figure 6.11.

## 6.4 Polymer as Corrosion Inhibitor for High-Temperature Naphthenic Acids Environment

Naphthenic acids accelerate the corrosion of crude oil, particularly, at high temperatures (200–400 °C), which can damage the piping and other processing equipment that is used in distillation, extraction, transportation, and processing of crude. The naphthenic acid corrosion becomes more serious due to the presence of sulfide compounds, such as hydrogen sulfide, sulfides, disulfides, polysulfides, and mercaptan. At lower temperatures (below 200 °C), naphthenic acid does not show a corrosive nature. However, at high temperatures, naphthenic acid causes the corrosion of metals. Hence, this is a big challenge to develop inhibitors to control high-temperature corrosion. Because, most of the organic corrosion inhibitors are thermally unstable, which can decompose at higher temperatures and deposit on the surface of the crude oil processing unit and create problems. Therefore, a thermally stable inhibitor will be useful for the industries to control naphthenic acid corrosion. Polymer compounds have been found thermally stable and exhibit a high degree of protection of metal alloys in naphthenic acids environment [34–36].

Petersen et al. [34] investigated that organic polysulfide (type R-(S)x-R′) exhibits effective inhibition at high temperatures (400 °F) for mild steel corrosion in naphthenic acids. The studies were carried out in the absence and presence of $H_2S$. It was found that alicyclic polysulfide exhibits better inhibition (80% IE at 1000 ppm) compared to aliphatic polysulfide (58% IE at 1000 ppm). Generally, commercially available nitrogen corrosion inhibitor does not show any inhibition effect in absence and presence of $H_2S$ in naphthenic acids. In another study, the organic polysulfide was mixed with phosphate ester to formulate a more effective film-forming corrosion inhibitor at high temperatures (500 °F) [35]. The combination preferable ratio of polysulfide and phosphate ester was 1:1 to 1:4. Subramaniyam [36] patented a file on the corrosion inhibition studies of phosphate ester polyisobutylene succinic ester and oxides polyisobutylene succinic ester as positive corrosion inhibitors for low-carbon steel CS 1010 at 290 °C in naphthenic acids environment. It was found that the oxide derivative of polyisobutylene succinic ester reduces the corrosion significantly more (99% IE at 200 ppm) compared to the phosphate derivative of polyisobutylene succinic ester (79% IE at 300 ppm).

## 6.5 Computational Studies of Polymeric Corrosion Inhibitors

Computational modeling as a tool in the design and development of corrosion inhibitors has significantly attracted a great deal of attention from corrosion scientists. The use of computational modeling in corrosion inhibition research minimizes the cost and can enhance the understanding of the inhibition mechanism. Among the computational techniques, density functional theory (DFT) and molecular dynamics simulations (MD) are widely used to analyze the corrosion inhibitors [37–40]. DFT has enabled corrosion scientists to accurately predict the interaction mechanism between corrosion inhibitor and metal surface with the analysis of the commonly used parameters, such as energy of highest occupied molecular orbital ($E_{\mathrm{HOMO}}$), energy of lowest unoccupied molecular orbital ($E_{\mathrm{LUMO}}$), and energy difference between HOMO and LUMO [41]. MD simulations can very well predict the adsorption behavior and orientation of inhibitors on the metal

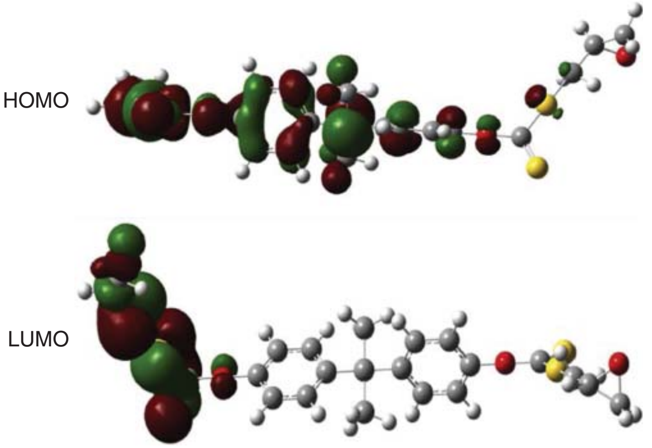

**Figure 6.12** HOMO and LUMO orbitals of the DGDCBA epoxy polymer. Source: Reproduced with permission from Hsissou et al. [44]. Copyright 2018 Elsevier.

surface with the analysis of interaction energy between corrosion inhibitors and metals [42, 43].

Hsissou et al. [44] studied inhibition effect of epoxy polymer *S*,*S*′-diglycidyl *O*,*O*′- dicarbonodithioate of bisphenol A (DGDCBA) on the corrosion of the E24 carbon steel in 1.0 M HCl using experimental and computational techniques. DFT studies were carried out using Gaussian 09 software with DFT method on the 6-31G (d,p) basis sets. The results show the reactive electron-donor sites; HOMO of difunctional DGDCBA epoxy inhibitor is distributed on aromatic ring, α-methylene of epoxy and epoxy group (Figure 6.12). Whereas in the reactive electron-acceptor sites, LUMO is epoxy group and localized in C=S group (Figure 6.12). These donor and acceptor sites can effectively interact with metal surfaces.

The MD simulation has been performed using materials studio version 6.0 software in ($40.537 \times 40.537 \times 4.753\,\text{Å}^3$) simulation box. It is mentioned that the DGDCBA epoxy polymer potentially adsorbs over the metal surface resulting obtained high values of the adsorption energies, which may be due to the flatness of inhibitor molecule and presence of a pair of electrons on the heteroatoms (–S– and –O–) (Figure 6.13).

Singh et al. studied the corrosion inhibition efficiency of aniline, formaldehyde, and piperazine-based polymer (ADPD) on N80 steel in 3.5% NaCl solution saturated with carbon dioxide [31]. The effective inhibition performance of ADPD has been predicted using the DFT and MD studies. In both neutral and protonated forms of inhibitor, the highest occupied molecular orbital (HOMO) orbitals are distributed around the benzene ring (Figure 6.14). The results show that the inhibitor molecule effectively interacts with the metal surface through the benzene ring. Moreover, the lowest unoccupied molecular orbital (LUMO) also distributed over the benzene ring indicates that the benzene ring can accept the lone pair electron from the metal d-orbital resulted overcome the positive charge and enhancing the bonding strength. BIOVIA Materials Studio® commercial software was used to perform the

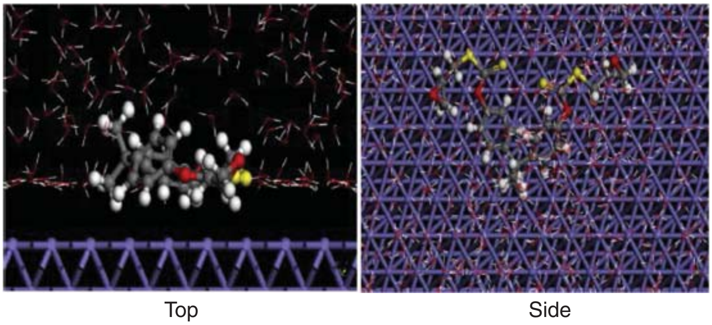

**Figure 6.13** Side and top views of stable adsorption configuration for Fe (110)/DGDCBA/50H2O system obtained using the adsorption locator module. Source: Reproduced with permission from Hsissou et al. [44]. Copyright 2018 Elsevier.

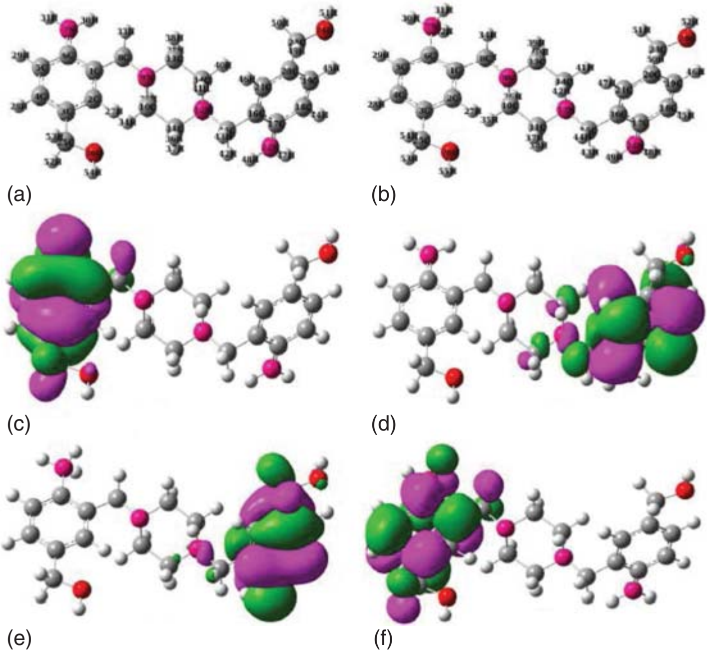

**Figure 6.14** Optimized geometries (a) Neutral (b) Protonated. Frontier molecular orbitals of neutral inhibitor (c) HOMO (d) LUMO. Frontier molecular orbitals of protonated (e) HOMO (f) LUMO. Source: Reproduced with permission from Singh et al. [31]. Copyright 2019 Elsevier.

MD simulation. The simulation was done using the box size 24.82 × 24.82 × 35.69 Å3 with $9Cl^-$, $491H_2O$, $9CO_3^{2-}$, and inhibitor molecules. The interaction results disclose that neutral form of inhibitor is more effectively interacts with metal surface compared to protonated form.

Chitosan derivatives are environment-friendly and thermally stable corrosion inhibitors [24]. It has multiple adsorptions and can effectively mitigate metal corrosion. Haque et al. studied corrosion inhibition of Schiff bases (CSBs) of chitosan and aldehydes [benzaldehyde (CSB-1), 4-(dimethylamino)benzaldehyde (CSB-2), and 4-hydroxy-3-methoxybenzaldehyde (CSB-3)] on mild steel in 1 M HCl solution using experimental and theoretical studies [45]. DFT calculations were carried out using Materials Studio software package (version 6.0) DFT/GGA level using BOP functional and DNP basis set. In this work, the author studied the effect of different substituents present in aromatic rings of chitosan Schiff bases. The DFT results disclosed that CSB-3 (having, —OH and —$OCH_3$) exhibits highest interaction with metal surfaces compared to other two inhibitors (CSB-1 and CSB-2). The performance of inhibitors was further studied with MD simulations using BIOVIA Materials Studio commercial software. MD simulation results show that chitosan Schiff bases adsorb on parallel and cover the maximum surface area (Figure 6.15). Generally, amine group (presence in CSB-2) is more effective electron-donor group compared to the hydroxyl and methoxy. However, the DFT and MD results show that presence of both hydroxyl and methoxy group in same aromatic ring (CSB-3) increase electron-donor tendency of CSB-3 compared to CSB-2 (having —$N(CH_3)_2$ group). Further, Chauhan et al. studied the corrosion inhibition of a Schiff base of chitosan with cinnamaldehyde (Cinn-Cht) on N-80 steel in 15% HCl using experimental and theoretical studies [24]. DFT study was performed using the Gaussian 09 software with 6-31G(d,p) basis set and the B3LYP

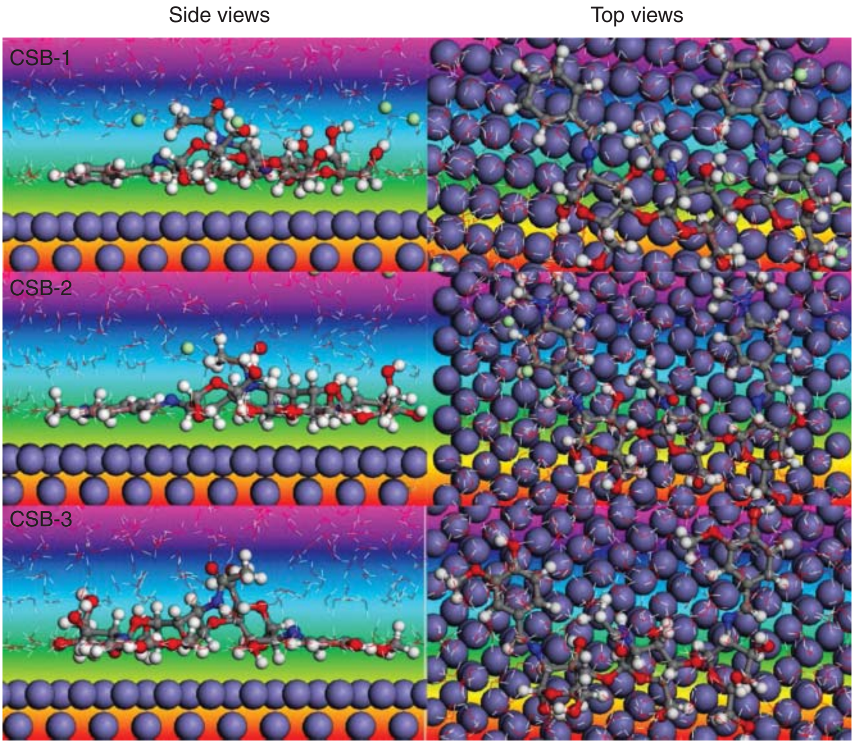

**Figure 6.15** Side and top views of the final adsorption of tested inhibitors on the Fe (110) surface in solution. Source: Reproduced with permission from Haque et al. [45]. Copyright 2018 American Chemical Society.

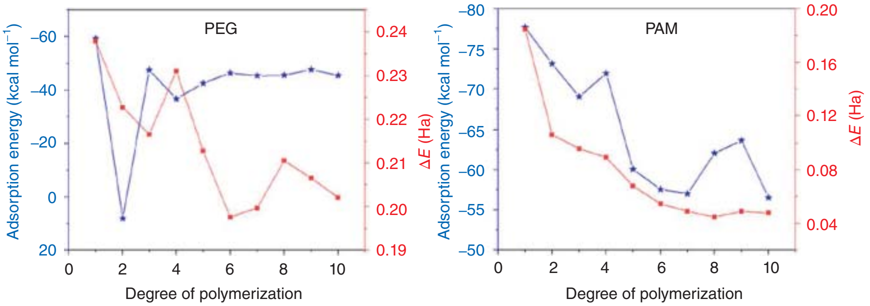

**Figure 6.16** Comprehensive comparison of the normalized adsorption energy and Δ*E* (poly) ethylene glycol (PEG) and (poly) acrylamide (PAM). Source: Reproduced with permission from ]. Liu et al. [47]. Copyright 2020 Elsevier.

correlation functional. The results show that the protonated form of Cinn-Cht is more effective (having less HOMO–LUMO energy gap) compared to chitosan and neutral Cinn-Cht.

On the development of computation techniques and getting a good agreement on corrosion inhibitors inhibition performance with experimental results [24, 45, 46]. Liu et al. theoretically analyzed the corrosion inhibition of (poly) ethylene glycol (PEG) and (poly) acrylamide (PAM) as well as degree of polymerization (DP) on the adsorption behavior on metal [47]. It is found that the effective interaction and adsorption of inhibitor molecules on metal surfaces do not always increase with increasing the degree of polymerization. As we can see in the results (Figure 6.16), the most effective PEG and PAM are obtained with DP 6 and DP 8, respectively.

## 6.6 Conclusions and Outlook

This chapter is focused on the effectiveness and environmentally benign polymeric corrosion inhibitor for high-temperature corrosive environments in industries, such as oil-well acidizing, sweet and sour corrosion, and oil refineries (naphthenic acids corrosion) (Table 6.1 and Table 6.2). With characteristic properties of macromolecules, such as multiple adsorption cites, good film-forming tendency, high thermal stability, and variety of derivatives, polymers exhibit potential corrosion inhibition and can replace the commercial using inhibitors. The polymer was mixed with another molecule to formulate a potential corrosion inhibitor.

For high-temperature corrosion inhibition, nitrogen-containing polymers were found more effective for oil-well acidizing and sweet and sour corrosion. However, for naphthenic acid corrosion, sulfur and phosphorous polymers are more effective. In oil-well acidizing, higher temperature polymeric corrosion inhibitors and quaternary amines are highly effective at lower concentrations (Table 6.1). Moreover, the presence of the cationic group in the molecule enhances its solubility. It was also found that quaternary amine polymer is more effective compared to the quaternary monomer [23]. In sweet and sour corrosion, *N*-imidazolinylpolymeric

**Table 6.2** High-temperature corrosion inhibitors for sweet and sour corrosion.

| Inhibitors | Metal/medium | Inhibition performance | Reference |
|---|---|---|---|
| 3000 Mw Sodium polyaspartate | Mild steel in brine solution with $CO_2$ | Conc.: 25 ppm<br>CR: 20 mpy at 56 °C | [30] |
| 3000 Mw Sodium polyaspartate: cysteine (99:1 ratio w/w) | Mild steel, brine solution with $CO_2$ | Conc.: 25 ppm<br>CR: 1.4 mpy at 56 °C | [30] |
| Aniline, formaldehyde and piperazine based polymer (ADPD) | N-80 steel in 3.5% NaCl with saturated $CO_2$ | Conc.: 400 ppm<br>IE: 93% at 30 °C<br>IE: 68% at 60 °C | [31] |
| Reaction product of *N*-imidazolinylpolymeric acid amides | Mild steel in 10% light gas oil; 90% brine saturated with $H_2S$ or $CO_2$ | Conc.: 25 ppm, 30 rpm<br>CR: 2.3 mpy at 120 °F (sour corrosion)<br>CR: 1.2 mpy at 160 °F (sweet corrosion) | [32] |
| Reaction product of polyepihalohydrin with a tertiary | Mild steel in NACE brine and $H_2S$ (90:10) | Conc.: 15 ppm<br>IE: 89% at 39 °C | [33] |

acid amides have been found a potential corrosion inhibitor. For naphthenic acid corrosion, phosphate ester polyisobutylene succinic ester exhibits a high degree of corrosion protection at low dosages [47]. Computations studies (DFT and MD simulations) are most advanced techniques to illustrate the mechanism of inhibitors adsorption on metal surfaces. DFT and MD simulations can also predict the inhibition performance of inhibitors. Hence, it can reduce the time and minimize the experimental cost.

## Acknowledgements

Thankfully acknowledge the University Malaysia Terengganu for proving necessary facilities to complete the book chapter.

## References

1 Palmer, J.W., Hedges, W., Dawson, J.L., and Institute of Materials, Minerals, and Mining, & European Federation of Corrosion. (2004). *The Use of Corrosion Inhibitors in Oil and Gas Production*, 2. Leeds: Maney Publishing.

2 Chukwuike, V.I. and Barik, R.C. (2022). Inhibitors for high-temperature in oil and gas fields. In: *Corrosion Inhibitors in the Oil and Gas Industry* (ed. V.S. Saji and S.A. Umoren), 271–288. Weinheim, Germany: Wiley.

3 US Public Health Service (1989). Toxicological profile for chromium, agency for toxic substance. Report No. ATSDR/TP-88/10.

**4** Cao, S., Liu, D., Ding, H. et al. (2019). Task-specific ionic liquids as corrosion inhibitors on carbon steel in 0.5 M HCl solution: an experimental and theoretical study. *Corrosion Science* 153: 301–331.

**5** Umoren, S.A. and Solomon, M.M. (2020). Polymeric corrosion inhibitors for oil and gas industry. *Corrosion Inhibitors in the Oil and Gas Industry* 303–320.

**6** Ansari, F.A. and Siddiqui, Y.S. (2018). A review on corrosion problems in context to oil and gas industries and application of suitable corrosion inhibitors. *Research Journal of Recent Science* 7 (7): 1.

**7** Sullivan III, D.S., Strubelt, C.E., and Becker, K.W. (1977). High temperature corrosion inhibitor (No. US 4028268).

**8** Finšgar, M. and Jackson, J. (2016). Electrochemical study of AISI C1018 steel in methanesulfonic acid containing an acetylenic alcohol–based corrosion inhibitor formulation. *Journal of Laboratory Automation* 21 (5): 632–641.

**9** Fiaud, C., Harch, A., Mallouh, D., and Tzinmann, M. (1993). The inhibition of iron corrosion by acetylenic alcohols in acid solutions at high temperature. *Corrosion Science* 35 (5–8): 1437–1444.

**10** Vishwanatham, S. and Haldar, N. (2007). Corrosion inhibition of N80 steel in hydrochloric acid by phenol derivatives.

**11** Vishwanatham, S. and Sinha, P.K. (2009). Corrosion protection of N80 steel in HCl by condensation products of aniline and phenol. *Anti-Corrosion Methods and Materials* 56: 139–144.

**12** Chen, H.J., Jepson, W.P., and Hong, T. (2000). High temperature corrosion inhibition performance of imidazoline and amide. In: *CORROSION 2000*. Orlando, Florida, USA: OnePetro.

**13** Quaraishi, M.A., Jamal, D., and Saeed, T.M. (2000). Fatty acid derivatives as corrosion inhibitors for mild steel and oil-well tubular steel in 15% boiling hydrochloric acid. *Journal of the American Oil Chemists' Society* 77 (3): 265–268.

**14** Quraishi, M.A. and Jamal, D. (2001). Corrosion inhibition by fatty acid oxadiazoles for oil well steel (N-80) and mild steel. *Materials Chemistry and Physics* 71 (2): 202–205.

**15** Sathiya Priya, A.R., Muralidharan, V.S., and Subramania, A. (2008). Development of novel acidizing inhibitors for carbon steel corrosion in 15% boiling hydrochloric acid. *Corrosion* 64 (6): 541–552.

**16** Bouklah, M., Hammouti, B., Lagrenee, M., and Bentiss, F. (2006). Thermodynamic properties of 2,5-bis (4-methoxyphenyl)-1,3,4-oxadiazole as a corrosion inhibitor for mild steel in normal sulfuric acid medium. *Corrosion Science* 48 (9): 2831–2842.

**17** Zhang, J., Sun, X., Ren, Y., and Du, M. (2015). The synergistic effect between imidazoline-based dissymmetric bis-quaternary ammonium salts and thiourea against $CO_2$ corrosion at high temperature. *Journal of Surfactants and Detergents* 18 (6): 981–987.

**18** Farahati, R., Ghaffarinejad, A., Rezania, H.J. et al. (2019). Sulfonated aromatic polyamide as water-soluble polymeric corrosion inhibitor of copper in HCl. *Colloids and Surfaces A: Physicochemical and Engineering Aspects* 578: 123626.

**19** Umoren, S.A. (2009). Polymers as corrosion inhibitors for metals in different media-A review. *The Open Corrosion Journal* 2 (1): 175–188.

**20** Hsissou, R., Benhiba, F., Abbout, S. et al. (2020). Trifunctional epoxy polymer as corrosion inhibition material for carbon steel in 1.0 M HCl: MD simulations, DFT and complexation computations. *Inorganic Chemistry Communications* 115: 107858.

**21** Annand, R.R. and Woodson, A.E. (1976). Method of inhibiting acid corrosion of ferrous metals with polyquaternary amino polymers. US Patent 3,982,894 filed 22 December 1971 and issued 28 September 1976.

**22** Quinlan, P.M. (1980). Quaternary polyvinyl heterocyclc compositions and use as corrosion inhibitors. US Patent 4,212,764 filed 03 July 1971 and issued 15 July 1980.

**23** Odewunmi, N.A., Solomon, M.M., Umoren, S.A., and Ali, S.A. (2020). Comparative studies of the corrosion inhibition efficacy of a dicationic monomer and its polymer against API X60 steel corrosion in simulated acidizing fluid under static and hydrodynamic conditions. *ACS Omega* 5 (42): 27057–27071.

**24** Chauhan, D.S., Mazumder, M.J., Quraishi, M.A., and Ansari, K.R. (2020). Chitosan-cinnamaldehyde Schiff base: a bioinspired macromolecule as corrosion inhibitor for oil and gas industry. *International Journal of Biological Macromolecules* 158: 127–138.

**25** Solomon, M.M., Gerengi, H., Kaya, T., and Umoren, S.A. (2017). Performance evaluation of a chitosan/silver nanoparticles composite on St37 steel corrosion in a 15% HCl solution. *ACS Sustainable Chemistry & Engineering* 5 (1): 809–820.

**26** Solomon, M.M., Gerengi, H., and Umoren, S.A. (2017). Carboxymethyl cellulose/silver nanoparticles composite: synthesis, characterization and application as a benign corrosion inhibitor for St37 steel in 15% $H_2SO_4$ medium. *ACS Applied Materials & Interfaces* 9 (7): 6376–6389.

**27** NACE MR0175/ISO 15156-1 (2001). *Petroleum and Natural Gas Industries—Materials for Use in $H_2S$-Containing Environments in Oil and Gas Production*. NACE International/ISO.

**28** Brondel, D., Edwards, R., Hayman, A. et al. (1994). Corrosion in the oil industry. *Oilfield Review (Netherlands)* 6 (2).

**29** Sharland, S.M. (1987). A review of the theoretical modelling of crevice and pitting corrosion. *Corrosion Science* 27 (3): 289–323.

**30** Fan, J.C., Fan, L.D.G. and Mazo, J. (2003). Composition for inhibition of metal corrosion. US 6,620,338 B2.

**31** Singh, A., Soni, N., Deyuan, Y., and Kumar, A. (2019). A combined electrochemical and theoretical analysis of environmentally benign polymer for corrosion protection of N80 steel in sweet corrosive environment. *Results in Physics* 13: 102116.

**32** Maddox Jr, J. and Schoen, W. (1971). Composition and Process for Inhibiting corrosion in oil wells. US Patent No. 3,623,979. Washington, DC: US Patent and Trademark Office.

**33** Naraghi, A. and Obeyesekere, N. (2006). Polymeric quaternary ammonium salts useful as corrosion inhibitors and biocides. US Patent Application No. 10/943,784.

**34** Petersen, P.R., III, Robbins, F.P. III, and Winston, W.G. (1993), Organic polysulfides, US 5,182,013 A.

**35** Babaian-Kibala, E., Hyatt, J.G. and Rose, T.J. (1997). Use of sulfiding agents for enhancing the efficacy of phosphorus in controlling high temperature corrosion attack. US Patent No. 5,630,964. Washington, DC: US Patent and Trademark Office.

**36** Subramaniyam, M. (2020). An effective novel polymeric additive for inhibiting napthenic acid corrosion and method of using the same. US Patent No. 10,787,619. Washington, DC: US Patent and Trademark Office.

**37** Zhang, J., Qiao, G., Hu, S. et al. (2011). Theoretical evaluation of corrosion inhibition performance of imidazoline compounds with different hydrophilic groups. *Corrosion Science* 53 (1): 147–152.

**38** Gece, G. and Bilgiç, S. (2010). A theoretical study on the inhibition efficiencies of some amino acids as corrosion inhibitors of nickel. *Corrosion Science* 52 (10): 3435–3443.

**39** Musa, A.Y., Jalgham, R.T., and Mohamad, A.B. (2012). Molecular dynamic and quantum chemical calculations for phthalazine derivatives as corrosion inhibitors of mild steel in 1 M HCl. *Corrosion Science* 56: 176–183.

**40** Xu, B., Yang, W., Liu, Y. et al. (2014). Experimental and theoretical evaluation of two pyridinecarboxaldehyde thiosemicarbazone compounds as corrosion inhibitors for mild steel in hydrochloric acid solution. *Corrosion Science* 78: 260–268.

**41** Srivastava, V., Haque, J., Verma, C. et al. (2017). Amino acid based imidazolium zwitterions as novel and green corrosion inhibitors for mild steel: Experimental, DFT and MD studies. *Journal of Molecular Liquids* 244: 340–352.

**42** Haque, J., Srivastava, V., Quraishi, M.A. et al. (2020). Polar group substituted imidazolium zwitterions as eco-friendly corrosion inhibitors for mild steel in acid solution. *Corrosion Science* 172: 108665.

**43** Xie, S.W., Liu, Z., Han, G.C. et al. (2015). Molecular dynamics simulation of inhibition mechanism of 3, 5-dibromo salicylaldehyde Schiff's base. *Computational and Theoretical Chemistry* 1063: 50–62.

**44** Hsissou, R., Abbout, S., Berisha, A. et al. (2019). Experimental, DFT and molecular dynamics simulation on the inhibition performance of the DGDCBA epoxy polymer against the corrosion of the E24 carbon steel in 1.0 M HCl solution. *Journal of Molecular Structure* 1182: 340–351.

**45** Haque, J., Srivastava, V., Chauhan, D.S. et al. (2018). Microwave-induced synthesis of chitosan Schiff bases and their application as novel and green corrosion inhibitors: experimental and theoretical approach. *ACS Omega* 3 (5): 5654–5668.

**46** El-Haddad, M.A., Bahgat Radwan, A., Sliem, M.H. et al. (2019). Highly efficient eco-friendly corrosion inhibitor for mild steel in 5 M HCl at elevated temperatures: experimental & molecular dynamics study. *Scientific Reports* 9 (1): 1–15.

**47** Liu, A., Guan, W., Zhao, X. et al. (2021). Investigation on the interfacial behavior of polyorganic inhibitors on a metal surface by DFT study and MD simulation. *Applied Surface Science* 541: 148570.

# 7

# Polyurethane Corrosion Inhibitor

*Mohammad M. Rahman*

*King Fahd University of Petroleum & Minerals, Interdisciplinary Research Center for Advanced Materials, Dhahran 31261, Saudi Arabia*

## 7.1 Introduction

Corrosion is a natural process that is seen on metal and alloys in a suitable environment [1, 2]. It can take place on metal structures in both external and internal sites. The rate of corrosion is faster internally than externally due to an aggressive environment, such as high temperature, high pressure, and toxic gases. Especially, internal corrosion is very aggressive in the oil and gas industry. Corrosion destroys the metals and alloys in infrastructures, pipelines, and storage tanks. It directly affects transportation, processing, and production. The corroded metal and its structure need to be rebuilt or replaced timely. If the corroded infrastructure is not replaced timely, there is a huge chance of sudden accidents. Thus, it makes a high risk to the industry [3, 4].

Usually, corrosion is protected by coatings (external corrosion) and chemicals (internal corrosion) [1, 5]. The chemicals used for corrosion protection purposes are usually called an inhibitor. The inhibitors are directly used for internal protection, whereas the inhibitors are mixed with a coating to enhance their external protection [6, 7]. In both cases, the long-lasting corrosion protection can help to avoid the unwanted shutdown of the production and supply. Thus, the industry always prefers long-lasting corrosion protection by using a proper inhibitor [6–10]. Different organic compounds are widely used as corrosion inhibitors. Especially, the heterocyclic compounds show very good performance to protect the metal from internal corrosion. Imidazole and its derivatives are particularly good for internal corrosion protection [11–13]. In many cases, mixed inhibitors are used to further improve corrosion protection in highly corrosive mediums. Many of them have excellent corrosion protection properties in ambient conditions. But their performance dropped down mostly under harsh conditions, such as high temperature, high salinity, and the presence of toxic gases; besides, most of the successful inhibitors are toxic. In these circumstances, most commercial inhibitors face challenges, and many of them have been restricted to use widely.

*Polymeric Corrosion Inhibitors for Greening the Chemical and Petrochemical Industry*, First Edition.
Edited by Mohammad A. Jafar Mazumder, Mumtaz A. Quraishi, and Amir Al-Ahmed.

Recently, polymers as an inhibitor are also used [14]. Though, the success of polymer as an inhibitor is not prominent. Very recently, polyurethane (PU), as an inhibitor, has been attracted by different groups. Their findings showed PU as a promising inhibitor. This chapter highlights a few recent works on PU corrosion inhibitors in different corrosive mediums.

## 7.2 Polyurethane (PU)

PU is mainly a urethane (–NHCOO–)/urea (–NHCONH–)-based multifunctional polymer. In many cases, it also contains esters, ethers, and aromatic groups [15, 16]. All the functional groups in PU mainly appeared from the monomers that are used during the synthesis. The main monomers are polyol, isocyanate, diamine, propionic acid, and tertiary amine. Each generic type of particular monomer has reactive and nonreactive functional groups. The reactive group directly reacted to make PU; at the same time, the nonreactive group also remained in PU. Thus, different functional groups can be attached to the PU main chain by changing the monomers. It boosts PU with multifunctional groups to work on different applications. Rahman et al. [17] synthesized PU by using four different polyols, such as polytetramethyleneoxide glycol (PTMG), polypropylene glycol (PPG), polytetramethyleneadipate glycol (PTAd), and PCL. The PTMG and PPG are polyether-based polyols, and the PTAd and PCL are polyester-based polyols. Each of the mentioned polyols can react with a diisocyanate to form a urethane group in PU; at the same time, the base polyether and polyester chain remain in PU. There are also different isocyanates to react with polyol to make urea groups, but the base aliphatic or aromatic group can also remain in PU. Huh et al. [16] used aliphatic, aromatic, and mixed aliphatic and aromatic isocyanates to synthesize PU. In all cases, the urea bond formed. The respective aliphatic and aromatic groups of isocyanates made different structures using differently structured isocyanates. The PU structures, thus, can be modified by changing the monomers. Though there are plenty of monomers available commercially, many research groups are still working to invent new monomers with new structures to have different functional groups in PU, which can also show different properties to broaden the PU applications.

There are many different polymerization techniques to synthesize the PU [15, 16]. However, the traditional synthesis methods are very challenging to control the molecular weight of PU. Recently, the atom transfer radical polymerization (ATRP) method has made a dramatic change in PU synthesis; this method can control PU molecular weight. Besides, different heteroatom-based PU synthesizing is also possible by the ATRP method, and thus it can be heavily contributed to broadening their applications [18]. The detailed polymerization methods have been described in the next sections.

In the last two decades, the properties of PU materials also improved by using nanofillers, hardeners, and crosslinkers [19–21]. However, the type and content of nanofillers, hardeners, and crosslinkers are important to improve the properties. Notably, different clay, carbonnanotube (CNT), and other carbon-based nanoparticles can improve the properties, which are only slightly deviated in harsh conditions [22].

Different fossil fuel-based monomers and organic solvents, which are toxic in nature, are mainly used in PU synthesis. Since the last decade, many industries have been facing challenges due to environmental legislation regarding using such monomers and solvents. Scientists in academia and industry made a huge effort to make environment-friendly PU by using less toxic monomers and water as a solvent. This trend started in this century in particular. Many monomers are now preparing for natural resources. Instead of organic solvents, water is being used in PU synthesis [23–26]. All these efforts make PU a green material.

The PU consists of soft and hard segments. The material's elastomeric properties mainly come from soft segments, whereas the mechanical strength comes from hard segments [27, 28]. These soft and hard segments formed from polyols and isocyanates, respectively. Mainly, the soft-segment and hard-segment ratios control the material properties. It has already been established that the PU's brilliant properties, such as high mechanical strength, high corrosion resistance, high chemical resistance, and good thermal stability, can be achieved by maintaining a proper ratio of soft segment and hard segment [29].

Currently, varieties of PU products are available commercially for many different applications. The major applications are summarized in Table 7.1.

### 7.2.1 PU Synthesis

PU synthesis is a simple reaction of monomers, and the synthesis process is easy to control (see Figure 7.1). The polyol, isocyanate, and diamine or low-molecular-weight diol are the typical monomers of PU.

Different types of PU can be prepared based on monomers and their contents. However, the polyol content (wt%) is usually much higher than other monomers. The common way to synthesize the PU is by reaction between a polyol and di/polyisocyanates, creating urethane groups repeatedly, and diamine reacts with di/polyisocyanates to create urea groups. Thus, the traditional PU consists of alternatives to urethane and urea groups. The isocyanate nature affects PU synthesis reaction rate and time. It is also common to use a very small amount of the

**Table 7.1** Main application of PU materials.

| PU product | Application | References |
|---|---|---|
| Coatings | Antifouling, anticorrosion, UV-degradation, decoration, wear resistant | [15, 22, 30] |
| Adhesives | Bonding of fiber, glass, rubber, ceramic, metal, and wood | [15, 17, 19] |
| Elastomers | Tubing, tire, patching, and cushion | [15, 16, 27] |
| Sealants | Sealing of electronic, buildings, and pavements | [15, 16, 27] |
| Foams | Building, insulation, and padding | [15–17, 27] |

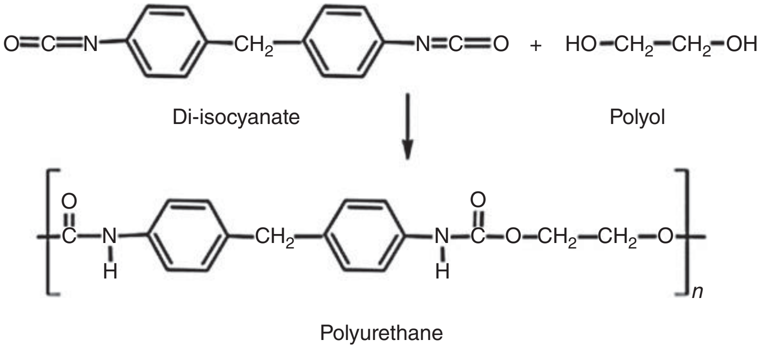

**Figure 7.1** A typical synthesis of polyurethane. Source: Akindoyo et al. [27]/Royal Society of Chemistry.

catalyst to accelerate the reaction. Aromatic isocyanates are very reactive; so, the PU synthesis reaction can be completed without any catalyst [29, 31–33].

There are plenty of available polyols for PU synthesis [34]. The widely used polyols are polyester polyol, polyether polyol, siloxane polyol, polycarbonate (PC), polycaprolactone (PCL), polysulfide (PS), and acrylate polyol. These polyols are boosts of very low- to high-molecular weight. The lower molecular weight has the advantage of rigidity, whereas the higher weight maintains the elastomeric property. Polyester polyol has advantage of higher mechanical strength, barrier resistance, and adhesive strength. The polyether polyol has advantage of a higher level of permeability and elastomeric properties. Siloxane polyol can make PU with a higher level of hydrophobicity, and also, it can make the surface smooth. The main advantage of polycaprolactone polyol is its biodegradability. It is also very common to use mixed polyols to achieve varieties of properties to use multipurpose applications. Recently, polyols are also prepared from natural resources. Especially castor oil, soya bean oil, and sunflower oil are hugely used to prepare polyols followed by PU materials.

Isocyanate is another important monomer of PU. Both aliphatic and aromatic isocyanates are used in industry, although aromatic isocyanate is preferable to aliphatic isocyanate due to cost-effectiveness. The aliphatic isocyanate has the advantage of keeping the color undamaged for a long time. All kinds of isocyanates are toxic, and they face challenges in using them for PU-based industrial products [31]. Scientists tried heavily to synthesize PU without isocyanate to get rid of this toxicity. Recently, the PU was synthesized without isocyanate. Such type of PU has almost the same properties as the traditional PU.

Two different methods are widely followed to prepare the PU dispersions. In one method, which is a single step, all the monomers are mixed together to prepare the PU. In another method, which is multisteps, the PU is made, followed by prepolymer, and chain extension steps. The reaction of polyol and diisocyanate forms the prepolymer. Later the prepolymer is chain extended using diamine or diol (low-molecular weight). In many cases, the PU dispersion is further mixed with polyisocyanate hardener to improve the properties. It is also common for postpolymerization and blending of PU dispersion to further enhance the properties [30].

Usually, the organic solvent is used during the PU synthesis. Unfortunately, organic solvents are toxic and expensive. Thus, the intention in the industry is to replace the organic solvent. In last two decades, many research groups used water as a primary solvent during the PU dispersion synthesis. This type of PU dispersion is called waterborne polyurethane (WBPU). The main trick to prepare this WBPU dispersion is to use a pendant hydrophilic salt group that is directly bonded with the polymer main chain. There must have a certain amount of hydrophilic group to prepare a stable dispersion. Though the content varied on monomer types, the minimum hydrophilic agent was mentioned above the 10 mol%. The widely used hydrophilic groups are dimethylolpropionic acid and dimethylolbutanoic acid. Usually, different tertiary amines are used to neutralize the acid group [30].

### 7.2.2 Structure

It is well-established that the PU can behave as elastomer, thermoplastic elastomer, and thermoplastic. Nature entirely depends on the monomers used in synthesis. The chemical structure (see Figure 7.1) of PU is an alternative to the soft segment and hard segment; the difference in glass-transition temperature of soft and hard segments makes a thermodynamic incompatibility in PU to lead to a microphase-separation structure. Overall, the properties depend on this microphase-separation structure. The higher the microphase separation, the material has higher the elastomeric character. The higher content of the soft segment contributes to a higher phase separation [15, 17, 30].

## 7.3 Polymer as an Inhibitor

There are many reports [35–37] available on different metals' corrosion and their inhibition by using any of the organic compounds, nanoparticles, and polymers in different corrosive environments. Earlier, the focus was mainly on different organic compounds as an inhibitor. Unfortunately, the widely used organic inhibitors are mostly toxic. Moreover, many of them have limitations at high temperatures. Later, many groups worked on green corrosion inhibitors. In the last decade, plenty of green polymers have been invented.

Most importantly, many green polymer inhibitors were prepared from natural resources. Recently, polymers, polymer composites, grafted polymers, and copolymers showed promising results in corrosion inhibition. Many of them are eco-friendly as well as cost-effective. The excellent efficiency can be ascribed due to the polymer's bigger size and sufficient and proper functional groups. This functional group can easily anchor to adsorb on the metal surface and thus protect corrosion. On a metal surface, the polymer can be adsorbed through the anchoring groups. Polymer is much larger than its monomers, and thus, the polymer can cover the metal surface compared to the corresponding monomers. In many cases, the higher the content (greater number of anchoring groups) of polymer, it can cover more surface and thus provides more protection. Though there is an optimum polymer content to achieve the maximum coverage, it will translate into the ultimate protection from corrosion. Other criteria, such as the polymer's monomer composition, the polymer's molecular weight, and the nature of the anchoring groups, have also contributed to the protection efficiency. The popular polymers as corrosion inhibitors are polyamines, polyimine, polyamides, and vinyl-based polymers. The polymers include grafted polymers, copolymers, and polymer-composites, which are less toxic or nontoxic, and recently received huge interest [38–41].

## 7.4 PU as Corrosion Inhibitor (PUCI)

Like other polymers, the PUCI also follows the exact mechanism to act as a corrosion inhibitor in different corrosive environments. The PUCI anchors on the metal surface following an adsorbed process to protect the metal from corrosion. The main advantage of PUCI is its available varieties of functional groups, which have different levels of protection ability in certain corrosive mediums. Thus, the variation of this PU structure gives a wide choice to perform in different corrosive mediums. The main challenge of PUCI is its solubility in water. This challenge has been faced by changing the traditional PUCI structure (see Table 7.2). The traditional PUCI structure has a shortage of hydrophilic salt groups in its base polymer chain. It makes them difficult to soluble in water. Recently, scientists [42] have chemically modified the PUCI structure to improve the solubility in water. Attaching proper and sufficient pendant hydrophilic group/salt groups can improve their inhibitors' performance. Banerjee et al. [42] made a sulfonated PUCI to change its structure. The modified PUCI performed excellently as an inhibitor. The traditional and modified structures are compared in Table 7.2 – the sulfonated groups attached to modified structure.

### 7.4.1 Plant-Resourced PUCI

Recently, few groups [43, 44] have shown a remarkable inhibition efficiency of PUCI, using natural resources (castor oil, soya bean oil, and sunflower oil) polyol to make

**Table 7.2** Compare of PUCI structures [42].

| PUCI | Structure |
|---|---|
| Traditional | 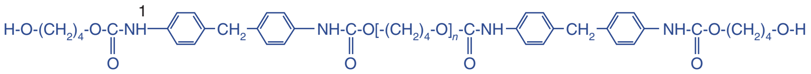 |
| Modified | 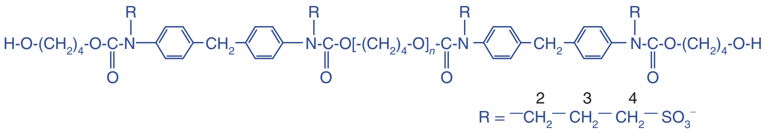 |

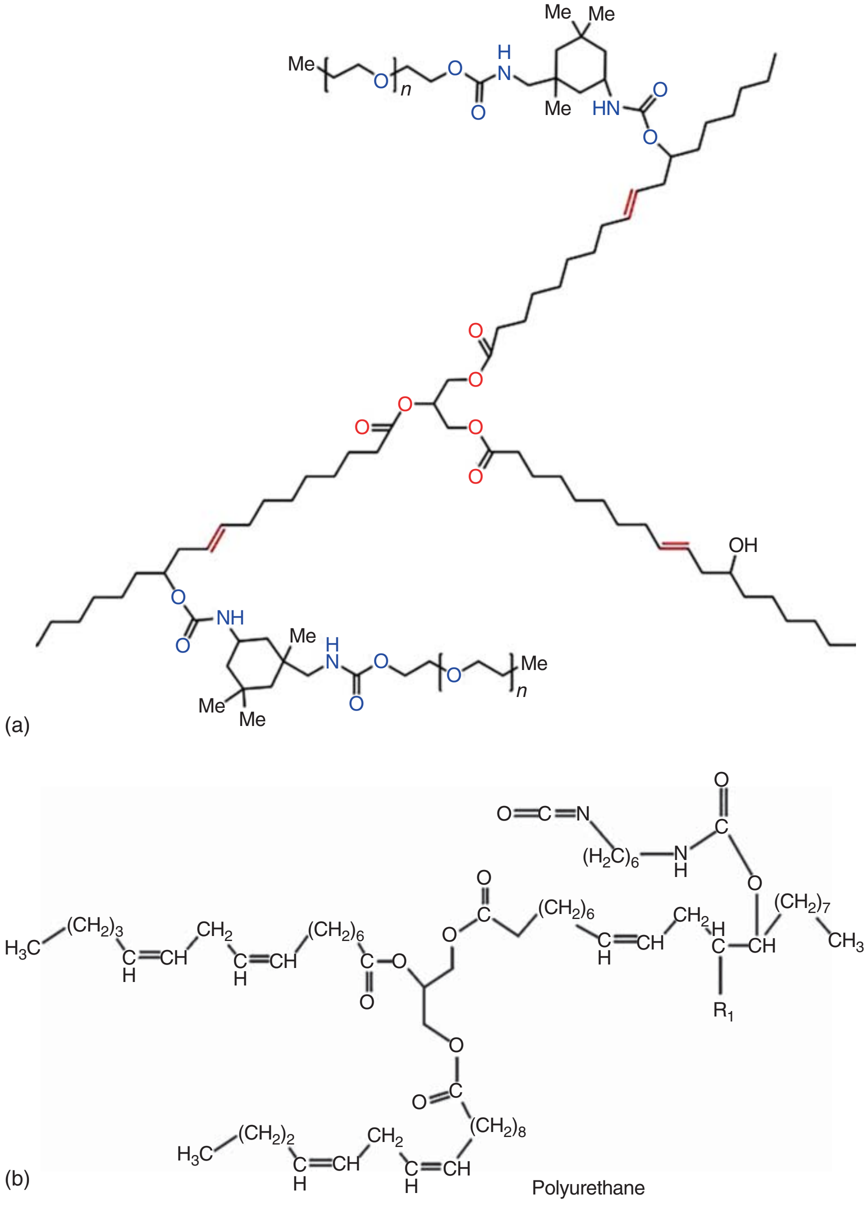

**Figure 7.2** PUCI using plant-sourced polyol (a) castor oil [43] and (b) soya bean oil. Source: Eswaramoorthi et al. [44]/Taylor & Francis.

less toxic inhibitors (see Figure 7.2). They used acid (HCl and $H_2SO_4$) as a corrosive medium [43–45]. The inhibition efficiency was found different at high temperatures. Farhadian et al. [43] mentioned almost the same efficiency at room temperature and high temperature at 80 °C, but Eswaramoorthi et al. [44] recorded lower efficiency at high temperature. Farhadian et al. [43] prepared PUCI using castor oil as a source of polyol. The corrosion protection efficiency was significant at room temperature and high temperature at 80 °C in 1 M HCl medium. PUCI has a remarkable control to suppress the corrosion in acidic medium. The high adsorption energy of PUCI mainly contributes to protecting the metal surface from acidic corrosion. Eswaramoorthi et al. [44] synthesized PUCI using soya bean oil as a source of polyol. They used 1 M $H_2SO_4$ as a corrosive medium. The PUCI adsorption follows the Langmuir adsorption isotherm. The higher the concentration, the higher the efficiency was recorded using PUCI. Farhadian et al. [45] also used sunflower oil to prepare polyol to synthesize another type of PUCI. Most importantly, this PUCI also acts as hydrate inhibition. The triglyceride group played an important role in improving inhibition efficiency. This study also used water as a primary solvent to synthesize PUCI. Such inhibitors are eco-friendly as they avoid toxic chemicals and solvents.

### 7.4.2 Nanocomposite

Many different types of polymer nanocomposites have been prepared in the last three decades. Varieties of polymers and nanofillers were used in preparing polymer nanocomposites. The widely used polymers are PU, acrylate, epoxy, and polyolefines. PU nanocomposite materials are also heavily attracted in academia and industry [1–4]. Nowadays, different PU nanocomposite materials are commercially available. Varieties of nanoparticles and their different contents are mixed with PU to improve the mechanical, thermal, barrier, and protective properties to extend the application of PU nanocomposite. One of their widely used is a coating material for corrosion protection [2–6].

The PU nanocomposites are prepared mainly by polymerization and blending processes [30]. In the polymerization process, the fillers are directly or solvently added to the polymer [30]. In the blending process, the fillers are added with preprepared PU dispersions [30]. The detailed preparation of PU nanocomposite is explained elsewhere [30]. The widely used nanofillers are clay, carbon nanotubes, graphene, and metal oxides. Both pristine and functionalized nanofillers were used in PU nanocomposite. In many cases, better properties were recorded for the polymerization method than the blending method. Rahman et al. [46, 47] used $CeO_2$ to improve the ultraviolet (UV)-degradation and corrosion resistance of PU. They prepared the materials separately by the polymerization and blending methods. They found a higher protective resistance in the polymerization method than the blending method. In another study [30], they found a higher protection capacity with a larger nanoparticle particle size. They also studied [48, 49] the distribution of nanoparticles. They found better protection with the homogeneous distribution of particles. The nanoparticle inclusion can also improve the self-healing property. Rahman et al. [50] found self-healing of PU material using $CeO_2$ nanoparticles.

Recently, Patel et al. [51] prepared a PU nanocomposite as a PUCI (see Figure 7.3). The functionalized graphene was directly bonded with the PUCI chain. The synthesis process and the PUCI structure are shown in Figure 7.2. The PUCI was a boost of the sulfonate group from graphene. They used 0.5 M $H_2SO_4$ as a corrosive medium.

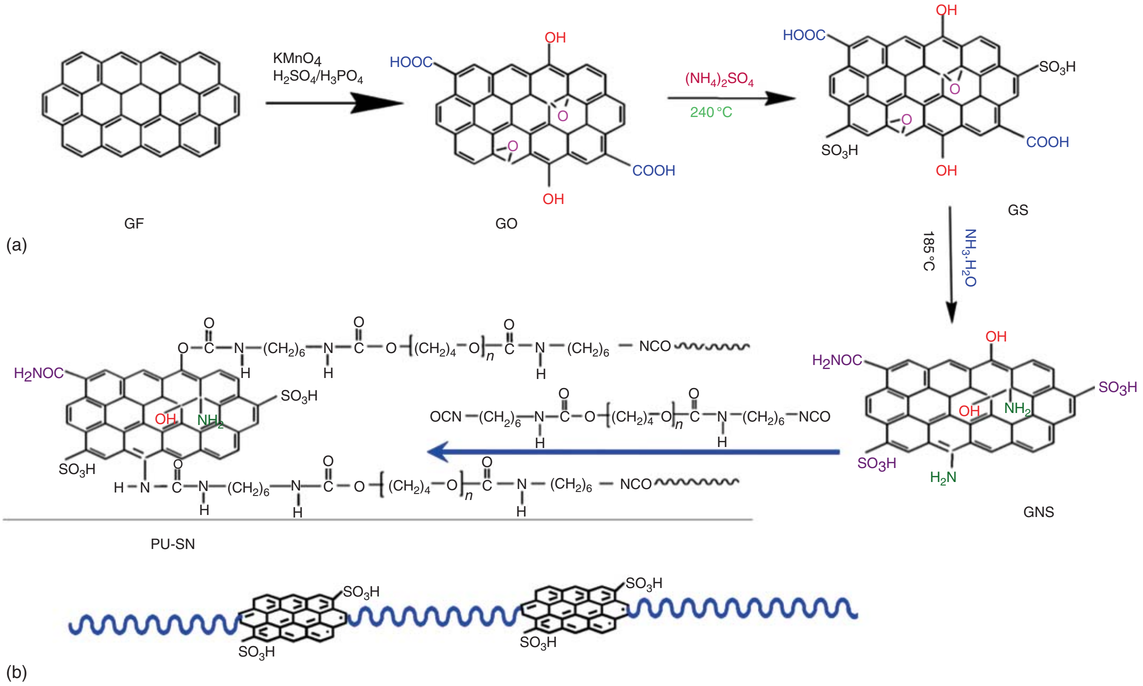

**Figure 7.3** Synthesis of graphene-based PUCI. Source: Patel et al. [51]/American Chemical Society.

The inhibition efficiency is significantly higher for nanocomposite compared to this for pristine PU material. A higher order of self-assembly improves the corrosion resistivity for nanocomposite than the pristine polymer. A more significant interaction between the sulfonate group and PU parent chain mainly increases this self-assembly.

### 7.4.3 Triblock Copolymers

A block copolymer is a linear arrangement of certain molecule's block units, and the units are repeated in an orderly manner. Kumar et al. synthesized different triblock copolymers as PUCI. A typical structure of triblock copolymer's PUCI is shown in Figure 7.4. They synthesized the PUCI by the ATRP method [52, 53]. They used 0.5 M $H_2SO_4$ and mild steel as a corrosive medium and a substrate. In their first study [52], they synthesized poly(dimethylaminoethyl methacrylate)-*b*-polyurethane-*b*-poly (dimethylaminoethylmethacrylate) and poly(*N*-vinylpyrrolidone)-*b*-polyurethane-*b*-poly(*N*-vinylpyrrolidone). The potentiodynamic polarization (PDP) analysis confirmed that these polymers are mixed corrosion inhibitors. The inhibition efficiency increased with increasing the polymer content. The chemisorption and physisorption process mainly works for PU as an inhibitor. However, the efficiency decreased with increasing the temperature. They conducted another study [53] based on their synthesized PUCI, namely, poly(*N*-isopropylacrylamide)-*b*-polyurethane-*b*-poly(*N*-isopropylacrylamide) (PIA–PU–PIA) and poly(*tert*-butylacrylate)-*b*-polyurethane-*b*-poly(*tert*-butylacrylate) (PtBA–PU–PtBA). These two polymers also acted as mixed inhibitors.

Interestingly, the PIA–PU–PIA and PtBA–PU–PtBA followed the Langmuir adsorption isotherm and El-Awady isotherm, respectively. A protective layer formed from a polymer on a metal surface by physisorption and chemisorption techniques, this protective layer protects the surface from acid corrosion. Higher efficiency was also recorded for PIA–PU–PIA compared to this for PtBA–PU–PtBA polymer. The attached functional groups made the difference for their different protection.

### 7.4.4 Polyurea-Based PUCI

Usually, the PU mainly consists of urethane groups [1, 2]. However, it is also common in PU with only urea groups in some cases. Abdulazeez et al. [54] synthesized

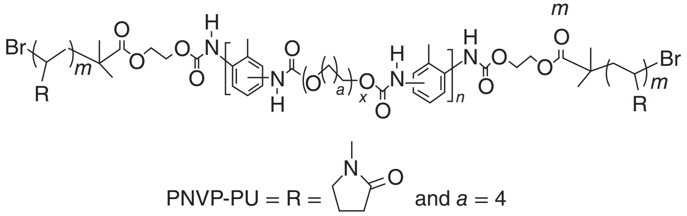

PDMAEMA-PU = R = $–COO-CH_2-CH_2-N-(CH_3)_2$ and *a* = 1

**Figure 7.4** A block copolymer of PUCI. Source: Kumar et al. [52]/Springer Nature/Licensed under CC BY 4.0.

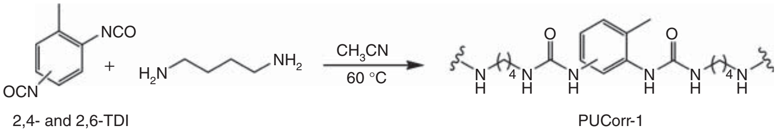

**Figure 7.5** Polyurea-based PUCI. Source: Abdulazeez et al. [54]/John Wiley & Sons.

PUCI (see Figure 7.5) based on urea groups. Their target was used to this PUCI in oil well, which is familiar for very aggressive corrosive environment. They prepared a simulated corrosive environment, saturated with toxic $H_2S$ and $CO_2$ gases. The mild steel bar (AISI 1018) was tested at 1.0 M HCl. By applying different techniques, such as electrochemical study and surface analysis as well as correlated with quantum chemical density-functional theory, they proved that PUCI can adsorb as a film onto the metal surface by a chemisorption mechanism. Their protection efficiency with 100 ppm PUCI was very high; the efficiency was 99.9% even at a temperature of 50 °C. Though the efficiency (>93%) was slightly lowered in the presence of $H_2S$ and $CO_2$ gases, the protection is still reasonable for oil wells.

### 7.4.5 Sulfonated-Based PUCI

One of the main challenges to using PUCI in different corrosive mediums is their less solubility character in the polar solvent [42, 55]. The traditional PU structure has no or less polar group and salt; it makes PU difficult to soluble in water. Banerjee et al. [55] modified the PU to make a structure with a pendant salt group in the base polymer chain (see Figure 7.6). They made a sulfonated PUCI (see Figure 7.6). They found an auspicious result using the synthesized PUCI. The corrosion efficiency was high using a small amount of sulfonated PUCI. They recorded 90% protection efficiency using only 20 ppm of sulfonated PUCI. They also found that the PUCI was inhibited through the Langmuir adsorption isotherm. Another study [42] of the same group also found a good corrosion protection efficiency using nanoparticles in PUCI. They used clay as a nanofiller in PUCI. The inhibition increased with increasing the clay content.

### 7.4.6 Waterborne PUCI

Recent environmental legislation has forced to use of an alternative to traditional toxic organic solvents during polymer synthesis in many countries. In the last two decades, many techniques have been invented to use water as a primary solvent during polymer synthesis. Unfortunately, many polymers sacrificed their protective properties by using water as the main solvent in many cases. Most of the PUCI is

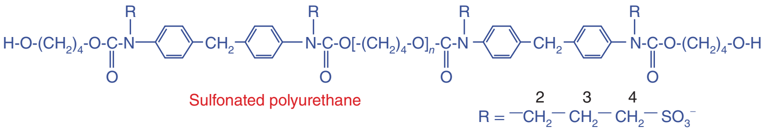

**Figure 7.6** Sulfonated-based PUCI. Source: Banerjee et al. [42]/Royal Society of Chemistry.

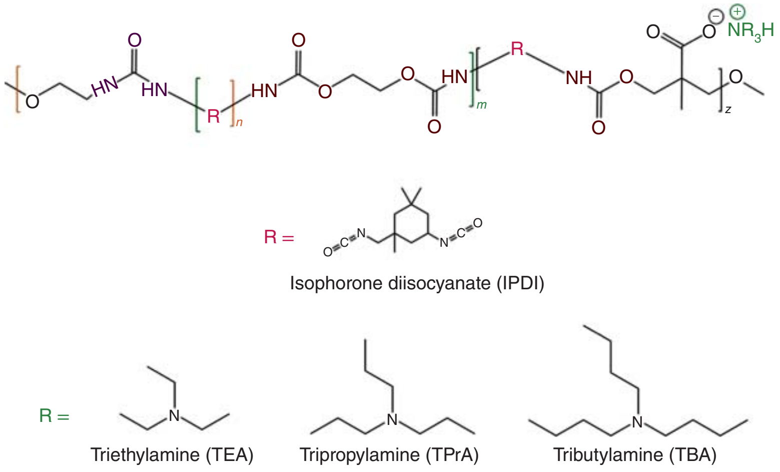

**Figure 7.7** Waterborne PUCI. Source: Farhadian et al. [40]/Elsevier.

also prepared by using organic solvents. Farhadian et al. have recently synthesized PUCI using water as the main solvent [40]. The structure is shown in Figure 7.7. The protective property was also improved using the prepared PUCI. In PUCI, they used two defined carboxyl acid salt contents, such as 34.64 and 17.32 mol%. The inhibition was higher with 34.64 mol% due to higher salt content. The inhibition was further improved by increasing the PUCI content. Their PUCI also worked fine to oppose the hydrate formation [40]. The dual action of this PUCI is also an excellent advancement for the oil and gas industry as corrosion and hydrate formation is common in many cases. The PUCI reduced the hydrate formation 7.7 times compared to water in a simulated corrosive medium. The prepared PUCI suppresses the corrosion process effectively in the presence of 2 M HCl.

## 7.5 Mechanism of PUCI Inhibition

The inhibition mechanism of PUCI was explained in different ways. Some of them [40, 42, 43, 45, 52–54] described the mechanism by computational study. Mainly, they used density functional theory (DFT), density-functional-based tight-binding (DFTB) approach, and the molecular dynamics (MD) simulation approaches.

Farhadian et al. [43] used the MD, DFTB, and DFT approaches to prove the anticorrosion mechanism of PUCI. They synthesized PUCI with urethane, urea, and triglyceride groups (see Figure 7.8). The highest occupied molecular orbital (HOMO) and lowest unoccupied molecular orbital (LUMO) study found that the triglyceride and urethane groups affect the molecular activity. The chemical adsorption was determined as the electron transition from the PUCI to metal. The proposed adsorbed configuration of the PUCI–Fe surface is shown in Figure 7.8. The PUCI is flat orientated on the metal surface. Thus, the PUCI reduced the open exposed area, thus preventing the corrosive medium from interacting with the metal

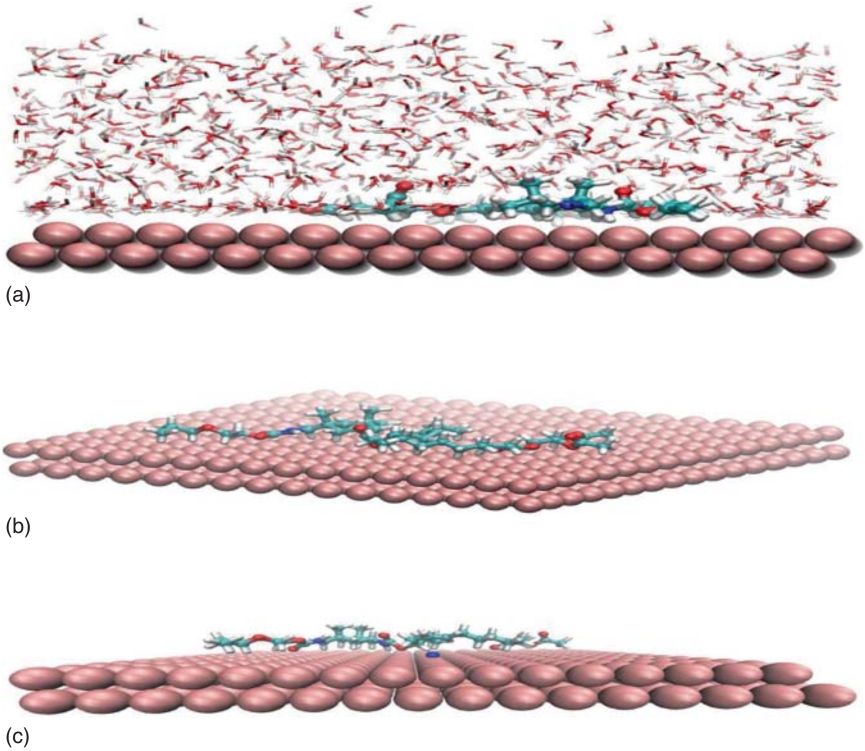

**Figure 7.8** Adsorbed configuration of the COCI–Fe surface in the presence of water using molecular dynamics simulation (a), the optimized structure of COCI–Fe (110) surface from DFTB calculation in water (b), and the optimized structure of COCI–Fe (110) surface from DFTB calculation in 1 M HCl (c). Source: Farhadian et al. [43], fig.11 (p. 12)/with permission of Elsevier.

surface. Such type of adsorption is the ultimate result of the donor (mainly from ether, ester, and urethane groups)–acceptor (metal vacant 3d orbital) interactions between the PUCI and metal surface.

Eswaramoorthi et al. [44] explain corrosion protection mechanism based on molecular adsorption. They found the adsorption of PUCI on the metal surface was physisorption. The PUCI adsorbed process was ascribed by donor–acceptor interactions (N and O lone pair electrons, aromatic rings/double bond of $\pi$-electrons, and metals vacant d orbitals).

## 7.6 Conclusions and Perspectives

The molecular structure is responsible for the corrosion inhibition performance of PUCI. Different functional groups in PUCI play an important role in having their corrosion protection property. Though PU has many applications for protection purposes, very few initiatives were found to use PU as an inhibitor in different corrosive mediums. It is good that most of the works found PUCI as an effective inhibitor. Especially, its capacity to cover a larger area of metals by its functional group makes PU a promising inhibitor. The protection efficiency is promising even at high temperatures as well as in the presence of highly corrosive gases. The PUCI can be a good choice for the oil and gas industry as this PUCI shows excellent efficiency in the presence of $H_2S$ and $CO_2$ gases.

## References

1 Solomon, M.M., Umoren, S.A., Obot, I.B. et al. (2018). Exploration of dextran for application as corrosion inhibitor for steel in strong acid environment: effect of molecular weight, modification, and temperature on efficiency. *ACS Applied Materials & Interfaces* 10: 28112–28129.

2 Paul, E., Egbuniwe, A., and Ekwumemgbor, P. (2018). The use of starch silver nanoparticles for the inhibition of mild steel corrosion using weight loss technique. *ATBU Journal of Science, Technology and Education* 6: 176–182.

3 Solomon, M.M., Gerengi, H., Kaya, T., and Umoren, S.A. (2017). Enhanced corrosion inhibition effect of chitosan for St37 in 15% $H_2SO_4$ environment by silver nanoparticles. *International Journal of Biological Macromolecules* 104: 638–649.

4 Srivastava, M., Srivastava, S.K., Nikhil et al. (2019). Chitosan based new nanocomposites for corrosion protection of mild steel in aggressive chloride media. *International Journal of Biological Macromolecules* 140: 177–187.

5 Fayomi, O., Akande, I., Oluwole, O., and Daramola, D. (2018). Effect of water-soluble chitosan on the electrochemical corrosion behaviour of mild steel. *Chemical Data Collections* 17: 321–326.

6 Chauhan, D.S., Mouaden, K.E., Quraishi, M.A., and Bazzi, L. (2020). Aminotriazolethiol-functionalized chitosan as a macromolecule-based bioinspired corrosion inhibitor for surface protection of stainless steel in 3.5% NaCl. *International Journal of Biological Macromolecules* 152: 234–241.

7 Chauhan, D.S., Quraishi, M.A., Sorour, A.A. et al. (2019). Triazole-modified chitosan: a biomacromolecule as a new environmentally benign corrosion inhibitor for carbon steel in a hydrochloric acid solution. *RSC Advances* 9: 14990–15003.

8 Chauhan, D.S., Ansari, K.R., Sorour, A.A. et al. (2018). Thiosemicarbazide and thiocarbohydrazide functionalized chitosan as ecofriendly corrosion inhibitors for carbon steel in hydrochloric acid solution. *International Journal of Biological Macromolecules* 107: 1747–1757.

9 Silverman, D., Kalota, D., and Stover, F. (1995). Effect of pH on corrosion inhibition of steel by polyaspartic acid. *Corrosion* 51: 818–825.

10 Zomorodian, A., Bagonyi, R., and Al-Tabbaa, A. (2021). The efficiency of eco-friendly corrosion inhibitors in protecting steel reinforcement. *Journal of Building Engineering* 38: 102171.

**11** Mobin, M., Khan, M., and Parveen, M. (2011). Inhibition of mild steel corrosion in acidic medium using starch and surfactants additives. *Journal of Applied Polymer Science* 121: 1558–1565.

**12** Shen, C., Alvarez, V., Koenig, J.D., and Luo, J.-L. (2019). Gum Arabic as corrosion inhibitor in the oil industry: experimental and theoretical studies. *Corrosion Engineering, Science and Technology* 54: 444–454.

**13** Azzaoui, K., Mejdoubi, E., Jodeh, S. et al. (2017). Eco friendly green inhibitor Gum Arabic (GA) for the corrosion control of mild steel in hydrochloric acid medium. *Corrosion Science* 129: 70–81.

**14** Dang, N., Wei, Y., Hou, L. et al. (2015). Investigation of the inhibition effect of the environmentally friendly inhibitor sodium alginate on magnesium alloy in sodium chloride solution. *Materials and Corrosion* 66: 1354–1362.

**15** Chattopadhyay, D.K. and Raju, K.V.S.N. (2007). Structural engineering of polyurethane coatings for high performance applications. *Progress in Polymer Science* 32: 352–418.

**16** Huh, J.H., Kim, H.I., Rahman, M.M., and Kim, H.D. (2008). Preparation and properties of MDI/$H_{12}$MDI-based water-borne poly(urethane-urea)s–effects of MDI content and radiant exposure. *Journal of Applied Polymer Science* 110: 3655–3663.

**17** Rahman, M.M., Hasneen, A., Chung, I.D. et al. (2013). Synthesis and properties of polyurethane coatings: the effect of different types of soft segments and their ratios. *Composite Interfaces* 20: 15–26.

**18** Xie, F., Xhang, T., Bryant, P. et al. (2019). Degradation and stabilization of polyurethane elastomers. *Progress in Polymer Science* 90: 211–268.

**19** Tao, C., Bao, J., Cheng, Q. et al. (2018). Preparation of waterborne polyurethane adhesives based on macromolecular-diols containing different diisocyanate. *The Journal of Adhesion* 95: 814–833.

**20** Su, X., Chen, Z., and Zhang, Y. (2017). Preparation and characterization of waterborne cellulose emulsion based on nitrocellulose modified with acrylic copolymer. *Chemical Papers* 71: 2145–2152.

**21** Che, J.Y., Cheon, J.M., Chun, J.H. et al. (2017). Kim Preparation and properties of emulsifier-/solvent-free slightly crosslinked waterborne polyurethane-acrylic hybrid emulsions for footwear adhesives (III)–effect of trimethylol propane (TMP)/ethylene diamine (EDA) content. *Journal of Adhesion* 31: 1872–1887.

**22** Cao, X., Ge, X., Chen, H., and W. (2017). Li effects of trimethylol propane and AAS salt on properties of waterborne polyurethane with low gloss. *Progress in Organic Coatings* 107: 5–13.

**23** Ryu, Y.S., Lee, Y.H., Kim, J.S. et al. (2017). Kim preparation and properties of emulsifier-/solvent-free polyurethane-acrylic hybrid emulsions for binder materials: effect of the glycidyl methacrylate/acrylonitrile content. *Journal of Applied Polymer Science* 134: 44497.

**24** Cakić, S.M., Ristić, I.S., Cincović, M.M. et al. (2016). Preparation and characterization of waterborne polyurethane/silica hybrid dispersions from castor oil polyols obtained by glycolysis poly(ethylene terephthalate) waste. *International Journal of Adhesion and Adhesives* 70: 329–341.

**25** Kim, H.L., Lee, Y.H., Kim, J.S. et al. (2016). Preparation and properties of crosslinkable waterborne polyurethane and polyurethane-acrylic hybrid emulsions and their crosslinked polymers. *Journal of Polymer Research* 23: 240.

**26** Llorente, O., Fernández-Berridi, M.J., González, A., and Irusta, L. (2016). Study of the crosslinking process of waterborne UV curable polyurethane acrylates. *Progress in Organic Coatings* 99: 437–442.

**27** Akindoyo, J.O., Beg, M.D.H., Ghazali, S. et al. (2016). Yuvaraj polyurethane types, synthesis and applications - a review. *RSC Advances* 6: 114453–114482.

**28** Li, Y., Noordover, A.J., Benthem, R.A., and Koning, C.E. (2015). Bio-based poly(urethane urea) dispersions with low internal stabilizing agent contents and tunable thermal properties. *Progress in Organic Coatings* 86: 134–142.

**29** Li, Y., Zheng, J., Luo, Y. et al. (2015). Effects of different ionizable groups on the thermal properties of waterborne polyurethanes used in bulletproof composites. *Journal of Applied Polymer Science* 132: 42374.

**30** Rahman, M.M. (2020). Polyurethane/zinc oxide (PU/ZnO) composite-synthesis, protective property and application. *Polymers* 12: 1535.

**31** Guo, Y.H., Guo, J.J., Miao, H. et al. (2014). Properties and paper sizing application of waterborne polyurethane emulsions synthesized with isophorone diisocyanate. *Progress in Organic Coatings* 77: 988–996.

**32** Li, Y., Noordover, B.A.J., Benthem, R.A.T.M., and Koning, C.E. (2014). Property profile of poly(urethane urea) dispersions containing dimer fatty acid-, sugar- and amino acid-based building blocks. *European Polymer Journal* 59: 8–18.

**33** Li, Y., Noordover, B.A.J., Benthem, R.A.T.M., and Koning, C.E. (2014). Reactivity and regio-selectivity of renewable building blocks for the synthesis of water-dispersible polyurethane prepolymers. *ACS Sustainable Chemistry & Engineering* 2: 788–797.

**34** Lei, L., Xia, Z., Cao, G., and Zhong, L. (2014). Synthesis and adhesion property of waterborne polyurethanes with different ionic group contents. *Colloid and Polymer Science* 292: 527–532.

**35** Nardeli, J.V., Fujiwara, C.S., Taryba, M. et al. (2020). Self-healing ability based on hydrogen bonds in organic coatings for corrosion protection of AA1200. *Corrosion Science* 177: 108984.

**36** Tourabi, M., Nohair, K., Traisnel, M. et al. (2013). Electrochemical and XPS studies of the corrosion inhibition of carbon steel in hydrochloric acid pickling solutions by 3,5-bis (2-thienylmethyl)-4-amino-1,2,4-triazole. *Corrosion Science* 75: 123–133.

**37** El-Haddad, M.A.M., Radwan, A.B., Sliem, M.H. et al. (2019). Highly efficient eco-friendly corrosion inhibitor for mild steel in 5 M HCl at elevated temperatures: experimental & molecular dynamics study. *Scientific Reports* 9: 3695.

**38** Olajire, A.A. (2017). Corrosion inhibition of offshore oil and gas production facilities using organic compound inhibitors-a review. *Journal of Molecular Liquids* 248: 775–808.

**39** Zhao, J., Zhou, T., Zhang, J. et al. (2014). Synthesis of a waterborne polyurethane-fluorinated emulsion and its hydrophobic properties of coating films. *Industrial & Engineering Chemistry Research* 53: 19257.

**40** Farhadian, A., Varfolomeev, M.A., Kudbanov, A. et al. (2020). Waterborne polymers as kinetic/anti-agglomerant methane hydrate and corrosion inhibitors: a new and promising strategy for flow assurance. *Journal of Natural Gas Science and Engineering* 77: 875–5100.

**41** Farhadian, A., Kudbanov, A., Varfolomeev, M.A., and Dalmazzone, D. (2019). Waterborne polyurethanes as a new and promising class of kinetic inhibitors for methane hydrate formation. *Scientific Reports* 9: 9797.

**42** Banerjee, S., Mishra, A., Singh, M.M. et al. (2011). Highly efficient polyurethane ionomer corrosion inhibitor: the effect of chain structure. *RSC Advances* 1: 199–210.

**43** Farhadian, A., Rahimi, A., Safaei, N. et al. (2020). A theoretical and experimental study of castor oil-based inhibitor for corrosion inhibition of mild steel in acidic medium at elevated temperatures. *Corrosion Science* 175: 108871.

**44** Eswaramoorthi, V., Jagadeesan, S., Palanisamy, S. et al. (2016). Soya bean oil based polyurethanes for corrosion inhibition of mild steel in acid medium. *Journal of Adhesion Science and Technology* 30: 468–493.

**45** Farhadian, A., Varfolomeev, M.A., Rezaeisadat, M. et al. (2020). Toward a bio-based hybrid inhibition of gas hydrateand corrosion for flow assurance. *Energy* 210: 118549.

**46** Rahman, M.M., Zahir, M.H., Helal, A. et al. (2021). UV-protected polyurethane/*f*-oil fly ash-$CeO_2$ coating: effect of pre-mixing of *f*-oil fly ash-$CeO_2$ with monomers. *Polymers* 13: 3232.

**47** Rahman, M.M. (2021). Polyurethane/f-oil fly ash-ZnO atmospheric corrosion protective coating. Corrosion 2021, Virtual Conference and Expo, April 19–30 2021.

**48** Rahman, M.M., Zahir, M.H., Arafat, M.E. et al. (2021). UV-shielding by a polyurethane/*f*-Oil fly ash-$CeO_2$ protective coating. *Journal of Applied Polymer Science* 138: 49904.

**49** Rahman, M.M., Zahir, M.H., Haq, M.B. et al. (2020). Silicone-enriched surface of immersed polyurethane-POSS antifouling coating. *International Journal of Polymer Analysis and Characterization* 25: 385–395.

**50** Rahman, M.M., Suleiman, R., Zahir, M.H. et al. (2020). Multi self-healable UV shielding polyurethane/$CeO_2$ protective coating: the effect of low-molecular-weight polyols. *Polymers* 12: 1947.

**51** Patel, D.K., Senapati, S., Mourya, P. et al. (2017). Functionalized graphene tagged polyurethanes for corrosion inhibitor and sustained drug delivery. *ACS Biomaterials Science & Engineering* 3: 3351–3363.

**52** Kumar, S., Vashisht, H., Olasunkanmi, L.O. et al. (2016). Experimental and theoretical studies on inhibition of mild steel corrosion by some synthesized polyurethane tri-block co-polymers. *Scientific Reports* 6: 30937.

**53** Kumar, S., Vashisht, H., Olasunkanmi, L.O. et al. (2017). Polyurethane based triblock copolymers as corrosion inhibitors for mild steel in 0.5 M $H_2SO_4$. *Industrial and Engineering Chemistry Research* 56: 441–456.

**54** Abdulazeez, I., AlHamouz, O.C.S., Khaled, M., and AlSaadi, A.A. (2020). Inhibition of mild steel corrosion in $CO_2$ and $H_2S$ saturated acidic media by a new polyurea based material. *Materials and Corrosion* 71: 646–662.

**55** Banerjee, S., Mishra, A., Singh, M.M., and Maiti, P. (2011). Effects of nanoclay and polyurethanes on inhibition of mild steel corrosion. *Journal of Nanoscience and Nanotechnology* 11: 966–978.

# 8

# Dual-Purpose Kinetic Hydrate and Corrosion Inhibitors

*Muhammad I. Ulhaq*

*Saudi Aramco, Research and Development Center, Dhahran 31311, Saudi Arabia*

## 8.1 Introduction

Corrosion is one of the biggest problems of the oil and gas industry, which affects pipelines (responsible for ~50% of pipeline failures) and seriously impacts the functioning of oil refineries and petrochemical plants [1]. Recurring shutdowns caused by corrosion due to repair and replacement of certain sections of the process cause a heavy economic burden on oil and gas exploration and production [2]. The majority of the equipment and processes involved in the drilling, exploration, transportation, refinement, and storage process potentially suffer from both internal and external corrosion leading to the weakening of metallic parts, which ultimately causes serious failures [3]. Environmental conditions, such as harsh weather, high humidity, and acidic condition, are the major cause of external corrosion, whereas corrosive fluid present in the pipeline is responsible for internal corrosion, which includes brine, organic acids, and acid gases, such as $CO_2$ and $H_2S$. [4–6]. Both types of corrosion have a strong ability to corrode carbon steel pipelines that are commonly used for the transportation and storage of oil and gas due to their low cost and strong mechanical properties (cf. Figure 8.1a) [7].

In this scenario, it is of utmost importance to continuously improve corrosion inhibition techniques to maximize the industry's economic viability [8]. Although it is almost impossible to completely eliminate the possibility of corrosion, it can be controlled to a greater extent by constant monitoring, maintenance, and proper choice of corrosion inhibitors (CIs) [9]. External corrosion can be inhibited by using alloys and stainless-steel materials suitable for a particular environment and contacting liquid [10]. Besides, polymer-based coatings, such as polyacrylates, polyurethanes, polyesters, epoxy, and alkyds, other resin or paint materials are also used that interact directly with external surface of metals and act as a barrier layer and insulation material [11]. These types of film-forming-coating materials are most commonly applied in the oil and gas industry [12]. Such materials also include organic molecules consisting of functional groups with heteroatoms, including nitrogen, sulfur, oxygen, phosphorus, and additional alkyl chains [13].

*Polymeric Corrosion Inhibitors for Greening the Chemical and Petrochemical Industry*, First Edition.
Edited by Mohammad A. Jafar Mazumder, Mumtaz A. Quraishi, and Amir Al-Ahmed.

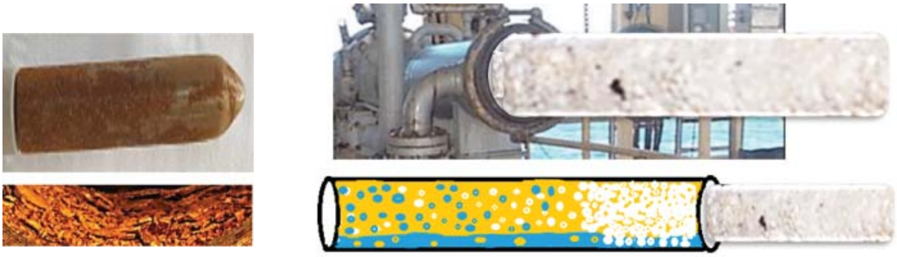

(a) Metal surface with corrosion and corrosion product

(b) Flow line blocked with gas hydrates

**Figure 8.1** The problems of (a) corrosion and (b) gas hydrate formation in the oil and gas industry. (a) https://www.worldofchemicals.com/media/oil-gas-corrosion-protection-underground-pipeline-protection-strategies/967.html and (b) https://www.arab-oil-naturalgas.com/tag/hydrate-formation/).

Heteroatoms facilitate organic molecules' adsorption on the metal surfaces by the transfer of lone pairs of electrons and protect metals from corrosive agents, whereas the alkyl chains provide additional thickness and strength to the protecting material [14].

On the other hand, internal corrosion can be inhibited by the inclusion of a variety of CIs and/or additives into the process stream [15]. Inhibitors (additives) are chemical substances that are typically classified in various categories based on their content and mode of action, such as neutralizing, scavenging, film-forming, and other miscellaneous materials [16]. These materials have a strong ability to tackle corrosion caused by the processing conditions and high concentration of water and salts during oil and gas production [17]. For instance, corrosion in refineries is often caused by concentrated acids, including HCl, $H_2SO_4$, and carbonic acid, which are usually inhibited by the inclusion of neutralizing inhibitors, such as ammonia, NaOH, amines, and polyamines, which effectively diminish the concentration of hydrogen ion in the environment [18]. Whereas scavengers, such as hydrazine and sodium sulfite, are often used to target dissolved oxygen, another major cause of corrosion during the production process [19, 20].

Another significant challenge of the petrochemical industries is the formation of gas hydrates, which possess serious problems by blocking the pipelines [21]. Gas hydrates are ice-like solid compounds that form naturally under particular environmental conditions [22]. These compounds usually consist of a mixture of gas ($CO_2$, methane, ethane, propane, etc.) and water. Water molecules trap the gaseous substances inside their cavities formed by the network of hydrogen bonds [23]. These types of crystalline lattices, which consist of 85 mol% of water and 15 mol% of guest(s) molecules (gas), are also known as hydrates or clathrates [24]. Gas hydrates are usually formed in subsea oil and gas flowlines at high pressures (more than 0.6 MPa) and low temperatures (less than 300 K) [25]. Gas hydrates have received enormous attention from both scientists and energy technologists due to their great potential as a massive energy source and a variety of other promising engineering applications, including hydrate-based carbon capture and storage, natural gas storage and transport, and seawater desalination [26–29].

However, in the petroleum industry, gas hydrates are considered a great nuisance due to their adverse effect on flow assurance. Despite great technological advancement, inhibition of gas hydrate formation still remains challenging [30]. Particularly, during the exploration, extraction, and transportation of oil and gas in the deeper and remote regions, the problem of gas hydrate formation considerably worsens [31, 32]. This seriously hampers the gas flow leading to the blockage of pipelines, which possess a greater risk of accidents and unbearable economic losses (cf. Figure 8.1b) [33, 34]. So far, various methods have been tried to prevent the formation of gas hydrates and remediate flow assurance [35]. These include pressure reduction and heating up of flow pipelines to keep the system out of the hydrate region. However, under the deep sea and harsh conditions, such methods are not ideal, economically viable, and pose safety concerns [36]. Chemical treatment is another commonly applied method for the prevention of hydrate formation [37]. In this technique, thermodynamic hydrate inhibitors (THIs), such as methanol, ethylene glycol, sodium chloride, and calcium chloride, are often applied to shift the hydrate equilibrium curve toward hydrate-free region [38]. However, it requires large quantities of THIs to achieve desired flow assurance, and to maintain these huge quantities, large storage capacities and recycling units are required, which also possess environmental concerns [39].

To address these issues, low-dosage hydrate inhibitors (LDHIs) are proposed, such as kinetic hydrate inhibitors (KHIs) and anti-agglomerants (AAs), which are highly effective even at lower concentrations, i.e. <3.0 wt% of active ingredients [40]. KHIs mostly include polymeric compounds that prevent hydrate formation by impeding hydrate crystals' nucleation and/or growth [41]. Whereas AAs are based on surfactants that allow the nucleation of small hydrate particles but inhibit their aggregation from forming large crystals, which ultimately facilitate the smooth flow of multiphase petroleum fluid [42]. Although KHIs and AAs are highly efficient in preventing hydrate formation, their large-scale applications are seriously affected due to their ineptness at lower temperatures [43]. Besides, KHIs with low deposition temperature are highly active, lacking a variety of polymeric structures leading to the precipitation of inhibitors during the injection process. Therefore, KHIs lose efficiency in warmer water, such as in the Gulf of Mexico, due to the insolubility of polymeric structures, which is important for effective inhibition [44].

Apart from this, most of the polymeric-structures-based KHIs also suffer from non-degradability, toxicity, and incompatibility with CIs [45, 46]. Thus, the simultaneous injection of KHIs and CIs usually diminishes the activity of both the components involved and increases the risk of hydrate formation in subsea pipelines [47]. Therefore, the development of multi-functional inhibitors capable of preventing the formation of gas hydrates and inhibiting corrosion will be highly desirable for the future of the oil and gas industry. In this chapter, we intend to briefly review three topics consecutively. Firstly, a brief overview of some of the commonly applied CIs will be presented. Subsequently, some of the gas hydrate fundamentals will be overviewed together with commonly applied KHIs and will be discussed including commercial KHIs. The latest examples will discuss an overview of the most studied dual-functional inhibitors that can prevent the formation of gas hydrates and inhibit corrosion. Their mechanism of action will also be highlighted, and the performance testing and evaluation of dual-purpose CI and KHI will also be briefly discussed. Finally, future prospects of dual-purpose CIs and KHIs for oil and gas industry will also be presented.

## 8.2 Corrosion Inhibitors (CIs)

The natural degradation of materials by chemical and/or electrochemical reactions with the substances in the environment is called corrosion [18]. Typically, it is the oxidation of atoms on the surface of metals, which convert them into more stable forms, such as oxides, hydroxides, sulfides, or carbonates, leading to the damaging of entire surfaces [48]. Highly humid and acidic environments promote corrosion under several complex conditions in oil and gas systems' production, processing, and transporting equipment [1]. The electrochemical process of corrosion often consists of three different components, including an electrolyte, an anode, and a cathode. The electrolyte is the corrosive medium that facilitates the transfer of electrons from an anode (point of corroding metal) to a cathode, which forms the electrical conductor in the cell that is not consumed in the corrosion process [49]. Crude fuel in pipelines and oil wells usually contains inherently corrosive substances, such as $CO_2$, $H_2S$, and free water, which potentially corrode the surfaces of the components involved in the extraction and production processes [50]. Due to this, components of pipelines and oil wells undergo degradation over time, leading to the weakening of mechanical properties of the materials, such as strength, ductility, and impact strength, causing loss of thickness and ultimate failure [51]. This requires the replacement of costly assembly components, which may lead to the stoppage of production and causes serious consequences [52].

So far, corrosion is responsible for several industrial catastrophes that have caused the loss of several billion dollars (~$1.372 billion) to crude industry [53, 54]. Besides, damaged pipelines and oil spills due to corrosion have also caused serious environmental hazards [55]. Due to this, a huge amount is spent by oil and gas companies globally to address the imminent problem of corrosion that occurs in several stages of oil production. Essentially, to maintain continuous flow assurance, necessary corrosion control practices are adopted by the authorities to avoid potential disasters that may cause loss of life, undesirable societal impacts, and serious environmental pollution [56]. A variety of corrosion occurs in oil and gas industry that is difficult to classify [57]. The type of corrosion is mostly based on the mechanism of attack, the appearance of corrosion damage, a section of industry, etc. [58]. The choice of preventive methods varies according to location, fluid composition, environmental conditions, and so forth. Notably, some common types of corrosion in the crude industry include oxygen corrosion, sweet and sour corrosion, crevice corrosion, galvanic corrosion, erosion–corrosion, microbiologically induced corrosion, and stress-corrosion cracking [59].

Corrosion in the crude industry is not a static phenomenon since the nature of fluid changes makes the corrosion inhibition programs less responsible over time [60]. Therefore, efficient monitoring and control of corrosion will contribute to the regular maintenance of oil flow, enhance asset integrity, and reduce unwanted losses. To date, several options are considered for corrosion control in the oil and gas industry, including the application of internal and external coatings, cathodic and anodic protection, material selection, and chemical-dosing-like application of inhibitors. Among several corrosion prevention methods, CIs are extensively used to provide effective corrosion protection during extraction, storage, and transportation [61]. Inhibitors are chemical substances added in small concentrations in the fluid to protect the surface of materials against corrosion, either by merging with them or by reacting with the impurities in the environment that may cause corrosion [62]. Mechanism of corrosion inhibition varies according to the conditions, in some cases, inhibitors limit the rate of the cathodic or anodic process by blocking active sites on the metal surface (inorganic inhibitors), while in others, the inhibitors may enhance the potential of the metal surface due to which metal enters the passivation region where a natural oxide film form [63]. Besides, inhibitors can also act by chemically adsorbing (organic inhibitors) on the surface of the metals (chemisorptions), leading to the formation of a protective thin film with inhibiting effect (cf. Figure 8.2) [64].

CIs are typically categorized into interface (or barrier) inhibitors and environmental conditioners (neutralizing and scavenging) based on their composition and mode of action. Barrier inhibitors (film-forming inhibitors) prevent penetration of corrosive substances by forming a protective layer on the metal surface via strong interfacial interactions, including electrostatic adsorption, chemisorption, and π-orbital adsorption [65]. These inhibitors typically consist of polar heads that interact with the metal surface and a hydrophobic group suspending away from the metal's surface to provide a protective layer against corrosive species. They are the most commonly applied inhibitors in the industry, and to be effective, they are not required to interact directly with corrosive elements [66]. The barrier inhibitors are further divided into two categories, such as liquid- and vapor-phase inhibitors.

The liquid-phase inhibitors are further divided into anodic, cathodic, and mixed inhibitors based on their mechanism of inhibition. Anodic inhibitors function by delaying the anodic reaction by forming a protective oxide film on the surface

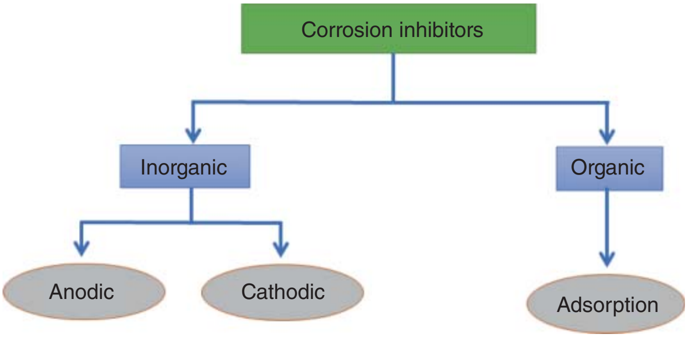

**Figure 8.2** Classification of commonly applied corrosion inhibitors.

of the metal. However, for this process, a critical concentration of inhibitor is required for the effective protection of metal since the anodic reaction involves the dissolution of the metal-to-metal cations. Anodic inhibitors are mostly made up of oxides, hydroxides, or salts in near-neutral solutions, which are able to form sparingly soluble deposits on the metal surface [67]. On the other hand, cathodic inhibitors either slow down the cathodic reaction or interrupt the flow of electrons from anode to cathode by selectively precipitating on cathodic regions [68]. The mixed-type inhibitor, which mainly includes organic compounds, protects metals from both anodic and cathodic reactions by physical adsorption (physisorption), chemisorption, and film formation. Physical adsorption occurs through interfacial interactions (ionic or electrostatic) between the metal surface and inhibitor. On the contrary, chemisorption involves the charge sharing or charge transfer between the metal surface and inhibitor. Unlike physisorption, chemisorption is the most effective method of metal protection from corrosion, which functions efficiently even at high temperature [69]. This chapter will only focus on a mixed type of liquid phase, organic CIs.

Organic compounds consisting of nitrogen, oxygen, and/or sulfur are potential industrial CIs, which have an excellent ability to form a protective film on the surface of metal against a corrosive environment via adsorption (both physical and chemical adsorption) [70]. The presence of lone pair and $\pi$-electrons in heteroatoms-based organic inhibitors facilitates the electron transfer, forming a coordinate covalent bond with metal (Fe). Thus, the performance and strength of adsorption of the inhibitor are associated with electron density and electronic structure of the inhibitor, cathodic and/or anodic overpotential, and the ability of the inhibitor to form a protective film. However, the ability of inhibition can be potentially influenced by the molecular size, chain length, aromaticity, cross-linking properties, and solubility of inhibitors. For instance, the increased chain length of hydrocarbon-based inhibitor has led to the decrease in inhibition properties of a compound due to the reduction in the aqueous solubility of the material [71]. In another case, the inhibition property of a substance is significantly enhanced when the H atom in the carbon skeleton is substituted with electron-rich substituents, such as $—NH_2$, $—NO_2$, —CHO, or —COOH [72]. So far, several simple organic substances, including amines; aldehydes; azoles such as imidazole and triazole; acids such as amino acid and succinic acid; and many others, have been successfully applied as CIs [73–75]. Chauhan et al. have designed novel amidoamine ammonium salts, which are embedded with motifs of quaternary ammonium, amide, and amine functionalities. The as-prepared molecules have displayed excellent aqueous solubility and high corrosion inhibition efficiency (more than 90%) for mild steel in 1 M HCl [76].

Apart from small organic molecules, polymers have also demonstrated excellent anticorrosion properties due to the possibility of the inclusion of a large number of heteroatom-based functional groups into the polymer matrix, which exhibits a strong ability to adhere to a large part of the metal surface [77]. Polymers constitute long chains of repeating units called monomers, which can be potentially fabricated into various architectures, including linear chains, branched, hyperbranched, comb-like, rotaxanes, cross-links, and dendrimeric structures. In comparison, polymeric CIs possess superior flexibility, solubility, multi-functionality, and film-forming ability than conventional small organic-molecules-based CIs [78]. Several types of polymers have been applied as CIs, including long-chain polyamines, polyanilines, polycarboxylic acids, polysulfides, and polyvinylamide derivatives polyaspartates and other polyaminoacids, heterocyclic functional groups and polymers adducts, and polymers nanocomposites [11, 79]. Besides, green CIs have been excessively explored due to the adverse environmental impact of synthetic materials, such as CIs, which are costly and toxic to humans and the environment. Green CIs are nontoxic, biodegradable, and environmentally friendly, and enormous studies have been published so far, which are mainly based on essential oils and purified compounds obtained from plant extracts [15].

## 8.3 Kinetic Hydrate Inhibitors (KHIs)

In oil and gas pipelines, small hydrocarbons surrounded by water molecules tend to accumulate in high-pressure and low-temperature conditions to form nonflowing crystalline solids known as gas hydrates [80]. Gas hydrates have a high tendency of causing serious operational and economic concerns and thus require novel, innovative techniques to reduce the costs associated with flow assurance, improving the overall recovery factors for deep-water, marginal, and mature fields [81]. A variety of gas hydrate inhibitors are usually applied, which as broadly classified into high-dosage hydrate inhibitors (HDGIs) and low-dosage inhibitors (LDGIs) (cf. Figure 8.3). The LDHIs are further divided into KHIs and anti-agglomerates (AA). Commonly, gas hydrates are inhibited by the utilization of thermodynamic "antifreeze" hydrate inhibitors (THIs), such as monoethylene glycol (MEG) and methanol (MeOH) to the aqueous phase. However, under challenging operational conditions, these inhibition techniques are not suitable, requiring enormous capital and operational expenditures. Moreover, these types of inhibitors have also caused

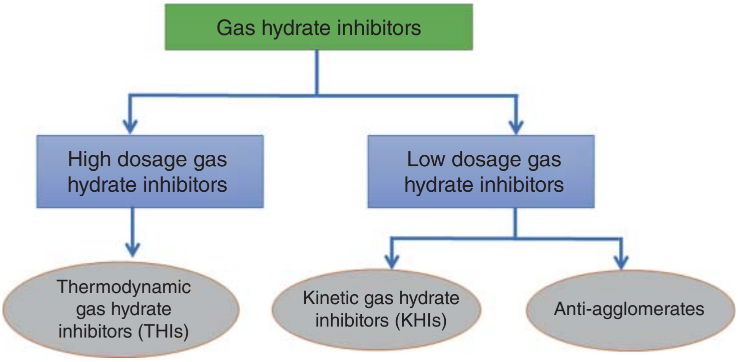

**Figure 8.3** Classification of gas hydrate inhibitors.

serious environmental concerns, as due to their large-scale applications, they require heavy-recycling and waste-handling costs.

Due to this, development of other suitable alternative inhibitors, which are low cost and easy to handle, is highly required for hydrate control. To minimize the use of THIs, Lederhos et al. proposed extending the metastable period prior to the nucleation phase of the hydrate by inserting a crystal stabilizer between metastable hydrate crystallite [82]. These types of crystal stabilizers are known as KHIs. Although the exact mechanism of KHI is still unclear, several studies suggest that they act by prolonging the hydrate nucleation and growth time [83]. The main component of KHIs is a water-soluble polymer or oligomer, which possesses both hydrophilic and hydrophobic functionalities, capable of preventing hydrate formation by interacting with both free water and water in hydrate particles. They are effective even at lower doses and function by prolonging hydrates' nucleation and growth phase without altering the gas-hydrate-phase equilibrium. Therefore, they offer several benefits over THIs and have attracted significant attention from scientists and technologists, which is clearly reflected by the increasing number of publications on this topic over a couple of decades [84].

Therefore, a variety of water-soluble polymers, such as poly(vinyl caprolactam) (PVCap), poly(vinyl pyrrolidone) (PVP), as well as hyperbranched poly(ester amide)s based on diisopropanolamine and carboxylic anhydrides, have been applied as KHIs [85]. Organic functionalities present in these KHIs facilitate the adsorption of these materials on the surface of hydrates and their interaction with water molecules responsible for the formation of cage structure. The KHIs are mainly divided into two categories, such as synthesized KHIs and natural KHIs [86]. Among synthesized KHIs, PVP and PVCap belonging to the lactam family of polymers are the most commonly applied materials in which PVP is a more effective inhibitor than PVCap [87]. For instance, Tang et al. have investigated the effect of PVP on the natural gas hydrate using Raman spectroscopy and cryo-scanning electron microscope (SEM). Results showed that PVP inhibited the occupancy of gas molecules in the large cages, and the hydrates dissociated faster in the presence of PVP than without PVP [88].

Thus, based on the structure of PVP and PVCap, lots of similar structure polymers and copolymers are applied as KHIs, such as carboxyl-acid-group-modified PVCap has been synthesized and used as an inhibitor against methane hydrate formation [89]. Besides, polyvinylpiperidinone (PVPip), VIMA/VP(*N*-vinyl-*N*-methyl acetamide and *N*-vinyl pyrrolidone copolymer), etc. containing one or more pendant lactam groups, which consist of oxygen atoms, form the hydrogen bonds with the water molecules to inhibit hydrate formation [90]. Furthermore, to enhance the water solubility and hydrogen-bonding ability of amide (—NH—C(=O)—) functional groups containing polymers, various polyvinylsulfonamides have been prepared by replacing the amide group with the sulfonyl moiety. When applied as KHIs, these polymers demonstrated excellent inhibition ability due to the presence of two oxygen atoms [91]. Some reports have suggested that hydrophilic moieties and hydrophobic end groups potentially alter the KHI properties, such as solubility and inhibition. To achieve this, various polymers have been grafted by the inclusion of various functional groups, such as hetero-cycles, chain or cyclic amides, betaines, and amine oxides, which have exhibited superior inhibition properties [92].

Although the aforementioned polymers have shown decent inhibition properties, they are costly and difficult to prepare. To overcome this, a variety of organic salts were applied as a synergist, strengthening the resultant material's inhibition properties due to the synergic effect between the components. These salts include tri-*n*-pentylamine oxide (TPAO), tetra(*n*-hexyl) ammonium bromide (THexAB), and mono fluoro ammonium salt, which have demonstrated synergistic effects with PVCap on hydrate formation [93]. Despite significant development, various challenges and uncertainties still prevent the large-scale application of synthesized polymers in the petroleum industry. Common problems are the lack of compatibility with other production chemicals, relatively low cloud point/fouling issues, poor repeatability of test results, performance concern under shut-in conditions, potential risk of hydrate formation at the top of pipelines, etc.

Apart from these problems, various environmental concerns have also limited synthesized polymers' widespread offshore field application. Thus, the focus on green hydrate inhibitors has been increasing steadily, typically based on polysaccharides, antifreeze proteins (AFPs), and other biomolecular materials that possess enhanced biodegradability. AFPs are obtained from deep ocean fish or frigid zone animals, which can protect organisms against freezing at low temperatures. As gas hydrate inhibitors, AFPs that can prevent the formation of ice crystals also have the ability to inhibit the hydrate formation, which is revealed in the tests of a series of AFPs from fishes and insects on the formation of hydrates that exhibited superior inhibition properties than PVP [94, 95]. AFPs act by controlling the morphology of hydrate crystals and not allowing them to grow into larger and well-dispersed particles. Despite the good inhibition properties of AFPs on hydrate formation, their high cost and low production hamper their applications in the oil and gas fields [96]. Therefore, other green inhibitors have been explored, such as starch, chitosan, and pectin, which consist of OH, $NH_2$, and COOH groups that can prevent hydrate formation by hydrogen bonding [97]. One such polysaccharide is alginate that is gaining popularity as a gas hydrate inhibitor. It is naturally derived from the brown seaweed *Phaeophyceae* and is produced as an extracellular material by bacteria, such as *Pseudomonas* and *Azotobacter*. Silva et al. have used alginate as a natural gas hydrate inhibitor and investigated the amount of methane hydrates formation over time [98]. Alginate exhibited a good inhibitory capacity and acted by delaying the formation of hydrates. Another polysaccharide is starch, which is obtained from different sources and exhibits different effects on the gas hydrate. For instance, Lee et al. investigated a variety of starch as an inhibitor in methane and methane/ethane mixture hydrate. However, most of them showed weak inhibiting effects except tapioca starch, which increased the induction time (delay of onset of crystallization) by order of magnitude. Further, the addition of polyethylene oxide (PEO) was found to enhance the performance of tapioca starch as well as some of the other starches [99]. Pectin is also used as a green inhibitor, which showed superior inhibition properties than PVCap [100]. Green inhibitors have decent inhibition properties and are biodegradable, but they have less applicability in the oil and gas industry due to various shortcomings. Natural inhibitors that are extracted from living organisms are costly and less available, while others are cheap and can be easily obtained, but they have low aqueous solubility and high viscosity and thus cannot be injected into pipelines.

## 8.4 Dual-Purpose Chemicals

In the petroleum industry, the protection of pipelines and other equipment is critical to maintaining flow assurance, often carefully managed to achieve economic and successful operations [101]. Particularly, in deep-water areas, the proper maintenance of pipelines is more challenging that is required to be addressed adequately. Both corrosion and the formation of gas hydrates are usually responsible for damaging the oil and gas pipelines, creating various safety and risking considerable economic loss [102]. During every stage of storage and transportation, apart from blocking the pipelines, the gas hydrates also interact with the composition of pipelines and other installations, which ultimately contribute to the process of internal corrosion [103]. While gas hydrate leads to the rupture of pipelines, the corrosion results in the degradation of the metal surface and deteriorates the pipelines' integrity [104]. Elimination of gas hydrate (NGH) and protection of pipelines from corrosion may lead to production shutdown, leading to huge economic losses. To overcome this problem, various strategies have been adopted by the industry, which are mainly beneficial and have several disadvantages, such as the separate application of a variety of gas hydrate and corrosion inhibitors (GHCIs) that cause further economic loss and create other environmental issues, including the requirement of large storage spaces, regeneration, and biodegradable problems besides adverse effects on each other performances [105]. For example, the separate injection of KHIs and CIs usually leads to the problem of compatibility. KHI performance is considerably reduced due to the presence of CIs and another way around [106]. Besides, the separate applications of KHIs and CIs chemicals require the development of extensive infrastructures, such as the installation of injection pumps, building large storage tanks, developing regeneration processes, and distribution pipelines in the deep-sea areas [107]. Therefore, there is an urgent need to develop low-cost and eco-friendly chemicals that can single-handedly tackle the two major flow assurance issues, including corrosion and gas hydrates. Most of the studies have investigated mainly the mechanism, types, and purpose of GHCI in the oil and gas industry. However, dual-purpose chemicals that have the ability to inhibit hydrate formation as well as prevent corrosion have been rarely studied. Therefore, developing a single chemical that can be used instead of multiple chemical dosages can potentially limit the cost of numerous chemicals and their infrastructure requirements, resulting in potential economic savings.

## 8.5 Dual-Purpose Corrosion Inhibitor and KHIs (GHCIs)

As mentioned earlier, the problems of gas hydrate formation and corrosion mitigation are often addressed individually using separate inhibitors. However, they usually suffer from compatibility issues. The CIs facilitate the nucleation of large gas hydrate crystals, particularly in deep-sea conditions, whereas GHIs enhance the corrosion rate. The negative interactions between KHIs and CIs are not well-understood due to various structures involved in testing. Still, competition between the components for the adsorption on the metal surface is mainly attributed [108]. To address this, initially, some of the known KHIs have been tested as potential CIs instead of designing multifunctional molecules. However, the results were not exciting [109]. This required the development of novel chemicals that can function as dual-purpose GHCIs. The idea is first proposed by Hoppe et al. Since then, scientists have striven hard to develop a variety of such single substance chemicals that can inhibit both gas hydrate formation and corrosion inhibition in a single dose [110]. This has addressed the compatibility issues and reduced the cost of chemicals, and offered several financial benefits. GHCIs should have the ability to connect with water molecules via hydrogen bonding and can also be able to adhere to the surface of the metal and form defensive film to inhibit both hydrate and corrosion formation, respectively (cf. Figure 8.4). This is typically achieved by modifying the functional group responsible for hydrate inhibition in GHIs using the corrosion inhibitor group in CIs. So far, different kinds of chemical substances have been developed, consisting of dual-purpose functionalities in offshore pipelines; these include synthetic and natural polymers (biopolymers), ionic liquids (ILs), amino acids, and other biomolecules.

Sheng et al. have designed single molecules based multifunctional polymers as GHCIs, which were prepared by modifying a base polymer with a key functional group, and investigated basic insights into the mode of action of these substances [46]. A copolymer based on vinylcaprolactam (VCap) and acrylic acid (PVCap-*co*-Na AA) was used as the base polymer. VCap effectively inhibited the hydrate formation, while the acrylic acid helped in coupling to known CIs. Besides, these copolymers were also modified with several other heteroatoms containing functionalities, such as taurine, which helped to bind via lone pair of electrons. In a similar study, Park et al. prepared several multifunctional polymers by further modifying PVCap-*co*-AA copolymer. The modification was performed by converting the acid groups to known CIs groups, such as imidazole (APIM) and quaternary ammonium (ATCH) moieties [111]. Farhadian et al. have introduced the concept of designing novel GHCIs using waterborne polyurea/urethanes (WPUUs) as efficient GHIs and CIs. These dual-purpose substances simultaneously delay onset nucleation time/temperature, reduce hydrae growth rate, prevent agglomeration of hydrate particles, and suppress corrosion [112]. Waterborne polyurethanes (WPU) of various hydrophobicity *N*-substituted diethanolamines (methyl, *n*-butyl, and *tert*-butyl) were used in another study by Pavelyev et al. for the fabrication

**Figure 8.4** Proposed functionality of dual-purpose corrosion inhibitor.

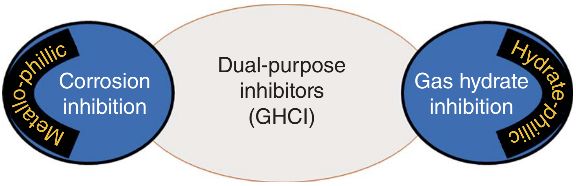

of GHCIs. In this work, the effect of the variation of diethanolamines differing in the size and branching of *N*-substituents and the amount of these groups on the structure of polymer molecules was investigated [113]. The study revealed a significant enhancement of inhibiting properties of dual-purpose inhibitors with the increase in the hydrophobicity of GHCIs. Very recently, waterborne polyurethanes (WPUs) with a varied length of the side substituents and polyethylene glycol-400 to 1,2-butanediol ratio were varied [114]. It was revealed that butyl derivatives (ethyl–butyl and methyl–butyl combinations) showed slightly better inhibition performance than commercial hydrate inhibitor PVCap

Apart from polymers, ILs exhibit fascinating properties, including low-melting point (less than 100 °C), low-vapor pressure, low toxicity, high polarity, and high chemical and thermal stability. This makes them suitable for substituting traditional toxic inhibitors [115]. Due to this, ILs were widely investigated for their corrosion inhibition properties that also exhibit hydrate inhibition abilities due to the presence of cations and anions [116]. In this regard, Xiao and Adidharma have five imidazolium-based ILs as a new class of GHIs has been investigated. Among various ILs, [EMIM] + [BF4] exhibited superior inhibition properties due to the presence of strong electrostatic and hydrogen-bonding affinity with water [117]. Due to these strong electrostatic charges and hydrogen-bonding ability, IL could shift the equilibrium hydrate dissociation/stability curve to a lower temperature and, at the same time, retard the hydrate formation by slowing down the hydrate nucleation rate and therefore act as both thermodynamic and kinetic inhibitors. A little later, Sasikumar et al. have theoretically investigated the same IL, namely, [EMIM] + [BF4] as CI, which has exhibited good inhibition properties due to strong adsorption properties, which was evaluated using Langmuir adsorption isotherm [118]. In another study, Yesudass et al. have studied some alkyl imidazolium-based Ils, namely, 1-ethyl-3-methylimidazolium ethyl sulfate [EMIM] + [EtSO4]−, 1-ethyl-3-methylimidazolium acetate [EMIM] + [Ac]−, 1-butyl-3-methylimidazolium thiocyanate [BMIM] + [SCN]−, 1-butyl-3-methylimidazolium acetate [BMIM] + [Ac]−, and 1-butyl-3-methylimidazolium dicyanamide [BMIM] + [DCA]. The studied ILs exhibited decent inhibition properties as mixed-type inhibitors, which inhibited both the anodic mild steel dissolution and cathodic hydrogen evolution reactions [119]. However, [EMIM] + [EtSO4] − demonstrated the highest corrosion inhibition, and the ADT value in THI is also the highest.

Apart from this, amino acids, such as alanine, glycine, and valine, have been investigated for thermodynamic and kinetic hydrate inhibition in the $CO_2$ system [120]. However, in other studies, these types of inhibitors have also been used as CIs [121]. For example, glycine and alanine were used as thermodynamic methane hydrate inhibitors in one study, whereas in another study, the same amino acids were applied as cathode type CIs for the metal in the acidic environment [122, 123]. Tyrosine has demonstrated effective corrosion inhibition properties on iron, which is electrochemically investigated in 0.1 M HCl; on the other hand, the same amino acid was used as a kinetic inhibitor of methane and ethane hydrates at very low concentrations up to 200 ppm [124, 125]. The corrosion inhibition property of serine was investigated on mild steel in $Na_2HPO_4$ solutions containing chloride ions as an aggressive ion using open-circuit potential (OCP), potentiodynamic polarization measurements, and pitting corrosion current measurements [126]. Recently, Sa et al. reported the effect of amino acids, including serine on gas hydrate formation. Serine changed its structure in the presence of water and thus interrupted the formation of methane and natural gas hydrates [127]. In addition, arginine was also tested separately for its corrosion inhibition properties in an acidic medium, wherein it functioned as a mixed-type inhibitor, while in a separate study, it acted as a thermodynamic inhibitor that suppressed the formation of methane hydrate crystals [123].

Due to environmental concerns, the focus is shifted more toward developing green inhibitors, which are nontoxic, cost-effective, and biodegradable. In this context, naturally occurring compounds and polymers, usually known as biomolecules, have gained significant attention. Farhadian et al. have recently used sunflower oil as a cost-effective and eco-friendly material to prepare a dual-function inhibitor to resolve incompatibility issues between anti-hydrate and anti-corrosion reagents [47]. Since the presence of long alkyl chains in KHIs enhance the inhibition performance and increase corrosion inhibition by forming a protective film, the alkyl chains of sunflower oil act as a protective layer. In contrast, triglyceride and its fatty acid chains can increase the strength of inhibition. In another study, the potential of glycerol as a dual function inhibitor has been tested, which is a well-known thermodynamic gas hydrate inhibitor in the oil and gas industry. The results revealed that glycerol has 66% corrosion inhibition efficiency at 10 000 ppm (1 wt%). The inhibition efficiency of glycerol shows the trend of proportionally increasing with the concentration [128].

Similarly, polysaccharides, which are biopolymers, have also been used in hydrate and corrosion inhibition applications. For instance, pectin acted as an effective inhibitor and suppressed steel corrosion in an acidic environment of 0.5 M HCl [129]. Whereas, it was also proved to be an exceptional naturally occurring KHI, which delayed methane hydrate production [100]. Another polysaccharide and carbohydrate-based biopolymer, namely, chitosan was found to block the actives sites of the metal and acted as a mixed type inhibitor [130]. On the other hand, its hydrogen-bonding ability in solution has successfully delayed the nucleation time of hydrate formation for methane and ethane [131]. Besides, cellulose derivatives also have great potential as a dual-purpose inhibitor. For instance, hydroxyethylcellulose inhibited the formation of methane hydrate [132]. And when applied as a CI in a separate study, it acted as a mixed type inhibitor in 3.5% NaCl for corrosion suppression of steel [133].

### 8.5.1 Mechanism of Action of GHCIs

As earlier stated, the application of single moiety as KHIs and CIs is the solution for incompatibility issues of separately applied inhibitors. Generally, individual KHIs and CIs are injected into the pipeline simultaneously to save production costs, creating negative interactions, and initiating compatibility problems. Therefore, the application of dual-purpose chemicals saves the storage area and reduces the cost of handling. Besides, individual application of KHIs and CIs, adversely affect each other performance [106]. Although some CIs are not interfered with by KHI in terms of general corrosion rate, the localized corrosion inhibition is usually comprised due to the presence of a KHI [134]. Similarly, several investigations have revealed the importance of performance testing of inhibitors before the simultaneous injection of individual inhibitors. Since a CI and a KHI, which exhibit effective performance on their own, can potentially fail the corrosion and the hydrate test protocols when applied in combination (co-inject).

Two possible mechanisms have been proposed by Moore et al. to explain the negative interactions between KHIs and CIs, which include the competition for the surface interface and chemical interaction at the molecular level. In the former case, both KHI and CI adhere to the surface interface via absorption. KHIs inhibit the growth of hydrate crystals by binding onto the surface of hydrates, whereas CIs block the active sites by absorbing onto the metal surface. Therefore, due to their high tendency to interact with the surfaces, it is highly likely that KHIs absorb onto the metal surface instead of gas hydrate and negatively impact the CI performance. Similarly, CI can also unwantedly absorb onto the surface of hydrate and inhibit KHI from interacting with the hydrate surface, which may lead to the lowering efficiency of KHI. In the latter case, the KHI molecules have specific anchoring centers that destroy the hydrate structure by interacting with the functional groups of hydrate molecules. Due to this, the energy requirement for the hydrate formation increases, which ultimately disturbs the reaction kinetics and delays the gas hydrate formation [108]. Therefore, when CI binds to these active centers of KHI, it may seriously affect the hydrate inhibition properties of KHI.

However, only a few studies have addressed this issue of incompatibility of KHIs and CIs, which requires a detailed investigation of the basic mechanism of both chemistries and development processes of the components [134]. For instance, Jones et al. have noted the reduced performance of both KHIs and CIs in the presence of each other, whereas, in other studies, the presence of KHIs did not affect the function of CI, which demonstrated enhanced performance [135, 136]. In another study, it is claimed that the incompatibility between KHIs and CIs is due to the competition among inhibitors to attach to the surface of pipeline and hydrate, and also the enhanced interaction between CIs and KHIs in aqueous solution can also be responsible for the incompatibility between the components [108].

Based on these observations, the application of those KHIs was encouraged, which also have corrosion inhibition properties. Indeed, Burgazli et al. investigated a variety of undisclosed chemicals as KHIs using an autoclave technique [109]. The result of the study suggested that the performance of inhibitors can be customized by selectively designing the molecules by manipulating the chemistry of the system. For example, to design an effective KHI, the size of the molecule, charge distribution, hydrogen-bonding ability, and surface-adsorption properties are the most critical aspects that determine the inhibition properties of KHIs. Whereas, in the case of CIs, the ability of the compound to adsorb onto the surface of the metal, forming a shielding layer, is a crucial factor in determining the system's corrosion behavior. Still, the interactions between KHIs and CIs have yet to be understood properly, which is a tedious process. All KHIs and CIs have to be validated together under similar conditions. To understand the mechanism of complex interactions of KHIs and CI with the pipelines and hydrates, the researchers have developed other strategies. Such as the development of multifunctional substances consisting of two different ends, including hydrate-philic and metallo-philic sides, significantly enhances the compatibility of the material [110]. Dual-purpose inhibitors typically act by forming hydrogen bonding with water molecules and simultaneously adsorb onto the surface of the pipeline to form a defensive layer that helps to mitigate hydrate and corrosion formations, respectively. In addition, KHI can be converted into GHCIs by modifying the hydrate inhibitor group of KHI with a CI group (which is usually achieved by attaching). For example, developing a copolymer of vinyl caprolactam (VCap) and acrylic acid (PVCap-*co*-Na AA) where the VCap provides hydrate inhibition, and the acrylic acid provides hydrate inhibition acid was used to couple on known CI groups.

### 8.5.2 Performance Testing and Evaluation of GHCIs

Experimental testing and screening inhibitors are essential from lab to pilot scale, which have been gradually improving over the years. Some of the commonly applied methods include autoclave, rocking cell, stirred reactor, batch or semi-batch crystallizers, high pressure-automated lag time apparatus (HP-ALTA) and (micro) differential scanning calorimetry (DSC or μ-DSC), pipe-wheel, and flow loop [21]. However, the choice of a suitable method is largely based on the inhibitor's purpose and properties, which need to be investigated. Stirred high-pressure autoclaves, HP-ALTA, flow loop, and other types of stirred reactors are frequently used in gas hydrate studies with adjustable agitation strength and pressure and temperature monitoring [137–139]. Stirred high-pressure autoclaves have been commonly used for years to determine the performance of KHIs [140]. This device is typically made in different sizes using various materials, such as steel, titanium, or sapphire. Since the hydrate formation process is stochastic, several experiments must be performed using the same parameters to obtain reliable results. For instance, Hase et al. have investigated the process of hydrate formation in the presence of five VP/VCap-based polymers using autoclave and rocking cell of hydrate methods [141]. The study has concluded the following order for testing KHIs. Initially, less effective KHIs can be eliminated using the constant cooling procedure; subsequently, the best performers among the screened KHIs can be selected using the crystal growth inhibition (CGI). Finally, most potential KHIs can be selected using the isothermal induction time measurements. Although the autoclave method is popular, it is a time-consuming process, leading to the development of other fast screening methods.

Such as the high-pressure rocking cell, which is made up of steel or sapphire, consists of a steel or glass ball that is rocked back and forth to create turbulence and mix the fluids [142]. This is a relatively fast process and can perform several experiments on each KHI to quickly screen a series of KHIs and determine their relative performance ranking [93]. However, to determine the absolute field performance of a KHI, an infinite number of tests at the field conditions are required. To overcome this problem, Lone et al. developed a 5-cell rocker rig technique to investigate the KHI performance by varying different parameters. Using rocking cells, several parameters were determined: rocking angle, rocking speed, aqueous volume added to the cell, steel versus glass balls, isothermal versus constant cooling test, cooling rate, and KHI concentration [143].

Usually, induction times are measured using these methods at constant sub-coolings and/or the maximum achievable sub-coolings while maintaining cooling ramps. In addition, these methods also require a large number of flammable gases, high pressures, and long data accumulation times. Moreover, the amount of sample required for testing is also large, which renders the use of the conventional technique challenging for precious inhibitors such as anti-freeze proteins [95, 144]. Due to these shortcomings in testing methods development of new inhibitors is seriously affected.

In this regard, Sheng et al. have developed a low cost, rapid method for the parallel screen of potential KHIs without using highly pressurized and potentially flammable/explosive fuel gases [46]. They have exploited the structure–property relationship knowledge to develop the understanding required for the control and prediction of hydrate formation. To achieve this, they have developed a rapid screening method to ascertain KHI efficiency based upon observing the inhibition of hydrate formation of structure II (sII)-forming cyclopentane (c-C5) hydrate under atmospheric pressure. This study introduces a flexible approach to generating libraries of novel polymers that can function as both hydrate and CIs. Applying this high-throughput method, the structure and properties of the polymers were successfully modulated to obtain information about the complex interplay of hydrate and corrosion. For this purpose, they have modified copolymers based on VCap and acrylic acid (PVCap-*co*-Na AA) with taurine. In combination with high throughput hydrate screen method with weight loss technique for corrosion, they have identified several promising GHCIs. Furthermore, using this proof-of-concept, other inhibitors' performance was also validated in other studies [43]. These studies suggest that developing a single polymer for dual purpose is more complex than mixing different inhibitors, but the idea of resolving compatibility issues using multi-purpose molecules is proved to be effective but still requires further investigations.

### 8.5.3 Factors Controlling the Performance of GHCIs

It is advantageous to use hydrate inhibitors that have potential applications in corrosion inhibition also. The key factors that affect the performance of the gas hydrate and corrosion inhibition behaviors of GHCIs are also depicted in Figure 8.5.

#### 8.5.3.1 Size/Molecular Weight of GHCIs

The size of the molecule in terms of the number of monomers added per reactive site played a significant role in both gas hydrate and corrosion inhibition. While additional monomers per reactive site appeared to improve the corrosion inhibition in all derivatives, gas hydrate inhibition appeared to be optimum at specific monomers added per reactive site depending upon the chemical. Polyaspartamides

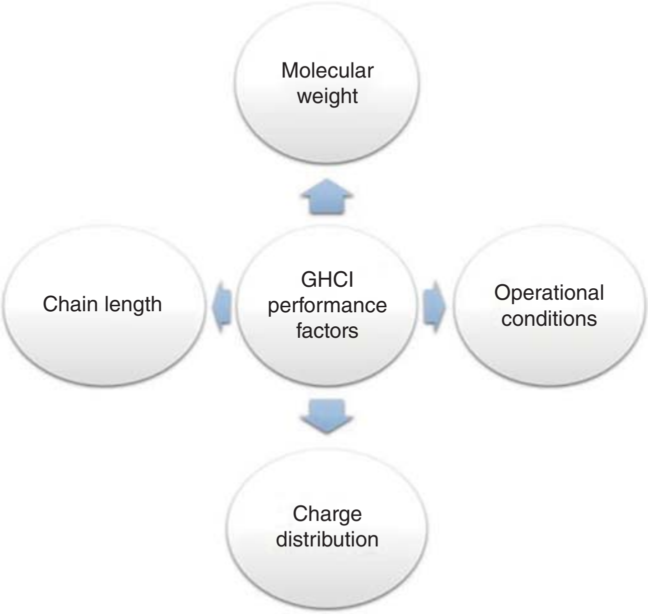

**Figure 8.5** Key factors controlling the performance of GHCIs as corrosion and gas hydrate inhibitors.

are a newly established category of KHIs with good biodegradability using polysuccinimide (PSI) [145].

The optimum molecular weight for KHI is reported around 1500–3000. At molecular weight lower than 100, the performance drops drastically, and at increasing molecular weights above 3000–4000, the performance drops slowly but does not disappear. The reason for the optimum range is related to the surface/volume ratio of the polymer as well as the high mobility of the polymer in the solution. The CIs are mainly based on small molecules; therefore, KHI with low-molecular weight will be ideal for the CI properties.

#### 8.5.3.2 Chain Length Specific to Corrosion Inhibitor

The impact of chain length changes the GHCI behavior of chemicals. The solubility of film-forming CIs can be changed by the hydrophilicity of the headgroup or by varying the length of the hydrophobic tail. However, if the tail is too short (less than 12 carbons), a good oily film of hydrocarbons with more than 20 carbons tails may be ripped off the walls at very high shear. Therefore, the CI part of the GHCI should have a reasonable size of the hydrophobic tail (more than 12 carbons) for better performance. Shorter chains are required for gas hydrate mitigation, whereas corrosion inhibition requires a relatively higher chain length.

#### 8.5.3.3 Charge Distribution of Corrosion Inhibitors

Some reported CIs are based on quaternary ammonium salts or cationic molecules. These cations of the CI adsorb on the surface of the metal through synergists, such as thiol-containing compounds. Similarly, the distribution of charge along the chain of the CHCI polymer is essential to get better adsorption on the metal surface. The second key point is that the charged surface should be exposed for better adsorption. Table 8.1 shows a list of biopolymers and synthetic polymers employed in GHCI applications. The chemical name, structure, and applications of polymers are highlighted in Table 8.1.

**Table 8.1** List of biopolymers and synthetic polymers as gas hydrate and corrosion inhibitor (GHCI).

| Chemicals | Structures | Corrosion inhibitor | Gas hydrate inhibitor specifi-cations | References |
|---|---|---|---|---|
| Polyaspartic acid | 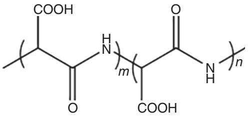 Polyaspartic acid | CI | KHI | Mobin et al. [146]<br>DelVillano et al. [147] |
| Pectin | 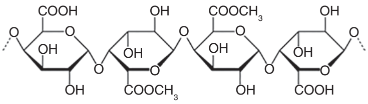 | CI | KHI | Umoren et al. [148]<br>Xu et al. [149] |
| Chitosan | 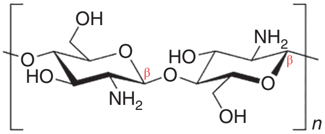 | CI | KHI | Gupta et al. [150]<br>Xu et al. [151] |
| Starch (in presence of DPMP) | 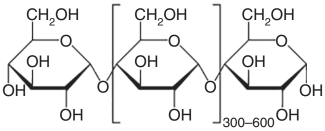 | CI | KHI | Brindha et al. [152]<br>Talaghet al. [153] |
| Hydroxyethyl cellulose | 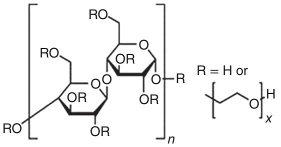 | CI | KHI | El-Haddad et al. [154]<br>Jokandan et al. [155] |
| Poly(vinyl caprolactam) (PVCap) | 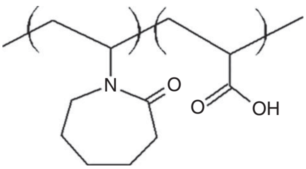 | CI | KHI | Park et al. [111] |
| Poly(vinyl caprolactam) (PVCap) | 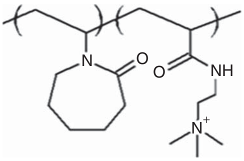 | CI | KHI | Park et al. [111] |

*(Continued)*

**Table 8.1** (Continued)

| Chemicals | Structures | Corrosion inhibitor | Gas hydrate inhibitor specifications | References |
|---|---|---|---|---|
| Poly(vinyl caprolactam) (PVCap) | 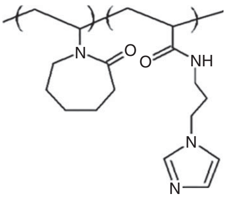 | CI | KHI | Park et al. [111] |
| Poly(vinyl caprolactam) (PVCap) | 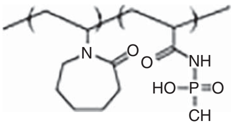 | CI | KHI | Sheng et al. [46] |
| Poly(vinyl caprolactam) (PVCap) | 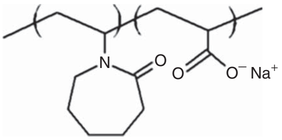 | CI | KHI | Sheng et al. [46] |
| Acryloyl-based polymers | 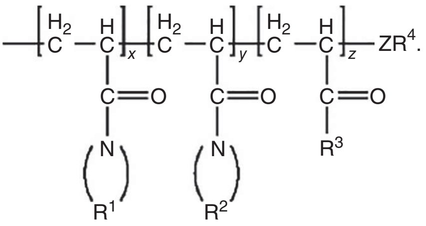 | CI | KHI | Ul-haq et al. [156] |

### 8.5.3.4 Operational Conditions

The operational conditions affect the performance of the GHCIs. One of the critical parameters is a gas mixture, especially $H_2S$ is the most accessible gas to form the gas hydrates. It forms gas hydrates at low temperatures compared to other gases, such as $CH_4$ or $CO_2$. Therefore, hydrates of $H_2S$ are more challenging to inhibit compared to other gases. Pressure and temperature are two additional parameters that impact the performance of KHIs, especially high pressure and lower subcooling temperatures.

Based on Figure 8.5 and above discussions, it is evident that a few key factors influence the performance of the GHCIs. Therefore, balanced or optimal parameters should be applied according to specific operating conditions to achieve the maximum performance of GHCIs.

## 8.6 Conclusion and Future Prospects

Herein, we have highlighted the problems of gas hydrate formation and corrosion in the oil and gas industry and the application of separate chemical inhibitors to resolve these issues. However, the concept of developing dual-purpose inhibitors that simultaneously inhibit both corrosion and gas hydrate formation has excellent potential in tackling the problems that occurred during the co-injection of separate KHIs and CIs. So far, very few dual-purpose inhibitors have been successfully developed that could inhibit both corrosion and gas hydrate formation simultaneously. However, there are plenty of materials available in the market that have demonstrated the ability to inhibit corrosion and hydrate formation separately. These types of materials have a huge potential to be modified and can be tested as dual-purpose inhibitors. Such materials include ILs, copolymers, and biomolecules, which have been successfully tested as KHIs and CIs. In contrast, very few, such as imidazolium and ammonium-based ILs, modified VCap and acrylic acid-based copolymers, have been tested as GHCI inhibitors. Furthermore, developing high throughput methods by exploiting the structure–properties relationship of the materials can accelerate the finding of novel GHCIs.

## Acknowledgments

The authors would like to thank Saudi Aramco for permission to publish this book chapter. Special thanks go to the R&DC management for their support and encouragement.

## List of abbreviation

| | |
|---|---|
| AFPs | antifreeze proteins |
| AA | anti agglomerate |
| CI | corrosion inhibitors |
| $CO_2$ | carbon dioxide |
| CGI | crystal growth inhibition |
| $Na_2HPO_4$ | disodium phosphate |
| GHCI | gas hydrate corrosion inhibitor |
| $H_2S$ | hydrogen sulfide |
| HCl | hydrochloric acid |
| KHI | kinetic hydrate inhibitor |
| LDHI | low-dose hydrate inhibitor |
| MPa | megapascal |
| MEG | monoethylene glycol |
| OCP | open-circuit potential |
| $H_2SO_4$ | sulfuric acid |
| TPAO | tri-*n*-pentylamine oxide (TPAO) |

| | |
|---|---|
| THexAB | tetra(*n*-hexyl) ammonium bromide |
| Vcap | vinyl caprolactam |
| Vp | vinyl pyrrolidine |
| WPUs | waterborne polyurethanes |

## References

**1** Popoola, L.T., Grema, A.S., Latinwo, G.K. et al. (2013). Corrosion problems during oil and gas production and its mitigation. *International Journal of Industrial Chemistry* 4: 1–15.

**2** Fayomi, O., Akande, I., and Odigie, S. (2019). Economic impact of corrosion in oil sectors and prevention: an overview. *Journal of Physics: Conference Series* 1378: 022037.

**3** Al-Janabi, Y.T. (2021). An overview of corrosion in oil and gas industry: upstream, midstream, and downstream sectors. *Corrosion Inhibitors in the Oil and Gas Industry* 7 (70): 1–18.

**4** Varela, F., Yongjun Tan, M., and Forsyth, M. (2015). An overview of major methods for inspecting and monitoring external corrosion of on-shore transportation pipelines. *Corrosion Engineering, Science and Technology* 50: 226–235.

**5** Castaneda, H. and Rosas, O. (2015). External corrosion of pipelines in soil. *Oil and Gas Pipelines* 265–274.

**6** Nešić, S. (2007). Key issues related to modelling of internal corrosion of oil and gas pipelines–a review. *Corrosion Science* 49: 4308–4338.

**7** Dwivedi, D., Lepková, K., and Becker, T. (2017). Carbon steel corrosion: a review of key surface properties and characterization methods. *RSC Advances* 7: 4580–4610.

**8** Olajire, A.A. (2017). Corrosion inhibition of offshore oil and gas production facilities using organic compound inhibitors–a review. *Journal of Molecular Liquids* 248: 775–808.

**9** Tamalmani, K. and Husin, H. (2020). Review on corrosion inhibitors for oil and gas corrosion issues. *Applied Sciences* 10: 3389.

**10** Amezhnov, A., Rodionova, I., Batsalev, A. et al. (2019). Effect of chemical composition and microstructure parameters on carbon and low-alloy steel corrosion resistance under oil industry pipeline operation conditions. *Metallurgist* 62: 1030–1038.

**11** Tiu, B.D.B. and Advincula, R.C. (2015). Polymeric corrosion inhibitors for the oil and gas industry: design principles and mechanism. *Reactive and Functional Polymers* 95: 25–45.

**12** Askari, M., Aliofkhazraei, M., Ghaffari, S., and Hajizadeh, A. (2018). Film former corrosion inhibitors for oil and gas pipelines–a technical review. *Journal of Natural Gas Science and Engineering* 58: 92–114.

**13** Verma, D.K., Dewangan, Y., Dewangan, A.K., and Asatker, A. (2021). Heteroatom-based compounds as sustainable corrosion inhibitors: an overview. *Journal of Bio-and Tribo-Corrosion* 7: 1–18.

**14** Chauhan, D.S., Verma, C., and Quraishi, M. (2021). Molecular structural aspects of organic corrosion inhibitors: experimental and computational insights. *Journal of Molecular Structure* 1227: 129374.

**15** Quraishi, M., Chauhan, D.S., and Ansari, A.F. (2021). Development of environmentally benign corrosion inhibitors for organic acid environments for oil-gas industry. *Journal of Molecular Liquids* 329: 115514.

**16** Ansari, K., Chauhan, D.S., Quraishi, M. et al. (2020). Chitosan Schiff base: an environmentally benign biological macromolecule as a new corrosion inhibitor for oil & gas industries. *International Journal of Biological Macromolecules* 144: 305–315.

**17** Camp, E. and Phillips, C. (1950). Neutralization as a means of controlling corrosion of refinery equipment. *Corrosion* 6: 39–46.

**18** Tang, Z. (2019). A review of corrosion inhibitors for rust preventative fluids. *Current Opinion in Solid State and Materials Science* 23: 100759.

**19** Gouda, V. and Shater, M. (1975). Corrosion inhibition of reinforcing steel by using hydrazine hydrate. *Corrosion Science* 15: 199–204.

**20** Emori, W., Jiang, S., Duan, D. et al. (2017). Corrosion behavior of carbon steel in amine-based CO2 capture system: effect of sodium sulfate and sodium sulfite contaminants. *Materials and Corrosion* 68: 674–682.

**21** Ke, W. and Kelland, M.A. (2016). Kinetic hydrate inhibitor studies for gas hydrate systems: a review of experimental equipment and test methods. *Energy & Fuels* 30: 10015–10028.

**22** Hassanpouryouzband, A., Joonaki, E., Farahani, M.V. et al. (2020). Gas hydrates in sustainable chemistry. *Chemical Society Reviews* 49: 5225–5309.

**23** Sloan, E.D. (2003). Fundamental principles and applications of natural gas hydrates. *Nature* 426: 353–359.

**24** Perrin, A., Musa, O.M., and Steed, J.W. (2013). The chemistry of low dosage clathrate hydrate inhibitors. *Chemical Society Reviews* 42: 1996–2015.

**25** Kvenvolden, K.A. (1993). Gas hydrates—geological perspective and global change. *Reviews of Geophysics* 31: 173–187.

**26** Makogon, Y.F. (2010). Natural gas hydrates–a promising source of energy. *Journal of Natural Gas Science and Engineering* 2: 49–59.

**27** Wang, X., Zhang, F., and Lipiński, W. (2020). Research progress and challenges in hydrate-based carbon dioxide capture applications. *Applied Energy* 269: 114928.

**28** Zhou, X., Zang, X., Long, Z., and Liang, D. (2021). Multiscale analysis of the hydrate based carbon capture from gas mixtures containing carbon dioxide. *Scientific Reports* 11: 1–9.

**29** Truong-Lam, H.S., Kim, S., Seo, S.D. et al. (2020). Water purifying by gas hydrate: potential applications to desalination and wastewater treatments. *Chemical Engineering Transactions* 78: 67–72.

**30** Sum, A.K., Koh, C.A., and Sloan, E.D. (2009). Clathrate hydrates: from laboratory science to engineering practice. *Industrial & Engineering Chemistry Research* 48: 7457–7465.

**31** Brewer, P.G., Orr, F.M., Friederich, G. et al. (1998). Gas hydrate formation in the deep sea: in situ experiments with controlled release of methane, natural gas, and carbon dioxide. *Energy & Fuels* 12: 183–188.

**32** Koh, C.A., Sum, A.K., and Sloan, E.D. (2012). State of the art: natural gas hydrates as a natural resource. *Journal of Natural Gas Science and Engineering* 8: 132–138.

**33** Zhang, H., Cheng, Y., Li, Q. et al. (2018). Numerical analysis of wellbore instability in gas hydrate formation during deep-water drilling. *Journal of Ocean University of China. JOUC* 17: 8–16.

**34** Olajire, A.A. (2020). Flow assurance issues in deep-water gas well testing and mitigation strategies with respect to gas hydrates deposition in flowlines—a review. *Journal of Molecular Liquids* 114203.

**35** Creek, J. (2012). Efficient hydrate plug prevention. *Energy & Fuels* 26: 4112–4116.

**36** Mokhatab, S., Wilkens, R.J., and Leontaritis, K. (2007). A review of strategies for solving gas-hydrate problems in subsea pipelines. *Energy Sources, Part A* 29: 39–45.

**37** Gao, S. (2009). Hydrate risk management at high watercuts with anti-agglomerant hydrate inhibitors. *Energy & Fuels* 23: 2118–2121.

**38** Kim, J., Kim, H., Sohn, Y.H. et al. (2017). Prevention of methane hydrate re-formation in transport pipeline using thermodynamic and kinetic hydrate inhibitors. *Journal of Petroleum Science and Engineering* 154: 114–125.

**39** Tang, C. and Liang, D. (2019). Inhibitory effects of novel green inhibitors on gas hydrate formation. *Chinese Journal of Chemical Engineering* 27: 2107–2117.

**40** Kelland, M.A. (2006). History of the development of low dosage hydrate inhibitors. *Energy & Fuels* 20: 825–847.

**41** Kelland, M.A. (2018). A review of kinetic hydrate inhibitors from an environmental perspective. *Energy & Fuels* 32: 12001–12012.

**42** Lv, Y., Guan, Y., Guo, S. et al. (2017). Effects of combined sorbitan monolaurate anti-agglomerants on viscosity of water-in-oil emulsion and natural gas hydrate slurry. *Energies* 10: 1105.

**43** da Silveira, K.C., Sheng, Q., Tian, W. et al. (2017). High throughput synthesis and characterization of PNIPAM-based kinetic hydrate inhibitors. *Fuel* 188: 522–529.

**44** Lim, V.W., Metaxas, P.J., Stanwix, P.L. et al. (2020). Gas hydrate formation probability and growth rate as a function of kinetic hydrate inhibitor (KHI) concentration. *Chemical Engineering Journal* 388: 124177.

**45** Luca, D., Villano, R., Kommedal, M. et al. (2009). A study of the kinetic hydrate inhibitor performance and seawater biodegradability of a series of poly (2-alkyl-2-oxazoline) s. *Energy & Fuels - ENERG FUEL* 23: 3665–3673.

**46** Sheng, Q., Silveira, K.C.d., Tian, W. et al. (2017). Simultaneous hydrate and corrosion inhibition with modified poly (vinyl caprolactam) polymers. *Energy & Fuels* 31: 6724–6731.

**47** Farhadian, A., Varfolomeev, M.A., Shaabani, A. et al. (2020). Sulfonated chitosan as green and high cloud point kinetic methane hydrate and corrosion inhibitor: experimental and theoretical studies. *Carbohydrate Polymers* 236: 116035.

**48** M.R. Simmons (2008). *Report of Offshore Technology Conference (OTC) presentation* (Houston, TX: NACE International Oil and Gas Production). USA.

**49** D. Corbin, E. Willson (2007). In New technology for real-time corrosion detection, Tri-service corrosion conference, USA.

**50** Lusk, D., Casserly, T., Gupta, M. et al. (2008). Armoured against corrosion. *Hydrocarbon Engineering* 13: 115–118.

**51** Amani, M. and Hjeij, D. (2015). A comprehensive review of corrosion and its Inhibition in the oil and gas industry, SPE Kuwait Oil and Gas Show and Conference, OnePetro.

**52** Okonkwo, P.C. and Mohamed, A.M. (2014). Erosion-corrosion in oil and gas industry: a review. *International Journal of Metallurgy Materials Science and Engineering* 4: 7–28.

**53** M. Simons (2008). *Report of offshore technology conference (OTC) presentation* (Houston, TX: NACE International Oil and Gas Production).

**54** Wood, M.H., Arellano, A.V., and Van Wijk, L. (2013). Corrosion related accidents in petroleum refineries, European Commission Joint Research Centre, report no. EUR, 26331.

**55** Zardasti, L., Hanafiah, N.M., Noor, N.M. et al. (2015). The consequence assessment of gas pipeline failure due to corrosion. In: *Solid State Phenomena*, vol. 227, 225–228. Switzerland: Trans Tech Publications, Ltd.

**56** Hou, B. (2019). Introduction to a study on corrosion status and control strategies in China. In: *The Cost of Corrosion in China*, 1–33. USA: Springer.

**57** Kermani, M.B. Morshed, A. (2003). Carbon Dioxide Corrosion in Oil and Gas Production—A Compendium. *CORROSION*, 59: 659–683.

**58** Devyaterikova, N., Nurmukhametova, M., Kharlashin, A., and Popov, Y. (2019). Types of corrosion damage of tubing in the oilfield. E3S Web of Conferences. 121. 03001 2019). https://doi.org/10.1051/e3sconf/201912103001.

**59** Sastri, V. (2014). Types of corrosion inhibitor for managing corrosion in underground pipelines. *Underground Pipeline Corrosion* 166–211.

**60** Whited, T., Yu, X.A., and Tems, R. (2013). Mitigating soil-side corrosion on crude oil tank bottoms using volatile corrosion inhibitors. In: *Corrosion 2013*, Paper No 2242. USA.

**61** Chugh, B., Thakur, S., and Singh, A.K. (2020). Microbiologically influenced corrosion inhibition in oil and gas industry. *Corrosion Inhibitors in the Oil and Gas Industry* 321–338.

**62** Rajeev, P., Surendranathan, A., and Murthy, C.S. (2012). Corrosion mitigation of the oil well steels using organic inhibitors–a review. *Journal of Materials and Environmental Science* 3: 856–869.

**63** Dariva, C.G. and Galio, A.F. (2014). Corrosion inhibitors–principles, mechanisms and applications. *Developments in Corrosion Protection* 16: 365–378.

**64** Ju, H., Kai, Z.-P., and Li, Y. (2008). Aminic nitrogen-bearing polydentate Schiff base compounds as corrosion inhibitors for iron in acidic media: a quantum chemical calculation. *Corrosion Science* 50: 865–871.

**65** Zhu, Y., Free, M.L., Woollam, R., and Durnie, W. (2017). A review of surfactants as corrosion inhibitors and associated modeling. *Progress in Materials Science* 90: 159–223.

**66** Verma, C., Haque, J., Quraishi, M., and Ebenso, E.E. (2019). Aqueous phase environmental friendly organic corrosion inhibitors derived from one step multicomponent reactions: a review. *Journal of Molecular Liquids* 275: 18–40.

**67** Sastri, V.S. (1998). *Corrosion Inhibitors: Principles and Applications*. New York: Wiley.

**68** Ai, J., Guo, X., Qu, J. et al. (2006). Adsorption behavior and synergistic mechanism of a cationic inhibitor and KI on the galvanic electrode. *Colloids and Surfaces A: Physicochemical and Engineering Aspects* 281: 147–155.

**69** Wombacher, F., Maeder, U., and Marazzani, B. (2004). Aminoalcohol based mixed corrosion inhibitors. *Cement and Concrete Composites* 26: 209–216.

**70** Goyal, M., Kumar, S., Bahadur, I. et al. (2018). Organic corrosion inhibitors for industrial cleaning of ferrous and non-ferrous metals in acidic solutions: a review. *Journal of Molecular Liquids* 256: 565–573.

**71** Solomon, M.M., Umoren, S.A., Quraishi, M.A. et al. (2020). Effect of akyl chain length, flow, and temperature on the corrosion inhibition of carbon steel in a simulated acidizing environment by an imidazoline-based inhibitor. *Journal of Petroleum Science and Engineering* 187: 106801.

**72** Yoo, S.-H., Kim, Y.-W., Chung, K. et al. (2013). Corrosion inhibition properties of triazine derivatives containing carboxylic acid and amine groups in 1.0 M HCl solution. *Industrial & Engineering Chemistry Research* 52: 10880–10889.

**73** Winkler, D.A. (2017). Predicting the performance of organic corrosion inhibitors. *Metals* 7: 553.

**74** Ma, Q., Qi, S., He, X. et al. (2017). 1, 2, 3-Triazole derivatives as corrosion inhibitors for mild steel in acidic medium: experimental and computational chemistry studies. *Corrosion Science* 129: 91–101.

**75** Obot, I., Solomon, M.M., Umoren, S.A. et al. (2019). Progress in the development of sour corrosion inhibitors: past, present, and future perspectives. *Journal of Industrial and Engineering Chemistry* 79: 1–18.

**76** Chauhan, D.S., Quraishi, M.A., Mazumder, M.A.J. et al. (2020). Design and synthesis of a novel corrosion inhibitor embedded with quaternary ammonium, amide and amine motifs for protection of carbon steel in 1 M HCl. *Journal of Molecular Liquids* 317: 113917.

**77** Hellberg, P.-E. (2011). Environmentally acceptable polymeric corrosion icnhibitors, SPE International Symposium on Oilfield Chemistry, OnePetro.

**78** Umoren, S.A. and Solomon, M.M. (2020). Polymeric corrosion inhibitors for oil and gas industry. *Corrosion Inhibitors in the Oil and Gas Industry* 303–320.

**79** Verma, C., Quadri, T.W., Ebenso, E.E., and Quraishi, M. (2021). Polymer nanocomposites as industrially useful corrosion inhibitors: recent developments. *Handbook of Polymer Nanocomposites for Industrial Applications* 419–435.

**80** Cha, M., Shin, K., Seo, Y. et al. (2013). Catastrophic growth of gas hydrates in the presence of kinetic hydrate inhibitors. *The Journal of Physical Chemistry A* 117: 13988–13995.

**81** Tohidi, B., Anderson, R., Mozaffar, H., and Tohidi, F. (2015). The return of kinetic hydrate inhibitors. *Energy & Fuels* 29: 8254–8260.

**82** Lederhos, J., Long, J., Sum, A. et al. (1996). Effective kinetic inhibitors for natural gas hydrates. *Chemical Engineering Science* 51: 1221–1229.

**83** Kelland, M. (2011). *A Review of Kinetic Hydrate Inhibitors: Tailormade Water-Soluble Polymers for Oil and Gas Industry Applications*, vol. 8, 171–210. New York: Nova Science Publishers, Inc.

**84** Ke, W. and Chen, D. (2019). A short review on natural gas hydrate, kinetic hydrate inhibitors and inhibitor synergists. *Chinese Journal of Chemical Engineering* 27: 2049–2061.

**85** Wang, Y., Fan, S., and Lang, X. (2019). Reviews of gas hydrate inhibitors in gas-dominant pipelines and application of kinetic hydrate inhibitors in China. *Chinese Journal of Chemical Engineering* 27: 2118–2132.

**86** O'Reilly, R., Ieong, N.S., Chua, P.C., and Kelland, M.A. (2011). Missing poly (N-vinyl lactam) kinetic hydrate inhibitor: high-pressure kinetic hydrate inhibition of structure II gas hydrates with poly (N-vinyl piperidone) and other poly (N-vinyl lactam) homopolymers. *Energy & Fuels* 25: 4595–4599.

**87** Roostaei, M., Javanmardi, J., Rasoolzadeh, A., and Mohammadi, A.H. (2021). Experimental determinations of the complete inhibition, the slow growth, and the rapid failure regions of methane hydrate formation in the presence of polyvinylpyrrolidone and polyvinylcaprolactam aqueous solutions. *Energy & Fuels* 35: 3780–3787.

**88** Tang, C., Zhou, X., Li, D. et al. (2018). In situ Raman investigation on mixed CH4-C3H8 hydrate dissociation in the presence of polyvinylpyrrolidone. *Fuel* 214: 505–511.

**89** Zhang, Q., Shen, X., Zhou, X., and Liang, D. (2017). Inhibition effect study of carboxyl-terminated polyvinyl caprolactam on methane hydrate formation. *Energy & Fuels* 31: 839–846.

**90** Singh, A. and Suri, A. (2021). Review of kinetic hydrate inhibitors based on cyclic amides and effect of various synergists. *Energy & Fuels*.

**91** Zhang, Q., Kelland, M.A., and Ajiro, H. (2020). Polyvinylsulfonamides as kinetic hydrate inhibitors. *Energy & Fuels* 34: 2230–2237.

**92** Roosta, H., Dashti, A., Mazloumi, S.H., and Varaminian, F. (2018). Effects of chemical modification of PVA by acrylamide, methacrylamide and acrylonitrile on the growth rate of gas hydrate in methane-propane-water system. *Journal of Molecular Liquids* 253: 259–269.

**93** Chua, P.C. and Kelland, M.A. (2012). Tetra (iso-hexyl) ammonium bromide the most powerful quaternary ammonium-based tetrahydrofuran crystal growth inhibitor and synergist with polyvinylcaprolactam kinetic gas hydrate inhibitor. *Energy & Fuels* 26: 1160–1168.

**94** Zeng, H., Wilson, L.D., Walker, V.K., and Ripmeester, J.A. (2003). The inhibition of tetrahydrofuran clathrate-hydrate formation with antifreeze protein. *Canadian Journal of Physics* 81: 17–24.

**95** Walker, V.K., Zeng, H., Ohno, H. et al. (2015). Antifreeze proteins as gas hydrate inhibitors. *Canadian Journal of Chemistry* 93: 839–849.

**96** Maddah, M., Maddah, M., and Peyvandi, K. (2021). Investigation on structural properties of winter flounder antifreeze protein in interaction with clathrate hydrate by molecular dynamics simulation. *The Journal of Chemical Thermodynamics* 152: 106267.

**97** Yaqub, S., Murtaza, M., and Lal, B. (2021). Towards a fundamental understanding of biopolymers and their role in gas hydrates: a review. *Journal of Natural Gas Science and Engineering* 103892.

**98** Silva, B.L.L.D., Ferraz, I.L., do Nascimento, D.F. et al. (2021). Sodium alginate polymer as a kinetic inhibitor of methane hydrate formation. *Journal of Materials Research and Technology* 12: 1999–2010.

**99** Lee, J.D., Wu, H., and Englezos, P. (2007). Cationic starches as gas hydrate kinetic inhibitors. *Chemical Engineering Science* 62: 6548–6555.

**100** Xu, S., Fan, S., Fang, S. et al. (2016). Pectin as an extraordinary natural kinetic hydrate inhibitor. *Scientific Reports* 6: 1–7.

**101** Gao, S. (2008). Investigation of interactions between gas hydrates and several other flow assurance elements. *Energy & Fuels* 22: 3150–3153.

**102** Joshi, S.V., Grasso, G.A., Lafond, P.G. et al. (2013). Experimental flowloop investigations of gas hydrate formation in high water cut systems. *Chemical Engineering Science* 97: 198–209.

**103** Zerpa, L.E., Salager, J.-L., Koh, C.A. et al. (2011). Surface chemistry and gas hydrates in flow assurance. *Industrial & Engineering Chemistry Research* 50: 188–197.

**104** Obanijesu, E., Gubner, R., Barifcani, A. et al. (2014). The influence of corrosion inhibitors on hydrate formation temperature along the subsea natural gas pipelines. *Journal of Petroleum Science and Engineering* 120: 239–252.

**105** Kamal, M.S., Hussein, I.A., Sultan, A.S., and von Solms, N. (2016). Application of various water soluble polymers in gas hydrate inhibition. *Renewable and Sustainable Energy Reviews* 60: 206–225.

**106** U. Klomp, A. Mehta. In Validation of kinetic inhibitors for sour gas fields, IPTC 2007: International Petroleum Technology Conference, 2007; European Association of Geoscientists & Engineers: pp cp-147-00088.

**107** Kelland, M.A. (2016). *Production Chemicals for the Oil and Gas Industry*, 2e. Boca Raton: CRC Press.

**108** Moore, J., Vers, L.V., and Conrad, P. (2009). Ss: flow assurance: understanding kinetic hydrate inhibitor and corrosion inhibitor interactions, Offshore Technology Conference, OnePetro.

**109** Burgazli, C., Navarrete, R., and Mead, S. (2005). New dual purpose chemistry for gas hydrate and corrosion inhibition. *Journal of Canadian Petroleum Technology* 44: 47–50.

**110** R. Hoppe, R.L. Martin, M.K. Pakulski, T.D. Schaffer (2006). In *Corrosion mitigation with gas hydrate inhibitors*, SPE Gas Technology Symposium; OnePetro.

**111** Park, J., Kim, H., Sheng, Q. et al. (2017). Kinetic hydrate inhibition performance of poly (vinyl caprolactam) modified with corrosion inhibitor groups. *Energy & Fuels* 31: 9363–9373.

**112** Farhadian, A., Varfolomeev, M.A., Kudbanov, A. et al. (2020). Waterborne polymers as kinetic/anti-agglomerant methane hydrate and corrosion inhibitors: a new and promising strategy for flow assurance. *Journal of Natural Gas Science and Engineering* 77: 103235.

**113** Pavelyev, R.S., Zaripova, Y.F., Yarkovoi, V.V. et al. (2020). Performance of waterborne polyurethanes in inhibition of gas hydrate formation and corrosion: influence of hydrophobic fragments. *Molecules* 25: 5664.

**114** Farhadian, A., Varfolomeev, M.A., Rahimi, A. et al. (2021). Gas hydrate and corrosion inhibition performance of the newly synthesized polyurethanes: potential dual function inhibitors. *Energy & Fuels* 35: 6113–6124.

**115** Verma, C., Alrefaee, S.H., Quraishi, M. et al. (2021). Recent developments in sustainable corrosion inhibition using ionic liquids: a review. *Journal of Molecular Liquids* 321: 114484.

**116** Kang, S.-P., Jung, T., and Lee, J.-W. (2016). Macroscopic and spectroscopic identifications of the synergetic inhibition of an ionic liquid on hydrate formations. *Chemical Engineering Science* 143: 270–275.

**117** Xiao, C. and Adidharma, H. (2009). Dual function inhibitors for methane hydrate. *Chemical Engineering Science* 64: 1522–1527.

**118** Sasikumar, Y., Adekunle, A., Olasunkanmi, L.O. et al. (2015). Experimental, quantum chemical and Monte Carlo simulation studies on the corrosion inhibition of some alkyl imidazolium ionic liquids containing tetrafluoroborate anion on mild steel in acidic medium. *Journal of Molecular Liquids* 211: 105–118.

**119** Yesudass, S., Olasunkanmi, L.O., Bahadur, I. et al. (2016). Experimental and theoretical studies on some selected ionic liquids with different cations/anions as corrosion inhibitors for mild steel in acidic medium. *Journal of the Taiwan Institute of Chemical Engineers* 64: 252–268.

**120** Sa, J.-H., Lee, B.R., Park, D.-H. et al. (2011). Amino acids as natural inhibitors for hydrate formation in CO2 sequestration. *Environmental Science & Technology* 45: 5885–5891.

**121** Hamadi, L., Mansouri, S., Oulmi, K., and Kareche, A. (2018). The use of amino acids as corrosion inhibitors for metals: a review. *Egyptian Journal of Petroleum* 27: 1157–1165.

**122** Aouniti, A., Khaled, K., and Hammouti, B. (2013). Correlation between inhibition efficiency and chemical structure of some amino acids on the corrosion of armco iron in molar HCl. *International Journal of Electrochemical Science* 8: 5925–5943.

**123** Bavoh, C.B., Partoon, B., Lal, B., and Keong, L.K. (2017). Methane hydrate-liquid-vapour-equilibrium phase condition measurements in the presence of natural amino acids. *Journal of Natural Gas Science and Engineering* 37: 425–434.

**124** Zor, S., Kandemirli, F., and Bingul, M. (2009). Inhibition effects of methionine and tyrosine on corrosion of iron in HCl solution: electrochemical, FTIR, and quantum-chemical study. *Protection of Metals and Physical Chemistry of Surfaces* 45: 46–53.

**125** Talaghat, M. (2014). Experimental investigation of induction time for double gas hydrate formation in the simultaneous presence of the PVP and l-tyrosine as kinetic inhibitors in a mini flow loop apparatus. *Journal of Natural Gas Science and Engineering* 19: 215–220.

**126** Rahuma, M.N., El-Sabbah, M.B., and Hamad, I.M. (2013). Effect of serine and methionine on electrochemical behavior of the corrosion of mild steel in aqueous solutions. *International Scholarly Research Notices* 2013: 1–7.

**127** Sa, J.-H., Kwak, G.-H., Han, K. et al. (2016). Inhibition of methane and natural gas hydrate formation by altering the structure of water with amino acids. *Scientific Reports* 6: 1–9.

**128** Sivabalan, V., Walid, B., Madec, Y. et al. (2020). Corrosion inhibition study on glycerol as simultaneous gas hydrate and corrosion inhibitor in gas pipelines. *Malaysian Journal of Analytical Sciences* 24: 62–69.

**129** Umoren, S.A., Obot, I.B., Madhankumar, A., and Gasem, Z.M. (2015). Performance evaluation of pectin as ecofriendly corrosion inhibitor for X60 pipeline steel in acid medium: experimental and theoretical approaches. *Carbohydrate Polymers* 124: 280–291.

**130** Gupta, N.K., Joshi, P., Srivastava, V., and Quraishi, M. (2018). Chitosan: a macromolecule as green corrosion inhibitor for mild steel in sulfamic acid useful for sugar industry. *International Journal of Biological Macromolecules* 106: 704–711.

**131** Xu, Y., Yang, M., and Yang, X. (2010). Chitosan as green kinetic inhibitors for gas hydrate formation. *Journal of Natural Gas Chemistry* 19: 431–435.

**132** Jokandan, E.F., Naeiji, P., and Varaminian, F. (2016). The synergism of the binary and ternary solutions of polyethylene glycol, polyacrylamide and hydroxyethyl cellulose to methane hydrate kinetic inhibitor. *Journal of Natural Gas Science and Engineering* 29: 15–20.

**133** El-Haddad, M.N. (2014). Hydroxyethylcellulose used as an eco-friendly inhibitor for 1018 c-steel corrosion in 3.5% NaCl solution. *Carbohydrate Polymers* 112: 595–602.

**134** Moloney, J., Mok, W.Y., and Gamble, C.G. (2009). Compatible corrosion and kinetic hydrate inhibitors for wet sour gas transmission lines. In: *Corrosion 2009*, paper no. 09350, NACE, Atlanta Georgia. OnePetro.

**135** Jones, R., Morales, N., Anthony, J. et al. (2013). Development of a novel kinetic hydrate inhibitor and corrosion inhibitor package for wet gas application. In: *OTC24375, Brasil*. USA: OnePetro.

**136** Fu, B. (2007). Development of non-interfering corrosion inhibitors for sour gas pipelines with co-injection of kinetic hydrate inhibitors. In: *Corrosion 2007*, paper 07666, NACE Corrosion conference Nashville, TN. USA: OnePetro.

**137** Duchateau, C., Glénat, P., Pou, T.-E. et al. (2010). Hydrate precursor test method for the laboratory evaluation of kinetic hydrate inhibitors. *Energy & Fuels* 24: 616–623.

**138** Duchateau, C., Pou, T.-E., Hidalgo, M. et al. (2012). Interfacial measurements for laboratory evaluation of kinetic hydrate inhibitors. *Chemical Engineering Science* 71: 220–225.

**139** Maeda, N. (2014). Measurements of gas hydrate formation probability distributions on a quasi-free water droplet. *Review of Scientific Instruments* 85: 065115.

**140** Chua, P.C. and Kelland, M.A. (2018). Study of the gas hydrate antiagglomerant performance of a series of mono-and bis-amine oxides: dual antiagglomerant and kinetic hydrate inhibition behavior. *Energy & Fuels* 32: 1674–1684.

**141** Hase, A., Cadger, S., Meiklejohn, T., and Smith, R. (2014). Comparison of different testing techniques for the evaluation of low dosage hydrate inhibitor performance, *Proceedings of the 8th International Conference on Gas Hydrates*.

**142** Eaton, M., Lachance, J., and Talley, L. (2011). Kinetic hydrate inhibitors performance. In: *Natural Gas Hydrates in Flow Assurance* (ed. D. Sloan, C. Koh, A.K. Sum, et al.), 105–143. UK: Elsevier.

**143** Lone, A. and Kelland, M.A. (2013). Exploring kinetic hydrate inhibitor test methods and conditions using a multicell steel rocker rig. *Energy & Fuels* 27: 2536–2547.

**144** Sharifi, H., Walker, V.K., Ripmeester, J., and Englezos, P. (2014). Insights into the behavior of biological clathrate hydrate inhibitors in aqueous saline solutions. *Crystal Growth & Design* 14: 2923–2930.

**145** Chua, P.C., Saebo, M., Lunde, A., and Kelland, M.A. (2011). Dua; kinetic hydrates and scale inhibition by polyaspartamides. *Energy & Fuels* 25: 5165–5172.

**146** Mobin, M. and Rizvi, M. (2017). Polysaccharide from Plantago as a green corrosion inhibitor for carbon steel in 1 M HCl solution. *Carbohydrate Polymers* 160: 172–183.

**147** Villano, L.D., Kommedal, R., and Kelland, M.A. (2008). Class of kinetic hydrate inhibitors with good biodegradability. *Energy Fuels* 22: 3143–3149.

**148** Umoren, S.A., Obot, I.B., Madhankumar, A., and Gasem, Z.M. (2015). Performance evaluation of pectin as ecofriendly corrosion inhibitor for X60 pipeline steel in acid medium: experimental and theoretical approaches. *Carbohydrate Polymers* 124: 280–291.

**149** Xu, S., Fan, S., Fang, S. et al. (2016). Pectin as an extraordinary natural kinetic hydrate inhibitor. *Scientific Reports* 6: 1–7.

**150** Gupta, N.K., Joshi, P.G., Srivastava, V., and Quraishi, M.A. (2018). Chitosan: a macromolecule as green corrosion inhibitor for mild steel in sulfamic acid useful for sugar industry. *International Journal of Biological Macromolecules* 106: 704–711.

**151** Xu, Y., Yang, M., and Yang, X. (2010). Chitosan as green kinetic inhibitors for gas hydrate formation. *Journal of Natural Gas Chemistry* 19: 431–435.

**152** Brindha, T., Mallika, J., and Moorthy, V.S. (2015). Synergistic effect between starch and substituted piperidin-4-one on the corrosion inhibition of mild steel in acidic medium. *Journal of Materials and Environmental Science* 6: 191–200.

**153** Talaghat, M.R. (2014). Enhancement of the performance of modified starch as a kinetic hydrate inhibitor in the presence of polyoxides for simple gas hydrate formation in a flow mini-loop apparatus. *Journal of Natural Gas Science and Engineering* 18: 7–12.

**154** El-Haddad, M.N. (2014). Hydroxyethylcellulose used as an eco-friendly inhibitor for 1018 c-steel corrosion in 3.5% NaCl solution. *Carbohydrate Polymers* 112: 595–602.

**155** Jokandan, E.F., Naeiji, P., and Varaminian, F. (2016). The synergism of the binary and ternary solutions of polyethylene glycol, polyacrylamide and Hydroxyethyl cellulose to methane hydrate kinetic inhibitor. *Journal of Natural Gas Science and Engineering* 29: 15–20.

**156** Ul-haq, I., Al-Malki, A., Al-Eid, M. et al. Acryloyl based polymers with active end cap as corrosion inhibitors. US Patent 2021/0171687A1.

# 9

# Polymers as Corrosion Inhibitors for Sweet Environment

*Dheeraj S. Chauhan*[1,2], *Vandana Srivastava*[3], *Yuanhua Lin*[4], *and*
*Mumtaz A. Quraishi*[5]

[1] *Modern National Chemicals, Second Industrial City, Dammam 31421, Saudi Arabia*
[2] *King Fahd University of Petroleum & Minerals, Center of Research Excellence in Corrosion, Dhahran 31261, Saudi Arabia*
[3] *Banaras Hindu University, Indian Institute of Technology, Department of Chemistry, Varanasi 221005, India*
[4] *Southwest Petroleum University, State Key Laboratory of Oil and Gas Reservoir Geology and Exploitation, Chengdu, Sichuan 610500, China*
[5] *King Fahd University of Petroleum and Minerals, Interdisciplinary Research Center for Advanced Materials, Dhahran 31261, Saudi Arabia*

## 9.1 Introduction

Corrosion of alloy steels in the oil and gas industry is a major concern [1, 2]. Due to their low cost and good mechanical properties, alloy steels are used as the materials of choice. However, during the storage and transport of oil, the carbon dioxide gas comes in contact with moisture and leads to the creation of carbonic acid, which is considerably corrosive [3–6]. In combination with the highly saline conditions and the turbulent flow, an extremely corrosive medium is generated that is detrimental to the structural integrity of the steel structures. Further, the presence of any dissolved organic acids, $H_2S$ gas, etc., can make the medium more aggressive. The term sweet corrosion is given to the corrosion caused by the dissolved $CO_2$ in the aqueous medium, without the presence of high levels of sulfide (otherwise known as Sour corrosion) [7, 8]. These aggressive environments are known to create corrosion issues in downhole completions during production, especially for sweet gas wells with high temperature, high pressure, and produced water containing high total dissolved solid (TDS). Further, with increase in the depth of oil and gas wells, there is a concomitant increase in the operating temperatures and pressures. Few corrosion inhibitor chemistries can withstand this aggressive environment and they fail as the temperature exceeds 200 °C. The sweet corrosion of alloy steels renders the material vulnerable to failure and causes huge economic impact. Significant potential corrosion problems can occur in downhole completions during production, especially for sweet gas wells with high temperature, high pressure, and produced water containing high TDS. Therefore, there is an urgent need to

*Polymeric Corrosion Inhibitors for Greening the Chemical and Petrochemical Industry*, First Edition.
Edited by Mohammad A. Jafar Mazumder, Mumtaz A. Quraishi, and Amir Al-Ahmed.

develop corrosion inhibitors for sweet gas wells that withstands this challenging corrosive environment.

To address this issue, one of the most effective strategies is the application of organic molecules as corrosion inhibitors. To control the corrosion of mild steel and tubular steels, such as N80 and L80, the solutions need to be inhibited by effective corrosion inhibitors, which are commonly organic compounds [9–12]. The organic compounds act by adsorption on the target metallic substrate and form a protective film, which imparts protection from the aggressive environment. Several organic corrosion inhibitors have been reported earlier to counter sweet corrosion, including quaternary ammonium salts, amines, surfactants, amides, and betaines. This chapter presents a brief overview of corrosion and corrosion inhibitors. Details of the economic issues of corrosion in oil and gas industry are given with the available inhibitor choices. Mechanistic details of sweet corrosion with the limitation of existing corrosion inhibitors are provided. Significance of polymeric corrosion inhibitors is described. A review of literature on the application of polymers as corrosion inhibitors is provided. The importance of chemical functionalization of polymers and their application in corrosion inhibitors is given. It is expected that the present chapter would benefit the scientists and researchers working in the area and provide a tool of reference.

## 9.2 An Overview of Corrosion

### 9.2.1 Corrosion and Its Economic Impact

The term corrosion describes an attack on a given metallic material by the aggressive surrounding environment, e.g. soil, moisture, and water vapor that results in the loss of material and the formation of corrosion products. The metallic materials are formed by purification of different metals by their corresponding ore forms by the application of a lot of energy following complex metallurgical procedures. On the other hand, during the process of corrosion, a metal surface reverts to the original ore form, which can describe corrosion as the reverse of metallurgy. Several industries, such as paper and pulp, power generation, oil and gas, batteries, reactors, and heat exchangers, operate in certain environmental extremes of high temperatures, pressures, high acidity, salinity, alkalinity, etc., that cause huge corrosion damage to the underlying metal surface. In addition, the presence of humidity, organic/inorganic salts, and other impurities aggravate the corrosion rate due to the increase in the conductivity of the electrolyte [13, 14]. Moreover, the deposition of corrosion products also considerably influences the corrosion rate [15–17]. In general, there are eight forms of corrosion that have been identified in various environments for different metals and alloys, namely, uniform corrosion (general corrosion), galvanic corrosion (two metals corrosion), pitting, crevice formation, selective leaching (parting corrosion), inter-granular corrosion, stress corrosion, and erosion–corrosion have been identified for corrosion of metals and alloys in different corrosive environments. The annual global losses of corrosion amount to approximately 3.4 trillion

USD as estimated by the National Association of Corrosion Engineers (NACE) [18]. Of this, the annual losses encountered in the oil and gas industry account for about 1372 billion USD [19]. A number of techniques are in practice to counter corrosion, namely, cathodic protection, anti-corrosion coatings, corrosion-resistant alloys, and corrosion inhibitors.

### 9.2.2 Corrosion Inhibitors

A corrosion inhibitor can be described as a chemical additive, which upon introduction to a corrosive environment, retards the rate of corrosion without modifying the concentration, pH, or chemical composition. Several inorganic and organic molecules have been reported as effective corrosion inhibitors [20–22]. The inorganic corrosion inhibitors include nitrates, chromates, and phosphates, whereas the organic corrosion inhibitors generally include acetylenic alcohols, imidazolines (IMs), quaternary ammonium salts, and betaines. The inhibitors in general, act by adsorption on the target metallic surface and form a protective film that brings down the rate of corrosion. Generally, anodic or passivating types of inhibitors precipitate on the anodic sites via forming surface oxide layers. These can be subdivided into oxidizing anion types that can form surface oxides in the absence of atmospheric oxygen (e.g. chromate, nitrite, and nitrates). Other types of anodic inhibitors can be nonoxidizing anion types that can passivate the metallic substrate in the presence of atmospheric oxygen only (e.g. molybdate, tungstate, and phosphate). Generally, the cathodic corrosion inhibitors precipitate at the cathodic sites and retard the hydrogen evolution taking place at the cathode, leading to mitigation of corrosive dissolution [23, 24]. These inhibitors can be categorized as oxygen scavengers (e.g. hydrazine and sodium sulfite), cathodic precipitates (e.g. magnesium, calcium, and zinc), and cathodic poisons (e.g. arsenic and antimony) [25–28]. According to the literature reports, organic inhibitors are extensively applied due to the ease of synthesis, high protection performance, and ease of application in a variety of corrosive media. According to a 2019 study, the global market for corrosion inhibitors was about 7.2 billion USD and is expected to reach 9.6 billion USD by 2026 [29].

## 9.3 Sweet Corrosion

### 9.3.1 Mechanism Details of $CO_2$ Corrosion

Carbon dioxide corrosion was first faced with gas and gas-condensate fields in the USA in the 1940s [11]. Carbon dioxide corrosion takes place in the operation of gasher, pumping and gas-lift oil, gas condensate, and gas wells and in recovering oil underwater drives with the use of freshwater containing 3%–4% $CO_2$. Produced oil and gas always contain some water mixed with brines and contain varying amounts of carbon dioxide (sweet gas), hydrogen sulfide (sour gas), and organic acids [30]. The dissolution of carbon dioxide in the aqueous phase of crude oil leads to the formation of carbonic acid. Conventionally, acid corrosion describes the corrosion of metallic surfaces due to mineral acids, such as HCl and $H_2SO_4$. However, it should be noted that the mineral acids undergo complete dissociation in the aqueous medium, while the carbonic acid, being weak, undergoes partial dissociation. The carbonic acid dissociates to afford hydrogen ions [31–33]:

$$CO_{2(g)} + H_2O_{(l)} \leftrightarrow H_2CO_{3(aq)} \tag{9.1}$$

$$H_2CO_{3(aq)} \rightarrow H^+_{(aq)} + HCO_3^-{}_{(aq)} \tag{9.2}$$

$$HCO_3^-{}_{(aq)} \rightarrow H^+_{(aq)} + CO_3^{2-}{}_{(aq)} \tag{9.3}$$

The electrochemical mechanism of sweet corrosion comprises cathodic hydrogen evolution as shown below (Eqs. (9.4)–(9.6)) and anodic dissolution of Fe metal (Eq. (9.7)) [31, 34]:

$$2H^+{}_{(aq)} + 2e^- \rightarrow H_{2(g)} \tag{9.4}$$

$$2H_2CO_{3(aq)} + 2e^- \rightarrow H_{2(g)} + 2HCO_3^-{}_{(aq)} \tag{9.5}$$

$$2HCO_3^-{}_{(aq)} + 2e^- \rightarrow H_{2(g)} + 2CO_3^{2-}{}_{(aq)} \tag{9.6}$$

$$Fe_{(s)} \rightarrow Fe^{2+}{}_{(aq)} + 2e^- \tag{9.7}$$

The rate of mass transfer of $H^+$ ions from the bulk solution to the metal/solution interface limits the corrosion rate of metal in the mineral acids. On the other hand, in case of $CO_2$ corrosion, since the pH is ~4, therefore, the transport of $H^+$ ions to the metal surface is small, and hence the carbonic acid causes a greater extent of hydrogen gas evolution at the electrode surface (alloy steel). Therefore, at a given pH, the corrosion rate in carbonic acid is greater than that observed in the mineral acids. Further, the presence of highly concentrated saline environment combined with acidic medium, makes the $CO_2$ corrosion extremely detrimental to the underlying metallic substrate and leads to great damage to the target metallic substrate [11, 35, 36].

### 9.3.2 Key Parameters Governing Sweet Corrosion

The sweet corrosion of steel is considerably affected by several parameters, including pH, temperature, partial pressure of carbon dioxide ($pCO_2$), steel surface chemical composition, $O_2$ concentration, rate of flow, deposition of corrosion products, and presence of organic acids. [34]. A summary of the influence of important factors is given below:

#### 9.3.2.1 Temperature

With increase in the temperature, corrosion rate at first rises until about 60 °C (saturation point), after which there is a steep decline in the corrosion rate observed to about 80 °C. From there onward, the corrosion rate becomes almost constant due to the formation of protective $FeCO_3$ layers. At temperatures <90 °C, the corrosion products include $Fe_2(OH)_2CO_3$, $Fe_6(OH)_{12}CO_3 \cdot H_2O$, $Fe_6(OH)_{12}CO_3$, and $Fe_2O_2CO_3$. The protective $FeCO_3$ layer formation takes place at >90 °C. From 90 to 150 °C, the major corrosion product is $FeCO_3$. $Fe_3O_4$ formation begins above 150 °C. From 150 to 200 °C both $FeCO_3$ and $Fe_3O_4$ are the corrosion products, whereas at >200 °C, $Fe_3O_4$ becomes the dominant corrosion product.

#### 9.3.2.2 $CO_2$ Partial Pressure

The rate of corrosion rises with rise in $pCO_2$ (from 4 to 18 bar) from 3 to 8 mmpy ($pH \sim 4$). This can be called the *film-free condition*, in which the corrosion rate increases with increase in $CO_2$ partial pressure. On the other hand, the corrosion rate declines with rise in $pCO_2$ (from 3.8 to 10.6 bar) from 15 to 0.8 mmpy (at $pH > 5.2$). This can be called the *film-forming condition*, in which the corrosion rate decreases with increase in the $CO_2$ partial pressure.

#### 9.3.2.3 pH

In general, the acidic pH range ($pH < 4$), causes the dissolution of $FeCO_3$ layers thereby promoting the corrosion rates. Thereafter, the corrosion rate becomes constant until the attainment of pH 5 and starts to decrease beyond this value due to the formation of stable layers of corrosion products.

The rise in temperature has, in general, a promoting effect on the corrosion rate until the condition of the deposition of corrosion products ($FeCO_3$) is satisfied, (e.g. high $pCO_2$, increase in pH, etc.) [37]. At $pH \sim 4$, the corrosion product formation starts at a temperature ≥120 °C, whereas at $pH \sim 6$, it can start even at 80 °C, and in this condition, the corrosion product layer is of a protective nature. The study of the different controlling parameters of sweet corrosion of steel is itself a major area of research. In addition to pH and temperature, another major factor is $pCO_2$ [31]. High $pCO_2$ (>3 bar) favors the formation of protective layers of $FeCO_3$. Further, at elevated temperatures of ≥150 °C, there could be simultaneous deposition of $Fe_3O_4$ as well, which can have a protective effect. The rate of flow, in general, has a promoting effect on the corrosion rate. The flowing electrolyte continuously removes the loosely bound corrosion product layers, leading to a fresh surface of steel in contact with the aggressive environment. On the other hand, the turbulent flow inside the steel pipelines has a considerable influence on both corrosion and corrosion inhibition. The flow can promote the mass transport of corrosion inhibitors from solution bulk to the electrochemical interface, rendering a favorable effect on corrosion inhibition [38, 39]. The increase in wall shear stress, however, can pose a negative hydro-mechanical effect that can cause erosion of the adsorbed inhibitor film [38, 39]. Figure 9.1 shows the interrelationship of the major factors governing $CO_2$ corrosion of steel.

### 9.3.3 Survey of Literature on Sweet Corrosion Inhibitors

The scientific and technical corrosion literature has descriptions and lists numerous chemical compounds that exhibit inhibitive properties. A schematic presentation of

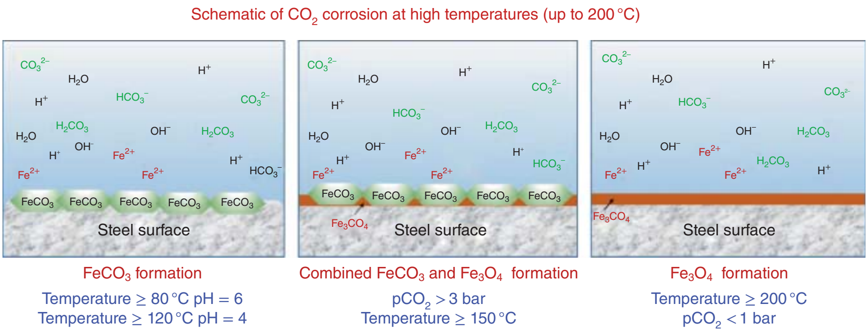

**Figure 9.1** Interrelationship of various factors governing the sweet corrosion of steels. Source: Reproduced with permission from Chauhan et al. [6]; Copyright 2021 © Elsevier.

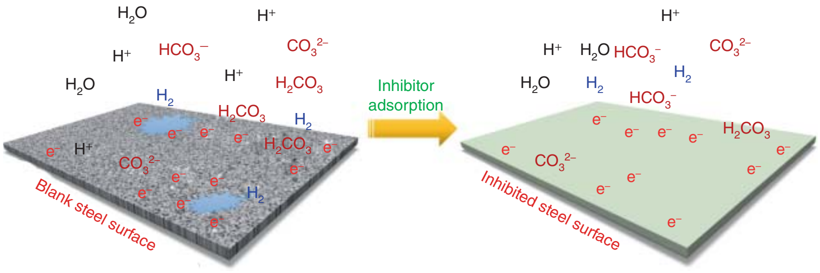

**Figure 9.2** Schematic representation of adsorption and protection performance of a corrosion inhibitor in sweet environment.

the adsorption and protective performance of a corrosion inhibitor in sweet medium is shown in Figure 9.2. A perusal of literature on high-temperature acid corrosion inhibitors indicated that effective corrosion inhibitors for $CO_2$ corrosion are based on IM-based organic compounds. These are most frequently used to protect pipelines from $CO_2$ corrosion because of their good adsorption characteristics and their ability to form film on metal surfaces [40–43].

Apart from IM derivatives, other classes of organic compounds are tested as corrosion inhibitors for high-temperature sweet corrosion, including amide, amidoamines, anhydrides, carboxylates, esters, ethylene glycol, amines, imidazoles, and quaternary amine derivatives. These include amides, IMs, phosphate esters, amines, quaternary ammonium salts, acetylenic alcohols, dimeric/trimeric acids, and surfactants. [38, 39, 44, 45]. However, these inhibitors are often criticized due to the drawbacks of high cost, multiple-step synthesis, high toxicity, etc. Generally, commercial corrosion inhibitor formulations (CIFs) consist of one or more inhibitor compounds with other additives, such as surfactants, film enhancers, de-emulsifiers, and oxygen scavengers. The inhibitor solvent package used can be

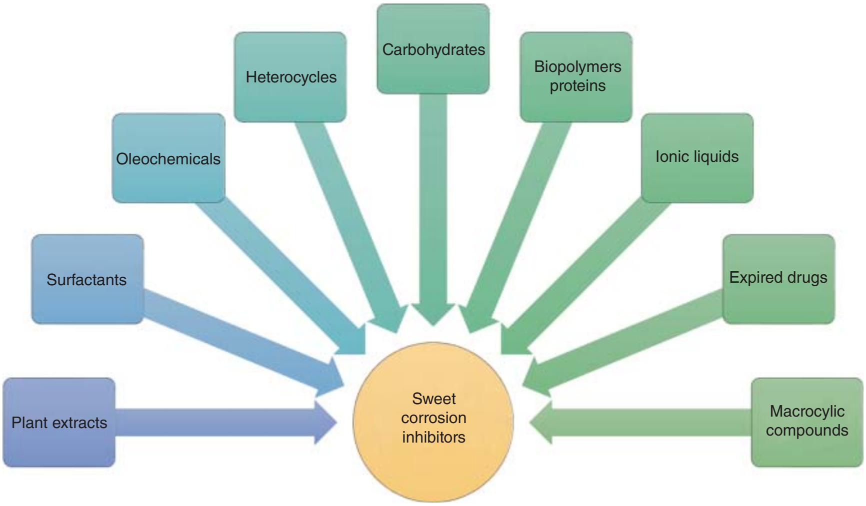

**Figure 9.3** Different types of sweet corrosion inhibitors.

critical with respect to the solubility/dispersibility characteristics and hence the application and performance of the products. As an inhibitor, the CIF must be stable (dispersive – not separated) in the acid/corrosive medium for at least 24–72 h, which is the duration of time the acid/CIF is stored onsite. Additionally, it needs to be liquid over a wide temperature range for field use in both cold and hot climates and there should not be any separation or solidification issues. Other criteria that are often required include the pour point (−20 °C), shelf life (one year), viscosity, additive, and other compatibility requirements. The most important factors that have to be taken into consideration in CIF design are performance criteria, which include performance at various temperatures and pressures, exposure time, steel metallurgy, acid type and concentration, and the surfactant used. The performance cost of a particular CIF can also be a very important deciding factor. The main constituent of an inhibitor formulation is the active inhibitor substance that is mainly responsible for the inhibition of metal corrosion. Most of the existing commercial inhibitors are toxic, suffer from poor solubility, and have low corrosion inhibition efficiency. The poor solubility of an active component presents issues in designing a suitable inhibitor formulation. On the other hand, the poor performance of the inhibitors renders an undesirable increase in the required amount of the active component that has direct influence on the cost of the inhibitor package or the inhibitor formulation used. Considering these issues, some of the modern categories of organic corrosion inhibitors include synthetic environmentally safer heterocycles, biopolymers, plant extracts, amino acids, ionic liquids, pharmaceutical products, oleochemicals, and macrocycles (Figure 9.3). Table 9.1 lists the performance of various corrosion inhibitors for sweet environments.

**Table 9.1** Protection performance of different types of inhibitors on sweet corrosion of steels.

| Name and structure of inhibitor | Metal Surface | IE%/ Concentration | Nature of Adsorption | Reference |
|---|---|---|---|---|
| 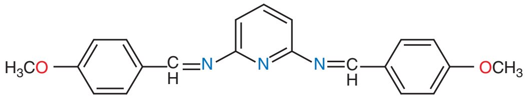<br>N,N'-(pyridine-2,6-diyl)bis(1-(4-methoxyphenyl) methanimine) | J55 steel,<br>N80 steel | 92/ 400 $mgL^{-1}$<br>90/ 400 $mgL^{-1}$ | Langmuir; mixed type | [35] |
| 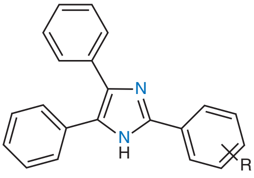<br>R= 4-$OCH_3$, 4-$CH_3$, 4-$NO_2$<br>Imidazole derivatives | J55 steel | 90/ 400 $mgL^{-1}$<br>84/ 400 $mgL^{-1}$<br>77/ 400 $mgL^{-1}$ | Langmuir; mixed type | [46] |
| 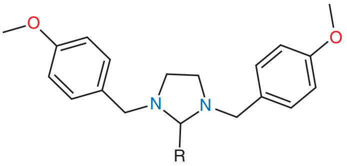<br>R = $C_6H_5$-$OCH_3$, $C_6H_5$-, $C_6H_5$-$NO_2$<br>Imidazolidine derivatives | J55 steel | 90.2/ 400 $mgL^{-1}$<br>84.9/ 400 $mgL^{-1}$<br>80.6/ 400 $mgL^{-1}$ | Langmuir; mixed type | [47] |

|  |  |  |  |  |
|---|---|---|---|---|
| 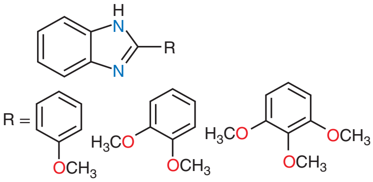<br>Benzimidazole derivatives | J55 steel | 94.5/ 1.407 mM<br>83.6/ 1.407 mM<br>79.0/ 1.407 mM | Langmuir; mixed type | [48] |
| 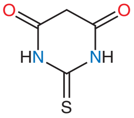<br>2-thiobarbituric acid | X60 steel | 91.8/ 100 mgL$^{-1}$ (pH 4)<br>93.7/ 100 mgL$^{-1}$ (pH 6) | Langmuir; mixed type | [49] |

(*continued*)

**Table 9.1** (Continued)

| Name and structure of inhibitor | Metal Surface | IE%/ Concentration | Nature of Adsorption | Reference |
|---|---|---|---|---|
| 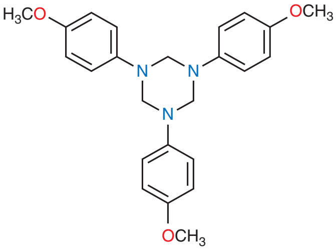 <br>1,3,5-tris(4-methoxyphenyl)-1,3,5-triazinane | API-X60 steel | 97.0/ 100 mg$L^{-1}$ (Static)<br>90.0/ 100 mg$L^{-1}$ (Hydrodynamic) | Langmuir; mixed type | [50] |
| 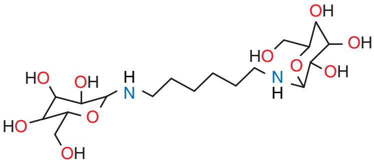 <br>Hexamethylene-1, 6-bis (N–D-glucopyranosylamine) | API X60 steel | 91.82/ 100 mg$L^{-1}$ | Langmuir; mixed type | [51] |

|  |  |  |  |  |
|---|---|---|---|---|
| *Gingko biloba* fruit extract<br>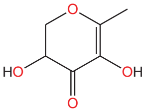<br>4H-Pyran-4-one, 2,3-dihydro-3,5-dihydroxy-6-methyl<br>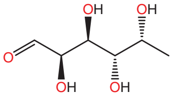<br>D-Galactose, 6-deoxy | J55 steel | 97/ 1000 mgL$^{-1}$ | Langmuir; mixed type | [52] |
| 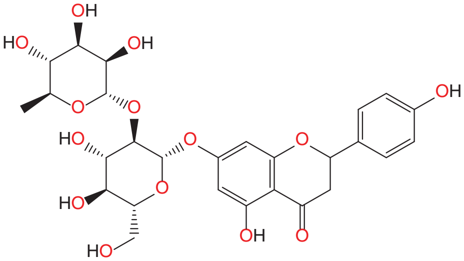<br>Naringin (Pomelo peel extract) | N80 steel | 91/ 400 mgL$^{-1}$ | Langmuir; mixed type | [53] |

(*continued*)

**Table 9.1** (Continued)

| Name and structure of inhibitor | Metal Surface | IE%/ Concentration | Nature of Adsorption | Reference |
|---|---|---|---|---|
| 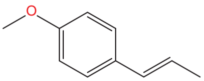<br>trans-Anethol (Anise extract) | Carbon steel | 93/ 400 $mgL^{-1}$ | Langmuir; mixed type | [54] |
| 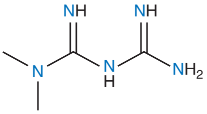<br>Metformin | C1018 steel | 90.0/ 100 $mgL^{-1}$ | Langmuir; mixed type | [55] |
| 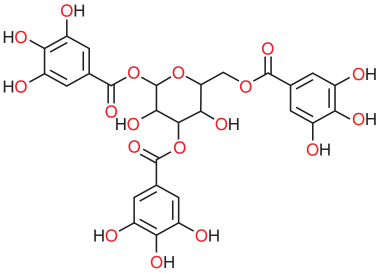<br>Tannic acid | API 5L X60 | 90%/ 500 $mgL^{-1}$ + 2 $gL^{-1}$ KI | - | [56] |

## 9.4 Polymers as Sweet CI

### 9.4.1 Significance of Polymers as Sweet CI

Polymers find significance in corrosion inhibition due to the high coverage of metal surfaces and the presence of abundance of adsorption active sites that allow interaction with the metallic surface. Different classes of polymers have been reported as corrosion inhibitors, including some common polymers (e.g. polyamines, polysulfides, polyvinylamide derivatives, polycarboxylates/polycarboxylic acids, and phosphate esters of polymeric corrosion inhibitors), conducting polymers (e.g. polyanilines and polypyrroles), macrocycles (e.g. porphyrins, phthalocyanines, crown ethers, and calixarenes), polysaccharides (e.g. chitosan, starch, cellulose, alginate, pectin, dextran, gums, and cyclodextrin), proteins, and polyaminoacids (e.g. gelatin, casein, gluten, soy, and polyaspartate) [57, 58]. In case of sweet corrosion, most of the available reports target polymers having natural origin or source. These bio-derived polymers or biopolymers have gained their market share by their intrinsic biodegradable nature in combination with the exciting properties that have been applied for specific applications. The biological polymers can be extracted from natural resources, synthesized by living organisms, or chemically produced from biological materials [59]. Having a natural origin, these biopolymers present a considerable advantage over plastic-based materials. Further benefits include biocompatibility, barrier action against moisture/gases, low toxicity, and cost-effectiveness, besides being green and environmentally safe. A detailed account of the corrosion inhibitors developed from these polymers and their application in mitigation of sweet corrosion of alloy steels is provided below.

### 9.4.2 Literature Survey of Polymers as Sweet CI

A polymer of aniline, piperazine, and formaldehyde was prepared and evaluated in sweet medium [60]. A mixed type of behavior with cathodic predominance was observed via potentiodynamic polarization (PDP) investigation. A decrease in the current densities was observed via scanning electrochemical microscopy (SECM) analysis. Surface investigation via scanning electron microscopy (SEM) studies revealed the formation of adsorbed inhibitor film and smooth surface morphology of the N80 steel. Density functional theory (DFT) and molecular dynamics (MD) studies supported the experimentally determined results. The influence of static and hydrodynamic conditions (0–2000 rpm) were investigated on SAE1018 steel surface in NACE 1D196 brine solution (3.5% NaCl, 0.305% $CaCl_2$, and 0.186% $MgCl_2$), $CO_2$-saturated solution using a water-based acrylic terpolymer, and methyl methacrylate/butyl acrylate/acrylic acid as corrosion inhibitor [61]. It was observed that an increase in the rotation speed led to an increase in the corrosion rate, while the inhibition efficiency also increased. Optical microscopy examinations indicated a decreased extent of attack on the metallic substrate in the presence of inhibitor. The inhibitor followed Langmuir isotherm with chemical mode of adsorption. Poly(methyl methacrylate-*co*-*N*-vinyl-2-pyrrolidone) polymer was prepared and studied on J55 steel corrosion in 3.5% NaCl saturated with $CO_2$ [62]. PDP studies indicated a mixed-type behavior. SEM revealed a smooth surface morphology of the steel substrate in the presence of inhibitor.

Considerable research work has been reported on the application of naturally occurring polymeric molecules as corrosion inhibitors. Several research reports are available on starch, chitosan, cellulose, glycogen, dextran, exudate gums, etc. Carboxymethyl cellulose (CMC) or cellulose gum, is derived from cellulose-containing carboxymethyl groups bound to some of the –OH groups of the glucopyranose units making the cellulose framework. Chitosan is a polymer extracted via N-deacetylation process of naturally occurring chitin that constitutes the exoskeletons of insects, mollusks, etc. Chitosan and CMC were studied for API 5L X60 steel surface in sweet environment via electrochemical impedance spectroscopy (EIS), PDP, and surface analysis [63]. The inhibitor performance was also compared with a commercial inhibitor formulation and encouraging results were noted. EIS study revealed the existence of a two-time constant process, and the PDP studies indicated anodic predominance, with a mixed type of inhibition performance. However, the inhibitors showed moderate inhibition efficiencies when compared with the commercial formulation. Gum Arabic is a biodegradable and nontoxic polymer of natural origin. It was studied for N80 steel surface in 0.5 M KCl solution saturated with $CO_2$ via weight loss measurements and electrochemical investigations [64]. At $500\,\mathrm{mg\,l^{-1}}$, 70.27% protection was achieved as noticed from the EIS measurements with the PDP studies, indicating a mixed nature of performance. Surface analysis via Fourier transform infrared spectroscopy (FTIR) and SEM–EDX (energy-dispersive X-ray) supported the inhibitor adsorption and the development of a protective film of inhibitor molecules on the steel surface. Maltodextrin (MDL) is a carbohydrate polymer that is commonly utilized as a food ingredient. It is derived from vegetable starch via partial hydrolysis and is generally obtained as a white hygroscopic spray-dried powder. MDL was investigated as inhibitor for P110 steel surface in $CO_2$-saturated NACE brine 1D196 using gravimetric and electrochemical analyses [65]. PDP indicated a mixed type of adsorption behavior. Atomic force microscopy (AFM) results indicated a lowering in the surface roughness of steel from 43 nm (blank) to 10.5 nm (inhibited). Synergistic improvement in the adsorption was revealed in the presence of potassium iodide (KI). The water contact angles increased from 61.28° (blank) to 84.08° (MDL)/92.17° (KI + MDL). X-ray photoelectron spectroscopy (XPS) revealed the metal–inhibitor interaction via –OH groups of the inhibitor.

In addition to polysaccharides, some proteins and polyamino acids have also been explored as corrosion inhibitors. Polyaspartic acid (PAsp) is an aqueous soluble biodegradable copolymer of acetoacetamide and 3-carboxypropionamide, α- and β-forms of L-Asp, and occasionally contains cyclic imide (succinimide) moieties, and glutamic acid [66]. For mild steel in a simulated brine medium, this polymer was utilized as corrosion inhibitor in the absence of any dissolved oxygen. About 40% protection was achieved at room temperature, which rose to 70% at an elevated temperature of 50 °C [57]. Table 9.2 lists the performance of various polymeric corrosion inhibitors for sweet environments.

**Table 9.2** Performance of some polymeric inhibitors for sweet corrosion of steels.

| **Name and structure of inhibitor** | **Metal surface** | **IE%/ concentration** | **Nature of adsorption** | **Reference** |
|---|---|---|---|---|
| 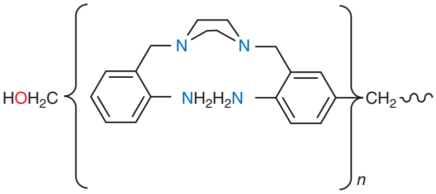<br>Polymeric ligand (APDP) | N80 steel | 93/400 mg $l^{-1}$ | Langmuir; mixed type | [60] |
| Water-base acrylic terpolymer (ATP), methyl methacrylate/ butyl acrylate/acrylic acid | SAE1018 steel | >90%/ 0.8 mmol $l^{-1}$ | Langmuir; anodic type | [61] |
| 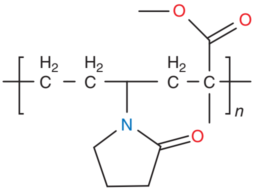<br>Poly(methyl methacrylate-*co*-*N*-vinyl-2-pyrrolidone) | J55 steel | 95%/1000 mg $l^{-1}$ | Langmuir; mixed type | [62] |

(*continued*)

Table 9.2 (Continued)

| Name and structure of inhibitor | Metal surface | IE%/ concentration | Nature of adsorption | Reference |
|---|---|---|---|---|
| 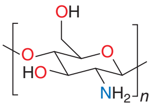<br>Chitosan<br>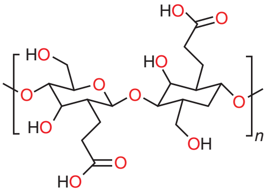<br>Carboxymethyl cellulose<br>Commercial inhibitor formulation | API 5L X60 | 55/100 $mg\,l^{-1}$<br>54/100 $mg\,l^{-1}$<br>93/100 $mg\,l^{-1}$ | Langmuir; mixed type | [63] |
| Gum arabic | N80 steel | 70.27%/ 500 $mg\,l^{-1}$ | Temkin; mixed type | [64] |

| | | | | |
|---|---|---|---|---|
| 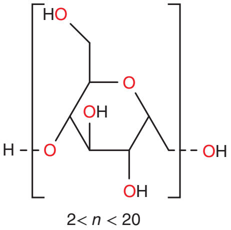<br>Maltodextrin | P110 steel | 95.1/300 $mg\,l^{-1}$<br>+ 0.5 mM KI | Langmuir;<br>cathodic type | [65] |
| Polyaspartic acid (PAsp) | Mild steel | 40%/— | — | [57] |
| 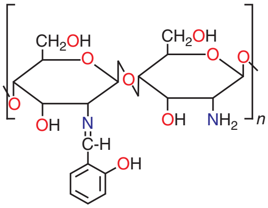<br>Chitosan–salicylaldehyde Schiff base | J55 steel | 95.2/150 $mg\,l^{-1}$ | Langmuir;<br>mixed type | [67] |

(*continued*)

**Table 9.2** (Continued)

| Name and structure of inhibitor | Metal surface | IE%/ concentration | Nature of adsorption | Reference |
|---|---|---|---|---|
| 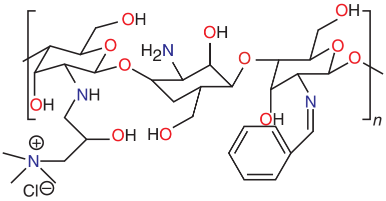 *N*-Benzyl chitosan oligosaccharide quaternary ammonium salt (BHC) | P110 Steel | 93.35/100 mg $l^{-1}$<br>91.62/100 mg $l^{-1}$ | Mixed type | [68] |
| 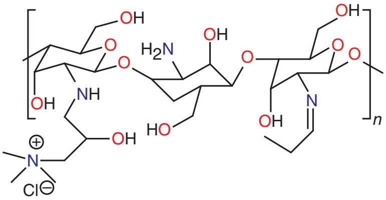 *N*-Propyl chitosan oligosaccharide quaternary ammonium salt (PHC) | | | | |

| | | | | |
|---|---|---|---|---|
| 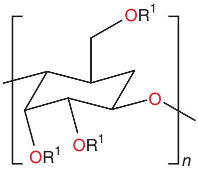 LDT ($R^1$ = $-COCHNH_2CH_2SH$)<br>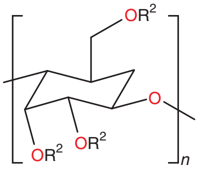 LDT ($R^2$ = $-COCHNH_2CH_2SH$) | Carbon steel | 86.6/250 mg $l^{-1}$<br>99.5/250 mg $l^{-1}$ | Langmuir; mixed type | [69] |
| 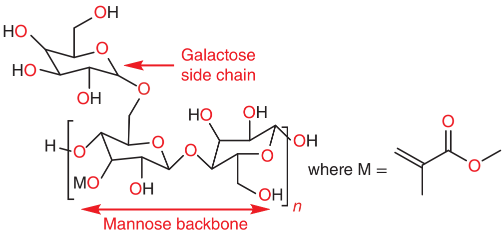 Guar gum and methyl methacrylate (GG-MMA) composite | P110 steel | 96.8%/300 mg $l^{-1}$ + 0.5 mM KI | Langmuir; mixed type | [70] |

### 9.4.3 Modified Polymers as Sweet CI

Salicylaldehyde–chitosan Schiff base (SCSB) was prepared via a single-step chemical transformation and utilized for J55 steel surface in 3% NaCl [67]. Various techniques, including weight loss, electrochemical measurements, and surface characterization, were undertaken to perform the inhibitor evaluation. The inhibition behavior was of a mixed type nature and kinetic control of the inhibition was observed. Chitosan oligosaccharides, namely, benzaldehyde-modified chitosan oligosaccharide quaternary ammonium salt (BHC) and propionaldehyde-modified chitosan oligosaccharide quaternary ammonium salt (PHC) were investigated for P110 steel in $CO_2$-saturated chloride medium [68]. Following quaternization of chitosan, reactions with benzaldehyde and propionaldehyde, two Schiff base derivatives, namely, BHC and PHC were prepared. The inhibitors were evaluated in static as well as hydrodynamic conditions. BHC showed higher inhibition efficiencies in both conditions. The water contact angle for the steel substrate rose from 14.7° in the blank to 95.5° and 80.7° in the presence of BHC and PHC, respectively, following a three-day immersion period. Dextran is a branched poly-α-ᴅ-glucoside having microbial origin and predominantly composed of glycosidic bonds C-1 → C-6. Dextran was chemically functionalized with amino acids to afford derivatives LDT and S-LDT [69]. The resulting corrosion inhibitors were evaluated for $CO_2$-saturated oilfield produce water employing electrochemical and surface analytical measurements. After a prolonged immersion time of 72 h, high inhibition efficiencies were observed for the inhibitors indicating strong and stable adsorption. The adsorption of the inhibitors followed both physical and chemical modes. High efficiencies of 86.6% and 99.5% for LDT and S-LDT were observed at a concentration of 250 $mg\,l^{-1}$. In another study, Guar gum and methyl methacrylate (GG–MMA) composite were evaluated for the protection of P110 steel surface in 3% NaCl solution saturated with $CO_2$ [70]. EIS indicated a kinetic control of the adsorption and inhibition performance. PDP measurements revealed a cathodic type inhibition behavior. At a concentration of 400 $mg\,l^{-1}$, high efficiency of 90% was achieved that increased further to 96.8% upon introduction of 300 $mg\,l^{-1}$ of GG-MMA and 5 mM KI. Thermodynamic parameters indicated spontaneous adsorption with mixed physical and chemical modes of adsorption.

## 9.5 Computational Modeling of Polymeric Inhibitors for Sweet Corrosion

Comprehensive testing and evaluation of corrosion inhibitors are generally accomplished by employing experimental techniques, e.g. weight loss tests, electrochemical measurements, and surface analysis. However, this consumes a considerable amount of time, is cumbersome, requires trained scientific staff, and dedicated, and expensive equipment. Even then, the obtained results sometimes are insufficient to properly explain the correlation between molecular structure and adsorption/inhibition potential. In recent years, several computational studies have emerged that can facilitate the analysis of reactivity parameters of the corrosion inhibitors that are key to adsorption on the target metallic substrate [2]. The structural aspects of an organic molecule to be used as corrosion inhibitor have a considerable influence on the adsorption and protection performance. These features include the presence and nature of attached functional groups, alkyl chains, heteroatoms, phenyl rings, π-bonds, etc. [71]. In this context, thorough computational analyses are required that can provide means to design and develop effective corrosion inhibitors. The major computational studies in this area are the DFT, Fukui indices, Monte Carlo simulations, and MD simulations. Herein we have provided an overview of literature presenting the computational studies that have been performed on polymeric molecules acting as sweet corrosion inhibitors.

For the polymer prepared using aniline, piperazine, and formaldehyde, the DFT studies indicated that the neutral form of the inhibitor had a greater propensity to adsorb on the steel surface compared to protonated molecule [60]. MD simulations revealed greater binding energy of the neutral inhibitor compared to the protonated molecule supporting the DFT-derived results. The inhibitor acted by sharing the lone pair electrons present on the N, and O atoms with the vacant d-orbital atoms of the Fe atoms on metal surface and also via donor–acceptor interactions between π-electrons of benzene ring and vacant d-orbitals of Fe. On the other hand, the protonated form of inhibitor underwent adsorption on metal surfaces via formation of chloride bridges. For MDL, computational studies indicated the predominant adsorption of the neutral form of MDL on the steel surface [65]. Authors screened the monomeric, dimeric, and tetrameric forms of neutral MDL via $pK_a$ analysis for their potential ability to inhibit corrosion. From the DFT studies, it was revealed that increase in the number of glucose units containing –OH groups having higher electron density resulted in an increased likelihood of adsorption on the steel surface. The $E_{\mathrm{HOMO}}$ increased, while the $E_{\mathrm{LUMO}}$ decreased at the same time resulting in a lower energy gap ($\Delta E$) with an increase in the number of monomeric units. For SCSB inhibitor discussed above, computational techniques suggested the inhibitor adsorption via salicylaldehyde moieties on the metallic substrate [67]. The electrostatic potential maps revealed a greater electron density around the heteroatoms indicating their involvement in the adsorption. The O atoms of –OH group were proposed to be site of electron donation, whereas the N atoms of $-NH_2$ group became protonated in the aqueous environment and behaved as the major sites for electron acceptance. The greater size and planarity of structure after chemical modification was attributed to better adsorption and inhibition performance. For amino acid-modified dextran discussed above, computational studies indicated that the studied inhibitors could undergo adsorption on the steel surface in an almost flat manner via the N, O, and S heteroatoms [69]. This supports the involvement of the heteroatoms in adsorption and corrosion protection [2, 72]. The adsorbed inhibitor films could prevent the diffusion of corrosive electrolytes to the surface of carbon steel. The introduction of the benzyl moieties in S-LDT inhibitor, π–π conjugation in the benzene ring, and the σ–π hyperconjugation between the benzene ring and the methylene group lead to a considerable rise in the electron density at the S atom. This resulted in greater chemical adsorption of the S-LDT inhibitor compared to LDT.

## 9.6 Mechanism of Adsorption and Inhibition

The presence of abundant amount of functional groups provides efficient capability to coordinate with metal ions and allows the formation of the metallic complexes of polymers with metal surfaces. This capability can be exploited to be used in the development of effective corrosion inhibitors. Moreover, the inhibition performance can be controlled by employing suitable electron-donating or withdrawing functional groups, π-bonds, phenyl rings, alkyl side chains, etc., attached to the polymeric backbone. A corroding metallic surface in sweet environment shows two kinds of corrosion reactions: (i) anodic metal dissolution and (ii) cathodic hydrogen evolution. A corrosion inhibitor when introduced to the acidic solution, can undergo protonation as follows [73]:

$$\mathrm{Inh_{neutral}} \rightleftarrows \mathrm{Inh_{protonated}} \tag{9.8}$$

The protonated inhibitor molecule can adsorb at the anodic sites on the metal surface via electrostatic interactions with the anions of the electrolyte via a bridge type of linkage. On the cathodic sites, the protonated inhibitor can directly adsorb via electrostatic interactions. The neutral form of the inhibitor molecules can adsorb at the metal surface via π-interactions, lone pair of the heteroatoms, polar functional groups, and back-donation of the electrons from the partially filled d-orbitals of the

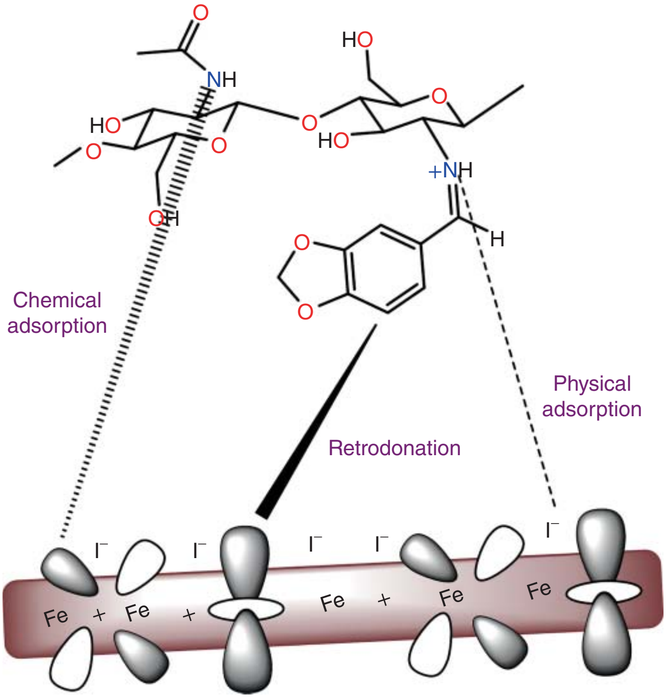

**Figure 9.4** Adsorption and corrosion protection behavior of chitosan–piperonal on steel surface in 15% HCl. Source: Reproduced with permission from Chauhan et al. [74]; Copyright 2020 © Elsevier.

metallic surface. The experimental and computational techniques are quite useful in the elucidation of the adsorption performance of the inhibitor. The adsorption of the inhibitor at the metal/electrolyte interface can be visualized in the form of a lowering in the weight loss and corrosion rate (gravimetric measurements), increase in the charge transfer resistance (EIS) and lowering in the corrosion current densities (PDP), and damping in the currents as a function of applied frequencies (electrochemical frequency modulation [EFM]) [51]. Furthermore, the shift in the corrosion potential (PDP) can elucidate the anodic/cathodic/mixed type of inhibitor behavior. The choice of a suitable adsorption isotherm can explain the metal–inhibitor interaction. The adsorption of a polymeric corrosion inhibitor is schematically represented in Figure 9.4. The computational techniques can provide further information on the adsorption sites located in the inhibitor molecules and the probable orientation of the inhibitor molecule on a given metal surface [75].

## 9.7 Conclusions and Prospects

The sweet corrosion of steel surfaces is a serious concern. In general, the available organic inhibitor classes are from the category of nitrogen-containing heterocycles. However, considering the toxicity issues and high cost associated with these molecules, researchers have explored alternative inhibitor molecules. On the other hand, there is a growing interest in the area of corrosion inhibitors based on polymers. One of the primary categories is the polymeric corrosion inhibitors derived from carbohydrates and polyamino acids. This chapter outlines briefly the significance of corrosion and its economic impact followed by a discussion on mechanistic aspects of sweet corrosion and major factors affecting sweet corrosion. Furthermore, in recent years, to improve the adsorption and the inhibition effect of the polymeric corrosion inhibitors on the metallic surface, the chemical modification of the inhibitor backbone has been applied as a strategy. A separate section on significance of computational studies in sweet corrosion environments employing polymers as inhibitors is provided. The comprehensive experimental studies have been well supported using appropriate computational modeling analysis of the corrosion inhibitors. It is noteworthy to mention that computational studies are often time-consuming due to the large and complex nature of polymers. Therefore, instead of using the whole polymer chain, researchers often focus on a small part of the same containing the representative functional groups, side chains, etc., to obtain an acceptable understanding of the nature of adsorption and corrosion inhibition. However, the collected literature also shows some knowledge gaps specifically in the realms of the influence of different functional groups, more detailed synergism studies, the effect of temperature, etc. Furthermore, another aspect is the development of inhibitor formulations using the desired surfactant, oil, synergistic agent, etc., as an additive along with the active corrosion inhibitors. Also, detailed comparisons of the newly developed corrosion inhibitors with the literature-reported corrosion inhibitors must be carried out before they can be considered for potential applications.

## References

1 Zhang, Y., Gao, K., and Schmitt, G. (2011). Inhibition of steel corrosion under aqueous supercritical $CO_2$ conditions. *CORROSION 2011, OnePetro*.

2 Quraishi, M.A., Chauhan, D.S., and Saji, V.S. (2020). *Heterocyclic Organic Corrosion Inhibitors: Principles and Applications*. Elsevier.

3 Xhanari, K., Wang, Y., Yang, Z., and Finšgar, M. (2021). A review of recent advances in the inhibition of sweet corrosion. *The Chemical Record* 21: 1845–1875.

4 Fioravante, I.A., Nunes, R.S., Acciari, H.A., and Codaro, E.N. (2019). Films formed on carbon steel in sweet environments-a review. *Journal of the Brazilian Chemical Society* 30: 1341–1349.

5 Onyebuchi, V.E., Kolios, A., Hanak, D.P. et al. (2018). A systematic review of key challenges of $CO_2$ transport via pipelines. *Renewable and Sustainable Energy Reviews* 81: 2563–2583.

6 Chauhan, D.S., Quraishi, M., and Qurashi, A. (2021). Recent trends in environmentally sustainable sweet corrosion inhibitors. *Journal of Molecular Liquids* 326: 115117.

7 Al-Janabi, Y.T. and Al-Ajwad, H.A. (2015). Corrosivity and corrosion inhibition of wet-sour crude oil wells. *CORROSION*, NACE paper No. 5759.

8 Askari, M., Aliofkhazraei, M., Ghaffari, S., and Hajizadeh, A. (2018). Film former corrosion inhibitors for oil and gas pipelines-a technical review. *Journal of Natural Gas Science and Engineering* 58: 92–114.

9 Schmitt, G. and Horstemeier, M. (2006). Fundamental aspects of $CO_2$ metal loss corrosion-part II: influence of different parameters on $CO_2$ corrosion mechanisms. *CORROSION 2006*. NACE International.

10 Dugstad, A. (2006). Fundamental aspects of $CO_2$ metal loss corrosion-part 1: mechanism. *CORROSION 2006*. NACE International.

11 Moiseeva, L. (2005). Carbon dioxide corrosion of oil and gas field equipment. *Protection of Metals* 41: 76–83.

12 Gregg, M. and Ramachandran, S. (2004). Review of corrosion inhibitor developments and testing for offshore oil and gas production systems. *CORROSION 2004*. NACE International.

13 Glass, G., Page, C., and Short, N. (1991). Factors affecting the corrosion rate of steel in carbonated mortars. *Corrosion Science* 32: 1283–1294.

14 Abd El Aal, E., Abd El Wanees, S., Farouk, A., and Abd El Haleem, S. (2013). Factors affecting the corrosion behaviour of aluminium in acid solutions. II. Inorganic additives as corrosion inhibitors for Al in HCl solutions. *Corrosion Science* 68: 14–24.

15 Zakowski, K., Narozny, M., Szocinski, M., and Darowicki, K. (2014). Influence of water salinity on corrosion risk—the case of the southern Baltic Sea coast. *Environmental Monitoring and Assessment* 186: 4871–4879.

16 Mazères, B., Desgranges, C., Toffolon-Masclet, C., and Monceau, D. (2016). Experimental study and numerical simulation of high temperature

(1100–1250 °C) oxidation of prior-oxidized zirconium alloy. *Corrosion Science* 103: 10–19.

**17** Yu, X., Jiang, B., Yang, H. et al. (2015). High temperature oxidation behavior of Mg-Y-Sn, Mg-Y, Mg-Sn alloys and its effect on corrosion property. *Applied Surface Science* 353: 1013–1022.

**18** Koch, G., Varney, J., Thompson, N. et al. (2016). International measures of prevention, application, and economics of corrosion technologies study. NACE International.

**19** Perez, T.E. (2013). Corrosion in the oil and gas industry: an increasing challenge for materials. *JOM* 65: 1033–1042.

**20** Sørensen, P.A., Kiil, S., Dam-Johansen, K., and Weinell, C.E. (2009). Anticorrosive coatings: a review. *Journal of Coatings Technology and Research* 6: 135–176.

**21** Sastri, V.S. (1998). *Corrosion Inhibitors: Principles and Applications*. Wiley.

**22** Sastri, V.S. (2012). *Green Corrosion Inhibitors: Theory and Practice*. Wiley.

**23** Sakai, T., Matsuoka, M., and Iwakura, C. (1995). Rare earth intermetallics for metal-hydrogen batteries. In: *Handbook on the Physics and Chemistry of Rare Earths* (ed. Vitalij Pecharsky, Jean-Claude Bunzli), vol. 21, 133–178. ELSEVIER. https://doi.org/10.1016/S0168-1273(05)80111-4.

**24** Bin-Dahbag, M.S., Al Quraishi, A.A., Benzagouta, M.S. et al. (2014). Experimental study of use of ionic liquids in enhanced oil recovery. *Journal of Petroleum & Environmental Biotechnology* 4: 1–7.

**25** Park, H., Kim, K.Y., and Choi, W. (2002). Photoelectrochemical approach for metal corrosion prevention using a semiconductor photoanode. *The Journal of Physical Chemistry B* 106: 4775–4781.

**26** Ihara, M., Nishihara, H., and Aramaki, K. (1992). The inhibition of iron corrosion in acid solutions using bismuth (III) chloride. *Corrosion Science* 33: 1267–1279.

**27** Finšgar, M. and Jackson, J. (2014). Application of corrosion inhibitors for steels in acidic media for the oil and gas industry: a review. *Corrosion Science* 86: 17–41.

**28** Abd El-Maksoud, S. (2008). The effect of organic compounds on the electrochemical behaviour of steel in acidic media. A review. *International Journal of Electrochemical Science* 3: 528–555.

**29** Hossain, N., Chowdhury, M.A., and Kchaou, M. (2020). An overview of green corrosion inhibitors for sustainable and environment friendly industrial development. *Journal of Adhesion Science and Technology* 1–18.

**30** Kahyarian, A., Brown, B., and Nesic, S. (2017). Electrochemistry of $CO_2$ corrosion of mild steel: effect of $CO_2$ on iron dissolution reaction. *Corrosion Science* 129: 146–151.

**31** Usman, B.J. and Ali, S.A. (2018). Carbon dioxide corrosion inhibitors: a review. *Arabian Journal for Science and Engineering* 43: 1–22.

**32** Mazumder, M.A., Al-Muallem, H.A., and Ali, S.A. (2015). The effects of *N*-pendants and electron-rich amidine motifs in 2-(*p*-alkoxyphenyl)-2-imidazolines on mild steel corrosion in $CO_2$-saturated 0.5 M NaCl. *Corrosion Science* 90: 54–68.

**33** Mazumder, M.A., Al-Muallem, H.A., Faiz, M., and Ali, S.A. (2014). Design and synthesis of a novel class of inhibitors for mild steel corrosion in acidic and carbon dioxide-saturated saline media. *Corrosion Science* 87: 187–198.

**34** Nešić, S. (2007). Key issues related to modelling of internal corrosion of oil and gas pipelines–a review. *Corrosion Science* 49: 4308–4338.

**35** Singh, A., Ansari, K., Xu, X. et al. (2017). An impending inhibitor useful for the oil and gas production industry: weight loss, electrochemical, surface and quantum chemical calculation. *Scientific Reports* 7: 14904.

**36** Singh, A., Lin, Y., Obot, I. et al. (2015). Corrosion mitigation of J55 steel in 3.5% NaCl solution by a macrocyclic inhibitor. *Applied Surface Science* 356: 341–347.

**37** Tanupabrungsun, T., Brown, B., and Nesic, S. (2013). Effect of pH on $CO_2$ corrosion of mild steel at elevated temperatures. *CORROSION/2013*, paper.

**38** Obot, I.B., Onyeachu, I.B., and Umoren, S.A. (2019). Alternative corrosion inhibitor formulation for carbon steel in $CO_2$-saturated brine solution under high turbulent flow condition for use in oil and gas transportation pipelines. *Corrosion Science* 159: 108140.

**39** Onyeachu, I.B., Obot, I.B., Sorour, A.A., and Abdul-Rashid, M.I. (2019). Green corrosion inhibitor for oilfield application I: electrochemical assessment of 2-(2-pyridyl) benzimidazole for API X60 steel under sweet environment in NACE brine ID196. *Corrosion Science* 150: 183–193.

**40** Chen, H.J., Jepson, W.P., and Hong, T.J. (2000). High temperature corrosion inhibition performance of imidazoline and amide. *CORROSION 2000*.

**41** He, Y., Zhou, Y., Yang, R. et al. (2015). Imidazoline derivative with four imidazole reaction centers as an efficient corrosion inhibitor for anti-$CO_2$ corrosion. *Russian Journal of Applied Chemistry* 88: 1192–1200.

**42** Porcayo-Calderon, J., De La Escalera, L.M., Canto, J., and Casales-Diaz, M. (2015). Imidazoline derivatives based on coffee oil as $CO_2$ corrosion inhibitor. *International Journal of Electrochemical Science* 10: 3160–3176.

**43** Guan, X. and Hu, Y. (2012). Imidazoline derivatives: a patent review (2006–present). *Expert Opinion on Therapeutic Patents* 22: 1353–1365.

**44** Onyeachu, I.B., Obot, I.B., and Adesina, A.Y. (2020). Green corrosion inhibitor for oilfield application II: the time–evolution effect on the sweet corrosion of API X60 steel in synthetic brine and the inhibition performance of 2-(2-pyridyl) benzimidazole under turbulent hydrodynamics. *Corrosion Science* 150: 108589.

**45** Singh, A., Ansari, K.R., Quraishi, M.A. et al. (2019). The effect of an *N*-heterocyclic compound on corrosion inhibition of J55 steel in sweet corrosive medium. *New Journal of Chemistry* 43: 6303–6313.

**46** Singh, A., Ansari, K., Kumar, A. et al. (2017). Electrochemical, surface and quantum chemical studies of novel imidazole derivatives as corrosion inhibitors for J55 steel in sweet corrosive environment. *Journal of Alloys and Compounds* 712: 121–133.

**47** Singh, A., Ansari, K., Lin, Y. et al. (2019). Corrosion inhibition performance of imidazolidine derivatives for J55 pipeline steel in acidic oilfield formation water: electrochemical, surface and theoretical studies. *Journal of the Taiwan Institute of Chemical Engineers* 95: 341–356.

**48** Singh, A., Ansari, K., Haque, J. et al. (2018). Effect of electron donating functional groups on corrosion inhibition of mild steel in hydrochloric acid:

experimental and quantum chemical study. *Journal of the Taiwan Institute of Chemical Engineers* 82: 233–251.

**49** Usman, B.J., Gasem, Z.M., Umoren, S.A., and Solomon, M.M. (2019). Eco-friendly 2-thiobarbituric acid as a corrosion inhibitor for API 5L X60 steel in simulated sweet oilfield environment: electrochemical and surface analysis studies. *Scientific Reports* 9: 1–17.

**50** Onyeachu, I.B., Chauhan, D.S., Quraishi, M.A., and Obot, I.B. (2021). Influence of hydrodynamic condition on 1,3,5-tris(4-methoxyphenyl)-1,3,5-triazinane as a novel corrosion inhibitor formulation for oil and gas industry. *Corrosion Engineering, Science and Technology* 56: 154–161.

**51** Onyeachu, I.B., Chauhan, D.S., Ansari, K.R. et al. (2019). Hexamethylene-1, 6-bis (*N*-D-glucopyranosylamine) as a novel corrosion inhibitor for oil and gas industry: electrochemical and computational analysis. *New Journal of Chemistry* 43: 7282–7293.

**52** Singh, A., Lin, Y., Ebenso, E.E. et al. (2015). *Gingko biloba* fruit extract as an eco-friendly corrosion inhibitor for J55 steel in $CO_2$ saturated 3.5% NaCl solution. *Journal of Industrial and Engineering Chemistry* 24: 219–228.

**53** Sun, Z., Singh, A., Xu, X. et al. (2017). Inhibition effect of pomelo peel extract for N80 steel in 3.5% NaCl saturated with $CO_2$ solution. *Research on Chemical Intermediates* 43: 6719–6736.

**54** Peimani, A. and Nasr-Esfahani, M. (2018). Application of anise extract for corrosion inhibition of carbon steel in $CO_2$ saturated 3.0% NaCl solution. *Protection of Metals and Physical Chemistry of Surfaces* 54: 122–134.

**55** Onyeachu, I.B., Abdel-Azeim, S., Chauhan, D.S., and Quraishi, M.A. (2021). Electrochemical and computational insights on the application of expired metformin drug as a novel inhibitor for the sweet corrosion of C1018 steel. *ACS Omega* 6: 65–76.

**56** Usman, B.J., Umoren, S.A., and Gasem, Z.M. (2017). Inhibition of API 5L X60 steel corrosion in $CO_2$-saturated 3.5% NaCl solution by tannic acid and synergistic effect of KI additive. *Journal of Molecular Liquids* 237: 146–156.

**57** Tiu, B.D.B. and Advincula, R.C. (2015). Polymeric corrosion inhibitors for the oil and gas industry: design principles and mechanism. *Reactive and Functional Polymers* 95: 25–45.

**58** Aljeaban, N., Goni, L., Alharbi, B. et al. (2020). Polymers decorated with functional Motifs for mitigation of steel corrosion: an overview. *International Journal of Polymer Science* 2020: 1–23.

**59** Jha, A. and Kumar, A. (2019). Biobased technologies for the efficient extraction of biopolymers from waste biomass. *Bioprocess and Biosystems Engineering* 42: 1893–1901.

**60** Singh, A., Soni, N., Deyuan, Y., and Kumar, A. (2019). A combined electrochemical and theoretical analysis of environmentally benign polymer for corrosion protection of N80 steel in sweet corrosive environment. *Results in Physics* 13: 102116.

**61** Azghandi, M.V., Davoodi, A., Farzi, G.A., and Kosari, A. (2012). Water-base acrylic terpolymer as a corrosion inhibitor for SAE1018 in simulated sour petroleum solution in stagnant and hydrodynamic conditions. *Corrosion Science* 64: 44–54.

**62** Lin, Y., Singh, A., Ebenso, E.E. et al. (2015). Effect of poly (methyl methacrylate-*co-N*-vinyl-2-pyrrolidone) polymer on J55 steel corrosion in 3.5% NaCl solution saturated with $CO_2$. *Journal of the Taiwan Institute of Chemical Engineers* 46: 214–222.

**63** Umoren, S.A., AlAhmary, A.A., Gasem, Z.M., and Solomon, M.M. (2018). Evaluation of chitosan and carboxymethyl cellulose as ecofriendly corrosion inhibitors for steel. *International Journal of Biological Macromolecules* 117: 1017–1028.

**64** Palumbo, G., Górny, M., and Banaś, J. (2019). Corrosion inhibition of pipeline carbon steel (N80) in $CO_2$-saturated chloride (0.5 M of KCl) solution using gum Arabic as a possible environmentally friendly corrosion inhibitor for shale gas industry. *Journal of Materials Engineering and Performance* 28: 6458–6470.

**65** Singh, A., Ansari, K., Alanazi, A.K. et al. (2022). Biological macromolecule as an eco-friendly high temperature corrosion inhibitor for P110 steel under sweet environment in NACE brine ID196: experimental and computational approaches. *Journal of Molecular Liquids* 345: 117866.

**66** Roweton, S., Huang, S., and Swift, G. (1997). Poly (aspartic acid): synthesis, biodegradation, and current applications. *Journal of Environmental Polymer Degradation* 5: 175–181.

**67** Ansari, K.R., Chauhan, D.S., Quraishi, M.A. et al. (2020). Chitosan Schiff base: an environmentally benign biological macromolecule as a new corrosion inhibitor for oil & gas industries. *International Journal of Biological Macromolecules* 144: 305–315.

**68** Cui, G., Guo, J., Zhang, Y. et al. (2019). Chitosan oligosaccharide derivatives as green corrosion inhibitors for P110 steel in a carbon-dioxide-saturated chloride solution. *Carbohydrate Polymers* 203: 386–395.

**69** Zhang, Q., Hou, B., Li, Y. et al. (2021). Dextran derivatives as highly efficient green corrosion inhibitors for carbon steel in $CO_2$-saturated oilfield produced water: experimental and theoretical approaches. *Chemical Engineering Journal* 424: 130519.

**70** Singh, A., Ansari, K., and Quraishi, M. (2020). Inhibition effect of natural polysaccharide composite on hydrogen evolution and P110 steel corrosion in 3.5 wt% NaCl solution saturated with $CO_2$: combination of experimental and surface analysis. *International Journal of Hydrogen Energy* 45: 25398–25408.

**71** Chauhan, D.S., Verma, C., and Quraishi, M. (2021). Molecular structural aspects of organic corrosion inhibitors: experimental and computational insights. *Journal of Molecular Structure* 1227: 129374.

**72** Quraishi, M.A., Chauhan, D.S., and Saji, V.S (341, 2021). Heterocyclic biomolecules as green corrosion inhibitors. *Journal of Molecular Liquids* 117265.

**73** Haque, J., Srivastava, V., Chauhan, D.S. et al. (2020). Electrochemical and surface studies on chemically modified glucose derivatives as environmentally benign corrosion inhibitors. *Sustainable Chemistry and Pharmacy* 16: 100260.

**74** Chauhan, D.S., Mazumder, M.J., Quraishi, M.A. et al. (2020). Microwave-assisted synthesis of a new piperonal-chitosan Schiff base as a bio-inspired corrosion inhibitor for oil-well acidizing. *International Journal of Biological Macromolecules* 158: 231–243.

**75** Obot, I., Haruna, K., and Saleh, T. (2019). Atomistic simulation: a unique and powerful computational tool for corrosion inhibition research. *Arabian Journal for Science and Engineering* 44: 1–32.

# 10

# Green Polymeric Inhibitors for Corrosion of Metals in Alkaline Media

*Refat M. Hassan (El-Moushy)*

*Assiut University, Chemistry Department, Faculty of Science, Assiut 71516, Egypt*

## 10.1 Definitions of Corrosion

The broad definition of corrosion can be defined as the degradation, deterioration, or destruction of metals by chemical surface reactions in the presence of atmospheric moisture and air. Fontana is defined the corrosion as extractive metallurgy in reverse [1]. This means that, when a corrosive metal, such as copper or iron, itself or a piece of its derivatives is left in an open atmosphere, a reddish-brown, greenish coating layer will be formed on the surface of such materials, which is termed the corrosion. Whereas in case of aluminum, a coherent surface oxide is formed, which impedes further reaction inside the surface forming the so-called pitting corrosion. On the other hand, the scientific definition of corrosion in chemistry is "the chemical or electrochemical reaction occurs between the metal and its environment," which leads to a remarkable deterioration of both the metal and its physicochemical properties. This means the occurrence of undesired attack on the surrounding surface of the corrosive metal [2–7].

The destruction of metals is mainly occurred by a direct chemical attack, especially at either elevated temperatures in dry environment or by an electrochemical process in wet-water or moist environment at low temperatures. Most of metals, in general, exhibit corrosion behavior in the presence of alkaline environmental atmospheric conditions except noble metals, such as gold and platinum. Indeed, all corrosion reactions are obeying to the thermodynamic laws.

### 10.1.1 Influence of Corrosion on the Economy Sector

The term corrosion is basically "the influence of corrosion on the economy sector" as well as represents to the rationalized corrosion phenomena and the methods of control. It was represented by the high financial losses, especially in industrialized countries. This appeared as a clutch for technological developments in strategic industry-related activities for the future of humanity, such as oil and gas, nuclear,

*Polymeric Corrosion Inhibitors for Greening the Chemical and Petrochemical Industry*, First Edition.
Edited by Mohammad A. Jafar Mazumder, Mumtaz A. Quraishi, and Amir Al-Ahmed.

deep water, and many others. Some metals, such as iron and aluminum, and their derivative alloys have wide applications in industrial sectors owing to their low cost and excellent mechanical properties. Unfortunately, these materials are suffering some severe damage during the industrial production either in case of operations or during the cleaning processes. The use of detergents leads to distinct destructive effects on the metal surfaces, especially during the process of cleaning. Such corrosion causes severe economic loses and hampers the safety of equipment. Consequently, such corrosion leads to direct economic losses of money, which are being spent on maintenance and replacement of the corroded parts. For example, costs consumed in maintaining, painting, cathodic protection devices, and protection techniques, such as modifying external environment by de-aeration, dehumidification, and galvanization, all lead to heavy financial losses.

Since most of the corrosion process is relatively slow, it affects the metals drastically. Therefore, it was noticed that the developed countries suffer an annual loss equivalent to 2–4% of their gross national product (GNP) due to such corrosion [7–10]. Approximately 20–25% can be avoided by using appropriate anticorrosion technology on using inhibitors. Therefore, various preventive techniques were developed by using inhibitors against metallic dissolution. This takes place by reducing the corrosion rates to minimum and safe as much as possible the surrounding environmental conditions with low cost. Among these, techniques, there is the use of polymeric materials as efficiency inhibitors for inhibition the dissolution of metals in aqueous alkaline media.

## 10.2 Main Reasons for Metals Corrosion

Usually, metals exist as ores in nature, which are thermodynamically more stable than that of the free metals. Since some of the consumed energy is supplied to extract those metals from their ores, then the extracted metal is existed in higher energy level. This means, such a metal will be in unstable state nature, thermodynamically. However, corroded metals are thermodynamically more stable than pure metals; the corrosion will affect some of the principal properties of metals, such as malleability, ductility, and electrical conductivity.

Of course, the development in construction sector has accompanied by an increase in corrosion problems. Therefore, the developments in other sectors, such as offshore oil and gas extraction, nuclear power production, and medicinal health, will need careful stricter rules and more control.

## 10.3 Theories of Corrosion

Corrosion of metals in aqueous solutions is an electrochemical process as established in the first half of the nineteenth century. Many theories were suggested, but the most acceptable and logical one is as follows:

### 10.3.1 Electrochemical Theory

In chemistry, the corrosion can be explained by the anode reaction where dissolution of metal occurs to generate the corresponding metal cations and electrons. The corrosion of a metal, M, can be expressed by the following general reaction:

$$\text{Metal} + \text{Aggressive environment} \rightarrow \text{Corrosion products}$$

For example, wet corrosion is based on an electrochemical mechanism in which two reactions sum up to give the overall corrosion process; anodic reaction that releases electrons by the oxidation of metals and a cathodic reaction that consumes those released electrons (reduction). Evans [11] explained the role of these ions under the influence of the exchange of ionic charges in such corrosion of metals and alloys. This explanation has laid down the basis of the electrochemical theory of corrosion. When a metal object is immersed in a corrosive medium, the metallic surface is divided into regions with different potentials under the influence of different metallic phases, grain boundaries stress and strain, impurities, etc. in the electrolyte of the metal under disintegration. This phenomenon is attributed to the displacement of hydrogen ions into the electrolyte by those of the anode metal and, hence, it leads to the formation of a galvanic cell. These generated electrons at the anode will travel to the cathode via an electronic path through the metal and, hence, it leads to reducing the number of positively charged ions present there. Simultaneously, the positively charged ions present at the anode will move to the cathode by similar ionic current path. Thus, the current flows from the anode to the cathode by an ionic current path with simultaneous pass of current from the cathode to the anode by an electronic path, thereby completing the associated electrical circuit. Both the anode and cathode reactions will occur simultaneously at the same rate for such formed electrical circuits. The rates of either the anode or the cathode reactions are known as the corrosion rates. This is besides other affected side factors, such as the temperature, pH, associated fluid dynamics, concentrations of dissolved oxygen, and dissolved salts. In alkaline and neutral solutions, the evolved hydrogen gas molecules are produced via the following reactions:

$$2H_2O + 2e^- \rightarrow H_2 + 2OH^- \tag{10.1}$$

When the corrosion products, such as hydroxides, are deposited on the metal surface, a reduction of the oxygen supply will occur (since the oxygen has to diffuse), which is as follows:

$$O_2 + 2H_2O + 4e \rightarrow 4OH^- \tag{10.2}$$

Since the rate of metal dissolution is equal to the rate of oxygen reduction, a limited supply and limited reduction rates of oxygen will also lead to reducing the rate of corrosion. In this case, the corrosion is said to be under cathodic control [5].

In some other cases, the corrosion products will form a dense and continuous surface oxide film, which is closely related to the crystalline structure of the metal. The films of this type will primarily prevent the conduction of the metal ions from the metal–oxide interface to the oxide–liquid interface, resulting in a corrosion reaction under anodic control [5]. When this happens, passivation occurs and the metal

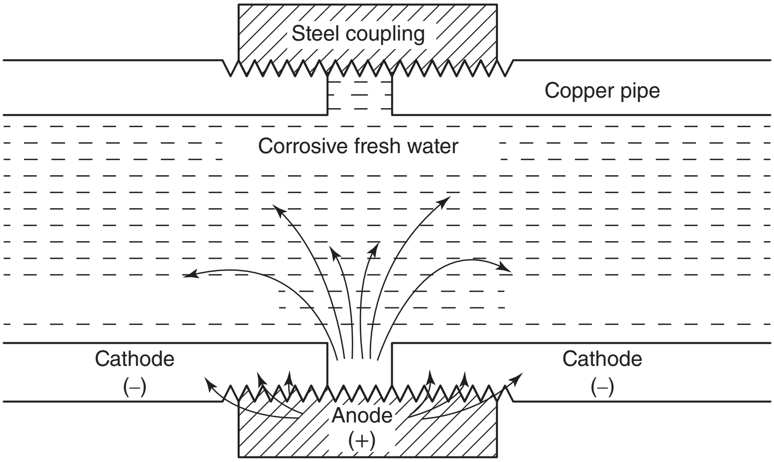

**Figure 10.1** The basic corrosion cell consists of an anode and cathode; a current enters the electrolyte at the anode and flows to the cathode, and a metallic path for electron flow. Note that the corrosion.

is referred to as in a passivized state. Examination of this fundamental reaction reveals that either loss of electrons or oxidation process will occur at the anode. The electrons lost at the anode are flowing through the metallic circuit to the cathode allowing a cathodic reaction (or reactions) to occur. A typical Galvanic cell is shown in Figure 10.1:

In the aerated solutions, the predominant corrosion reaction is usually characterized by the following:

i. The corrosion occurs by an electrochemical process where the electrical current is generated between the anode and the cathode passing through the environment electrolyte. This means that both anode and cathode are required for occurrence of the corrosion process with a simultaneous dissolution of the metal. The flow takes place from the anode to the cathode through the electrolyte by ion transportation with simultaneous passing of negative ions in the opposite direction.
ii. The lost number of electrons at the anode must equal the number of electrons that are gained at the cathode. This means that an electron flows within the metal from the anodic area at which the electrons are released to the cathodic zone, where such electrons are consumed. The flow of electrons takes place in direction opposite to the conventional current direction.

## 10.4 General Types of Corrosions

There are two main basic categories of the corrosion reactions, which have been recognized as follows:

### 10.4.1 Galvanic Corrosion

Galvanic corrosion occurs when two or more dissimilar metals of different electrochemical potential values, such as a noble metal and less noble metal [12–14], are placed in an electrolyte. This means that the presence of an electrolyte between the two metals is necessary to establish a closed circuit. The area ratio between cathode and anode is so important. For instance, if the more noble cathodic metal has a large surface area and the less noble metal has a relatively small area, a large cathodic reaction must be balanced by a correspondingly large anodic reaction concentrated in a small area, resulting in a higher anodic reaction rate [14], i.e. it leads to a higher metal dissolution rate or corrosion rate. Therefore, the ratio of cathodic to anodic area should be kept as low as possible. Since aluminum is thermodynamically more active than most of the other common structural materials the passive oxide, which protects aluminum, may easily be broken down locally when the potential is raised due to contact with a more noble material. This is particularly the case when aluminum and its alloys are exposed to waters containing chlorides or other aggressive species. Therefore, galvanic corrosion is one of the major practical corrosion problems of aluminum and aluminum alloys [15]. This leads to the generation of a potential difference with existing electrical differences between the metals, which result in the flow of the current between them. The series of standard reduction potentials of various metals can be used to explain the risk of galvanic corrosion; however, these potentials express thermodynamic properties, which do not take place to account the kinetic aspects [16]. Also, if the potential difference between the two metals in a galvanic couple is too large, the more noble metal does not take part in the corrosion process with its own ions. Thus, under this condition, the reduction potential of the more noble metal does not play any role. Again, if the two metals are electrically connected, the more active metal will act as the anode in the resulting galvanic cell and, hence, the corrosion of such metal will be increased. More details on the anodic and cathodic reactions have been described above.

Some precautions may be recommended when the ratio of area between the anode and cathode as well as the electrical isolation of the two dissimilar metals used are very larger. Hence, it recommended to use a suitable inhibitor as well as avoiding the existence of any moisture as much as possible.

### 10.4.2 Uniform Corrosion

This type of corrosion is resulting from the continual shifting of the anode and the cathode regions of metal surfaces that get in contact with the electrolyte. Thus, in turn, it leads to a nearly uniform corrosive attack on the entire surface. An example of such corrosion is the rusting of steel plates in seawater. If the rate of metal loss is known, it is possible to accommodate a design for corrosion maintenance.

### 10.4.3 Other Types of Corrosion

Another type of classification based on the corrosion mechanisms may be defined as follows:

### 10.4.3.1 General and Local Electrochemical Corrosion

The local electrochemical corrosion is occurred when two separate cells of different electrode potentials exist or a corrosion current with separate corrosion products appears on the anode and cathode. Whereas the general electrochemical corrosion occurs when separate anodic surfaces do not appear or are small dimensions (sub-micro cells) or fluctuate over the surfaces, the attack will be more uniform. Thus, there are possibilities for corrosion products to form a continuous film and delay the continuous attack. Therefore, the general electrochemical corrosion leads to a uniform attack whereas the local electrochemical corrosion leads to localized attacks [17, 18].

Many researchers [2, 19] have demonstrated that galvanic corrosion is directly proportional with respect to the area-ratio between the cathode-metal and the anode-metal and, hence, the galvanic corrosion is the maximum at the intersection of the two metals. The attack decreases as the distance from the intersection increases.

### 10.4.3.2 Crevice Corrosion

Crevice corrosion is a localized corrosion attack that occurs when crevices, formed by lapped joints, or areas of partial shielding, are exposed to corrosive environments, especially underneath deposits and in narrow crevices that obstruct oxygen supply [20–24]. This oxygen is initially required for the formation of the passive film and later for re-passivation and repair. Two common cases are oxygen cells and metal-ion cells. Oxygen concentration cells occur when the shielded area becomes depleted in oxygen and the area acts as an anode relative to the oxide region. In the case of an oxygen cell, we have an oxygen “gradient” that forces the formation of the anode and cathodes with respect to the oxygen levels. The metal-ion cell corrosion occurs when relative speeds of electrolytes over the metal surface are greater at one point than at another, thus resulting in metal-ion crevice corrosion. A good example is where a disc of metal is rotating at high speed in seawater. Corrosion occurs near the edge where linear velocities are the highest and the metal-ion concentration is low (since the ions are repeatedly swept away). The high velocity, higher than in regions closer to the hub of the disc, sweeps away the metal ions, thus forming anode regions. At the center of the disc, where velocities are lower, the metal acts as a cathode and is protected. Here, there is an equilibrium concentration and, hence, the metal ions continue to form because we cannot reach an equilibrium concentration. However, the two concentration cells corrode at different regions of the crevice. The oxygen cell corrodes under the shielded area while the metal-ion cell corrodes outside of the area. As stated before, the initial driving force behind the corrosion is either the oxygen or the metal-ion cell. Its continued growth is governed by the accumulation of corrosion products, calcareous deposits, and salts within the crevice design for easy account of the corrosion. A special form of crevice corrosion that occurs on steel and aluminum beneath a protecting film of metal or phosphate, such as in cans exposed to atmosphere, is called filiform corrosion [22].

### 10.4.3.3 Intergranular Corrosion

Here, the intergranular corrosion is the localized attack with propagation into the material structure with no major corrosion on the other parts of the surface [1, 19, 21–28]. This means, it usually occurs adjacent to gain boundaries with relatively little corrosion of the matrix. This attack is usually rapid because the ratio of the area between the cathode and anode is very large and penetrates deep into the metal resulting in loss of strength and causing catastrophic failures. Most metals and alloys are subject to intergranular corrosion when exposed to specific corrodes. The main cause of this type of corrosion is the presence of galvanic elements due to differences in concentration of impurities or alloying elements [1]. In most cases, there is a zone of less noble metal at or in the grain boundaries, which acts as an anode, while other parts of the surface form the cathode [26]. The most familiar example of intergranular corrosion is associated with austenitic steels [27]. A special form of intergranular corrosion in aluminum alloys is exfoliation corrosion [19]. Several reviews have appeared on this topic [29–32].

### 10.4.3.4 Pitting Corrosion

Pitting corrosion is an extremely deep localized attack on the metal surfaces, including perforation of thin-walled structures, which eventually results in holes formation in the metal. It is one of the most destructive and insidious forms of corrosion. Basically, the alloys subject to pitting are those that rely on an oxide film for protection, such as stainless steel. It is one of the most destructive and insidious forms of corrosion.

Basically, the alloys subject to pitting are those that rely on an oxide film for protection. This is also a form of intensive localized attack, the rate of attack being nonuniform. It is most destructive form of corrosion and results in sudden failure of the equipment due to the formation of pits or holes. In case of iron, it occurs in the presence of chloride ions depending upon the concentration of chloride ions.

If the oxide has low cathodic activity, the corrosion process is controlled by the cathodic reaction, which means that nature of the formed alloy is the most important. Therefore, if the cathodic reaction occurs on different metals, such as the deposition of Cu on the aluminum surface, the pitting rate may be very high. It has been found that high concentrations of aggressive anions in solutions of low-pH values strongly favor the process of pitting initiation. Whereas, the local thinning of the passive layer will lead to a complete breakdown giving pit formation. Pits can grow from a few nanometers to the micrometer ranges. In the propagation stage, the metal cations results from the dissolution reaction will diffuse toward the mouth of the pit or crevice (in the case of crevice corrosion) to react with OH∼ ions produced by the cathodic reaction. This, in turn, forms metal hydroxide deposits that may cover the pit to a varying extent. The corrosion products covering the pits may facilitate the faster corrosion since they prevent the exchange between the interior and the exterior electrolytes resulting in aggressive conditions in the pit [31, 33, 34].

#### 10.4.3.5 Stress Corrosion Cracking (SCC)

The cracking corrosion of metal or alloy due to the simultaneous presence of tensile stress and a specific corrosive environment is known as stress corrosion cracking (SCC). SCC occurs with specific alloys under the threshold conditions are the corrosive of environment solution composition, minimum tensile stress levels, temperature, metal composition, and metal structure. Some examples of such types of corrosion are brass and stainless steel alloys. Specific brass alloys will crack in ammonia-containing environments when a minimum threshold tensile stress is reached. Stainless steel alloys do not crack in ammonia environments but will crack in chloride solutions. The interplay of the conditions leading to SCC is not well understood. It is believed that the corrosion causes a pit or surface discontinuity to form on the metal, which then functions to act as a stress concentrator. The presence of a minimum threshold tensile stress, coupled with the corrosion, causes the crack to propagate. Additionally, during the initial corrosion, the tensile stresses could cause the protective films on the surface to rupture, thereby exposing the metal to the corrosive environment. This particularly dangerous corrosion type can be the result of environmental factors, such as SCC occurs with specific alloys under the following threshold conditions of composition of corrosive environment solution, metal composition, metal structure temperature conditions, levels of tensile stress, and corrosive environment solution composition.

There are various types of tracking attacks, such as corrosion fatigue, which correspond to the reduction in the fatigue strength due to the presence of a corrosive environment. It is owing to the combined action of cyclic stress and corrosive environment, where the accelerated failure of a metal that undergoes cyclic loading is owing to its presence in a corrosive environment [19, 27, 34–38].

#### 10.4.3.6 Fretting Corrosion

This type of corrosion occurs between two surfaces in contact with each other in dry or humid air when exposed to slight relative motion of small amplitude. Various alternate terms, such as friction oxidation, wear oxidation, and chafing. False brinelling is used to describe this phenomenon [27, 39, 40].

#### 10.4.3.7 Erosion–Corrosion

Erosion–corrosion is defined as an increase in the rate of corrosion to the relative movement between the metal surface and the liquid or gaseous environments. This type of corrosion is also known as impingement corrosion. This corrosion occurs in agitators, copper pipes, centrifuges, etc. Localized attack due to erosion–corrosion usually has bright surfaces from corrosion products, such as the pits rounded holes and valleys [1, 36].

#### 10.4.3.8 Stray Current Corrosion

Corrosion can be accelerated by the action of electrical currents entering a metal from some external sources, such as a generator or a battery, and leaving the metal to continue its flow in whole or part through the seawater electrolyte. As an example of stray current corrosion, consider the bilge pump illustrated below. The electrical connections were made **s**uch that the current found a path from the pump and its through-hull connection to the seawater and back through the propeller shaft and engine to the battery. To prevent such corrosion, all-metal surfaces exposed to bilge water or projecting through the hull should be electrically connected (bonded) to the negative side of the battery. Another example of stray current corrosion damage to a ship is through the use of an onshore welding generator below. If the return leads to the onshore generator does not have ample current carrying capacity, some of the current will find its way back through discontinuities in the paint on the submerged hull, resulting in corrosion of the hull. To avoid such corrosion, the generator should have been placed on the ship's deck and its AC lines could have been run from shore. Any AC stray current to shore would have caused little damage. Stray current corrosion can also occur when the current from a cathodic protection system passes from the anode to a metal object that was not designed to be protected before going to the object, which was intended to be protected. The result can be severe local attack on the unprotected metal where the current exits. It can also attenuate the current to a point that the object to be protected is under-protected.

### 10.4.3.9 Cavitation Corrosion

This is a special type of erosion–corrosion caused by the formation of vapor bubbles in a corrosive environment near a metal surface and when a bubbles collapse attack arises; for example, hydraulic turbulence and ship propellers. [41]. Usually, it occurs at fluid dynamic conditions, causing argue pressure variations due to high velocities, as often is the case for water turbines, propellers, pump rotors, and external surfaces of wet cylinder linings in diesel engines. While erosion–corrosion has a pattern reflecting flow direction, cavitation attacks are deep pits grown perpendicularly to the surface. Pits are often localized close to each other or grown together over smaller or larger areas, making a rough, spongy surface [1, 26, 27].

## 10.5 Corrosion Reactions of Al in Alkaline Media

Aluminum metal and its alloys are known as the most important materials used in chemical industry. It is a typical example of metals that are subjected to corrosion processes in alkaline environment atmosphere by formation of a thin layer of metal oxide on the surface of the metal or the appearance of pitting sites inside the cooking pots and articles. The anodic reaction is a primary reaction belongs to the reduction of water according to:

$$H_2O + e^- = \tfrac{1}{2}H_2 + OH^- \tag{10.3}$$

The overall anodic reaction for corrosion of Al in alkaline media is:

$$Al + 4OH^- = Al(OH)_4{}^- + 3e^- \tag{10.4}$$

## 10.6 Techniques for Prevention and Protection of Metals from Corrosion

Although, there are many different prevention methods to protect metals from corrosion occurrences, such as the selection of a material, which does not corrode in the surrounding environment, coatings the metal surface with paint which is providing a barrier between the metal surface and the corrosive environment. This in addition to some other limited prevention techniques based on the prevention of water accumulation on the metal surfaces or changing the potential toward more negative metal and thus prevents the transfer of positive metal ions from the metal to the environment. Corrosion inhibitors are active chemical species that help to slow down, delay or prevent corrosion, via different mechanisms, such as adsorption onto the metal surface that blocks active surface sites.

Therefore, the use of inhibitors still remains the most common and widely technique applied in the engineering industry and other sectors for protection of most metals and their derivative alloys. This is owing to the high performance, eco-friendly, nontoxicity, and safety of such polymers.

### 10.6.1 Green Polymeric Inhibitors for Inhibition of Al Metal Dissolution in Alkaline Media

Of course, there are many compounds, such as synthetic [42–44], organic [45–50], and inorganic [51–54] molecules, that have been applied as inhibitors to decrease the dissolution of aluminum metal in alkaline medium. In this chapter, we shall concern only with the green water-soluble polymeric inhibitors applied to inhibit the corrosion of Al in aqueous alkaline solutions [51–55]. A corrosion inhibitor is used to prevent the corrosion of embedded metal. The mechanism of inhibition is complex, and there is no general theory applicable to all situations. Some of these chemicals have been suggested as being effective; others have produced conflicting results in laboratory screening tests. Many inhibitors that appear to be chemically effective produce adverse effects on the physical properties. However, some drawbacks have been noticed with respect to the inhibitors toxicity for healthcare of human beings and the inhibitors high cost. This fact encourages numerous investigators to pay more attention to solving this problem. Hence, great development of the inhibitors has been recognized for reducing the dissolution of metals in the presence of aqueous alkaline environmental atmosphere, especially when the metal acts as a galvanic anode [12–17].

In view of our interest through various studies on natural polymers in particularly the coordination biopolymer metal-alginate complexes (ALG) in either hydrogel or granule gel nature as well as on the derivatives of polysaccharides, such as the kinetics of sol–gel transformations, electrical properties, thermal degradations, ion exchanges, heterogeneous chemical equilibria, chromatographic separations, morphology, rheology, and synthesis, which were reviewed in more details earlier [52]. Again, the kinetics and mechanistic of oxidation of such water-soluble macromolecules such inhibitors have been investigated in detail and presented elsewhere [53, 54]. Hence, we expected that such water-soluble macromolecules may be considered good examples to be used as green inhibitors for inhibiting the metals dissolution, especially aluminum in alkaline media. Fortunately, such water-soluble polymeric macromolecules were manifested as green corrosion inhibitors for Al dissolution in aqueous alkaline solutions [55–57]. This may be owing to its excellent and distinct advantages as well as the high-performance inhibition with high safety compared to the available classical inhibitors.

Here, in this chapter, we are concerned with green natural polymers as inhibitors in particularly the polysaccharides that are used for inhibition of Al dissolution in alkaline solutions.

## 10.6.2 Natural Polymers

Generally, the polymers are large molecules built of high-molecular weights built up by the repetition of small simple chemical units called monomers. The polymers can be basically classified into two main categories named biological and nonbiological macromolecules. However, each of them is of great importance, we concern with the biological one in this chapter. Unfortunately, the most available inhibitors applied were synthetic polymers, which are suffering from some drawbacks, such as the nonbiodegradability, non-eco-friendly, and high cost. Therefore, seeking high-performance inhibitor polymers avoided from such disadvantages is the main challenge to solve this problem. It has been recognized that the biomaterials in particularly the polysaccharides, are the typical examples to be used as inhibitors for metal dissolution in aqueous media. This fact may be attributed to their remarkable physical advantages, such as biodegradability, biocompatibility, eco-friendly, nontoxicity, hydrophilicity, and low cost.

### 10.6.2.1 Polysaccharides

The repetition manner in polysaccharides is linear and each monomer is linked to another by ether linkage. The length of the polysaccharide is dependent on the source of reagent, which is specified by the number of repeated units in the macromolecular chain. This is usually called the degree of polymerization in case of synthetic polymers.

### 10.6.2.2 Solubility of Polysaccharides

ALG and pectates (PEC) polysaccharides as natural polymers and poly(vinyl alcohol) (PVA) as synthetic polymers are water-soluble macromolecules to form viscous colloidal solutions when dissolved in water. The resulting solutions are hydrophilic in nature. The high solubility is owing to the presence of –OH and $-COO^-$ moieties(s), which have a high tendency to interact with water. In aqueous solutions, swelling (orientation) of the spherical or coiled colloids will transfer them to linear block copolymer structures. Therefore, an interface between the macromolecule and water is formed through such existed moiety group(s). However, all polysaccharides are known to be water-soluble, and the solubility is relatively slow for high-molecular-weights macromolecules. Therefore, it needs agitations, such as vigorously stirring in case of preparation of high concentration solutions, to avoid the aggregate formation which swells with difficulty. Indeed, the solubility of polysaccharides is related to the thermodynamic laws stated in Eq. 10.5,

$$\Delta G = \Delta H - T\Delta S \tag{10.5}$$

The free energy of mixing must be of negative sign. This fact was achieved by the remarkably high negative $\Delta S$ values of the water as solvent. Generally, two stages occurred for dissolving the polysaccharides. The first stage concerns a slow diffusion of the solvent molecules into the polymer to produce swollen jellies, followed by disintegration of such formed jellies into a colloidal sol.

All applied polymeric inhibitors of either natural or synthetic nature were used without further purifications. Stock solutions of such polymer solutions (2%, 3%, and 4%) were prepared by stepwise addition of the reagent powder to deionized water (w/w) while rapidly and vigorously stirring the solution to prevent the formation of coagulate lumps, which swell with difficulty. The prepared 2% solutions were left at room temperature (25 °C) for about 24 h to become air bubbles-free. Then, it was kept in a refrigerator to avoid any bacterial attack. The validity of the prepared ALG, PEC, and PVA sol for using is about two weeks. After removing the ALG, PEC, and PVA solution from the refrigerator, it should be kept at room temperature for about one to two hours to be easy for handling before using in experiments should be taken and left at room temperature for about one to two hours before using.

### 10.6.2.3 Behavior of Water-Soluble Polymeric Macromolecules in Alkaline Media

In strong alkaline solutions, the primary and secondary alcoholic groups of polysaccharides, such as ALG [58, 59] and PEC [60, 61], as natural polymers have high affinity for deprotonating (proton donor) forming the corresponding more reactive negative alkoxides (Eq. 10.6).

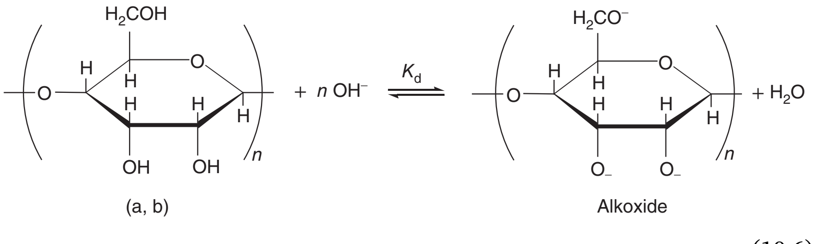

(10.6)

Similarly, the synthetic polymer, such as PVA [62, 63], deprotonated in the alkali to give the corresponding enolate form, as illustrated by (Eq. 10.7)

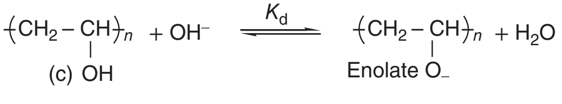

$$\underset{\text{(c) OH}}{-\!\!\left(\mathrm{CH_2-CH}\right)\!\!-_n} + \mathrm{OH^-} \xrightleftharpoons{K_d} \underset{\text{Enolate O}^-}{-\!\!\left(\mathrm{CH_2-CH}\right)\!\!-_n} + \mathrm{H_2O} \tag{10.7}$$

where $K_d$ is the deprotonating constant.

### 10.6.2.4 Types of Polysaccharides

Polysaccharides are classified into two main categories depending on the nature of moieties functional groups present with the monomers of the macromolecular chains:

#### *10.6.2.4.1 Non-sulfated Polysaccharides*

**I-Alginates (ALG)** Sodium ALG reagent is a naturally occurring polysaccharide [64–71]. It is a water-soluble anionic polyelectrolyte composed of two glycan monomers named α-L-guluronic acid (G block) and β-D-mannuronic (D block) acid units linked in (1$^{®}$ 4) positions of linear block copolymer structure. The configurations structures of both (M) and (G) blocks can be illustrated, as shown in Scheme 10.1,

Studies of ALG indicated that the two different uronic acids residues exist as blocks of homopolymeric sequences of (M blocks) and (G-blocks), separated by long sequences of heteropolymeric sequences (MG-blocks), arranged in a nearly alternating fashion. The M and G blocks are distributed within the polymer chain in varying proportions to produce heterogeneous alternating (MG) and homogeneous (MM or GG) sequences in the primary structure of algae. These sequences are illustrated below:

**_M_M_M_M_M_M … M_G_M_G_M_G_M_G_ … G_G_G_G_G_G_**

**M – block MG – block G – block**

The monomers are arranged in clock-wise manner around the macromolecular chains, but the distribution of arrangements is not random. It demands that the relatively long sequences should contain only one hexauronic acid residue (mainly G block). The presence of multiple hydroxyl functionality enhances the formation of linear-linked chains. The biological and physical properties in aqueous solutions depend not only on the G/M ratio but also on the distribution of these blocks along with the chain [68]. On the other hand, the G/M ratio is dependent on the source of ALG reagent. The ALGs have widespread in industrial applications due to its high ability for forming hydrogels in different shapes, such as pellets, beads, membranes, columns, fibers, and films, in the presence of divalent metal ions owing to

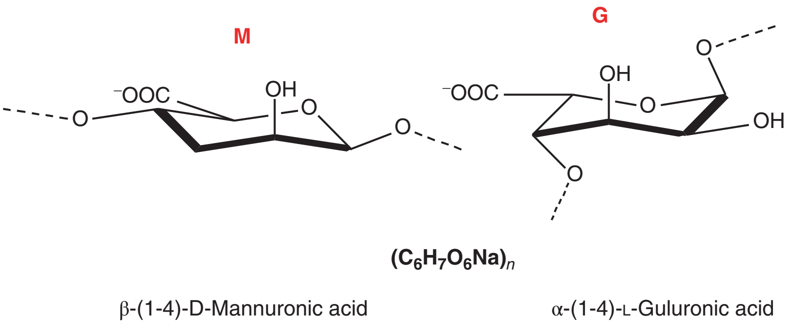

**Scheme 10.1** Geometrical structure of non-sulfated alginate.

the presence of zones rich in GG blocks [64–67]. The geometrical configuration of (G) and (M) glycoside units of ALG.

Recently, ALG has been chemically modified to increase its hydrophilicity. It has a number of free hydroxyl and carboxyl groups distributed along with the backbone; therefore, it is an ideal candidate for chemical functionalization [69]. ALG absorbs water quickly, which makes it useful as an additive in dehydrated products, such as slimming aids, and the manufacture of paper and textiles. It is also used for waterproofing and fireproofing fabrics, in the food industry as a thickening agent for drinks, ice cream and cosmetics, and as a gelling agent for jellies. ALG is used as an ingredient in various pharmaceutical preparations in which it combines with bicarbonate to inhibit reflux. Sodium ALG is used as an impression-making material in dentistry, prosthetics, life casting, and for creating positives for small-scale casting.

**ii-Pectates (PEC)** Pectates (PEC) as a sustainable natural polymer macromolecules are the methylated ester of polygalacturonic acids, which were commercially extracted from citrus peels and apple under mildly acidic conditions [70–72]. It comprises a core of alternating β-D-mannuronic acid with α-L-guluronic acid units linked in one to four positions. The geometrical configuration of pectin polysaccharides has a great similarity to that of the ALG structure. The principal structural difference is the C-2 and C-3 hydroxyl group positions, which are in trans-position in the former and cis-position in the latter, if the conformational is considered it will be equatorial–equatorial and axial–equatorial, respectively.

Pectin is widely used in food industry as gelling and thickening agent for preparing the gums and jellies and stabilizers in food. The classical application is giving main use for pectin is as a gelling agent, the jelly-like consistency to jams or marmalades, which would otherwise be sweet juices. Pectin also reduces syneresis in jams and marmalades and increases the gel strength of low-calorie jams. For household use, pectin is an ingredient in gelling sugar (also known as "jam sugar") where it is diluted to the right concentration with sugar and some citric acid to adjust pH. In some countries, pectin is also available as a solution or an extract, or as a blended powder, for home jam making.

#### *10.6.2.4.2 Sulfated Polysaccharides*

Sulfated polysaccharides are natural polymers, which contain many sulfur-atoms within their macromolecular chains, such as carrageenan and chondroitin-4-sulfate.

## 10.6.3 Synthetic Polymers

The synthetic polymers represent another type of water-soluble polymers, which were used as green inhibitors for inhibition of the dissolution of metals, especially aluminum in alkali solutions, such as the PVA [57], and in acid solutions, such as poly(ethylene glycol) [73].

### 10.6.3.1 Poly (Vinyl Alcohol) (PVA)

PVA used was 72 000 (D) [74–89]. The PVA was used in a variety of medical applications because of its biocompatibility, low tendency for protein adhesion, and low toxicity and low cost. Recently, PVA-based polymers are used widely in additive manufacturing. For example, 3D-printed oral dosage forms demonstrate great potential in the pharmaceutical industry. It is possible to create drug-loaded tablets with modified drug-release characteristics where PVA is used as a binder substance. Specific uses include cartilage replacements, contact lenses, and eye drops. PVA is used as an aid in suspension polymerizations. The chemical structure of PVA is as follows:

$$-\left(\mathrm{CH_2}-\mathrm{CHOH}\right)_n-$$
$$-\left(\mathrm{C_2H_4O}-\right)_n$$

Although the natural polymers in particularly, the polysaccharides have been used as green inhibitors of high efficiency for inhibition the dissolution of metals in aqueous alkaline or acidic media, other inorganic, natural products, and organic compounds were applied as inhibitors for metal corrosion.

## 10.7 Applied Methodologies for Measurements of Corrosion Rates

### 10.7.1 Methodology Techniques

There are two main methodologies used for studying the rates of Al corrosion depending on nature of corrosion rates whether is fast or slow.

#### 10.7.1.1 Hydrogen Gas Evolution (Gasometric Technique)

Generally, this technique is used for fast corrosion processes, such as the dissolution of aluminum in alkaline solutions. The rates of corrosion are determined volumetrically. This process takes place by measuring the evolved hydrogen produced from dissolution of aluminum in alkali solutions. Rectangular specimens of metal aluminum 3 cm long and 1.9 cm in diameter were used without further polishing to ensure reproducible surface. However, they were washed with carbon tetra chloride and absolute ethyl alcohol, and then dried in acetone and stored in free desiccators prior to the use in corrosion testing. The specimen was suspended by means of glass hook in the tested solutions of NaOH, which were previously placed into conical flask fitted with graded side-arm burette filled with doubly distilled water as described elsewhere [55–57, 90–93]. The conical flasks were thermostated in controlled water bath at the desired temperature within ±0.1 °C. When the NaOH solution had attained the temperature of the thermostat, the Al specimen was immersed into the alkali solution. The volume of the evolved (or the loss in weight of Al metal) as a function of time may be taken as the rate of dissolution of aluminum in the corrosive media as expressed by Eq. (10.8):

$$R_c = \frac{V_{H_2}}{St} \tag{10.8}$$

where $R_c$ is the rate of corrosion, $S$ is the surface area of Al metal (cm$^2$), $t$ is the time (min), $V_{H_2}$ is the volume of evolved hydrogen (ml)

#### 10.7.1.2 Weight-loss Method

The weight-loss method was commonly applied for slow corrosion processes, such as the corrosion of aluminum in alkaline solutions [94–100]. The loss in weight of metal as a function of time may be taken as the rate of Al dissolution in the corrosive media using Eq. (10.9):

$$R_c = \frac{\Delta W}{St} \tag{10.9}$$

where $R_c$ is the rate of corrosion, $S$ is the surface area of Al metal ($cm^2$), $t$ is the time (min), $V_{H_2}$ is the volume of evolved hydrogen (ml), and $\Delta W$ is the loss in mass (mg) of Al metal into the corrosive medium. Plots of the evolved active hydrogen $V_{H2}$ vs. time (Eq. 10.14) or the change in weight $\Delta W$ vs. time (Eq. 10.15) were found to be linear. This linearity is indicative of the absence of formation of soluble surface films during the corrosion process. The corrosion rates ($R_c$) can be determined from the slopes of such linear plots.

The experimental results of the corrosion rates using the above two techniques were found to be in good agreement with each other within the experimental errors ($4 \pm 1\%$). This fact recognizes that the volumetric procedure is a reproducible technique for application in all other experimental kinetic measurements. Typical plots for applying the above two techniques for corrosion of Al in alkaline solutions using inhibitors are shown in Figure 10.2a,b (ALG and PEC) and Figure 10.3a,b (PVA).

## 10.8 Factors Affecting the Corrosion Process

To elucidate a suitable mechanism for the corrosion process, the influence of several factors, such as the nature of the metal, nature, and pH of the corrosive medium, the nature of the inhibitor and its concentration, the range of temperature as well as the kinetic isotherm models that matches the corrosion kinetics. This means that two main factors play the main role in the nature of the corrosion of a metal, such as Al in aqueous solutions.

### 10.8.1 Nature of the Metal

In our case of Al, the purity of the corrosive metal is the most important factor. However, it is incorrect to assume that pure metals do not corrode at all. For example, water saturated with air high purity iron corrodes at almost the same rate as impure commercial iron. This is because corrosion depends on several other factors, such as variation in temperature and availability of oxygen to different parts of the metal, which lead to the setting up of local action cells. For other metals, several factors, such as the position of the metal into the electrochemical series, such as the physical state of the metals (particle size, orientation of grains, localized stresses, and smooth or rough surface), the nature of film formed on the metal surface, the nature of areas ratios between the cathodic and anodic regions and the stability of the corrosion films.

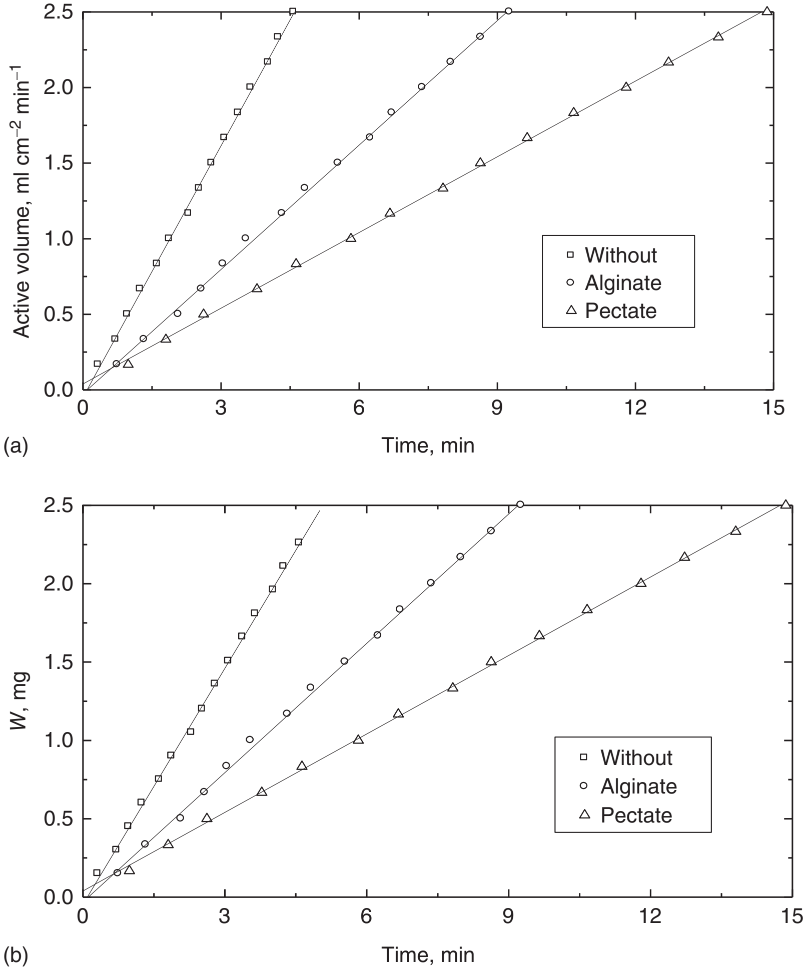

**Figure 10.2** Plots of $H_2$-gas evolution and weight-loss vs. time for the corrosion of aluminum in alkaline media in the absence and presence of $2 \times 10^{-2}$ M of ALG and PEC inhibitors weight-loss techniques in alkaline media at $[OH^-] = 4.0$ M and $I = 4.0$ M and 25 °C. (a) Applying $H_2$-gas evolution; (b) applying weight loss.

### 10.8.2 Nature of the Corroding Environment

These are the most important factors, which influenced the corrosion rates of metals, such as aluminum metal, and can be explained as follows:

#### 10.8.2.1 Dependence of Corrosion Rates on Nature and Concentration of Corrosive Media

The experimental results obtained from the influence of the nature (acid or base) and the concentration (pH) of the corrosive media on the corrosion rates of Al at fixed of all other reagents concentration indicated that the corrosion rates were increased

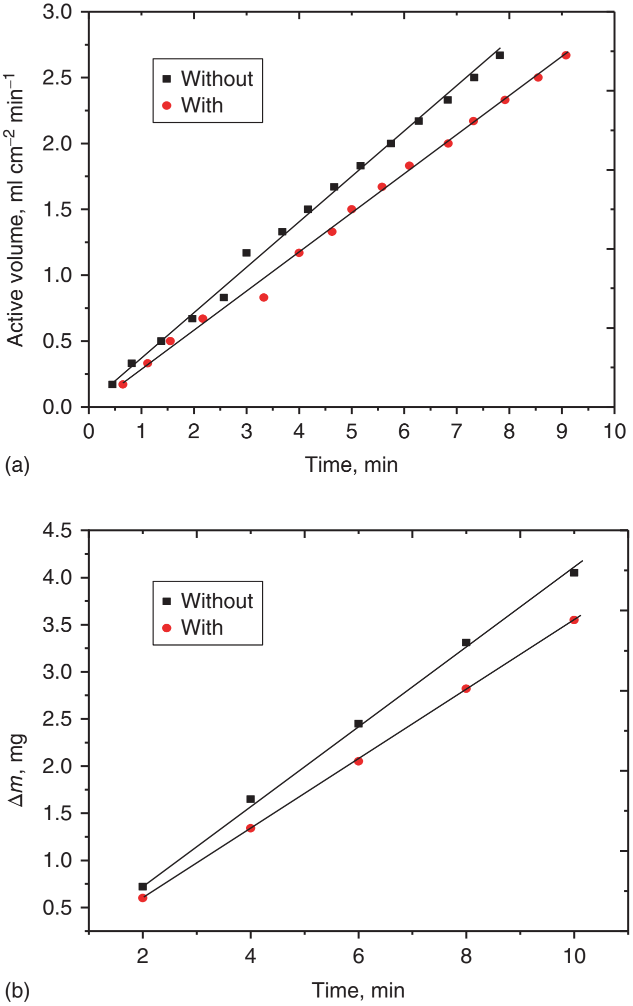

**Figure 10.3** Plots of $H_2$-gas evolution (a) and weight-loss (b) as functions of time (min) in the corrosion of aluminum in sodium hydroxide in the absence and presence of 0.002 M of PVA inhibitor. $[OH^-] = 4.0$ M, $I = 4.0$ M at 25 °C.

with increasing the concentration of either the acid or the base as well as increasing in temperature, as shown in Table 10.1.

This means that the rates of corrosions of Al in aqueous alkaline media are function of the concentration of the corrosive media as well as the corrosion processes are of base-catalyzed nature. The fractional positive orders with respect to the concentration of the corrosive media were obtained from (log $R_c$ vs. log [corrosive media]). On the other hand, the corrosion rates were found to be larger in the acidic media rather than that in the alkaline solutions of similar experimental conditions. This means that corrosion process increases with lowering the pH's values of the corrosive media.

**Table 10.1** Dependence of the corrosion rate ($R_c$, ml cm$^{-2}$ min$^{-1}$) on nature and concentration of the corrosive medium and temperature in the corrosion of Al in the absence of inhibitors.

| | $[OH^-]$ (M) | | | |
|---|---|---|---|---|
| **Temp. (°C)** | **2.0** | **3.0** | **4.0** | **5.0** |
| 25 | 0.25 | 0.30 | 0.38 | 0.42 |
| 30 | — | — | 0.52(0.95)$^{a)}$ | — |
| 35 | — | — | 0.87(1.22)$^{a)}$ | — |
| 40 | — | — | 1.15(1.39)$^{a)}$ | — |

Experimental errors ±4%.
a) Values between brackets for $[H^-]$ [55, 56].
Source: Adapted from Refs. [55, 56].

#### 10.8.2.2 Dependence of Corrosion Rates on Nature and Concentration of Inhibitors

The influence of the nature and concentration of the inhibitors used on the corrosion rates of Al in alkaline solutions as corrosive media indicated that corrosion rates are decreased with increasing the inhibitors concentration. This means that the inhibition was strengthened by increasing the inhibitors concentration. Negative fractional orders in the inhibitors concentration was obtained from the equation ($R_c = [\text{inhibitor}]^n$). The experimental results indicated that the rate of corrosion was increased with increasing the temperature and followed the order PEC < ALG < PVA with respect to the type of the examined inhibitors, as listed in Table 10.2.

Again, the values of the corrosion rates were found to decrease with increasing the concentration of various examined inhibitors examined in alkaline solutions. The results in alkaline media are summarized in Table 10.3.

A comparison of the results obtained for the influence of PEC as inhibitor in acidic and alkaline media along with other activation parameters are listed in Table 10.4.

**Table 10.2** Dependence of the corrosion rates ($R_c$, ml cm$^{-2}$ min$^{-1}$) on the nature of inhibitor and the temperature in the corrosion of Al in alkaline media.

| | | Temp. (°C) | | |
|---|---|---|---|---|
| **Rate (ml cm$^{-2}$ min$^{-1}$)** | **Inhibitor** | **30 °C** | **35 °C** | **Reference** |
| $R_c^-$ | Free | 0.52 (0.95)$^{a)}$ | 0.87 | [55, 56] |
| $R_c^-$ | PVA | 0.33 | 1.02 | [57] |
| $R_c^-$ | ALG | 0.28 | 0.40 | [56] |
| $R_c$ | PEC | 0.15 (0.5) | 0.28 (0.59) | [55, 56] |

$[\text{Inhibitor}] = 0.4 \times 10^{-2}$ M and $[OH^-] = I = 4.0$ M at different temperatures.
Experimental errors ±4%.
a) The value between brackets in HCl.

**Table 10.3** Dependence of the corrosion rate ($R_{c,}$ ml cm$^{-2}$ min$^{-1}$) on the inhibitor concentration using various inhibitors in the corrosion of Al in alkaline medium.

| $10^2$ [Inhibitor] (M) | PVA | Alginate | Pectate |
|---|---|---|---|
| 0.0 | 0.52 | 0.52 | 0.52 (0.95) |
| 0.2 | 0.34 | 0.24 | 0.17 (0.63) |
| 0.4 | 0.28 | 0.16 | 0.08 (0.50) |

$[OH^-] = I = 4.0$ M at 30 °C.
Experimental errors ±4%.

**Table 10.4** A comparison between the activation parameter, the corrosion rates, and inhibition efficiency of pectin (PEC) as a natural polymeric inhibitor on the Al corrosion in both acidic [103] and alkaline [56, 57] solutions.

| $10^2$ [PEC] (M) | $\Delta H$$^{a)}$ (kJ mol$^{-1}$) | $\Delta S$$^{a)}$ (J mol$^{-1}$ K$^{-1}$) | $\Delta G$$^{a)}$ (kJ mol$^{-1}$) | $E_a$$^{a)}$ (kJ mol$^{-1}$) | A (mol$^{-1}$ s$^{-1}$) | $R_c$$^{b)}$ (ml cm$^{-2}$ min$^{-1}$) | I.E$^{b)}$ (%) |
|---|---|---|---|---|---|---|---|
| *Activation parameters in acidic solutions*$^{c)}$ | | | | | | | |
| 0.0 | 30.90 | −177.44 | 83.78 | 33.51 | $9.51 \times 10^3$ | 0.95 | — |
| 0.4 | 23.37 | −207.84 | 85.31 | 24.08 | $1.19 \times 10^2$ | 0.50 | 44.44 |
| *Activation parameters in alkaline solutions*$^{d)}$ | | | | | | | |
| 0.0 | 58.85 | +61.97 | 77.31 | 61.15 | $1.20 \times 10^{11}$ | 0.52 | — |
| 0.4 | 92.63 | 11.13 | 89.31 | 95.15 | $6.46 \times 10^{13}$ | 0.11 | 72.67 |

a) Experimental errors ±4%.
b) [Media] = 4.0 M at 30 °C.
c) The activation parameters in acidic solutions (Ref. 103).
d) The activation parameters in alkaline solutions (Refs. 56, 57).
Source: Adapted from Refs. [56, 57, 103].

It has been noticed that the values of the corrosion rates for PEC as inhibitor for the dissolution of Al in alkaline solutions were smaller rather than in acidic media. This means that the inhibitors have high efficiency in alkaline solutions more than that in acidic media. This fact can be explained on the basis of the tendency of the alcoholic functional groups, which are present within the monomers of the polymeric inhibitor macromolecular chains for either deprotonating in alkaline solutions or protonating in the acidic solutions (acceptor), respectively, i.e. the magnitudes of the deprotonation and protonation constants values. It is well-known that the functional alcoholic groups of such polymeric inhibitors have high affinity to form the more reactive negative alkoxides by deprotonating in alkaline solutions as indicated by Eqs. (10.6) and (10.7). Therefore, the alkoxides formed in alkaline solution with negative charge will have high tendency to react with the positive ions formed on the surface of the corrosive metals to form the protective thin layers on the metal surface. This was supported by the evaluated thermodynamic values.

**Table 10.5** Percentage inhibition efficiency (%I.E) for the corrosion of Al in NaOH medium.

| | $10^2$ [Inhibitor] (M) | | | | |
|---|---|---|---|---|---|
| **Inhibitor** | **0.2** | **0.3** | **0.4** | **0.6** | **Reference** |
| Alginate | 26.5 | 44.66 | 58.33 | 78.17 | [56] |
| Pectate | 46.67 | 62.23 | 72.67 | 81.67 | [55, 56] |
| PVA | 19.16 | 26.67 | 35.17 | 41.17 | [57] |

Experimental errors ±4%.
$[\mathrm{OH}^-] = \mathrm{I} = 4.0\,\mathrm{M}^3$ at 30 °C.

The percentage of inhibitions efficiency (%I.E) of the inhibitors can be calculated using the following equation

$$\%\mathrm{I.E} = \frac{R_c{}^{o} - R_c'}{R_c{}^{o}} \times 100 \tag{10.10}$$

where $R_c{}^{o}$ and $R_c{}'$ are the corrosion rates of Al metal in the absence and presence of inhibitors. The corrosion rates were found to decrease in the orders PVA > ALG > PEC in alkaline solutions (Tables 10.2 and 10.3). This means that the inhibition efficiency (%I.E) should be increased in the same order, i.e. PVA < ALG < PEC in alkaline media (Table 10.5). This result was found to be in good agreement with the evaluated values of the deprotonating constants for such inhibitors in alkaline media [58–62, 101].

#### 10.8.2.3 Dependence of Corrosion Rate on Temperature

It is of great importance to evaluate the activation and kinetic parameters of corrosion of Al in alkaline media to elucidate suitable corrosion mechanisms and identify the models of adsorption isotherms that match the corrosion kinetics. Therefore, experimental measurements were performed at different temperatures for Al dissolution in alkaline media at fixed of all other reagents concentrations. The corrosion rates were found to increase with increasing the temperature in either the absence or presence of the inhibitors (Tables 10.1–10.4).

The activation parameters, such as the activation enthalpies $\Delta H^{\neq}$, the activation entropies, $\Delta S^{\neq}$, and the activation free energy $\Delta G^{\neq}$ changes, of the corrosion processes of Al in different corrosive media for both free and inhibited conditions were calculated by the method of least-squares from the well-known Arrhenius and Eyring equations of the transition state theory [102],

$$-\ln \frac{Nh}{RT} R_c = \frac{\Delta H^{\neq}}{RT} - \frac{\Delta S^{\neq}}{R} \tag{10.11}$$

$$\Delta G^{\neq} = \Delta H^{\neq} - T\Delta S^{\neq} \tag{10.12}$$

where the symbols $h$ is the Plank's constant, $N$ is the Avogadro's number, $R$ is the gas constant, and $T$ is the absolute temperature, respectively (the term $R/N$ is equal to the Boltzmann's constant $k_b$). These activation parameters in the alkaline

**Table 10.6** The activation parameters and corrosion rates for the corrosion of Al in the absence and presence of natural (PEC, ALG) and synthetic (PVA) polymeric inhibitors in alkaline medium.

| Inhib. | $10^2$ [Inhib.] (M) | $\Delta H$ a) (kJ mol$^{-1}$) | $\Delta S$ a) (J mol$^{-1}$ K$^{-1}$) | $\Delta G$ a) (kJ mol$^{-1}$) | $E_a$ a) (kJ mol$^{-1}$) | $R_c$ b) (ml cm$^{-2}$ min$^{-1}$) | $A$ (mol$^{-1}$ s$^{-1}$) | Reference |
|---|---|---|---|---|---|---|---|---|
| Without | 0.0 | 58.85 | +61.97 | 77.31 | 61.15 | 0.52 | $1.20 \times 10^{11}$ | [55] |
| PEC | 0.4 | 92.63 | +11.13 | 79.01 | 79.94 | 0.11 | $8.01 \times 10^{12}$ | [56] |
| ALG | 0.4 | 68.93 | −22.02 | 89.31 | 95.15 | 0.16 | $6.46 \times 10^{13}$ | [56] |
| PVA | 0.4 | 51.56 | −82.44 | 76.13 | 53.15 | 0.33 | $1.69 \times 10^{9}$ | [57] |

a) Experimental errors ±4%.
b) $[OH^-] = 4.0$ M at 30 °C.

solutions were calculated by the method of least-squares and are summarized in Table 10.6.

It is well-known from the thermodynamics that the negative values of entropies of activation, $\Delta S^{\neq}$, are indicative of the compactness of the formed intermediates (formed thin film on the metal surface) rather than the reactants that mean more orders of the intermediates than that of the reactants. Again, the positive values of the free energy of activations, $\Delta G^{\neq}$, is indicating the non-spontaneity processes of the intermediates for decomposition, and vice versa for positive and negative values of both $\Delta S^{\neq}$ and $\Delta G^{\neq}$, respectively. The evaluated $\Delta S^{\neq}$ and $\Delta G^{\neq}$ values along with the other $\Delta G^{\neq}$ and $E^{\neq}$ activation parameters are listed in Tables 10.4 and 10.6. Again, the relatively higher values of the activation energies, $E^{\neq}$, in case of the inhibited conditions (i.e. in present of inhibitors) rather than that of uninhibited ones (free), especially in alkaline solutions, indicate the inhibitive action of the influence of the inhibitors by decreasing the energy barrier for the corrosion process, emphasizing the electrostatic character of the inhibitor's adsorption on Al surface. Again the observed decrease in the apparent activation energy, $E^{\neq}$, at higher inhibitor efficiency may arise from the shift of the net corrosion reaction from that on the uncovered surface to one involving the adsorbed sites [55–57, 103–106].

### 10.8.3 Corrosion Mechanisms

Although, the presence of remarkable differences between the $\Delta H^{\neq}$ and $\Delta S^{\neq}$ values, the free energy of activation $\Delta G^{\neq}$ values seem to be nearly similar when considering the experimental errors (Tables 10.4 and 10.6). This result means that these various inhibitors may exhibit similar mechanisms of corrosion with respect to the inhibition behavior of Al into alkaline corrosive media.

In view of the above interpretations and the reported experimental observations, suitable mechanisms for dissolution of Al in aqueous alkaline solutions may be suggested.

The anodic and cathodic processes in NaOH as alkali can be expressed by Eqs. (10.13) and (10.14), respectively:

$$\mathrm{Al} + 4\mathrm{OH}^- \overset{\mathrm{Ox}}{\rightleftharpoons} \mathrm{Al(OH)}_{4^-} + 3\mathrm{e} \tag{10.13}$$

$$\mathrm{H_2O} + \mathrm{e} \overset{\mathrm{Red}}{\rightleftharpoons} \tfrac{1}{2}\mathrm{H_2} + \mathrm{OH}^- \tag{10.14}$$

The overall electrochemical process is

$$2\,\mathrm{Al} + 2\,\mathrm{OH}^- + 6\,\mathrm{H_2O} = 2\,\mathrm{Al(OH)_4}^- + 3\,\mathrm{H_2} \tag{10.15}$$

It was reported that the inhibitor can affect the corrosion rate of metals in the corrosive media if the inhibitor is able to affect the kinetics of dissolution or alter the position of electrochemical behavior [100]. This effect takes place when a thin film of the inhibitor is formed on the surface of the metal by either the interaction or adsorption processes. Generally, this film is formed by the adsorption in case of using anionic inhibitors on the positive sites, which may be formed as a result of the liberation of electrons in the anodic process (Eq. 10.12). The net result of adsorption is the formation of an inhibitor thin film on the aluminum metal surface. The protective film will isolate the metal from further dissolution into the corrosive medium. This takes place by preventing more Al atoms from leaving the metal surface toward the corrosive medium. This means that net process is the decreasing of the corrosion rates. Therefore, the anodic reaction may be suggested to be the rate-determining step in such corrosion processes. Again, it is well-known that a relationship exists between the structure of the inhibitor and adsorption, which depends on the nature of adsorption and corrosion inhibition performance [55, 69–72]. Again, it was recognized that the presence of sulfur, nitrogen, or oxygen atoms via the inhibitors leads to strong adsorption of the inhibitor on the metal surface. Therefore, the presence of alcoholic functional groups –OH within the cited macromolecule inhibitors could result in remarkable inhibition effect. This may be explained by the formation of bridges between the polymer inhibitor and the Al metal surface. Moreover, the presence of lone pairs of electrons on the oxygen atoms of the hydroxyl groups may enhance the interaction between the inhibitors and the positive sites that formed on Al surface in case of the oxidation process at the anode surfaces (Eq. 10.12) [107]. Hence, we expect that the polymers are adsorbed more strongly than that of the monomers. This means that the inhibition efficiency should be larger for polymers of high-molecular weight than that of low-molecular ones [107–109] where the inhibition efficiency (%I.E) was decreased in the order PVA < ALG < PEC, respectively (Table 10.6).

### 10.8.4 Absorption Isotherm Models Identification

Adsorption isotherms provide basic information on the nature of interaction between the inhibitor and the Al metal through applying some adsorption models. This means that the mechanism of corrosion inhibition can be explained on the basis of adsorption behavior [110, 111]. There are two types of interactions for describing the adsorption of inhibitors on the metal surface. The first type corresponds to physisorption, whereas the second type is corresponding to the chemisorption. Such type depends on the chemical structure of the inhibitor, nature of the corrosive medium, and the valence and nature of corrosive metal.

The cathodic reaction produces by picking up an electron released from the anodic reaction in alkaline solutions ($H_2O + e^- = H + OH^-$) was defined by Eqs. (10.13)–(10.15). In such solutions, the chemisorbed atom on the metal surface reacts by combining with other adsorbed atoms to form $H_2$ gas molecule, which bubbles from the metal surface. A very small amount of the uncombined atoms will remain; however, this amount does not affect the whole process. Therefore, the rates of combination and absorption of atoms are nearly the same for all inhibitor levels. This fact is confirmed by the identical results obtained for the corrosion rates calculated for hydrogen gas evolution in either the gasometric methods or from the weight-loss techniques.

In aqueous solutions, the metal surface was always covered with adsorbed water molecules. Therefore, the adsorption of inhibitor from the aqueous solution is a quasi-substituted process and the inhibitor that has the ability to be desorbed strongly on the metal surface will hinder the dissolution of the metal into the corrosive medium [112, 113]. Here, the degree of surface coverage ($\theta$) considered as the determining factor that plays the main role in the inhibition efficiency and, hence, it can be enhanced in the interpretation of the corrosion mechanism [114]. This depends on the magnitude of the calculated values of the surface coverage's using the following relationship:

$$\theta = 1 - \left(R'_{\mathrm{c}}\right)_{\mathrm{inh}} / \left(R^{\mathrm{o}}{}_{\mathrm{c}}\right)_{\mathrm{free}} \tag{10.16}$$

where $(R'{}_{\mathrm{c}})_{\mathrm{inh}}$ and $(R^{\mathrm{o}}{}_{\mathrm{c}})_{\mathrm{free}}$ are the corrosion rates in the presence and absence of inhibitor. It was observed that the ($\theta$) values were decreased with increasing the temperature as a result of the increase in the adsorption of inhibitor molecules. On the other hand, the ($\theta$) values increased with the increase in the inhibitor concentration as a result of the decrease in the corrosion rates $(R_{\mathrm{c}})_{\mathrm{inh}}$ (numerator in Eq. 10.16). Theoretically, the adsorption process can be regarded as a single substitution of (X) molecule of the water molecules adsorbed on the metal surface by the following reaction:

$$I_{(\mathrm{aq})} + X\,H_2O = I_{(\mathrm{Sur})} + X\,H_2O_{(\mathrm{aq})} \tag{10.17}$$

where $X$ is the size ratio and equals the number of adsorbed water molecules replaced by a single inhibitor molecule. The extent of adsorption depends on many factors, such as the conditions of metal surface, the chemical structure of the inhibitor and the nature of functional groups within the inhibitor, pH and type of corrosive medium, and temperature [115–117].

The adsorption also provides some information about the interaction among the inhibitor molecules themselves as well as their interaction with the metal surface. Actually, the adsorbed molecules may cause some difficulty for the surface to adsorb further molecules from neighboring sites, and hence, a multilayer-adsorption may take place. The net result is the formation of various surface sites with varying degrees of activation. For this reason, a number of mathematical adsorption expressions have been developed to fit the degree of surface coverage through adsorption isotherms to provide some knowledge on the nature of interaction of the adsorbed molecules.

Langmuir isotherm suggests that each site holds one adsorbed species [117, 118] and can be represented by Eq. (10.18).

$$\frac{C}{\theta} = \frac{1}{K_{\text{ads}}} + C \tag{10.18}$$

where $C$ is the concentration of inhibitor and $K_{\text{ads}}$ is the equilibrium constant of adsorption process. Equation (10.19) required that plots of $C/\theta$ against $C$ should be linear with a positive intercept on $C/\theta$ axes and of unity slope. Some of the experimental studies were tested by fitting to the Freundlich adsorption isotherm [117, 119], which is defined by the following relationship:

$$\log\theta = \log K_{\text{ads}} + n\log[C] \quad (0 < n < 1) \tag{10.19}$$

According to Eq. (10.19), plotting the log $\theta$ against log $[C]$ should be linear with intercepts on log $\theta$ axis. Furthermore, the values of n and $K_{\text{ads}}$ can be evaluated from the slopes and intercepts of such plots, respectively. These calculated parameters are calculated by the method of least-squares and are summarized in Table 10.7.

Some other experimental results were tested by the El-Wady adsorption models,

$$\log(\theta/(1-\theta)) = \text{Log}K - n\,\text{Log}\,C \tag{10.20}$$

Equation (10.20) requires that plotting of the left-hand side against log $C$ to be linear with intercepts on the left-hand side axis from whose slopes and intercepts the values of $n$ and $K$ can be evaluated. The results are summarized in Table 10.7.

Temkin postulates another form of the adsorption isotherm models through the following relationship:

$$\ln KC = a\theta \tag{10.21}$$

**Table 10.7** The adsorption and thermodynamic parameters using adsorption isotherm models for the Al corrosion in alkaline medium.

| Inhibitor | Isotherm | Slope ($n$) | K ($M^{-1}$) | $-\Delta G^\circ_{\text{ads}}$ (kJ mol$^{-1}$) | $-\Delta H^\circ$ (kJ mol$^{-1}$) | $-\Delta S^\circ$ (J mol$^{-1}$ K$^{-1}$) | Reference |
|---|---|---|---|---|---|---|---|
| PVA | Freundlich | 0.59 | 0.55 | 8.46 | 38.29 | 100.15[a)] | [57] |
| PVA | El-Wady | 0.88 | 0.20 | 3.39 | 34.92 | 105.80[b)] | [57] |
| ALG | Langmuir | 1.004 | 0.50. | 20.74 | 45.05 | 217.15 | [56] |
| ALG | Freundlich | 0.45 | 0.36 | 7.38 | — | — | [56] |
| PEC | Langmuir | 1.042 | 0.98 | 22.02 | 20.98 | 141.91 | [56] |
| PEC | Freundlich | 0.31 | 0.48 | 8.15 | — | — | [56] |

$[OH^-] = 4.0$ M and I = 4.0 M at 30 °C.

a) $R^2 > 099$.

b) At temperature 25 °C.

where ($a$) is the interaction parameter [2]. According to Eq. (10.21), plots of ln$C$ vs. $\theta$ should be linear with slope of equal to $K$ and intercept equal to the interaction parameter ($a$), respectively.

The standard adsorption free energy ($\Delta G°$) can be calculated from the well-known relationship [94, 95, 120], which relates the adsorption equilibrium constant to the adsorption free energy as follows:

$$\log K_{\text{ads}} = -\log C_{\text{H}_2\text{O}} - \left(\Delta G°\right)_{\text{ads}}/2.303RT \tag{10.22}$$

where $C_{\text{H}_2\text{O}}$ is the molar concentration of water (55.5), $R$ is the gas constant, and $T$ is the absolute temperature.

The observed negative values of $\Delta H°_{\text{ads}}$ indicated that the adsorption process of the inhibitor on Al surface is of spontaneous nature and vice versa for the positive values.

Thermodynamically, $\Delta G°_{\text{ads}}$ is related to the enthalpy ($\Delta H°_{\text{ads}}$) and entropy ($\Delta S°_{\text{ads}}$) of the adsorption process by the famous equation.

$$\Delta G°_{\text{ads}} = \Delta H°_{\text{ads}} - T\Delta S°_{\text{ads}} \tag{10.23}$$

From Eqs. (10.22) and (10.23), the following equation may be obtained:

$$\log K_{\text{ads}} = \left(-\log C_{\text{H}_2\text{O}} + \frac{\Delta S°_{\text{ads}}}{2.303R}\right) - \frac{\Delta H°_{\text{ads}}}{2.303RT} \tag{10.24}$$

Plots of log $K_{\text{ads}}$ vs. $1/T$ gave good straight lines for all cited inhibitors from which slopes and intercepts the values $\Delta H°_{\text{ads}}$ and $\Delta S°_{\text{ads}}$ can be evaluated. These values were calculated by using the least-squares method and are summarized in Table 10.7.

The experimental results indicated that the adsorption processes of the corrosion of Al in aqueous alkaline solutions obey the relationships models of both Langmuir and Freunlich for the ALG and PEC inhibitors [56]; whereas obeys both Freundlich and El-Wady relationship models for the PVA inhibitor [57] in alkaline media.

### 10.8.5 Electrochemical Measurements

Unfortunately, no data were available on such measurements using the cited natural and synthetic polymeric inhibitors for aluminum corrosion in aqueous alkaline media except for galvanic polarization measurements in case of poly(ethylene glycol) in the acidic media [73].

## 10.9 Conclusion

This chapter introduces new green inhibitors of alcoholic macromolecules as alternative future promising materials for protection of the equipment and instruments from the corrosion processes in presence of alkaline atmospheric conditions present in the industrial technology environment. These green natural inhibitors are present in abundance in either the coasts of the Red and Mediterranean seas (ALG) or in the apple and lemon fruits (PEC) as polysaccharides. It also includes PVA synthetic polymer as water-soluble green inhibitor. The experimental results indicated that these green inhibitors exhibited the Langmuir and Freundlich isotherm adsorption models for both ALG and PEC; whereas the PVA inhibitors obeyed the Freundlich and El-Wady adsorption model. Such green inhibitors are characterized by their obvious advantages, such as nontoxicity biodegradability, eco-friendly, and low cost. Applying these inhibitors will save thousand millions of dollars for the economic sectors, which are consumed in maintaining, painting, cathodic protection devices, and protection techniques, such as modifying external environment by de-aeration, dehumidification, and galvanization, which lead to heavy financial losses in strategic industry sectors.

## Acknowledgment

The author would like to present his grateful acknowledgment with thanks to Professor Dr. Metwally Abdalla, Professor of Physical Chemistry, Chemistry Department, Faculty of Science, Benha University, Benha, Egypt for his great support and encouragement during the preparation of this chapter.

## References

1. Fontana, M.G. and Greene, N.D. (1986). *Corrosion Engineering*. New York/Singapore: McGraw-Hill.
2. Davis, J.R. (2000). *Corrosion: Understanding the Basics*, 182. ASM International.
3. Roberge, P.R. (1999). *Handbook of Corrosion Engineering*. London: McGraw-Hill.
4. Shreir, L.L., Jarman, R.A., and Burstein, G.T. (1994). *Corrosion*. London: Butterworth-Heinemann.
5. Winston, R. (2000). *Revie Uhlig's Corrosion Handbook*, 2e. London: Wiley.
6. Cicek, V. and Al-Numan, B. (2011). *Corrosion Chemistry*. Hoboken, NJ/Canada: Wiley.
7. Pedeferri, P. (2018). *Corrosion Science and Engineering*. Switzerland, AG: Springer Nature.
8. Jacobson, G. (2016). *IMPACT Report International Measure of Prevention, Application and Economics of Corrosion Technologies Study*. NACE International.
9. Houston NBS Publication 511-1-2-3 (1978). Economic effects of metallic corrosion in the United States. Report to Congress by the National Bureau of Standards. Washington, DC.
10. Koch, G.H., Brongers, M.B.H., Thomson, N.G. et al. (2004). *Corrosion Costs and Preventative Strategies in the United States*. Houston, TX: National Association of Corrosion Engineers Publications; *Corrosion Costs and Preventive Strategies in the United States*. 2001. CC Technologies Laboratories, Inc. in Dublin, Ohio with support from the Federal Highway Administration and National Association of Corrosion Engineers.

**11** Evans, U.R. (1948). *An Introduction to Metallic Corrosion*. London, UK: Edward Arnold.

**12** Wallen, B. and Anderson, T. (1986). Galvanic corrosion of copper alloys in contact with a highly alloyed stainless steel in sea water. 10th Scandinavian Corrosion Congress.

**13** Dexter, S.C. (1999). *Galvanic Corrosion*. University of Delaware Sea Grant College Program.

**14** Bardal, E., Drugli, J.M., and Gartland, P.O. (1974). A review: the behavior of corrosion resistant steels in seawater. *Corrosion Science* 30: 343–353.

**15** Valen, S., Bardal, E., Rogne, T., and Drugli, J.M. (1989). New galvanic series based upon long duration testing in flowing seawater. Scandinavian Corrosion Congress.

**16** Valen S, Bardal E, Rogne T, Drugli JM. New galvanic series based upon long duration testing in flowing seawater. Stavanger: 11th Scandinavian Corrosion**.**

**17** Prjor, M.J. and Keir, D.S. (1957). Galvanic corrosion: I. Current flow and polarization characteristics of the aluminum-steel and zinc-steel couples in sodium chloride solution. *Journal of the Electrochemical Society* 104: 269.

**18** Compton, K.G. (1971). *NACE Basic Corrosion Course*. Houston, TX: National Association of Corrosion Engineers.

**19** Bardal, E. (2003). *Corrosion and Protection*, 131–132. Springer.

**20** Hammonds, P. (1989). Introduction to corrosion and its prevention. In: *Comprehensive Chemical Kinetics*, chapter 4, vol. 28, 233–297. Elsevier.

**21** Rezenfeld, I.L. (1981). *Corrosion Inhibitors*. New York: McGraw-Hill Inc.

**22** Combrade, P. (2002). *Crevice Corrosion of Metallic Materials in Corrosion Mechanisms in Theory and Practice*, 2e. New York/Basel: Marcel Dekker.

**23** Leidheiser, H. (1987). *Coatings in Corrosion Mechanisms*, 183–186. New York/Basel: Marcel Dekker.

**24** Ljsseling, F.P. (2000). *Survey of Literature on Crevice Corrosion*. London: The Institute of Materials.

**25** De Vivekanand Kani, P.K. and Banerjee, S. (1997). Proceedings of the International Conference on Corrosion, 125.

**26** Kooch, R. (1972). *Annual Book of ASTM Standards, Part 10*. Philadelphia, PA: ASTM.

**27** Uhlig, H.H. (1971). *Corrosion and Corrosion Control*. New York/London: Wiley.

**28** Hatch, J.E. (1984). *Aluminum: Properties and Physical Metallurgy*, 301. Metals Park, OH: ASM International.

**29** Strehblow, H.H. (2002). *Mechanisms of Pitting Corrosion in Corrosion Mechanisms in Theory and Practice*, 2e. New York/Basel: Marcel Dekker.

**30** Pou, T.E., Murphy, Q.J., Bockris, J.O.M., Tongson, L.L., and Monkowsk, M. (1984). Proceedings, 9th International Congress on Metallic Corrosion Toronto, 141.

**31** Bertocci, U.(1987). Advances in localized corrosion. Proceedings of 2nd International Conference on Localized Corrosion, Orlando, PL. National Association of Corrosion Engineers, 127.

**32** Wranglen, G. (1985). *An Introduction to Corrosion and Protection of Metals*. London/New York: Chapman and Hall.

**33** Kruger, J., Long, G.G., Kuriyama, M., and Goldman, A.J. (1983). *Passivity of Metals and Semiconductors*, 163. Amsterdam: Elsevier Science Publishers.

**34** Kaesche, H. (1966). *The Corrosion of Metals; Physico-Chemical Principles and Actual Problems*, 474. Berlin: Springer-Verlag.

**35** Bardal, E. (2003). *Corrosion and Protection*, 135–136. Springer.

**36** Hutchings, I.M. (1986). *The Erosion of Materials by Liquid Flow*, 25. Columbus, OH: Materials Technological Institute of the Chemical Processing Industry.

**37** Lees, D.J. (1982). Characteristics of stress corrosion fracture initiation and propagation. *Metallurgist and Materials Technology* 141: 29–38.

**38** Bardal, E. (2003). *Corrosion and Protection*, 170. Springer.

**39** Narayan, R. (1998). *An Introduction to Metallic Corrosion and its Prevention*. Oxford: IBH Publishing Co. Pvt. Ltd.

**40** Bardal, E. (2003). *Corrosion and Protection*, 154. Springer.

**41** Waterhouse, R.B. (1972). *Fretting Corrosion*. Pergamon Press.

**42** Muller, B. and Schmelich, T. (1955). High-molecular weight styrene-maleic acid copolymers as corrosion inhibitors for aluminum pigments. *Corrosion Science* 37: 877–883.

**43** Muller, B., Oughourlian, C., and Schubert, M. (2000). Amphiphilic copolymers as corrosion inhibitors for zinc pigment. *Corrosion Science* 42: 578–584.

**44** Abd El-Wanees, S., Abd El-Aal, A., and Abd El-Aal, E.E. (1993). Effect of poly(ethylene glycol) on pitting of cadmium in alkaline solutions. *British Corrosion Journal* 28: 222–226.

**45** Ramakrishnaih, K. and Subramanyan, N. (1976). Effect of some nitrogen containing organic compounds on the corrosion and polarization behaviour of aluminium in 1M solutions of sodium hydroxide and hydrochloric acid with and without calcium. *Corrosion Science* 16: 307–316.

**46** Talati, J.D. and Modi, R.M. (1979). P-substituted phenols as corrosion inhibitors for aluminum-copper alloy in sodium hydroxide. *Corrosion Science* 19: 35–48.

**47** Daufin, G., Labre, J.P., and Pagetti, J. (1977). Corrosion inhibition of an aluminium-silicon-magnesium alloy in alkaline media. *Corrosion Science* 17: 901–912.

**48** Solyneos, K.G., Varhegyi, B., Kalman, E. et al. (1993). Inhibition of aluminum corrosion in alkaline solutions by silicon and nitrogen containing compounds. *Corrosion Science* 35: 1455–1457; 1459–1462.

**49** Muller, B. and Fisher, S. (2006). Epoxy ester resins as corrosion inhibitors for aluminum and zinc pigments. *Corrosion Science* 48: 2406–2414.

**50** Lunarska, E. and Chernagayeva, O. (2016). Effect of frictional-mechanical treatment of the low alloy steels on some exploitation properties in sea water simulated solution. *Solid State Phenomena* 250: 56–60.

**51** Hassan, R.M., Khairou, K.S., and Awad, A. (2018). New aspects physicochemical properties of polymer-gels in particularly the coordination biopolymeric metal-alginate ionotropic hydrogels. In: *Polymer Gels: Synthesis and Characterization* (ed. V.K. Thakur and M.K. Thakur), 275–354. Springer Publisher, chapter 10.

**52** Hassan, R.M. (2016). Oxidation of some sulfated macromolecules using various oxidizing agents: focusing on the nature of electron-transfer process and oxidation mechanistics with synthesis of coordination biopolymer oxidation precursors as novel chelating agents. In: *Advances in Chemistry Research*, vol. 30 (ed. J.C. Taylor), 141–211. New York, chapter 8: Nova Publishers.

**53** Hassan, R.M. (2016). Kinetics and mechanistic orientation to the nature of electron-transfer process of oxidation of biodegradable water-soluble polymers by chromic acid in aqueous perchlorate solutions: a linear free- energy correlation. In: *Handbook of Sustainable Polymers: Structure and Chemistry* (ed. V.J. Thakur and M.K. Thakur), 413–455. Pan Stanford Publishers, chapter 12.

**54** Hassan, R.M. (2013). A mechanstic approach to the kinetics of electron-transfer reactions in oxidation of water–soluble macromolecules in particularly carbohydrates by alkaline permanganate with spectrophotometric detection of blue hypomanganate(V) and green manganite (VI)short-lived transient species. A linear free energy correlation. In: *Recent Development in Carbohydrate Research*, vol. 3 (ed. S.G. Pandalai), 27–63. Transworld Research Network A Review.

**55** Zaafarany, I. (2012). Corrosion inhibition of aluminum in aqueous alkaline solutions by alginate and pectate water-soluble natural anionic polyelectrolytes. *Portugaliae Electrochimica Acta* 30: 419–426.

**56** Hassan, R.M., Zaafarany, I.A., Gobouri, A., and Takagi, H.D. (2013). A revisit to the corrosion inhibition of aluminum in aqueous alkaline solutions by water-soluble alginates and pectates as anionic polyelectrolyte inhibitors. *International Journal of Corrosion* 1–8.

**57** Hassan, R.M., Zaafarany, I., Hazzay, O.A., and Takagi, H.D. (2013). Kinetics of corrosion inhibition of aluminum in alkaline solutions by water-soluble poly (vinyl alcohol) as synthetic polymer. *Journal of Electrochemistry & Plating Technology* 1: 3–14.

**58** Hassan, R.M. (1993). Alginate polyelectrolyte ionotropic gels. XVIII. Oxidation of alginate polysaccharide by potassium permanganate in alkaline solutions. Kinetics of decomposition of the intermediate complex. *Journal of Polymer Science: Part A* 31: 1147.

**59** Khairou, K.S. and Hassan, R.M. (2000). Pectate polyelectrolyte ionotropic gels. I. Kinetics and mechanism of formation of manganite (VI)-pectate intermediate complex during oxidation of pectate polysaccharide by alkaline permanganate. *European Polymer Journal* 36: 2021–2030.

**60** Khairou, K.S. (2003). Kinetics and mechanism of decomposition of intermediate complex during oxidation of pectate polysaccharide by potassium permanganate in alkaline solutions. *International Journal of Chemical Kinetics* 35: 67–72.

**61** Hassan, R.M. (1993). New coordination polymers. III: oxidation of poly(vinyl alcohol) by permanganate ion in alkaline solutions. Kinetics and mechanism of formation of intermediate complex with a spectrophotometric detection of manganate(vi) transient species. *Polymer International* 30: 5–9.

**62** Hassan, R.M., El-Gaiar, S., and El-Summan, A.M. (1993). New coordination polymers. IV. Oxidation of poly (vinyl alcohol) by permanganate ion in alkaline solutions. Kinetics and mechanism of decomposition of intermediate complex. *Polymer International* 32: 39–42.

**63** Schweiger, R.G. (1962). Acetylation of alginic acid. I. Preparation and viscosities of align acetate. *The Journal of Organic Chemistry* 27: 1786–1789.

**64** Schweiger, R.G. (1962). Reaction of align acetates with calcium and other divalent ions. *The Journal of Organic Chemistry* 27: 1786–1179.

**65** Haugh, A. (1964). Composition and properties of alginate. Thesis. Norwegian Institute of Technology, Trondheim, Norway.

**66** Haugh, A. and Larsen, B. (1971). Biosynthesis of alginate: part III. Polymannuronicacid C-5 epimerase from azotobacter vinelandii (Lipman). *Carbohydrate Research* 17: 297–308.

**67** Smidsrod, O. (1973). Some physical properties of alginates in solution and in the gel state. Thesis, Norwegian Institute of Technology, Trondheim.

**68** Khon, R. (1975). Ion binding of polyuronates-alginate and pectin. *Pure and Applied Chemistry* 42: 371–397.

**69** Badawy, W.A., El-Kharafi, F.M., and Al-Hassan, A.S.E.Y. (1998). The electrochemical behavior of cadmium in aqueous solutions. *Current Topics in Electrochemistry* 6: 33–74.

**70** Minzanova, S.T., Mironova, V.F., Arkhipova, D.M. et al. (2018). Biological activity and pharmacological application of pectic polysaccharides: a review. *Polymers* 10: 1407–1419.

**71** Kumar, V. and Singh, L. (2018). Pectin from fruit peels and its uses as pharmaceutical and food grade: a descriptive review. *European Journal of Biomedical and Pharmaceutical Sciences* 5: 185–199.

**72** Paulsen, B.S. and Barselt, S. (2005). Bioactive pectic polysaccharides. *Advances in Polymer Science* 186: 69–101.

**73** Abdalla, M., Megahed, H.E., Radwan, M.A., and Abdfattah, E. (2012). Poly (ethylene–glycol) compounds as corrosion inhibitors for aluminum in 0.5 M hydrochloric acid solution. *Journal of American Science* 8: 49–55.

**74** Muppalaneni, S. (2013). Polyvinyl alcohol in medicine and pharmacy: a perspective. *Journal of Developing Drugs* 2: 112.

**75** Gajra, B., Pandya, S.S., Vidyasagari, G. et al. (2012). Poly vinyl alcohol hydrogel and its pharmaceutical and biomedical applications: a review. *International Journal of Pharmaceutical Research* 4: 20–27.

**76** Gaaz, T., Sulong, A., Akhtar, M.N. et al. (2015). Properties and applications of polyvinyl alcohol, halloysite nanotubes and their nanocomposites. *Molecules* 20: 22833–22847.

**77** Shahini, M.H., Ramezanzadeh, B.B., and Mohammadloo, H.E. (2021). Recent advances in biopolymers/carbohydrate polymers as effective corrosion inhibitive macro-molecules: a review study from experimental and theoretical views. *Journal of Molecular Liquids* 325: 115110.

**78** Kim, Y.S., Park, I.J., An, B.S. et al. (2020). Improvement of corrosion penetration resistance for aluminum heat exchanger by alloying zirconium. *Materials Chemistry and Physics* 241: 122275.

**79** Nardeli, V.J., Fugivara, S.F., Taryba, M. et al. (2019). Tannin: a natural corrosion inhibitor for aluminum alloy. *Progress in Organic Coating* 135: 368.

**80** Laleh, R.R., Savaloni, H., Abdi, F., and Abdi, Y. (2019). Corrosion inhibition enhancement of Al alloy by grapheme oxide coating in NaCl solution. *Progress in Organic Coating* 1: 300–307.

**81** Solomon, M.M., Umoren, S.A., Quraishi, M.A., and Salman, M. (2019). Myristic acid based imidazoline derivative as effective corrosion inhibitor for steel in 15% HCl medium. *Journal of Colloid and Interface Science* 551: 47–61.

**82** Abd El-Rehim, S.S. and Hassan, H.H. (2016). Experimental and theoretical investigations of adsorption and inhibitive properties of Tween 80 on corrosion of aluminum alloy (A5754) in alkaline media. *Zeitschrift Fur Physikalische Chemie* 230: 67–78.

**83** Verma, C., Ebenso, E., and Quraishi, M.A. (2017). Ionic liquids as green and sustainable inhibitors for metal and alloys: an overview. *Journal of Molecular Liquids* 233: 403–414.

**84** Abdallah, M., Kamar, E.M., El-Etre, A.Y., and Eid, S. (2016). Gelatin as corrosion inhibitor for aluminum and aluminum silicon alloys in sodium hydroxide solutions. *Protection of Metals and Physical Chemistry of Surfaces* 52: 140–148.

**85** Wang, J.D., Gao, L., Zhang, D. et al. (2016). Experimental and theoretical investigation on corrosion inhibition of AA5052 aluminium alloy by L-cysteine in alkaline solution. *Materials Chemistry and Physics* 169: 142–151.

**86** Xhanari, K. and Finsgar, M. (2019). Organic corrosion inhibitors for aluminum and its alloys inchloride and alkaline solutions: a review. *Arabian Journal of Chemistry* 12: 4646–4663.

**87** Abdallah, M., Kamar, E.M., Eid, E., and El-Etre, A.Y. (2016). Animal glue as green inhibitor for corrosion of aluminum and aluminum-silicon alloys in sodium hydroxide solutions. *Journal of Molecular Liquids* 220: 755–761.

**88** Abdallah, M. and Atwa, S.T. (2014). Corrosion inhibition of aluminum in NaOH solutions using some bidentate azo dyes compounds and synergistic action with some metal ions. *International Journal of Electrochemical Science* 9: 4747–4760.

**89** Abdallah, M. and Hazazi, O.A. (2014). Influence of *N*-thiazolyl-2-cyanoacetamide derivatives on the corrosion of aluminum in 0.01 M sodium hydroxide. *Protection of Metals and Physical Chemistry of Surfaces* 50: 659–666.

**90** Hassan, R.M. and Ibrahim, S. (2021). Performance and efficiency of methyl cellulose polysaccharide as a green promising inhibitor for inhibition of corrosion of magnesium in acidic solutions. *Journal of Molecular Structure* 1246: 131180.

**91** Muller, B. (1999). Polymeric corrosion inhibitors for aluminum pigment. *Reactive and Functional Polymers* 39: 165–177.

**92** Muller, B. and Schmelich, T. (1995). High-molecular weight styrene-maleic acid copolymers corrosion inhibitors for aluminum pigments. *Corrosion Science* 37: 877–883.

**93** Abdel Gaber, A.M., Khamis, E., Abo El-Dahab, H., and Adel, S. (2008). Inhibition of aluminum corrosion in alkaline solutions using natural compound. *Materials Chemistry and Physics* 109: 297–305.

**94** El-Wady, G.Y., El-Said, I.A., and Fouda, A.S. (2008). Anion surfactants as corrosion inhibitors for aluminum dissolution in HCl solutions. *International Journal of Electrochemical Science* 3: 177–190.

**95** Amin, M.A., Hazzazi, O.A., Abd El-Rhim, S. et al. (2009). Polyacrylic acid as a corrosion inhibitor for aluminum in weakly alkaline solutions. Part I: weight loss, polarization, impedance EFM and EDX studies. *Corrosion Science* 51: 658–667.

**96** Arenos, M.A., Bethencourt, M., Botana, F.G. et al. Inhibition of aluminum alloy and galvanized steel by lanthanide salts. *Corrosion Science* 43: 157–170.

**97** Awad, S.A., Kamal, K.M., and Kassab, A. (2001). Effect of anions on the corrosion of aluminum in sodium hydroxide: part I. The chromate ion. *Journal of Electroanalytical Chemistry* 127: 203–209.

**98** Lunarska, E. and Chernagayeva, O. (2006). Effect of corrosion inhibitors on hydrogen uptake by Al from NaOH solution. *International Journal of Hydrogen Energy* 31: 285–293.

**99** Maayta, A.K. and Al-Rawashdeh, N.A.F. (2004). Inhibition of acidic corrosion of pure aluminum by some organic compounds. *Corrosion Science* 46: 1129–1140.

**100** McCafferty, E. (1979). *Corrosion Control by Coating* (ed. H. Leidheiser Jr.,). Princeton, NJ: Science Press.

**101** Hassan, R.M. (1993). Alginate polyelectrolyte ionotropic gels. XIV. Kinetics and mechanism of formation of intermediate complex during the oxidation of alginate polysaccharide by alkaline permanganate with a spectrophotometric evidence of manganate (VI) transient species. *Journal of Polymer Science Part A* 31: 51–59.

**102** Glasston, S., Laidler, K.J., and Eyring, H. (1941). *The Theory of Rate Processes*, 41. New York: McGraw-Hill.

**103** Hassan, R.M. and Zaafarany, I.A. (2013). Kinetics of corrosion inhibition in acidic media by water-soluble natural polymeric pectates as anionic polyelectrolyte inhibitors. *Materials* 6: 1–16.

**104** Hassan, R.M., Ibrahim, S.M., Takagi, H.D., and Sayed, S.A. (2018). Kinetics of corrosion inhibition of aluminum in acidic media by water-soluble natural polymeric chondroitin-4-sulfate as anionic polyelectrolyte inhibitor. *Carbohydrate Polymers* 192: 356–363.

**105** Hassan, R.M., Ibrahim, S.M., Salman, S.A., and Takagi, H.D. (2019). A promising water-soluble synthetic polymer of high efficiency and low cost as inhibitor for inhibition of metals corrosion: inhibition of magnesium corrosion by poly (ethylene glycol) in acidic media. *Journal of Bio- and Tribo-Corrosion* 101: 1–10.

**106** Noor, E.A. (2009). Potential of aqueous extract of *Hibiscus sabdariffa* leaves for inhibiting the corrosion of aluminum in alkaline solutions. *Journal of Applied Electrochemistry* 39: 1465–1475.

**107** Khairou, K.S. and El-Sayed, A. (2003). Inhibition effect of some polymers on the corrosion of cadmium in a hydrochloric acid solution. *Journal of Applied Polymer Science* 88: 866–871.

**108** Fouda, A.S., Elewady, G.Y., Ibrahim, R.R., and Salim, E.A. (2015). New antipyrine derivatives as corrosion inhibitors for C-steel in 1.0M hydrochloric acid solutions. *Pharma Chemica* 7: 260–274.

**109** Popova, A., Christov, M., Raicheva, S., and Sokolova, E. (2004). Adsorption and inhibitive properties of benzimidazole derivatives in acid mild steel corrosion. *Corrosion Science* 46: 1333–1350.

**110** Popova, A., Christov, M., and Vasilev, M. (2007). Inhibitive properties of quaternary ammonium bromides of *N*-containing heterocycles on acid mild steel corrosion. Part I: gravimetric and voltammetric results. *Corrosion Science* 49: 327–331.

**111** Raicheva, S.N., Aleksiev, B.V., and Sokolova, E. (1993). The effect of the chemical structure of some nitrogen- and sulphur-containing organic compounds on their corrosion inhibiting action. *Corrosion Science* 34: 343-350.

**112** Hassan, R.M., Ibrahim, S.M., Salman, S.A., and Takagi, H.D. (2019). A promising water-soluble synthetic polymer of high efficiency and low cost as inhibitor for inhibition of metals corrosion: inhibition of magnesium corrosion by poly (ethylene glycol) in acidic media. *Journal of Bio-and Tribo-Corrosion* 5 (4): 1–10.

**113** Chauban, R.L. and Gunsekaran, G. (2007). Corrosion inhibition of mild steel by plant extract in dilute HCl medium. *Corrosion Science* 49: 1143–1161.

**114** Keles, H., Keles, M., Dehri, I., and Serindag, O. (2008). Adsorption and inhibitive properties of aminobiphenyl and its Schiff base on mild steel corrosion in 0.5 M HCl medium. *Colloids and Surfaces A* 320: 138–145.

**115** Zaafarany, I.A. (2006). Inhibition of acidic corrosion of iron by some carrageenan compounds. *Current World Environment: An International Research Journal of Environmental Sciences* 12: 101–108.

**116** Khairou, K.S. and Zaafarany, I.A. (2006). Some sulfated water soluble natural polymer compounds as corrosion inhibitors for dissolution of iron in hydrochloric acid solution. *Material Science Research India* 3: 135–140.

**117** Solomon, M.M., Umoren, S.A., Udsoro, I.I., and Udoh, A.P. (2010). Synergistic and antagonistic effects between halide ions and carboxymethyl cellulose for the corrosion inhibition of mild steel in sulphuric acid solution. *Cellulose* 17: 635–644.

**118** Mazhar, M.A., Badawy, W.A., and Abou Romia, R.M. (1986). Impedance studies of corrosion resistance of aluminium in chloride media. *Surface and Coating Technology* 29: 335–345.

**119** Kliskic, M., Radosevic, J., Gudic, S., and Kotalinik, V. (2000). Aqueous extract of *Rosmarinus officinalis* L. as inhibitor of Al–Mg alloy corrosion in chloride solution. *Journal of Applied Electrochemistry* 30: 823–830.

**120** Yurt, A., Ulutaas, S., and Dal, H. (2006). Electrochemical and theoretical investigation on the corrosion of aluminum in acidic solution containing some Schiff bases. *Applied Surface Science* 253: 919–925.

# 11

# Polymeric Corrosion Inhibitors for Acid Media

*Nurudeen A. Odewunmi*[1]*, Mohammad A. Jafar Mazumder*[1,2]*, and*
*Shaikh A. Ali*[1,2]

[1] *King Fahd University of Petroleum & Minerals, Chemistry Department, Dhahran 31261, Saudi Arabia*
[2] *King Fahd University of Petroleum & Minerals, Interdisciplinary Research Center for Advanced Materials, Dhahran 31261, Saudi Arabia*

## 11.1 Background

Abstaining from the use of acidic solutions (hydrochloric acid; HCl, sulfuric acid; $H_2SO_4$, hydrofluoric acid; HF, formic acid; HCOOH, sulfamic acid; $H_2NSO_3H$, nitric acid; $HNO_3$, phosphoric acid; $H_3PO_4$), and mixtures of two or more of acids in the transportation, processing, and production of consumer products and services is practically unavoidable in the human daily and industrial activities. Acid corrosion has been one of the major challenges for industrialized countries in sustaining their economic influence. The interactions of metallic materials, such as copper (Cu), zinc (Zn), aluminum (Al), iron (Fe), and their alloys, with acids-related chemicals at some extreme or harsh operational (temperature, pressure, and moisture) conditions due to their economic importance increase their chance of corrosion vulnerability in acidic media. The most utilized of these metals for engineering parts, pipelines, submarines, and building constructions are low-carbon steel (CS) owing to their unique economic advantages and attractive metallurgical and mechanical properties [1, 2]. The effort of the National Association of Corrosion Engineers (NACE) and the Federal Highway Administration (FHWA) of the United States (US), with the support of the US Congress, revealed that 3.1% of the US gross domestic product (GDP) amounted to US$276 billion was the cost associated to corrosion in the United States [3]. The cost implication of corrosion is alarming, but some industrial operations, such as acid cleaning of boilers, acid pickling, degreasing, and rinsing, lead to gradual degradation or deterioration of different materials due to their interaction with acidic solutions, which are unavoidable in many industries. The involvement of acids in the forms of $CO_2$, $SO_2$, HCl, and other states as a major corrosive agent depends on the concentration, interaction time, and operational conditions. A relatively lower concentration usage of acids and mild operating conditions are involved in some manufacturing industries where

*Polymeric Corrosion Inhibitors for Greening the Chemical and Petrochemical Industry*, First Edition.
Edited by Mohammad A. Jafar Mazumder, Mumtaz A. Quraishi, and Amir Al-Ahmed.

parts are deepened into $H_2SO_4$, $HNO_3$, HF, and mixtures of acids before a finished product can be achieved. Chemical descaling, degreasing, precleaning, cleaning, acid dip, rinsing, and pickling are popular in the metal manufacturing industry [4]. Acid corrosion of pipelines and other related materials is more pronounced in oil and gas exploration, where activities, such as drilling, transportation, and storage of petroleum products, in extreme operational conditions [5] necessitate the use of acid to mitigate the corrosion process. The effects of petroleum products on pipelines due to gradual equipment deterioration are sudden and complete system failure, a catastrophic accidents, wastage of materials, and even loss of life [6]. In acidizing, high-concentrated acid solutions are used in oil and gas wells to enhance oil well flow by removing unwanted materials from oil bore surfaces, accessing blocked oil well channels by rock formations, and general stimulating practices to enhance oil recovery. The majority of acidizing procedures are carried out using HCl among the convectional acids to improve flow and permeability capacity of oil and gas mitigation of the fouling process. These procedures include gel breaking, matrix acidizing, sandstone and carbonate matrix, fracture acidizing, damage removal, stimulation, and completion of horizontal well [7, 8].

The following steps are represented by Eqs. (11.1)–(11.3), which have demonstrated the general electrochemical anodic and cathodic reactions of metal (using Fe as an example) in an acidic medium [9]:

The dissolution of metal shows the oxidation reaction of Fe

$$\mathrm{Fe} \rightarrow \mathrm{Fe}^{2+} + 2\mathrm{e}^{-} \text{ (Anodic reaction)} \tag{11.1}$$

The corrosive environment determines the cathodic reactions. In acidic media, two cathodic reactions are expected: hydrogen evolution and oxygen reduction.

$$2\mathrm{H}^{+} + 2\mathrm{e}^{-} \rightarrow \mathrm{H}_2 \text{ (Hydrogen evolution)} \tag{11.2}$$

$$\mathrm{O}_2 + 4\mathrm{H}^{+} + 4\mathrm{e}^{-} \rightarrow 2\mathrm{H}_2\mathrm{O} \text{ (Oxygen reduction)} \tag{11.3}$$

In acid pickling and other enhanced oil wells recovery process where HCl is used, Eqs. (11.4)–(11.7) represent the corrosion reactions.

$$\mathrm{Fe} + \mathrm{Cl}^{-} \rightleftharpoons \mathrm{FeCl}^{-}_{\mathrm{ads}} \tag{11.4}$$

$$\mathrm{FeCl}^{-}_{\mathrm{ads}} + \mathrm{Fe} \rightleftharpoons \mathrm{FeCl}^{-}_{\mathrm{ads}}\mathrm{Fe} \tag{11.5}$$

$$\mathrm{FeCl}^{-}_{\mathrm{ads}}\mathrm{Fe} + \mathrm{OH}^{-} \rightarrow \mathrm{FeOH}^{+} + \mathrm{Fe} + \mathrm{Cl}^{-} + 2\mathrm{e}^{-} \tag{11.6}$$

$$\mathrm{FeOH}^{+} + \mathrm{H}^{+} \rightleftharpoons \mathrm{Fe}^{2+} + \mathrm{H}_2\mathrm{O} \tag{11.7}$$

## 11.2 Outward and Inward Acid Corrosion

The vulnerability of metals (mostly steel) and other materials to the acidic solution are not limited to their contact with fluid or other electrolytes during some important operational procedures in the industries but extended to their exposure to the immediate environments, such as the soil, groundwater, and the atmosphere. In the oil and gas industries, where structures erected for offshore exploration are being exposed to seawater, condensation and rain can lead to acid corrosion of the outer part of metallic structures. Aside from that, many pipelines, storage tanks, and other pieces of equipment are exposed to acid corrosion externally through their interaction with moisture, humidity, and acidic soil contents. Cathodic protection is an effective technique, which is used to protect the external surface of ferrous materials, such as steel, in an aqueous corrosive environment where a sacrificial anode is electrochemically engineered to corrode instead of the structure by application of an impressed current [10]. However, the use of external coatings that consist of polymeric materials, such as polyesters, epoxy, polyurethanes, polyacrylates, resins, and conducting polymers composites [11–13] that can serve as a protective barrier for corrosion have been adapted to mitigate external structures corrosion.

Besides, the objective of this chapter is to emphasize the inward (internal) corrosion of materials that are susceptible to acid corrosion and the use of polymeric material to mitigate acid corrosion. During oil exploration, oil-based drilling mud, which is not naturally corrosive, is encountered, but the introduction of some additives to enhance drilling procedures makes acid gas, oxygen, and other corrosive contaminants available in the mud system that will eventually decrease the pH and induce acid corrosion. Acetic acid is one of the additives used to retard acid devoid of viscosity, perforating fluid, stimulating treatment, an aqueous solution to drive surfactant, an initial treatment fluid before the use of concentrated HCl and HF in acidizing, and as a temporary bridging agent (transitory emulsion or true gel) for well completion process [14]. These activities will make acid corrosion persistence throughout the casing, refining, and distribution of products that are all cut across low-, moderate-, and high-temperature working conditions. The encounter of naphthenic acid mostly at very high temperatures and other crude-oil constituents leads to complex acid corrosion in the oil and gas refinery industry that is not yet understood [15]. The most straightforward approach that proved economically viable to mitigate acid corrosions in metal manufacturing, oil, and gas industries is the use of corrosion inhibitors.

## 11.3 Organic and Inorganic Corrosion Inhibitor in Acid Media

The uniqueness of ferrous materials, such as mild steel (MS) for numerous industrial applications owing to their ability to withstand harsh operating conditions is not enough to acquit it and other nonferrous (Zn, Al, and Cu) metallic material from gradual disintegration by corrosion process [16–20] due to their interaction with acidic media. The presence of low concentrations of corrosion inhibitors in acidic solutions involved in many industrial operations has proven to be effective in reducing the corrosion rate of metal to a reasonable amount. Corrosion inhibitors have been classified as precipitation, adsorption, anodic or oxidizing passivation, phase (volatile or vapor), and scavenger inhibitors based on how the corrosion process is controlled and many other factors [21]. However, for a corrosion inhibitor to be effective for metal surface protection in corrosive media, the following requirement must possess as enumerated by Umoren and Solomon [22].

(i) Ability to form a compact and waterproof film after metal oxidation;
(ii) The film formed should be able to cover a large surface area of the metal;
(iii) High disposable site of adsorption (preferably chemisorption) on the metal surface;
(iv) It should be able to build up (polymerized) in situ on the metal surface;
(v) It should be environment-friendly; and
(vi) It must be easy to handle, cheap, and readily available.

These highlighted requirements and the characteristics adapted for the classifications of corrosion inhibitors are often embedded in what constitutes another grouping of corrosion inhibitors as inorganic and organic corrosion inhibitors. For a corrosion inhibitor to possess an adsorption center for metal surface, it should either contain some inorganic components, such as heteroatom (oxygen, nitrogen, phosphorous, and other electron-rich center atoms), or electron-rich functional groups from an organic compound. In the oilfield applications, multicomponent inhibitors containing film-forming organic compounds or chemicals along with some inorganic components (oxygen, $H_2S$ scavengers, and metals), oxidizing agents in small quantities to promote adsorption of inhibitor and formation of a hydrophobic film on metal surface for adequate protection of metal from corrosive environments.

### 11.3.1 Challenges of the Organic and Inorganic Components in Corrosion Inhibitor

There are some challenges associated with the use of corrosion inhibitors considering their effectiveness, unfavorable chemical properties, and influence on environmental pollution management. Inhibitors containing some inorganic components, such as chromium, are effective for corrosion mitigation of different steels in acidified chloride solutions [23, 24]. Chromium compounds have been found to exhibit high toxicity properties. This characteristic has led to the prohibition of chromium-base compounds to minimize the threat of toxic material to the environment to enhance public protection [24]. Despite this action, attempts have been made to develop an efficient corrosion inhibitor with a relatively lower chromium concentration to reduce its adverse toxicity effect on the environment [25], but still highly discouraged due to the toxicological profiles of chromium [26]. Several efforts channels toward the replacement of chromium in the formulations of corrosion inhibitors by several advanced technologies, such as plasma deposition at low temperature, sol–gel application, and the use of many inorganic inhibitors, have not provided the level of protection offered by chromates inhibitors [27]. The closest accomplishment in the search for a chromate-free corrosion inhibitor system is the discovery of lanthanide compounds. Lanthanides corrosion inhibitors have proven to be an exceptional candidate that achieved the requirement of an acceptable protection capacity, low toxicity, and more environment-friendly inhibitors. But its application is still restricted on account of its toxicity level [28].

Organic corrosion inhibitors in acidic media, on the other hand, are very active metal surface adsorbates characterized by both hydrophobic and hydrophilic moieties within the same molecules in the corrosive media. They are effective corrosion inhibitors in all aqueous media owing to their high solubility, formation of stable film that is effective as a protection film against corrosive environments, and more environment-friendly than the inorganic corrosion inhibitors [9, 29]. The ease of adsorption of organic corrosion inhibitors in acidic media on metal is promoted by their strong polar constituent primarily based on nitrogen atoms from amines [29], amides [30], imidazole [31], quaternary ammonium salts [32, 33], and other compounds containing oxygen [34], sulfur [35, 36] and phosphorus [36]. However, despite the ability of organic corrosion inhibitors to prevent acid corrosion in both anodic and cathodic corrosion reaction sites of metals, there are challenges of the exposure to hazardous materials, needs for qualified experts, and high-cost implications (expensive) in their complicated synthesis procedures. The use of natural resources has been suggested as an alternative consideration for environment-friendly corrosion inhibitors in acidic media [37].

### 11.3.2 Polymeric Corrosion Inhibitor in Acidic Media

The ability of a molecule of an inhibitor to build up in situ on the metal surface as part of the requirement for improved and more effective protection of metal in a corrosive environment [22] is practically impossible for an organic inhibitor. Hence, the search for a perfect replacement of inorganic and organic corrosion inhibitors that can meet all the requirements of an effective corrosion inhibitor by natural resources, as suggested by Yang [38], considers polymeric material as a corrosion inhibitor in acidic media. Polymeric materials occur naturally and are synthesized in the laboratory to suit the desired application. They are molecules generally characterized by the repetition of one or more organic species (atom or group of atoms), functionalities linked together in a sufficient amount that can provide an improved desired property. The superior inhibition efficiency (IE) ability of a polymer compound than its corresponding single repeating unit (monomer) has been demonstrated on the surface of MS in 15% HCl solution. A di-cationic monomer, namely, $N^1$, $N^1$-diallyl-$N^6$, $N^6$, and $N^6$-tripropylhexane-1,6-diaminium chloride (mono-NTHDC), has been reported to offer 79.1% IE for API CS in 15% HCl solution at $1000\,\text{mg}\,\text{l}^{-1}$ concentration, while $100\,\text{mg}\,\text{l}^{-1}$ of the poly-NTHDC compounds (10% amount of the monomer) provides a better IE of 86.1% in the corrosive acidic media [38]. Several research outcomes have justified the use of polymeric materials as efficient corrosion inhibition of metals in corrosive media [39–41] owing to some functional groups' hydrophobic moieties that acted as an adsorptions center protective layer on metal surface in the corrosive media, respectively.

## 11.4 Natural Polymeric Materials

All organic compounds, such as carbohydrates, proteins, and essential oils, that originated through a biological process from plants and animals are naturally polymeric materials. Any natural occurring substance, such as pectin, gum arabic, cellulose, starch, oils, gellan gum, and chitosan, consists of aromatic compounds, multiple bonds, carbohydrates, and/or amino acids as a single repeating unit are natural polymeric materials [41].

## 11.5 Essential Oils

The essential oil molecules contain a single monomer unit that is predominantly aromatics and aliphatic unsaturated hydrocarbon, utilizing the multiple bond unpaired electron center as an adsorption center for metal in corrosive media.

### 11.5.1 Terpenes and Isoprene

Most herbs, plants, and some animals' smells are characterized by the presence of aromatic compounds commonly referred to as terpene. The essential oil extracted from plants and animals contains terpene and other organic compounds identified to possess an inhibiting property of metals and alloys of metals in acidic media [42]. Limonene is a major terpene that has been used as a corrosion inhibitor of MS in HCl solution [43]. The potency of essential oil as a corrosion inhibitor in acidic media has been attributed to the presence of several terpenes' monomers, such as limonene, β-caryophyllene, α-pinene, myrcene, α-terpineol, terpinolene, and terpinen-4-ol [44, 45].

Polyterpenes are low-molecular weight organic compounds that are used to develop adhesives owing to their stickiness. Polyterpenes contain a repeated unit of isoprene, which can be regarded as polyisoprene with general formula $(C_5H_8)_n$, as shown in Figure 11.1. They are an integral part of natural rubber, which contains about 97% *cis* 1,4-polyisoprene and exist naturally in latex form in *Hevea braziliensis* [45]. The use of rubber leaf extract has been reported to be an effective corrosion inhibitor of MS in an acidic environment due to the presence of multiple bond compounds as indicated by the photochemical of the rubber leaf [46].

### 11.5.2 Tannins and Flavonoids

Tannins are derivatives of phenol resulting from the product obtained by the secondary metabolic process of the plant. They are water-soluble polyphenols with molecular weight between 500 and 3000 Da depending on the particular plant species' metabolic product. Besides, the molecular weight of tannins can be up to 2000 Da when in complex with alkaloids, saccharides, and proteins [47]. Flavonoids are a class of polyphenol compounds consisting of 15-carbon atoms with two phenyl rings separated by a heterocyclic ring, as shown in Figure 11.2a. Regarding the

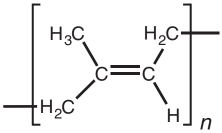

**Figure 11.1** The chemical structure of polyisoprene.

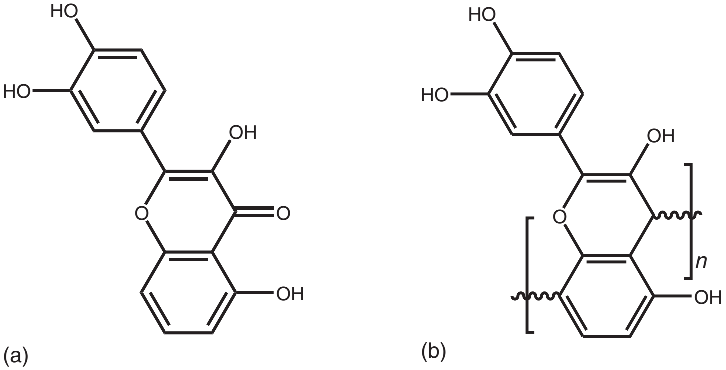

**Figure 11.2** The representative chemical structure of (a) flavonoids and (b) condensed tannins; polymeric flavonoids.

relatively lower number of phenolic compounds in flavonoids compared to tannins, tannins are regarded as polymeric flavonoids (Figure 11.2b). A series of four monomer flavonoids, namely, epigallocatechin, epicatechin, epicatechin gallate, and catechin, constituted mangrove tannins, are effective corrosion inhibitors of metal in an acidic medium. However, tannins are more effective corrosion inhibitors of metal than the individual flavonoids, probably due to polymeric and synergistic effects of flavonoids in different tannins compounds [48]. Due to tannins' effectiveness as corrosion inhibitors in acidic mediums, some natural, biodegradable, and cost-effective vegetal tannins have been evaluated and patented as an effective anticorrosive agent of steel and iron in the acidic medium [49]. A polymeric structure of mimosa tannins was reported to constitute a few repeated units of flavonoids that were found to be effective for protecting low CS in $H_2SO_4$ solution [50].

## 11.6 Carbohydrates (CHO)

The naturally occurring compounds consisting of carbon, hydrogen, and oxygen atoms are called carbohydrates (CHO) with the general formula $C_n(H_2O)_n$. They are classified according to the number of carbon atoms from 3 to 10 as triose, tetrose, pentose, hexose, heptoses, octose, nonose, and decose, respectively; where $n$ is between 3 and 10. Each compound of this classification is regarded as a monosaccharide. However, monosaccharides are polyhydroxyketone (ketoses) or polyhydroxylaldehyde (aldoses) compounds due to ketone's presence; C=O, or carbonyl aldehyde; H–C=O functional groups in their molecular structure.

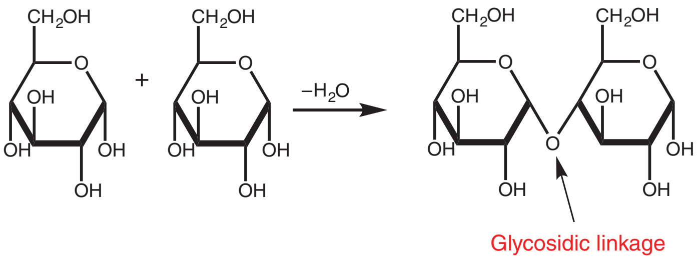

**Scheme 11.1** The condensation reaction of α-D-glucose shows the glycosidic linkage in the maltose backbone structure.

Disaccharides, oligosaccharides, and polysaccharides, also referred to as ketal or acetal, are formed by forming a series of glycosidic linkages or bonds, as shown in Scheme 11.1, through the condensation reaction of two or more monosaccharides [51]. The chemical structures of CHOs used as corrosion inhibitors in the acidic medium are shown in Figure 11.3, and the summary of their performances in different modifications is listed in Table 11.1.

### 11.6.1 Starch

Starch is a very complex CHO molecule consisting of glycosidic bonds connecting different glucose units. It is a heteropolysaccharide molecule with different weight percentages of linear, branch, and, helical molecules that depend on its derived source [92]. The representative structure of starch shown in Figure 11.3a is an abundant CHO that is present virtually in every human diet, such as cassava, yam, tapioca, potatoes, oats, cereals, peas, and nuts. The utilization of molecular starch as corrosion inhibition application is limited owing to its low surface adhesion strength and solubility. The anticorrosive ability of molecular starch reports in a corrosive medium is based on either its physical or chemical modifications to enhance the possibility of the electron-rich hydroxyl group in its molecular structure to undergo coordinate bond with the empty d-orbital of the metal substrate. The physically modified sweet potato starch by extrusion method was found to be anticorrosive active for galvanized steel in 1 M HCl solution. The IE was time, temperature, and concentration-dependent with a maximum corrosion IE of 64.26% for $0.7\,g\,l^{-1}$ concentration. The efficacy of the starch inhibitor was found to be reduced with an increase in time of immersion and temperature [52]. The effectiveness of sodium dodecylsulfate (SDS) and cetyltrimethylammonium bromide (CTAB) as an additive to improve the performance of starch as a corrosion inhibitor on MS in 0.1 M $H_2SO_4$ was evaluated. The pure starch was found to achieve 66.21% efficiency at $0.2\,g\,l^{-1}$ concentration. However, the addition of a small amount of SDS and CTAB was found to improve the corrosion IE of the starch in the acidic medium [53]. The glycerin-grated maize starch was successfully evaluated on carbon–manganese (C-Mn) steel in a 1 M HCl solution. The IE was found to increase with an increase in the concentration of the glycerine-grafted starch up to 94% for $0.3\,g\,l^{-1}$ concentration [54]. The effect of potassium iodide (KI) on the starch extracted from millet

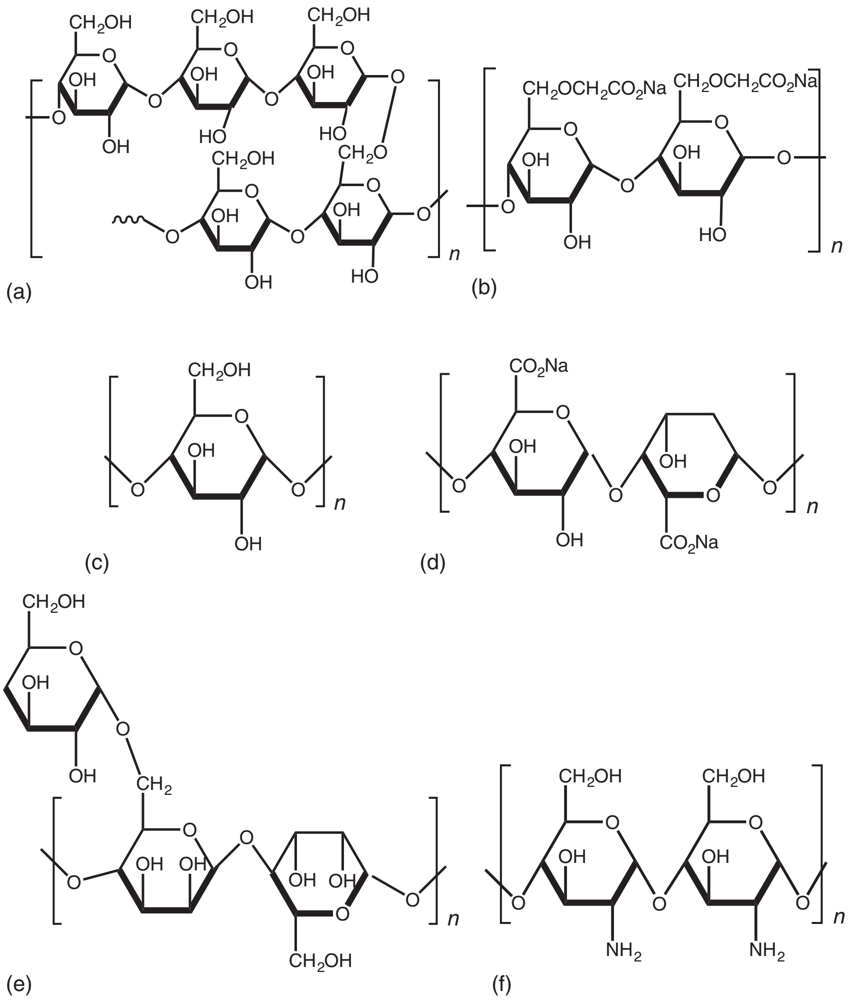

**Figure 11.3** The chemical structure of some selected CHO corrosion inhibitors in acidic media (a) starch, (b) sodium carboxymethylcellulose (Na-CMC), (c) dextrin, (d) alginate, (e) guar gum (GG), and (f) chitosan.

grain by the physical method was evaluated as a corrosion inhibitor of MS in 0.5 M $H_2SO_4$. It was found that the pure millet starch attained a corrosion inhibition of 87.14% in the absence of KI. In the presence of KI, the IE increases to 94.03% indicating a synergistic effect of iodide ion on the corrosion inhibition efficacy of millet starch on MS in 0.5 M $H_2SO_4$ solution [55].

### 11.6.2 Cellulose

Cellulose is an abundant water-insoluble polysaccharide constituted by a glucose repeating unit linked by a glycosidic bond. It is available with a reactive carboxymethyl group attached to its hydroxyl group of the glucopyranosyl cellulosic

**Table 11.1** The performance of CHOs as polymeric corrosion inhibitors in acid media.

| CHOs | Inhibitor source/composition | Performance indicator by $IE_{max}$ | References |
|---|---|---|---|
| Starch | • Sweet potato starch on galvanized steel in 1 M HCl | 64.3% | [52] |
| | • Starch modified with CTAB and SDS on MS in 0.1 M $H_2SO_4$ | 66.2% | [53] |
| | • Maize starch-modified glycerin C-Mn steel in 0.5 M $H_2SO_4$ | 94.0% | [54] |
| | • Millet grain starch with KI on MS in 0.5 M $H_2SO_4$ | 94.0% | [55] |
| Sodium carboxymethyl-cellulose (Na-CMC) | • Na-CMC as corrosion inhibitor on MS in 1 M HCl, Al in 0.5 M $H_2SO_4$, and MS in 2 M $H_2SO_4$ | 78.0%, 86.0%, and 65.0%, respectively | [56–58] |
| | • Gemini surfactant (diester) –Na-CMC composite on MS in 1 M HCl | 57.3% enhanced to 90.1% | [59] |
| | • AgNps-Na-CMC composite on ST37 steel in 15% $H_2SO_4$ | 93.4% | [60] |
| | • CMC with KI on Al in 2 M $H_2SO_4$ | 65.2% enhanced to 80.4% | [61] |
| Pectin | • Pectin from citrus peel on Al in 2 M $H_2SO_4$ | 91.0% | [62] |
| | • Commercial pectin on Al alloy in 0.025 M HCl | 95.0% | [63] |
| | • Pectin from sugar beet pulp, sunflower head, and Opuntia cladode on MS in 1 M HCl | 91.6%, 92.0%, and 95.0%, respectively | [64–66] |
| | • Pectin from apple fruit on X-60 MC in 0.5 M HCl | 96.0% | [67] |
| Exudates fluids | • Commercial guar gum on CS in 2 M $H_3PO_4$, 1 M $H_2SO_4$, and 15% HCl | 95.8%, 93.9%, and 94.9%, respectively | [68–70] |
| | • Gum arabic on MS in 1 M $H_2SO_4$ and Al in 1 M $H_2SO_4$ | 37.9% and 79.7%, respectively | [71] |
| | • Xanthan gum-SDS, CDC, and Triton X-100 composites on MS in 1 M HCl | 74.2% enhanced to 83.2%, 75.9%, and 82.3%, respectively | [72] |
| | • Xanthan gum grated co-polyacrylamide on MS in 15% HCl | 90.8% enhanced to 93.2% | [73] |
| Carrageenan | • Iota, lambda, and kappa carrageenan on Fe in 1 M HCl | 76.1%, 80.4%, and 72.0% respectively | [74] |
| | • Iota carrageenan on MS in 0.5 M $H_2SO_4$ | 86.8% | [75] |
| | • Iota carrageenan/pefloxacin mesylate composite on Al in 2 M HCl | 66.7% enhanced to 91.8% | [76] |

*(Continued)*

**Table 11.1** (Continued)

| CHOs | Inhibitor source/composition | Performance indicator by IE$_{max}$ | References |
|---|---|---|---|
| Dextrin | • Acrylonitrile-modified β-cyclodextrin on X70 MS in 0.5 M $H_2SO_4$ | 85.0% | [77] |
| | • Dextrin grafted with PVAc on MS in 15% HCl | 84.6% enhanced to 98.4% | [78] |
| | • Floxacin-mediated dextrin on MS in 0.5 M $H_2SO_4$ | 70.4% enhanced to ~90.0% by each of the floxacins | [79] |
| Alginate | • Sodium alginate on Cu in 1 M HCl | 78.2% | [80] |
| | • Sargassum muticum alginate extract on CS in 1 M HCl | 97.0% | [81] |
| | • Hydrquinoline-grated alginate (HQ-g-Alg) on MS in 1 M HCl | 92.6% | [82] |
| | • Alginate-cationic surfactant CS in 1 M HCl | 96.2% | [83] |
| Chitosan | • Chitosan on Cu in 0.5 M and 1 M HCl | 94% and 87% | [84, 85] |
| | • Chitosan on MS in 1 M HCl | 96.0% | [86] |
| | • Chitosan-cinnamaldehyde composite on Cu on 1 M HCl | 89.0% | [87] |
| | • PEG cross-linked chitosan (PEG-chi) on MS in 1 M $H_2NSO_3H$ | 93.0% | [88] |
| | • PANI-chitosan on MS in 0.5 M HCl | 79.8% | [89] |
| | • Oligosaccharide chitosan-grated glucose (COS-g-Glu) on MS in 1 M HCl | 97% | [90] |
| | • Chitosan enhance KI on MS in 1M $H_2NSO_3H$ | 73.8% enhanced to 90% | [91] |

component and thereby referred to as carboxymethylcellulose (CMC) or simply cellulose gum (CG). CG can be easily synthesized by the reaction of cellulose and chloroacetic acid in an alkali medium. In an acidic environment, the protonation of the carbonyl group of the CMC will form polycation centers, which can be weakly attracted by the negative charge of MS, resulting in a physisorption reaction between CMC and MS in the corrosive acidic media [93]. This assumption is expected to be a promising corrosion inhibitor of the metal substrate in acidic media. The assessment of sodium carboxymethylcellulose (Na-CMC) as an effective polymeric inhibitor in 0.5 M and 1 M HCl on Al sheet, respectively, and MS have been reported and revealed that Na-CMC (Figure 11.3b) is a concentration-dependent inhibitor with diminished IE at elevated temperature owing to its physical adsorption on the metal surface [59, 60]. A similar report of the physisorption adsorption behavior of CMC on MS in 2 M $H_2SO_4$ has been reported with an increase in IE as the concentration of CMC increases and inability to retain the efficiency at elevated temperature [58]. The evaluation of biodegradable cationic diester gemini surfactant has proven to improve the IE of Na-CMC from 57.3% to 90.1% in the presence of the gemini surfactant [59]. The use of silver nanoparticles (AgNps) obtained by reducing $AgNO_3$ with natural honey to modify CMC as an effective corrosion inhibitor composite has been successfully synthesized, characterized, and evaluated on ST37 steel in 15% $H_2SO_4$. Despite the aggressive corrosive environment (15% $H_2SO_4$), $1\,g\,l^{-1}$ AgNp/CMC composite inhibitor could achieve 93.4% IE at 60 °C by weight-loss technique [60]. The synergistic effect of 5 mM KI on the IE of CMC on Al in 2 M $H_2SO_4$ has been reported to be impressive to validate CMC as a potential active ingredient for the development of effective corrosion inhibitor [61].

### 11.6.3 Pectin

Pectin is a class of heteropolysaccharides consisting of galacturonic acid and its corresponding methyl ester with natural abundance in the nonwoody terrestrial plant's cell wall. The representative molecular structure of pectin is shown in Figure 11.4b. Its component predominantly consists of partially methyl ester of polygalacturonic acid and pectic acid (Figure 11.4a) in nonspecific varying proportion and neutral sugar side chain. Pectic acid is a transparent water-soluble gelatinous acid consisting of the galacturonic acid repeating unit (polygalacturonic acid). Pectin is a natural CHO whose composition and structure depend on the plant species, plant parts, and the plant's growth stage [94]. The presence of the carboxylic acid group (–COOH) and its corresponding esters (–$COOCH_3$) groups in the backbone structure of pectin makes it a promising molecule that reduces the corrosion rate of metal in corrosive media. The pectin extracted from citrus peel was evaluated for the corrosion protection of Al sheet in 2 M HCl solution and was found to be effective at a relatively lower temperature. The results show that the IE of 91% was achieved at 10 °C and reduced to 31% at 40 °C [62]. The use of commercial pectin on Al alloy sheet as a corrosion inhibitor in HCl solution was reported to be concentration-dependent and achieved IE of 95% at $2\,g\,l^{-1}$ concentration [63]. The effect of acids and enzymes hydrolysis extraction methods for pectin from sugar beet pulp was investigated for their anticorrosive property of MS in 1 M HCl solution. The pectin extracted by enzyme hydrolysis possessed superior anticorrosive properties than the pectin extracted by acid hydrolysis [64]. Three different molecular weights of sunflower head pectin (SFHP), 4.50,

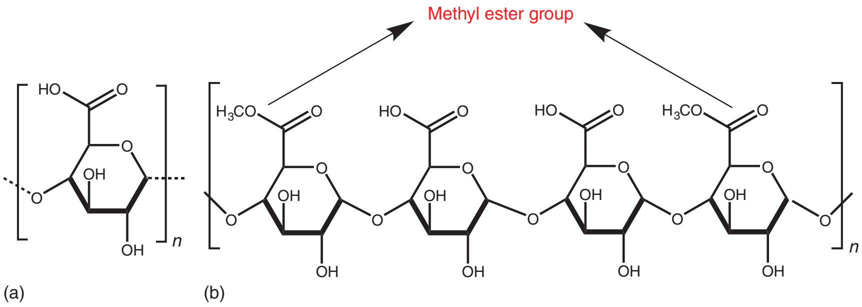

Figure 11.4 The representative chemical structure of (a) pectic acid and (b) pectin.

97.23, and 254.64 kDa, were evaluated for corrosion inhibition of MS in 1 M HCl solution. The lowest molecular weight (4.50 kDa) of SFHP was the most promising inhibitor with a superior efficiency of 92%, and the medium SFHP achieved a slightly lower efficiency of about 90% [65]. The performance of pectin from apple and Opuntia cladodes on MS and X-60 steel were evaluated in HCl solution with impressive corrosion IE 96% and 95%, respectively [66, 67].

### 11.6.4 Exudates' fluids

Generally, exudates' fluids are referred to as gum owing to their characteristics sticky and/or moist properties in liquid form (wet) and harden when dried. Usually, they are water-soluble polysaccharide secretion of varying composition and viscosity depending on the source of the viscous tree. Guar gum (GG) extracted from the seed of guar beans (Figure 11.3e) has been evaluated to be a promising anticorrosive fluid for the protection of CS in phosphoric acid, $H_2SO_4$, and 15% HCl solutions [68–70]. Another significant class of exudate fluid from the sap material of *Leguminosae* (acacia tree) is gum arabic (GA). GA consists of a mixture of some CHO (disaccharide, polysaccharide, and oligosaccharides), proteins backbone with numerous amino acids that can be construed to make GA potential protection of metal in the corrosive environment [95]. The evaluation of GA as a corrosion inhibitor of MS and Al in 1 M $H_2SO_4$ solutions shows that GA is more effective for the protection of Al than MS in the testing solution [71]. The analysis of the surface of MS by gas chromatography–mass spectroscopy (GCMS) and Fourier-transform infrared spectroscopy (FTIR) after evaluating the potency of exudates gum extracted from *Daniella Ollivierre* (DO) as corrosion inhibition of MS in 0.1 M HCl solution has revealed the adsorption of some nitrophenol, sucrose, phthalate, and stearic acids. Some carboxylic compounds function as active corrosion inhibition agents [96]. The lists of gums that can serve as corrosion inhibitors of metal in acidic media are inexhaustible. Besides, Xanthan gum needs to be mentioned owing to its effectiveness as a corrosion inhibitor of MS in 1 M HCl and a very aggressive 15% HCl acidic environment [78, 79].

### 11.6.5 Carrageenan

Carrageenan is a gel-like polysaccharide primarily found in the Rhodophydeae seaweed family. It consists of both sulfated α- and substituted 3,6 anhydro β-D-galactose backbone. They are mainly linear polysaccharides classified as iota, lambda, and kappa derivatives of carrageenan, as shown in Figure 11.5, according to the degree of substituted hydroxyl group and the degree of linear chain sulfation. This characteristic makes carrageenan possess a flexible molecular symmetry with unstable helical conformation that makes it exist as a gel at ambient temperature [93]. The presence of free hydroxyl and sulphonic acid groups endowed carrageenan with the ability to donate an electron to the empty d-orbital of iron (Fe) from metal, thereby functioning as an effective corrosion inhibitor by complexation of metal ions on the substrate surface in a corrosive environment. The effectiveness of some

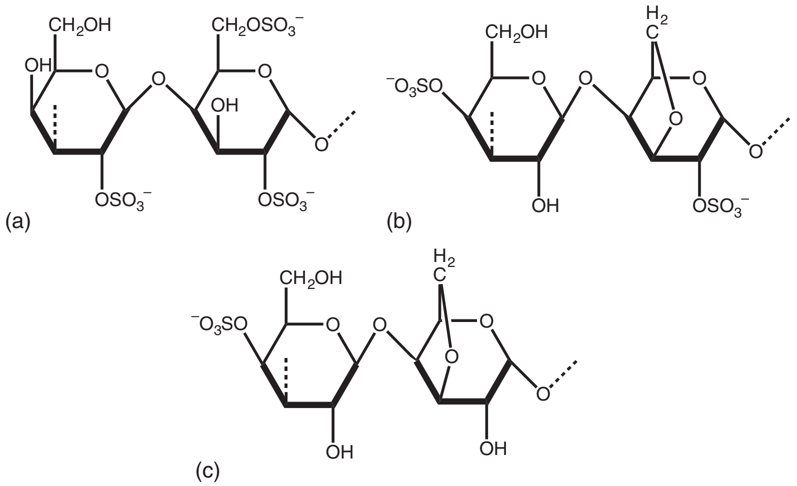

**Figure 11.5** The representative chemical structure of (a) lambda-carrageenan, (b) iota-carrageenan, and (c) kappa-carrageenan.

carrageenan compounds (iota, kappa, and lambda) as corrosion inhibitors of Fe in 1 M HCl solution was found to increase with an increase in inhibitor concentration and a decrease in efficiency with increasing temperature [74]. The corrosion IE of iota-carrageenan on Al sheet in 1–2 M HCl solution in the presence of zwitterions mediator has been evaluated and reported to improve from 67% to 92% due to mediator/carrageenan synergic effect [76]. The inulin and iota-carrageenan copolymer as a potential inhibitor of MS in $H_2SO_4$ solution have been successfully evaluated to possess a strong adsorption characteristic [75] on MS in the corrosive environment. The kinetic and thermodynamic investigations on the roles of five different amino acids (alanine, glycine, serine, cysteine, and isoleucine) on the improved adhesion property of iota-carrageenan on Al surface in 2 M HCl solution were established to improve in the presence of amino acids [97].

### 11.6.6 Dextrin

Dextrin is an inclusive term for various products obtained by controlled heating of any form of starch (de-polymerization by heating) in the presence of acid and moisture [98]. It can occur naturally by starch hydrolysis catalyzed by amylase in the human digestive system. The representative structure of dextrin is shown in Figure 11.3c. They are CHO polymers with low-molecular weight characterized by D-glucose monomer links by either α-1,4 or α-1,6 glycosidic bonds. Dextrin exists in different forms, such as cyclic dextrin, amylodextrin, maltodextrin, and α,β-dextrin. The corrosion inhibition potency of isolated dextrin is less effective in acidic media but can be at optimum performance in the presence of mediators or modifiers. The isolated β-cyclodextrin and modified β-cyclodextrin with acrylamide (ACM) polymer was evaluated as an inhibitor for the dissolution of X70 MS in 0.5 M $H_2SO_4$ solution. The modified β-cyclodextrin was found to offer better protection (up to

85% efficiency) than the isolated β-cyclodextrin [77]. A grafted copolymer consisting of polyvinyl acetate (PVAc) and dextrin has been reported as an efficient corrosion inhibitor of MS in HCl solution [78]. The use of different floxacin, such as levoflocaxin, ciprofloxacin, and norfloxacin, as a mediator for enhanced performance of dextrin in 0.5 M $H_2SO_4$ solution as corrosion protection of MS revealed the tremendous reduced dissolution of MS in the presence of floxacin than pure dextrin in the absences of floxacin [79].

### 11.6.7 Alginates

Alginate is an anionic polysaccharide colloidal gum that binds with molecular water in the cell wall of algae. Alginates consist of covalently bonded C-5 epimer of α-L-guluronate and D-monnurolate homopolymeric bond. This sugar group is called alginic acid due to the carboxylic acid (–COOH) functional group in its backbone structure, as shown in Figure 11.3d. Owing to the anionic state of alginate, it is often available as sodium alginate (Na Alginate) salt form. The alginate extracted from *Sargassum muticum* (Japanese wireweed algae) by the methanolic crude method was evaluated as a corrosion inhibitor of CS in 1 M HCl. The result revealed that the extracted alginate undergoes a chemisorption adsorption process on the substrate in the corrosive environment, with 1 $g\,l^{-1}$ achieving 97% IE [81]. An alginate bioactive inhibitor grafted with 5-methyl-8-hydroxyquinoline by green condensation reaction in water between alginate and 5-chloromethyl-8-hydroxyquinoline was successfully synthesized and confirmed structurally with FTIR, $^{1}H$, and $^{13}C$ NMR. The modified alginate (HQ-g-Alg) possessed a superior IE than the unmodified alginate [82]. Sodium alginate has been evaluated for the protection of Cu substrate in 1 M HCl solution. The result reveals that Na alginate is a concentration-dependent inhibitor that undergoes physisorption adsorption process on Cu substrate due to the reduction in the efficiency as the temperature increases [80]. The synthesis of a cationic surfactant; (*N*-(2-hydroxyethyl)-*N*,*N*-dimethyldodecan-1-aminium bromide from Na alginate was reported and evaluated for the anticorrosive property on CS in 1 M HCl. The result obtained shows that the IE of Na alginate cationic surfactant increases with an increase in concentration of 0.005 M achieving 96.2% IE and exhibiting a positive trend at elevated temperature [83].

### 11.6.8 Chitosan

Chitosan is a polysaccharide consisting of glucosamine (Figure 11.3f), a compound with a substituted amine (–$NH_2$) group in the glucose-repeating unit of its backbone structure. It is a naturally occurring polymer extracted from the chitin of fungal cell walls and arthropods (crabs, shrimps, crustaceans, insects, and lobsters). It is mainly used for skin infection treatment and advanced therapeutic procedures due to its antifungal and antibacterial activities [99]. However, the anticorrosion activities of chitosan can be derived from the electron-rich amine and hydroxyl functional groups that can serve as adsorption centers for metal. The potency of chitosan as an effective corrosion inhibitor of different metal substrates, such as Cu, MS, and some other CS substrates, in the acidic medium, has been evaluated. The IE of chitosan on Cu substrate in 0.5 M HCl solution was revealed to increase as the concentration of chitosan increased in the corrosive medium to a maximum of 94% [84], while in 1 M HCl solution, similar behavior was observed with optimum efficiency of 87% [85] at relatively lower concentration of chitosan. The chitosan modified with cinnamaldehyde by microwave synthesis was reported to be very effective for Cu with efficiency greater than 89% IE at a dose of $1\,\mathrm{g\,l^{-1}}$. The computational studies evaluation further indicates the superior adsorption property of chitosan modified with cinnamaldehyde than the isolated cinnamaldehyde molecule and the parent chitosan [87]. The performance of chitosan as corrosion inhibitor of MS is not so impressive in acidic media unless it is chemically modified at a very low concentration of 0.1 M HCl solution, where 96% IE is achieved at 60 °C and later reduced to 93% efficiency at 70 °C [86]. The anticorrosion performance of polyethylene glycol (PEG) cross-linked chitosan on MS in 1 M sulfamic acid ($H_2NSO_3H$) for sugar industry application reveals the PEG-modified chitosan inhibitor is concentration-dependent and that $0.2\,\mathrm{g\,l^{-1}}$ could achieve 93.9% efficiency on MS in 1 M $H_2NSO_3H$ [88]. A polyaniline (PANI) chitosan composite prepared in the presence of acetic and sulfamic acid was reported to achieve 79.87% IE for MS in 0.5 M HCl solution [89]. The evaluation of oligosaccharide glucose moiety grafted on chitosan (COS-g-Glu) on MS in 1 M HCl solution revealed the concentration-dependence of COS-g-Glu, and as low as 0.001 M of COS-g-Glu could achieve 97% efficiency [90]. The effect of KI on the performance of chitosan was found to be synergistic with MS in $H_2NSO_3H$ solution. It was reported that $0.2\,\mathrm{g\,l^{-1}}$ chitosan could only possess 73.8% IE, but in the presence of $0.005\,\mathrm{g\,l^{-1}}$ KI, the IE was found to increase to 90% owing to the synergistic effect of KI [91]. The modification of chitosan with triazole, thiosemicarbazide, and thiocarbohydrazide has been revealed to be effective for improving corrosion inhibition of chitosan of CS in 1 M HCl solution with impressive corrosion inhibition efficiencies of 95%, 92.5%, and 93.2%, respectively [100, 101]. The evaluation of thiocarbohydrazide-modified chitosan using formaldehyde linkage has also been reported on 304 steel in 2% acetic acid with $0.06\,\mathrm{g\,l^{-1}}$ of the thiocarbohydrazide-modified chitosan achieving 92% IE [101].

## 11.7 Natural Proteins

Natural proteins are polymeric compounds of amino acids and imino acids. Amino acids constitute 20 natural proteins; one of them is an imino acid (nitrogen atom forms a double bond with another molecule or two single bonds with alkyl groups), while 19 others are α-amino acids [102]. Mainly, they produce from animal products, such as milk, meat, dairy products, eggs, poultry products, fish, and other natural sources, including plants (almond, chickpeas, and peanuts), products consisting of an appreciable repeating unit of peptide bonds from amino acids. An amino acid is an organic compound composed of carboxylic; –COOH and amine; $-NH_2$ functional group in a single unit that forms a peptide bond (–CONH–) through a

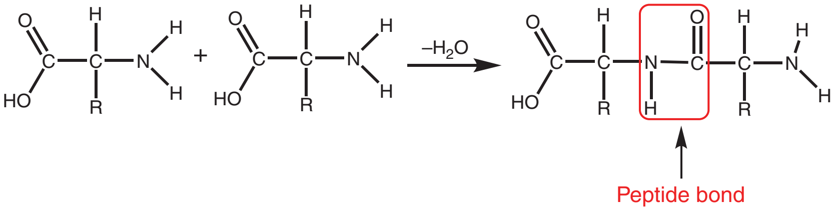

**Scheme 11.2** The condensation reaction between two amino acids shows the formation of a peptide bond.

condensation reaction between –COOH and $–NH_2$ functional groups, as shown in Scheme 11.2. A repeated polypeptide unit of different amino acid sequences characterizes the structure of a protein. The polyamides, amino acids, polypeptides, and polynucleotides (DNA and RNA) are all related to the functionalities of protein structure [103].

### 11.7.1 Soy Polymer

Soy polymer (SP) is a natural protein from soybean, an edible seed from the pea family called Fabaceae. The presence of peptide bonds in the backbone structure of the protein will make it a suitable candidate for corrosion inhibition of metal in an acidic medium. SP has been evaluated as a corrosion inhibitor of CS in 1 M $H_2SO_4$ solution in different temperatures from 30 to 60 °C [104]. The IE of SP increases with increased concentration in all temperatures; however, the maximum IE obtainable is 89.51% at 30 °C with $5\,g\,l^{-1}$ concentration. Different extracts of SP (glycine maximum meal) from a Brazilian soybean meal were evaluated as corrosion inhibitors of MS in 0.5 M $H_2SO_4$ solution. The aqueous extract (AE), high-molecular-weight fraction (HMWF), and the commercially isolated soy polymer (CIP) were all revealed to be concentrated-dependent corrosion inhibitors [105]. The IE of AE, HMWF, and CIP at $0.8\,g\,l^{-1}$ concentration extracts were 85.2%, 88.7%, and 94.8%, respectively. The evaluation of SP and polyvinyl pyrrolidone (PVP) composite has demonstrated a better corrosion inhibitor than the individual compounds on CS in 1 M $H_2SO_4$ solution. The optimal IE of 84% was obtainable for SP, while SP-PVP composite achieved 96%IE [104].

### 11.7.2 Casein

Casein is a phosphoprotein (αS1. αS2, β, and k) related to natural protein abundant in mammalian milk. It constitutes between 20% and 60% of the protein in human milk and 80% of the proteins in cow's milk [106]. The casein content is higher in sheep and buffalo milk than in human and other mammalian's milk [107]. The characteristic of many food products, such as texture, nutrition, water binding, fat stabilization, and taste, is determined by their caseinates percentages during food formulation [108]. The electrodeposition of casein layer on zinc substrate to improve the corrosion resistance of the Zn alloy [109] and its function in the synthesis of self-healing corrosion protective coating [110] can be attributed to the existence of polypeptide bond in protein, owing to the availability of –$NH_2$ and –COOH functional group in their backbone structure allows casein to function as a corrosion inhibitor. The effect of casein as a corrosion inhibitor of MS in 0.1 M HCl solution has been evaluated to reduce the corrosion rate of MS in the acidic medium. Casein achieved 65.03% corrosion inhibition at $50\,\mathrm{mg\,l^{-1}}$ concentration and 96.02% corrosion efficiency at $400\,\mathrm{mg\,l^{-1}}$ concentrations.

### 11.7.3 Zein

Zein is an abundant natural protein present in the corn tissue. It is a natural polymeric material that constitutes 80% of the whole proteins in the endosperm tissue of corn [111]. The presence of hydrophobic and hydrophilic groups in the zein backbone has been attributed to the possibility of obtaining materials with varying properties for pharmaceutical, biomedical, and food packing applications by mixing zein with a polymeric and nonpolymeric material [112]. However, zein is a water-insoluble material and thereby makes its application as corrosion inhibition challenging. Besides, SDS surfactant has been reported to aid its application as corrosion inhibition in acidic medium. The evaluation of corrosion inhibition of MS in 0.5 M $H_2SO_4$ by zein–SDS aggregate has been revealed to be dependent on the SDS–zein ratio in the zein–SDS complex formation. The presence of zein–SDS aggregate formed with 4 μM SDS and $500\,\mathrm{mg\,l^{-1}}$ zein achieved 90% IE protection for MS in 0.5 M $H_2SO_4$ [113].

### 11.7.4 Hydrolysate from Shrimp By-products

The process of obtaining di- and tri-polypeptides from whole protein, leaving the protein intact and making available some free amino acid, is termed protein hydrolysate [114] in contrast to protein hydrolysis, where protein-digesting enzymes are used to break down proteins [115]. Hydrolysate remains the available free amino source for protein biosynthesis since hydrolysis decreases the peptide bond of the protein molecule. The edible part of shrimps is just 65%, and the remaining components, exoskeleton, and cephalothorax are discarded as a waste product and consist of protein tissue [116]. The use of exoskeleton and cephalothorax by-products of shrimps have been established to be a significant constituent for the preparation of liquid protein-rich hydrolysates by lactic acid fermentation and was successfully converted to a human and animal diet rich in amino acid [117]. The extraction of protein hydrolysate containing amino acids was successfully carried out on recovered shrimps waste products (RSWP) and evaluated for corrosion inhibition of CS in 1 M HCl solution [118]. The evaluation outcome reveals that the IE of RSWP increases with an increase in the concentration of RSWP in the corrosive medium and achieves 95.01% efficiency at $5\times10^{-3}$ M concentration. The presence of free amino acid on the RSWP hydrolysate can be attributed to the chemisorption adsorption energy level estimated for the RSWP on CS in 1 M HCl solution.

## 11.8 Synthetic Polymeric Materials

The choice of determining a desired functional group for the selective and specific chemical reaction from naturally occurring polymers is a challenge due to their heterogeneous nature. Synthetic polymers are materials designed with specific functionalities for desired applications by chemical reactions terms polymerization reactions. A polymer can be engineered to contain a repetitive bonding of some molecules called monomers and can also be designed to consist of two or more monomers in the polymer's backbone by the process called copolymerization. Synthetic polymers made of different monomers containing functional groups, such as amine, amide, aniline, carboxylic, and many more have been considered corrosion inhibitors of metals in the corrosive medium.

### 11.8.1 Polyglycols

Polyglycols, polyols, or polyether glycols are polymers with two hydroxyl groups attached to different carbon atoms. Besides, polyacetal (polyoxymethylene), a highly crystalline polymer, is insoluble in water [119]; polyglycols can either be waxy solid or viscous liquid depending on their molecular weight. They are part of many functional fluids (hydraulic fluids, transmission fluids, and process oils) owing to their impressive lubricity. The three most important polyglycols are PEG, polypropylene glycol (PPG), and polytetrahydrofuran (PTHF). Out of the three polyglycols, PEG (Figure 11.6a) and PPG (Figure 11.6b) are very important polymeric materials for corrosion inhibitors of metal in acidic medium.

PEG is polymers with a molecular weight greater than 20 000 Da and can also be referred to as polyethylene oxide (PEO) when the molecular weight is less than 20 000 Da. PEG is soluble in water and many organic solvents (ethanol, benzene, acetonitrile, and dichloromethane). They are available in different structural forms (linear and branched) [120]. The use of PEG as a corrosion inhibitor of α-brass alloy in 1 M $HNO_3$ solution has been reported by Fouda et al. [121] to be concentration-dependent and achieved a corrosion IE of 80.0%. The effects of different molecular weights of PEG on the corrosion inhibition of different metal substrates in an acidic medium have been demonstrated. Three PEG compounds of 600, 2000, and 6000 Da molecular weight (Mwt) were evaluated as corrosion inhibitors of Al in 0.5 M HCl solution. The result of the investigation revealed that the efficacy of PEG as a corrosion inhibitor increases with increasing the concentration of PEG in the corrosive medium. Higher the Mwt of the PEG, the better the corrosion IE as revealed in this order; 6000 Da > 2000 Da > 600 Da [122]. The outcome of similar studies with eight PEG compounds of Mwt between 200 and

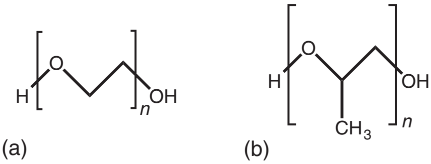

**Figure 11.6** The chemical structure of (a) polyethylene glycol (PEG) and (b) polypropylene glycol (PPG).

10 000 Da CS in 1.5 M $H_2SO_4$ solution revealed the same trend of the efficacy of PEG depending on the molecular weight. However, it was established that the low concentration of high Mwt PEG exhibited approximately the same corrosion efficiency of 90% as the high concentration of low Mwt PEG [123]. The influence of flow rates between 250 and 500 rpm on the performance of PEG (6000 Da) as corrosion inhibitor on rotating disk steel (RDS) in 0.5 M $H_2SO_4$ solution has been evaluated. The study revealed that PEG exhibited an impressive corrosion IE in the hydrostatic state. Still, efficiency cannot be retained in the hydrodynamic state owing to a drastic reduction in the corrosion inhibition efficiencies probably by the restriction of the formation of the protective film on the RDS by different flow rates [124]. Attempts to improve the effectiveness of PEG as a corrosion inhibitor in acidic solutions have been reported with further modifications. The polymer of PEG–anthranilic acid composite synthesized in oxalic acid medium with ammonium persulphate was found to be highly effective on MS in 1 M HCl with an achievement of 97% IE [125]. The synthesis of three gemini surfactants (PEG bromoester) based on PEG of different Mwt, namely, G600Br, G1000Br, and G1500Br, for PEG of 600, 1000, and 1500 Da, respectively, have been reported and evaluated as corrosion inhibition of MS in 1 M HCl solution. The best performance of the PEG bromoesters was exhibited by G1500Br with an IE of 94% [126]. The cross-linked of PEG (4000 Da) with chitosan (PEG-Chi) to improve the efficiency of PEG as corrosion inhibition of MS in 1 M $H_2NSO_3H$ was successful with an impressive outcome of 94% IE at 0.2 $g\,l^{-1}$ concentration [88]. The copolymerization of PEG with different triethanolamine prepared by the condition of triethanolamine in the presence of NaOH as a catalyst for different hours (3, 4, and 6) to produce polytriethanolamine of 8, 10, and 12 polymeric chains, namely, $P_8$, $P_{10}$, and $P_{12}$. The evaluation of PEG/polytriethanolamine ($P_8$, $P_{10}$, and $P_{12}$) reveals that the three compounds offer considerable promising protection for CS against 1 M $H_2SO_4$ solution with corrosion IE of 86.5%, 90.9%, and 94.7% for $P_8$, $P_{10}$, and $P_{12}$, respectively.

The comparative studies of PPG and polymethacrylic acid (PMAA) to evaluate their potency as corrosion inhibitors of MS in 0.5 M $H_2SO_4$ solution were explored [127]. PPG was found to be a better inhibitor than PMAA with a 1 $g\,l^{-1}$ concentration achieving 71.0% and 44.9% IE for PPG and PMAA, respectively. It was further revealed that corrosion inhibition of both polymers increases with an increase in concentration but could not be sustained as the temperature of the corrosive medium increases. The effect of KI on the adsorption property of PPG on Al sheet in 0.5 M $H_2SO_4$ solution was evaluated. The IE obtained for 1 $g\,l^{-1}$ concentration of PPG was estimated to be 50.3%. This efficiency was found to increase with an increase in the concentration of KI in the corrosive medium. The addition of 2 mM KI increases the IE to 54.1%, while 5 mM KI increases it to 75.6%, indicating a synergistic effect of 5 mM of KI with PPG on Al in 0.5 M $H_2SO_4$ solution [128]. The impressive performance of PPG as an effective corrosion inhibition of X-60 MS in15% HCl solution was reported by Umoren [129]. The result indicated the IE of PPG increased with an increase in concentration and attained 90% at 55 °C with 1 $g\,l^{-1}$ concentration.

## 11.8.2 Polyamines Derivatives

The presence of some electron-rich functional groups and amine (–$NH_2$) functionality in the backbone structures of polyaniline, polyimines, and polyamides make polyamines derivatives suitable candidates that can serve as polymeric inhibitors of the metal substrate in a corrosive environment. The ease of protonation of the nitrogen atom site (–N–) of the amines in an acidic medium makes polyamines derivatives favorable for the adsorption mechanism of inhibitors in an acidic medium.

### 11.8.2.1 Polyethyleneimine (PEI)

Imines are functional groups of amines compounds consisting of carbon–nitrogen double bond (C=N) in the backbone of their structure. However, polyethyleneimine (PEI) is of a different kind, the linear PEI consisting of a repeating unit of secondary amine (Figure 11.7a). At the same time, the branched macromolecules PEI is a kind of polyamine consisting of the primary, secondary, and tertiary amines in its backbone structure, as shown in Figure 11.7b, for the commercially available water-soluble branched macromolecules PEI. The branched macromolecules have been analyzed to consist of an approximately ratio 1 : 2 : 1 of the primary, secondary, and tertiary amine groups, respectively [130]. The potency of PEI as an effective corrosion inhibitor of CS in different concentrations of $H_3PO_4$ solution has been examined at 30 °C. It was found that IE of $5\times10^{-5}$ M PEI increased as $H_3PO_4$ increased. The IE of PEI was found to be 81% in 3 M $H_3PO_4$ solution, increased to 90% IE in 7 M $H_3PO_4$ solution, and remained 90% as the concentration increased to 9 M $H_3PO_4$ solution [131]. The quaternary polyethyleneimine (QPEI) prepared by tertiary amination reaction of the macromolecular PEI followed by quaternization reaction has been evaluated as an effective corrosion inhibitor of CS in 0.5 M $H_2SO_4$ solution. At 0.005 g $l^{-1}$ concentration, QPEI offered 92% IE for CS in $H_2SO_4$ solution [132]. The PEI was able to withstand a concentrated HCl solution when chemically modified with graphene oxide (GO) with enhanced performance in the presence of KI [133]. The presence of 0.05 g $l^{-1}$ polyethyleneimine-grafted graphene oxide (PEI-GO) in 15% HCl solution was found to be adsorbed effectively on CS at 65 °C with an estimated 89.75% IE. This IE was later enhanced owing to the synergistic effect of 0.005 M KI in the aggressive corrosive medium to 97.77% IE.

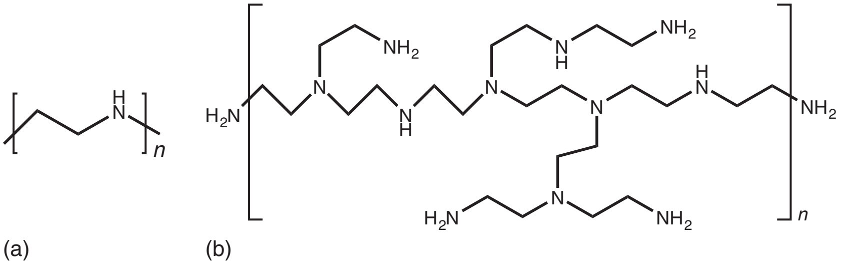

**Figure 11.7** The chemical structure of (a) linear polyethyleneimine (PEI) repeating unit and (b) branched PEI consists of primary, secondary, and tertiary amine groups, respectively.

#### 11.8.2.2 Polyaniline (PANI) and Polydiamines (PDAs)

The linear polydiamines (PDAs) are relatively water-soluble polyamines derivatives with two terminals $-NH_2$ functional groups in their backbone structures and can be represented as $[NH_2-(CH_2)_n-NH_2]$. Some linear PDAs have demonstrated effective corrosion inhibition properties in acidic media. The effect of polymethylene diamines for $n = 1-12$ was synthesized, but polymethylene diamines of $n = 1-8$ were evaluated as corrosion of Fe in 6 M HCl solution in deaerated condition at ambient temperature owing to the solubility challenges in the testing solution [134]. The result revealed that 1,3-propane diamine was a better corrosion inhibitor than ethylene diamine. This superior performance is attributed to the effect of chain length of the diamine compounds as evince by increase in IE from $n = 3$ to $n = 8$.

The influence of counterions on gemini surfactant with dimeric amines platform as corrosion inhibitor of American Iron and Steel Institute (AISI) stainless steel (SS) specimen in 3 M HCl solution was investigated, according to Pakiet et al. [135]. The effectiveness of dimeric amines surfactants as corrosion inhibitors was influenced by the nature of counterions in the surfactant-dimeric amines platform. The iodide counter ion was revealed to provide better performance than its corresponding bromide counterions as a corrosion inhibitor in 3 M HCl solution. Three polyamine derivatives, namely, $P_4$, $P_6$, and $P_8$, were obtained by the condensation polymerization of triethanolamine at 245 °C for 4, 6, and 8 h, respectively. The polyamines were ethoxylated and then esterified with oleic acid. The esterified products were evaluated for an anticorrosion property on CS in 1 M HCl solution [136]. The result revealed that the IE of the esterified polyamines increases with an increase in concentration, and $P_8$ could achieve 95% IE at $0.6\,g\,l^{-1}$ concentration.

PANI is another class of polyamines consisting of a repeating unit of a benzene ring and $-NH_2$. PANI is a water-soluble conducting polymer. The benzene ring and the $-NH_2$ can serve as the source of electrons for adsorption on a metal surface to form a protective barrier for diffusing corrosive ions in an acidic medium. The PANI synthesized by persulfate oxidation of aniline was evaluated for effective corrosion inhibition of pure Fe in 0.5 M $H_2SO_4$ solution. The effect of polymerization on the efficacy of PANI was demonstrated by comparing the effectiveness of the aniline (monomer) with the PANI as corrosion inhibitors in an acidic medium [137]. It was revealed that aniline was, in contrast, accelerating the corrosion of pure Fe in 0.5 M $H_2SO_4$ solution, whereas $0.1\,g\,l^{-1}$ concentration of PANI was estimated to achieve 84% IE of Fe in the corrosive medium. To improve the IE of PANI in the acidic medium, attempts at doping, blending, and compositing PANI with other materials have been explored. The effects of cerium ion on the performance of PANI as corrosion inhibitor of Fe in 0.5 M $H_2SO_4$ solution have been investigated [138]. The IE of 53% of $0.01\,g\,l^{-1}$ concentration of PANI was found to increase to 88% IE in the presence of $1 \times 10^{-3}$ M cerium ion concentration. In the presence of the same concentration of cerium ion, the IE of 71% for $0.05\,g\,l^{-1}$ concentration of PANI has enhanced to 90% IE. The composite consisting of nanodiamonds (NDs) and PANI synthesized using ammonium peroxydisulfate under a controlled oxidative polymerization condition was successfully reported to exhibit an excellent corrosion inhibition of steel and Al due to their electronics and chain conformation properties [139]. The copolymerization of aniline and anthranilic acid to form poly-(aniline-*co*-anthranilic acid) solution as an effective corrosion inhibitor of CS in 1 M HCl has been evaluated [140]. The PANI-anthranilic acid copolymer IE was found to increase with an increase in the inhibitor concentration until a maximum of 90.54% IE was achieved with 0.02 $\text{g l}^{-1}$ concentration of poly-(aniline-*co*-anthranilic acid). The performance of copolymerized *o*-toluidine and aniline compounds doped with *p*-toluene sulfonic acid (PSA) as an effective corrosion inhibition of MS in 0.5 M $H_2SO_4$ solution. The resulting poly (aniline-*co*-*o*-toluidine)-doped *p*-toluene sulfonic acid (PAT-PSA) was found to protect MS effectively at a very low concentration of 0.001 $\text{g l}^{-1}$ with IE of 78.9%. The IE was found to increase with an increase in PAT-PSA concentration to an optimum IE value of 95.3% at 0.02 $\text{g l}^{-1}$ concentration [141].

Some PANI derivatives, PDAs, are also reported to possess corrosion inhibition of metal in acidic media. The superior performances of polymeric material over its monomer counterpart have been demonstrated with *p*-phenylenediamine on MS in 1 M HCl solution. The evaluation of *p*-phenylenediamine and poly(*p*-phenylenediamine) was found to be concentration-dependent. However, 5 $\text{g l}^{-1}$ concentration of *p*-phenylenediamine monomer was found to achieve 73.0% IE while about 100-fold lesser concentration (0.05 $\text{g l}^{-1}$) of chemically synthesized poly(*p*-phenylenediamine) acquired 85% IE [142]. The electrochemical polymerization of *ortho*-phenylene diamine (*o*-phenylene diamine) has been reported to function as an effective corrosion inhibitor of MS in 1 M HCl solution. The IE of poly(*o*-phenylenediamine) was found to increase with an increase in concentration until an optimum IE of 95% for 0.6 $\text{g l}^{-1}$ concentration of poly(*o*-phenylene diamine) in the acidic medium [143].

#### 11.8.2.3 Polydopamine (PDM)

The ease of oxidation of dopamine to form PDM (Scheme 11.3) that consist of dopamine in different oxidation states, indole, and relatively lesser unit of pyrrole is an intrinsic characteristic that makes PDM an excellent adsorbent on any surface owing to the existence of abundant catechol moieties (dihydroxy benzene) [144]. The uniform-sized spherically shaped PDM nanoparticles PDM-sph-nps) from dopamine in Tris–buffer solution was synthesized and used as corrosion inhibitor of MS in 1 M HCl solution with an IE of 86% at 40 M concentration [145]. The control synthesis of PDM corrosion inhibitors by three different methods to obtain PDM-1, PDM-2, and PDM-3 with different surface chemistry was explored and evaluated for corrosion inhibition of MS in 1 M HCl solution [146]. The IE of 93%, 99%, and 96% was achieved with 0.005 $\text{g l}^{-1}$ concentration PDM-1, PDM-2, and PDM-3. The superior performance of PDM-2 was attributed to its high hydrophilic property owing to the presence of large –COOH group moieties in its repeating unit structure.

### 11.8.3 Polyamides Derivatives

Amides are organic compounds characterized by a carbonyl functional group (O=C) attached to the nitrogen atom of an amine. The presence of both O=C and $-NH_2$

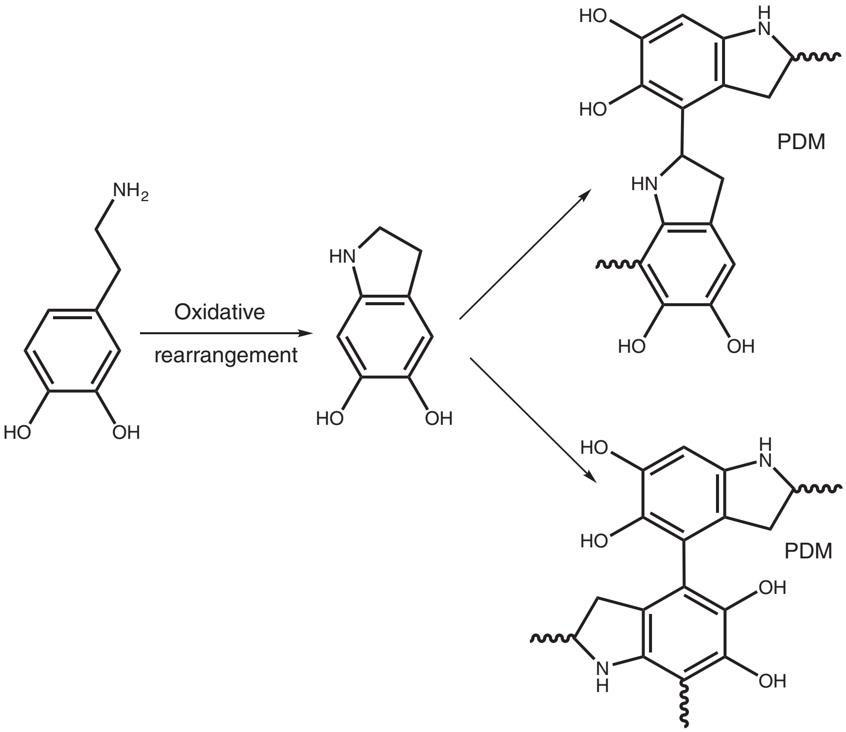

**Scheme 11.3** The representative polymerization reaction of dopamine to form PDM derivatives. Source: Liebscher [144]/John Wiley & Sons.

functional groups in the backbone structure of an amide makes all amino acids, urea, and other related compounds, such as glutamic acid, and is classified as amide derivatives.

Urea is an organic compound also known as carbamide with a chemical formula $CO(NH_2)_2$. The product form from the reaction between isocyanate and diamine is called polyurea owing to the presence of urea linkage in the product [147], as shown in Scheme 11.4. The corrosion inhibitor derived from urea and phosphate derivative guanidine copolymerization (PGUC) was synthesized and evaluated for its ability to

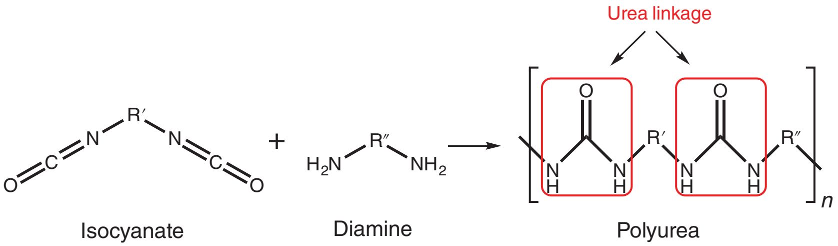

**Scheme 11.4** The representative reaction for the formation of polyurea. Source: Sánchez-Ferrer et al. [147]/John Wiley & Sons.

inhibit Armco Fe 1 M HCl solution from corrosion at 30 °C [148]. It was found that PGUC physically adsorbed on Armco Fe and that the IE of PGUC increases as its concentration increases in the acidic solution until it reaches 91% IE at a relatively high concentration (11.5 $g\,l^{-1}$) of PGUC. The use of polyurea derivatives synthesized with diaryl ether monomer by polycondensation reaction was very soluble in polar aprotic solvents and acted as cathodic type corrosion inhibitor of MS in 0.5 M $H_2SO_4$ at 40 °C [149]. The polyurea could not achieve more than 78.52% IE at 0.002 $g\,l^{-1}$ concentration. Any increase in the concentration of the inhibitor yielded lower IE. Attempt to improve the performance of polyurea as corrosion inhibitors led to the synthesis of polyurea derivatives based on diarylidenecyclopentanone. The effect of polymerization was demonstrated on CS in 0.5 M $H_2SO_4$ at 40 °C by comparing the IE of the monomer and the polyurea [150]. The monomer achieved 89.99% IE at 0.002 $g\,l^{-1}$ concentration, and the polyurea at lower concentration (0.05 $g\,l^{-1}$) attained 95.31% IE. The comparison of this impressive polyurea based on diarylidenecyclopentanone (Polyurea-Pent) with another derivative of polyurea based on diarylidenecyclohexanone (polyurea-Hex) as corrosion inhibitors of MS in 0.5 M $H_2SO_4$ at 40 °C was evaluated [151]. The performance monomer of polyurea-Pent (89.99% IE at 1 $g\,l^{-1}$ concentration) as corrosion inhibitor was far superior to the monomer of polyurea-Hex (34.51% IE at 1 $g\,l^{-1}$ concentration). Moreover, similar anticorrosive performance was exhibited by 0.03 $g\,l^{-1}$ polyurea-Pent and 0.05 $g\,l^{-1}$ polyurea-Hex with 88.26% and 39.26% IE, respectively.

Polyaspartic acid (PASP), as shown in Figure 11.8, is a representative of polyaminoacids. It has also been investigated for its anticorrosive property in acidic media. The PASP synthesized from L-aspartic acid by thermal condensation reaction was evaluated for the corrosion inhibition of CS in 0.5 M $H_2SO_4$ at different temperatures [152]. The IE of PASP increases with an increase in the concentration of PASP in the corrosive medium. However, 4 $g\,l^{-1}$ PASP was found to attain the optimal IE of 80.33% after 48 h of complete immersion in 0.5 M $H_2SO_4$ solution at 20 °C. Effort on improving IE of PASP in acidic medium was extended to exploring the synergistic interaction of PASP with iodide ion ($I^-$) from KI on MS in 0.5 M $H_2SO_4$ solution [153]. The investigation revealed that in the absence of KI, 2 $g\,l^{-1}$ PASP achieved 88.0% IE while the IE was found to increase to 98.8% in KI, indicating a synergistic interaction of KI with PASP. Two functional PASP eco-friendly inhibitors were successfully synthesized and evaluated for their corrosion inhibition of MS in 0.5 M $H_2SO_4$ solution. The PASP functionalized with *N*-(3-aminopropyl)imidazole and then copolymerized with n-dodecyl amine to form PASP/*N*-(3-aminopropyl)imidazole and

**Figure 11.8** The representative chemical structure of polyaspartic (PASP) repeating unit.

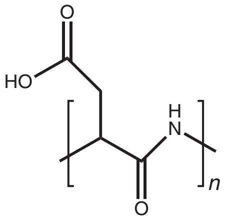

PASP/*N*-(3-aminopropyl)imidazole-*co*-*n*-dodecyl amine referred to as PD-1 and PD-2, respectively [154]. The performance of corrosion inhibition of MS 0.5 M $H_2SO_4$ solution of PD-2 was superior to PD-1. They are both concentration-dependent with IE of 89.4% and 94.0% at 0.1 $g\,l^{-1}$ concentration for PD-1 and PD-2, respectively at 20 °C. The use of dopamine as a mediator to improve the corrosion IE of PASP in 0.5 M $H_2SO_4$ solution has been demonstrated to be effective on MS with 0.1 $g\,l^{-1}$ PASP-dopamine achieving 90.9% IE [155].

### 11.8.4 Polyvinyl Derivatives

Polyvinyls are groups of polymers derived from a polyethylene backbone structure $CH_2$=CHR. The substituent R in the polyethylene background is the major factor that is used to classify polyvinyl compounds, as shown in the homologous polyvinyl structure in Figure 11.9a. The polyvinyl alcohol (PVOH) (Figure 11.9b), PVAc (Figure 11.9c), polyacrylonitrile (PACN) (Figure 11.9d), polyacrylic acid (PACA) (Figure 11.9e), and polyacrylamide (PACM) (Figure 11.9f) can be obtained from the homologous structure repeating unit when R is OH, $COOCH_3$, COOH, CN, and $CONH_2$, respectively.

PVOH, as shown in Figure 11.9b, is one of the most utilized polyvinyl polymers as corrosion inhibitors of the metal substrate in acidic media. The effect of different concentrations of PVOH and PEG as corrosion inhibitors on Al sheet in 0.1 M

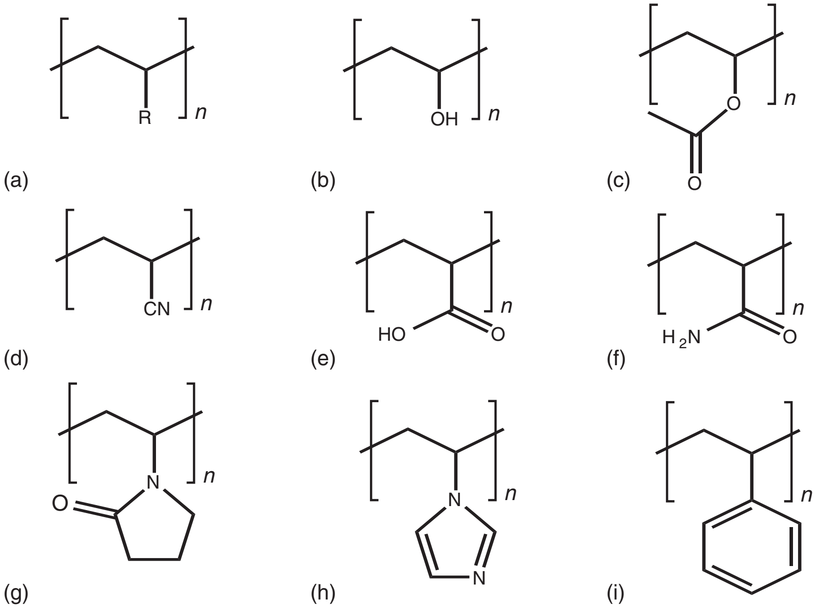

**Figure 11.9** The chemical structure of polyvinyl polymers corrosion inhibitors in acidic media (a) polyvinyl homologous, (b) polyvinyl alcohol (PVOH), (c) polyvinyl acetate (PVAc), (d) polyacrylonitrile (PACN), (e) polyacrylic acids(PACA), (f) polyacrylamide (PACM), (g) polyvinyl pyrrolidone, (h) polyvinyl imidazole (PVI), and (i) polystyrene repeating units.

$H_2SO_4$ solution was studied at different temperatures between 30 and 60 °C [156]. The effectiveness of both inhibitors was found to decrease as the temperature and concentration increased. The optimum performance for both inhibitors was observed at $1 \times 10^{-3}$ M concentration at 30 °C (PVOH; 43.52% and PEG; 50.93%). Investigating different Mwt of PVOH (14 000 g $mol^{-1}$; PVOH-I, 72 000 g $mol^{-1}$; PVOH-II, and 125 000 g $mol^{-1}$; PVOH-III) has been explored on MS in 0.5 M HCl solution [157]. The IE of 66.01%, 74.58%, and 79.87% were achieved at 0.1 g $l^{-1}$ concentration, indicating the increased influence the IE of PVOH in its Mwt. On the contrary, the influence of the degree of hydrolysis of PVOH was also investigated to gain insight into the adsorption property of PVOH on MS in 1 M HCl solution. The PVOH with a lower percentage of hydrolysis despite its lower Mwt (80%; 6000 g $mol^{-1}$) was found to achieve more IE (79.7%) than the PVOH with a higher percentage of hydrolysis and higher Mwt (99.7%; 78 000 g $mol^{-1}$) with an IE of 60.3% [158]. Owing to the observed low IE of PVOH in acidic medium, the effect of different halide ions ($Cl^-$, $Br^-$ and $I^-$) from their corresponding potassium salts (KCl, KBr, and KI) on the IE of PVOH on MS in 0.1 M $H_2SO_4$ solution was evaluated. The result revealed that KI improves the IE of PVOH better than KBr and KCl, probably due to the size of atomic radii and electronegativity of halides ions [159]. Several organic-based additives, such as surfactants (SDS and cetylpyridinium chloride, CPC) [160], sulfanilic acid [161], leucine [162], proline [163], aniline [164], *o*-methoxy aniline [165], and threonine [166], have been used to synthesize composites of PVOH, an enhanced and effective corrosion inhibitor of MS in acidic media. The performance of a grafted terpolymer synthesized with polyvinyl alcohol, acrylic acid, and vinyl sulfonic acid (PVOH-*p*-poly(AA-VSA)) has been explored on MS in 1 M HCl solution at 25 °C with an IE of 98.8% [167]. Besides, the effect of polymerization has been demonstrated with the comparison of the effectiveness of vinyl alcohol (VOH) monomer, and PVOH as corrosion inhibition of CS in 1 M HCl solution with E of 53.6% and 91.5% was obtained for the VOH and PVOH [168].

Short-time-interval techniques by differential pulse polarography (DPP) and differential pulse anodic stripping voltammetric (DPASV) to evaluate the potency of PVAc corrosion inhibitor as corrosion inhibitor of CS in 1 M $H_2SO_4$ solution have been explored [169]. The volumetric procedure revealed that the corrosion rate of CS in the presence of PVAc (Figure 11.9c) attained 91% IE after 24 hours of immersion. The evaluation of PVAc to prevent the corrosion rate of Al in 2 M $H_2SO_4$ and 0.5 M HCl solutions was investigated. It was found that the dissolution of Al is faster in HCl solution than in $H_2SO_{4,}$ which is responsible for the discrepancy in the concentration of acid used for the investigation [170]. The IE of PVAc increases with the increase in concentration but decreases with an increase in temperature. The optimum performance was achieved at 35 °C with IE of 90.3% and 78.4% IE for Al in 2 M $H_2SO_4$ and 0.5 M HCl solutions, respectively, in the presence of 2.5 g $l^{-1}$ concentration of PVAc. The sulfonated poly(acrylamide-vinyl acetate) copolymer consisting of vinyl acetate and ACM monomers was successfully synthesized and evaluated as an efficacy corrosion inhibitor of CS in 1 M HCl solution [171]. The copolymer was estimated to achieve 96.71% IE in the presence of 0.5 g $l^{-1}$ concentration of PVAc in the corrosive medium at 30 °C. The grated PVAc dextrin copolymer (Dxt-g-PVAc) was explored and found to be effective as a corrosion inhibitor of MS in a 15% HCl solution. The IE of isolated dextrin was found to be 84.56%; however, Dxt-g-PVAc could attain 98.39% IE at the same concentration of 0.15 $g\,l^{-1}$ [78].

PACA, as represented in Figure 11.9e, has been evaluated to exhibit poor anticorrosive properties on Al and Fe in 0.5 M $H_2SO_4$ solution with an IE of 79% and 53% at 30 °C, respectively [172, 173]. It was revealed from the investigation that KI improved IE of Al (79–87%) and Fe (53–95%) owing to the synergistic interaction of PACA and KI. The synergistic action of iodide ion on PACA as a corrosion inhibitor in $H_2SO_4$ solution was further elucidated on the Al sheet by the in situ atomic force microscopy (AFM) monitoring technique [173]. The microstructure of Al and Fe was identified to be a major factor responsible for their susceptibility to drastic dissolution in $H_2SO_4$ solution [174, 175]. However, PACA was evaluated to exhibit a considerable anticorrosion property in HCl solution. The water-soluble PACA and PANI composite corrosion inhibitor on 316 SS in 0.5 M HCl solution was estimated to achieve 91.68% IE at 0.5 $g\,l^{-1}$ concentration [175]. The PACA on MS in the same corrosive acidic medium was estimated to attain 96.8% IE at 0.1 $g\,l^{-1}$ concentration [176]. The comparison study of PACA and poly (sodium acrylate) (PACNa) revealed that both inhibitors are effective corrosion inhibitors of MS in HCl solution with IE above 90%, but PACA is slightly better than PANa [177].

The acid corrosion resistance of PACN, as shown in Figure 11.9d, has been demonstrated in the honeycomb Al alloy bipolar plate membrane for fuel cells that are highly susceptible to corrosion due to high proton exchange in the acidic medium. The PACN film prepared by infusion was smooth and dense with an enhanced mechanical engagement with the Al alloy to provide an improved corrosion resistance of the Al alloy in the corrosive medium [178].

The effect of KBr and KI on enhancing the anticorrosive property of PACM has been explored on Al in 2 M HCl solutions at different temperatures. The improvement in the IE of PACM (Figure 11.9f) by KI was found to exceed KBr; this can be attributed to differences in the atomic radii and electronegativity of the two halide ions [179]. The use of KI as a superior mediator for the enhancement of PACM IE in acidic medium (1 M $H_2SO_4$ solution) has been consolidated to improve IE of PACM of Fe [180] and in different Mwt of PACM mixed with poly 4-vinyl pyridine (P4VPyd) on MS in 1 M $H_2SO_4$ solution [181]. The presence of KI in 0.1 $g\,l^{-1}$ concentration of PACM was found to increase IE from 52.2% to 87%, while in PACM/P4VPyd mixture, the presence of KI in 0.1 $g\,l^{-1}$ concentration PACM increased IE from 63.12% to 94.5%, indicating the superior performance of PACN/P4VP mixture. The contribution of natural products, such as GG and fenugreek mucilage, to improving the anticorrosive property of PACM on MS in acidic medium has been explored. It was revealed that the 0.001 $g\,l^{-1}$ concentration of fenugreek–PACM achieves 78% IE and 0.1 $g\,l^{-1}$ concentration reaches 96% IE in 0.5 M $H_2SO_4$ solution [182] and GG grafting with GG with PACM also revealed more than 90% IE [183] in 1 M HCl solution. The synthesis of high Mwt of PACM (1 400 000 $g\,mol^{-1}$) by inverse emulsion polymerization was successfully reported and evaluated as corrosion inhibition of CS in 1 M HCl and 0.5 M $H_2SO_4$ solution [184, 185]. The result indicated that high Mwt PACM could achieve 85% IE at $4 \times 10^{-6}$ M concentration in $H_2SO_4$ solution, and the 6 hours of immersion time was achieved with 96% IE in HCl solution at $3\times10^{-6}$ M concentration. The evaluation of nanogel polymer by dispersion of magnetic core–shell of poly (2-acrylimido-2-methyl propane sulfonic acid) (PAMPS) and its copolymerization with ACM and acrylic acid (ACA) was explored their anticorrosive property on CS in 1 M HCl solution [184]. The PAMPS, PAMPS/AA, and PAMPS/ACM inhibitors 0.25 g l$^{-1}$ concentration were found to attain 81%, 89%, and 91% IE, respectively, revealing that PAMPS and ACM copolymerization yielded an effective corrosion inhibitor CS in 1 M HCl solution. The experimental and theoretical study of PACM as an effective corrosion inhibitor of MS in 2 M $H_3PO_4$ solution revealed that PACM IE increases with an increase in concentration and decreases with an increase in temperature of the testing medium [185]. The optimal concentration of 0.6 g l$^{-1}$ PACM was found to be adsorbed effectively on the MS with an IE of 91.02% at 30 °C. The grafting of poly 2-methoxyaniline (P2MePANI) with an average viscosity—molecular weight PACM of 177 858 g mol$^{-1}$ obtained by the radical polymerization of ACM using ammonium per-sulfate were evaluated on MS in 1 M HCl solution [186] at different temperatures (25–55 °C). The resulting grafted polymer (PACM-g-P2MePANI) against the expected outcome at all tested temperatures exhibited lower performance than P2MePANI inhibitor but better than PACM inhibitor. The IE at 0.8 g l$^{-1}$ concentration for PACM, P2MePANI, and PACM-g-P2MePANI at 55 °C was 71.00%, 92.17%, and 82.88%, respectively.

The evaluation of PVP, as represented in Figure 11.9g, as corrosion inhibitor of MS and CS in 1 M $H_2SO_4$ has revealed that IE of PVP increases with increased concentration and decreased temperature [105, 187]. The evaluation of PVP as corrosion inhibitor of CS in different concentrations of $H_3PO_4$ solution has revealed that PVP IE increases with an increase in concentration in the corrosive medium at 30 °C [131]. The IE of $5\times10^{-5}$ M concentration level of PVP was found to be 81% in 3 M $H_3PO_4$, increase to 89% in 7 M $H_3PO_4$, and reduced to 86% in 9 M $H_3PO_4$, indicating 7 M $H_3PO_4$ as the optimal concentration for the effective performance of PVP in $H_3PO_4$ solution. The stabilization of PVP film formed on CS surface by AgNps for effective and improved corrosion inhibition performance in 1 M HCl solution has been explored. The IE of Ag-PVP film at $7.5\times10^{-2}$ M concentration in 1 M HCl solution on CS was estimated to be approximately 90% for both electrochemical impedance and polarization technique [188]. To improve the solubility and corrosion inhibition performance of polymethylaniline (PMA) in 1 M HCl solution on MS substrate, a water-soluble inhibitor consisting of PVP and PMA composite (PVP–PMA) has been synthesized [187]. The IE of the resulting PVP–PMA was evaluated to increase with an increase in concentration and temperature of the corrosive medium. The optimum IE achieved at 60 °C was 87.01% at 5 g l$^{-1}$ concentration. The evaluation of the different molecular weights of PVP inhibitors (PVP-10; 10 000 g mol$^{-1}$ and PVP-45; 45 000 g mol$^{-1}$) in $H_2SO_4$ solution has revealed that the IE of inhibitor increases with an increase in molecular weight of PVP. The IE of 42.7% and 94.9% were estimated for PVP-10 and PVP-45 at $1\times10^{-2}$ M concentration, respectively [189]. The blend of PVP and PEG (PVP–PEG) and PACM (PVP–PACM) in the different ratios have been explored and revealed to exhibit better corrosion inhibition performances than the individual polymers as corrosion inhibition of Al in HCl solution [190, 191].

The polyvinyl imidazole (PVI), as shown in Figure 11.9h, derivative was synthesized from *N*-vinyl imidazole with azobisisobutyronitrile initiator in benzene and evaluated as a corrosion inhibitor of Q235 steel in 1 M HCl solution. The resulting PVI attained 90.1% IE at $0.002\,\mathrm{g\,l^{-1}}$ concentration at 25 °C [190]. The effect of PVI on the corrosion inhibition performance of chitosan and carboxymethyl chitosan (CMch)was investigated on API X70 steel in 1 M HCl solution [191]. The grafted polyvinyl imidazole with carboxymethyl chitosan (PVI-g-CMch) has been evaluated to exhibit better performance as a corrosion inhibitor than chitosan and carboxymethyl chitosan at the same concentration. The IE of 73.9%, 75.7%, and 80.6% were achieved by $0.2\,\mathrm{g\,l^{-1}}$ concentration of chitosan, CMch, and PVI-g-CMch, respectively; and an increase in the concentration of PVI-g-CMch to $1\,\mathrm{g\,l^{-1}}$ attained 92% IE. Besides, the evaluation of a vinyl imidazole monomer and PVI revealed a corrosion inhibitor of stainless steel in 0.5 M $H_2SO_4$ solution reported not to favor polymerization reaction as the monomer vinyl imidazole seems to exhibit better performance than the PVI [192].

The introduction of polystyrene (PS) into HCl and $H_2SO_4$ solutions to reduce the corrosion rate of MS has been suggested and revealed to be an economical way of preventing metal corrosion in an acidic medium [193]. The PS sulfonic acid doped with polypyrrole (PS-dppy) has also been revealed to be an effective corrosion inhibitor of CS in 1 M HCl solution [194]. An impressive IE of 87.1% could be achieved with a $0.04\,\mathrm{g\,l^{-1}}$ concentration of PS-dppy in the corrosive acidic medium.

As a whole, the anticorrosive properties of some polyvinyl's polymers, namely, PVOHs, PVAcs, PACA, PACN, PACM, PVP, PVI, and PS, in acidic media are tabulated in Table 11.2.

### 11.8.5 Polyzwitterion

The class of polymer compounds consisting of equal numbers of positively charged (cations) and negatively charged (anions) ions in the backbone of their structure is generally referred to as polyzwitterion (PZ). The cations are typical quaternary nitrogen atoms from ammonium ion ($NH_4^+$), and the base of PZ classification as sulfobetaine (SB), phosphorylcholine (PC), and carboxy betaine (CB) are according to the anion's functional groups. As shown in Figure 11.10a–c, the PZs consisting of sulfonates ($RSO_3^-$), phosphates ($PO_4^{3-}$), and carboxylates ($RCO_2^-$) anions are classified as SB, PC, and CB PZ, respectively [200, 201]. The presence of charged moieties in PZ compared with other polymeric materials makes PZ exhibit super hydrophilicity, greater stability, and better functionalization for the development of corrosion inhibitors in acidic media. The influence of sulfur (S), nitrogen (N), and oxygen (O) in a residual methionine (an amino acid) and P, N, and O on phosphoric acid has been considered in the preparation of copolymer and homo zwitterions compounds evaluated the corrosion inhibition of MS in 1 M HCl solution at different temperatures [201]. It was revealed that the presence of phosphoric acid and methionine residue was responsible for effective adsorption of the PZ on mild steel

**Table 11.2** The performance of polyvinyl's polymers as corrosion inhibitors in acid media.

| Polyvinyls | Inhibitor, substrate, and medium | Performance indicator by $IE_{max}$ | References |
|---|---|---|---|
| Polyvinyl alcohol (PVOH) | • PVOH on Al in 0.5 M $H_2SO_4$ | 43.5% | [156] |
| | • Influence of different molecular weights of PVOH; 14 000, 72 000, and 125 000 g mol$^{-1}$ on MS in 0.5 M HCl. The higher the molecular weight, the better the IE of PVOH | 66.0%, 74.6%, and 79.9%, respectively | [157] |
| | • Effect of degree of hydrolysis (80 and 99.7%) of PVOH on MS in 1 M HCl. The lower the hydrolysis, the better the IE of PVOH | 79.7% and 60.3%, respectively | [158] |
| | • PVOH-based terpolymer as corrosion inhibitor of MS in 1 M HCl | 98% | [167] |
| | • Effect of polymerization of vinyl alcohol (VOH) on CS in 1 M HCl | 53.6% (VOH) and 91.5% (PVOH) | [168] |
| Polyvinyl acetate (PVAc) | • PVAc as corrosion inhibitor of CS in 1 M $H_2SO_4$ | 91% | [169] |
| | • PVAc as an inhibitor for Al in 2 M $H_2SO_4$ and 0.5 M HCl | 90.3% and 78.4% for $H_2SO_4$ and HCl, respectively | [170] |
| | • Sulfonated poly(acrylamide-vinyl acetate) copolymer on CS in 1 M HCl. Dextrin grafted PVAc copolymer on MS in 15% HCl | 96.7%<br>98.4% | [171]<br>[78] |
| Polyacrylic acid (PACA) | • PACA exhibits a better efficiency than poly (sodium acrylate) on MS in 0.1 M HCl | 90.0% | [177] |
| | • PACA on MS in 0.5 M HCl | 96.8% | [176] |
| | • PANI-PACA composite on 316 SS in 0.5 M HCl | 91.75% | [175] |
| | • Synergistic effect of KI on the corrosion efficacy of PACA on Fe and Al in 0.5 M $H_2SO_4$ | 53% enhanced to 95% on Fe<br>79% enhanced to 87% on Al | [195]<br>[172] |
| Polyacrylonitrile (PACN) | • PACN inhibiting corrosion of bipolar plate honeycomb made of Al alloy for fuel cell in 0.5 M $H_2SO_4$ plus 0.002 g l$^{-1}$ HF | 99.5% | [178] |
| Polyacrylamide (PACM) | • Effectiveness of the mixture of polyvinyl pyridine with PACM on Fe in 1 M $H_2SO_4$ and the synergy of KI | 52.2% IE of PACM to 87% by KI and the mixture was enhanced from 63.1% to 94.5% | [181] |
| | • PACM grated with Fenugreek Mucilage on MS in 0.5 M $H_2SO_4$ | 96% | [196] |
| | • Guar gum-grated PACM (GG-g-PACM) on MS in 1 M HCl | 90.7% | [183] |

*(Continued)*

**Table 11.2** (Continued)

| Polyvinyls | Inhibitor, substrate, and medium | Performance indicator by $IE_{max}$ | References |
|---|---|---|---|
| | • High-molecular weight PACM ($1.4 \times 10^6$ g mol$^{-1}$) on CS in 1 M HCl and 0.5 M $H_2SO_4$ | 85% and 96% for $H_2SO_4$ and HCl, respectively | [182, 197] |
| | • Poly2-acrylimido-2-methyl propane sulfonic acid (PAMPS) copolymerized with acrylic acid (ACA) and acrylamide (ACM) on CS in 1 M HCl | 81% (PAMPS), 89% (PAMPS-ACA), and 91% (PAMPS-ACM) | [184] |
| | • PACM as corrosion inhibitor of MS in 2 M $H_3PO_4$ solution | 91.0% | [185] |
| | • The grafting of poly 2-methoxylaniline (P2MePANI) with PACM efficacy on MS in 1 M HCl | 71% (PACM) and 82.9% (PACM-g-P2MePANI) | [186] |
| Polyvinyl pyrrolidone (PVP) | • Evaluation of PVP as corrosion inhibitor of CS in different concentrations of $H_3PO_4$ | 89% optimal in 7 M $H_3PO_4$ | [131] |
| | • Silver nanoparticle PVP (AgNp-PVP) thin on CS in 1 M HCl | 90% | [188] |
| | • Polymethylaniline (PMA)–PVP composite on MS in 1 M HCl | 87% | [187] |
| | • Effect of molecular weight PVP-10 and PVP-45 (10 000 and 45 000 g mol$^{-1}$ respectively) of PVP on SS in $H_2SO_4$ solutions | 42.7% (PVP-10) and 94.9% (PVP-45) | [189] |
| | • The blend of PVP and PEG in the different ratios on Al in 0.1 M HCl | 80% | [198] |
| | • The blend of PVP and PACM in the different ratios on Al in 0.1 M HCl | 58% | [199] |
| | • PVP–Soy polymer composite on CS in 1 M $H_2SO_4$ | 96% | [104] |
| Polyvinyl imidazole (PVI) | • PVI on Q235 steel in 1 M HCl solution | 90.1% | [190] |
| | • Effect of grafting PVI on carboxymethyl chitosan (PVI-g-CMCh) on IE of chitosan (Ch) and carboxymethyl chitosan on API X70 steel in 1 M HCl | 73.9% (Ch), 75.7% (CMCh), and 81.6–92% (PVI-g-CMCh) | [191] |
| Polystyrene (PS) | • Introduction of PS to reduce the corrosion rate of MS in HCl and $H_2SO_4$ solutions | 90% (HCl) and 84% ($H_2SO_4$) | [193] |
| | • PS-sulfonic acid doped with polypyrrole (PS-ddpy) on CS in 1 M HCl | 87.1% | [194] |

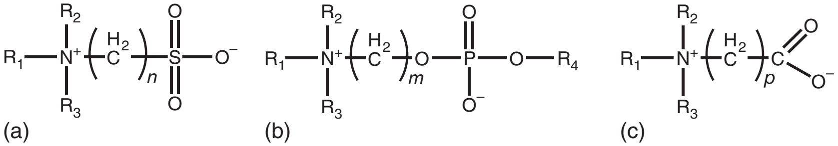

**Figure 11.10** The chemical structures of polyzwitterion (PZ) consist of ammonium ion ($NH_4^+$) cation classified according to the anionic compounds (a) sulfobetaine (SB), (b) phosphorylcholine (PC), and (c) carboxy betaine (CB).

in the acidic medium. A di-cationic polymer, namely, poly($N^1$, $N^1$-diallyl-$N^6$, $N^6$, $N^6$-tri propyl hexane-1,6-diammonium chloride) (poly-NDTHDC), that was counterbalanced with chloride ions ($Cl^-$) to make it a PZ was synthesized, and the comparative study for the efficacy of the PZ and its corresponding monomer (NDTHDC) as corrosion inhibitor was investigated on the surface of API X60 MS on hydrodynamic condition in 15% HCl solution [38]. The effect of polymerization of the PZ was demonstrated, as revealed by IE of 86.1% for 0.1 $g\,l^{-1}$ concentration of poly-NDTHDC compared to the 79.1% of 1 $g\,l^{-1}$ concentration of NDTHDC. The synthesis of poly (bis-zwitterion) (PBZ) consisting of *N*-(2-aminoethyl)iminodiacetic acid chelating motif by one-pot, two-step cyclo-polymerization reaction of diallyl amine, ethyl bromoacetate, and 2-bromoethylamine hydrobromide, and its application as corrosion inhibitor for MS in 1 M HCl solution was successfully explored [202]. The resulting PBZ was aided with KI to achieve 99% IE at 0.02 $g\,l^{-1}$ concentration in 1 M HCl solution. The cysteine-based diallylamine PZ that was synthesized from the homo and copolymer of cysteine residues and diallyldimethylammonium chloride (DADMAC) was evaluated as effective corrosion inhibitors of MS in 1 M HCl at temperature [203]. The resulting PZ polymers were reported to be very effective as corrosion inhibitors of MS 60 °C.

## 11.9 Conclusion

Polymeric compounds are an alternative to the existing corrosion inhibitors in an acidic medium that is found wanting or inadequate owing to their toxicity, non-biodegradable, expensive, and noncompatible with green chemistry for a safer environment. Most polymeric materials, such as polyvinyl, are suitable for corrosion inhibitors at elevated temperatures between 40 and 60 °C, while some of them are high-heat resistance and can survive up to 150 °C or more. The ability of polymeric materials to cover a larger surface area owing to their repeated unit of functional group or groups when adsorbed on the surface of the metal substrate in a corrosive environment makes them a unique material to be considered for the formulation of advanced corrosion inhibitors as demonstrated with 10% relative amount of mono-NTHDC compounds on API CS provides a better IE of 86.1% in 15% HCl solution [38] and several others.

However, the low mechanical property of polymeric materials (mainly, the naturally occurring polymers) is a challenge that limits its usage in the industry. An effort to improve on this deficiency can be continuously addressed by incorporating appropriate motifs, functionalities, additives, and mediators in the backbone structures of polymeric materials as corrosion inhibitors in acid media during polymerization to mention a few of numerous modifications, some of them are presented in Tables 11.1 and 11.2. Xanthan gum IE on MS in 15% HCl solution was improved from 90% to 93.2% owing to the grafting of PACM into the backbone of the Xanthan gum [73], the grafting of dextrin with PVAc was found to enhance IE of dextrin in 15% HCl solution on MS from 84.6% to 98.4% [78], and the tremendous improvement of IE of PACA in 0.5 M $H_2SO_4$ solutions on Fe and Al by KI synergistic effect [172, 173].

## Acknowledgments

The authors gratefully acknowledge the research facilities provided by King Fahd University of Petroleum & Minerals (KFUPM), Dhahran, Saudi Arabia.

## References

1. Vidyarthy, R.S. and Sivateja, P. (2019). Influence of activating flux tungsten inert gas welding on mechanical and metallurgical properties of the mild steel. *Materials Today: Proceedings* 28: 977–981.
2. Wang, F.C. and Han, L.H. (2019). Analytical behavior of carbon steel-concrete-stainless steel double-skin tube (DST) used in submarine pipeline structure. *Marine Structures* 63: 99–116.
3. Koch, G.H., Brongers, M., Thompson, N.G., Virmani, Y.P., and Payer, J.H. (2002). Corrosion cost and preventive strategies in the United States. pp. 1–12.
4. Woodard & Curran, Inc. (2006). Wastes from industries (Case Studies). In: *Industrial Waste Treatment Handbook*, 409–496. Woodard & Curran, Inc.
5. Tamalmani, K. and Husin, H. (2020). Review on corrosion inhibitors for oil and gas corrosion issues. *Applied Sciences* 10 (10): 3389.
6. Wu, W., Cheng, G., Hu, H., and Zhou, Q. (2013). Risk analysis of corrosion failures of equipment in refining and petrochemical plants based on fuzzy set theory. *Engineering Failure Analysis* 32: 23–34.
7. Singha, A. and Quraishi, M.A. (2015). Acidizing corrosion inhibitors: a review. *Journal of Materials and Environmental Science* 6 (1): 224–235.
8. Pourabdollah, K. (2020). Matrix acidizing: a fouling mitigation process in oil and gas wells. *Reviews in Chemical Engineering* 36 (2): 311–331.
9. El-Maksoud, S.A.A. (2008). The effect of organic compounds on the electrochemical behaviour of steel in acidic media: a review. *International Journal of Electrochemical Science* 3 (5): 528–555.

**10** Ashworth, V. (2010). Principles of cathodic protection. In: *Shreir's Corrosion* (ed. L.L. Shreir), 2747–2762. Elsevier.

**11** Golgoon, A., Aliofkhazraei, M., Toorani, M. et al. (2015). Corrosion and wear properties of nanoclay- polyester nanocomposite coatings fabricated by electrostatic method. *Procedia Materials Science* 11: 536–541.

**12** Ates, M. (2016). A review on conducting polymer coatings for corrosion protection. *Journal of Adhesion Science and Technology* 30 (14): 1510–1536.

**13** Palimi, M.J., Rostami, M., Mahdavian, M., and Ramezanzadeh, B. (2015). The corrosion protection performance of the polyurethane coatings containing surface modified $Fe_2O_3$ nanoparticles. *Corrosion* 71 (8): 1012–1026.

**14** Harris, F.N. (1961). Applications of acetic acid to well completion, stimulation and reconditioning. *Journal of Petroleum Technology* 13 (07): 637–639.

**15** Slavcheva, E., Shone, B., and Turnbull, A. (1999). Review of naphthenic acid corrosion in oil refining. *British Corrosion Journal* 34 (2): 125–131.

**16** Feng, Q., Yan, B., Chen, P., and Shirazi, S.A. (2019). Failure analysis and simulation model of pinhole corrosion of the refined oil pipeline. *Engineering Failure Analysis* 106: 104177.

**17** Seghier, M., Keshtegar, B., Correia, J. et al. (2018). Structural reliability analysis of corroded pipeline made in X60 steel based on M5 model tree algorithm and monte carlo simulation. *Procedia Structural Integrity* 13: 1670–1675.

**18** Döner, A., Yüce, A.O., and Kardaş, G. (2013). Inhibition effect of rhodanine-N-acetic acid on copper corrosion in acidic media. *Industrial and Engineering Chemistry Research* 52 (29): 9709–9718.

**19** El-Haddad, M.N. and Fouda, A.S. (2015). Electroanalytical, quantum and surface characterization studies on imidazole derivatives as corrosion inhibitors for aluminum in acidic media. *Journal of Molecular Liquids* 209: 480–486.

**20** Ali, S.M. and Al Lehaibi, H.A. (2016). Control of zinc corrosion in acidic media: Green fenugreek inhibitor. *Transactions of Nonferrous Metals Society of China* 26 (11): 3034–3045.

**21** Bradford, S.A. (2001). *Corrosion Control*, 2e|INIS., 345–371. Edmonton, Alberta, Canada: CASTI.

**22** Umoren, S.A. and Solomon, M.M. (2014). Recent developments on the use of polymers as corrosion inhibitors-a review. *The Open Materials Science Journal* 8 (1): 39–54.

**23** Ilevbare, G.O. and Burstein, G.T. (2003). The inhibition of pitting corrosion of stainless steels by chromate and molybdate ions. *Corrosion Science* 45 (7): 1545–1569.

**24** Environmental Policy Tools (1995). A User' s Guide September 1995. *Environ. Prot.*, (September).

**25** Bahadur, A. (1998). Development and evaluation of a low chromate corrosion inhibitor for cooling water systems. *Canadian Metallurgical Quarterly* 37 (5): 459–468.

**26** Services, H. (2002). Toxicological profile for chromium. ATSDR's Toxicol. Profiles, September.

**27** Twite, R.L. and Bierwagen, G.P. (1998). Review of alternatives to chromate for corrosion protection of aluminum aerospace alloys. *Progress in Organic Coatings* 33 (2): 91–100.

**28** Bethencourt, M., Botana, F.J., Calvino, J.J. et al. (1998). Lanthanide compounds as environmentally-friendly corrosion inhibitors of aluminium alloys: a review. *Corrosion Science* 40 (11): 1803–1819.

**29** Stupnisek-Lisac, E., Brnada, A., and Mance, A.D. (2000). Secondary amines as copper corrosion inhibitors in acid media. *Corrosion Science* 42 (2): 243–257.

**30** Elsharif, A.M., Abubshait, S.A., Abdulazeez, I., and Abubshait, H.A. (2020). Synthesis of a new class of corrosion inhibitors derived from natural fatty acid: 13-docosenoic acid amide derivatives for oil and gas industry. *Arabian Journal of Chemistry* 13 (5): 5363–5376.

**31** Odewunmi, N.A., Mazumder, M.A.J., and Ali, S.A. (2021). Evaluation of 1-hexadecylbenzimidazole as a corrosion inhibitor on low carbon steel 15% HCl solution interface. *ChemistrySelect* 6 (13): 3199–3217.

**32** Odewunmi, N.A., Mazumder, M.A.J., Aldahdooh, M.K., and Ali, S.A. (2021). N1,N1,N12,N12-Tetramethyl-N1, N12-dioctyldodecane-1,12-diaminium bromide: Its synthesis and application in inhibition of mild steel corrosion in 15% HCl. *Journal of Molecular Liquids* 338: 116630.

**33** Odewunmi, N.A., Mazumder, M.A.J., Ali, S.A., and Alharbi, B.G. (2021). Hydroquinone decorated with alkyne, quaternary ammonium, and hydrophobic motifs to mitigate corrosion of X-60 mild steel in 15 wt.% HCl. *Chemistry: An Asian Journal* 16 (7): 801–821.

**34** Bothi Raja, P. and Sethuraman, M.G. (2008). Atropine sulphate as corrosion inhibitor for mild steel in sulphuric acid medium. *Materials Letters* 62 (10–11): 1602–1604.

**35** Karakurt, T. (2018). Investigation of the molecular structure of 4-(3-methyl-3-phenylcyclobutyl)-2-[2-(3-methylbenzylidene)hydrazinyl]thiazole in the gas and solid phases. *Acta Crystallographica Section C: Structural Chemistry* 74 (11): 1502–1508.

**36** Verma, C., Verma, D.K., Ebenso, E.E., and Quraishi, M.A. (2018). Sulfur and phosphorus heteroatom-containing compounds as corrosion inhibitors: an overview. *Heteroatom Chemistry* 29 (4): e21437.

**37** Yang, H.-M. (2021). Role of organic and eco-friendly inhibitors on the corrosion mitigation of steel in acidic environments—a state-of-art review. *Molecules* 26 (11): 3473.

**38** Odewunmi, N.A., Solomon, M.M., Umoren, S.A., and Ali, S.A. (2020). Comparative studies of the corrosion inhibition efficacy of a dicationic monomer and its polymer against API X60 steel corrosion in simulated acidizing fluid under static and hydrodynamic conditions. *ACS Omega* 5 (42): 27057–27071.

**39** Saleh, R.M., Badran, M.M., El Hosary, A.A., and El Dahan, H.A. (1988). Corrosion inhibition of 304 stainless steel in H3PO4-CI− solutions by chromium, molybdenum, nitrogen, tungsten, and boron anions. Part 1: polarisation measurements. *British Corrosion Journal* 23 (2): 105–108.

**40** Fathima Sabirneeza, A.A., Geethanjali, R., and Subhashini, S. (2015). Polymeric corrosion inhibitors for iron and its alloys: a review. *Chemical Engineering Communications* 202 (2): 232–244.

**41** Gandini, A. and Belgacem, M.N. (2002). Recent contributions to the preparation of polymers derived from renewable resources. *Journal of Polymers and the Environment* 10 (3): 105–114.

**42** Bathily, M., Ngom, B., Gassama, D., and Tamba, S. (2021). Review on essential oils and their corrosion-inhibiting properties review on essential oils and their corrosion-inhibiting properties. *Journal of Applied Chemistry* 9 (June): 65–73.

**43** Chaieb, E., Bouyanzer, A., Hammouti, B., and Berrabah, M. (2009). Limonene as green inhibitor for steel corrosion in hydrochloric acid solutions. *Wuli Huaxue Xuebao/ Acta Physico - Chimica Sinica* 25 (7): 1254–1258.

**44** El Ouariachi, E., Paolini, J., Bouklah, M. et al. (2010). Adsorption properties of Rosmarinus of ficinalis oil as green corrosion inhibitors on C38 steel in 0.5 M H2SO4. *Acta Metallurgica Sinica (English Letters)* 23 (1): 13–20.

**45** Rudin, A. and Choi, P. (2013). Biopolymers. *Elements of Polymer Science and Engineering* 521–535.

**46** Okewale, A.O. (2017). The use of rubber leaf extract as a corrosion inhibitor for mild steel in acidic solution. *International Journal of Materials and Chemistry* 7 (1): 5–13.

**47** Krzyzowska, M., Tomaszewska, E., Ranoszek-Soliwoda, K. et al. (2017). Tannic acid modification of metal nanoparticles: possibility for new antiviral applications. *Nanostructures for Oral Medicine* 335–363.

**48** Rahim, A.A., Rocca, E., Steinmetz, J. et al. (2007). Mangrove tannins and their flavanoid monomers as alternative steel corrosion inhibitors in acidic medium. *Corrosion Science* 49 (2): 402–417.

**49** Rahim, A.A. and Kassim, J. (2010). Recent development of vegetal tannins in corrosion protection of iron and steel. *Recent Patents on Materials Science* 1 (3): 223–231.

**50** Martinez, S. and Štern, I. (2001). Inhibitory mechanism of low-carbon steel corrosion by mimosa tannin in sulphuric acid solutions. *Journal of Applied Electrochemistry* 31 (9): 973–978.

**51** Ouellette, R.J. and Rawn, J.D. (2015). Carbohydrates. In: *Organic Chemistry Study Guide*, 539–567. Elsevier.

**52** Anyiam, C.K., Ogbobe, O., Oguzie, E.E. et al. (2020). Corrosion inhibition of galvanized steel in hydrochloric acid medium by a physically modified starch. *SN Applied Sciences* 2 (4): 1–11.

**53** Mobin, M., Khan, M.A., and Parveen, M. (2011). Inhibition of mild steel corrosion in acidic medium using starch and surfactants additives. *Journal of Applied Polymer Science* 121 (3): 1558–1565.

**54** Lahrour, S., Benmoussat, A., Bouras, B. et al. (2019). Glycerin-grafted starch as corrosion inhibitor of C-Mn steel in 1 M HCl solution. *Applied Sciences* 9 (21): 1–18.

**55** Nwanonenyi, S., Madufor, I., Uzoma, P., and Chukwujike, I. (2016). Corrosion inhibition of mild steel in sulphuric acid environment using millet starch and potassium iodide. *International Research Journal of Pure and Applied Chemistry* 12 (2): 1–15.

**56** Bayol, E., Gürten, A.A., Dursun, M., and Kayakirilmaz, K. (2008). Adsorption behavior and inhibition corrosion effect of sodium carboxymethyl cellulose on mild steel in acidic medium. *Wuli Huaxue Xuebao/ Acta Physico - Chimica Sinica* 24 (12): 2236–2243.

**57** Egbuhuzor, O.M., Madufor, I.C., Nwanonenyi, S.C., and Bokolo, J.O. (2020). Adsorption behavior and corrosion rate model of sodium carboxymethyl cellulose (Na-CMC) polymer on aluminium in HCl solution. *Nigerian Journal of Technology* 39 (2): 369–378.

**58** Solomon, M.M., Umoren, S.A., Udosoro, I.I., and Udoh, A.P. (2010). Inhibitive and adsorption behaviour of carboxymethyl cellulose on mild steel corrosion in sulphuric acid solution. *Corrosion Science* 52 (4): 1317–1325.

**59** Aslam, R., Mobin, M., Aslam, J. et al. (2019). Inhibitory effect of sodium carboxymethylcellulose and synergistic biodegradable gemini surfactants as effective inhibitors for MS corrosion in 1 M HCl. *Journal of Materials Research and Technology* 8 (5): 4521–4533.

**60** Solomon, M.M., Gerengi, H., and Umoren, S.A. (2017). Carboxymethyl cellulose/silver nanoparticles composite: synthesis, characterization and application as a benign corrosion inhibitor for St37 Steel in 15% $H_2SO_4$ medium. *ACS Applied Materials & Interfaces* 9 (7): 6376–6389.

**61** Sovizi, M.R. and Abbasi, R. (2020). Effect of carboxymethyl cellulose on the corrosion behavior of aluminum in $H_2SO_4$ solution and synergistic effect of potassium iodide. *Journal of Adhesion Science and Technology* https://doi.org/10.1080/01694243.2020.1717803 34 (15): 1664–1678.

**62** Fares, M.M., Maayta, A.K., and Al-Qudah, M.M. (2012). Pectin as promising green corrosion inhibitor of aluminum in hydrochloric acid solution. *Corrosion Science* 60: 112–117.

**63** Charitha, B.P. and Rao, P. (2020). Pectin as a potential green inhibitor for corrosion control of 6061Al–15%(V) SiC(P) composite in acid medium: electrochemical and surface studies. *Journal of Failure Analysis and Prevention* 20 (5): 1684–1696.

**64** Abou-Elseoud, W.S., Abdel-karim, A.M., Hassan, E.A., and Hassan, M.L. (2021). Enzyme- and acid-extracted sugar beet pectin as green corrosion inhibitors for mild steel in hydrochloric acid solution. *Carbohydrate Polymer Technologies and Applications* 2: 100072.

**65** Ma, X., Wang, J., Xu, J. et al. (2019). Sunflower head pectin with different molecular weights as promising green corrosion inhibitors of carbon steel in hydrochloric acid solution. *ACS Omega* 4 (25): 21148–21160.

**66** Saidi, N., Elmsellem, H., Ramdani, M. et al. (2015). Using pectin extract as eco-friendly inhibitor for steel corrosion in 1M HCl media. *Der Pharma Chemica* 7 (6): 87–94.

**67** Umoren, S.A., Obot, I.B., Madhankumar, A., and Gasem, Z.M. (2015). Performance evaluation of pectin as ecofriendly corrosion inhibitor for X60 pipeline steel in acid medium: experimental and theoretical approaches. *Carbohydrate Polymers* 124: 280–291.

**68** Messali, M., Lgaz, H., Dassanayake, R. et al. (2017). Guar gum as efficient non-toxic inhibitor of carbon steel corrosion in phosphoric acid medium: electrochemical, surface, DFT and MD simulations studies. *Journal of Molecular Structure* 1145: 43–54.

**69** Abdallah, M. (2004). Guar gum as corrosion inhibitor for carbon steel in sulfuric acid solutions. *Portugaliae Electrochimica Acta* 22 (2): 161–175.

**70** Biswas, A., Pal, S., and Udayabhanu, G. (2017). Effect of chemical modification of a natural polysaccharide on its inhibitory action on mild steel in 15% HCl solution. *Journal of Adhesion Science and Technology* 31 (22): 2468–2489.

**71** Umoren, S.A. (2008). Inhibition of aluminium and mild steel corrosion in acidic medium using Gum Arabic. *Cellulose* 15 (5): 751–761.

**72** Mobin, M. and Rizvi, M. (2016). Inhibitory effect of xanthan gum and synergistic surfactant additives for mild steel corrosion in 1 M HCl. *Carbohydrate Polymers* 136: 384–393.

**73** Biswas, A., Pal, S., and Udayabhanu, G. (2015). Experimental and theoretical studies of xanthan gum and its graft co-polymer as corrosion inhibitor for mild steel in 15% HCl. *Applied Surface Science* 353: 173–183.

**74** Zaafarany, I. (2006). Inhibition of acidic corrosion of iron by some Carrageenan compounds. *Current World Environment: An International Research Journal of Environmental Sciences* 1 (2): 101–108.

**75** Gowraraju, N.D., Jagadeesan, S., Ayyasamy, K. et al. (2017). Adsorption characteristics of Iota-carrageenan and Inulin biopolymers as potential corrosion inhibitors at mild steel/sulphuric acid interface. *Journal of Molecular Liquids* 232: 9–19.

**76** Fares, M.M., Maayta, A.K., and Al-Mustafa, J.A. (2012). Corrosion inhibition of iota-carrageenan natural polymer on aluminum in presence of zwitterion mediator in HCl media. *Corrosion Science* 65: 223–230.

**77** Zou, C., Yan, X., Qin, Y. et al. (2014). Inhibiting evaluation of β-cyclodextrin-modified acrylamide polymer on alloy steel in sulfuric solution. *Corrosion Science* 85: 445–454.

**78** Biswas, A., Das, D., Lgaz, H. et al. (2019). Biopolymer dextrin and poly (vinyl acetate) based graft copolymer as an efficient corrosion inhibitor for mild steel in hydrochloric acid: electrochemical, surface morphological and theoretical studies. *Journal of Molecular Liquids* 275: 867–878.

**79** Devi, G.N., Unnisa, C.B.N., Roopan, S.M. et al. (2020). Floxacins: as mediators in enhancing the corrosion inhibition efficiency of natural polymer dextrin. *Macromolecular Research* 28 (6): 558–566.

**80** Jmiai, A., El Ibrahimi, B., Tara, A. et al. (2018). Alginate biopolymer as green corrosion inhibitor for copper in 1 M hydrochloric acid: experimental and theoretical approaches. *Journal of Molecular Structure* 1157: 408–417.

**81** Nadi, I., Belattmania, Z., Sabour, B. et al. (2019). *Sargassum muticum* extract based on alginate biopolymer as a new efficient biological corrosion inhibitor for carbon steel in hydrochloric acid pickling environment: gravimetric, electrochemical and surface studies. *International Journal of Biological Macromolecules* 141: 137–149.

**82** Fardioui, M., Rbaa, M., Benhiba, F. et al. (2021). Bio-active corrosion inhibitor based on 8-hydroxyquinoline-grafted-Alginate: experimental and computational approaches. *Journal of Molecular Liquids* 323: 114615.

**83** Tawfik, S.M. (2015). Alginate surfactant derivatives as an ecofriendly corrosion inhibitor for carbon steel in acidic environments. *RSC Advances* 5 (126): 104535–104550.

**84** El-Haddad, M.N. (2013). Chitosan as a green inhibitor for copper corrosion in acidic medium. *International Journal of Biological Macromolecules* 55: 142–149.

**85** Jmiai, A., El Ibrahimi, B., Tara, A. et al. (2017). Chitosan as an eco-friendly inhibitor for copper corrosion in acidic medium: protocol and characterization. *Cellulose* 24 (9): 3843–3867.

**86** Umoren, S.A., Banera, M.J., Alonso-Garcia, T. et al. (2013). Inhibition of mild steel corrosion in HCl solution using chitosan. *Cellulose* 20 (5): 2529–2545.

**87** El Mouaden, K., Chauhan, D.S., Quraishi, M.A. et al. (2020). Cinnamaldehyde-modified chitosan as a bio-derived corrosion inhibitor for acid pickling of copper: microwave synthesis, experimental and computational study. *International Journal of Biological Macromolecules* 164: 3709–3717.

**88** Chauhan, D.S., Srivastava, V., Joshi, P.G., and Quraishi, M.A. (2018). PEG cross-linked Chitosan: a biomacromolecule as corrosion inhibitor for sugar industry. *International Journal of Industrial Chemistry* 9 (4): 363–377.

**89** Kong, P., Feng, H., Chen, N. et al. (2019). Polyaniline/chitosan as a corrosion inhibitor for mild steel in acidic medium. *RSC Advances* 9 (16): 9211–9217.

**90** Rbaa, M., Benhiba, F., Hssisou, R. et al. (2021). Green synthesis of novel carbohydrate polymer chitosan oligosaccharide grafted on D-glucose derivative as bio-based corrosion inhibitor. *Journal of Molecular Liquids* 322: 114549.

**91** Gupta, N.K., Joshi, P.G., Srivastava, V., and Quraishi, M.A. (2018). Chitosan: a macromolecule as green corrosion inhibitor for mild steel in sulfamic acid useful for sugar industry. *International Journal of Biological Macromolecules* 106: 704–711.

**92** Copeland, L., Blazek, J., Salman, H., and Tang, M.C. (2009). Form and functionality of starch. *Food Hydrocolloids* 23 (6): 1527–1534.

**93** Umoren, S.A. and Eduok, U.M. (2016). Application of carbohydrate polymers as corrosion inhibitors for metal substrates in different media: a review. *Carbohydrate Polymers* 140: 314–341.

**94** Limberg, G., Körner, R., Buchholt, H.C. et al. (2000). Quantification of the amount of galacturonic acid residues in blocksequences in pectin homogalacturonan by enzymatic fingerprinting with exo- and endo-polygalacturonase II from *Aspergillus niger*. *Carbohydrate Research* 327 (3): 321–332.

**95** Verbeken, D., Dierckx, S., and Dewettinck, K. (2003). Exudate gums: occurrence, production, and applications. *Applied Microbiology and Biotechnology* 63 (1): 10–21.

**96** Eddy, N.O., Odiongenyi, A.O., Ameh, P.O., and Ebenso, E.E. (2012). Corrosion inhibition potential of daniella oliverri gum exudate for mild steel in acidic medium. *International Journal of Electrochemical Science* 7 (8): 7425–7439.

**97** Ashassi-Sorkhabi, H. and Kazempour, A. (2020). Thermodynamic and kinetic insights into the role of amino acids in improving the adhesion of iota-carrageenan as a natural corrosion inhibitor to the aluminum surface. *Journal of Adhesion Science and Technology* 34 (9): 961–975.

**98** Tomasik, P., Wiejak, S., and Pałasiński, M. (1989). The thermal decomposition of carbohydrates. Part II. The decomposition of starch. *Advances in Carbohydrate Chemistry and Biochemistry* 47 (C): 279–343.

**99** Periayah, M.H., Halim, A.S., and Saad, A.Z.M. (2016). Chitosan: a promising marine polysaccharide for biomedical research. *Pharmacognosy Reviews* 10 (19): 39–42.

**100** Chauhan, D.S., Quraishi, M.A., Sorour, A.A. et al. (2019). Triazole-modified chitosan: a biomacromolecule as a new environmentally benign corrosion inhibitor for carbon steel in a hydrochloric acid solution. *RSC Advances* 9 (26): 14990–15003.

**101** Li, M., Xu, J., Li, R. et al. (2014). Simple preparation of aminothiourea-modified chitosan as corrosion inhibitor and heavy metal ion adsorbent. *Journal of Colloid and Interface Science* 417: 131–136.

**102** Kunugi, S. (2015). Proteins as polymers and polyelectrolytes. In: *Encyclopedia of Polymeric Nanomaterials* (ed. S. Kobayaschi and K. Müllen), 1–6. Springer.

**103** Canalle, L.A., Löwik, D.W.P.M., and van Hest, J.C.M. (2009). Polypeptide – polymer bioconjugates. *Chemical Society Reviews* 39 (1): 329–353.

**104** Nwanonenyi, S.C., Obasi, H.C., Chukwujike, I.C. et al. (2018). Inhibition of carbon steel corrosion in 1 M $H_2SO_4$ using soy polymer and polyvinylpyrrolidone. *Chemistry Africa* 2 (2): 277–289.

**105** De Lima, K.C.D.S., Paiva, V.M., Perrone, D. et al. (2020). Glycine max meal extracts as corrosion inhibitor for mild steel in sulphuric acid solution. *Journal of Materials Research and Technology* 9 (6): 12756–12772.

**106** Kunz, C. and Lönnerdal, B. (1990). Human-milk proteins: analysis of casein and casein subunits by anion-exchange chromatography, gel electrophoresis, and specific staining methods. *The American Journal of Clinical Nutrition* 51 (1): 37–46.

**107** Robinson, R.K. (2005). *Dairy Microbiology Handbook*, 3e, 765. Wiley.

**108** O'Kennedy, B.T. (2011). Caseins. *Handbook of Food Proteins* 13–29.

**109** Berrekhis, F., Roques, Y., Aries, L., and Hajjaji, M. (1997). Electrodeposition of casein coatings on zinc alloy. *Progress in Organic Coatings* 31 (4): 341–345.

**110** Yabuki, A. and Sakai, M. (2011). Self-healing coatings of inorganic particles using a pH-sensitive organic agent. *Corrosion Science* 53 (2): 829–833.

**111** Zhang, H. and Mittal, G. (2010). Biodegradable protein-based films from plant resources: A review. *Environmental Progress & Sustainable Energy* 29 (2): 203–220.

**112** Corradini, E., Curti, P.S., Meniqueti, A.B. et al. (2014). Recent advances in food-packing, pharmaceutical and biomedical applications of zein and zein-based materials. *International Journal of Molecular Sciences* 15 (12): 22438–22470.

**113** Roy, P. and Sukul, D. (2015). Protein-surfactant aggregate as a potential corrosion inhibitor for mild steel in sulphuric acid: Zein-SDS system. *RSC Advances* 5 (2): 1359–1365.

**114** Manninen, A.H. (2009). Protein hydrolysates in sports nutrition. *Nutrition & Metabolism (London)* 6 (1): 38.

**115** Vidotti, R.M., Viegas, E.M.M., and Carneiro, D.J. (2003). Amino acid composition of processed fish silage using different raw materials. *Animal Feed Science and Technology* 105 (1–4): 199–204.

**116** Gildberg, A. and Stenberg, E. (2001). A new process for advanced utilisation of shrimp waste. *Process Biochemistry* 36 (8–9): 809–812.

**117** Bueno-Solano, C., López-Cervantes, J., Campas-Baypoli, O.N. et al. (2009). Chemical and biological characteristics of protein hydrolysates from fermented shrimp by-products. *Food Chemistry* 112 (3): 671–675.

**118** Farag, A.A., Ismail, A.S., and Migahed, M.A. (2018). Environmental-friendly shrimp waste protein corrosion inhibitor for carbon steel in 1 M HCl solution. *Egyptian Journal of Petroleum* 27 (4): 1187–1194.

**119** Samanta, S., Bogdanowicz, D.R., Lu, H.H., and Koberstein, J.T. (2016). Polyacetals: water-soluble, pH-degradable polymers with extraordinary temperature response. *Macromolecules* 49 (5): 1858–1864.

**120** Zarrintaj, P., Saeb, M.R., Jafari, S.H., and Mozafari, M. (2020). Application of compatibilized polymer blends in biomedical fields. *Compatibilization of Polymer Blends* 2020: 511–537.

**121** Fouda, A.S., El-Dossoki, F.I., and Shady, I.A. (2018). Adsorption and corrosion inhibition behavior of polyethylene glycol on α-brass alloy in nitric acid solution. *Green Chemistry Letters and Reviews* 11 (2): 67–77.

**122** Abdallah, M., Megahed, H.E., Radwan, M.A., and Abdfattah, E. (2012). Polyethylene glycol compounds as corrosion inhibitors for aluminium in 0.5M hydrochloric acid solution. *Journal of American Science* 8 (11): 49–55.

**123** Ashassi-Sorkhabi, H. and Ghalebsaz-Jeddi, N. (2005). Inhibition effect of polyethylene glycol on the corrosion of carbon steel in sulphuric acid. *Materials Chemistry and Physics* 92 (2–3): 480–486.

**124** Ashassi-Sorkhabi, H. and Kazempour, A. (2020). Influence of fluid flow on the performance of polyethylene glycol as a green corrosion inhibitor. *Journal of Adhesion Science and Technology* 34 (15): 1653–1663.

**125** Banumathi, N., Subhashini, S., and Rajalakshmi, R. (2010). Polyethelene glycol-anthranilic acid composite as corrosion inhibitor for mild steel in acid medium. *E-Journal of Chemistry* 7 (SUPPL. 1).

**126** Abd-Elaal, A.A., Shaban, S.M., and Tawfik, S.M. (2017). Three Gemini cationic surfactants based on polyethylene glycol as effective corrosion inhibitor for mild steel in acidic environment. *Journal of the Association of Arab Universities for Basic and Applied Sciences* 24: 54–65.

**127** Umoren, S., Solomon, M.M., Israel, A.U. et al. (2015). Comparative study of the corrosion inhibition efficacy of polypropylene glycol and poly (methacrylic acid) for mild steel in acid solution. *Journal of Dispersion Science and Technology* 36 (12): 1721–1735.

**128** Solomon, M.M., Umoren, S.A., Israel, A.U., and Etim, I.G. (2016). Synergistic inhibition of aluminium corrosion in H2SO4 solution by polypropylene glycol in the presence of iodide ions. *Pigment & Resin Technology* 45 (4): 280–293.

**129** Umoren, S.A. (2016). Polypropylene glycol: a novel corrosion inhibitor for × 60 pipeline steel in 15% HCl solution. *Journal of Molecular Liquids* 219: 946–958.

**130** Amara, M. and Kerdjoudj, H. (2003). Modification of the cation exchange resin properties by impregnation in polyethyleneimine solutions application to the separation of metallic ions. *Talanta* 60 (5): 991–1001.

**131** Schweinsberg, D.P., Jianguo, Y., Lin, W., and Otienoalego, V. (1995). Polyvinylpyrrolidone and polyethylenimine as inhibitors for the corrosion of a low carbon steel in phosphoric acid. *Corrosion Science* 37 (6): 975–985.

**132** Gao, B., Zhang, X., and Sheng, Y. (2008). Studies on preparing and corrosion inhibition behaviour of quaternized polyethyleneimine for low carbon steel in sulfuric acid. *Materials Chemistry and Physics* 108 (2–3): 375–381.

**133** Ansari, K.R., Chauhan, D.S., Quraishi, M.A. et al. (2020). The synergistic influence of polyethyleneimine-grafted graphene oxide and iodide for the protection of steel in acidizing conditions. *RSC Advances* 10 (30): 17739–17751.

**134** McCafferty, E. and Hackerman, N. (1972). Double layer capacitance of iron and corrosion inhibition with polymethylene diamines. *Journal of the Electrochemical Society* 119 (2): 146.

**135** Pakiet, M., Kowalczyk, I.H., Leiva Garcia, R. et al. (2018). Influence of different counterions on gemini surfactants with polyamine platform as corrosion inhibitors for stainless steel AISI 304 in 3 M HCl. *Journal of Molecular Liquids* 268: 824–831.

**136** Al-Sabagh, A.M., Elsabee, M., Elazabawy, O.E., and El-Tabey, A.E. (2010). Corrosion inhibition efficiency of polytriethanolamine surfactants for pipe-lines carbon steel in 1M HCL. *Journal of Dispersion Science and Technology* 31 (10): 1288–1297.

**137** Jeyaprabha, C., Sathiyanarayanan, S., and Venkatachari, G. (2006). Polyaniline as corrosion inhibitor for iron in acid solutions. *Journal of Applied Polymer Science* 101 (4): 2144–2153.

**138** Jeyaprabha, C., Sathiyanarayanan, S., and Venkatachari, G. (2006). Effect of cerium ions on corrosion inhibition of PANI for iron in 0.5 M $H_2SO_4$. *Applied Surface Science* 253 (2): 432–438.

**139** Gomez, H., Ram, M.K., Alvi, F. et al. (2010). Novel synthesis, characterization, and corrosion inhibition properties of nanodiamond−polyaniline films. *Journal of Physical Chemistry C* 114 (44): 18797–18804.

**140** Fuhua, S., Xiutong, W., Jianqiang, Y., and Baorong, H. (2011). Corrosion inhibition by polyaniline copolymer of mild steel in hydrochloric acid solution. *Anti-Corrosion Methods and Materials* 58 (3): 111–115.

**141** Srivastava, V. and Singh, M.M. (2010). Corrosion inhibition of mild steel in acidic medium by poly (aniline-co-o-toluidine) doped with p-toluene sulphonic acid. *Journal of Applied Electrochemistry* 40 (12): 2135–2143.

**142** Manivel, P., Sathiyanarayanan, S., and Venkatachari, G. (2008). Synthesis of poly(p-phenylene diamine) and its corrosion inhibition effect on iron in 1M HCl. *Journal of Applied Polymer Science* 110 (5): 2807–2814.

**143** Abd El Rehim, S.S., Sayyah, S.M., El-Deeb, M.M. et al. (2010). Poly(o-phenylenediamine) as an inhibitor of mild steel corrosion in HCl solution. *Materials Chemistry and Physics* 123 (1): 20–27.

**144** Liebscher, J. (2019). Chemistry of polydopamine – scope, variation, and limitation. *European Journal of Organic Chemistry* 2019 (31–32): 4976–4994.

**145** Yang, F., Li, X., Dai, Z. et al. (2017). Corrosion inhibition of polydopamine nanoparticles on mild steel in hydrochloric acid solution. *International Journal of Electrochemical Science* 12 (8): 7469–7480.

**146** Habibiyan, A., Ramezanzadeh, B., Mahdavian, M., and Kasaeian, M. (2020). Facile size and chemistry-controlled synthesis of mussel-inspired bio-polymers based on polydopamine nanospheres: application as eco-friendly corrosion inhibitors for mild steel against aqueous acidic solution. *Journal of Molecular Liquids* 298: 111974.

**147** Sánchez-Ferrer, A., Rogez, D., and Martinoty, P. (2010). Synthesis and characterization of new polyurea elastomers by sol/gel chemistry. *Macromolecular Chemistry and Physics* 211 (15): 1712–1721.

**148** Lebrini, M., Bentiss, F., Chihib, N.E. et al. (2008). Polyphosphate derivatives of guanidine and urea copolymer: inhibiting corrosion effect of Armco iron in acid solution and antibacterial activity. *Corrosion Science* 50 (10): 2914–2918.

**149** Aly, K.I., Abbady, M.A., Mahgoub, S.A., and Hussein, M.A. (2009). New polymer syntheses, Part 44: synthesis, characterization, and corrosion inhibition behavior of new polyurea derivatives based on diaryl ether in the polymers backbone. *Journal of Applied Polymer Science* 112 (2): 620–628.

**150** Aly, K.I., Wahdan, M.H., and Hussein, M.A. (2009). New polymer syntheses, Part 43: novel polyamides-based diarylidenecyclopentanone: synthesis, characterization, and corrosion inhibition behavior. *Journal of Applied Polymer Science* 112 (1): 513–523.

**151** Aly, K.I. and Hussein, M.A. (2010). New polymer syntheses, part 45: corrosion inhibition behavior of novel polyurea derivatives based on diarylidenecycloalkanone moieties in the polymers backbone. *Journal of Polymer Research* 17 (5): 607–620.

**152** Cui, R., Gu, N., and Li, C. (2011). Polyaspartic acid as a green corrosion inhibitor for carbon steel. *Materials and Corrosion* 62 (4): 362–369.

**153** Qian, B., Wang, J., Zheng, M., and Hou, B. (2013). Synergistic effect of polyaspartic acid and iodide ion on corrosion inhibition of mild steel in $H_2SO_4$. *Corrosion Science* 75: 184–192.

**154** Chai, C., Xu, Y., Shi, S. et al. (2018). Functional polyaspartic acid derivatives as eco-friendly corrosion inhibitors for mild steel in 0.5 M $H_2SO_4$ solution. *RSC Advances* 8 (44): 24970–24981.

**155** Chai, C., Xu, Y., Xu, Y. et al. (2020). Dopamine-modified polyaspartic acid as a green corrosion inhibitor for mild steel in acid solution. *European Polymer Journal* 137 (July): 109946.

**156** Umoren, S.A., Ogbobe, O., Okafor, P.C., and Ebenso, E.E. (2007). Polyethylene glycol and polyvinyl alcohol as corrosion inhibitors for aluminium in acidic medium. *Journal of Applied Polymer Science* 105 (6): 3363–3370.

**157** Umoren, S. and Gasem, Z. (2014). Influence of molecular weight on mild steel corrosion inhibition effect by polyvinyl alcohol in hydrochloric acid solution. *Journal of Dispersion Science and Technology* 35 (8): 1181–1190.

**158** Umoren, S.A., Obot, I.B., Madhankumar, A., and Gasem, Z.M. (2015). Effect of degree of hydrolysis of polyvinyl alcohol on the corrosion inhibition of steel: theoretical and experimental studies. *Journal of Adhesion Science and Technology* 29 (4): 271–295.

**159** Umoren, S.A., Ogbobe, O., Ebenso, E.E., and Ekpe, U.J. (2006). Effect of halide ions on the corrosion inhibition of mild steel in acidic medium using polyvinyl alcohol. *Pigment & Resin Technology* 35 (5): 284–292.

**160** Mobin, M. and Khan, M.A. (2013). Synergistic influence of polyvinyl alcohol and surfactants on the corrosion inhibition of mild steel in 0.1 M $H_2SO_4$. *Chemical Engineering Communications* 200 (9): 1149–1169.

**161** Srimathi, M., Rajalakshmi, R., and Subhashini, S. (2014). Polyvinyl alcohol-sulphanilic acid water soluble composite as corrosion inhibitor for mild steel in hydrochloric acid medium. *Arabian Journal of Chemistry* 7 (5): 647–656.

**162** Sabirneeza, A.A.F., Subhashini, S., and Rajalakshmi, R. (2013). Water soluble conducting polymer composite of polyvinyl alcohol and leucine: an effective acid corrosion inhibitor for mild steel. *Materials and Corrosion* 64 (1): 74–82.

**163** Sabirneeza, A.A.F. and Subhashini, S. (2014). Poly(vinyl alcohol–proline) as corrosion inhibitor for mild steel in 1M hydrochloric acid. *International Journal of Industrial Chemistry* 5 (3–4): 111–120.

**164** Karthikaiselvi, R., Subhashini, S., and Rajalakshmi, R. (2012). Poly (vinyl alcohol - aniline) water soluble composite as corrosion inhibitor for mild steel in 1 M HCl. *Arabian Journal of Chemistry* 5 (4): 517–522.

**165** Karthikaiselvi, R. and Subhashini, S. (2014). Study of adsorption properties and inhibition of mild steel corrosion in hydrochloric acid media by water soluble composite poly (vinyl alcohol-o-methoxy aniline). *Journal of the Association of Arab Universities for Basic and Applied Sciences* 16: 74–82.

**166** Subhashini, S. and Sabirneeza, A.A.F. (2011). Gravimetric and electrochemical investigation of water soluble poly(vinyl alcohol-threonine) as corrosion inhibitor for mild steel. *Lecture Notes in Computational Science and Engineering* 2194 (1): 657–662.

**167** Geethanjali, R. and Subhashini, S. (2014). Synthesis of water soluble polyvinyl alcohol-based terpolymer and evaluation of corrosion inhibition property on mild steel in hydrochloric acid. *Research Journal of Recent Sciences* 3 (March): 170–176.

**168** Alaoui, K., El Kacimi, Y., Galai, M. et al. (2016). Anti-corrosive properties of polyvinyl-alcohol for carbon steel in hydrochloric acid media: electrochemical and thermodynamic investigation. *Journal of Materials and Environmental Science* 7 (7): 2389–2403.

**169** Shukla, J. and Pitre, K.S. (2005). Corrosion and inhibition kinetics of PVA polymer on carbon steel in sulfuric acid solution. *Indian Journal of Chemistry - Section A* 44 (11): 2270–2273.

**170** Nwanonenyi, S.C., Obasi, H.C., Oguzie, E.E. et al. (2017). Inhibition and adsorption of polyvinyl acetate (PVAc) on the corrosion of aluminium in sulphuric and hydrochloric acid environment. *Journal of Bio- and Tribo-Corrosion* 3 (4): 1–13.

**171** Noor El-Din, M.R.N. and Khamis, E.A. (2015). Utilization of sulfidated poly (acrylamide-vinyl acetate) as a new corrosion inhibitor for carbon steel in acidic media. *Journal of Industrial and Engineering Chemistry* 24: 342–350.

**172** Umoren, S.A., Li, Y., and Wang, F.H. (2010). Effect of polyacrylic acid on the corrosion behaviour of aluminium in sulphuric acid solution. *Journal of Solid State Electrochemistry* 14 (12): 2293–2305.

**173** Umoren, S.A., Pan, C., Li, Y., and Wang, F.H. (2014). Elucidation of mechanism of corrosion inhibition by polyacrylic acid and synergistic action with iodide ions by in-situ AFM. *Journal of Adhesion Science and Technology* 28 (1): 31–37.

**174** Umoren, S.A., Li, Y., and Wang, F.H. (2011). Effect of aluminium microstructure on corrosion and inhibiting effect of polyacrylic acid in $H_2SO_4$ solution. *Journal of Applied Electrochemistry* 41 (3): 307–315.

**175** Syed, J.A., Tang, S., Lu, H., and Meng, X. (2015). Water soluble polyaniline-polyacrylic acid composites as efficient corrosion inhibitors for 316SS. *Industrial and Engineering Chemistry Research* 54 (11): 2950–2959.

**176** Dwivedi, A., Bharti, P.K., and Shukla, S.K. (2018). Interaction of water soluble polyacrylic acid with mild steel/hydrochloric acid interface. *IOP Conference Series: Materials Science and Engineering* 404 (1): 012044.

**177** Ouass, A., Galai, M., Ouakki, M. et al. (2021). Poly(sodium acrylate) and poly(acrylic acid sodium) as an eco-friendly corrosion inhibitor of mild steel in normal hydrochloric acid: experimental, spectroscopic and theoretical approach. *Journal of Applied Electrochemistry* 51 (7): 1009–1032.

**178** Zeng, Y., He, Z., Hua, Q. et al. (2020). Polyacrylonitrile infused in a modified honeycomb aluminum alloy bipolar plate and its acid corrosion resistance. *ACS Omega* 5 (27): 16976–16985.

**179** Umoren, S.A. and Solomon, M.M. (2010). Effect of halide ions additives on the corrosion inhibition of aluminum in HCl by polyacrylamide. *Arabian Journal for Science and Engineering* 35 (2A): 115–129.

**180** Umoren, S.A., Li, Y., and Wang, F.H. (2010). Electrochemical study of corrosion inhibition and adsorption behavior for pure iron by polyacrylamide in $H_2SO_4$: synergistic effect of iodide ions. *Corrosion Science* 52 (5): 1777–1786.

**181** Mansri, A., Bouras, B., Tennouga, L., and Medjahed, K. (2012). Effect of iodide ion on corrosion inhibition of mild steel in 1M $H_2SO_4$ by polyacrylamide with different macromolecular weight and polyacrylamide poly4-vinylpyridine mixture. *Der Pharma Chemica* 4 (5): 1803–1811.

**182** Beniken, M., Driouch, M., Sfaira, M. et al. (2018). Anticorrosion activity of a polyacrylamide with high molecular weight on C-steel in acidic media: part 1. *Journal of Bio- and Tribo-Corrosion* 4 (3): 1–14.

**183** Roy, P., Karfa, P., Adhikari, U., and Sukul, D. (2014). Corrosion inhibition of mild steel in acidic medium by polyacrylamide grafted Guar gum with various grafting percentage: effect of intramolecular synergism. *Corrosion Science* 88: 246–253.

**184** Atta, A.M., El-Azabawy, O.E., Ismail, H.S., and Hegazy, M.A. (2011). Novel dispersed magnetite core-shell nanogel polymers as corrosion inhibitors for carbon steel in acidic medium. *Corrosion Science* 53 (5): 1680–1689.

**185** Jadaa, R.J., Abd, A.N., and Khadom, A.A. (2021). Polyacrylamide as a corrosion inhibitor for mild steel in 2 M phosphoric acid: experimental and theoretical studies. *Chemical Papers* 75 (10): 5375–5386.

**186** Azzam, E.M.S., El-Salam, H.M.A., Mohamed, R.A. et al. (2018). Control the corrosion of mild steel using synthesized polymers based on polyacrylamide. *Egyptian Journal of Petroleum* 27 (4): 897–910.

**187** Karthikaiselvi, R. and Subhashini, S. (2017). The water soluble composite poly(vinylpyrrolidone–methylaniline): a new class of corrosion inhibitors of mild steel in hydrochloric acid media. *Arabian Journal of Chemistry* 10: S627–S635.

**188** Atta, A.M., Allohedan, H.A., El-Mahdy, G.A., and Ezzat, A.R.O. (2013). (2013) Application of stabilized silver nanoparticles as thin films as corrosion inhibitors for carbon steel alloy in 1M hydrochloric acid. *Journal of Nanomaterials* .

**189** Khaled, M. (2010). The effect of molecular weight on the corrosion protection properties of polyvinylpyrrolidone polymers on stainless steel. *Arabian Journal for Science and Engineering* 35 (1): 29.

**190** Ding, Q. and Chen, S. (2015). Corrosion inhibition of poly N-vinyl imidazole for Q235 steel in HCl solution. *Journal of Chinese Society for Corrosion and Protection* 35 (1): 55–60.

**191** Eduok, U., Ohaeri, E., and Szpunar, J. (2018). Electrochemical and surface analyses of X70 steel corrosion in simulated acid pickling medium: effect of poly (N-vinyl imidazole) grafted carboxymethyl chitosan additive. *Electrochimica Acta* 278: 302–312.

**192** Öncül, A., Çoban, K., Sezer, E., and Şenkal, B.F. (2011). Inhibition of the corrosion of stainless steel by poly-N-vinylimidazole and N-vinylimidazole. *Progress in Organic Coatings* 71 (2): 167–172.

**193** Shittu, M.D., Olawale, J.O., Adeoye, M.O. et al. (2014). Investigation of corrosion resistance of polystyrene as an inhibitor in hydrochloric and tetra-oxo sulphate VI acids. *International Journal of Materials and Chemistry* 4 (1): 9–13.

**194** Wang, X. and Xing, J. (2020). Polystyrene sulfonic acid-doped polypyrrol (dppy) as a corrosion inhibitor for carbon steel in 1.0 M HCl solution. *International Journal of Electrochemical Science* 15 (2): 1606–1621.

**195** Umoren, S.A., Li, Y., and Wang, F.H. (2010). Synergistic effect of iodide ion and polyacrylic acid on corrosion inhibition of iron in $H_2SO_4$ investigated by electrochemical techniques. *Corrosion Science* 52 (7): 2422–2429.

**196** Srivastava, V. and Sitashree Banerjee, M.M.S. (2010). Inhibitive effect of polyacrylamide grafted with fenugreek mucilage on corrosion of mild steel in 0.5 M $H_2SO_4$ at 35 °C. *Journal of Applied Polymer Science* 116: 810–816.

**197** Beniken, M., Driouch, M., Sfaira, M. et al. (2018). Kinetic–thermodynamic properties of a polyacrylamide on corrosion inhibition for C-steel in 1.0 M HCl medium: part 2. *Journal of Bio- and Tribo-Corrosion* 4 (3): 1–13.

**198** Umoren, S.A. and Ebenso, E.E. (2008). Blends of polyvinyl pyrrolidone and polyacrylamide as corrosion inhibitors for aluminium in acidic medium. *Indian Journal of Chemical Technology* 15 (4): 355–363.

**199** Umoren, S.A., Eduok, U.M., and Solomon, M.M. (2014). Effect of polyvinylpyrrolidone-polyethylene glycol blends on the corrosion inhibition of aluminium in HCl solution. *Pigment & Resin Technology* 43 (5): 299–313.

**200** Schlenoff, J.B. (2014). Zwitteration: coating surfaces with zwitterionic functionality to reduce nonspecific adsorption. *Langmuir* 30 (32): 9625–9636.

**201** Jafar Mazumder, M.A. (2019). New, amino acid based zwitterionic polymers as promising corrosion inhibitors of mild steel in 1 M HCl. *Coatings* 9 (10): 675.

**202** Aldahdooh, M.K. and Ali, S.A. (2020). Synthesis and application of a poly(bis-zwitterion) containing chelating motifs of N-(2-aminoethyl)iminodiacetic acid. *European Polymer Journal* 141 (September): 110071.

**203** Jafar Mazumder, M.A. (2019). Synthesis, characterization and electrochemical analysis of cysteine modified polymers for corrosion inhibition of mild steel in aqueous 1 M HCl. *RSC Advances* 9 (8): 4277–4294.

# 12

# Polymeric Corrosion Inhibitors for Microbiologically Influenced Corrosion

*Chaitanya Kumar, Mohan Yama, and Jaya Rawat*

*Bharat Petroleum Corporate R&D Centre, Corrosion & Fouling Division, Plot No. 2A, Udyog Kendra, Surajpur (PO), Gautam Buddha Nagar (Dist), Greater Noida, Uttar Pradesh 201306, India*

## 12.1 Introduction to Microbiologically Influenced Corrosion (MIC)

The accelerated deterioration of metal due to the metabolic activity of microorganisms is referred to as microbiologically influenced or induced corrosion (MIC), also known as Bio-corrosion. MIC is a major problem in most of the industries. It is caused by microbes in biofilms. The microbes in bulk fluid initially attach to the surface and form metabolically active colonies in presence of water and a carbon/energy source. In course of time, microbial growth in these colonies leads to the formation of a biofilm. Metabolic activity of microbes within biofilms formed on metallic surfaces affect the kinetics of cathodic and/or anodic reactions and also considerably modifies the chemistry of any protective layers, leading to either acceleration or inhibition of corrosion [1]. Through physiologically different metabolic processes, the microbes in such biofilms can grow either aerobically or anaerobically and generate metabolites such as hydrogen sulfide, methane, organic acids, carbon dioxide, and iron oxides. This results in electron transfer and corrosion directly or indirectly via numerous mechanisms. The exact types of microorganisms involved in a particular case depend on the nature of the material, the environmental conditions, and the content of certain impurities e.g. sulfur content and moisture content. MIC is basically a result of interactions between microorganisms (microbiology) and their surrounding environment comprising of media (chemical composition and physical parameters like temperature and flow) and the metals (metallurgy) [2]. Heterogeneous reactions inside a biofilm cause negative effects like material deterioration, increase in corrosion rate, and heat transfer resistance [3]. The development of a biofilm is aided by the production of extracellular polymeric substances (EPS) comprising microbial biopolymers such as polysaccharides, lipids, proteins, and nucleic acids. The binding of EPS to metal ions is critical in MIC and depends both on the type of metal ion and the microbial species. Depending on the environment, proliferation of microbes

*Polymeric Corrosion Inhibitors for Greening the Chemical and Petrochemical Industry*, First Edition.
Edited by Mohammad A. Jafar Mazumder, Mumtaz A. Quraishi, and Amir Al-Ahmed.

and EPS production results in a mature biofilm within a relatively short time [4]. The biofilm ameliorates corrosion at the interface between the metal and bulk solution by altering the chemistry such as pH, oxygen levels, and nutrients. This alteration of the chemistry leads to major changes in the active or passive properties of the metal as well as the corrosion products formed. Some of the important microbes considered to play a crucial role in the MIC are discussed in the following section.

## 12.2 Microbes in MIC

Although a variety of microorganisms including archaea, fungi, and algae are considered to be directly or indirectly influencing the process of corrosion only few classes of bacteria shall be discussed here. The major organisms responsible for MIC are broadly identified as sulfur reducing bacteria (SRB), sulfur oxidizing bacteria (SOB), acid producing bacteria (APB), manganese and iron oxidizing bacteria (MFOB), iron reducing bacteria (IRB), slime producing bacteria, and methanogens. These microbes typically coexist forming a complex biofilm on the corroding metal surfaces. A complete understanding of the exact mechanism of the MIC is still not known.

### 12.2.1 Sulfur Reducing Bacteria

SRB is widespread in many natural environments and considered to be one of the main culprits of MIC. In addition to sulfates, SRB also could reduce sulfite, thiosulfate, and elementary sulfur to sulfides. Under anaerobic conditions, these bacteria gain energy by reduction of the sulfate to hydrogen sulfide using the electrons derived from the oxidation of organic matter [5]. Majority of SRB belongs to Deltaproteobacteria and some gram positive *Clostridia* [6]. It is proposed that these electrons are transported from the metal surface to the sulfate reduction pathway via a hydrogen intermediate which is produced by the action of hydrogenase enzymes. The hydrogenases in SRB are among the most well-studied group of enzymes in MIC [7]. SRB-mediated corrosion is reported to be primarily of two types – electrical MIC (EMIC) and chemical MIC (CMIC). EMIC is considered more prevalent in which direct electron transfer occurs between the metal substrate and SRB. In CMIC, corrosion is induced by hydrogen sulfide formed due to sulfate reduction [8]. Almost all metals form metal oxides under aqueous environments. Copper alloys and carbon steel used in the pipelines and storage tanks in industries are prone to SRB-induced corrosion due to the reaction between the sulfide produced by SRB and the metal oxides resulting in the formation of metal sulfides [9].

### 12.2.2 Metal Oxidizing Bacteria (MOB)

Metal oxidizing organisms like manganese (Mn) and iron (Fe) oxidizing bacteria are also often reported to be causative microorganisms for MIC. These two groups of organisms can attach to surfaces and produce metal oxide/hydroxide/oxyhydroxide deposits. Under certain favorable conditions, such deposits can induce corrosion of few metals and alloys.

Aerobic iron-oxidizing bacteria like *Pseudomicrobium* sp. and *Gallionella* sp. obtain their energy by oxidizing ferrous ($Fe^{2+}$) to ferric ion ($Fe^{3+}$). They deposit ferric oxide on carbon steel pipeline surfaces and promote tubercle formation which has a steep pH gradient, the pH at the bottom being the lowest. At very low pH, ferric salts cannot protect the metal surface from further corrosion due to chemical activity. Some of the *Pseudomonas* sp. has also been implicated in the reduction of $Fe^{3+}$ to $Fe^{2+}$ ion. This reduction results in the removal of protective layer since most of the ferrous salts are soluble in nature. Thus, iron oxidizing/reducing microbes promotes corrosion directly. Manganese-oxidizing bacteria (MnOB) oxidize soluble divalent manganese ($Mn^{2+}$) to the insoluble manganic ($Mn^{3+}$ and $Mn^{4+}$) oxides. Some bacteria such as *Leptothrix* sp., can oxidize both soluble $Fe^{2+}$ and $Mn^{2+}$. The deposition of manganic oxides creates an anaerobic environment that favors the growth of SRB [10].

### 12.2.3 Acid Producing Bacteria (APB)

APB is another major group of microbes involved in MIC. The most corrosive metabolites are produced by these types of bacteria. Acetic and butyric acid are the example of such corrosive microbial products. Sulfur oxidizing bacteria like *Thiobacillus* sp. produce sulfuric acid from sulfur or sulfide. Though the exact mechanism of MIC is not clearly known it is widely accepted and reported that the first and foremost significant activity of all the microbes is to form a biofilm on the metal surface.

## 12.3 Biofilms

Biofilms are defined as heterogeneous populations of different types of microorganisms like bacteria, algae, protozoa, and fungi which accumulate at interfaces and excrete extra polymeric substances (EPS) resulting in microbial cells entrapment in a highly hydrated slime. EPS is a heterogeneous mixture of various biomolecules like polysaccharides, proteins, amphiphilic polymers, lipids, and nucleic acids which facilitates the attachment of microbial communities on the surface. In contrast to single-celled organisms which freely float or swim in the bulk liquid (planktonic form), biofilms form predominantly on solid surface (substratum) interfaces in aqueous systems [3]. The presence of a biofilm results in formation of localized environments with distinct characteristics of pH and redox conditions which results in the transport of reactive chemical species from or toward the metal surface [11]. This consortium of microbes, EPS, and solid corrosion by-products form a complex reactive surface that induces corrosion mechanism (Figure 12.1).

Formation of bacterial biofilms on metal surface may hasten or hinder corrosion. Microbial biofilms formed due to colonization of various microbes form

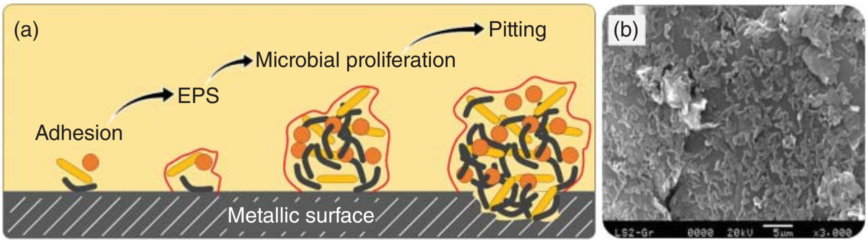

**Figure 12.1** (a) Steps involved in biofilm formation (b) scanning electron micrograph (SEM) of a biofilm.

nonuniform patches on the metallic surface. Areas below thicker patches are proposed to become anodic in nature due to higher respiration activity and lower oxygen concentration while areas under thinner patches become cathodic in nature due to less respiration and relatively higher oxygen concentrations. This formation of distinct aeration areas induces corrosion below the biofilms. Javaherdashti proposed an alternative term "temenos" to indicate biofilm since the terminology was misleading [12]. The Greek word "temenos" means to cut off which emphasizes that the conditions under the biofilm are completely different from the bulk solution. Further, the biological content of the biofilm is relatively smaller compared to the nonorganic content which is estimated to be 60–70% of the total dry weight of a biofilm.

### 12.3.1 Biofilm Studies and Characterization

Biofilm studies are highly interdisciplinary in nature involving researchers from various backgrounds like microbiologists, chemists, modeling, and simulation engineers. The analysis of biofilms includes microscopic studies, microbiological, and molecular biological studies and also physicochemical methods. Microbiologists study the biofilm in laboratories through microcosms of bacterial consortia which present a simplified in vitro ecosystem simulating natural environments under controlled laboratory conditions. Experimental setup of microcosms to check the MIC by different bacterial group has been studied extensively. It helps to understand the microbiological influence to propagate corrosion in actual system. In laboratory conditions, MIC studies in microcosm setups of microbial consortia with iron/carbon steel coupons are evaluated by weight loss method, pit formation analysis, and biofilm composition evaluation after few days to months of incubation. Molecular biology techniques like denaturing gradient gel electrophoresis (DGGE), polymerase chain reaction (PCR), and fluorescence in situ hybridization (FISH) are some of the major techniques used to study and analyze biofilms. Confocal laser scanning microscopy, atomic force microscopy, SEM, and nuclear magnetic resonance spectroscopy are some of the surface characterization techniques employed to characterize the biofilms [3].

## 12.4 MIC Issues in Industry: Oil and Gas

Microbial presence in processing units of industries is mainly observed in aqueous/hydrated zones where there are ambient conditions for growth of microbes. In various hydrocarbon systems, these problems are getting alleviated due to presence of hydrocarbon-degrading bacteria along with APB and SRB. The major cases observed in hydrocarbon industry related to MIC are:

### 12.4.1 Pipeline Internal Corrosion

(a) Off-shore and on-shore pipelines where major failures are observed in low-lying areas where there are probabilities of stagnation or low liquid flow/velocities.
(b) Many of the pipelines face problems of lower capacity utilization and suffer from being idle for some days. These operational issues favor microbes for their better growth and increase corrosion thereafter.
(c) During the project execution of pipeline laying, there may be some time delay in project completion resulting in exposure of pipeline material to atmosphere. Further, improper drying of pipeline after hydrotesting can also create problems of MIC.
(d) Several products either crude oils or finished hydrocarbon products like gasoline, diesel, or kerosene may also have some contaminations of water/dissolved oxygen/acidic or sulfur compounds which may initiate internal corrosion and attract microbial growth and proliferation in some areas [10, 13, 14].

### 12.4.2 Water Network Systems

Water network is highly prone to microbial growth. In refineries and installations, the MIC issues are observed in coolers, cooling water, or ETP network and other related utilities.

### 12.4.3 Hydrocarbon Product Storage Tanks

Microbial presence in sludge samples of tank bottom of crude oil and other hydrocarbons is generally observed while cleaning. This is mostly due to moisture contaminations in bottom areas.

There is no established relationship between the number of microorganisms and the corresponding corrosion rate. However, presence of these MIC causing microbes requires suitable measures to be taken for alleviation of the microbes. Mechanical scraping of pipelines using pigs, use of expensive metal alloys like carbon steel for storage and transportation, use of antimicrobial coatings, injection of chemical biocides, and corrosion inhibitors are some of the current methodologies practiced in the industry to mitigate MIC. The details of application of corrosion inhibitors to mitigate MIC is discussed below.

## 12.5 Corrosion Inhibitors for MIC

Corrosion inhibitors are chemical substances that reduce or retard corrosion processes when added in minimal quantities into the corrosive medium. The category and quantity of corrosion inhibitor depends on aggressiveness of the environment. Corrosion inhibition is dependent on the shielding structures formed on metal surface. If cathodic reaction is retarded by corrosion inhibitor, then it is called as cathodic inhibitor and if anodic reaction is retarded it is called as anodic corrosion inhibitor. Some moieties affect both cathodic and anodic corrosive reactions and these are called as mixed corrosion inhibitors. There are two classes of corrosion inhibitors – organic and inorganic inhibitors. Chromate is used as inorganic type to mitigate the corrosion of iron and its alloys. However, chromate ions are not recommended due to environmental concerns. Organic corrosion inhibitors typically have three fundamental structural requirements, which include (i) an anchoring functional group, (ii) backbone structure, and (iii) substituent functional group. The anchoring groups are helpful in attachment of corrosion inhibitors onto the surface of metal and change the metal/solution interface due to nonuniform scattering of electrical charges [15]. These functional groups usually comprise one or more heteroatoms, viz., sulfur, nitrogen, oxygen, or phosphorous [16]. The backbone feature of the corrosion inhibitor provides bonding strength and surface coverage over metal surface. The backbone generally comprises additional substituent atoms and groups. The common corrosion inhibiting additives employed in oil and gas industry are surface-active, polar organic moieties and most of them are amines or amine salt by-products [17]. These groups interact with several interfaces, which include metal–oil, metal–water, oil–water, oil–gas, water–gas, and metal–gas.

Corrosion inhibition is achieved by two different mechanisms, viz. (i) by decreasing the aggressive nature of corrosive medium and (ii) via adsorption of corrosion inhibitor molecules on metal surfaces as barriers [15]. There are four different types of corrosion inhibitors employed in MIC, which are discussed below.

### 12.5.1 Inorganic Corrosion Inhibitors

Arsenic and selenium species retard the cathodic reaction by arresting the oxygen diffusion. Oxyanions of chromates, molybdates, nitrites, tungstates, and rare earth metals are helpful in filling the passive iron oxide film defects [18, 19]. Zhong et al. studied the inhibiting effect of free nitrous acid over microbial corrosion in a simulated water injection system. 0.49 ppm of free nitrous acid exhibited an inhibition efficiency (IE) of 31% [20]. The authors have also demonstrated the synergistic effect of free nitrous acid and *N*-*b*-hydroxyethyl oleyl imidazoline as corrosion inhibitors and an IE of 50% achieved [20].

### 12.5.2 Organic Corrosion Inhibitors

Imidazoline and its derivative corrosion inhibitors have been extensively used in oilfield pipelines for last few decades [21]. Forsyth et al. and other researchers extensively studied the corrosion inhibition of steel by a variety of rare earth environment friendly organic compounds [22–28]. Lanthanum 4-hydroxycinnamate and imidazolinium 4-hydroxycinnamate have shown significant abiotic corrosion inhibition on the HY80 high strength steel in artificial seawater environment [29]. Cetrimonium nalidixate is also reported as microbial corrosion inhibitor for single strain bacteria on mild steel in chloride environment [30]. However, the rare earth metal type corrosion inhibitors are unstable in nature and it is a big limitation in these type of corrosion inhibitors [31].

Sheng et al. have employed 2-methyl-benzimidazole as corrosion inhibitor to mitigate MIC caused by SRB for both mild steel and 316 stainless steel [32]. Sodium pyrithione and benzyldimethyl-dodecylammonium chloride are also employed as corrosion inhibiting agent for X80 carbon steel and stainless steel respectively to mitigate MIC caused by SRB [33, 34]. ZnO-interlinked chitosan nanoparticles are employed for mixed-type SRB corrosion inhibition of pipeline steel [35]. Polyacrylamide inhibitor is used for L360 pipeline steel to control SRB and total general bacteria growth on metal surface [36]. Cationic gemini surfactant inhibitor is employed to block the biofilm development of sulfidogenic bacteria on mild steel surface [37, 38]. Alginates polymeric corrosion inhibitors are useful in controlling the growth of Gram +ve, Gram −ve bacteria, and also fungi on mild steel surface [39]. Different types of amino acids in combination with tetra-hydroxyl methylphosphonium sulfate (THPS), successfully inhibited the microbial corrosion caused by SRB [40].

### 12.5.3 Green Corrosion Inhibitors

As the chemical corrosion inhibitors are environmentally hazardous, there is demand for environmentally friendly green corrosion inhibitors in many industries, due to their renewable characteristics, ease of availability, lower costs, biodegradable, and biocompatible nature. These are attained from various natural products, such as plant extracts, herbs, and extracellular substances from bacteria [41, 42].

The inhibitive mechanism of green corrosion inhibitors depend on heterocyclic organic moieties viz., alkaloids, flavonoids, cellulose, tannins, and polycyclic molecules, which are helpful in film formation on metal surface [43]. The eco-friendly green corrosion inhibitors are classified according to their availability in different origins as follow [44],

1. Amino acids
2. Biosurfactants
3. Carbohydrates
4. Medicines
5. Natural gums
6. Oleochemicals
7. Plant extracts
8. Polymers.

The research focused on green corrosion inhibitors was initiated in 1900s. *Chelidonium majus* was used as the first green corrosion inhibitor, which has

**Table 12.1** Green corrosion inhibitors on different metals.

| S. No. | Metal | Corrosion inhibitor | References |
|---|---|---|---|
| 1 | Aluminum | Cassava starch, exudate gum | [47, 48] |
| 2 | Carbon steel | Neem extract, chitosan-based nanocomposite, Etoricoxib, *Daphne gnidium* | [49–52] |
| 3 | Copper | Chitosan polymer, tobacco | [53, 54] |
| 4 | Mild steel | *Artemisia pallens*, *Moringa oleifera* leaves, *Carica papaya* peels, ginger extract, *Musa paradisiaca* peel extract, *M. oleifera* leaf extract, *Polyalthia longifolia* plant extract | [55–60] |
| 5 | Austenitic steels | *Allium cepa* extract, *Cistus ladanifer* leaf, *Aloe vera* extract, *Myrtus communis* extract, sodium pyrithione, *Salvia officinalis*, *Costus afar* leaves extract, *Aloe barbadensis* extract, *Citrus reticulata* peels extract mediated copper nanoparticles composite | [33, 45, 60–64] |
| 6 | Zinc | Chitosan polymer, tobacco | [53, 54] |

shown better efficiency than synthetic corrosion inhibitors [45, 46]. Few of the green corrosion inhibitors on different metals are shown in Table 12.1.

## 12.6 Polymeric Corrosion Inhibitors

Enactment of polymers as corrosion mitigating agents is found to be an innovative methodology due to their architecture which includes branched and linear chains, rotaxanes, crosslinks, comb-like, and dendrimeric structures. Polymers have certain leads of multi-functionality, solubility, malleable viscosity, improved adherence to metal surfaces, and superior film-developing abilities in comparison to general corrosion inhibitors (organic or inorganic), which are at small molecular level [65]. Smart crafting features of repetitive functional groups in the polymer chain with many number of binding groups provide large surface area over metal surface, which leads to efficient corrosion inhibition. The anchoring moiety may be cationic, anionic, nonionic, or ampholytic in nature [66, 67]. Several researchers have already reported on polyamines with long-chain molecules as film-forming corrosion inhibitors [68, 69]. Based on type of functional groups of anchoring side, polymeric corrosion inhibitors are divided into different types, which are shown in Table 12.2.

### 12.6.1 Polymeric Corrosion Inhibitors for Microbial Corrosion

MIC is a severe concern in oil and gas as well as other industries. The worldwide projected economic damage is 20% with a direct cost of 30–50 billion dollars

**Table 12.2** Different types of polymeric corrosion inhibitors.

| Type of polymeric CI | Common types and examples | Reference |
|---|---|---|
| Amine, imine, and amide polymers | (a) *Polyaniline and its derivatives:*<br>Poly(*o*-ethoxy aniline) and $Cl^-$, sulfamic acid–doped poly(*o*-ethoxy aniline), poly(styrene sulfonic acid)–doped polyaniline, pernigraniline, polyanthranilic acid, poly(aniline-formaldehyde), poly(aniline-*co*-orthotoluidine), poly(vinylpyrrolidone-aniline), poly(aniline-*co*-4-amino-3-hydroxy-naphthalene-1-sulfonic acid), poly(vinyl pyrrolidone-methyl aniline), poly(vinyl pyrrolidone-*o*-methoxy aniline), poly(*N*-methyl aniline) + histidine | [70–83] |
| | (b) *Polyamines and its derivatives:*<br>Polymethylene diamines, poly(aminoquinone), poly(diphenylamine), poly(*p*-amino benzoic acid), poly(*p*-toluidine), poly(*p*-phenylenediamine), poly triethanol amine | [78, 84–88] |
| | (c) *Polyimines:*<br>Polyethyleneimine and its quaternary ammonium salts | [89–93] |
| | (d) *Polyamides:*<br>Polyurea derivatives, diarylidene cyclopentanone | [94, 95] |
| Vinyl polymers | (a) *Polyvinylpyridines:*<br>Poly(4-vinylpyridine), poly(4-vinyl pyridine-poly (3-oxide-ethylene) tosyle), poly(vinyl caprolactone-*co*-vinyl pyridine), poly(vinyl imidazol-*co*-vinyl pyridine), poly(4-vinylpyridine-hexadecyl bromide) | [96–99] |
| | (b) *Polyvinyl pyrrolidines:*<br>Polyvinylpyrrolidone and its derivatives | [96, 100] |
| | (c) *Polyvinyl alcohols, acetates, benzenes:*<br>Polyvinyl benzyl trimethyl ammonium chloride, polyvinyl acetate, polyvinyl alcohol | [101, 102] |
| Acryl polymers | (a) *Polyacrylamide:*<br>Polyacrylamide, *N*-(methacryloyloxymethyl) benzotriazole, polymethyl methacrylate, polyethyleneoxide, polyacrylamide-phenyl phosphonate + 50 ppm $Zn^{2+}$, copolymer of acrylamide and 4-vinyl pyridine, fenugreek-g-polyacrylamide, polyacrylamide-g-okra mucilage (polysaccharide), poly(acrylamide-*co*-4-vinylpyridine) + potassium iodide, pectin-g-polyacrylamide and acrylic acid, acrylate copolymer + isothiazolone + zinc phosphonates, terpolymer of methyl methacrylate/butyl acrylate/acrylic acid | [103–113] |
| | (b) *Polyacrylic acid* | [114] |

*(Continued)*

**Table 12.2** (Continued)

| Type of polymeric CI | Common types and examples | Reference |
|---|---|---|
| Phosphate esters polymers | *Poly-oxyalkylated thiolates, polyisobutylene succinic esters* | [115–118] |
| Polysulfides | *Polysulfides* | [119–123] |
| Bio-polymers | (a) Chitosan derivatives: acetyl thiourea chitosan polymer, (b) *Cellulose derivatives:* carboxy methylcellulose, hydroxyl ethyl cellulose, starch, (c) Guar gum, (d) carrageenan, (e) medipolymorphol, (f) dextran, (g) kraft lignin, (h) soda lignin | [100, 124–131] |
| Other polymers | (a) Polymaleic acid derivatives<br>(b) Polyethylene glycol derivatives<br>(c) Polyaspertic acid derivatives<br>(d) Terpolymers derivatives | [42, 132–135] |

per annum [136, 137]. Various microbial corrosion inhibition methods such as biocides, cathodic protection, bacterial biofilms, and coatings have been employed in many industries [138–141]. Due to characteristics like impermeability, good adhesion, abrasion resistance, flexibility, and biocompatibility, polyurethanes have been used to retard microbial corrosion for past few decades [139–143]. However, polyurethanes undergo degradation in microbial matrix [144–146].

Tiwari and Hihara demonstrated the incorporation of polyisocyanate-modified graphene oxide nanosheets into the polyurethane matrix coating, which showed significant corrosion inhibition properties on aluminum [147]. The increased amount of grafting and crosslinking in its coating retarded the interaction of aqueous environment with aluminum. This coating also exhibited good resistance to salt spray corrosion even after 694 hours. The authors have also reported corrosion protection ability of silicones grafted polymeric coatings over aluminum. These comprise polydimethylsiloxane and its by-products which are used for mitigation of micro-fouling and corrosion [146]. Fourier transform infrared spectroscopy (FTIR) and Raman spectroscopic studies exhibited good bonding nature of silicones with metal surface, which acts as good protection barrier. Thermal studies, X-ray photoelectron spectroscopy (XPS), and field emission scanning electron microscopy (FE-SEM) studies also inferred that these coatings show excellent protection over corrosion for aluminum. Microbial corrosion studies with SRB were also studied by using these silicone backbone coatings. These silicone coating specimens exhibited better protection efficiency than uncoated specimens even after 90 days of immersion in soil (Figure 12.2).

Sugama and Cook studied the effect of natural polysaccharides namely chitosan and poly(itaconic acid) condensation products on aluminum alloy microbial corrosion inhibition by employing thermgravimetric analysis (TGA), FTIR, XPS, contact angle measurements, and electrochemical impedance studies [148]. The FTIR

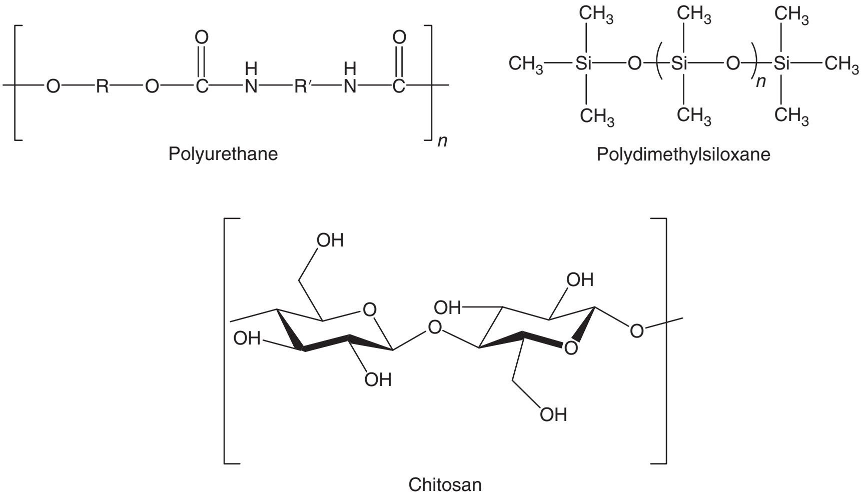
Polyurethane

Polydimethylsiloxane

Chitosan

**Figure 12.2** Structure of polyurethane, polydimethylsiloxane, and chitosan.

and XPS studies confirmed the molecular interactions of grafted chitosan and poly(itaconic acid) over aluminum surface by forming stable bonds. TGA studies were carried out to analyze the moisture uptake of both non-modified chitosan and poly(itaconic acid) modified chitosan coatings over aluminum for 24 hours at 70% humidity. It is evidenced that poly(itaconic acid) modified chitosan coating was less susceptible to moisture than non-modified chitosan coating. Contact angle measurements inferred the good hydrophobicity of poly(itaconic acid) modified chitosan coatings even after 10 days of exposure to aqueous environment. From pore resistance values, which were obtained from EIS studies, it was inferred that poly(itaconic acid) (20%) modified chitosan (80%) coatings have shown excellent corrosion protection efficiency of 99.7% in NaCl environment. Similarly, salt spray resistance of 694 hours was also obtained by using same composition (Figure 12.3).

Quaternary ammonium compounds have been extensively employed as biocides and corrosion inhibitors to mitigate MIC. The synergistic combination of positive quaternary ammonium ions and halide anions shows a raise in corrosion protection. This is accredited to the cohesive Van der Waals' attraction between quaternary ammonium ion/halide ion complex and the positively charged metal ionic surface [149–151]. The quaternary ammonium cations viz., *N*-decyl-*iso*-quinolinium (DIQ), *N*-decyl-triethyl ammonium (DTEA), *N*-decyl-quinolinium (DQ), and *N*-decyl-pyridinium (DP) have shown >90% IE in both sulfuric acid and hydrochloric acid environments. The IEs were obtained by measuring the corrosion current values from EIS data and iron dissolution values in the solution [149]. Qi et al. [151] successfully employed dodecyl dimethyl benzyl ammonium chloride quaternary ammonium salt along with hydroxyethane-1,1-diphosphonic acid (HEDP) and NaClO to retard microbial corrosion by SRB in cooling water network of thermal power plants. The authors have employed potentiodynamic polarization studies and XPS studies to study the effect of above inhibitors on corrosion inhibition of SS316L steel. The degradation mechanisms of quaternary ammonium compounds

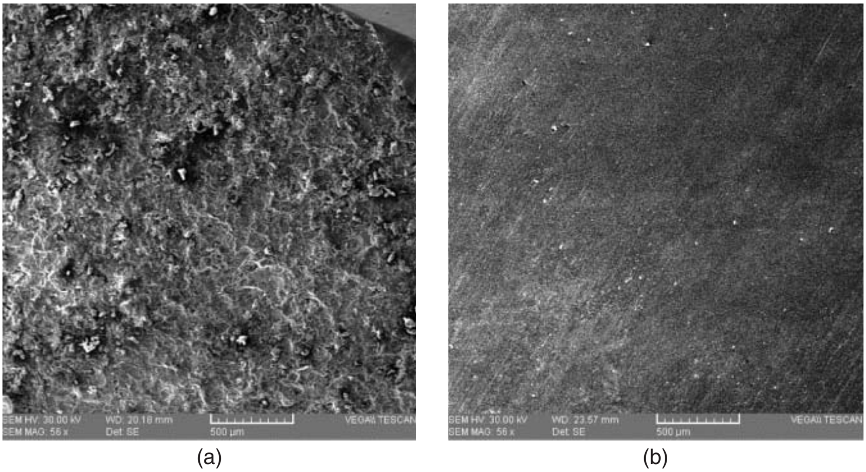

(a) (b)

**Figure 12.3** SEM images of SS316 specimens immersed in saline environment inoculated with SRB after seven days in the (a) absence and (b) presence of copolymer of chitosan.

over plasma membranes of bacterial cells by dissolution of lipids and the discharging of intracellular materials prove that these also act as biocides. Ethambutol hydrochloride nalidixate and cetrimonium nalidixate quaternary ammonium salts were also reported to suppress the growth of *Vibrio alginolyticus* species by acting as biocides [152].

The conducting polymers, polypyrrole (PPy), polyaniline (PANI), and polythiophene (PBT) have good anticorrosion properties over aluminum, mild steel, stainless steels, copper, and its alloys. PANI retards the microbial corrosion with its electrostatic interaction with Gram-negative *Escherichia coli* and Gram-positive *Staphylococcus aureus* by forming positively charged nitrogen [153].

Poly(*N*-methylaniline) microspheres are reported to suppress the growth and proliferation of SRB and remarkably reduced the corrosion rate of carbon steel [153, 154]. Poly(vinyl-*N*-hexylpyridinium bromide) (hexyl-polyvinyl pyridinium) are also employed as corrosion inhibitors to mitigate microbial growth to >99% [155].

#### 12.6.1.1 Corrosion Inhibition by Extracellular Polymeric Substances of Biofilms

Corrosion mitigation by EPS produced by bacteria present within biofilms has shown good efficiency for carbon steel [136, 156], stainless steel [156], aluminum [156–159], and copper [157]. The EPS mainly include polysaccharides, proteins, nucleic acids, and other metabolites. The general mechanisms involve following pathways,

(i) Formation of diffusion barrier layer by biofilms on metal surface, which retards the reaction of corrosive species with metal surface,
(ii) Decreasing the concentration of oxygen in environment by aerobic bacteria. So that the cathodic oxygen reduction reaction in corrosion will be arrested at metal/solution interface,

(iii) Metabolic products that act as corrosion inhibitors (e.g. siderophores),
(iv) Production of antibiotics by certain bacteria sometimes prevents the growth of corrosive microorganisms.

Purwasena et al. [160] studied the corrosion inhibiting effect of polymeric bio-surfactant produced by *Bacillus* sp. on carbon steel. A bio-surfactant produced by *Bacillus* sp. from oil reservoir was used as an antimicrobial agent. Weight loss experiments by using carbon steel coupons inferred that an IE of 48% was obtained by using extracellular polymeric material. SEM examination studies revealed less corrosion in the presence of this bio-surfactant. It is also reported that the EPS produced by *Desulfovibrio alaskensis* mitigated the attachment of the corrosive species of *Desulfovibrio indonesiensis* on steel surfaces. Polarization studies and biofilm studies on stainless steel coupons showed above inhibitive properties of *D. alaskensis* [161]. Quartz crystal microbalance studies showed the deposition of *Desulfovibrio vulgaris* extracellular polymeric substance on high alloy steel surface which alleviates the biofilm adhesion on metal surface [162, 163]. Similar effect was also reported with *Lactobacillus helveticus*'s polymeric substances, which retarded the attachment of *Listeria*. EPS of *Lactobacillus* sp. was also reported as corrosion inhibitor for pathogenic *Enterococcus* [164].

## 12.7 Conclusions

In many industries like oil and gas, thermal power plants, steel, and textile microbiological and chemical corrosion problems coexist at several locations which require proper monitoring and dosage of appropriate additives. Selection of different types of green and polymeric corrosion inhibitors plays major role in general and microbial corrosion mitigation of different metallurgies in various environments. Use of appropriate techniques viz. electrochemical studies, weight loss experiments, XPS, Raman spectroscopy, FTIR, biofilm characterization, and SEM–energy dispersive X-ray (EDX) studies are helpful in selection and evaluation of these polymeric corrosion inhibitors for different metals in different environments. The extracellular polymeric substances of *D. alaskensis*, *D. vulgaris,* and *Lactobacillus* sp. are also used as polymeric corrosion inhibitors to suppress the biofilm formation on metal surfaces. Many of the microbial growth can be controlled or retarded using these types of green and polymeric corrosion inhibitors to a larger extent. In some locations, where microbiological corrosion is found to be severe, use of specific biocide in optimum dosage along with these polymeric corrosion inhibitors at a definite period can reduce corrosion issues substantially.

## References

**1** Beech, I.B. and Sunner, J. (2004). Biocorrosion: towards understanding interactions between biofilms and metals. *Current Opinion in Biotechnology* 15 (3): 181–186.

**2** Little, B.J., Blackwood, D.J., Hinks, J. et al. (2020). Microbially influenced corrosion—any progress? *Corrosion Science* 170 (March): 108641.

**3** Denkhaus, E., Meisen, S., Telgheder, U., and Wingender, J. (2007). Chemical and physical methods for characterisation of biofilms. *Microchimica Acta* 158 (1–2): 1–27.

**4** Penesyan, A., Paulsen, I.T., Kjelleberg, S., and Gillings, M.R. (2021). Three faces of biofilms: a microbial lifestyle, a nascent multicellular organism, and an incubator for diversity. *NPJ Biofilms and Microbiomes* 7 (1): 1–9.

**5** Butlin, K.R., Adams, M.E., and Thomas, M. (1949). The isolation and cultivation of sulphate-reducing bacteria. *Journal of General Microbiology* 3 (1): 46–59.

**6** Muyzer, G. and Stams, A.J.M. (2008). The ecology and biotechnology of sulphate-reducing bacteria. *Nature Reviews Microbiology* 6 (6): 441–454.

**7** Beech, I.B. (2003). Biocorrosion: role of sulfate reducing bacteria. In: *Encyclopedia of Environmental Microbiology* (ed. G. Bitton). Wiley.

**8** Enning, D. and Garrelfs, J. (2014). Corrosion of iron by sulfate-reducing bacteria: new views of an old problem. *Applied and Environmental Microbiology* 80 (4): 1226–1236.

**9** Macdonald, D.D. (1999). Passivity - the key to our metals-based civilization. *Pure and Applied Chemistry* 71 (6): 951–978.

**10** Muthukumar, N., Rajasekar, A., Ponmariappan, S. et al. (2003). Microbiologically influenced corrosion in petroleum product pipelines - a review. *Indian Journal of Experimental Biology* 41 (9): 1012–1022.

**11** Vargas, I.T., Alsina, M.A., Pavissich, J.P. et al. (2014). Multi-technique approach to assess the effects of microbial biofilms involved in copper plumbing corrosion. *Bioelectrochemistry* 97: 15–22.

**12** Javaherdashti, R. (2020). Some thoughts about misconceptions surrounding the term ‘biofilm’. *Corrosion Engineering, Science and Technology* 55 (8): 681–684.

**13** Khan, M.A.A., Hussain, M., and Djavanroodi, F. (2021). Microbiologically influenced corrosion in oil and gas industries: a review. *International Journal of Corrosion and Scale Inhibition* 10 (1): 80–106.

**14** Salgar-Chaparro, S.J., Darwin, A., Kaksonen, A.H., and Machuca, L.L. (2020). Carbon steel corrosion by bacteria from failed seal rings at an offshore facility. *Scientific Reports* 10 (1): 1–15.

**15** Sastri, V.S., Perumareddi, J.R., and Elboujdaini, M. (2005). Selection of corrosion inhibitors. *Corrosion Engineering, Science and Technology* 40 (3): 270–272.

**16** Kelland, M.A. (2014). *Production Chemicals for the Oil and Gas Industry*. Boca Raton, FL: CRC Press.

**17** Fink, J. (2012). *Petroleum Engineer’s Guide to Oil Field Chemicals and Fluids*, 2e. Amsterdam: Gulf Professional Publishing.

**18** Jones, D.A. (1996). *Principles and Prevention of Corrosion*. Prentice Hall.

**19** Roberge, P.R. (2012). *Handbook of Corrosion Engineering*. McGraw-Hill Education.

**20** Zhong, H., Shi, Z., Jiang, G., and Yuan, Z. (2020). Synergistic inhibitory effects of free nitrous acid and imidazoline derivative on metal corrosion in a simulated water injection system. *Water Research* 184: 116122.

**21** Wang, B., Du, M., Zhang, J., and Gao, C.J. (2011). Electrochemical and surface analysis studies on corrosion inhibition of Q235 steel by imidazoline derivative against $CO_2$ corrosion. *Corrosion Science* 53 (1): 353–361.

**22** Blin, F., Koutsoukos, P., Klepetsianis, P., and Forsyth, M. (2007). The corrosion inhibition mechanism of new rare earth cinnamate compounds - electrochemical studies. *Electrochimica Acta* 52 (21): 6212–6220.

**23** Blin, F., Leary, S.G., Wilson, K. et al. (2004). Corrosion mitigation of mild steel by new rare earth cinnamate compounds. *Journal of Applied Electrochemistry* 34 (6): 591–599.

**24** Deacon, G.B., Forsyth, M., Junk, P.C., and Leeb, W.W. (2008). From chromates to rare earth carboxylates: a greener take on corrosion inhibition. *Chemistry in Australia* 75 (9): 18–21.

**25** Forsyth, M., Seter, M., Hinton, B. et al. (2011). New “green” corrosion inhibitors based on rare earth compounds. *Australian Journal of Chemistry* 64 (6): 812–819.

**26** Catubig, R., Seter, M., Neil, W. et al. (2011). Effects of corrosion inhibiting pigment lanthanum 4-hydroxy cinnamate on the filiform corrosion of coated steel. *Journal of the Electrochemical Society* 158 (11): C353–C358.

**27** Seter, M., Hinton, B., and Forsyth, M. (2012). Understanding speciation of lanthanum 4-hydroxy cinnamate and its impact on the corrosion inhibition mechanism for AS1020 steel. *Journal of the Electrochemical Society* 159 (4): C181–C189.

**28** Blin, F., Leary, S.G., Deacon, G.B. et al. (2006). The nature of the surface film on steel treated with cerium and lanthanum cinnamate based corrosion inhibitors. *Corrosion Science* 48 (2): 404–419.

**29** Catubig, R.A., Neil, W.C., McAdam, G. et al. (2020). Multifunctional inhibitor mixtures for abating corrosion on HY80 steel under marine environments. *Journal of the Electrochemical Society* 167 (2): 021503.

**30** Seter, M., Thomson, M.J., Chong, A. et al. (2013). Cetrimonium nalidixate as a multifunctional inhibitor to combat biofilm formation and microbiologically influenced corrosion. *Australian Journal of Chemistry* 66 (8): 921–929.

**31** Gece, G. (2011). Drugs: a review of promising novel corrosion inhibitors. *Corrosion Science* 53 (12): 3873–3898.

**32** Sheng, X., Ting, Y.P., and Pehkonen, S.O. (2007). Inhibition of microbiologically influenced corrosion of mild steel and stainless steel 316 by an organic inhibitor. *Advances in Materials Research* 20–21: 379–382.

**33** Wang, J., Hou, B., Xiang, J. et al. (2019). The performance and mechanism of bifunctional biocide sodium pyrithione against sulfate reducing bacteria in X80 carbon steel corrosion. *Corrosion Science* 150: 296–308.

**34** Hsu, C.W., Chen, T.E., Lo, K.Y., and Lee, Y.L. (2019). Inhibitive properties of benzyldimethyldodecylammonium chloride on microbial corrosion of 304 stainless steel in a desulfovibrio desulfuricans-inoculated medium. *Materials (Basel)* 12 (307): 1–12.

**35** Rasool, K., Nasrallah, G.K., Younes, N. et al. (2018). “Green” ZnO-interlinked chitosan nanoparticles for the efficient inhibition of sulfate-reducing bacteria in inject seawater. *ACS Sustainable Chemistry & Engineering* 6 (3): 3896–3906.

**36** Feng, S., Li, Y., Liu, H. et al. (2020). Microbiologically influenced corrosion of carbon steel pipeline in shale gas field produced water containing $CO_2$ and polyacrylamide inhibitor. *Journal of Natural Gas Science and Engineering* 80: 103395.

**37** Labena, A., Hegazy, M.A., Horn, H., and Müller, E. (2014). Cationic Gemini surfactant as a corrosion inhibitor and a biocide for high salinity sulfidogenic bacteria originating from an oil-field water tank. *Journal of Surfactants and Detergents* 17 (3): 419–431.

**38** Labena, A., Hegazy, M.A., Horn, H., and Müller, E. (2015). The biocidal effect of a novel synthesized gemini surfactant on environmental sulfidogenic bacteria: planktonic cells and biofilms. *Materials Science and Engineering: C* 47: 367–375.

**39** Shaban, S.M., Aiad, I., Moustafa, A.H., and Aljoboury, O.H. (2019). Some alginates polymeric cationic surfactants; surface study and their evaluation as biocide and corrosion inhibitors. *Journal of Molecular Liquids* 273: 164–176.

**40** Aiad, I.A., Tawfik, S.M., Shaban, S.M. et al. (2013). Enhancing of corrosion inhibition and the biocidal effect of phosphonium surfactant compounds for oil field equipment. *Journal of Surfactants and Detergents* 17 (3): 391–401.

**41** Wei, H., Heidarshenas, B., Zhou, L. et al. (Ken)(2020). Green inhibitors for steel corrosion in acidic environment: state of art. *Materials Today Sustainability* 10: 100044.

**42** Alrefaee, S.H., Rhee, K.Y., Verma, C. et al. (2021). Challenges and advantages of using plant extract as inhibitors in modern corrosion inhibition systems: recent advancements. *Journal of Molecular Liquids* 321: 114666.

**43** Palou, L., Ali, A., Fallik, E., and Romanazzi, G. (2016). GRAS, plant- and animal-derived compounds as alternatives to conventional fungicides for the control of postharvest diseases of fresh horticultural produce. *Postharvest Biology and Technology* 122: 41–52.

**44** El Ibrahimi, B., Jmiai, A., Bazzi, L., and El Issami, S. (2020). Amino acids and their derivatives as corrosion inhibitors for metals and alloys. *Arabian Journal of Chemistry* 13 (1): 740–771.

**45** Kokilaramani, S., Al-Ansari, M.M., Rajasekar, A. et al. (2021). Microbial influenced corrosion of processing industry by re-circulating waste water and its control measures - a review. *Chemosphere* 265: 129075.

**46** Miralrio, A. and Vázquez, A.E. (2020). Plant extracts as green corrosion inhibitors for different metal surfaces and corrosive media: a review. *Processes* 8 (942): 1–27.

**47** Umoren, S.A., Obot, I.B., Ebenso, E.E., and Obi-Egbedi, N.O. (2009). The Inhibition of aluminium corrosion in hydrochloric acid solution by exudate gum from *Raphia hookeri*. *Desalination* 247 (1–3): 561–572.

**48** Anaee, R.A., Tomi, I.H.R., Abdulmajeed, M.H. et al. (2019). Expired Etoricoxib as a corrosion inhibitor for steel in acidic solution. *Journal of Molecular Liquids* 279: 594–602.

**49** El Mouaden, K., El Ibrahimi, B., Oukhrib, R. et al. (2018). Chitosan polymer as a green corrosion inhibitor for copper in sulfide-containing synthetic seawater. *International Journal of Biological Macromolecules* 119: 1311–1323.

**50** AlAbbas, F.M., Bhola, S.M., Spear, J.R. et al. (2013). The shielding effect of wild type iron reducing bacterial flora on the corrosion of linepipe steel. *Engineering Failure Analysis* 33: 222–235.

**51** Korenblum, E., Regina, F., Goulart, D.V. et al. (2013). Antimicrobial action and anti-corrosion effect against sulfate reducing bacteria by lemongrass (*Cymbopogon citratus*) essential oil and its major component, the citral. *AMB Express* 3 (44): 1–8.

**52** Singh, A., Dayu, X., Ituen, E. et al. (2020). Tobacco extracted from the discarded cigarettes as an inhibitor of copper and zinc corrosion in an ASTM standard D1141-98(2013) artificial seawater solution. *Journal of Materials Research and Technology* 9 (3): 5161–5173.

**53** Deng, S., Li, X., and Du, G. (2021). An efficient corrosion inhibitor of cassava starch graft copolymer for aluminum in phosphoric acid. *Chinese Journal of Chemical Engineering* 37: 222–231.

**54** Ituen, E., Singh, A., and Yuanhua, L. (2020). Inhibitive effect of onion mesocarp extract-nickel nanoparticles composite on simultaneous hydrogen production and pipework corrosion in 1 M HCl. *International Journal of Hydrogen Energy* 45 (18): 10814–10825.

**55** Zadeh, F.M.H., Khaleghi, M., Bordbar, S., and Jafari, A. (2021). *Myrtus communis* extract: a bio-controller for microbial corrosion induced by sulphate reducing bacteria. *Corrosion Engineering, Science and Technology* 56 (3): 269–278.

**56** Agarry, S.E., Oghenejoboh, K.M., Aworanti, O.A., and Arinkoola, A.O. (2019). Biocorrosion inhibition of mild steel in crude oil-water environment using extracts of *Musa paradisiaca* peels, *Moringa oleifera* leaves, and *Carica papaya* peels as biocidal-green inhibitors: kinetics and adsorption studies. *Chemical Engineering Communications* 206 (1): 98–124.

**57** Nwigwe, U.S., Mbam, S.O., and Umunakwe, R. (2019). Evaluation of *Carica papaya* leaf extract as a bio-corrosion inhibitor for mild steel applications in a marine environment. *Materials Research Express* 6: 105107.

**58** Rasheed, P.A., Pandey, R.P., Jabbar, K.A. et al. (2020). Chitosan/lignosulfonate nanospheres as “green” biocide for controlling the microbiologically influenced corrosion of carbon steel. *Materials (Basel)* 13 (11): 2484.

**59** Vaithiyanathan, S., Chandrasekaran, K., and Barik, R.C. (2018). Green biocide for mitigating sulfate-reducing bacteria influenced microbial corrosion. *3 Biotech* 8 (12): 495.

**60** Narenkumar, J., Parthipan, P., Usha Raja Nanthini, A. et al. (2017). Ginger extract as green biocide to control microbial corrosion of mild steel. *3 Biotech* 7 (2): 133.

**61** Anadebe, V.C., Okafor, C.S., and Onukwuli, O.D. (2020). Electrochemical, molecular dynamics, adsorption studies and anti-corrosion activities of *Moringa Leaf* biomolecules on carbon steel surface in alkaline and acid environment. *Chemical Data Collections* 28: 100437.

**62** Agwa, O.K., Iyalla, D., and Abu, G.O. (2017). Inhibition of bio corrosion of steel coupon by sulphate reducing bacteria and iron oxidizing bacteria using *Aloe Vera* (*Aloe barbadensis*) extracts. *Journal of Applied Sciences and Environmental Management* 21 (5): 833–838.

**63** Ituen, E., Ekemini, E., Yuanhua, L., and Singh, A. (2020). Green synthesis of *Citrus reticulata* peels extract silver nanoparticles and characterization of structural, biocide and anticorrosion properties. *Journal of Molecular Structure* 1207: 127819.

**64** Ibisi, N. and Ozoinyiama, C. (2017). The inhibitive behaviors of *Costus afar* leaves extract on sulphur reducing bacteria. *Asian Journal of Chemical Sciences* 3 (1): 1–9.

**65** Jeyaprabha, C., Sathiyanarayanan, S., and Venkatachari, G. (2006). Polyaniline as corrosion inhibitor for iron in acid solutions. *Journal of Applied Polymer Science* 101 (4): 2144–2153.

**66** Tiu, B.D.B. and Advincula, R.C. (2015). Polymeric corrosion inhibitors for the oil and gas industry: design principles and mechanism. *Reactive and Functional Polymers* 95: 25–45.

**67** Fathima Sabirneeza, A.A., Geethanjali, R., and Subhashini, S. (2015). Polymeric corrosion inhibitors for iron and its alloys: a review. *Chemical Engineering Communications* 202 (2): 232–244.

**68** Go, T.S. (1974). Use of alkylene polyamines in distillation columns to control corrosion. US Patent 3819328A, issued 1974.

**69** Olen, L. and Riggs, J. (1996). Process of reacting equimolar amounts of a monosaturated diol, a polyalkylene polyamine and a monocarboxylic acid and product. US Patent 3282970A, issued 1996.

**70** Jeyaprabha, C., Sathiyanarayanan, S., Phani, K.L.N., and Venkatachari, G. (2005). Influence of poly(aminoquinone) on corrosion inhibition of iron in acid media. *Applied Surface Science* 252 (4): 966–975.

**71** Jeyaprabha, C., Sathiyanarayanan, S., Phani, K.L.N., and Venkatachari, G. (2005). Investigation of the inhibitive effect of poly(diphenylamine) on corrosion of iron in 0.5 M $H_2SO_4$ solutions. *Journal of Electroanalytical Chemistry* 585 (2): 250–255.

**72** Manivel, P., Sathiyanarayanan, S., and Venkatachari, G. (2007). Influence of $H^+$ and $Cl^-$ ions on inhibitive performance of poly(aniline) for iron corrosion in acid. *Journal of Applied Polymer Science* 106: 3988–3993.

**73** Sathiyanarayanan, S., Balakrishnan, K., Dhawan, S.K., and Trivedi, D.C. (1994). Prevention of corrosion of iron in acidic media using poly (*o*-methoxy-aniline). *Electrochimica Acta* 39 (6): 831–837.

**74** Sathiyanarayanan, S., Dhawan, S.K., Trivedi, D.C., and Balakrishnan, K. (1992). Soluble conducting poly ethoxy aniline as an inhibitor for iron in HCl. *Corrosion Science* 33 (12): 1831–1841.

**75** Shukla, S.K., Quraishi, M.A., and Prakash, R. (2008). A self-doped conducting polymer "polyanthranilic acid": an efficient corrosion inhibitor for mild steel in acidic solution. *Corrosion Science* 50 (10): 2867–2872.

**76** Mekki Daouadji, M. and Chelali, N. (2004). Influence of molecular weight of poly(ortho-ethoxyaniline) on the corrosion inhibition efficiency of mild steel in acidic media. *Journal of Applied Polymer Science* 91 (2): 1275–1284.

**77** Quraishi, M.A. and Shukla, S.K. (2009). Poly(aniline-formaldehyde): a new and effective corrosion inhibitor for mild steel in hydrochloric acid. *Materials Chemistry and Physics* 113 (2–3): 685–689.

**78** Benchikh, A., Aitout, R., Makhloufi, L. et al. (2009). Soluble conducting poly(aniline-*co*-orthotoluidine) copolymer as corrosion inhibitor for carbon steel in 3% NaCl solution. *Desalination* 249 (2): 466–474.

**79** Karthik, G. and Sundaravadivelu, M. (2013). Inhibition of mild steel corrosion in sulphuric acid using esomeprazole and the effect of iodide ion addition. *ISRN Electrochemistry* 2013: 1–10.

**80** Karthikaiselvi, R. and Subhashini, S. (2017). The water soluble composite poly(vinylpyrrolidone–methylaniline): a new class of corrosion inhibitors of mild steel in hydrochloric acid media. *Arabian Journal of Chemistry* 10: S627–S635.

**81** Karthikaiselvi, R. and Subhashini, S. (2014). Study of adsorption properties and inhibition of mild steel corrosion in hydrochloric acid media by water soluble composite poly (vinyl alcohol-*o*-methoxy aniline). *Journal of the Association of Arab Universities for Basic and Applied Sciences* 16: 74–82.

**82** Bhandari, H., Choudhary, V., and Dhawan, S.K. (2011). Influence of self-doped poly(aniline-*co*-4-amino-3-hydroxy-naphthalene-1-sulfonic acid) on corrosion inhibition behaviour of iron in acidic medium. *Synthetic Metals* 161 (9–10): 753–762.

**83** Menaka, R., Nandhini, M., and Subhashini, S. (2014). Histidine as synergistic additive on poly (*N*-methyl aniline) for mild steel corrosion in 0.5 M $H_2SO_4$. *Research Journal of Recent Sciences* 3: 177–184.

**84** Manivel, P., Sathiyanarayanan, S., and Venkatachari, G. (2008). Synthesis of poly(*p*-phenylene diamine) and its corrosion inhibition effect on iron in 1M HCl. *Journal of Applied Polymer Science* 110: 2807–2814.

**85** Manivel, P. and Venkatachari, G. (2006). The inhibitive effect of para-amino benzoic acid and its polymer on corrosion of iron in 1 mol/L HCl solution. *Journal of Materials Science and Technology* 22 (3): 301–305.

**86** McCafferty, E. and Hackerman, N. (1972). Double layer capacitance of iron and corrosion inhibition with polymethylene diamines. *Journal of the Electrochemical Society* 119 (2): 146–154.

**87** Al-Sabagh, A.M., Elsabee, M., Elazabawy, O.E., and El-Tabey, A.E. (2010). Corrosion inhibition efficiency of polytriethanolamine surfactants for pipe-lines carbon steel in 1 M HCl. *Journal of Dispersion Science and Technology* 31 (10): 1288–1297.

**88** Abd El Rehim, S.S., Sayyah, S.M., El-Deeb, M.M. et al. (2010). Poly(*o*-phenylenediamine) as an inhibitor of mild steel corrosion in HCl solution. *Materials Chemistry and Physics* 123 (1): 20–27.

**89** Finšgar, M., Fassbender, S., Nicolini, F., and Milošev, I. (2009). Polyethyleneimine as a corrosion inhibitor for ASTM 420 stainless steel in near-neutral saline media. *Corrosion Science* 51 (3): 525–533.

**90** Gao, B., Zhang, X., and Sheng, Y. (2008). Studies on preparing and corrosion inhibition behaviour of quaternized polyethyleneimine for low carbon steel in sulfuric acid. *Materials Chemistry and Physics* 108 (2–3): 375–381.

**91** Sekine, I., Sanbongi, M., Hagiuda, H. et al. (1992). Corrosion inhibition of mild steel by cationic and anionic polymers in cooling water system. *Journal of the Electrochemical Society* 139 (11): 3167–3173.

**92** Zhang, X., Wu, X., Li, J. et al. (2009). Anticorrosion behaviors of quaternary polyethyleneimine in acidic environment. *Materials Science Forum* 610–613: 136–141.

**93** Zhang, X., Wu, X.D., and Gao, B.J. (2011). Studies on cationic property of quaternary polyethyleneimine. *Materials Science Forum* 689: 432–439.

**94** Lebrini, M., Bentiss, F., Chihib, N.E. et al. (2008). Polyphosphate derivatives of guanidine and urea copolymer: inhibiting corrosion effect of Armco iron in acid solution and antibacterial activity. *Corrosion Science* 50 (10): 2914–2918.

**95** Kamal, I.A., Abbady, M.A., Mahgoub, S.A., and Hussein, M.A. (2009). New polymer syntheses, part 44: synthesis, characterization, and corrosion inhibition behavior of new polyurea derivatives based on diaryl ether in the polymers backbone. *Journal of Applied Polymer Science* 112 (2): 620–628.

**96** Schweinsberg, D.P., Jianguo, Y., Lin, W., and Otienoalego, V. (1995). Polyvinylpyrrolidone and polyethylenimine as inhibitors for the corrosion of a low carbon steel in phosphoric acid. *Corrosion Science* 37 (6): 975–985.

**97** Chetouani, A., Medjahed, K., Sid-Lakhdar, K.E. et al. (2004). Poly(4-vinylpyridine-poly(3-oxide-ethylene) tosyle) as an inhibitor for iron in sulphuric acid at 80°C. *Corrosion Science* 46 (10): 2421–2430.

**98** Benabdellah, M., Ousslim, A., Hammouti, B. et al. (2007). The effect of poly(vinyl caprolactone-*co*-vinyl pyridine) and poly(vinyl imidazol-*co*-vinyl pyridine) on the corrosion of steel in $H_3PO_4$ media. *Journal of Applied Electrochemistry* 37 (7): 819–826.

**99** Belkaid, S., Tebbji, K., Mansri, A. et al. (2012). Poly(4-vinylpyridine-hexadecyl bromide) as corrosion inhibitor for mild steel in acid chloride solution. *Research on Chemical Intermediates* 38 (9): 2309–2325.

**100** Mbin, M., Khan, M.A., and Parveen, M. (2011). Inhibition of mild steel corrosion in acidic medium using starch and surfactants additives. *Journal of Applied Polymer Science* 121: 1558–1565.

**101** Bereket, G., Yurt, A., and Türk, H. (2003). Inhibition of the corrosion of low carbon steel in acidic solution by selected polyelectrolytes and polymers. *Anti-Corrosion Methods and Materials* 50 (6): 422–435.

**102** Umoren, S.A., Ogbobe, O., Igwe, I.O., and Ebenso, E.E. (2008). Inhibition of mild steel corrosion in acidic medium using synthetic and naturally occurring polymers and synergistic halide additives. *Corrosion Science* 50 (7): 1998–2006.

**103** Srikanth, A.P., Lavanya, A., Nanjundan, S., and Rajendran, N. (2006). Synthesis, characterization, and corrosion protection properties of poly(*N*-(methacryloyloxymethyl) benzotriazole-*co*-methyl methacrylate) on mild steel. *Applied Surface Science* 253 (4): 1810–1816.

**104** Yurt, A., Bütün, V., and Duran, B. (2007). Effect of the molecular weight and structure of some novel water-soluble triblock copolymers on the electrochemical behaviour of mild steel. *Materials Chemistry and Physics* 105 (1): 114–121.

**105** Atta, A.M., El-Azabawy, O.E., Ismail, H.S., and Hegazy, M.A. (2011). Novel dispersed magnetite core-shell nanogel polymers as corrosion inhibitors for carbon steel in acidic medium. *Corrosion Science* 53 (5): 1680–1689.

**106** Rajendran, S., Apparao, B.V., and Palaniswamy, N. (1998). Synergistic and antagonistic effects existing among polyacrylamide, phenyl phosphonate and $Zn^{2+}$ on the inhibition of corrosion of mild steel in a neutral aqueous environment. *Electrochimica Acta* 44 (2–3): 533–537.

**107** Srivastava, V., Banerjee, S., and Singh, M.M. (2010). Inhibitive effect of polyacrylamide grafted with fenugreek mucilage on corrosion of mild steel in 0.5 M $H_2SO_4$ at 35°C. *Journal of Applied Polymer Science* 116: 810–816.

**108** Han, T. and Liu, J. (2010). Facile synthesis of palmitic acid polyacrylamide and its application for steel protection from corrosion using electrochemical determination. *Procedia Engineering* 7: 404–409.

**109** Banerjee, S., Srivastava, V., and Singh, M.M. (2012). Chemically modified natural polysaccharide as green corrosion inhibitor for mild steel in acidic medium. *Corrosion Science* 59: 35–41.

**110** Mansri, A., Bouras, B., Hammouti, B. et al. (2013). Synergistic effect of AM-4VP-9 copolymer and iodide ion on corrosion inhibition of mild steel in 1 M $H_2SO_4$. *Research on Chemical Intermediates* 39 (4): 1753–1770.

**111** Geethanjali, R., Sabirneeza, A.A.F., and Subhashini, S. (2014). Water-soluble and biodegradable pectin-grafted polyacrylamide and pectin-grafted polyacrylic acid: electrochemical investigation of corrosion-inhibition behaviour on mild steel in 3.5% NaCl media. *Indian Journals of Materials Science* 2014: 1–9.

**112** Choi, D.J., Kim, Y.W., and Kim, J.G. (2001). Development of a blended corrosion, scale, and microorganism inhibitor for open recirculating cooling systems. *Werkstoffe und Korrosion* 52 (9): 697–704.

**113** Vakili Azghandi, M., Davoodi, A., Farzi, G.A., and Kosari, A. (2012). Water-base acrylic terpolymer as a corrosion inhibitor for SAE1018 in simulated sour petroleum solution in stagnant and hydrodynamic conditions. *Corrosion Science* 64: 44–54.

**114** Kavitha, A.L., Vasudevan, T., and Prabu, H.G. (2011). Evaluation of synthesized antiscalants for cooling water system application. *Desalination* 268 (1–3): 38–45.

**115** Outlaw, B.T, Alink, B.A.O, Kelly, J.A, and Claywell, C.S. (1985). Corrosion inhibition in deep gas wells by phosphate esters of poly-oxyalkylated thiols. US Patent 4511480A issued 1985.

**116** Richard, L.M., Gene, F.B., and James, B.D. (2005). Corrosion inhibitors and methods of use. US patent 6866797B1, issued 2005.

**117** Naraghi, A. and Grahmann, N. (1997). Corrosion inhibitor blends with phosphate esters. US Patent 5611992A, issued 1997.

**118** Subramaniyam, M. (2010). An effective novel polymeric additive for inhibiting napthenic acid corrosion and method of using the same. WO2010023628A1, issued 2010.

**119** Subramaniyam, M. (2009). A new additive for inhibiting acid corrosion and methods of using the new additive. EP2340296B1, issued 2009.

**120** Howland, W.W. (1961). Process for preventing corrosion in ferrous systems. US patent 2659693A, issued 1961.

**121** Gay, R.J., Gay, C.C., Matthews, V.M. et al. (1993). Dynamic polysulfide corrosion inhibitor method and system for oil field piping. US Patent 5188179A, issued 1993.

**122** Babaian-Kibala, E., Hyatt, J.G., and Rose, T.J. (1997). Use of sulfiding agents for enhancing the efficacy of phosphorous in controlling high temperature corrosion attack. CA2176182C, issued 1997.

**123** Petersen, P.R., Robbins, F.P., and Winston, W.G. (1993) Naphthenic acid corrosion inhibition. US Patent 5182013A, issued 1993.

**124** Umoren, S.A., Banera, M.J., Alonso-Garcia, T. et al. (2013). Inhibition of mild steel corrosion in HCl solution using chitosan. *Cellulose* 20 (5): 2529–2545.

**125** Deyab, M.A. and Abd El-Rehim, S.S. (2013). Influence of polyethylene glycols on the corrosion inhibition of carbon steel in butyric acid solution: weight loss, EIS and theoretical studies. *International Journal of Electrochemical Science* 8 (12): 12613–12627.

**126** Arukalam, I.O., Madufor, I.C., Ogbobe, O., and Oguzie, E. (2014). Experimental and theoretical studies of hydroxyethyl cellulose as inhibitor for acid corrosion inhibition of mild steel and aluminium. *Open Corrosion Journal* 6 (1): 1–10.

**127** Umoren, S.A., Solomon, M.M., Udosoro, I.I., and Udoh, A.P. (2010). Synergistic and antagonistic effects between halide ions and carboxymethyl cellulose for the corrosion inhibition of mild steel in sulphuric acid solution. *Cellulose* 17 (3): 635–648.

**128** Abdallah, M. (2004). Guar gum as corrosion inhibitor for carbon steel in sulfuric acid solutions. *Portugaliae Electrochimica Acta* 22: 161–175.

**129** Zaafarany, I. (2006). Inhibition of acidic corrosion of iron by some *Carrageenan* compounds. *Current World Environment: An International Research Journal of Environmental Sciences* 1 (2): 101–108.

**130** Oyaizu, K., Yamaguchi, A., Hayashi, T. et al. (2006). Controlled oxidation of dextran for evolution of polyether segment bearing pendant carboxyl groups for corrosion inhibition applications. *Polymer Journal* 38 (4): 343–348.

**131** Akbarzadeh, E., Ibrahim, M.N.M., and Rahim, A.A. (2011). Corrosion inhibition of mild steel in near neutral solution by Kraft and Soda lignins extracted from oil palm empty fruit bunch. *International Journal of Electrochemical Science* 6 (11): 5396–5416.

**132** Li, Y.J., Wu, B., Zeng, X.P. et al. (2002). The voltammetry-photocurrent response study of passivation of carbon steel in slightly alkaline solutions containing the corrosion inhibitor phosphor-polymaleic acid-$ZnSO_4$. *Thin Solid Films* 405: 153–161.

**133** Xu, Y., Zhang, B., Zhao, L., and Cui, Y. (2013). Synthesis of polyaspartic acid/5-aminoorotic acid graft copolymer and evaluation of its scale inhibition and corrosion inhibition performance. *Desalination* 311: 156–161.

**134** Ashassi-Sorkhabi, H., Ghalebsaz-Jeddi, N., Hashemzadeh, F., and Jahani, H. (2006). Corrosion inhibition of carbon steel in hydrochloric acid by some polyethylene glycols. *Electrochimica Acta* 51 (18): 3848–3854.

**135** Migahed, M.A., Aly, R.O., and Al-Sabagh, A.M. (2004). Impact of gamma-ray-pre-irradiation on the efficiency of corrosion inhibition of some novel polymeric surfactants. *Corrosion Science* 46 (10): 2503–2516.

**136** Hamandez, G., Kucera, V., Thierry, D. et al. (1994). Corrosion inhibition of steel by bacteria. *Corrosion* 50 (8).

**137** Javaherdashti, R. (1999). A review of some characteristics of MIC caused by sulfate-reducing bacteria: past, present and future. *Anti-Corrosion Methods and Materials* 46 (3): 173–180.

**138** Videla, H., Guiamet, P., Gómez de Saravia, S. et al. (2004). Environmentally friendly approaches to inhibit biocorrosion: an overview. *Corrosion*, (NACE-04574).

**139** Videla, H.A. (2002). Prevention and control of biocorrosion. *International Biodeterioration and Biodegradation* 49 (4): 259–270.

**140** Little, B., Lee, J., and Ray, R. (2007). A review of "green" strategies to prevent or mitigate microbiologically influenced corrosion. *Biofouling* 23 (2): 87–97.

**141** Zuo, R. (2007). Biofilms: strategies for metal corrosion inhibition employing microorganisms. *Applied Microbiology and Biotechnology* 76 (6): 1245–1253.

**142** Bentham, R.H., Morton, L.H.G., and Allen, N.G. (1987). Rapid assessment of the microbial deterioration of polyurethanes. *International Biodeterioration* 23 (6): 377–386.

**143** Cere, S. and Vazquez, M. (2002). Properties of the passive films present on copper and copper-nickel alloys in slightly alkaline solutions. *Journal of Materials Science Letters* 21 (6): 493–495.

**144** Kay, M.J., McCabe, R.W., and Morton, L.H.G. (1993). Chemical and physical changes occurring in polyester polyurethane during biodegradation. *International Biodeterioration and Biodegradation* 31 (3): 209–225.

**145** Ramezanzadeh, B., Ghasemi, E., Mahdavian, M. et al. (2015). Covalently-grafted graphene oxide nanosheets to improve barrier and corrosion protection properties of polyurethane coatings. *Carbon* 93: 555–573.

**146** Gu, J.D., Mitton, D.B., Ford, T.E., and Mitchell, R. (1998). Microbial degradation of polymeric coatings measured by electrochemical impedance spectroscopy. *Biodegradation* 9 (1): 39–45.

**147** Tiwari, A. and Hihara, L.H. (2010). High performance reaction-induced quasi-ceramic silicone conversion coating for corrosion protection of aluminium alloys. *Progress in Organic Coatings* 69 (1): 16–25.

**148** Sugama, T. and Cook, M. (2000). Poly(itaconic acid)-modified chitosan coatings for mitigating corrosion of aluminum substrates. *Progress in Organic Coatings* 38 (2): 79–87.

**149** Frignani, A., Tassinari, M., Mesazaros, L., and Trabanelli, G. (1991). The use of electrochemical impedance spectroscopy to study armco iron corrosion in acid solutions inhibited by quaternary ammonium compounds. *Corrosion Science* 32 (8): 903–911.

**150** Tiller, J.C., Lee, S.B., Lewis, K., and Klibanov, A.M. (2002). Polymer surfaces derivatized with poly(vinyl-*N*-hexylpyridinium) kill airborne and waterborne bacteria. *Biotechnology and Bioengineering* 79 (4): 465–471.

**151** Qi, Y., Li, J., Liang, R. et al. (2017). Chemical additives affect sulfate reducing bacteria biofilm properties adsorbed on stainless steel 316L surface in circulating cooling water system. *Frontiers of Environmental Science & Engineering* 11 (2): 1–14.

**152** Seter, M., Thomson, M.J., Stoimenovski, J. et al. (2012). Dual active ionic liquids and organic salts for inhibition of microbially influenced corrosion. *Chemical Communications* 48 (48): 5983–5985.

**153** Liu, H., Huang, L., Huang, Z. et al. (2008). Preparation of conducting poly *N*-methylaniline microsphere and its antibacterial performance to sulfate reducing bacteria. *Journal of Wuhan University of Technology Materials Science Edition* 23 (4): 536–540.

**154** Nanlin, S., Xuewei, G., Hemin, J. et al. (2006). Antibacterial effect of the conducting polyaniline. *Journal of Materials Science and Technology* 22 (3): 289–290.

**155** Tiller, J.C., Liao, C.J., Lewis, K., and Klibanov, A.M. (2001). Designing surfaces that kill bacteria on contact. *Proceedings of the National Academy of Sciences of the United States of America* 98 (11): 5981–5985.

**156** Jayaraman, A., Hallock, P.J., Carson, R.M. et al. (1999). Inhibiting sulfate-reducing bacteria in biofilms on steel with antimicrobial peptides generated in situ. *Applied Microbiology and Biotechnology* 52 (2): 267–275.

**157** Jayaraman, A., Ornek, D., Duarte, D.A. et al. (1999). Axenic aerobic biofilms inhibit corrosion of copper and aluminum. *Applied Microbiology and Biotechnology* 52 (6): 787–790.

**158** Örnek, D., Jayaraman, A., Syrett, B. et al. (2002). Pitting corrosion inhibition of aluminum 2024 by *Bacillus* biofilms secreting polyaspartate or γ-polyglutamate. *Applied Microbiology and Biotechnology* 58 (5): 651–657.

**159** Zuo, R., Kus, E., Mansfeld, F., and Wood, T.K. (2005). The importance of live biofilms in corrosion protection. *Corrosion Science* 47 (2): 279–287.

**160** Purwasena, I.A., Astuti, D.I., Ardini Fauziyyah, N. et al. (2019). Inhibition of microbial influenced corrosion on carbon steel ST37 using biosurfactant produced by *Bacillus* sp. *Materials Research Express* 6: 115405.

**161** Stadler, R., Fuerbeth, W., Harneit, K. et al. (2008). First evaluation of the applicability of microbial extracellular polymeric substances for corrosion protection of metal substrates. *Electrochimica Acta* 54 (1): 91–99.

**162** Stadler, R., Wei, L., Fürbeth, W. et al. (2010). Influence of bacterial exopolymers on cell adhesion of *Desulfovibrio vulgaris* on high alloyed steel: corrosion inhibition by extracellular polymeric substances (EPS). *Materials and Corrosion* 61 (12): 1008–1016.

**163** Grooters, M., Harneit, K., Wöllbrink, M. et al. (2007). Novel steel corrosion protection by microbial extracellular polymeric substances (EPS) – biofilm-induced corrosion inhibition. *Advances in Materials Research* 20–21: 375–378.

**164** Velraeds, M.M.C., Van Der Mei, H.C., Reid, G., and Busscher, H.J. (1996). Inhibition of initial adhesion of uropathogenic *Enterococcus faecalis* by biosurfactants from *Lactobacillus* isolates. *Applied and Environmental Microbiology* 62 (6): 1958–1963.

# 13

# Smart Polymers Coating for Upstream Oil and Gas Industry to Slow Down the Corrosion

*Rabia Nazar, Umer Mehmood, Hassan Ahmed, Aimen Imran, and Syed A. Raza*

*University of Engineering and Technology (UET) Lahore, Polymer and Process Engineering (PPE) Department,*
*G. T. Road, Lahore, Punjab 39161, Pakistan*

## 13.1 Introduction

Corrosion, also known as the corrosion of a metal or its attributes, affects every component of an oil and gas field at every stage of its life. Corrosion is an obstacle worthy of all advanced technology and research we can throw at it, from casting strings to production platforms, drilling to abandonment. The presence of oxygen, which is critical for corrosion, is rare in developing formation [1]. Only during the drilling stage are polluted fluids supplemented with oxygen introduced. If drilling muds are not treated, they will damage not just well covering but also mining equipment, tubing, and heavy machinery. Water and $CO_2$ created or inserted for secondary recovery might severely damage completion threads. Metal is easily attacked by acid used to decrease formation damage all around well or to eliminate scale. High production velocities can corrode completions and surface pipes, and formation sand can blast them away. Other issues arise from hydrogen sulfide ($H_2S$). Because of the added complexity of high temperatures, pressures, and stresses involved with mining or manufacturing, a material engineer, an increasingly powerful figure in the industry, is necessary to manage all of these corrosion situations.

### 13.1.1 Corrosion in the Primary Manufacturing Processes

Downstream, midstream, and upstream are the three key components of the oil and gas sector. The upstream sector is responsible for discovering, locating, and producing natural gas and crude oil from both onshore and offshore fields. Therefore, the upstream industry is sometimes known as the production and exploration (E&P) sector. Wells of water, gas, and oil are all explored in the upstream industry. Transportation, storage, processing, and wholesale marketing of refined or crude petroleum products are all part of the midstream sector. Natural gas and crude oil

*Polymeric Corrosion Inhibitors for Greening the Chemical and Petrochemical Industry*, First Edition.
Edited by Mohammad A. Jafar Mazumder, Mumtaz A. Quraishi, and Amir Al-Ahmed.

are transported from production locations to petrochemical plants and refineries via pipelines and other transportation systems. Natural gas pipeline systems transport gas from natural gas generating wells, purification plants, and separation plants to consumers in the downstream region, like local utilities. Midstream operations frequently crossover into the upstream and downstream industries. Natural gas processing plants, for example, may be included in the midstream sector if they refine raw natural gas along with natural gas liquids (NGLs) extraction and production and elemental sulfur. The downstream industry, which comprises petrochemical facilities, crude oil processing plants, and petroleum product distribution, is the third major sector. The processing of crude oil into diesel, petrol, airplane fuel, and other fuels is an important component of the downstream industry. Hundreds of consumer products, like asphalt, lubricants, heating oil, jet fuel, plastic, synthetic rubber, fertilizers, antifreeze agents, insecticides, medicines, propane, and natural gas, are also produced by the downstream industry.

The produced fluid streams are generally dry in the initial phases of the production of oil products from a newfound field. The corrosion process at low temperatures, on the other hand, requires the presence of water. Thus, most of the oil-production equipment is made of carbon steel, which is very inexpensive and has the needed strength for pressure containment. If the streams stay dry or subjugated by the hydrocarbon phase, the life of these facilities can easily surpass 50 years without the need for any corrosion management measures. Over time, nothing remains in the same condition. For instance, the volume of produced water rose as gas and oil fields matured, either naturally or because of water flooding. This increase in water content necessitated the use of a corrosion management approach that was both effective and practical to implement. Corrosion inhibition has been the preferred strategy for allowing production from fields that were on the verge of being abandoned due to increased activity of corrosion. The cumulative experience of employing carbon steel for corrosion prevention promoted the expansion of this strategy to places with more aggressive corrosion conditions, like wells with greater $H_2S$ levels.

Interior corrosion of carbon steel equipment and piping in oil and gas processing, production, and transport, has been controlled using continuous and batch corrosion inhibitor treatments. There are many commercial oxidation agents in the market, and chemical companies are always developing new compounds. For corrosion inhibitor selection and evaluation, numerous global guidelines have been established and are being developed.

Corrosion in the gas and oil industry is exceedingly costly, involving direct and indirect expenses such as wasted time, replacement of construction materials, and ongoing employee participation in corrosion management, along with safety and environmental effects. The research looked at corrosion-related cost studies executed in Finland, China, Australia, Japan, India, Germany, Sweden, Kuwait, the United States, and the United Kingdom. According to this research, the annual corrosion expenses in each country varied from 1% to 5% of their gross national product (GNP). The costs of corrosion failures and their repercussions on safety and the environment are not included in these analyzes. According to the International Measures of Prevention, Application, and Economics of Corrosion Technologies

(IMPACT) study, corrosion control measures can save between 15% and 35% of the cost of damage, equating to an international corrosion cost reduction of US$375–875 billion per year.

Table 13.1 briefly summarizes the predominant corrosion types in upstream production operations.

**Table 13.1** Predominant corrosion types in upstream production operations [2].

| Sr. No. | Component | Predominant material of construction | Predominant corrosion type | Main environmental factors influencing corrosion | Internal or external both |
|---|---|---|---|---|---|
| 1 | Drill pipe | Carbon steel | Sulfide stress cracking (SSC)<br>Corrosion fatigue | $H_2S$ | External |
| 2 | Casing pipe | Carbon steel | SSC | $H_2S$<br>Temperature | Internal |
| 3 | Downhole tubular | Carbon steel | SSC<br>Chloride SCC | $H_2S$<br>Chloride<br>Temperature | Internal |
| 4 | Sucker rods | Carbon steel | Corrosion fatigue<br>SSC | $H_2S$<br>Temperature | External |
| 5 | Acidizing pipe | Carbon steel | General corrosion | Acids (organic and inorganic) | Internal |
| 6 | Water generator | Carbon steel | Localized pitting corrosion | $O_2$<br>Microbes<br>$H_2S$<br>$CO_2$ | Internal |
| 7 | Gas generator | Carbon steel | Localized pitting corrosion | Chloride SCC<br>$O_2$<br>Chloride | Internal |
| 8 | Open mining | Carbon steel | Erosion–corrosion | Sand | Internal |
| 9 | In situ production | Carbon steel | Erosion–corrosion | Temperature<br>Sand | Internal |
| 10 | Wellhead | Carbon steel | Localized pitting corrosion<br>SSC | $CO_2$<br>$H_2S$<br>$O_2$ | External |
| 11 | Production pipeline | Carbon steel | Hydrogen-induced cracking (HIC)<br>Localized pitting corrosion | $H_2S$<br>$CO_2$ | Internal |

*(Continued)*

**Table 13.1** (Continued)

| Sr. No. | Component | Predominant material of construction | Predominant corrosion type | Main environmental factors influencing corrosion | Internal or external both |
|---|---|---|---|---|---|
| 12 | Heavy crude oil pipelines | Carbon steel | Localized pitting corrosion | Crude oil | Internal |
| 13 | Hydro-transportation pipeline | Carbon steel | Erosion–corrosion | Sand | Internal |
| 14 | Gas dehydration facility | Carbon steel | Localized pitting corrosion | $CO_2$<br>$H_2S$<br>$O_2$ | Internal |
| 15 | Oil separator | Carbon steel | Localized pitting corrosion | Crude oil | Internal |
| 16 | Recovery center (extraction) | Carbon steel | Erosion–corrosion | Sand<br>Temperature | Internal |
| 17 | Upgrader lease tank | See refinery carbon steel | HIC<br>Localized pitting corrosion | $H_2S$<br>$CO_2$ | Internal |
| 18 | Wastewater pipeline | Carbon steel | Localized pitting corrosion | $O_2$ | Internal |
| 19 | Tailing pipeline | Carbon steel | Erosion–corrosion | Sand | Internal |

Source: Papavinasam [2]/with permission of Elsevier.

## 13.2 Mechanism of Corrosion

$H_2S$, $CO_2$, organic acids, bacteria, water, and sand are among the substances found in the fluid streams flowing in oil and gas pipes. These components are among the most common reasons for pipeline corrosion. In the presence of water, $CO_2$ dissolves and forms an acidic oxide, which reacts with Fe. Sweet corrosion is the name for this form of corrosion. In gas and oil pipelines, sweet corrosion is accountable for the majority of the corrosion annihilation. Sour corrosion takes place when $H_2S$ levels in the oil and gas exceed 100 parts per million, causing corrosion and pitting in the pipeline [3, 4].

### 13.2.1 Electrochemical Nature of Corrosion

Electrochemical mechanisms cause metal and alloy corrosion in water or any ionically conducting medium. A cathode, an anode, an electrolytic conductor, and a metallic conductor are required for an electrochemical corrosion reaction to occur (Figure 13.1). At the electrode, a metal ion escapes the metal and enters

**Figure 13.1** Basic four elements for corrosion to take place. Source: Papavinasam [2]/with permission of Elsevier.

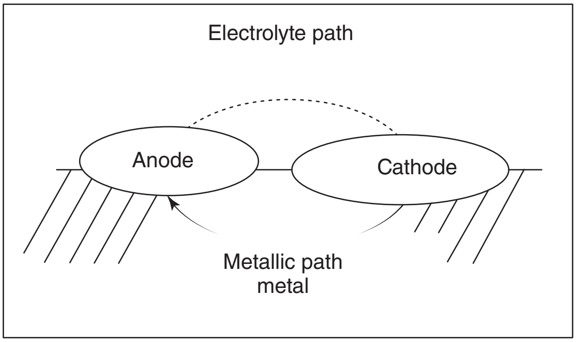

the solution. As a result of this action, electrons are left on the metal surface. As a result, the metal is oxidized at the anode, losing electrons. Corrosion is the term for this process. A distinctive corrosion reaction taking place at the anode is shown by Eq. (13.1):

$$\mathrm{M} \rightarrow \mathrm{M}^{n} + n\mathrm{e}^{-} \tag{13.1}$$

The metal ions are carried from the anode to the cathode by the solution. Most electrolytes are liquids; however, they can also be solids. Electrical conductivities are higher in electrolytes with a higher ion concentration. An electrolyte is made up of two types of ions: anions and cations. Negatively charged anions go toward the anode, where they may be oxidized. Positively charged cations travel towards the cathode, where they may be reduced. Deionized water, for instance, contains fewer ions and hence is a poor electrolyte. Seawater, in contrast, includes numerous dissolved ions, making it an excellent electrolyte that sustains corrosion. If metallic ions are reduced at the cathode, they may exit the solution and deposit on the cathode. It obtains electrons from the metal surface during this process.

The reaction occurring at the cathode is shown in Eq. (13.2):

$$\mathrm{M}^{n} + n\mathrm{e}^{-} \rightarrow \mathrm{M} \tag{13.2}$$

To produce $H_2CO_3$ (carbonic acid), $CO_2$ existing in gas and oil will dissolve in water [5, 6]. This acid dissolves steel to yield hydrogen and iron carbonate [7]. This reaction that happens at the cathode is shown by Eq. (13.3):

$$\mathrm{Fe} + \mathrm{H_2CO_3} \rightarrow \mathrm{FeCO_3} + \mathrm{H_2} \tag{13.3}$$

Carbonic acid, despite its weakness, is particularly corrosive to carbon steel. The iron carbonate coatings are formed via the chemical reaction described above. Depending on the circumstances at the time of manufacture, these films might be non-protective or protective at the anode [shown in Eq. (13.4)].

$$\mathrm{Fe} \rightarrow \mathrm{Fe}^{2+} + 2\mathrm{e}^{-} \tag{13.4}$$

$CO_2$ functions as a catalyst, enhancing hydrogen production and thus enhancing the corrosion rate of metallic materials in an aqueous environment [6].

According to Eqs. (13.5) and (13.6), ($H_2CO_3$) carbonic acid either acts as an additional source of $H^+$ or is directly decreased:

$$2H^+ + 2e^- \rightarrow H_2(g) \tag{13.5}$$

$$2H_2CO_3 + 2e^- \rightarrow H_2(g) + 2HCO_3^- \tag{13.6}$$

The concentration of dissolved iron will rise until the $Fe^{2+}$ precipitation rate equals the $FeCO_3$ precipitation rate [8].

The double volume of bicarbonate is obtained when $Fe^{2+}$ is liberated during the corrosion reaction, according to Eq. (13.7):

$$Fe + 2H_2CO_3 \rightarrow Fe^{2+} + H_2 + 2HCO_3^- \tag{13.7}$$

As the pH rises, the concentrations of bicarbonate and carbonate rise to the point where solid $FeCO_3$ precipitates as illustrated in Eq. (13.8):

$$Fe^{2+} + 2HCO_3^- \rightarrow FeCO_3\,(s) + H_2CO_3 \tag{13.8}$$

The pH remains constant until all the ferrous ions generated by corrosion precipitate as $FeCO_3$, and the whole reaction enters the condition in which iron carbonate and hydrogen are produced [9].

There should be passivity to regulate the pace of the pipeline's corrosion. The condition of passivity on the surface of the metal is caused by the existence of a protective coating. When a protective film develops on a metal surface, it creates a coating that protects the material from further corrosion [4]. At high temperatures, the inert layer formed on carbon steel oxidizes and breaks into two layers. The interior layer is dense, has a uniform thickness, and adheres effectively to steel. The exterior film is a permeable aggregate of crystals with a nonuniform thickness that would scale off the steel at a location (Figure 13.2).

Erosion, dissolution, and turbulence remove this protective film from the pipeline's surface, resulting in additional corrosion. The following are some of the mechanisms that could lead to the protective coating being removed:

(i) When the shear tension between the substrate and the layer is greater than the adhesive force, the protective layer dissolves or is removed by hydrodynamic shear stress. This is a result of a mechanical erosion process in the pipeline triggered by the multiphase flow control [9, 11].

(ii) Relative near-wall turbulence density assists in the removal of the protective coating in a dispersed flow condition. The increased corrosion rate [11] is caused by the disturbance of the mass transfer boundary layer [12].

(iii) Mass transfer is used to control the film's dissolution. As a result, the breakaway velocity may represent situations where the film's dissolving rate exceeds its growth rate. Corrosion types such as stress corrosion, intergranular, crevice, and pitting are a few of the principal sources of corrosion failures caused by the breakdown of the protective film [13, 14]. Electrochemical and mechanical breakdown processes are the most common. Mechanical collapse appears when the protecting film is broken because of tension or abrasive wear, whereas electrochemical breakdown occurs when the fluid constituent reacts chemically with the steel.

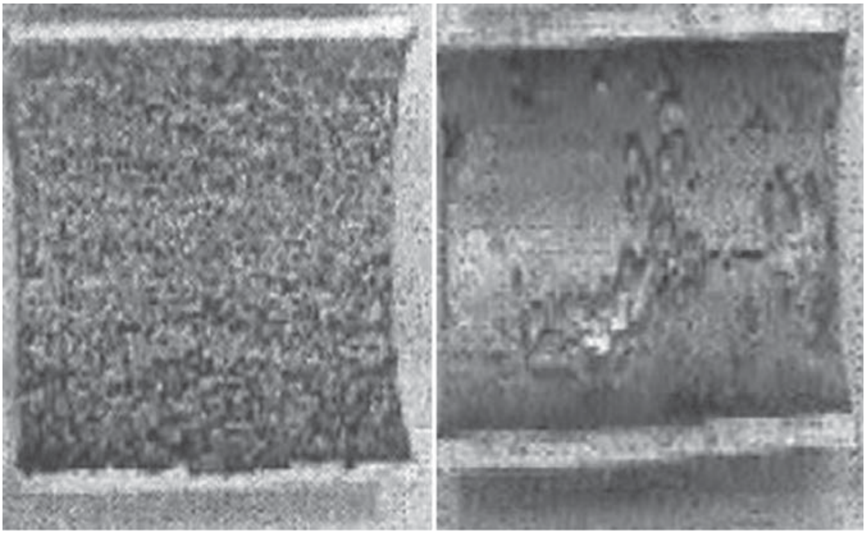

Uniform corrosion Mesa corrosion

**Figure 13.2** The typical form of mesa corrosion caused by $CO_2$, moisture, and flow. Source: Nalli [10]/John Wiley & Sons, Inc.

## 13.3 Kinds of Corrosion in Industry

In the industry, corrosion may be classed as electrical and chemical, or mechanical.

### 13.3.1 Electrochemical Corrosion

#### 13.3.1.1 Corrosion due to Galvanic Reaction

This kind of corrosion, also known as bimetal corrosion, occurs when two dissimilar metals with different electrochemical potency contact and are exposed to an electrochemical environment (illustrated in Figure 13.3). Because of the electric potential between them, electrons move between them. The metal with the least reactivity is the cathode, whereas the material with the greatest reactivity is the anode. The potential difference between the two metals is directly related to the rate of electrochemical reactions. The cathode metal is uncorroded, while the anode metal is corroded. Pipe and tubular sheet, corrosion-resistant pipe with paneling, and the vessel's deck coming into contact with brass or bronze blades are all examples of galvanic couplings in heat pumps.

#### 13.3.1.2 Pitting Corrosion

It's a kind of localized warfare in which metal is quickly penetrated and removed in a limited, specified region (shown in Figure 13.4). A pit forms when a small portion of a metal surface is exposed to hazardous species such as the chloride ion as a result of electrochemical or chemical breakdown. Pitting occurs more often when environmental conditions differ from the overall metal surface. On steel, conjunction of

**Figure 13.3** Galvanic corrosion on aluminum hose barb. Source: Popoola et al. [15]/Springer Nature.

**Figure 13.4** Pitting corrosion on the internal surface of the wet gas pipeline. Source: Mansoori et al. [16]/Elsevier.

chlorine and $H_2S$ creates localized pitting. Because of the massive electron transport over vast areas of the surface of the metal, which is the cathode, this pitting region, which is usually the anode, is often severely damaged. Pit development rate is influenced by a variety of factors including transportation, moisture, permeability, ion type, pH level, and ionic strength. When it produces perforation or generates stress in critical areas, it is the most prevalent cause of device, construction, and transportation failure [4, 17].

### 13.3.2 Mechanical Corrosion

#### 13.3.2.1 Stress Corrosion Cracking (SCC)

SCC occurs when tensile stress and corrosive conditions interact, culminating in failure that would not have happened if either of the two were prevalent at that level

**Figure 13.5** SCC has affected an oil and gas pipeline. Source: Popoola et al. [15]/Springer Nature.

alone (shown in Figure 13.5). Stress may be applied or inherent, and the more stress a material is subjected to, the more probable it is to fail. Because residual pressures may have gone unreported during the total load assessment, they are more harmful. When a metal degrades due to SCC, there may or may not be extensive corrosion, but there can be pits that operate as applied load, with the pit's base acting as the site of crack initiation. SSC may take several forms, including corrosive stress cracking (CSC) and sulfide stress cracking (SSC) [17, 18].

### 13.3.3 Chemical Corrosion

#### 13.3.3.1 $H_2S$ Corrosion

Sour corrosion is another name for it. Because it includes hydrogen ions, $H_2S$ is abrasive when dissolved in water. Hydrogen sulfide is a common by-product of oil extraction that poses a significant health risk, mainly in crude oil and gas locations. Iron sulfides (FeSx) and hydrogen are two corrosion by-products. At low temperatures, iron sulfide form a scale that functions as a corrosion barrier. Because the existence of $H_2S$ mixed with tensile strength may induce sulfide stress cracking, selecting the appropriate material is critical. Sour corrosion may be classified into three types: homogeneous, etching, and progressive cracking (shown in Figure 13.6) [18].

#### 13.3.3.2 $CO_2$ Corrosion

Sweet corrosion is another name for it. In oil extraction systems, $CO_2$ is a primary corrosive element (shown in Figure 13.7). At the temperatures found in most oil extraction systems, dry $CO_2$ gas is not corrosive; however, when absorbed in aqueous solutions, it becomes corrosive, causing a redox reaction between steel and the contacting aqueous solution. Carbonic acid is formed when $CO_2$ combines with water, making the fluid acidic. In certain circumstances, the corrosion result is $FeCO_3$, which might function as a protective coating. When carbon dioxide is generated, corrosion pitting develops. $CO_2$ corrosion, which is probably the most prevalent kind of attack in the oil and gas sector, is influenced by the temperature, acidity rise, aqueous

**Figure 13.6** Oil and gas pipeline in sour condition. Source: Popoola et al. [15]/Springer Nature.

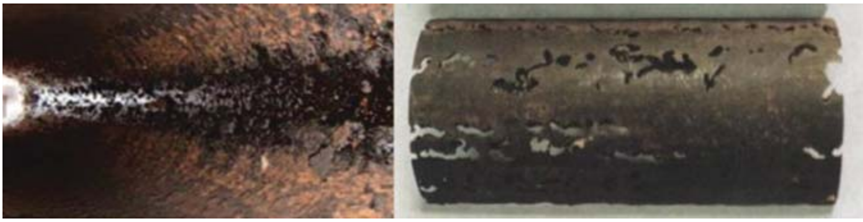

**Figure 13.7** Corrosion due to $CO_2$. Source: Shi et al. [19]/Elsevier.

flow content, the existence of non-constituents, flow condition, and metal properties [20, 21].

#### 13.3.3.3 Oxygen Corrosion

In the petroleum industry, the corrosion damage caused by oxygen on inner surfaces is very severe (shown in Figure 13.8). At depths higher than 100 m below ground, oxygen is commonly unavailable (330 ft). Oxygen contamination is more prevalent in activities that produce oil at near-ambient pressure. Pump seals,

**Figure 13.8** Corrosion due to oxygen. Source: Popoola et al. [15]/Springer Nature.

casings, processed vents, and exposed valves all have the potential to let oxygen into good fluids. As an ion donor in cathodic processes, oxygen increases metal anodic degradation. The passage of elevated drilling fluids through the edges of a drill pipe continued to deliver oxygen to the metal, rendering it hazardous, even at low small concentrations as 5 ppb. When oxygen is present, the destructive impacts of acid gases ($H_2S$ and $CO_2$) are increased. Controlling corrosion caused by oxygen in the hydraulic system seems to be difficult and ineffective. Preventing corrosion induced by oxygen in a drilling fluid system is challenging and inefficient. Homogeneous and pitting corrosion are the two most frequent kinds of corrosion.

## 13.4 Conventional Corrosion Prevention Methods

Many corrosion problems in the oil and gas sectors can be solved using protective coatings and other protective techniques. Every year, millions of paints are utilized as a coating material around the world. One of the easiest and cheapest methods to prevent corrosion is to use protective coatings such as paints, polymer, or powders. Urethane plastic, waxes, and paints are among them [22]. Some of the conventional methods are discussed below.

### 13.4.1 Tar Coatings

Tar coatings are the most ancient coatings utilized in the oil and gas sector (shown in Figure 13.9). They have several distinguishing characteristics, including resistance to water and moisture penetration, good corrosion resistance, low price, and ease of use. While fragility tracked and adhesion dropped, less mechanical strength in cold weather and flexibility in hot weather, perhaps surviving loss or damage during transportation and installation, and poorer resistance to UV rays are all regarded as drawbacks [24].

### 13.4.2 Alloyed Steel (Stainless)

Alloying of steels is one of the most effective corrosion prevention methods known, combining the properties of many metals to increase the wear and corrosion

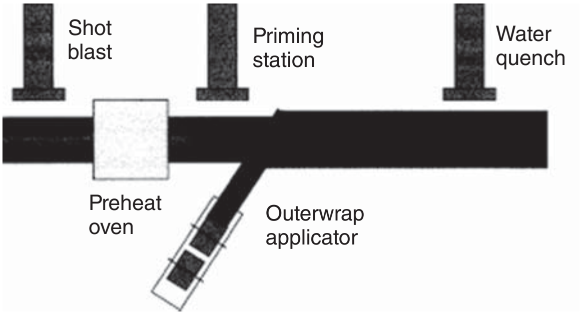

**Figure 13.9** Coating of epoxy Coal Tar. Source: Papavinasam [23]/with permission of Elsevier.

resistance of the final product. When corrosive environment nickel and oxide layer chromium are mixed, an alloy that can be employed in both the oxidative or reduced chemical states is created. Varying alloys provide different degrees of durability in different situations, providing companies with more options. Alloyed steel is rather costly, given its efficacy. They also can't produce films.

### 13.4.3 Cathodic Protection

Electrochemical protection is known as cathodic protection. To prevent corrosion, chemical reactions on metal substrates are converted to inactive sites by feeding ions from another resource, often galvanic anodes are attached just above the surface. Metals such as aluminum, magnesium, and zinc are used to make anodes. While cathodic protection is effective, anodes degrade over time and must be replaced or repaired often, resulting in higher maintenance expenses. In high-resistance circumstances, they also contribute to the structure's mass and are ineffectual.

### 13.4.4 Galvanic Coatings

Galvanic coatings are also being used because they contain metal particles that are non-noble. These coatings form a physical barrier and act as highly active metals that prevent the surface from corrosion when the barrier gets damaged. Zinc coatings may be considered galvanic. These are classified as inorganic zinc coatings based on ethyl silicates and organic zinc coatings based on epoxy resins.

The zinc is present in dust particle form in both these types. The amount of zinc present decides the degree of corrosion protection. Inorganic coatings can be used to provide corrosion protection across a wide range of temperatures typically up to 400 °C due to their silicate backbone. Epoxy zinc coatings give a more limited temperature range not more than 120 °C due to the organic backbone. Due to the wider range, inorganic coatings are preferred over epoxy. However, inorganic coatings have some drawbacks:

- It has a working temperature range of 20–25 °C. Conditions outside this temperature can increase its drying time and productivity.
- Cracking can occur if the applied coating is too thick.
- They continue to degrade over time and their repairing process is very expensive.

### 13.4.5 Polyolefin Coatings

These include coatings made of polyethylene or polypropylene, which have good mechanical strength, a low price, and strong corrosion resistance. One of the major issues with these coatings is that they are less adherent to steel pipes. Polyethylene coating has some limitations, including limited impact resistance, especially at high temperatures, mud crackup because of soil stress, and low thermal resistance. To tackle this problem, a three-layer coating method with epoxy liner, middle layer, enhanced copolymer polyolefin, and polyolefin surface coating is suggested.

Epoxy lining provides cohesiveness and resistance to cathodic disbandment in this system, while polyolefin provides mechanical characteristics, chemical resistance, and penetration to water and oxygen. Extrusion is used to apply these coatings. Polyurethane (PU) coatings are also utilized, and they produce better outcomes than polyethylene and polypropylene. They have good chemical resistance, high impact resistance, good flexibility, and strong adherence to metal surfaces. However, the issue of its long-term stability persists. Ultraviolet (UV) radiation can cause polymeric coatings to degrade over time. These coatings can develop micro-cracks and have a shorter lifespan therefore these are not the best solution to slow down the corrosion process [24].

### 13.4.6 Fusion Bonded Epoxy (FBE) Coating

Pipelines, steel pipes, and a variety of piping fittings are all protected by fusion bonded epoxy (FBE) coatings, which is a thermoset powder or resin coatings. FBE coatings are thermoset polymers by nature. This coating is mainly composed of a powder or polymeric resin that is applied to the surface of the pipes and then heated to a high temperature to initiate cross-linking. FBE coating, unlike conventional paint, involves resin cross-linking.

FBE provides enhanced quality control, uniform coating thickness, and excellent coating-to-steel bonding due to its superior adhesive properties. FBE coatings, on the other hand, should be treated with caution since even minor damage/defects can have a substantial influence on the coating's performance because patching in the damaged area is not always effective, and slight damage in the coating might cause corrosion in a harsh atmosphere. Both UV degradation and alkali resistance are poor [25].

## 13.5 Smart Coatings

The above-described coatings are a reasonable solution to corrosion prevention however they fail over long period and have some disadvantages. Therefore, to incorporate this, smart coatings are now being developed. Some of the smart coatings are discussed below.

### 13.5.1 Polymer Composite Coating

In this technique, microcapsules as reinforcement are mixed into a coating matrix allowing active agents to be released in a controlled manner. This allows the repairing agent to be released quickly as the crack propagates through the coatings, resulting in self-healing. Nanoparticles include $SiO_2$, $Al_2O_3$, $TiO_2$, ZnO, and ZnS. Among these, zinc oxide and titanium oxide are used as UV blocking agents due to their lower photocatalytic ability [26].

Lowry et al. [27] investigated the effects of nano-ZnO incorporated coatings with low nano-ZnO particle dispersion in a PU/acrylic coating. Madidi et al. [28] developed a silicone rubber/$TiO_2$ coating via spray coating method and tested its stability under UV light. Results showed that the coating's superhydrophobicity was retained after 212 hours of UV exposure and 80 hours of condensation with no appreciable color change. Graphene is a good UV light-absorbing material that is commonly employed for polymer coatings in addition to metal oxide nanoparticles. Furthermore, the high UV-shielding characteristic of graphene can be attained with reduced graphene content in polymer coatings due to its large surface area.

Nuraje et al. [29] added graphene in PU coating with an epoxy-based primer for improved weathering. Results revealed that the inclusion of graphene increased resistance to UV degradation.

### 13.5.2 Conducting Polymer Coating

Conducting polymers are commonly used as protective coatings on metals to decrease the rate of corrosion and increase protection efficiency values. In recent years, conducting polymers encapsulated in Montmorillonite (MMT) layers has attracted a lot of research attention. Conducting polymers, such as polyacetylene, polyaniline (PANI), polypyrrole (PPy), and polythiophene have attracted a lot of theoretical attention and practical applications in various sectors, particularly in corrosion protection for metals. They have oxidizing properties which cause steel passiveness. The electro-active interface can be displaced from its regular location by conductive polymers in their conducting state [30].

#### 13.5.2.1 Polyaniline

PANI is being considered a potential corrosion-resistant material for metals. PANI is a good anticorrosive coating candidate to substitute chromium-containing coatings, which have negative health and ecological consequences [31]. Tallman and coworkers [32] gave an overview of the consumption of conducting polymers for corrosion management, with a focus on the protection provided by PANI to aircraft structural alloys such as 2024-T3, 6061, and 7075. Because of its good electrical conductivity, simplicity of production, cheap monomer, enhanced stability, and potential implementation, PANI is the most potential conducting polymer contender. PANI-epoxy mix coating provided remarkable protection against Mild Steel corrosion, according to Talo et al. [33].

#### 13.5.2.2 Polypyrrole

PPy is a potential conducting polymer due to its high conductance, resilience, simplicity of manufacture, and environmental friendliness [31]. Bilayer PPy coatings for steel corrosion prevention were investigated by Kowalski et al. [34]. According to the findings, the bilayered coating kept the steel in a passive (inactive) state and prevented corrosion for a longer length of time.

#### 13.5.2.3 Polycarbazole and its Derivatives

Conducting polymers of polycarbazole (PCz) and poly (*N*-vinyl carbazole) (PVCz) were electro-coated over a natural iron sulfide ($FeS_2$) surface. Electrochemical coating reduced photoactivity by inhibiting corrosion and photo corrosion of $FeS_2$, whereas chemical coating of thin, transparent PVCz on the surface increased the photoactivity while inhibiting corrosion and photo corrosion [31].

### 13.5.3 Self-healing Polymers for Coatings

Self-healing polymers have the most satisfactory performance among the smart polymers. They can return to their original shape after damage without losing their properties. They are generally classified as extrinsic and intrinsic. In extrinsic, a self-healing agent is introduced into the polymer in the form of microcapsules or hollow fibers. They consist of a catalyst, cross-linker, and a healing agent. Healing occurs due to diffusion or any chemical reaction. Therefore, a catalyst acts to promote that chemical reaction to heal the surface. Usually, the microcapsule approach has been very successful in which micron-sized particles of solids and liquids are enclosed in an inert shell that protects them from the external environment while allowing them to release the healing agent at the specific damaged area, resulting in a more controlled healing process. Microcapsules or hollow fibers are used to contain various components such as monomers, dyes, catalysts, corrosion inhibitors, and hardeners. These reservoirs can be put into systems during polymer or coating manufacture, and they can be broken if a crack occurs. The healing agent is then released into the fractures, which hardens, and cures the cracks through capillary force [35].

In intrinsic, the polymer itself has self-healing properties although an external stimulus is required such as heat, light, current, pH, or moisture. These polymers include poly (*N*-acetyl ethyleneimine), poly(urea–urethane), polylactic acid (polylactide), and polyhydroxy urethanes. Healing occurs due to the mobility of polymeric chains and their surface approaching ability after the damage. The main applications for self-healing polymers are in the development of smart coatings to slow down corrosion. In Figure 13.10, a polymeric coating of polyethylene having an encapsulated healing agent is applied on steel pipe with a primer i.e. usually, a paint that improves the adhesion of coatings with the metal substrate. As the UV light starts to degrade the coating, the capsule breaks and releases the healing agent which then repairs the damage.

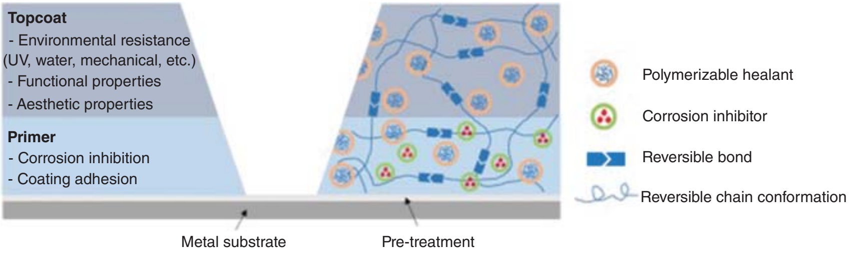

**Figure 13.10** Self-healing coatings for corrosion protection. Source: Zhang et al. [36]/Public Domain CC BY.

#### 13.5.3.1 Synthesis of Micro/Nano-Capsule

Microencapsulation is the process of enclosing micron-sized solid, liquid, or gas groups in inert shells to protect them from the surroundings. The production of microcapsules is the final result of this work. Microcapsules are made up of two parts: a core and a shell, and they can vary in size (micro, nano) and shape [37].

Small particles (3–800 m) with a liquid-filled center and a coated topmost layer are known as micro-/nano-capsules. The most prevalent methods for making microcapsules include interlayer polymerization, ejection, in situ polymerization, and solgel procedures. Interfacial polymerization is the most common approach for encapsulating inhibitors in polymeric shells. At the intersection of two immiscible liquid phases, interfacial polymerization occurs. For this reason, the active monomer must first be saturated in a first solvent. The solution may then be emulsified in a second solvent with the help of a surfactant. The second stage of the polymerization process is to introduce another reactive monomer to the polymerization phase. Micro/nano-capsules may be made via the polymerization of two monomers on the surface of emulsion droplets. This may be done using several emulsions with various qualities. Oil-in-water emulsions are often used for interfacial polymerization [38, 39]. The reactants may be swirled at different speeds throughout the emulsification process to generate capsules of varied sizes. As the stirring speed is raised, the average diameter of the capsules falls.

#### 13.5.3.2 Mechanism of Self-healing Polymers

Figure 13.11 depicts the mechanism of a self-healing polymer. Self-healing coatings work by releasing corrosion inhibitors on-demand from smart micro/nano-capsules embedded in organic coatings. The corrosion inhibitors may be released from the capsules by physical activation, acidity, or temperature-controlled stimulation.

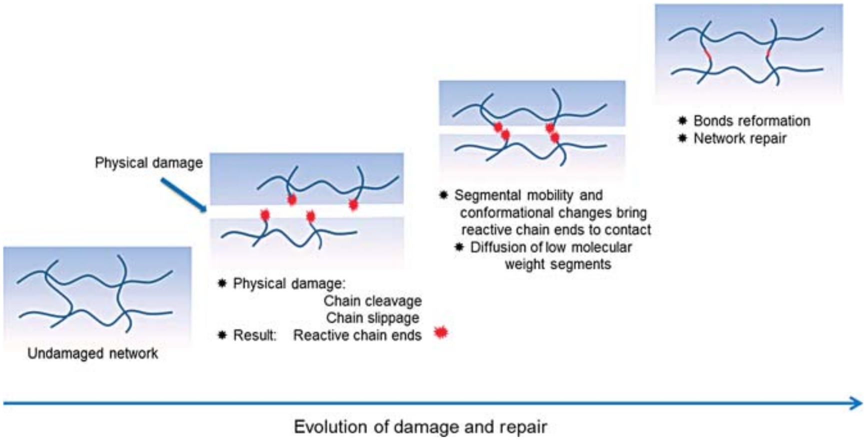

**Figure 13.11** Healing mechanism of self-healing polymers. Source: Yang and Urban [40]/Royal Society of Chemistry.

The capsules' composition, as well as the susceptibility of the capsules' shell to pH, determine the degree of healing. Physical impact or a shift in the external environment trigger the capsules to discharge the reducing agents at the appropriate locations (e.g. pH). Chloride ions may pass through the covering to the metallic substrate because of the fracture. As a consequence, corrosion processes commence on the metal substrate. During cathodic processes, the hydroxyl ion ($OH^-$) is formed, causing localized pH increases at the metallic surface's cathodic sites. The inhibitors from the capsules seep into the defect when the pH increases, breaking down the polyelectrolyte shell and enhancing the defect's permeability. The corrosion inhibitors that are generated both cure the damage and prevent it from happening again [35].

The self-healing properties of PU-based microcapsules injected with isosorbide derivative were investigated by Koh et al. [41]. In an interfacial polymerization procedure, they synthesized the microcapsules by combining a mixture of 2,6 diethyl-1,3-diisocyanato-4-methylbenzene and 4,6 diethyl-1,3-diisocyanato-2-methylbenzene (DETDI) copolymer with 1,4-butanediol. They created the microcapsules by combining a DETDI prepolymer with 1,4-butanediol in an interfacial polymerization process. Corrosion inhibitors at values of 25–200 ppm were observed to display potential resistance to corrosion and a low decaying degree in microcapsules (0.47%) (Figure 13.12).

Raps et al. [42] investigated the self-healing characteristics of epoxy water-based coatings supplemented with corrosion inhibitor-loaded nano-capsules such as 2-methylbenzothiazole (BT) and 2-mercaptobenzothiazole (BMBT) (MBT). By including liquid core nano-capsules packed with a natural heterogeneous catalyst into the coating matrix [43], they exhibited acceptable self-healing. Raps and colleagues looked at the healing mechanisms of a polyurea microcapsule-doped epoxy primer. This system received active corrosion protection thanks to the discharge of the inhibitor solution and the formation of a passive layer within micro-cracks on the surface layer.

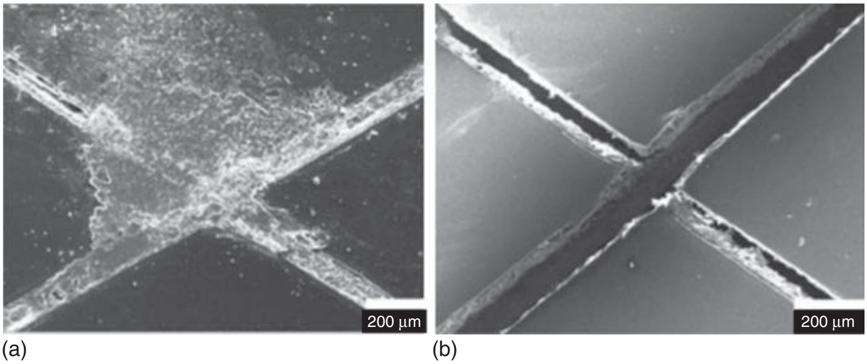

(a) (b)

**Figure 13.12** SEM micrographs of (a) the itched region of the control panel and (b) the self-healing anticorrosion coating after healing. Source: Koh et al. [41]/American Chemical Society.

White et al. used an epoxy matrix and Grubbs' catalyst to scatter dicyclopentadiene (DCPD) as a liquid healing agent. A loop-breaking metathesis polymerization occurs when DPCD interacts with the Grubbs' catalyst, producing a strongly merge tough polydicyclopentadiene that repairs the fracture.

Alexander et al. [44] created acrylate polycaprolactone (PCL) polyurethane-based UV-cure self-healing coatings. The results revealed that these coatings have excellent mechanical qualities and self-healing abilities. The majority of the coating composition is usually made up of two main structural components in such coatings. A reactive diluent, usually a low molecular mass (multi)functional acrylate monomer, is usually combined with an oligomeric acrylate resin. Irradiation formed a complex system in which both the reacting diluent and the resin may function as cross-linkers, resulting in an impermeable, static coating. There are many approaches for incorporating movement into the end coating material. To begin, use a monofunctional active diluent to produce larger linear acrylate chains. Second, a molecular mass acrylate resin with limited functionality may be utilized to keep the overall cross-link density low. On the other side, these techniques will lower the coating's resistance and strength. To mitigate these adverse effects, a volatile diluent was selected that, when cured, creates a polymer with a reduced cross-link density but a $T_g$ much above ambient temperature, accounting for the negative effects without adding excessive stiffness.

Isobornyl acrylate is a monomer commonly utilized in industrial applications where the final cured product must have a high $T_g$. As a cross-linker, a commercial PCL diol with a reasonably high molecular weight was employed as the starting material. The synthesis of a PCL–urethane prepolymer was acrylate end-capped by adding 2-hydroxyethyl acetate to a dibutyltin dilaurate (DBTL)-catalyzed reaction with 2-hexamethylene diisocyanate at 90 °C in dry toluene, generating polypropylene nonwoven fabrics (PPNF).

Huang et al. [45] prepared an intrinsic epoxy system with bifunctional adducts by Diels–Alder reaction. Diels–Alder epoxy resins are resilient in harsh environments such as oxidation agents, air, and water. Microscopy studies showed that the coating had recovered its structural integrity. Immersion testing also showed complete restoration of corrosion protection of the healed sample.

Chen et al. [46] studied the effects of self-healing coatings on steel reinforcement. Tung oil i.e. a triglyceride drying oil was encapsulated and inserted into an epoxy matrix and coating was prepared. These coatings were applied to steel reinforcement and given time to cure. The samples were then damaged and tested. The optical microscopy test confirmed the self-healing ability of these coatings.

By strengthening a composite material with halloysite nanotubes (HNTs) equipped with sodium nitrate and urea–formaldehyde microparticles packed with a self-healing agent, Habib et al. [47] produced a multifunctional polymeric smart coating (linseed oil). The produced coatings were applied to the refined mild steel substrate using the doctor's blade method. It was discovered that HNTs release inhibitors in a pH-dependent manner. According to the findings, the produced coatings might offer adequate protection against corrosion for steel in the oil and gas sector.

Shchukina and Shchukin [48] linked the corrosion protection of poly epoxy powder coatings with 8-hydroxyquinoline loaded into HNTs and mesoporous silica and found that both successfully resisted pitting corrosion.

To develop self-healing acrylic and polyurethane composite coatings for Cu, Abdullayev et al. employed organic inhibitors 2-mercaptobenzothiazole (MBT), benzotriazol (BTA), and 2-mercaptobenzimidazole (MBI) as alloying elements in halloysite clay nanotubes. The release behavior of doped halloysites indicated that BTA and MBT were produced in two stages (fast and slow), whereas MBI was released in one. For coatings with modeled 5 mm scratches, MBT and MBI showed the greatest self-healing capabilities.

## 13.6 Conclusion

This chapter has provided discussions about smart coatings as a solution to long-term flaws in conventional methods of preventing corrosion. The main function of the smart coating is corrosion protection. The literature has shown that using self-healing polymers in coatings is the most reasonable method to develop smart coatings due to their ability to repair the fractures or scratches without losing the original properties as soon as the damage occurs in the coating.

Although the approach of using self-healing polymers in coatings mentioned in this chapter has shown good performance to prevent corrosion for longer times which is the main challenge in oil and gas industries, the approach is still in the preliminary development stage and hasn’t gotten a lot of attention. This is due to the complexity of the processing techniques, the restricted time and ranges for their healing capability, and the negative effects of the healing agents on the quality of the coating. As a result, current and future advancements in self-healing coatings are concentrated on optimizing techniques to alleviate difficulties.

## Acknowledgment

The authors acknowledge the support provided by PPE Department, UET Lahore, Pakistan.

## References

1 Mohamed, E.A., Saleh, R.A., and Yagub, M.T. (2015). The effect of acetate ions on $CO_2$ corrosion of mild steel at different pHs. *University Bulletin* 17: 35–54.

2 Papavinasam, S. (2014). “Mechanisms.” *Corrosion Control in the Oil and Gas Industry*, 1 *Gulf Professional Publishing* Houston, TX, USA: 249-300. https://doi.org/10.1016/B978-0-12-397022-0.00005-4

3 Buchanan, R.A. and Stansbury, E.E. (2012). Electrochemical corrosion. In: *Handbook of Environmental Degradation of Materials* (ed. M. Kutz), 87–125. Elsevier.

4 Ossai, C.I. (2012). Advances in asset management techniques: an overview of corrosion mechanisms and mitigation strategies for oil and gas pipelines. *ISRN Corrosion* 2012: 1–10.

5 Xiao, Y. and Nesic, S. (2005). A stochastic prediction model of localized $CO_2$ corrosion, OnePetro. http://www.icmt.ohio.edu/documents/publications/8140.pdf.

6 Fajardo, V., Canto, C., Brown, B., and Nesic, S. (2007). Effect of organic acids in $CO_2$ corrosion, OnePetro.

7 Hedges, B., Chen, H.J., Bieri, T.H., and Sprague, K. (2006). A review of monitoring and inspection techniques for $CO_2$ and $H_2S$ corrosion in oil & gas production facilities, OnePetro.

8 Dugstad, A., Gulbrandsen, E., Seiersten, M., et al. (2006). Corrosion testing in multiphase flow, challenges and limitations, OnePetro.

9 Nesic, S., Cai, J., and Lee, K.-L. (2005). A multiphase flow and internal corrosion prediction model for mild steel pipelines, OnePetro.

10 Nalli, K. (2012). Appendix VI: corrosion and its mitigation in the oil and gas industries. *Process Plant Equipment* 673–679. https://doi.org/10.1002/9781118162569.APP6.

11 Keating, A. and Nesic, S. (1999). Prediction of two-phase erosion-corrosion in bends.

12 Nesic, S. and Postlethwaite, J. (1990). Relationship between the structure of disturbed flow and erosion—corrosion. *Corrosion* 46: 874–880.

13 Wen, J., Gu, T., and Nesic, S. (2007). Investigation of the effects of fluid flow on Srb biofilm.

14 Fang, H., Brown, B., and Nescaronicacute, S. (2011). Effects of sodium chloride concentration on mild steel corrosion in slightly sour. *Environments* 67: 015001-1–015001-12.

15 Popoola, L.T., Grema, A.S., Latinwo, G.K. et al. (2013). Corrosion problems during oil and gas production and its mitigation. *International Journal of Industrial Chemistry* 4: 1–15.

16 Mansoori, H., Mirzaee, R., Esmaeilzadeh, F. et al. (2017). Pitting corrosion failure analysis of a wet gas pipeline. *Engineering Failure Analysis* 82: 16–25.

17 Kumar, S., Harsimran, S., Santosh, K., and Rakesh, K. (2021). Overview of corrosion and its control: a critical review. 3: 13–24.

18 Tuttle, R.N. (1987). Corrosion in oil and gas production. *Journal of Petroleum Technology* 39: 756–762.

19 Shi, L., Wang, C., and Zou, C. (2014). Corrosion failure analysis of L485 natural gas pipeline in $CO_2$ environment. *Engineering Failure Analysis* 36: 372–378.

20 Al-Janabi, Y.T. (2020). An overview of corrosion in oil and gas industry. In: *Corrosion Inhibitors in the Oil and Gas Industry* (ed. V.S. Saji and S.A. Umoren), 1–39. Wiley.

21 Amani, M. and Hjeij, D. (2015). A comprehensive review of corrosion and its inhibition in the oil and gas industry. *Society of Petroleum Engineers*. SPE Kuwait Oil and Gas Show and Conference, Mishref, Kuwait, Paper Number: SPE-175337-MS.

**22** Weiss, K.D. (1997). Paint and coatings: a mature industry in transition. *Progress in Polymer Science* 22: 203–245.

**23** Papavinasam, S. (2014). Mitigation – external corrosion. In: *Corrosion Control in the Oil and Gas Industry*, 529–620. Elsevier.

**24** Samimi, A. (2012). Use of polyurethane coating to prevent corrosion in oil and gas pipelines transfer. *International Journal of Innovation and Applied Studies* 1: 186–193.

**25** Nayyar, M.L. (2000). Fusion-bonded epoxy internal linings and external coatings for pipeline corrosion protection. In: *Piping Handbook*. McGraw-Hill Education.

**26** Ching, Y.C., Udenni Gunathilake, T.M.S., Ching, K.Y. et al. (2019). Effects of high temperature and ultraviolet radiation on polymer composites. In: *Durability and Life Prediction in Biocomposites, Fibre-Reinforced Composites and Hybrid Composites*, 407–426. https://doi.org/10.1016/B978-0-08-102290-0.00018-0.

**27** Lowry, M.S., Hubble, D.R., Wressell, A.L. et al. (2008). Assessment of UV-permeability in nano-ZnO filled coatings via high throughput experimentation. *Journal of Coatings Technology and Research* 5: 233–239.

**28** Madidi, F., Momen, G., and Farzaneh, M. (2016). Development of a stable $TiO_2$ nanocomposite self-cleaning coating for outdoor applications. *Advances in\break Materials Science and Engineering* 2016.

**29** Nuraje, N., Khan, S.I., Misak, H., and Asmatulu, R. (2013). The addition of graphene to polymer coatings for improved weathering. *ISRN Polymer Science* 2013: 1–8.

**30** Stankiewicz, A., Szczygieł, I., and Szczygieł, B. (2013). Self-healing coatings in anti-corrosion applications. *Journal of Materials Science* 48: 8041–8051.

**31** Ates, M. (2016). A review on conducting polymer coatings for corrosion protection. *Journal of Adhesion Science and Technology* 30: 1510–1536.

**32** Spinks, G.M., Dominis, A.J., Wallace, G.G., and Tallman, D.E. (2001). Electroactive conducting polymers for corrosion control. *Journal of Solid State Electrochemistry* 62 (6): 85–100.

**33** Talo, A., Forsen, O., and Ylasaari, S. (1999). Corrosion protective polyaniline epoxy blend coatings on mild steel. *Synthetic Metals* 102: 1394–1395.

**34** Kowalski, D., Ueda, M., and Ohtsuka, T. (2007). Corrosion protection of steel by bi-layered polypyrrole doped with molybdophosphate and naphthalenedisulfonate anions. *Corrosion Science* 3: 1635–1644.

**35** Kardar, P., Yari, H., Mahdavian, M., and Ramezanzadeh, B. (2016). Smart self-healing polymer coatings: mechanical damage repair and corrosion prevention. *Industrial Applications for Intelligent Polymers and Coatings* 511–535.

**36** Zhang, F., Ju, P., Pan, M. et al. (2018). Self-healing mechanisms in smart protective coatings: a review. *Corrosion Science* 144: 74–88.

**37** Benita, S. (2006). *Microencapsulation Methods Industrial Applications*. AbeBooks.

**38** Alexandridou, S., Kiparissides, C., Mange, F., and Foissy, A. (2008). Surface characterization of oil-containing polyterephthalamide microcapsules prepared by interfacial polymerization. *Journal of Microencapsulation (Micro and Nano Carriers)* 18: 767–781.

**39** Hong, K. and Park, S. (1999). Preparation of polyurethane microcapsules with different soft segments and their characteristics. *Reactive and Functional Polymers* 42: 193–200.

**40** Yang, Y. and Urban, M.W. (2013). Self-healing polymeric materials. *Chemical Society Reviews* 42: 7446–7467.

**41** Koh, E., Lee, S., Shin, J., and Kim, Y.W. (2013). Renewable polyurethane microcapsules with isosorbide derivatives for self-healing anticorrosion coatings. *Industrial and Engineering Chemistry Research* 52: 15541–15548.

**42** Raps, D., Hack, T., Kolb, M. et al. (2010). Development of corrosion protection coatings for AA2024-T3 using micro-encapsulated inhibitors. *ACS Symposium Series* 1050: 165–189.

**43** Kopeć, M., Szczepanowicz, K., Mordarski, G. et al. (2015). Self-healing epoxy coatings loaded with inhibitor-containing polyelectrolyte nanocapsules. *Progress in Organic Coatings* 84: 97–106.

**44** Lutz, A., van den Berg, O., Wielant, J. et al. (2016). A multiple-action self-healing coating. *Frontiers in Materials* 2: 73.

**45** Huang, M., Zhang, H., and Yang, J. (2012). Synthesis of organic silane microcapsules for self-healing corrosion resistant polymer coatings. *Corrosion Science* 65: 561–566.

**46** Chen, Y., Xia, C., Shepard, Z. et al. (2017). Self-healing coatings for steel-reinforced concrete. *ACS Sustainable Chemistry & Engineering* 5: 3955–3962.

**47** Habib, S., Khan, A., Nawaz, M. et al. (2019). Self-healing performance of multifunctional polymeric smart coatings. *Polymers (Basel)* 11.

**48** Shchukina, E. and Shchukin, D.G. (2019). Nanocontainer-based active systems: from self-healing coatings to thermal energy storage. *Langmuir* 35: 8603–8611.

# 14

# Surface Characterization Techniques in Corrosion Inhibition Research

*Ambrish Singh*[1], *Kashif R. Ansari*[2], *Shivani Singh*[3], *Mumtaz A. Quraishi*[2], *and Yuanhua Lin*[1]

[1] *Southwest Petroleum University, School of New Energy and Materials, Chengdu 610500, Sichuan, China*
[2] *King Fahd University of Petroleum and Minerals, Interdisciplinary Research Center for Advanced Materials, Dhahran 31261, Saudi Arabia*
[3] *Lovely Professional University, School of Bioengineering and Biosciences, Phagwara 144402, Punjab, India*

## 14.1 Introduction

The introduction of a corrosion inhibitor into the aggressive solution undergoes adsorption onto the selected surface of metal. For complete understanding of the corrosion inhibitor adsorption and corresponding inhibition efficiency of inhibitor film, it is important to go through specific experimental methods. The methods consist of an evaluation of inhibition efficiency of corrosion inhibitor, elucidating adsorption mechanism methods, different electrochemical methods, and characterization of surface methods. The corrosion evaluation methods may be categorized into many types depending upon the principle of operation and methods of data obtained. In general, the primary reference for these tests is based on ASTM standards [1].

The first method category is the immersion (weight loss) where information about the inhibitor concentration is gathered at which inhibitor provides the maximum inhibition efficiency [2–4]. In the present time, different methods that are advanced have come but the weight-loss method is the simplest and most trusted method for evaluation of inhibitor performance. The second category consists of electrochemical methods for the investigation of corrosion inhibition of inhibitors that are electrochemical impedance spectroscopy (EIS), electrochemical frequency modulation (EFM), electrochemical frequency modulation trend (EFMT), and polarization resistance. These methods give information on real-time electrochemical behavior of corrosion and are nondestructive [5, 6]. The other electrochemical method is potentiodynamic polarization (PDP), which is a destructive method and after performing this experiment, the metal surface is no longer of use. The electrochemical methods give measurable information about adsorption of corrosion inhibitors, and additionally, the electrochemistry occurs over the corroding metal surface. The third method category evaluates the surfaces of the corroded and protected metal samples. This method includes scanning electron microscopy (SEM),

*Polymeric Corrosion Inhibitors for Greening the Chemical and Petrochemical Industry*, First Edition.
Edited by Mohammad A. Jafar Mazumder, Mumtaz A. Quraishi, and Amir Al-Ahmed.

atomic force microscopy (AFM), scanning electrochemical microscopy (SECM), X-ray photoelectron spectroscopy (XPS), and contact angle measurements. These methods are very useful by providing direct information on the inhibitor structure as well as the adsorbed inhibitor composition elemental status over surface of metal [7–11]. Additionally, these experimental techniques support to assist in explaining inhibitor mechanism adsorption and inhibitor–metal interaction.

In the present chapter, we try to describe the commonly used experimental methods for the examination of corrosion inhibitor performance. The above-mentioned methods have been explained using typical examples.

## 14.2 Method of Weight Loss

The weight loss is simplest, affordable, and commonly used method for the evaluation of the corrosion inhibition efficiency of corrosion inhibitor. Initially, the metal samples were cut into desired coupon sizes and were polished using different grit abrasive papers. The rinsed and cleaned coupons were kept in desiccator. Then the coupon samples were immersed into the aggressive medium and after the known time (6/12/24 hours) samples were removed and washed as per the ASTM standard [12–15]. The weight-loss difference before and after the immersion gives average weight loss [16].

The speed of the metal destruction in the given specific corrosive environment is known as the corrosion rate ($C_\mathrm{R}$). The corrosion rate (mm/y) is estimated as per Eq. (14.1):

$$C_\mathrm{R} = \frac{8.76 \times 10^4 \times \Delta m}{s \times t \times \rho} \tag{14.1}$$

where $C_\mathrm{R}$ is corrosion rate (mm/y), $\Delta m$ is weight loss (g), $\rho$ is steel density (g cm$^{-3}$), $A$ is steel exposed area (cm$^2$), and $t$ is testing duration (h).

The application of corrosion rate was used for the estimation of surface coverage ($\theta$) (Eq. 14.2) and the inhibition efficiency ($\eta\%$) (Eq. 14.3):

$$\theta = \frac{C_{\mathrm{R}(a)} - C_{\mathrm{R}(p)}}{C_{\mathrm{R}(a)}} \tag{14.2}$$

$$\eta\% = \frac{C_{\mathrm{R}(a)} - C_{\mathrm{R}(p)}}{C_{\mathrm{R}(a)}} \times 100 \tag{14.3}$$

(14.2)(14.3)where $C_{\mathrm{R}(a)}$ and $C_{\mathrm{R}(p)}$ are corrosion rates without and with corrosion inhibitors, respectively.

Alternatively, the corrosion rate ($C_\mathrm{R}$) in mpy (Eq. 14.4) and mg cm$^{-2}$ h$^{-1}$ (Eq. 14.5) can also be calculated as follows:

$$C_\mathrm{R} = \frac{3.45 \times 10^3 \times \Delta m}{\rho A t} \tag{14.4}$$

$C_\mathrm{R}$, $A$, $t$, and $\Delta m$ correspond to the corrosion rate (mm/y), steel area (cm$^2$), immersion time (h), and change in mass loss (g). 3.45 is a constant.

$$C_\mathrm{R} = \frac{\Delta m}{At} \tag{14.5}$$

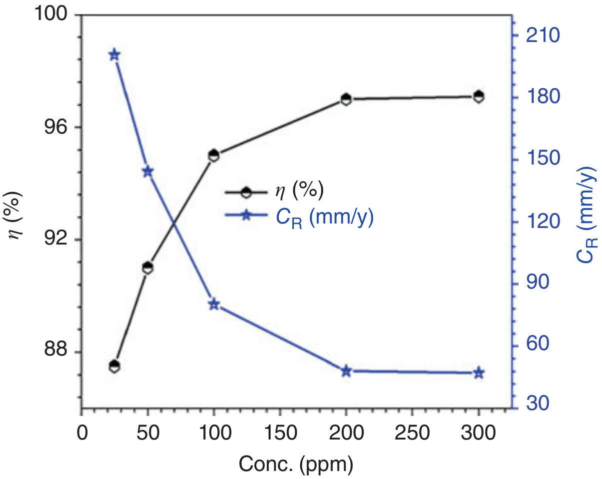

**Figure 14.1** Variation of inhibitor concentration with $\eta$% and $C_R$.

### 14.2.1 Concentration of Inhibitor

The method of weight loss was used to analyze the inhibition efficiency ($\eta$%) and corrosion rate ($C_R$). Figure 14.1 represents the $\eta$% and $C_R$ variation with an increasing concentration of inhibitor [17].

The inhibitor addition leads to increase in $\eta$% and decrease in $C_R$ values, respectively. After reaching the maximum values, the increase in the concentration does not produce any significant change in the values. Thus, value has supposed to optimum inhibitor concentration. The increase in $\eta$% and decrease in $C_R$ with increasing inhibitor concentration suggest the formation of an inhibitor protective layer that covers more surface area at optimum concentration and minimize the contact of corrosive medium with metal active sites. This supports the adsorption of inhibitor molecules.

### 14.2.2 Temperature Effect and Parameters of Activation

Temperature plays an important role in terms of kinetics of corrosion reaction behavior of corroding metal by changing the adsorption strength of inhibiting compounds. It is a well-known fact that an increase in temperature can break weak electrostatic adsorption bonds among metal and corrosion inhibitor [18]. This process mainly occurs by an increase in the kinetic energy of corrosion inhibitor by an increase in temperature that makes the molecules to desorb from the metal surface that finally lowers the performance of the corrosion inhibitor [19]. However, whenever the increase in temperate causes no change/increase in corrosion inhibitor performance then the adsorption is said as chemical adsorption. In this way, chemical/coordinate bonds have formed between the metal and corrosion inhibitor.

The dependency of corrosion inhibitor performance on temperature can be justified using Arrhenius and the transition state equations [20]:

$$C_\mathrm{R} = A \exp\left(\frac{-E_\mathrm{a}}{RT}\right) \tag{14.6}$$

$$C_\mathrm{R} = \frac{RT}{Nh} \exp\left(\frac{\Delta S^*}{R}\right) \exp\left(-\frac{\Delta H^*}{RT}\right) \tag{14.7}$$

where $E_\mathrm{a}$, $T$, $A$, and $R$ are energy of activation, temperature, pre-exponential factor, and gas constant, respectively; $N$, $h$, $\Delta H^*$, and $\Delta S^*$ are Avogadro number, Plank's constant, enthalpy, and entropy of activation, respectively.

Figure 14.2a represents Arrhenius plots. The values of $E_\mathrm{a}$ are calculated from the slope of the plots i.e. $E_\mathrm{a}/2.303R$. A plot of $\log C_\mathrm{R}/T$ vs. $1/T$ (Figure 14.2b) provides a straight line with a slope of $\Delta H^*/2.303R$ and intercept of $\log (R/Nh) + \Delta S^*/2.303R$ known as the transition-state plot, which allows the calculation of $\Delta H^*$ and $\Delta S^*$.

The higher value of $E_\mathrm{a}$ in presence of inhibitor as compared to the absence of inhibitor reveals toward increment in the thickness of double-layer thickness, which ultimately increases the barrier of activation energy of corrosion reaction and thus reduces the corrosion process [21]. In general, the increment in the activation energy with the addition of inhibitor represents the physical nature of corrosion inhibition adsorption, and this is the initial stage of corrosion inhibitor adsorption [22]. However, chemical adsorption of inhibitors is represented by the lower $E_\mathrm{a}$. But the adsorption type cannot be judged only on the basis of $E_\mathrm{a}$ values because the adsorption process is competitive in nature and it is taking place by the replacement of the pre-adsorbed water molecules that also require some activation energy [23].

The positive value of $\Delta H^*$ reveals the slower dissolution of metal [24]. The increasing value of $\Delta H^*$ in presence of inhibitor suggests that the energy barrier that governed the corrosion reaction has increased. In the same way, an increase in the values of $\Delta S^*$ with the addition of corrosion inhibitor reveals toward the adsorption of inhibitor over the metal surface [25]. The inhibitor adsorption is by replacing pre-adsorbed water molecules. Thus, an increase in entropy of solvent reflects the increase in the value of $\Delta S^*$ [25].

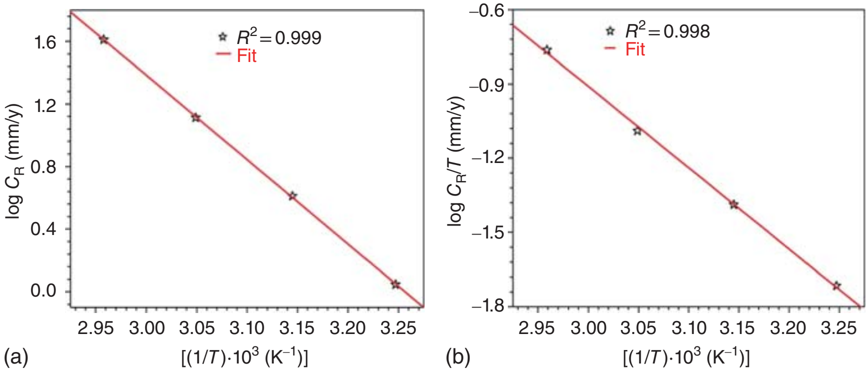

**Figure 14.2** (a) Arrhenius plot (b) transition-state plot.

## 14.3 Parameters of Adsorption

### 14.3.1 Isotherms

The interactive nature of corrosion inhibitor and metal surface is analyzed using various kinds of adsorption isotherms models [26]. The selection isotherm plays a key role in the understanding of the adsorptive nature of corrosion inhibitors. The parameters obtained from the fitting of isotherm are used for the calculation of standard free energy of adsorption, which helps to determine whether the corrosion reaction is spontaneous or not and also inhibitor adsorption is physical or chemical [27]. Some adsorption isotherms models are explained briefly in this section:

(a) **Langmuir isotherm model:** The isotherm assumes that a single inhibitor layer has formed over the metal surface with the number of localized equilibrium sites are fixed. It also assumes that there is no lateral interaction that takes in between adsorbed and free inhibitor molecules. The below equation describes Langmuir isotherm model [28]:

$$\frac{C_{\mathrm{inh}}}{\theta} = \frac{1}{K_{\mathrm{ads}}} + C_{\mathrm{inh}} \tag{14.8}$$

where $C_{\mathrm{inh}}$ and $K_{\mathrm{ads}}$ are concentration and equilibrium constant. The typical Langmuir isotherm graph is given in Figure 14.3

(b) **Temkin isotherm model:** The equation used for the calculation of this model is as follows:

$$\exp(-2a\theta) = K_{\mathrm{ads}}C \tag{14.9}$$

where $C$ = inhibitor concentration, $\theta$ = fraction of site occupied by inhibitor molecules, and $a$ = interaction parameter between adsorbing species and the metal surface [29]. The Temkin isotherm is plotted using the values of surface coverage ($\theta$) vs. log $C$ (Figure 14.4).

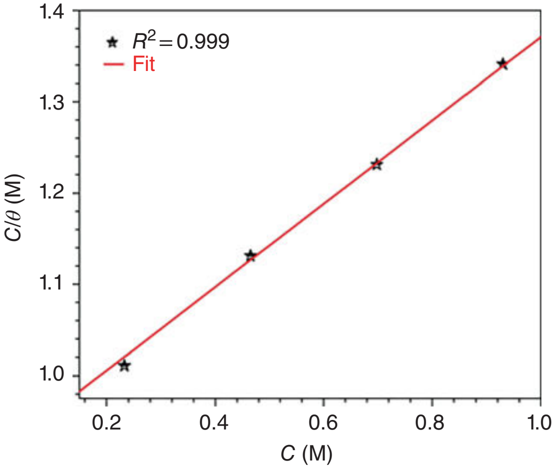

**Figure 14.3** Langmuir isotherm for the adsorption.

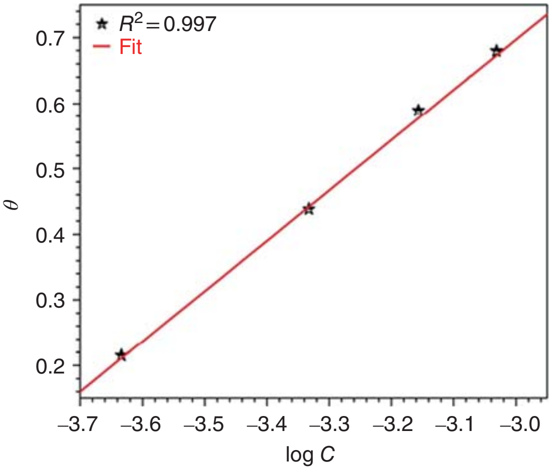

**Figure 14.4** Temkin adsorption isotherm.

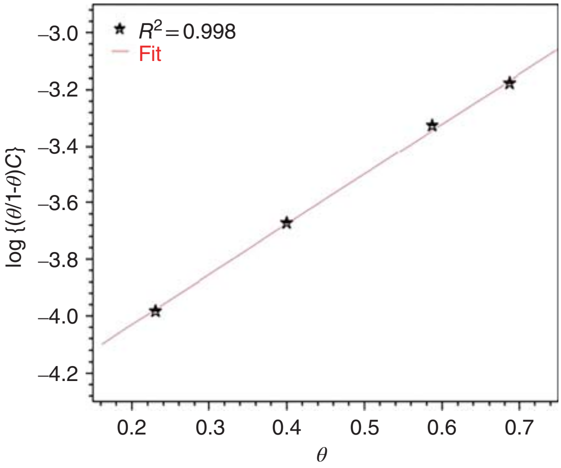

**Figure 14.5** Frumkin isotherm model.

(c) **Frumkin isotherm model:** The below equation represents the Frumkin adsorption isotherm model:

$$KC = \frac{\theta}{1-\theta} e^{-f\theta} \tag{14.10}$$

where $f$ = lateral interaction parameter among adsorbed inhibitor molecules and the positive or negative values of $f$ represents the attraction or repulsive, respectively. An example of the Frumkin isotherm model is depicted in Figure 14.5.

(d) **Flory–Huggins isotherm:** The below equation represents this model (Figure 14.6) [30]:

$$\frac{\theta}{x(1-\theta)^x} = K_{\text{ads}} C \tag{14.11}$$

**Figure 14.6** Flory–Huggins isotherm model.

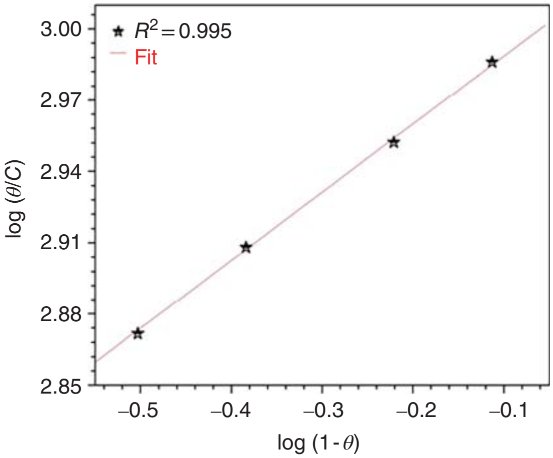

**Figure 14.7** El-Awady isotherm model.

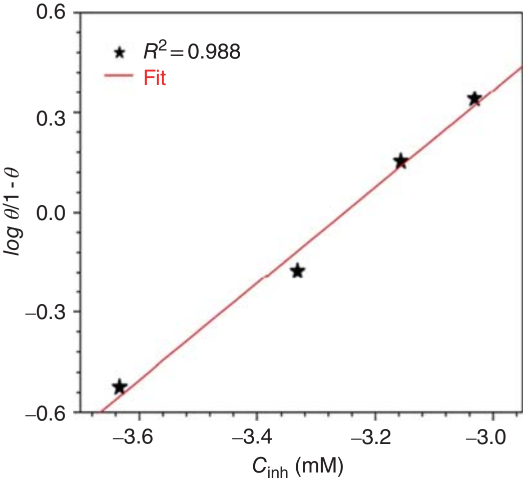

(e) **El-Awady isotherm model:** The El-Awady isotherm model is given by Eq. (14.12) (Figure 14.7) [31]

$$\log\left(\frac{\theta}{1-\theta}\right) = \log K + y \log C_{\text{inh}} \tag{14.12}$$

where $K_{\text{ads}} = K^{1/y}$ and $y$ represents occupied number of molecules of inhibitors at reactive centers. Generally, value of $1/y$ less or greater one corresponds to multilayer adsorption and more than one site occupation, respectively.

### 14.3.2 Energy of Adsorption

The isotherm models help in the calculation of standard free energy of adsorption ($\Delta G^0{}_{\text{ads}}$) and adsorption equilibrium constant ($K_{\text{ads}}$). The $K_{\text{ads}}$ and $\Delta G^0{}_{\text{ads}}$ are related mathematically as per the below equations: [32]:

$$\Delta G^0{}_{\text{ads}} = -2.303RT\log(55.55 \times K_{\text{ads}}) \tag{14.13}$$

$$\Delta G^0{}_{\text{ads}} = -2.303RT\log(10^6 \times K_{\text{ads}}) \tag{14.14}$$

where $\Delta G^0{}_{\text{ads}}$, $T$, $R$, and $55.55/10^6$ are standard adsorption free energy, temperature, gas constant, and concentration of water molecules, respectively.

In general, the negative values of $\Delta G^0{}_{\text{ads}}$ represent the spontaneity of the adsorption process. If the value of $\Delta G^0{}_{\text{ads}}$ is $-20$ kJ mol $\text{l}^{-1}$ or lower, then the adsorption is physical in nature. However, if the value is $-40$ kJ mol $\text{l}^{-1}$ or higher, then the adsorption is chemical in nature [33]. But, if the value is in between $-20$ and $-40$ kJ mol $\text{l}^{-1}$, then combined adsorption, i.e. physical and chemical, is observed. Additionally, we can also calculate parameters, such as adsorption enthalpy and entropy [34].

The heat of adsorption ($Q_{\text{ads}}$) was calculated using the below-mentioned equation [35]:

$$Q_{\text{ads}} = 2.303\left[\log\left(\frac{\theta_2}{1-\theta_2}\right) - \log\left(\frac{\theta_1}{1-\theta_1}\right)\right] \times \left(\frac{T_1T_2}{T_2 - T_1}\right) \tag{14.15}$$

where $\theta_1$, and $\theta_2$ are the surface coverage at temperatures $T_1$ and $T_2$ (65 °C), respectively. The positive values of $Q_{\text{ads}}$ represent the chemical adsorption mechanism [35].

## 14.4 Electrochemical Techniques

### 14.4.1 Open-Circuit Potential Curves

Figure 14.8 represents open-circuit potential curves in absence and presence of different concentrations of inhibitor. It could be observed that in 30 min, the curves achieve steady state. Adsorption of inhibitor molecules onto metal surface with inhibitor addition is represented by curves shifting.

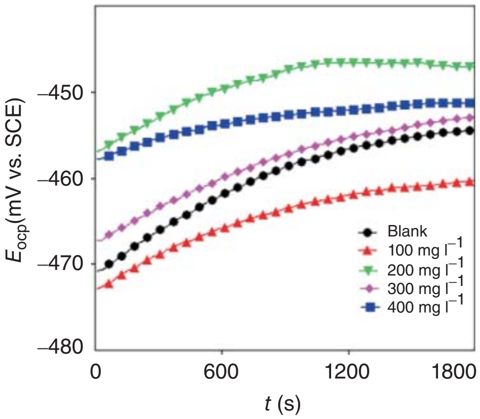

**Figure 14.8** Open-circuit potential without and with different concentrations of inhibitor.

### 14.4.2 Electrochemical Impedance Spectroscopy

Impedance technique is used for the measurement of capacitance of double-layer ($C_{\mathrm{dl}}$) and resistance of charge transfer ($R_{\mathrm{ct}}$). In this technique, alternate current (AC) is applied. The application of complex numbers helps to resolve the impedance into two parts, i.e.

$$\text{Real part} = |Z'| = |Z\cos\theta| \tag{14.16}$$

$$\text{Imaginary part} = |Z''| = |Z\sin\theta| \tag{14.17}$$

The total resistance for the AC flow is given by $Z$,

$$Z = Z' - Z'' \tag{14.18}$$

where

$$Z' = R_{\mathrm{s}} + \frac{R_{\mathrm{ct}}}{1 + \omega^2 C_{\mathrm{dl}} {R_{\mathrm{ct}}}^2} \tag{14.19}$$

$$Z'' = \frac{\omega C_{\mathrm{dl}} {R_{\mathrm{ct}}}^2}{1 + \omega {C_{\mathrm{dl}}}^2 {R_{\mathrm{ct}}}^2} \tag{14.20}$$

From the above equations, a plot is generated between $Z'$ and $Z''$ that looks like semicircle and that intersects real axis at higher and lower frequencies. The intersection at higher and lower frequencies sides represents $R_{\mathrm{s}}$ and $R_{\mathrm{s}} + R_{\mathrm{ct}}$, i.e. $R_{\mathrm{p}}$. The capacitance of double-layer capacitance is calculated as per Eq. (14.21):

$$\omega\left(Z''_{\max}\right) = \frac{1}{C_{\mathrm{dl}} \times R_{\mathrm{ct}}} \tag{14.21}$$

Inhibition efficiency by using impedance measurements is carried out by using the formula:

$$\eta\% = \frac{R_{\mathrm{ct(inh)}} - R_{\mathrm{ct(blank)}}}{R_{\mathrm{ct(inh)}}} \times 100 \tag{14.22}$$

where $R_{\mathrm{ct(inh)}}$ and $R_{\mathrm{ct\,(blank)}}$ are inhibitor-containing and inhibitor-free resistance of charge. A general example of fitted Nyquist plots without and with different concentrations of inhibitor in an acidic medium at 308 K temperature is shown in Figure 14.9a. The inspection of this figure represents a depressed semicircle, which is due to the surface imperfection and inhomogeneity. The semicircle's appearance also represents the capacitive behavior both in the absence and in presence of inhibitor. As it can be seen from the figure that as the inhibitor concentration increased, the semicircle size increased, which is due to the increase in charge-transfer resistance ($R_{\mathrm{ct}}$) of the metal. The equivalent circuit is represented in Figure 14.9b. The equivalent circuit is modeled using elements of constant phase (CPE), resistance in charge transfer ($R_{\mathrm{ct}}$), and resistance in solution ($R_{\mathrm{s}}$). The double-layer capacitance ($C_{\mathrm{dl}}$) and thickness of the adsorbed layer are calculated using the below equations [36]:

$$C_{\mathrm{dl}} = \left(Y_{\mathrm{o}} {R_{\mathrm{ct}}}^{1-n}\right)^{1/n} \tag{14.23}$$

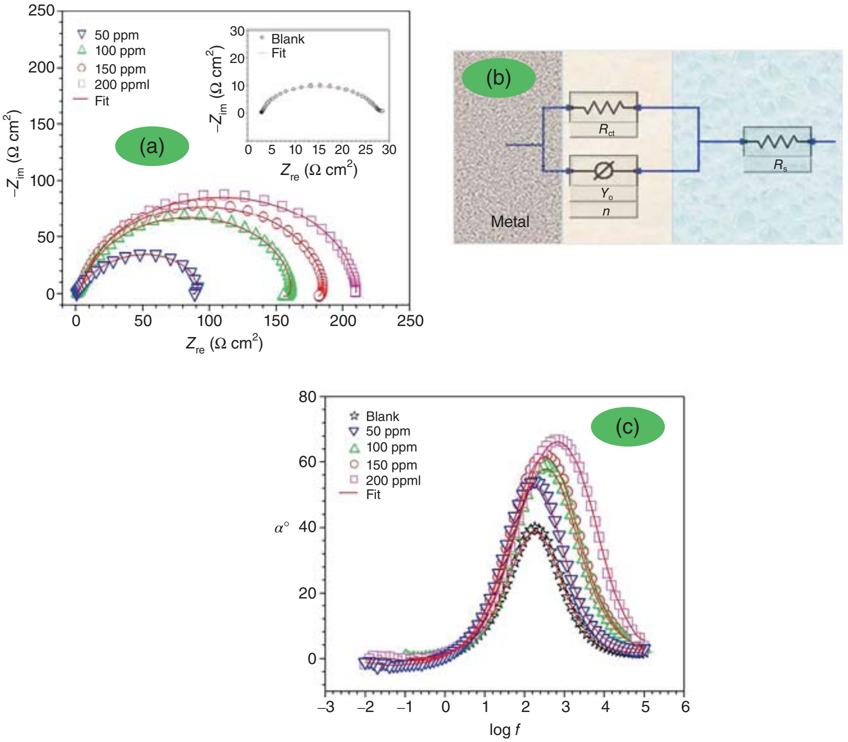

**Figure 14.9** A general EIS measurements images: (a) Nyquist plots, (b) equivalent circuit, and (c) phase angle plot.

The plots of phase angle are represented in Figure 14.9c. The phase angle plots suggest the increasing values of phase angles with increasing inhibitor concentrations at an intermediate frequency, which indicate that inhibitor molecules adsorbed over the metal surface and inhibit the dissolution of metal.

### 14.4.3 Potentiodynamic Polarization

The technique is for the measurement of anodic and cathodic polarization. Figure 14.10 represents the anodic and cathodic reactions as metal dissolution and hydrogen evolution, respectively. It is notable that at high-applied current, the hydrogen evolution process becomes identical. The Tafel regions were extrapolated for the determination of polarization parameters (Figure 14.10). The hydrogen evolution and metal dissolution rates are equal at corrosion potential, which provides the value of corrosion current density. Tafel constant can also be calculated from the anodic and cathodic Tafel curves.

This technique governed the kinetics of the corrosion process and could be explained on the basis of the below points.

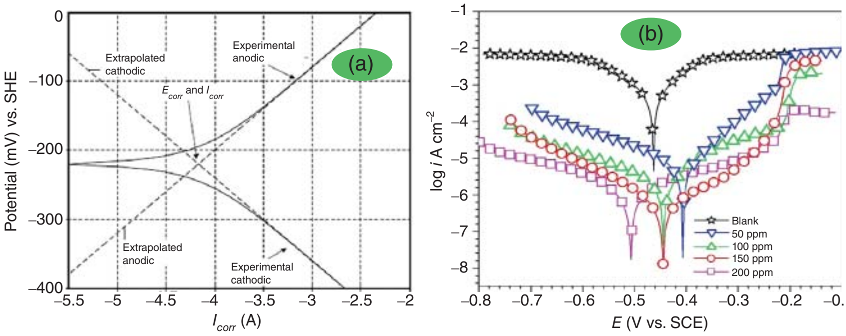

**Figure 14.10** (a) Extrapolated Tafel curves; (b) Tafel for corrosion of carbon steel in acidic in absence and presence of inhibitor.

#### 14.4.3.1 Kinetics of Corrosion

Consider an electrochemical reaction, where the reaction takes place at the metal–solution interface, and the rate of reaction is proportional to current–potential dependence. Overvoltage (polarization) $\eta$ is the potential change, $E - E_r$, from the equilibrium half-cell electrode potential $E_r$, caused by a net surface reaction rate for the half-cell reaction and was introduced by Nernst and Caspari. The dependence of $\eta$ on the current density for a hydrogen evolution reaction has been shown to be $\eta = a + b \log i$ by Tafel. Butler gave the kinetic treatment of a reversible electrode in which the concepts of the partial anodic and cathodic currents are related to $\eta$ through an exponential equation.

##### *14.4.3.1.1 Activation-Controlled Corrosion*

Generally, activation polarization is caused by a slow electrode reaction. The reaction at the electrode requires activation energy to proceed. The most important example of activation-controlled corrosion reaction is that of hydrogen ion reduction at cathode. The relationship between current and potential for a corroding system in which anodic reaction is metal dissolution and cathodic reaction is hydrogen evolution can be derived by the application of electrochemical kinetic theory.

For the metal dissolution reaction,

$$\mathrm{M} \rightarrow \mathrm{M}^{+2} + 2\mathrm{e}^- \tag{14.24}$$

$$i_c = i_c^{o} \left\{ \exp\left( \frac{\alpha_c F}{RT} \left(E - E_c^{\,r}\right) \right) - \exp\left( \frac{-\beta_c F}{RT} \left(E - E_c^{\,r}\right) \right) \right\} \tag{14.25}$$

where $E_c^{\,r}$ is the reversible potential of cathodic dissolution reaction, $i_c^{o}$ is the exchange current density for cathodic reaction, and $\alpha_c$, $\beta_c$ is transfer coefficients of reduction reaction.

Normally, the corrosion potential ($E_{corr}$) will be far away from the equilibrium potential of the reversible reaction. Hence, the contribution from the deposition reaction of metal dissolution and the reduction reaction is negligible. Therefore, the net current of the mixed electrode system is given as follows:

$$i = i_\mathrm{a} - i_\mathrm{c} \tag{14.26}$$

$$= i_\mathrm{a}^{\,\mathrm{o}} \left\{ \exp\left( \frac{\alpha_\mathrm{a} F}{RT} \left(E - E_\mathrm{a}^{\,\mathrm{r}}\right) \right) - \exp\left( \frac{-\beta_\mathrm{a} F}{RT} \left(E - E_\mathrm{a}^{\,\mathrm{r}}\right) \right) \right\} \tag{14.27}$$

At corrosion potential $E = E_\mathrm{corr}$, $i = 0$

$$\text{i.e. } i_\mathrm{corr} = i_\mathrm{a}^{\,\mathrm{o}} \left( \exp \frac{\alpha_\mathrm{a} F}{RT} \left(E_\mathrm{corr} - E_\mathrm{a}^{\,\mathrm{r}}\right) \right) \text{ (for anodic reaction)} \tag{14.28}$$

$$\text{i.e. } i_\mathrm{corr} = i_\mathrm{c}^{\,\mathrm{o}} \left( \exp \frac{\alpha_\mathrm{c} F}{RT} \left(E_\mathrm{corr} - E_\mathrm{c}^{\,\mathrm{r}}\right) \right) \text{ (for cathodic reaction)} \tag{14.29}$$

Substituting the terms $E_\mathrm{a}^{\,\mathrm{r}}$ and $E_\mathrm{c}^{\,\mathrm{r}}$ in terms of $E_\mathrm{corr}$

$$i = i_\mathrm{corr} \left\{ \exp\left( \frac{\alpha_\mathrm{a} F}{RT} (E - E_\mathrm{corr}) \right) - \exp\left( \frac{-\beta_\mathrm{c} F}{RT} (E - E_\mathrm{corr}) \right) \right\} \tag{14.30}$$

The above equation can be rewritten in terms of Tafel slopes $\beta_\mathrm{a}$ and $\beta_\mathrm{c}$ as

$$i = i_\mathrm{corr} \left\{ \exp\left( \frac{2.3(E - E_\mathrm{corr})}{\beta_\mathrm{a}} \right) - \exp\left( \frac{-2.3(E - E_\mathrm{corr})}{\beta_\mathrm{c}} \right) \right\} \tag{14.31}$$

Since $E - E_\mathrm{corr} = \eta$

$$i = i_\mathrm{corr} \left\{ \exp\left( \frac{2.3\eta}{\beta_\mathrm{a}} \right) - \exp\left( \frac{-2.3\eta}{\beta_\mathrm{c}} \right) \right\} \tag{14.32}$$

The above expression forms the basis of measuring corrosion rate by electrochemical method.

#### 14.4.3.1.2 Diffusion-Controlled Reaction

Concentration polarization or diffusion overpotential is the potential difference of a cathode in the absence and presence of an external current. The corrosion process in neutral media consists of metal dissolution reaction as anodic and oxygen reduction as a cathodic reaction. In such cases,

$$i_\mathrm{a} = i_\mathrm{corr} \left( \exp \frac{\alpha_\mathrm{a} F}{RT} (E - E_\mathrm{corr}) \right) \tag{14.33}$$

$$i_\mathrm{c} = i_\mathrm{d} = \frac{\eta F D C_\mathrm{b}}{\delta} \tag{14.34}$$

where $D$ is diffusion coefficient, $\delta$ is diffusion layer thickness, and $C_\mathrm{b}$ is the concentration of reduced species.

$$i = i_\mathrm{a} - i_\mathrm{c} \tag{14.35}$$

$$i_\mathrm{a} = i_\mathrm{corr} \left( \exp \frac{\alpha_\mathrm{a} F}{RT} (E - E_\mathrm{corr}) \right) - i_\mathrm{d} \tag{14.36}$$

$i_\mathrm{d}$ = limiting diffusion current density.

At corrosion potential, $E = E_\mathrm{corr}$, $i = 0$; therefore, $i_\mathrm{corr} = i_\mathrm{d}$.

It follows that the $i_\mathrm{d}$ is the most significant parameter in the corrosion reaction in which the cathodic reaction is diffusion-controlled and any factor that increases $i_\mathrm{d}$ will increase the corrosion rate.

The extrapolation of the Tafel curves helps in the determination of kinetic parameters, such as $i_{\mathrm{corr}}$, $E_{\mathrm{corr}}$, $\beta_{\mathrm{a}}$, $\beta_{\mathrm{c}}$, and $\eta_{\mathrm{PDP\%}}$ [37]:

$$\eta_{\mathrm{PDP\%}} = \frac{i_{\mathrm{corr}} - i_{\mathrm{corr(inh)}}}{i_{\mathrm{corr}}} \times 100 \tag{14.37}$$

where $i_{\mathrm{corr}}$ = corrosion current density without inhibitor and $i_{\mathrm{corr(inh)}}$ = corrosion current density with inhibitor. In general, if the shift in $E_{\mathrm{corr}}$ is less than 85 mV, i.e. in a positive direction as compared to without inhibitor, then the inhibitor is anodic type. However, if the shifts in greater than 85 mV, i.e. in a negative direction, then the inhibitor is cathodic type. Nevertheless, if the shift in both is more/less than 85 mV, then the inhibitor is said to be mixed type. But there are conflicts among the scientists above this type of shifting. According to this community, a prominent shift in either anodic or cathodic direction helps to decide the action of the inhibitor is anodic or cathodic.

### 14.4.4 Electrochemical Frequency Modulation Trend (EFMT)/Electrochemical Frequency Modulation Trend (EFM)

Both EFMT and EFM are nondestructive and very sensitive electrochemical technique that helps in the calculation of various parameters. The below equations are used for kinetic parameters calculation [5]:

$$i_{\mathrm{corr}} = \frac{i_{\omega}^{2}}{\sqrt{48(2i_{\omega}i_{3\omega} - i_{2\omega})}} \tag{14.38}$$

$$\text{Causality factor (2)} = \frac{i_{\omega_2 \pm \omega_1}}{i_{2\omega_1}} = 2.0 \tag{14.39}$$

$$\text{Causality factor (3)} = \frac{i_{\omega_2 \pm \omega_1}}{i_{3\omega_1}} = 3.0 \tag{14.40}$$

It helps in the simultaneous measurement of corrosion rate and corrosion current. Figure 14.11 represents the EFMT in the absence and presence of inhibitor to the corrosive medium. It is observed in Figure 14.11 that the values of corrosion rate and corrosion current are very high. However, the addition of inhibitor causes a significant reduction in corrosion rate and corrosion current value [38]. This observation supports the protective nature of inhibitor molecules. Similarly, in EFM, value of corrosion current decreases with the addition of corrosion inhibitor as compared to a blank (Figure 14.12).

The causality factors (CFs) provide the validation of the EFMT measurements. The theoretical values of CFs, i.e. CF-2 and CF-3, are 2.0 and 3.0, respectively. If the experimentally obtained values are close to the theoretical value, then the obtained results are in good agreement.

### 14.4.5 Linear Polarization Resistance

It is also called linear polarization resistance (LPR) in short. The polarization resistance of a material is defined as the $\Delta E/\Delta i$ slope of a potential–current density

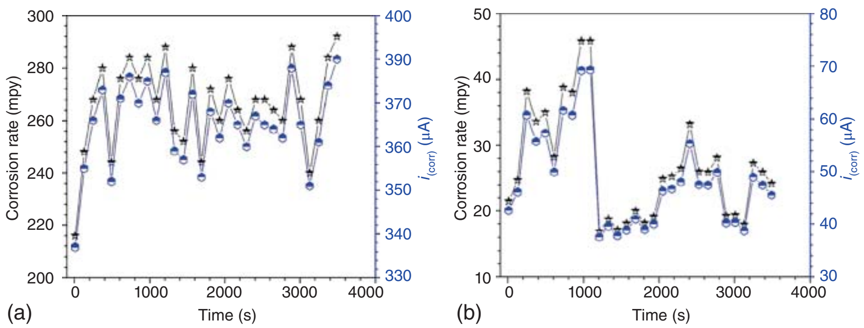

**Figure 14.11** EFMT curves for (a) without inhibitor (b) with inhibitor.

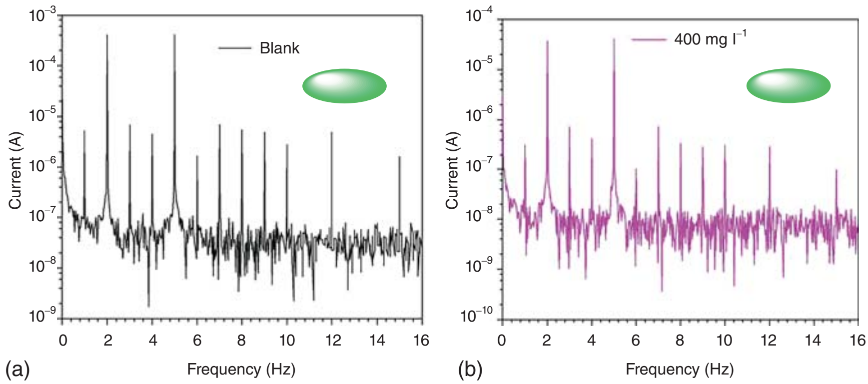

**Figure 14.12** EFM curves for (a) without inhibitor (b) with inhibitor.

curve at the free corrosion potential (Figure 14.13), yielding the polarization resistance $R_{\mathrm{p}}$ that can be itself related to the corrosion current ($i_{\mathrm{corr}}$) with the help of the Stern–Geary approximation in Eq. (14.41) [39].

$$R_{\mathrm{p}} = \frac{B}{i_{\mathrm{corr}}} = \frac{(\Delta E)}{(\Delta i)_{\Delta E \to 0}} \tag{14.41}$$

where $R_{\mathrm{p}}$ is the polarization resistance, $i_{\mathrm{corr}}$ is the corrosion current, and $B$ is an empirical polarization resistance constant that can be related to the anodic ($b_{\mathrm{a}}$) and cathodic ($b_{\mathrm{c}}$) Tafel slopes with Eq. (14.42).

$$B = \frac{b_{\mathrm{a}} \times b_{\mathrm{c}}}{2.3(b_{\mathrm{a}} + b_{\mathrm{c}})} \tag{14.42}$$

The corrosion inhibition efficiency can be calculated as given below:

$$\eta_{LPR\%} = \frac{R_{\mathrm{p}}^{\mathrm{inh}} - R_{\mathrm{p}}}{R_{\mathrm{p}}^{\mathrm{inh}}} \times 100 \tag{14.43}$$

where the terms $R_{\mathrm{p}}$ and $R^{\mathrm{inh}}{}_{\mathrm{p}}$ represent the polarization resistance without and with the inhibitor, respectively.

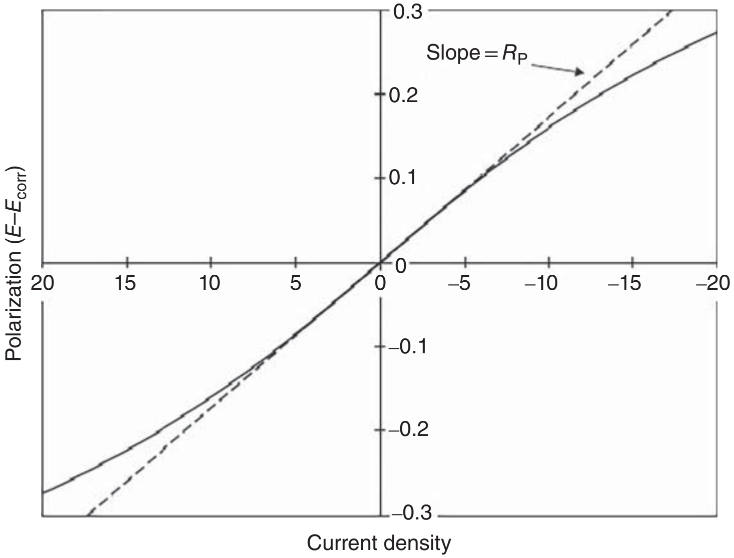

**Figure 14.13** Hypothetical linear polarization plot.

## 14.5 Surface Analytical Techniques

Surface characterization techniques are commonly used for understanding the corrosion inhibition mechanism and interaction among the surface of metals and corrosion inhibitor molecules [40]. The most commonly used techniques are discussed in brief:

### 14.5.1 Scanning Electron Microscopy

The SEM is the most commonly used technique for understanding the surface morphology of metal. It can provide images of the surface whose magnification could range from 10 × to $10^6$ ×. In the SEM, a fine probe is used for focusing the electrons in a rectangular pattern of parallel scanning lines for scanning the metals sample surface [41]. In the SEM, the metals samples, such as carbon steel, Zn, and Cu, are dipped into the corrosive solution without and with inhibitor for an appropriate period of time (3–24 h). After that, the samples are taken out, washed with distilled water, and analyzed. It is observable that the metal sample without inhibitor was severely damaged due to the direct contact of metal and corrosive solution. However, the metal sample with inhibitor was smooth with very little damage due to the formation of a protective film of inhibitor molecules over the metal surface that could act as a barrier between the metal surface and corrosive solution (Figure 14.14). Although no quantitative information about the surface, smoothness could be obtained using the SEM technique.

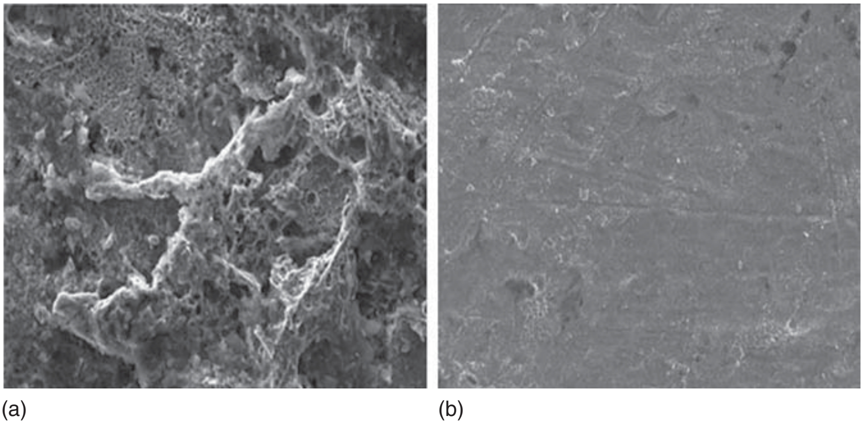

(a) (b)

**Figure 14.14** SEM images of carbon steel (a) without inhibitor (b) with inhibitor.

### 14.5.2 Energy-Dispersive X-ray Spectroscopy

The energy-dispersive X-ray spectroscopy (EDX) provides the chemical composition of the adsorbed inhibitor film and thus provides some quantitative data. The EDX data are presented as the energy vs. intensity (counts) plots and the X-rays characterized the respective elements from where they come, such as from Fe, Cu, and Al. If the inhibitor layer is formed over the metal surface, then the respective peaks of elements, such as C, O, N, S, and P, could also appear that support corrosion inhibitor adsorption onto the metal surface (Figure 14.15) [41].

The second way of EDX representation is in the form of a table that consists of atomic weight % of the different elements. The limitation of EDX analysis is it could not provide any information about the metal and corrosion inhibitor interaction.

### 14.5.3 Water Contact Angle

The adsorption of organic inhibitor molecules over the metal surface causes to change in the wetting properties and the degree of wettability could be determined

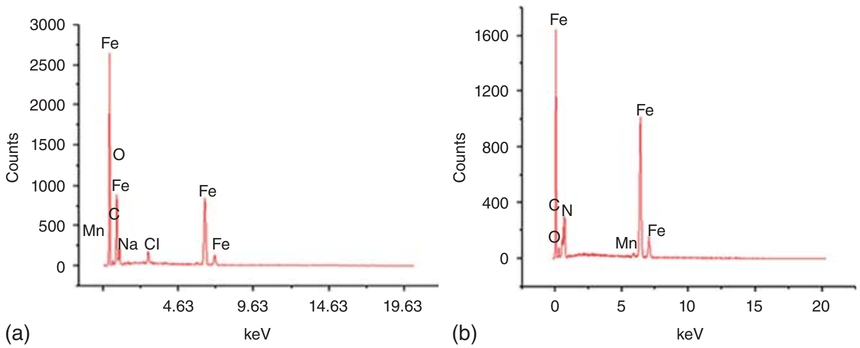

**Figure 14.15** EDX images of carbon steel (a) without inhibitor (b) with inhibitor.

by measuring the water contact angle (WCA) of the surface [42]. Thus, the corrosion inhibitor film's hydrophilicity or hydrophobicity can be differentiated using WCA measurement. The measurement of WCA is done using the tensiometer that is popularly known as contact angle meter. This instrument has various modes for estimation of WCA but studying the wettability of inhibitor films over the metal surface sessile drop method is most commonly used. In the sessile method, a water drop (5 ml) is applied over the metal sample surface and WCA is measured immediately after locating. The drops images are analyzed and a contact angle with a precision of ±0.1° is calculated depending upon the shapes of the drops. Figure 14.16 represents the WCA without and with the addition $n$ of inhibitor molecules. Here, it is noticeable that without additional inhibitor the WCA is very less. However, with the inhibitor addition, the value of WCA is increased corresponding to the decrease in the metal surface wettability due to the presence of a hydrophobic film of organic corrosion inhibitor molecules [43].

### 14.5.4 Atomic Force Microscopy

The AFM technique is similar to the SEM where in both we get the surface roughness. However, in AFM, we can get some quantitative data. As in SEM, the metal samples are dipped into the corrosive solution in the presence and absence of corrosion inhibitor for the appropriate time. The measurement could be done in contact, semicontact (tapping), or noncontact modes, respectively. However, due to the rough and damaged metal surface, the last modes are more preferred. The advantage of AFM is that it provides the values of surface roughness (i.e. root-mean-square roughness and average roughness) along with the surface profile images (Figure 14.17). Thus, in the observation of roughness values, it is easy to differentiate the performance of the corrosion inhibitor with respect to blank. It also helps to compare the inhibition performance among the series of corrosion inhibitors. However, the AFM technique gives no information about the chemical composition of adsorbed inhibitor film.

### 14.5.5 X-Ray Photoelectron Spectroscopy

XPS is the most commonly used surface analysis technique for the estimation of materials composition [44]. The basic principle of XPS is photoelectric effect phenomenon. The energy of X-rays is strong enough to kick out the electrons from the

**Figure 14.16** WCA images of carbon steel (a) without inhibitor (b) with inhibitor.

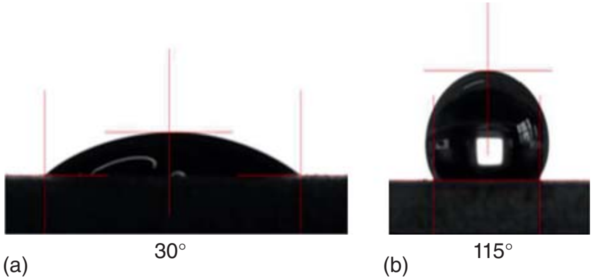

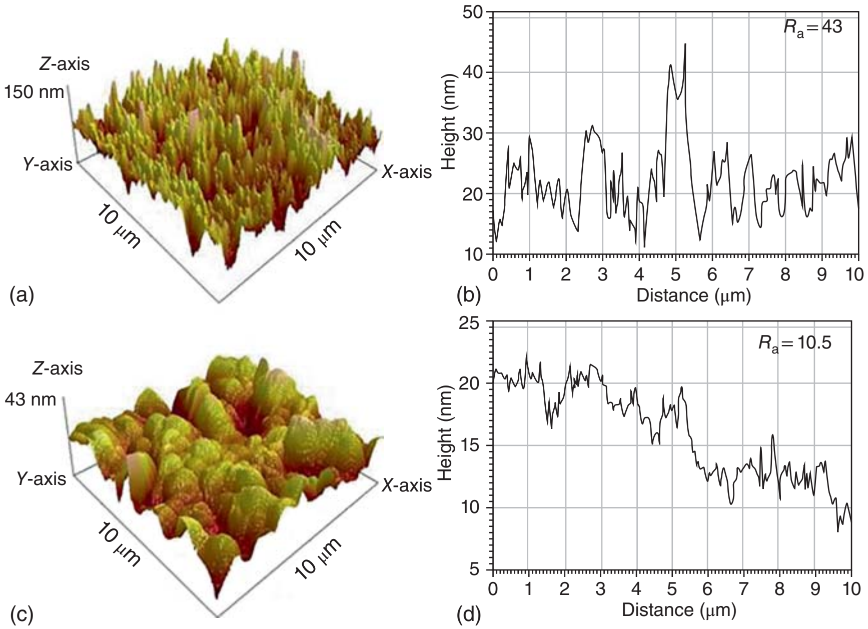

**Figure 14.17** Three dimension AFM images and corresponding height profile diagram of carbon steel: (a, b) without inhibitor (c, d) with inhibitor.

core orbitals. Depending upon the binding energy of the electrons, different energy is used for the removal and thus an energy spectrum is formed. The X-rays can easily penetrate deep into the materials and they can remove the electrons up to the first 4 nm thickness. Thus, the commonly formed layer of inhibitor films is of few nm and thus can be easily probed. The mathematical relation between the binding energy ($E_B$) of an electron and kinetic energy ($E_k$) of the ejected photoelectron is as follows:

$$E_B = h\upsilon - (E_k + \phi) \tag{14.44}$$

where $h\upsilon$ and $\phi$ are X-ray energy and spectrometer work function.

The XPS spectra of adsorbed inhibitor over carbon steel are represented in Figure 14.18. The Fe$_{2p}$ spectrum consists of two peaks at the binding energy of 711.25 eV (Fe$_{2p3/2}$) and 724.61 eV (Fe $_{2p1/2}$). These peaks correspond to iron oxide, i.e. $Fe_2O_3$, FeOOH, and FeO(OH) [45]. The Fe$_{2p3/2}$ peak has two satellite peaks at 711.13 and 713.54 eV [46]. The Fe$_{2p1/2}$ also consists of one satellite peak at 725.37 eV [46]. Also, one satellite peak at 718.01 eV was observed [46]. The spectrum of N1s (Figure 14.6b) consists of three peaks. The peak at 398.46 and 399.16 eV corresponds to C—N and C—N—Fe coordination, respectively [9]. The peak at 400.11 eV reveals protonated nitrogen (=N$^+$—) [9]. The C 1s spectra show five peaks. The peak from 284.38 to 285.1 eV represents C—C and C—H bonds [47]. The peak at 285.9 and 288.1 eV is attributed to C—O—C, C=N bond, and O—C=O, respectively [48]. The O1s deconvoluted spectra have four peaks. The peak at 529.8–530.8 eV represents $O^{2-}$ and it represents that $Fe^{3+}$ is in the form of $Fe_2O_3$ and $Fe_3O_4$ [10]. The peak

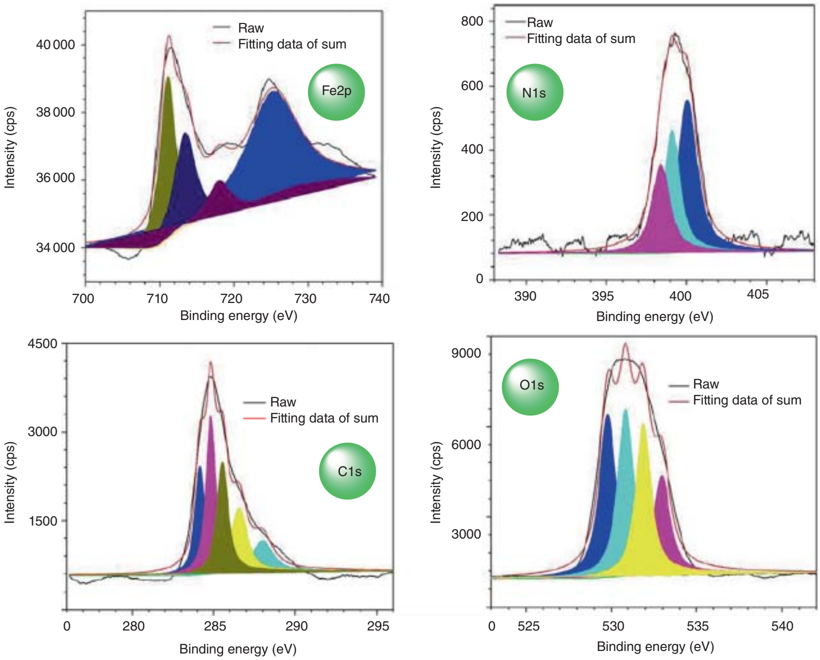

**Figure 14.18** XPS spectra images for adsorbed inhibitor on carbon steel.

at 531.8 eV corresponds to $OH^-$ and it represents the presence of iron oxides, i.e. FeOOH [10]. The peak at 532.9 eV corresponds to oxygen molecules adsorbed in the form of water [49]. XPS results confirmed the inhibitor adsorption onto the carbon steel surface.

## 14.5.6 X-Ray Diffraction

X-ray diffraction (XRD) comes in the category of nondestructive technique for the investigation of a varying range of materials [50]. In this method, monochromatic X-rays with constructive interference and crystalline sample are used. The XRD instrument produces X-rays via the cathode ray tube that generates the monochromatic radiation, which is passed toward the testing sample. The interaction between the testing sample and incident X-ray beam generates constructive interference that satisfies the Bragg's law condition [51]:

$$n\lambda = 2d \sin \theta \tag{14.45}$$

where $n$, $\lambda$, $d$, and $\theta$ are integers, X-ray wavelength, inter-planar spacing, and angle of diffraction. Since every sample has a unique "$d$" spacing that helps to identify the characteristic of that sample.

Figure 14.19 represents the XRD images of corrosion product that is present over the surface of carbon steel samples. In absence of corrosion inhibitor different peaks at $2\theta = 33°$, $40°$, $44°$, $48°$, $51°$, $52°$, and $66°$ are observed that correspond to iron

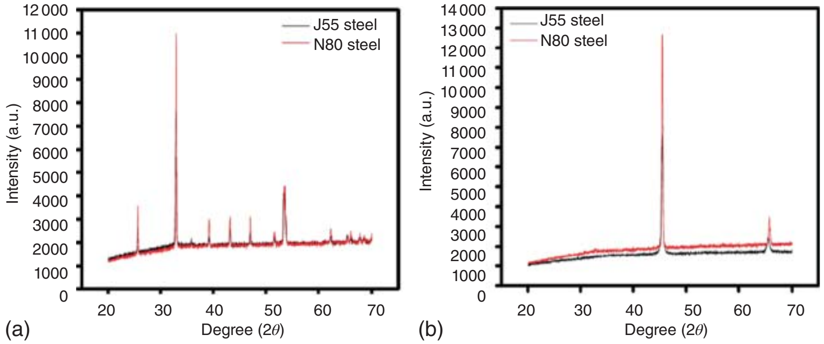

**Figure 14.19** XPS spectra images of carbon steel (a) without inhibitor (b) with inhibitor.

oxide (Figure 14.19a). However, only iron peaks are observed in the XRD patterns in presence of inhibitor (Figure 14.19b). The absence of iron oxide peaks with the addition of inhibitors suggests the formation of inhibitor protective film over the metal surface.

### 14.5.7 Scanning Electrochemical Microscopy (SECM)

SECM is a versatile and powerful technique for the investigation of the local electrochemical activity that is ongoing over the corroding metal surface using an ultramicroelectrode tip. Here, the tip of ultramicroelectrode is moved over the surface of the studied metal sample using precise positioning systems. The pictorial presentation of SECM in feed-back mode for the corrosion of carbon steel in 3.5% NaCl solution in the present and absence of corrosion inhibitor is shown in Figure 14.20a,b. According to Figure 14.20a, in absence of corrosion inhibitor, the value of corrosion current increases as the micro-tip probe comes close to the carbon steel surface, which suggests that the metal surface is conductive in nature [52]. However, in presence of inhibitor, the value of corrosion current decreased as the probe comes close to a metal surface (Figure 14.20b), which suggests that the surface metal becomes insulating due to the adsorption and formation inhibitor film [53].

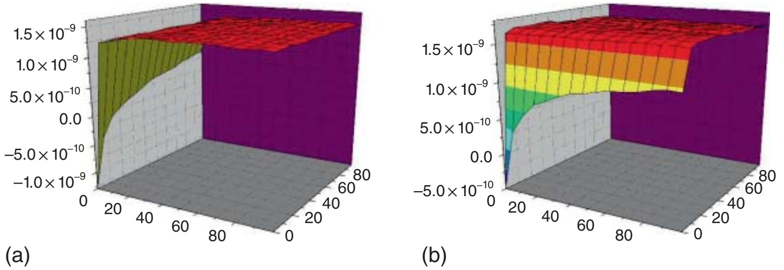

**Figure 14.20** SECM images (a) without inhibitor (b) with inhibitor; x-axis, distance; y-axis, current.

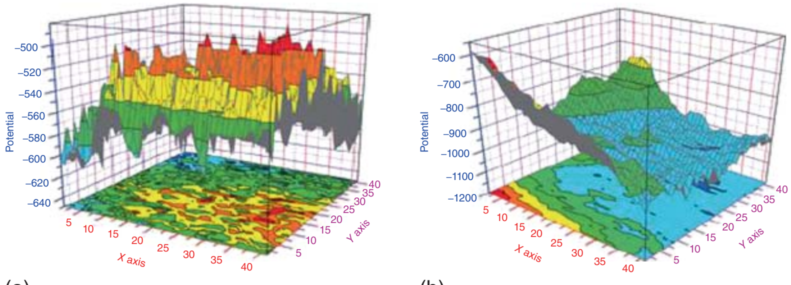

(a) (b)

**Figure 14.21** SKP images (a) without inhibitor (b) with inhibitor.

### 14.5.8 Scanning Kelvin Probe (SKP) Method

The scanning Kelvin probe (SKP) technique gives beneficial information about the micro-corrosion process involving a metallic probe that vibrates over the working electrode surface. The vibration creates an alternative capacitor and produces an AC that flows between the probe and the working electrode periphery [54]. The active anodic sites may obliquely be associated with chloride accumulation and can be distinguished by lower corrosion potentials, as shown in Figure 14.21 [55]. The figures reveal that during contact the potential of the metal surface is irregular without an inhibitor film due to the initiation of corrosion causing pits and cracks on the surface (Figure 14.21a). The development of the cathodic activity on the surface with the addition of inhibitor is likely to be due to the time taken by the corrosive solution to break through the inhibitor film that is formed over the metal surface (Figure 14.21b). That the anodic potential covered more surface without an inhibitor and the cathodic potential covered more area with an inhibitor film.

### 14.5.9 Scanning Vibrating Electrode Technique (SVET)

Scanning vibrating electrode technique (SVET) has provided a useful contribution to the study of the initiation of pitting corrosion evolving overtime on the metal surface, which was not possible before. Inhibition of corrosion corresponds to a very sluggish process, which involves various pH levels and different potentials incurred on the surface of the metal [56]. The first pit was detected in the initial scan and after that heavy pit continued to be formed from 0 to 10 h at the surface (Figure 14.22a–c). Moreover, the pits were evenly distributed on the surface for both without and with inhibitors. The SVET maps show that the pits developed at a very fast rate during 0–10 h for a metal surface without an inhibitor (Figure 14.22a–c). The rate of development of the pits was slow and lower for the metal surface with inhibitor. Once the pit begins to form the anodic activity becomes intense close to the pit and several counter cathodic activities start at the periphery of the pit (Figure 14.22d–f). For a metal surface with inhibitor, the anodic activity increased with time (5–10 h) near the pits and gradually covered most of the cathodic areas. The delay in the progress of the pits on the surface of the metal was due to the inhibitor film, which mitigated

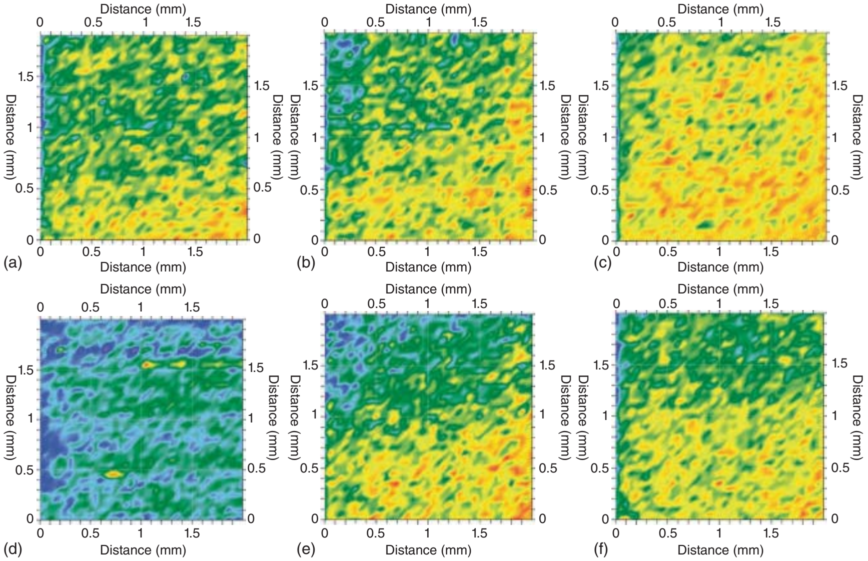

**Figure 14.22** SVET images (a–c) without inhibitor (d–f) with inhibitor.

the anodic reaction. But, gradually, the film started to break down and as the corrosive solution started to infiltrate the inhibitor film, the anodic activities started to increase.

### 14.5.10 Time-of-Flight Secondary Ion Mass Spectrometry

Any atomic or molecular species that can be ionized and transported into a gas phase can be, in principle, analyzed by mass spectrometry. At its basis, the secondary ion mass spectrometry (SIMS) is the measurement of the mass-to-charge ratio ($m/z$) of secondary ions generated from a target surface via ion beam bombardment. The formation of the secondary ions, i.e. ionization, occurs at or very close to the emission of the particles from the surface. The ionization process is, therefore, strongly influenced by the chemical state of the surface; this is known as the matrix effect [57, 58]. Time-of-flight secondary ion mass spectrometry (ToF-SIMS) is a technique used to analyze the chemistry of materials. An energetic beam of primary ions ($0.1 \times 10^{20}$ keV) is used to bombard a sample surface. The bombarding primary ion produces a variety of sputtered particles: monoatomic and polyatomic particles of the sample are produced along with electrons and photons and resputtered primary ions. The secondary ions are formed to carry negative, positive, and neutral charges. The desired secondary ions are extracted and detected using mass spectrometry. A schematic of the instrumental components of a dual-beam ToF-SIMS IS is shown in Figure 14.23 [59].

In the field of corrosion inhibition, the ToF-SIMS measurements can provide knowledge of elemental and molecular species existing on a metal surface and can provide high chemical sensitivity in a short time. The major benefit of

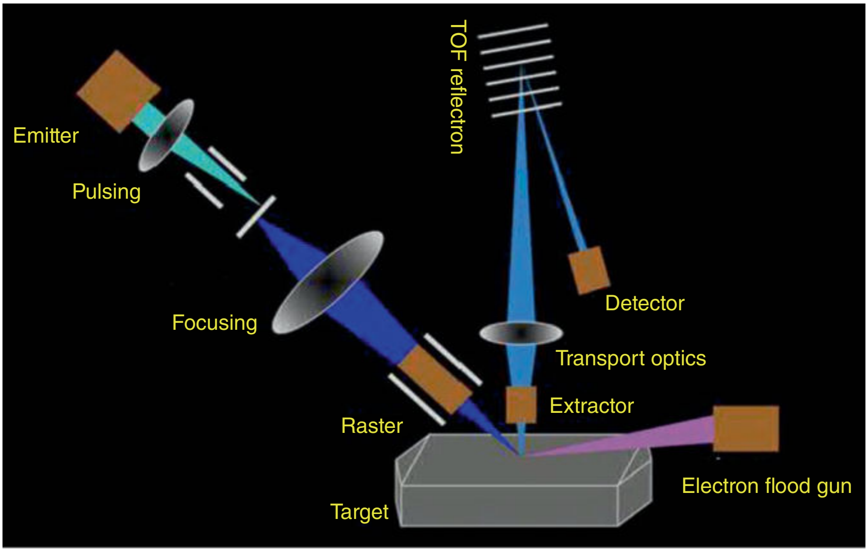

**Figure 14.23** Schematic of the major components of a time-of-flight secondary ion mass spectrometer.

ToF-SIMS is that (i) it offers greater sensitivity than XPS, (ii) direct evidence related to inhibitor adsorption can be obtained via analyzing the mass spectra, and (iii) the ToF-SIMS can detect the whole organic inhibitor molecule and also its characteristic fragments on the metal surface [59]. Figure 14.24 depicts the adsorption of 4-amino-5-methyl-4*H*-1,2,4-triazole-3-thiol (AMTT) on the surface of copper in 3.5% NaCl [59]. Evidence of the inhibitor ($C_3H_6N_4S^-$) on the metal surface can be visualized by the presence of characteristic negative ions: $C_3H_5N_4S^-$ ($m/z = 129.0260$), $C_3H_4N_4S^-$ ($m/z = 128.0213$), and $C_3H_3N_4S^-$ ($m/z = 127.0120$). The figure shows the spectra of the blank and the Cu-AMTT samples that show the existence of fragments $C_3H_4N_4S^-$ (Figure 14.24a) and $C_3H_5N_4S^-$ (Figure 14.24b) only on the inhibited sample supporting the inhibitor adsorption. The results shown in Figure 14.25 reveal the metal–inhibitor interaction. The fragment ions $C_3H_4N_4SCu^-$ ($m/z = 190.9529$), $C_3H_2N_4SCu^-$ ($m/z = 188.9270$), and $C_3HN_4SCu^-$ ($m/z = 187.9253$) provide support for the AMTT molecule bonded to the Cu surface. Additional fragments, e.g. $CuS^-$, $CSCu^-$, and $CuN_2^-$, observed for the Cu-AMTT sample suggest that the inhibitor binds with the Cu surface via its thiol group/amino group and/or the involvement of the triazole ring in the adsorption [60].

### 14.5.11 Fourier-Transform Infrared Spectroscopy

The Fourier-transform infrared (FTIR) spectroscopy is a quick and reliable method to obtain information related to the inhibitor adsorption on a metal surface. The FTIR technique is dedicated to the detection and identification of organic compounds using the functional groups and the nature of bonding in a molecule. Therefore, the FTIR spectra of the metal samples are recorded after immersion in

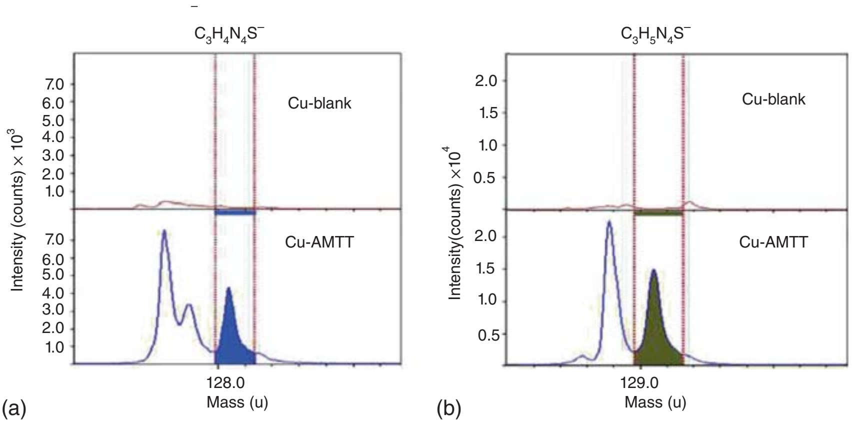

**Figure 14.24** Global negative ion mass spectra obtained on blank and AMTT samples. Source: Reproduced with permission from Chauhan et al. [60]; Copyright 2019 © Elsevier.

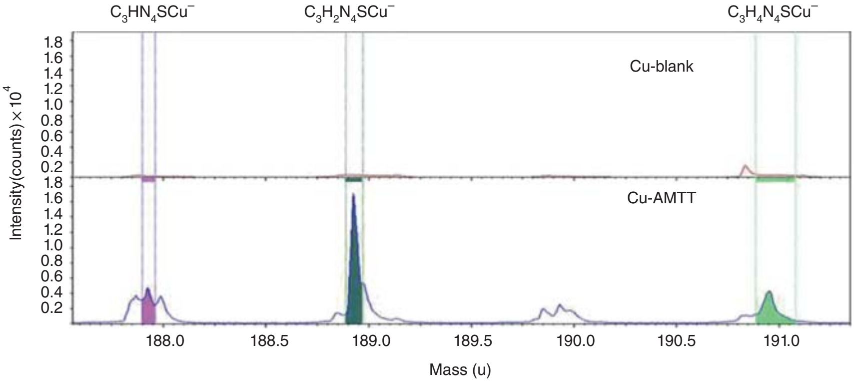

**Figure 14.25** Evidence of inhibitor AMTT bonded to copper. Source: Reproduced with permission from Chauhan et al. [60]; Copyright 2019 © Elsevier.

the corrosive solution without and with the inhibitors. The spectra of the blank metal samples show the features related to the presence of the corrosion products [5]. The FTIR characteristics of the Triazines film formed on the N80 steel surface are presented in Figure 14.26. In the case of the pure TZs, characteristic peaks are shown in Figure 14.27. In the adsorbed TZs, broadband around 3300 $\text{cm}^{-1}$ is attributed to the O—H stretching, which suggests the formation of FeOOH. However, the aromatic C—H stretching, C—N, and C=C bands intensities in the region between 1600 and 600 $\text{cm}^{-1}$ become weaker after the adsorption of TZs over the N80 steel surface (Figure 14.26). This result confirms the involvement of these centers in the adsorption phenomenon, which further leads to the formation of TZs film onto the N80 steel surface [61, 62].

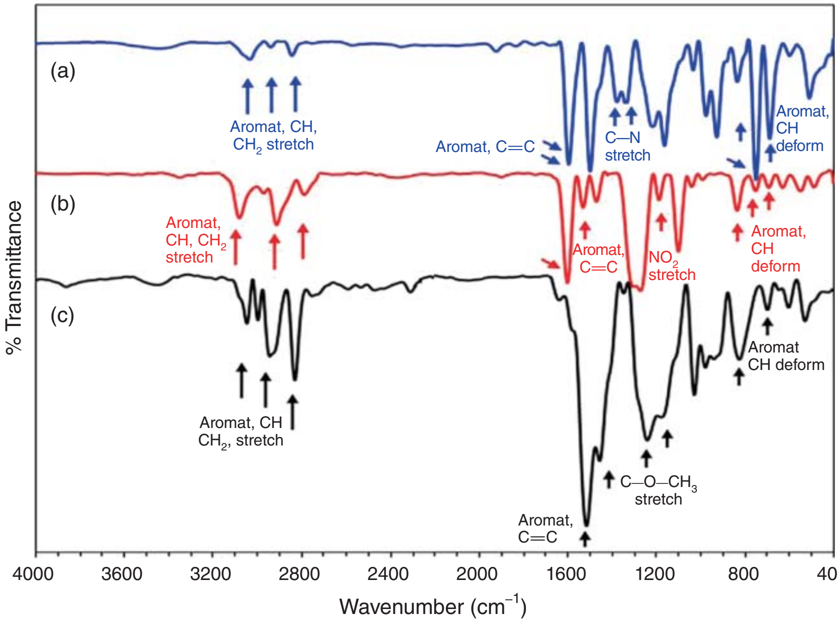

**Figure 14.26** FTIR spectra of pure inhibitors (a) TZ-1, (b) TZ-2, and (c) TZ-3.

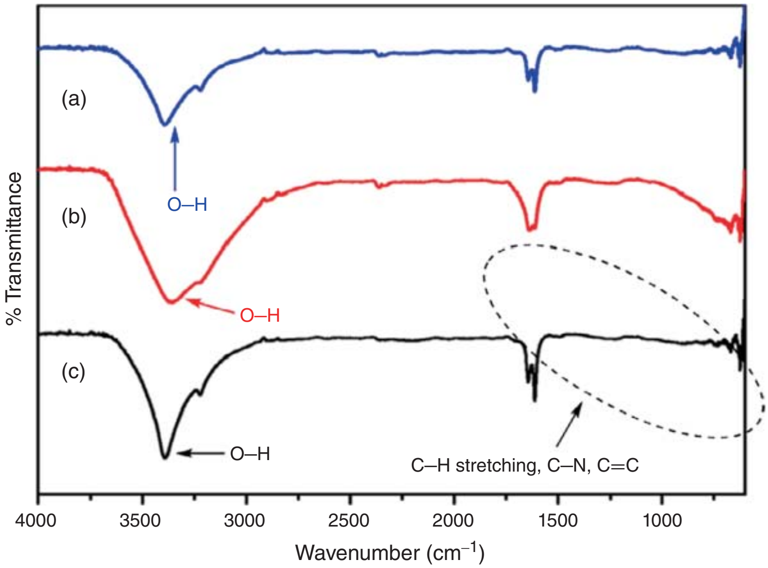

**Figure 14.27** FTIR spectra of adsorbed inhibitor molecules on the N80 steel surface. (a) TZ-1, (b) TZ-2, and (c) TZ-3.

## 14.6 Conclusion

In the present chapter, different techniques have been applied for successful study of metallic corrosion inhibition. In practical cases, satisfactory results were obtained from weight-loss and electrochemical methods for determination of protection ability of metal. However, to understand the proper mechanism of corrosion inhibitor performance, surface analytical techniques that include AFM, SEM, and XPS should use. The application of surface techniques provides the exact nature of adsorbed inhibitor film composition, thickness, and types of bonds between inhibitor molecules and metal surfaces.

## Acknowledgment

The authors acknowledge the financial support provided by the King Fahd University of Petroleum and Minerals (KFUPM), Kingdom of Saudi Arabia, under the Deanship of Scientific Research (DSR) project number DF191051. Ambrish Singh is thankful to the Sichuan 1000 Talent Fund, financial assistance provided by the Youth Scientific and Innovation Research Team for Advanced Surface Functional Materials, Southwest Petroleum University number-2018CXTD06, and open fund project number-X151517KCL42.

## Important Websites

https://onlinelibrary.wiley.com/doi/abs/10.1002/9781118015438.ch4
https://link.springer.com/chapter/10.1007/978-1-4757-4825-3_6
https://www.sciencedirect.com/topics/engineering/surface-corrosion

## References

1. Baboian, R. (2005). *Corrosion Tests and Standards: Application and Interpretation, ASTM Manual Series 20*. ASTM International.
2. Chauhan, D.S., Ansari, K., Sorour, A. et al. (2018). Thiosemicarbazide and thiocarbohydrazide functionalized chitosan as ecofriendly corrosion inhibitors for carbon steel in hydrochloric acid solution. *International Journal of Biological Macromolecules* 107: 1747–1757.
3. Ansari, K.R., Chauhan, D.S., Quraishi, M.A., and Saleh, T.A. (2020). Bis(2-aminoethyl)amine-modified graphene oxide nanoemulsion for carbon steel protection in 15% HCl: effect of temperature and synergism with iodide ions. *Journal of Colloid and Interface Science* 564: 124–133.
4. Ambrish Singh, K.R., Ansari, M.A.Q., and Kaya, S. (2020). Theoretically and experimentally exploring the corrosion inhibition of N80 steel by pyrazol derivatives in simulated acidizing environment. *Journal of Molecular Structure* 1206: 127685.

**5** Onyeachu, B., Chauhan, D.S., Ansari, K.R. et al. (2019). Hexamethylene-1,6-bis (NeD-glucopyranosylamine) as a novel corrosion inhibitor for oil and gas industry: electrochemical and computational analysis. *New Journal of Chemistry* 43: 7282–7293.

**6** Ambrish Singh, K.R., Ansari, M.A.Q., Lgaz, H., and Lin, Y. (2018). Synthesis and investigation of pyran derivatives as acidizing corrosion inhibitors for N80 steel in hydrochloric acid: theoretical and experimental approaches. *Journal of Alloys and Compounds* 762: 347–362.

**7** Ambrish Singh, K.R., Ansari, M.A.Q., Kaya, S., and Guo, L. (2020). Aminoantipyrine derivatives as a novel eco-friendly corrosion inhibitors for P110 steel in simulating acidizing environment: experimental and computational studies. *Journal of Natural Gas Science and Engineering* 83: 103547.

**8** Kang, E., Neoh, K., and Tan, K. (1992). The intrinsic redox states in polypyrrole and polyaniline: a comparative study by XPS. *Surface and Interface Analysis* 19: 33–37.

**9** Mazumder, M.A., Al-Muallem, H.A., Faiz, M., and Ali, S.A. (2014). Design and synthesis of a novel class of inhibitors for mild steel corrosion in acidic and carbon dioxide-saturated saline media. *Corrosion Science* 87: 187–198.

**10** Temesghen, W. and Sherwood, P. (2002). Analytical utility of valence band X-ray photoelectron spectroscopy of iron and its oxides, with spectral interpretation by cluster and band structure calculations. *Analytical and Bioanalytical Chemistry* 373: 601–608.

**11** Jamalia, S.S., Moulton, S.E., Tallman, D.E. et al. (2014). Applications of scanning electrochemical microscopy (SECM) for local characterization of AZ31 surface during corrosion in a buffered media. *Corrosion Science* 86: 93–100.

**12** Wade, S. and Lizama, Y. (2015). Clarke's solution cleaning used for corrosion product removal: effects on carbon steel substrate. *Corrosion and Prevention 2015, Conference Paper e 050*, Australasian Corrosion Association.

**13** ASTM (2004). *G1e03: Standard Practice for Preparing, Cleaning, and Evaluating Corrosion Test Specimens*. ASTM International.

**14** Kina, A. and Ponciano, J. (2013). Inhibition of carbon steel $CO_2$ corrosion in high salinity solutions. *International Journal of Electrochemical Science* 8: 12600–12612.

**15** Finsgar, M. and Jackson, J. (2014). Application of corrosion inhibitors for steels in acidic media for the oil and gas industry: a review. *Corrosion Science* 86: 17–41.

**16** ASTM (2001). *G4-01, Standard Guide for Conducting Corrosion Tests in Field Applications*. ASTM International.

**17** Ansari, K.R., Quraishi, M.A., and Singh, A. (2017). Chromenopyridin derivatives as environmentally benign corrosion inhibitors for N80 steel in 15% HCl. *Journal of the Association of Arab Universities for Basic and Applied Sciences* 22: 45–54.

**18** Rajeswari, V., Kesavan, D., Gopiraman, M., and Viswanathamurthi, P. (2013). Physicochemical studies of glucose, gellan gum, and hydroxypropyl cellulosed inhibition of cast iron corrosion. *Carbohydrate Polymers* 95: 288–294.

**19** Luo, X., Ci, C., Li, J. et al. (2019). 4-Aminoazobenzene modified natural glucomannan as a green eco-friendly inhibitor for the mild steel in 0.5 M HCl solution. *Corrosion Science* 151: 132–142.

**20** Aoun, S.B. (2017). On the corrosion inhibition of carbon steel in 1 M HCl with a pyridinium-ionic liquid: chemical, thermodynamic, kinetic and electrochemical studies. *RSC Advances* 7: 36688–36696.

**21** Ansari, K., Quraishi, M., Singh, A. et al. (2016). Corrosion inhibition of N80 steel in 15% HCl by pyrazolone derivatives: electrochemical, surface and quantum chemical studies. *RSC Advances* 6: 24130–24141.

**22** Solmaz, R. (2014). Investigation of adsorption and corrosion inhibition of mild steel in hydrochloric acid solution by 5-(4-dimethylaminobenzylidene) rhodanine. *Corrosion Science* 79: 169–176.

**23** Vracar, L.M. and Drazic, D. (2002). Adsorption and corrosion inhibitive properties of some organic molecules on iron electrode in sulfuric acid. *Corrosion Science* 44: 1669–1680.

**24** Ansari, K. and Quraishi, M. (2014). Bis-Schiff bases of isatin as new and environmentally benign corrosion inhibitor for mild steel. *Journal of Industrial and Engineering Chemistry* 20: 2819–2829.

**25** Ateya, B., El-Anadouli, B., and El-Nizamy, F. (1984). The adsorption of thiourea on mild steel. *Corrosion Science* 24: 509–515.

**26** Fateh, A., Aliofkhazraei, M., and Rezvanian, A. (2017). Review of corrosive environments for copper and its corrosion inhibitors. *Arabian Journal of Chemistry* 13: 481–544. https://doi.org/10.1016/j.arabjc.2017.05.021.

**27** El-Hajjaji, F., Messali, M., Aljuhani, A. et al. (2018). Pyridazinium-based ionic liquids as novel and green corrosion inhibitors of carbon steel in acid medium: electrochemical and molecular dynamics simulation studies. *Journal of Molecular Liquids* 249: 997–1008.

**28** Singh, P., Singh, A., and Quraishi, M. (2016). Thiopyrimidine derivatives as new and effective corrosion inhibitors for mild steel in hydrochloric acid: electrochemical and quantum chemical studies. *Journal of the Taiwan Institute of Chemical Engineers* 60: 588–601.

**29** Oguzie, E., Li, Y., and Wang, F. (2007). Corrosion inhibition and adsorption behavior of methionine on mild steel in sulfuric acid and synergistic effect of iodide ion. *Journal of Colloid and Interface Science* 310: 90–98.

**30** Flory, P.J. (1942). Thermodynamics of high polymer solutions. *The Journal of Chemical Physics* 10: 51–61.

**31** Karthikaiselvi, R. and Subhashini, S. (2014). Study of adsorption properties and inhibition of mild steel corrosion in hydrochloric acid media by water soluble composite poly (vinyl alcohol-o-methoxy aniline). *Journal of the Association of Arab Universities for Basic and Applied Sciences* 16: 74–82.

**32** Singh, A., Ansari, K.R., Chauhan, D.S. et al. (2020). Anti-corrosion investigation of pyrimidine derivatives as green and sustainable corrosion inhibitor for N80 steel in highly corrosive environment: experimental and AFM/XPS study. *Sustainable Chemistry and Pharmacy* 16: 100257.

**33** Yadav, D.K., Chauhan, D., Ahamad, I., and Quraishi, M. (2013). Electrochemical behavior of steel/acid interface: adsorption and inhibition effect of oligomeric aniline. *RSC Advances* 3: 632–646.

**34** Mourya, P., Banerjee, S., Rastogi, R.B., and Singh, M.M. (2013). Inhibition of mild steel corrosion in hydrochloric and sulfuric acid media using a thiosemicarbazone derivative. *Industrial & Engineering Chemistry Research* 52: 12733–12747.

**35** Oguzie, E.E. (2007). Corrosion inhibition of aluminium in acidic and alkaline media by Sansevieriatrifasciata extract. *Corrosion Science* 49: 1527–1539.

**36** Fragoza-Mar, L., Olivares-Xometl, O., Domínguez-Aguilar, M.A. et al. (2012). Corrosion inhibitor activity of 1,3-diketone malonates for mild steel in aqueous hydrochloric acid solution. *Corrosion Science* 61: 171–184.

**37** Hosseini, M., Mertens, S.F., Ghorbani, M., and Arshadi, M.R. (2003). Asymmetrical Schiff bases as inhibitors of mild steel corrosion in sulphuric acid media. *Materials Chemistry and Physics* 78: 800–808.

**38** Singh, A., Dayu, X., Ituen, E. et al. (2020). Tobacco extracted from the discarded cigarettes as an inhibitor of copper and zinc corrosion in an ASTM standard D1141-98(2013) artificial seawater solution. *Journal of Materials Research and Technology* 9: 5161–5173. https://doi.org/10.1016/j.jmrt.2020.03.033.

**39** Grauer, R., Moreland, P.J., and Pini, G. (1982). *A Literature Review of Polarisation Resistance Constant (B) Values for the Measurement of Corrosion Rate*. Houston, TX: NACE International.

**40** Grosvenor, A., Kobe, B., Biesinger, M., and McIntyre, N. (2004). Investigation of multiplet splitting of Fe 2p XPS spectra and bonding in iron compounds. *Surface and Interface Analysis* 36: 1564–1574.

**41** Goldstein, J.I., Newbury, D.E., Michael, J.R. et al. (2017). *Scanning Electron Microscopy and X-Ray Microanalysis*. Springer.

**42** Singh, A., Lin, Y., Ansari, K. et al. (2015). Electrochemical and surface studies of some porphines as corrosion inhibitor for J55 steel in sweet corrosion environment. *Applied Surface Science* 359: 331–339.

**43** Murmu, M., Saha, S.K., Murmu, N.C., and Banerjee, P. (2019). Effect of stereochemical conformation into the corrosion inhibitive behaviour of double azomethine based Schiff bases on mild steel surface in 1 mol/L HCl medium: an experimental, density functional theory and molecular dynamics simulation study. *Corrosion Science* 146: 134–151.

**44** Briggs, D. (1979). *Handbook of X-Ray Photoelectron Spectroscopy* (ed. C.D. Wanger, W.M. Riggs, L.E. Davis, et al.). Eden Prairie, MN: Perkin-Elmer Corp., Physical Electronics Division.

**45** Roosendaal, S.J., van Asselen, B., Elsenaar, J.W. et al. (1999). The oxidation state of Fe(100) after initial oxidation in $O_2$. *Surface Science* 442: 329–337.

**46** Yuan, L., Wang, Y., Cai, R. et al. (2012). The origin of hematite nanowire growth during the thermal oxidation of iron. *Materials Science and Engineering B* 177: 327–336.

**47** Bentiss, F., Jama, C., Mernari, B. et al. (2009). Corrosion control of mild steel using 3,5-bis (4-methoxyphenyl)-4-amino-1,2,4-triazole in normal hydrochloric acid medium. *Corrosion Science* 51: 1628–1635.

**48** Arukalam, I., Madufor, I., and Oguzie, E. (2014). Inhibition of mild steel corrosion in sulfuric acid medium by hydroxyethyl cellulose. *Chemical Engineering Communications* 202 (1): 112–122.

**49** Babić-Samardžija, K., Lupu, C., Hackerman, N. et al. (2005). Inhibitive properties and surface morphology of a group of heterocyclic diazoles as inhibitors for acidic iron corrosion. *Langmuir* 21: 12187–12196.

**50** Stanjek, H. and Häusler, W. (2004). Basics of X-ray diffraction. *Hyperfine Interactions* 154: 107–119.

**51** Speakman, S.A. (2016). Basics of X-ray diffraction. Massachusetts Institute of Technology. http://prism.mit.edu/xray

**52** Izquierdo, J., Nagy, L., Santana, J.J. et al. (2011). A novel microelectrochemical strategy for the study of corrosion inhibitors employing the scanning vibrating electrode technique and dual potentiometric/amperometric operation in scanning electrochemical microscopy: application to the study of the cathodic inhibition by benzotriazole of the galvanic corrosion of copper coupled to iron. *Electrochimica Acta* 58: 707–716.

**53** Aouinaa, N., Balbaud-Célérier, F., Huet, F. et al. (2013). Initiation and growth of a single pit on 316L stainless steel: influence of $SO_4^{2-}$ and $ClO_4^-$ anions. *Electrochimica Acta* 104: 274–281.

**54** Nazarov, A., Romano, A.P., Fedel, M. et al. (2012). Filiform corrosion of electrocoated aluminium alloy: role of the pre-treatment. *Corrosion Science* 65: 187–198.

**55** Fuente, D.D.L., Chico, B., and Morcillo, M.A. (2006). A SEM/XPS/SKP study on the distribution of chlorides in contaminated rusty steel. *Corrosion Science* 48: 2304–2316.

**56** Simões, A.M., Battocchi, D., Tallman, D.E., and Bierwagen, G.P. (2007). SVET and SECM imaging of cathodic protection of aluminium by a Mg-rich coating. *Corrosion Science* 49: 3838–3849.

**57** Fearn, S. (2015). *An Introduction to Time-of-Flight Secondary Ion Mass Spectrometry (ToF-SIMS) and its Application to Materials Science*. Morgan & Claypool Publishers.

**58** Linford, M.R. (2013). An introduction to time-of-flight secondary ion mass spectrometry (ToF-SIMS). *Vacuum Technology and Coating* 2–7.

**59** Hofmann, J.P., Rohnke, M., and Weckhuysen, B.M. (2014). Recent advances in secondary ion mass spectrometry of solid acid catalysts: large zeolite crystals under bombardment. *Physical Chemistry Chemical Physics* 16: 5465–5474.

**60** Chauhan, D.S., Quraishi, M., Carrie, re, C. et al. (2019). Electrochemical, ToF-SIMS and computational studies of 4-amino-5-methyl-4*H*-1,2,4-triazole-3-thiol as a novel corrosion inhibitor for copper in 3.5% NaCl. *Journal of Molecular Liquids* 289: 111113.

**61** de Souza, F.S. and Spinelli, A. (2009). Caffeic acid as a green corrosion inhibitor for mild steel. *Corrosion Science* 51: 642.

**62** Vengatesh, G., Karthik, G., and Sundaravadivelu, M. (2017). A comprehensive study of ondansetron hydrochloride drug as a green corrosion inhibitor for mild steel in 1 M HCl medium. *Egyptian Journal of Petroleum* 26: 705.

# 15

# Guidelines for Designing Corrosion Inhibitors for Oil and Gas Production

*Nayef M. Alanazi and Muhammad I. Ulhaq*

*Research and Development Center, Saudi Aramco, Dhahran, Saudi Arabia*

## 15.1 Introduction

The use of corrosion inhibitors is the most cost-effective strategy to control internal corrosion in pipelines. Implementing a corrosion inhibition treatment program in the oil and gas industry is essential to control corrosion in pipelines and enable the long-term use of low-cost materials, such as carbon steel in corrosive environments [1–3]. These needs have also spurred the design of corrosion inhibitors and the development of new test protocols. Syntheses and formulation of new corrosion inhibitors change in the face of field maturation challenges, new recovery approach regulations, and unique field exposures (e.g. higher total dissolved solids [TDS], water cut, $H_2S$, and $CO_2$ contents). Further, to address higher integrity expectations, it has become essential to assure that field applied corrosion inhibitor maintains high efficiency and is designed within its integrity operating window.

The primary corrosion mechanism leading to failures in oil and gas pipelines is pitting corrosion along with the bottom line or at the water–gas interface. Other less common corrosion mechanisms are top-of-the-line corrosion (also known as vapor-phase corrosion), under deposit corrosion, stress-corrosion cracking, sulfide stress cracking, and hydrogen-induced cracking. These corrosion mechanisms are classified into two most important types of corrosion prevalent in oil and gas environments, which are sweet ($CO_2$-induced) corrosion and sour ($H_2S$-induced) corrosion [4]. The most common factors to internal corrosion pipelines are $H_2S$, $CO_2$, oxygen ingress, bacteria, water holdup, chlorides, solids deposition, polysulfides, elemental sulfur, and critical velocity. This chapter guides deigning corrosion inhibitors for different applications and services in the oil and gas industry, including corrosion inhibitor management and screening corrosion inhibitors, to ensure and improve the integrity of carbon steel applications.

*Polymeric Corrosion Inhibitors for Greening the Chemical and Petrochemical Industry*, First Edition.
Edited by Mohammad A. Jafar Mazumder, Mumtaz A. Quraishi, and Amir Al-Ahmed.

## 15.2 Classification of Corrosion

The environment in which is metal is present plays an essential part in corrosion, corrosion mechanisms, and type of corrosion depending on the environments to which a metal is exposed. Usually, corrosion is classified into four major categories, i.e. uniform corrosion, fretting corrosion, pitting corrosion, and stress corrosion. Uniform corrosion can be identified based on visual examination and is commonly known as general corrosion, whereas fretting, pitting, and stress-corrosion types are classified under localized corrosion. Figure 15.1 illustrates the general classification of corrosion.

### 15.2.1 Crevice and Pitting Corrosions

Crevice and pitting corrosions are related because of similar mechanisms, and both occur in stagnant water, chlorine, oxygen, or carbon dioxide environments. These are present in a confined area of the metal surface and are highly localized in nature. The pitting corrosion occurs mainly under sour and sweet settings, and it is difficult to detect the pitting corrosion because it is usually covered by the corrosion products, such as FeS or $FeCO_3$. It can result in the formation of unnoticed small narrow pits. Crevice corrosion occurs when a portion of metal comes in contact with another metal or with a nonmetal. It mainly takes place around protected areas, such as clamps, joints, and gaskets.

### 15.2.2 Stress-Corrosion Cracking (SCC)

Stress- corrosion cracking is the cracking that takes place due to the internal stress on the metal surface in a corrosive environment. The critical parameters that play an essential role in stress-corrosion cracking are temperature, stress, metal composition, and composition of the corrosion environment. In the solution phase or fluid phase, the pH and the composition of the media are two essential factors to impact the SCC. In addition to these factors, oxygen and salt (chloride) content increases the susceptibility of the metal to SCC and temperature.

### 15.2.3 Fretting and Erosion–Corrosion

Fretting corrosion, also called friction corrosion or oxidation corrosion, occurs when the fluid-flow rate inside the pipeline is very high. This corrosion takes place in

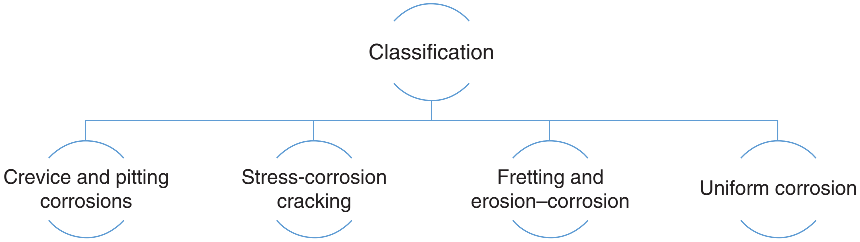

**Figure 15.1** General classification of corrosion.

the process of transportation when rough surfaces come in contact and experience vibration. At the same time, loaded metal surfaces impact each other in the environment they are present. Usually, it appears as pits or grooves surrounded by corrosion products (corrosion scales). This problem becomes more evident inside the oil and gas pipelines due to the movement of fluid that causes much more vibration. Erosion–corrosion is considered one of the five most widespread forms of corrosion deterioration in the oil and gas industry. In offshore applications, the transportation of liquids or fluids having slurries and other particles in pipelines spends a significant amount every year.

### 15.2.4 Uniform Corrosion

Uniform corrosion or general corrosion is a more common type of corrosion. It is predictable if the corrosion rate is known; therefore, it is the least damaging form of corrosion. Uniform corrosion is also known as homogenous form, and it occurs when the chemical composition and structure of the metal are uniform. The metal surface undergoes a uniform thinning onto the surface. The coating and chemical corrosion inhibitors are standard solutions to control general corrosion. General corrosion is most likely to occur due to exposure of the metal surface to strong acid and hot alkaline environments. Inorganic acids, such as hydrochloric acid, are more aggressive in inducing uniform corrosion than organic acids.

## 15.3 Corrosion Inhibitors

It is well-known in the literature [5, 6] that corrosion inhibitors are grouped into four general categories depending on their working mechanism to prevent the metal surface. They reduce corrosion by either acting as a barrier by forming an adsorbed layer or retarding the cathodic, the anodic, or both processes. These categories include anodic inhibitor, volatile corrosion inhibitor, cathodic inhibitor, and mixed inhibitor. Regardless of inhibitor category, they are applied in the oil and gas industry by either batch or continuous treatment methods. The batch treatment provides a way of laying down a film of inhibitor in one application. The life and strength of the film depend on many factors, including the type of inhibitor, acid gas concentration, temperature, velocity, and water cut, all of the latter affecting the corrosivity of the system [7]. Once the film is no longer protective, another batch treatment must be applied. Batch treatment also reduces scaling in the well. It also extends well life, improves well integrity, minimizes deferred gas impact, and maximizes gas recovery [8].

On the other hand, continuous treatment is generally the preferred treatment method since the concentration of the inhibitor can be controlled or changed at any given time. A higher concentration of inhibitor can be applied until a film is established, and then the concentration of inhibitor is reduced to a level sufficient to maintain the inhibitor film. However, the corrosion inhibitors used in the oil and gas industry are designed based on the environment that needs to be addressed. For instance, sour and sweet corrosion inhibitors are commonly used to address corrosion problems related to a corrosion mechanism due to the presence of $H_2S$ or/and $CO_2$ gases. The following sections discuss in detail the design of each type of corrosion inhibitor.

### 15.3.1 Sour Corrosion Inhibitor

Sour corrosion occurs when an excess of $H_2S$ (100 ppm) is present in the oil and gas, and predominantly it causes corrosion in the pipeline in the form of pitting [9]. $H_2S$ is a weak acid, readily soluble in water, and is a source of hydrogen ions. Under high $H_2S$ partial pressures, typically in gas formations, pH values of as low as 3 have been estimated. The sour corrosion mechanism is still not fully understood. Figure 15.2 illustrates the plausible general mechanism of carbon steel in a sour environment. It begins with the hydrolysis and dissociation of Hydrogen sulfide gas. The $H_2S$ gas dissolves in water cut, and the dissociation of $H_2S$(aq) produces $H^+$ and $HS^-$ ions [11, 12]. The secondary ionization of the bisulfide ($HS^-$) leads to the formation of $H^+$ and $S_2^-$ ions [13]. The general mechanism of $H_2S$ corrosion involves the gradual desorption of metallic Fe, the formation of FeS (mackinawite) in the anodic region, and the simultaneous $H^+$ ions reduction to $H_2$ in the cathodic region. A recent study [14, 15] on the assessment of corrosion under iron sulfide deposit in a sour environment noted that when iron sulfide, particularly mackinawite phase, was deposited on a steel surface, significant general and localized corrosion were observed. Compared with other iron sulfide phases, the mackinawite is considered an enemy form and can generate a high corrosion rate underneath iron sulfide film. The reason for that is that the mackinawite is a nonprotective and porous layer that is positively electro-potential higher than bare steel. Therefore, a sour corrosion inhibitor is needed to be designed to mitigate such a sour corrosion mechanism.

Obot et al. [10] conducted a review and analysis on the development of sour corrosion inhibitors and these corrosion inhibitors are grouped into four, namely amines, imidazolines, Gemini surfactants, and water-based polymers as shown in Figure 15.3. The percentage distribution of these four classes is in the order: amine-based 46% > imidazoline-based 31% > surfactant-based 20% > polymer-based 4%. It is pertinent to state that the inhibition efficiency of these compounds is in the

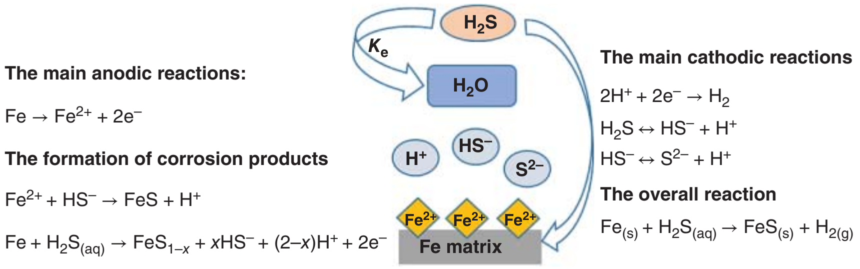

**Figure 15.2** General mechanism of iron oxidation in a sour environment. Source: Obot et al. [10]/with permission of Elsevier.

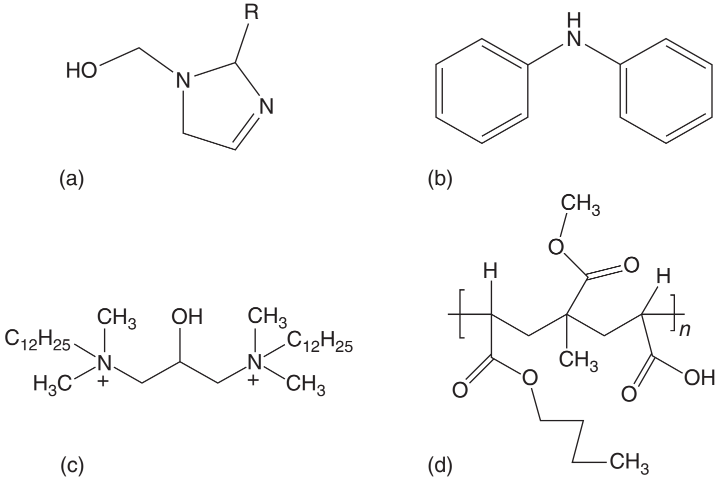

**Figure 15.3** Selected structures of the different chemistries were reported as sour corrosion inhibitors. (a) Hydroxyethyl imidazoline, where R is an alkyl chain derivative: imidazoline chemistry. Source: Rivera-Grau et al. [16]/ESG, (b) diphenylamine: amine chemistry. Source: Kashkovskiy et al. [17]/Elsevier, (c) 1,3-bis(dodecyl dimethyl ammonium chloride)-2-propanol: Gemini chemistry. Source: Zhao et al. [18], and (d) water-based terpolymer: corrosion science. Source: Azghandi et al. [22]/Elsevier.

range of 77%–99%, and the corrosion rate is reduced below the acceptable limit of 4 mpy (0.1 mm/y) in most cases [10, 16–25].

#### 15.3.1.1 Amine-Based Inhibitor

Amines are derived from ammonia and are grouped into primary, secondary, and tertiary amines based on their nature and the number of substituents on the nitrogen atom. Methylamine, dimethylamine, and trimethylamine are examples of primary, secondary, and tertiary amines, respectively. When a substituent is a cyclic group, the amine is said to be a cyclic amine. The electronic properties of the substituent and the degree of solvation have a profound effect on the basicity of amines. Amines gain numerous industrial applications as commodities for the manufacture of rubber, dyes, pharmaceuticals, synthetic resins, fibers, etc. [26–29]. The effectiveness of oil-soluble amine-type inhibitors in retarding carbon steel corrosion in sour environments has been established [30–32]. For instance, an oil-soluble filming amine corrosion inhibitor was developed for sweet and sour corrosion by Papir et al. [30]. The evaluation of the product was carried out both in the laboratory using the wheel test method and in the field. The developed amine-based inhibitor was compared with a Chevron sour commercial inhibitor. It was found that the developed inhibitor performed better than the commercial inhibitor at lower concentrations (500–2000 ppm), longer times (72 hours), and higher temperatures (86–150 °F). The average corrosion rate of the developed amine-based inhibitor was 1.6 mpy, whereas that of the commercial inhibitor was 2.5 mpy. Mok et al. [31] claimed that amine-based inhibitors are capable of providing up to 99% protection to carbon steel in sour conditions. Kashkovskiy et al. [17] presented tributylamine as an effective volatile inhibitor for sour corrosion of steel. In more specific terms, dibutylamine, cyclohexylamine, diphenylamine, phenyleneamine, and tributylamine [18, 33] are the most potent low-carbon steel inhibitors in sour environment.

#### 15.3.1.2 Imidazoline-Based Inhibitor

Imidazolines are nitrogen-containing heterocycles derived from imidazoles. Imidazoline structure can be divided into three parts; pendant group (hydrophilic head), imidazoline ring (five-membered heterocyclic ring), and the substituent (hydrophobic tail). It exists in three isomeric forms, namely, 2-imidazoline, 3-imidazoline, and 4-imidazoline. Of these three isomeric forms, the 2-imidazoline is the most commonly found as its ring occurs in some natural products and pharmaceuticals. This isomeric form has gained application as an antihyperglycemic, anti-inflammatory, antihypertensive, antihypercholesterolemic, and antidepressant reagent [34, 35]. Imidazoline and its derivatives are effective corrosion inhibitors [16, 23–25], and most of the commercial inhibitors are based on imidazoline chemistries and are explicitly designed for oilfield applications [36–39].

The mechanism of inhibition by imidazoline in a corrosive environment is one of the contentious issues among corrosion scientists. In the report of Edwards et al. [25], it was proposed that corrosion inhibition by imidazoline is primarily due to the bonding of the imidazoline ring in a planar orientation to the metal surface. According to the authors, the hydrophobic part plays a vital role in the inhibition performance, whereas the pendant group contributes less to the corrosion inhibition performance by imidazoline molecules as such variation in the chemistry of the group is unimportant. A study [40] agrees with Edwards et al. [25] on the strong interaction between the imidazoline ring and substrate surface, although the orientation was not considered but differed on the role of the pendant group. It was found that the pendant group could improve the inhibition performance by enhancing molecular adsorption. It was demonstrated in the works [41, 42], where an imidazoline inhibitor-containing three phenyl groups was designed and analyzed. The excellent inhibition efficiency of 94% was achieved for carbon steel in $H_2S/CO_2$ environment with $50\,\mathrm{mg\,l^{-1}}$ of this inhibitor.

#### 15.3.1.3 Gemini Surfactants-Based Inhibitor

The term “surfactant” is used to describe surface-active organic compounds tending to lower the interfacial tension (surface tension) between two interfaces that could be liquid–liquid, gas–liquid, or liquid–solid. Surfactants are amphiphilic; that is, they have both hydrophilic and hydrophobic portions. Usually, the hydrophilic part is the head, while the tail is the hydrophobic portion. This dual characteristic, often referred to as hydrophilic and lipophilic tendencies, makes surfactants to be compatible with oily materials and water. Surfactants gain a wide range of applications as detergents, wetting agents, emulsifiers, dispersants, foaming, and stabilizing agents. [43, 44]. Based on the type of polar head group, surfactants are classified as anionic, cationic, zwitterionic (amphoteric), and nonionic. Anionic surfactants are those having negatively charged hydrophilic head carboxylates (sodium stearate, sodium lauroyl sarcosinate, perfluorononanoate, etc.), sulfonates (perfluorooctanesulfonate, perfluorobutanesulfonate, etc.), sulfates (ammonium lauryl sulfate, sodium dodecyl sulfate, etc.), and phosphates (alkyl ether phosphates). Cationic surfactants have a positively charged hydrophilic head, and examples include lauryl amine hydrochloride and trimethyl dodecyl ammonium chloride. The hydrophilic head of zwitterionic surfactants carries both negative and positive charges. pH variation influences the behavior of this class of surfactants. For instance, in an alkaline medium, zwitterionic surfactants behave like anionic surfactants. They act like cationic surfactants and as amphoteric compounds in an acid environment in a neutral medium [43, 44]. Examples of zwitterionic surfactants are lauryl betaine and lauramidopropyl betaine. As the name implies, nonionic surfactants have no formal charge on the polar head. They can be subdivided into five groups: ethoxylates; fatty acid esters of polyhydroxy compounds; amine oxides, e.g. lauryldimethyl oxide, also called dodecyl dimethylamine oxide; sulfoxides, e.g. dimethyl sulfoxide; and phosphine oxides, e.g. phosphine oxide. The classification of surfactants is summarized in Figure 15.4.

Surfactants present interesting adsorption chemistry because of their dual tendencies. Like other organic molecules, ionic surfactants can adsorb on the metal surface via physical or chemical adsorption mechanism. The physisorption mechanism is driven by hydrophobic, literal, and electrostatic interaction [45]. Ionic surfactant's adsorption through the physisorption mechanism can be categorized into adsorption on hydrophobic solids and adsorption on hydrophilic solids. In the case of the adsorption of ionic surfactants on a hydrophobic surface, the driving force is the hydrophobic interaction between the hydrophobic solid surface and the hydrophobic surfactant tail. The driving force is the electrostatic force between the polar metal surface and the polar surfactant head for the adsorption of ionic surfactants on hydrophilic solids. Chemisorption of ionic surfactants occurs when

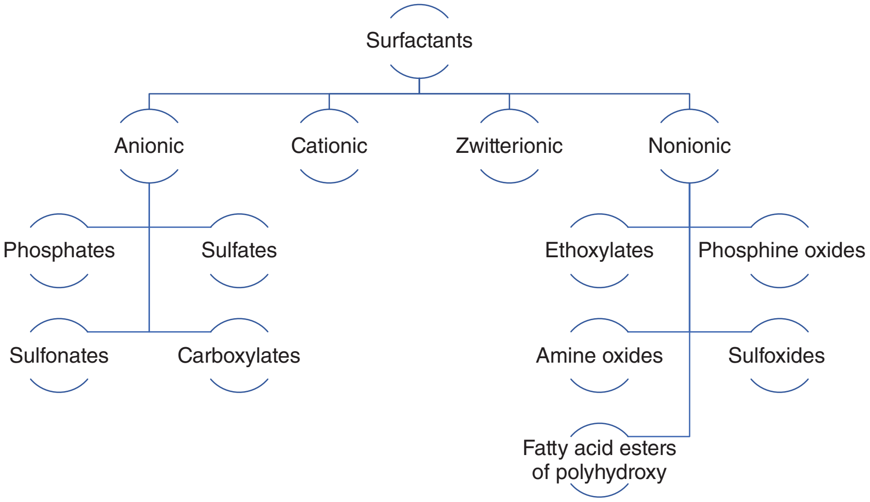

**Figure 15.4** Classification of surfactants.

the surfactants interact with hydrophilic solids electron sharing or transfer; that is, new bonds are formed. Ionic surfactant's adsorption through chemisorption mechanism is characterized by low-adsorption rate and monolayer coverage [45]. A typical example of chemisorption of ionic surfactant is the adsorption of xanthates on sulfide minerals in froth flotation, and it was [46] reported that ethyl xanthate adsorbed on sulfide mineral surfaces by covalent binding. Another work [47] also demonstrated the flotation of salt minerals, and fatty acid salts chemically bind on mineral surfaces. Generally, the adsorption of nonionic surfactants is physisorption, and the driving forces are hydrophobic attraction, lateral interaction, and hydrogen bonding. Detailed information on the adsorption behavior of surfactants on metal surfaces can be found elsewhere [45].

#### 15.3.1.4 Polymer-Based Inhibitor

Polymers are macromolecules characterized by repeating unit(s) called monomers, which are sufficient to give a set of characteristics. Based on origin, polymers are classified into natural, synthetic, and semisynthetic. Natural polymers are obtained from natural sources, typically plant and animal sources. Examples include shellac, silk, cellulose, and wool. Much emphasis is on this class of polymers recently due to their abundance in the environment and ecological friendliness [48, 49]. Synthetic polymers are manufactured polymers, and polyvinyl chloride, polyethylene, polystyrene, etc. are some examples. As the name implies, the semisynthetic is from natural sources but modified to get the final product. Generally, unmodified polymer fairly inhibits metals corrosion when used as an inhibitor [49, 50], due to their insolubility in an aqueous medium occasioned by their hydrophobic nature conferred on them mainly by the presence of methylene groups. Again, most polymers considered for corrosion inhibition cannot withstand high temperatures [48]. However, significant research efforts have been made, particularly in the present century, to overcome the shortcomings mentioned above and enhance the corrosion inhibition of polymers. Some of the approaches adopted are copolymerization, the combination with substances that exert synergistic influence [51], cross-linking [52], and compositing [53]. In a sour environment, acrylic terpolymers have been advocated for use as corrosion inhibitors because they satisfy the green corrosion inhibitor requirements (environment-friendly, nonbioaccumulative, biodegradable, and very low marine toxicity level). As mentioned earlier, the challenge with using polymers generally as metals corrosion inhibitors are their poor solubility in an aqueous medium and their decomposition at elevated temperatures [48].

### 15.3.2 Sweet Corrosion Inhibitor

Sweet corrosion is one of the significant challenges in the oil and gas industry, costing billions of dollars ($) every year. Great efforts have been exploited to control the corrosion business, safety, and environmental considerations. Sweet corrosion is caused by the dissolved carbon dioxide ($CO_2$) in water to form carbonic acid ($H_2CO_3$). The corrosion product ($FeCO_3$) layer formation is eventually triggered by the reaction between the free iron(II) ion ($Fe^{2+}$), released from the steel surface during dissolution, with the carbonate ion. The sweet corrosion mechanism of steel is detailed elsewhere [54]. The corrosion rate increases directly with temperature, system pressure, and concentration of $CO_2$. Sweet corrosion is typically slow and localized, and results in pitting attacks as well. Pits are usually covered under corrosion products, and their small size makes them difficult to detect. Corrosion inhibitors are always considered the first line of defense against internal corrosion in oil and gas production and processing industries. Inorganic inhibitors, such as sodium ferrocyanide and sodium arsenite ($Na_2HAsO_3$), were used in the early days to inhibit sweet corrosion in oil wells, but the treatment frequency and effectiveness were not satisfactory. This led to the development of organic corrosion inhibitors that are based on film-forming amines and their salts. Obot et al. [55] conducted a review and analysis of the distribution of the dominant sweet corrosion inhibitor chemistries, which were found to be in the descending order of magnitude: imidazolines > amines > amides/amido compounds > aldehydes/carboxylates.

#### 15.3.2.1 Imidazolines-Based Inhibitor

Imidazoline is an excellent film-former, and its derivatives constitute essential starting materials for many sweet corrosion inhibitor formulations. This is attributed to the efficient adsorption properties on the steel surface. They function as mixed-type corrosion inhibitors and impede both anodic and cathodic half-reactions during sweet corrosion. Low-temperature sweet corrosion inhibitor formulations based on imidazoline chemistry have been recognized since the 1940s [56]. However, high-temperature sweet corrosion is the most dominant problem in the $CO_2$ environment of the oil and gas industry. The first visible work for some imidazoline derivatives as high-temperature sweet corrosion inhibitors was reported by Jovanciecevic et al. [56]. The authors investigated the effect of hydrocarbon chain length on the inhibition behavior of the imidazoline derivative at 150 °C and 15 psi $CO_2$ partial pressure. It was found that the imidazoline could lower the corrosion rate of C1018 steel down to 2 mpy. Recent work [57] showed that gemini imidazolines were also promising candidates for the inhibition of high-temperature sweet corrosion of carbon steel whereas the gemini imidazoline reduced the corrosion rate down to 2 mpy when tested in a synthetic brine solution at 100 °C under 15 psi $CO_2$ partial pressure. Although some authors emphasized the effect of precorrosion on the performance of imidazolines, the mechanism behind the $FeCO_3$-imidazoline interaction still needs to be investigated more deeply. This is necessary, given that the corrosion inhibitors are usually added, not to the bare steel surface but the steel surface with fully or partially-formed sweet corrosion products layers (e.g. $FeCO_3$). For instance, it was shown that the inhibition performance of imidazoline-based high-temperature sweet corrosion inhibitors was significantly influenced by their application either on bare steel surfaces or steel surfaces with partially or fully-formed $FeCO_3$ layer [58, 59]. The findings from these works concluded that timing the injection of the imidazolines was important. Once a stable nonporous $FeCO_3$ scale was formed on the steel surface in $CO_2$-saturated, the addition of an imidazoline-based formulation did not significantly change the corrosion rate of X65 steel.

#### 15.3.2.2 Amines-Based Inhibitor

Amine-based inhibitors constitute another important class of film-forming adsorption-type $CO_2$ corrosion inhibitors. Depending on the number of alkyl groups substituted for the nitrogen, aliphatic amines can be classified as primary, secondary, tertiary, or quaternary. Amine-based compounds also possess nitrogen atoms as the active center for adsorption onto the steel surface, such as the imidazolines. The alkyl groups extend into the solution to create the hydrophobic layer, which repels the ingress of corrosive agents. They are cheaper and more affordable film-forming inhibitors compared to imidazolines. However, their application as active ingredients of high-temperature sweet corrosion inhibitor formulations can be hindered because they become less soluble as the number of carbon atoms in the alkyl chain increases. Again, although the amines have been tested inappreciably high temperatures, they have not been tested well enough in high pressure and high hydrodynamics conditions. This may be because, at high temperatures, most amines rearrange themselves to assume cyclic ring structures or become decomposed into insoluble products, which diminishes their high-temperature sweet corrosion inhibition performance. Nevertheless, the work of Ramachandran et al. [60] stands out, where an amine derivative was applied at 232 °C under 450 psi of $CO_2$ in a synthetic brine solution. The authors emphasized that the amine could not withstand higher $CO_2$ partial pressures up to 1500 psi at such a high temperature. Such high pressure could only be applicable at a lower temperature around 188 °C.

#### 15.3.2.3 Amides/Amido-Based Inhibitor

Amides are precursors of imidazolines. They also exhibit excellent corrosion inhibition. Their active centers include the carbonyl group bearing an oxygen atom and the amine group containing the nitrogen atom. The structure of amidoamine greatly modifies their chemistry and confers superior properties on them relative to alkyl amines and imidazoline [61]. They can receive more nitrogen. They have higher cationic coverage and also exhibit higher surface activity and capacity to neutralize most acids. They are also relatively cheaper to produce than imidazoline, which usually requires a two-step and more complex high-temperature procedure. It was reported [62] that water solubility was essential for imparting high efficiency on an amido imidazoline used as a high-temperature sweet corrosion inhibitor. The water-solubility enables effective inhibitor-substrate interaction via adsorption. This eventually reduces the occurrence of pitting corrosion compared with the oil-soluble amides. However, there is a lack of knowledge on precorrosion's effect on the amides, not determining their chemical stability at the working temperature. The water solubility advantage for amide-based formulations was also emphasized by Ramachandran et al. [63]. The authors showed that some newly developed high-temperature water-soluble amides exhibited higher density than oil-soluble counterparts, which aids the batch treatment of wells with high fluid levels. The water-soluble inhibitors also possess high-flash points, ensuring their safety for use with lower impact on the environment. Amidoamines appear to be the most reported high-temperature sweet corrosion inhibitors based on amides. However, the inhibitor performed poorly, even worse than the blank solution, in 100% water cut (without oil). The presence of the oil phase was incredibly beneficial for the effective dispersion of the inhibitor in the brine solution. It was concluded that approximately 0.1% of the oil was necessary to sustain the inhibition performance of the amides.

#### 15.3.2.4 Aldehydes/Carboxylates-Based Inhibitor

Recently, some high-temperature sweet corrosion inhibitors based on aldehydes and carboxylic acids/carboxylates have been reported [64]. Their interaction points include the carbonyl group, which contains an oxygen atom with lone pair electrons donated to the empty orbitals of the Fe atom in the steel. It was noted [64] that carboxylates exhibited higher inhibition efficiencies than amines. This was concluded, especially for 13Cr steel, after comparing some long-carbon-chain carboxylic acids with some amine-based formulations at a partial pressure of 150 °C and 479 psi $CO_2$. Unlike the nitrogen atom in an amine, the carboxylate provided its COO– group, which enhanced affinity for 13Cr steel. On the other hand, Mazumder et al. [65] fused a cinnamaldehyde moiety with propargyl and isoxazolidine moieties (both of which have well-established sweet corrosion inhibition properties). This fusion yielded a novel structure tested for its sweet corrosion inhibition for mild steel in 0.5 M NaCl solution at 120 °C and 10 bar $CO_2$ partial pressure. Its inhibition efficiency was 88%. These chemistries deserve remarkable attention because they deviate markedly from the overdependence on nitrogen-based chemistries. It is even more special since it is based on the fusion of multiple inhibitive chemistries [65, 66]. However, these chemistries have majorly been investigated in purely NaCl solutions, giving doubts about their efficiency in the actual field condition, consisting of very aggressive brine solutions with a high concentration of dissolved solids.

## 15.4 Corrosion Inhibitor Management

The application of effective corrosion inhibition in oil and gas production is essential to enable long-term use of carbon steel in corrosive systems. Carbon steel as a low-cost material requires proper validation of corrosion inhibition effectiveness to assure operational integrity. Sonke and Grimes [67] suggested a corrosion inhibition management process, which is outlined in Figure 15.5. They divided the corrosion inhibition management process into five major steps:

- Identify the application window.
- Define corrosion inhibition test program.
- Select corrosion inhibitors in the laboratory.
- Assure corrosion inhibitor performance in the field.
- Implementation and surveillance of corrosion inhibitor application.

These steps are further described in the following sections.

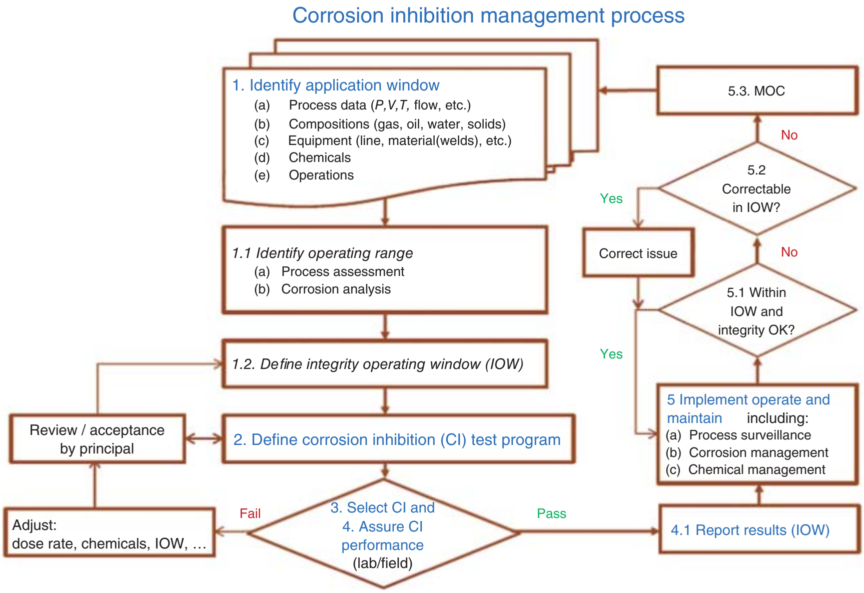

**Figure 15.5** Corrosion inhibition management process was suggested by Sonke and Grimes [67]. Source: Sonke and Grimes [67].

### 15.4.1 Identify Application Window

The process evaluation aims to define the integrity operating window needed for the corrosion inhibition designing and application. Identification of the application window involves data gathering, estimating, and filtering to an essential window based upon corrosion and corrosion inhibition impact and corrosion analysis to define testing needs within this window further. Initial steps to identify an application window are to identify scopes of interest (e.g. well, flow line, process facilities, and pipeline), including design requirements and estimated period of interest. To identify the operating range, field data that will have a specific impact on corrosion and corrosion mitigation efforts (corrosion inhibition effectiveness) need to be gathered. Data to be gathered includes process data, compositions of gas and liquids, other treatment chemicals, and field operating capabilities, as they may impact corrosion or corrosion inhibitor performance. Production changes that can be expected within the application period need to be incorporated in the data assessment, e.g. water breakthrough and its impact on salinity (TDS), sand production, pressure, temperature, velocity, and fluid composition (e.g. new wells). Based on the gathered data, an analysis shall be made that defines the range of integrity operating windows for high corrosion inhibition effectiveness.

### 15.4.2 Define Corrosion Inhibition Test/Validation Program

Based on the identified corrosion inhibitor within the integrity operating window, a test protocol can be formulated suitable for the specific application. There are two test program approaches to validate the corrosion inhibition performance within its integrity operating window. In one approach, a test program is developed that covers all possible combinations of the critical exposure conditions – all temperatures, salinities, oil/water ratios, treatment chemicals, flows, etc. A more efficient approach is to identify a few critical, severe, base case exposures, and worst-case scenarios, then validate the full corrosion inhibition performance within its integrity operating window at appropriate extended boundary excursions from these base conditions. Base case exposure conditions, critical for CI performance evaluation, are the highest corrosion rate, the highest exposure temperature, and the highest salinity/TDS). Based on the identified base case conditions, a test program can be designed to address these exposures and excursions from these conditions.

The base case parameters to define the integrity operating window of corrosion inhibition are those most strongly impacting corrosion and corrosion inhibition effectiveness. These are defined as the process conditions of (A) temperature, (B) partial pressures of acid gasses "$H_2S$, $CO_2$," (C) water chemistry, and (D) hydrocarbon "oil/water ratio." The base case typically needs to cover a range of conditions that often requires evaluation of more than one field exposure condition. Base case corrosion inhibition performance validation (e.g. parameters A–D) is often performed in a standard autoclave test. To validate the boundaries of full operating window of corrosion inhibition, other tests should be added to the program to cover additional parameters that can impact the corrosion inhibitor performance in the corrosion inhibitor within integrity operating window. The final test program should reflect the entire range of expected exposure conditions. In principle, the full window, including "boundary" exposures, should be tested/validated as extensions of all critical base case conditions as a matrix of required tests. For identification of a critical window of conditions for testing, the following criteria are recommended:

1. The maximum partial pressure of acid gasses, $pCO_2/pH_2S$, respectively, should generally be used for the test exposure.
2. For temperature, it is critical to look at both the full range of exposure temperatures and, potentially, intermediate temperature(s) at which the maximum unmitigated corrosion rate within this range would occur.
3. For water compositions, prior to acid gas saturation, the test water chemistry should reflect that measured from actual, depressurized field samples (if available) and include similar salinity/TDS, organic acids concentration, and pH.
4. Oil/condensate composition and water ratio range can impact corrosion inhibition performance due to natural surfactants in the oil (promoting emulsions), natural inhibitors in the oil, and partitioning between the oil and aqueous phase. Hydrocarbons can themselves contribute to corrosion inhibition performance, and the presence of hydrocarbons may be crucial to the performance of some corrosion inhibitor products. Water/hydrocarbon ratio has several effects. Low water cut reduces the corrosion rate by promoting hydrocarbon wetting of the steel. Some inhibitor types, e.g. oil-soluble/water-dispersible, may also require minimum flow turbulence to effectively partition into the water phase.
5. Partitioning of corrosion inhibitors between a hydrocarbon and aqueous phase can impact the available corrosion inhibitor presence at the wet metal substrate.

Corrosion inhibitor partitioning can be significantly impacted by process conditions, such as mixing energy at the injection point and turbulent versus stratified flow.

6. To assure chemical compatibility, since corrosion inhibitors are often used in operations with other chemicals to optimize and safeguard production, evaluation of the effectiveness of corrosion inhibitors in the presence of other substances is relevant.
7. Deposits can impair corrosion inhibitor effectiveness by physically impairing corrosion inhibitor access to the metal surface, but some deposits – FexSy and sulfur – may also directly enhance the corrosion. In sour conditions, the presence of deposits has a significant impact on the unmitigated corrosion rate

### 15.4.3 Selection of Corrosion Inhibitor

A large number of corrosion inhibitors are available commercially, and chemical manufacturers are continuously developing new products. The selection of the correct inhibitor depends on the type of system to be protected, whether a pumping oil well, a gas-lift well, a gas well, a waterflood system, or a flow line. For example, if a conventional inhibitor is injected upstream of a gas compressor, the heavier components could deposit and foul the compressor's valves. Both temperature and pressure should be considered when selecting an inhibitor. Higher temperature and pressure could lead to polymerization and sludge formation. The pressure levels will determine the corrosivity of $CO_2$ and $H_2S$. The inhibitor's thermal stability should be assessed during corrosion inhibitor evaluation. Factors that influence inhibitor selection include:

- Identifying the problem to be solved.
- Identifying the corrosive species.
- Pressure and temperature.
- Velocity.
- Production composition.
- Water/oil ratio.
- The salinity of the water.
- The acidity of water and oil.

Parameters to be considered when evaluating an inhibitor is whether the system is sweet or sour, the service pressure and temperature, water composition, and water cut, and the type of corrosion inhibitor treatment, e.g. batch or continuous treatments. Factors that affect the dosage and frequency of treatment include the severity of corrosion, the total amount of produced fluid, the percentage of water, the nature of corrodent, and the type of chemical selected. Based on the defined corrosion inhibitor within the integrity operating window and the required corrosion inhibitor test program, one or more corrosion inhibitor products need to be found to meet the corrosion inhibitor within the integrity operating window requirements. The first step in finding a suitable corrosion inhibitor is to communicate the corrosion inhibitor within integrity operating window requirements to the potential supplier(s). With this information at hand, a supplier should find product(s) that are suitable to cover the requirements. For selection, the supplier can use data from field experience in similar conditions, previous corrosion inhibitor test qualifications, using internal expertise, or develop a corrosion inhibitor specifically to meet the needed requirements. Selection of a candidate product based on matching experience or qualifications can be straightforward and lead to relatively fast product selection. If new product development is required, the process can be more time-consuming, and vendor testing might be needed to confirm the potential suitability. A product's performance qualification/validation program can be optimized based on the available data and relevance to the proposed corrosion inhibitor application. Corrosion inhibitor testing data for candidate product selection may be less demanding, and a relative performance assessment, based upon limited, less rigorous tests, may be performed to identify candidate products. However, a relative performance assessment usually does not provide complete and final assurance of corrosion inhibitor performance across the corrosion inhibition within the integrity operating window. With appropriate quality controls, a full validation assessment is required to ensure complete corrosion inhibitor within the integrity operating window. Test data should always seek to replicate actual field exposures in line with the defined corrosion inhibitor within the integrity operating window.

### 15.4.4 Assurance of Corrosion Inhibitor (Laboratory Testing/Field Trial)

Several international standards have been developed [68–70] and are developed [71] for corrosion inhibitor evaluation and selection. The mentioned factors in the previous section that influence inhibitor selection include identifying the problem to be solved and should be considered on the laboratory testing matrix. For example, the test exposures as defined in the base case are often performed by high temperature and high-pressure autoclave (vessel) rotating cage test design with test specimens exposed to a low, consistent shear. Inhibitor thermal stability, compatibility with used chemicals in the process, emulsion, and foaming tendency should be screened during corrosion inhibitors development. Based on the previous analyses, a full assessment program can be identified and documented as the basis for corrosion inhibitor verification and implementation. With the full corrosion inhibition of integrity operating window envelope identified, subsequent field and/or laboratory-based final performance assessments need to provide full coverage. These final assessments should be witnessed or performed by the user or a qualified and audited independent agency to ensure quality data. This full validation assessment should provide data that reliably indicates the performance of the corrosion inhibitor under all the field conditions that can be expected, as defined in its corrosion inhibition of integrity operating window.

Field validation of corrosion inhibitor performance may be performed to assure corrosion inhibition of integrity operating window suitability. Still, such assessments need to consider the practicality of assessing the entire identified integrity operating window. If future operational changes are incorporated in the integrity operating window, access to a suitable exposure will likely be limited or, perhaps, not yet actually present in the field. Field validation also requires accurate capture of the corrosion inhibitor performance, which may not be within the capability of existing field monitoring tools, requiring either upgrades or a move to laboratory assessment. An assessment program employing and potentially modifying a production side stream may expand the field validation capabilities if suitable field fittings and utilities are present for such a testing installation. A blend of field and laboratory approaches can also be considered. A laboratory validation assessment needs to be performed using test methods, protocols, and conditions that replicate the field conditions identified in the corrosion inhibition within the integrity operating window assessment envelope. The program is usually initiated by testing the base case exposures, followed by the balance of the test program to validate the full boundaries of the corrosion inhibition within the integrity operating window.

### 15.4.5 Implementation and Surveillance of Corrosion Inhibitor Application

Corrosion Inhibition performance shall be identified as a key performance indicator (KPI) as part of the corrosion management strategy. Once a corrosion inhibitor is selected as previously described, KPIs should be defined as follows:

1. Operate within the defined integrity operating window and in line with the corrosion inhibitor qualification, as identified in the process and liquid chemistry operating conditions, e.g. pressures, temperatures, gas composition, and oil/water ratio.
2. Apply proven corrosion inhibitor dose rate in line with the required corrosion inhibitor dosage based on total liquids, including oil–water partitioning. The application rates will require regular adjustment to compensate for fluctuations in liquid production rates and ratios.
3. Recording corrosion inhibitor availability uptime/downtime and regularly comparing actual injection performance against uptime and dose required by the corrosion inhibitor design and corrosion assessment. A corrosion inhibitor assessment that can be incorporated to reduce the estimated corrosion impact of short corrosion inhibitor injection downtime upsets is the validated corrosion inhibitor persistency.
4. Assessing and recording the total time of upsets within (or beyond) the integrity operating window design. The impact of such upsets should be shorter than the upset period incorporated in the design.
5. Implementing and recording special mitigations and risks relevant to the risk of under deposit corrosion, such as frequency treatment, scraping frequency, flow behavior below water, or deposit drop out limit, and documenting solids production events.
6. These KPIs need to be evaluated and reported to accountable management on a frequent (yearly or less) basis.
7. Alarms and surveillance activities need to be defined that trigger adjustment on time with respect to the unmitigated corrosion rate. Alarms should include injection availability and selected online critical corrosion inhibitor with integrity operating window parameters.

## 15.5 Safety on Designing Corrosion Inhibitor

The oil and gas industry is a high-risk industry, facing health and safety challenges in every aspect of production and operation. Safety is one of the major requirements to ensure no fire risk on the application of corrosion inhibitors as well as no health issue on plant staff. Therefore, the supplier should submit a safety data sheet of any corrosion inhibitor to chemical handlers and users. The safety data sheet is a standardized document that contains occupational safety and health data. The international hazard communication standard mandates that chemical manufacturers communicate hazard information to chemical handlers by providing a safety data sheet. Typically, it contains chemical properties, health and environmental hazards, protective measures, and safety precautions for storing, handling, and transporting chemicals. Hazardous chemicals management should be implemented over the production, operation, packaging, storage, transportation, use, and disposal of hazardous chemicals.

The chemical flashpoint is the safety aspect that should be considered in the initial stage of corrosion inhibitor development. Flashpoint is reported in a safety data sheet that assesses the flammability of a material. There are strict flash point parameters on chemicals at field locations. The flashpoint of a chemical is a measure of its tendency to form a flammable mixture with air under controlled laboratory conditions and its data indicates the possible presence of highly volatile and flammable material in a relatively nonvolatile or nonflammable material. The flashpoint is the lowest temperature corrected to a pressure of 15 psi, at which an ignition source causes the vapors of a sample to ignite under specified test conditions. National Association of Corrosion Engineers (NACE) report highlighted [72] that the corrosion inhibitor flash point should be higher than outside and stored temperatures. For instance, because of the high summer temperature in Middle East countries, an oil-field chemical's acceptable industrial flash point shall be higher than 65 °C. The flammable and combustible liquids are stored in atmospheric tanks or transferred at temperatures below their flashpoints. They shall be reviewed to ensure that fire and explosion hazards are addressed by fire prevention according to National Fire Protection Association (NFPA) NFPA 30 [73].

On the other hand, there are some corrosion inhibitors where methanol is a part of the final formulation and is not recommended for the coated pipelines. This is not because of the low flash point of methanol but of the incompatibility of methanol with epoxy coating. It was reported [63] that water-soluble inhibitors possess high-flash points, ensuring their safety for use with lower impact on the environment.

## 15.6 Conclusions

Over the years, several formulations of corrosion inhibitors have been developed to tackle diverse corrosion challenges in the oil and gas industries. A scientific and patent literature review reveals that the current sour corrosion inhibitors are amine-based, imidazoline-based, gemini surfactants, and terpolymers. For sweet corrosion inhibitor application, nitrogen-based chemistries, such as imidazolines, amines, and amides, are the most reported inhibitors for high-temperature sweet corrosion of steel. A method for selecting and validating corrosion inhibitor performance and operating a corrosion inhibition system is proposed using the concept of a corrosion inhibitor within the integrity operating window. The combined understanding of corrosion processes, oil and gas operations, and laboratory test methods are crucial for effective corrosion inhibitor selection, performance validation, deployment, and operational surveillance. Employing a combination of engineering, operational, and laboratory corrosion inhibitor experience and capability is necessary to define a corrosion inhibitor within the integrity operating window properly. This corrosion inhibitor within the integrity operating window is needed to properly identify needed testing, employing recognized methods developed for corrosion inhibitor performance validation. Corrosion inhibition management requires a defined work process to properly ensure corrosion inhibitor test program definition, testing, and implementation.

## Acknowledgment

The authors would like to thank Saudi Aramco for permission to publish this book chapter. Special thanks go to the R&DC management for their support and encouragement.

## List of Abbreviations

| | |
|---|---|
| CI | corrosion inhibitors |
| $CO_2$ | carbon dioxide |
| $FeCO_3$ | iron carbonate |
| $H_2CO_3$ | carbonic acid |
| $H_2S$ | hydrogen disulfide |
| Mpy | mils per year |
| $Na_2HAsO_3$ | sodium arsenite |
| NACE | National Association of Corrosion Engineers |
| NaCl | sodium chloride |
| NFPA | National Fire Protection Association |
| Psi | pound per square inch |
| SCC | stress crossing cracking |
| TDS | total dissolved solids |

## References

**1** Al-Otaibi, M.S., Al-Mayouf, A.M., Khan, M. et al. (2012). Corrosion inhibitory action of some plant extracts on the corrosion of mild steel in acidic media. *Arabian Journal of Chemistry* 7: 340–346.

**2** Dariva, C.G. and Galio, A. (2014). *Corrosion Inhibitors – Principles, Mechanisms and Applications, Developments in Corrosion Protection*, 366–376. IntechOpen. ISBN: 978-953-51-6359-6.

**3** Obot, I.B., Obi-Egbedi, N.O., and Umoren, S.A. (2009). Antifungal drugs as corrosion inhibitors for aluminum in 0.1 M HCl. *Corrosion Science* 51 (8): 1868–1875.

**4** Aslam, J., Aslam, R., Zehra, S., and Rizvi, M. (2022). Corrosion inhibitors for sweet ($CO_2$ corrosion) and sour ($H_2S$ corrosion) oilfield environment. In: *Environmentally Sustainable Corrosion Inhibitors*, ISBN: 978-0-323-85405-4, 165–181. Elsevier.

**5** Monticelli, C. (2018). Corrosion inhibitors. In: *Encyclopedia of Interfacial Chemistry*, ISBN: 9780128098943, 164–171. Elsevier.

**6** Aslam, J. and Aslam, R. (2022). Corrosion inhibitors for high temperature corrosion in oil and gas industry. In: *Environmentally Sustainable Corrosion Inhibitors*, ISBN: 978-0-323-85405-4, 423–437. Elsevier.

**7** Dougherty, J.A. (1997). Effect of treatment method on corrosion inhibitor performance. NACE Corrosion 97, Paper No. 344.

**8** Leal, J., Ramachandran, S., Wang, Q. et al. (2020). Successful long duration batch treatment of gas well to prevent corrosion challenges and solutions. IPTC-19640-MS (2020) 1-11.

**9** Nyborg, R. (2005). Controlling internal corrosion in oil and gas pipeline. *Business Briefing-Exploration & Production: The Oil & Gas Review* 2: 70–74.

**10** Obot, I.B., Solomon, M.M., Umoren, S.A. et al. (2019). Progress in the development of sour corrosion inhibitors: past, present, and future perspectives. *Journal of Industrial and Engineering Chemistry* 79: 1–18.

**11** Alanazi, N.M. and El-Sherik, A.M. (2018). Under-deposit corrosion behavior of a carbon steel. *Materials Performance* 57: 2–5.

**12** Wen, X., Bai, P., Luo, B. et al. (2018). Review of recent progress in the study of corrosion products of steels in a hydrogen sulphide environment. *Corrosion Science* 139: 124–140.

**13** Zhang, G.A., Zeng, Y., Guo, X.P. et al. (2012). Electrochemical corrosion behavior of carbon steel under dynamic high pressure $H_2S/CO_2$ environment. *Corrosion science* 65: 37–47.

**14** Memendez, C.M., Jovancicevic, V., Ramachandran, S. et al. (2013). Assessment of corrosion under iron sulfide deposits and $CO_2/H_2S$ conditions. *Corrosion Engineering* 69: 145–156.

**15** Alanazi, N.M., El-Sherik, A.M., Rasheed, A.H. et al. (2015). Corrosion of pipeline steel X-60 under field-collected sludge deposit in a simulated sour environment. *Corrosion Engineering* 71: 305–315.

**16** Rivera-Grau, L.M., Casales, M., Regla, I. et al. (2012). $H_2S$ corrosion inhibition of carbon steel by a coconut-modified imidazoline. *International Journal of Electrochemical Science* 7: 12391–12403.

**17** Kashkovskiy, R.V., Kuznetsov, Y.I., and Kazansky, L.P. (2012). Inhibition of hydrogen sulfide corrosion of steel in gas phase by tributylamine. *Corrosion Science* 64: 126–136.

**18** Zhao, J., Duan, H., and Jiang, R. (2015). Synergistic corrosion inhibition effect of quinoline quaternary ammonium salt and Gemini surfactant in $H_2S$ and $CO_2$ saturated brine solution. *Corrosion Science* 91: 108–119.

**19** Kudryavtsev, D.B., Panteleeva, A.R., Yurina, A.V. et al. (2009). Polymeric inhibitors of hydrogen sulfide corrosion. *Petroleum Chemistry* 49: 193–198.

**20** Raffa, P., Broekhuis, A.A., and Picchioni, F. (2016). Polymeric surfactants for enhanced oil recovery: a review. *Journal of Petroleum Science and Engineering* 145: 723–733.

**21** Jing-Mao, Z. and Jun, L. (2012). Corrosion inhibition performance of carbon steel in brine solution containing $H_2S$ and $CO_2$ by novel Gemini surfactants. *Acta Physico-Chemica Sinica* 28: 623–629.

**22** Vakili Azghandi, M., Davoodi, A., Farzi, G.A., and Kosari, A. (2012). Water-base acrylic terpolymer as a corrosion inhibitor for SAE1018 in simulated sour petroleum solution in stagnant and hydrodynamic conditions. *Corrosion Science* 64: 44–54.

**23** Pournazari, S., Moayed, M.H., and Rahimizadeh, M. (2013). In situ synthesis of 2-phenylbenzimidazole as hydrogen sulfide corrosion inhibitor of carbon steel. *Corrosion Engineering* 69: 1195–1204.

**24** Szyprowski, A.J. (2002). Impedance study of imidazoline inhibitors against hydrogen sulphide corrosion of steel. *British Corrosion Journal* 37: 141–146.

**25** Edwards, A., Osborne, C., Webster, S. et al. (1994). Mechanistic studies of the corrosion inhibitor oleic imidazoline. *Corrosion Science* 36: 315–325.

**26** Barczak, M. (2019). Amine-modified mesoporous silicas: morphology-controlled synthesis toward efficient removal of pharmaceuticals. *Microporous and Mesoporous Materials* 278: 354–365.

**27** Dai, Y.X., Lv, F.N., Wang, B., and Chen, Y. (2018). Thermoresponsive phenolic formaldehyde amines with strong intrinsic photoluminescence: preparation, characterization and application as hardeners in waterborne epoxy resin formulations. *Polymer* 145: 454–462.

**28** Ziarani, G.M., Moradi, R., Lashgari, N., and Kruger, H.G. (2018). *Amine Dyes, Metal-Free Synthetic Organic Dyes*, ISBN: 978-0-12-815647-6, 19–46. Elsevier.

**29** Farahani, M.H.D.A. and Chung, T.S. (2018). Solvent resistant hollow fiber membranes comprising P84 polyimide and amine-functionalized carbon nanotubes with potential applications in pharmaceutical, food, and petrochemical industries. *Chemical Engineering Journal* 345: 174–185.

**30** Papir, Y.S., Schroeder, A.H., and Stone, P.J. (1989). New downhole filming amine corrosion inhibitor for sweet and sour production. Society of Petroleum Engineers, Paper No. 18489-MS.

**31** Mok, W.Y., Jenkins, A.E., Keenan, S.R., and Gamble, C.G. (2005). Control of localized corrosion using green corrosion inhibitors. NACE International Corrosion Conference & Expo, Houston, TX, Paper No. 05289.

**32** Stewart, S., Jovancicevic, V., Menendez, C. et al. (2010). Evaluation of a new sour gas corrosion inhibitor for field applications via localized corrosion monitoring techniques. NACE International Corrosion Conference & Expo, Houston, TX, Paper No. 10274.

**33** Savoy, M.G. (1952). Inhibitors against hydrogen sulfide and brine corrosion. US Patent 2,593,057.

**34** Shetnev, A., Osipyan, A., Baykov, S. et al. (2018). Novel monoamine oxidase inhibitors based on the privileged 2-imidazoline molecular framework. *Bioorganic & Medicinal Chemistry Letters* 29: 40–46.

**35** Trulli, L., Sciubba, F., and Fioravanti, S. (2018). Chiral trans-carboxylic trifluoromethyl 2-imidazolines by a $Ag_2O$-catalyzed Mannich-type reaction. *Tetrahedron* 74: 572–577.

**36** Diaz, E.F., Gonzalez-Rodriguez, J.G., Martinez-Villafañe, A., and Gaona-Tiburcio, C. (2010). $H_2S$ corrosion inhibition of an ultra high strength pipeline by carboxyethyl-imidazoline. *Journal of Applied Electrochemistry* 40: 1633–1640.

**37** Szyprowski, A.J. (2000). Relationship between chemical structure of imidazoline inhibitors and their effectiveness against hydrogen sulphide corrosion of steels. *British Corrosion Journal* 35: 155–160.

**38** Galicia, P. and González, I. (2005). Modification of 1018 carbon steel corrosion process in alkaline sour medium with a formulation of chemical corrosion inhibitors. *Electrochimica Acta* 50: 4451–4460.

**39** Lucio-Garcia, M.A., Gonzalez-Rodriguez, J.G., Martinez-Villafañe, A. et al. (2010). A study of hydroxyethyl imidazoline as $H_2S$ corrosion inhibitor using electrochemical noise and electrochemical impedance spectroscopy. *Journal of Applied Electrochemistry* 40: 393–399.

**40** Gusmano, G., Labella, P., Montesperelli, G. et al. (2006). Study of the inhibition mechanism of imidazolines by electrochemical impedance spectroscopy. *Corrosion* 62: 576–583.

**41** Zhao, X., Chen, C., Yu, H., and Chen, Q. (2018). Evaluation and mechanism of corrosion inhibition performance of new corrosion inhibitor. NACE International Corrosion Conference & Expo, Houston, TX, Paper No. 11029.

**42** Ramachandran, S., Tsai, B.-L., Blanco, M. et al. (1996). Self-assembled monolayer mechanism for corrosion inhibition of iron by imidazolines. *Langmuir* 12: 6419–6428.

**43** Tripathy, D.B., Mishra, A., Clark, J., and Farmer, T. (2018). Synthesis, chemistry, physicochemical properties and industrial applications of amino acid surfactants. *Comptes Rendus Chimie* 21: 112–130.

**44** Alwadani, N. and Fatehi, P. (2018). Synthetic and lignin-based surfactants: challenges and opportunities. *Carbon Resources Conversion* 1: 126–138.

**45** Chang, Z., Chen, X., and Peng, Y. (2018). The adsorption behavior of surfactants on mineral surfaces in the presence of electrolytes – a critical review. *Minerals Engineering* 121: 66–76.

**46** Leppinen, J.O., Basilio, C.I., and Yoon, R.H. (1989). In-situ FTIR study of ethyl xanthate adsorption on sulfide minerals under conditions of controlled potential. *International Journal of Mineral Processing* 26: 259–274.

**47** Jong, K., Han, Y., and Ryom, S. (2017). Flotation mechanism of oleic acid amide on apatite. *Colloids & Surfaces a Physicochemical & Engineering Aspects* 523: 127–131.

**48** Umoren, S.A. and Solomon, M.M. (2016). Synergistic corrosion inhibition effect of metal cations and mixtures of organic compounds: a review. *Journal of Energy Environmental & Chemical Engineering* 5: 246–273.

**49** Fares, M.M., Maayta, A.K., and Al-Mustafa, J.A. (2012). Corrosion inhibition of Iota-Carrageenan natural polymer on aluminum in presence of zwitterion mediator in HCl media. *Corrosion Science* 65: 223–230.

**50** Jeyaprabha, C., Sathiyanarayanan, S., and Venkatachari, G. (2005). Co-adsorption effect of polyaniline and halide ions on the corrosion of iron in 0.5 M $H_2SO_4$ solutions. *The Journal of Electroanalytical Chemistry* 583: 232.

**51** Umoren, S.A. and Ebenso, E.E. (2007). The synergistic effect of polyacrylamide and iodide ions on the corrosion inhibition of mild steel in $H_2SO_4$. *Materials Chemistry and Physics* 106: 387.

**52** Umoren, S.A., Solomon, M.M., Udosoro, I.I., and Udoh, A.P. (2010). Synergistic and antagonistic effects between halide ions and carboxymethyl cellulose for the corrosion inhibition of mild steel in sulphuric acid solution. *Cellulose* 17: 635–648.

**53** Banerjee, S., Srivastava, V., and Singh, M.M. (2012). Chemically modified natural polysaccharide as green corrosion inhibitor for mild steel in acidic medium. *Corrosion Science* 59: 35–41.

**54** Sun, W. and Nesic, S. (2008). Kinetics of corrosion layer formation: Part 1-Iron carbonate layer in carbon dioxide corrosion. *Corrosion* 64: 334–346.

**55** Obot, I.B., Onyeachu, I.B., Umoren, S.A. et al. (2020). High temperature sweet corrosion and inhibition in the oil and gas industry: progress, challenges and future perspectives. *Journal of Petroleum Science and Engineering* 185: 106469.

**56** Jovanciecevic, V., Ramachandran, S., and Prince, P. (1998). Inhibition of $CO_2$ corrosion of mild steel by imidazolines and their precursors. *Corrosion* 55: 449–455.

**57** Yang, J., Gao, L., Liu, X. et al. (2016). A highly efficient corrosion inhibitor by use of Gemini imidazoline. SPE International Symposium on Oilfield Chemistry, Society of Petroleum Engineers, The Woodlands, TX, Paper No. SPE-173777-PA.

**58** Hirano, S., Sunaba, T., and Lto, T. (2019). Corrosion inhibitor performance under high temperature/high salinity sweet conditions. NACE International Corrosion Conference & Expo, Houston, TX, Paper No. 12756.

**59** Palenscar, A., Gulbrandsen, E., and Kosoru, K. (2016). Corrosion inhibition under $FeCO_3^-$ forming conditions at elevated temperatures. SPE International Oilfield Corrosion Conference and Exhibition, Society of Petroleum Engineers, Aberdeen, Scotland, Paper No. SPE-169614-MS.

**60** Ramachandran, S., Soo Ahn, Y., Greaves, M. et al. (2006). Development of high temperature, high pressure corrosion inhibitor. NACE International Corrosion Conference & Expo, San Diego, CA, Paper No. 06377.

**61** Askari, M., Aliofkhazraei, M., Ghaffari, S., and Hajizadeh, A. (2018). Film former corrosion inhibitors for oil and gas pipelines–a technical review. *Journal of Natural Gas Science & Engineering* 58: 92–114.

**62** Moiseeva, L.S. (2005). Carbon dioxide corrosion of oil and gas field equipment. *Journal of Protection of Metals* 41: 76–83.

**63** Ramachandran, S., Jovancicevic, V., and Jeff, L. (2009). Development of a new water soluble high temperature corrosion inhibitor. NACE International Corrosion Conference & Expo, Atlanta GA, Paper No. 09237.

**64** Tomoe, Y., Shimizu, M., Ito, T., and Sunaba, T. (2013). Inhibitor evaluation for 13Cr steel in high temperature, sweet corrosions, and the effects of co-existence of liquid hydrocarbons. NACE International Corrosion Conference & Expo Orlando, FL, Paper No. 2262.

**65** Mazumder, M.A.J., Al-Muallem, H.A., Faiz, M., and Ali, S.A. (2014). Design and synthesis of a novel class of inhibitors for mild steel corrosion in acidic and carbon dioxide-saturated saline media. *Corrosion Science* 87: 187–198.

**66** Lopez, D.A., Perez, T., and Simison, S.N. (2003). The influence of microstructure and chemical composition of carbon and low alloy steels in $CO_2$ corrosion. A state-of-the-art appraisal. *Materials and Design* 24: 561–575.

**67** Sonke, J. and Grimes, W.D. (2017). Guidelines for corrosion inhibitor selection for oil and gas production-Part2: corrosion inhibition performance validation. NACE International Corrosion Conference & Expo, Houston, TX, Paper No. 8842.

**68** ASTM G170 (2012). *Standard Guide for Evaluating and Qualifying Oilfield and Refinery Corrosion Inhibitors in the Laboratory*. West Conshohocken, PA: ASTM International.

**69** ASTM G184 (2016). *Standard Practice for Evaluating and Qualifying Oil Field and Refinery Corrosion Inhibitors Using Rotating Cage*. West Conshohocken, PA: ASTM International.

**70** ASTM G185 (2016). *Standard Practice for Evaluating and Qualifying Oil Field and Refinery Corrosion Inhibitors Using the Rotating Cylinder Electrode*. West Conshohocken, PA: ASTM International.

**71** TG 550 (2019). NACE New Standard on Corrosion inhibition management for oil and gas fields, Houston, TX.

**72** Technical Committee Report By NACE International Task Group (TG) 330 (2014). Laboratory evaluation of corrosion inhibitors used in the oil and gas industry, Item No. 24259.

**73** NFPA 30 (2018). National fire protection association technical committees on flammable and combustible liquids for tank storage and piping systems (FLC-TAN).

# Index

*Polymeric Corrosion Inhibitors for Greening the Chemical and Petrochemical Industry*, First Edition.
Edited by Mohammad A. Jafar Mazumder, Mumtaz A. Quraishi, and Amir Al-Ahmed.